TTF 680

ANALYSIS AND SYNTHESIS OF MECHANISMS

Editor-in-Chief
N.I. LEVITSKII

Published for the National Aeronautics and Space Administration
and the National Science Foundation, Washington, D.C.
byAmerind Publishing Co. Pvt. Ltd., New Delhi

This collection of articles deals with the analysis and synthesis of plane, and spatial mechanisms. Various theorteical and practical problems associated with the design of plane mechanisms as well as of adjustable lever and cam-lever mechanisms are considered.

A major part of the book is devoted to articles in which the problems of kinematic and dynamic analysis of cam mechanisms as well as problems of selecting optimum laws of movement of driven links are solved.

Mechanisms of certain machines and instruments, e.g., radialpiston multipath hydromotors, molding presses, pneumatic-hydraulic drives for stopcocks and electrical switches are also described in this collection.

The material presented in this book is intended for scientists and engineer-technicians engaged in the computation and design of mechanisms.

TT 71-58004
NASA TT F-680

AKADEMIYA NAUK SSSR
Otdelenie mekhaniki i protsessov upravleniya
Gosudarstvennyi Nauchno-issledovatel'skii Institut Mashinovedeniya

ACADEMY OF SCIENCES OF THE USSR
Department of Mechanics and Control Processes
State Scientific-Research Institute of Machine Design

ANALYSIS AND SYNTHESIS OF MECHANISMS

(Analiz i Sintez Mekhanizmov)

Editor-in-Chief
N. I. Levitskii

Nauka Publishers
Moscow 1970

Translated from Russian

Published for the National Aeronautics and Space Administration
and the National Science Foundation, Washington, D. C.
by Amerind Publishing Co. Pvt. Ltd., New Delhi
1975

Editorial Board:
Academician I. I. Artobolevskii (Chairman), G. G. Baranov,
A. P. Bessonov, V. A. Gavrilenko, E. V. Gerts,
V. A. Zinov'ev, A. E. Kobrinskii, L. V. Petrokas,
N. P. Raevskii, M. A. Skuridin, A. V. Shlyakhtin

© 1975 *Amerind Publishing Co. Pvt. Ltd., New Delhi*

Translated and Published for the National Aeronautics and Space Administration, pursuant to an agreement with the National Science Foundation, Washington, D. C. by Amerind Publishing Co. Pvt. Ltd.,
66 *Janpath, New Delhi* 110001

Translators: S. K. Goel & K. L. Awasthy
General Editor: Dr. V. S. Kothekar

Available from the U. S. Department of Commerce
National Technical Information Service
Springfield, Virginia 22161

Printed at Prem Printing Press, Lucknow, India
Production: M. L. Gidwani

UDC 62.23

The manual deals with the analysis and synthesis of plane, spatial and spherical mechanisms, problems of selection of optimal laws of movement of links of cam mechanisms.

Material presented in the manual is intended for scientists and engineer-technicians engaged in the computation and design of mechanisms.

FOREWORD

This collection of articles deals with the analysis and synthesis of plane and spatial mechanisms. Various theoretical and practical problems, associated with the design of plane mechanisms as well as of adjustable lever and cam-lever mechanisms, are considered in the articles of N. I. Aleksishvili, Yu. M. Zingerman, P. G. Mudrov and V. I. Kulyugin and others.

A major part of the book is devoted to articles (K. V. Tir and D. N. Senik, E. N. Dokuchaeva, Yu. V. Epshtein and V. A. Novgorodtsev and others) in which the problems of kinematic and dynamic analysis of cam mechanisms as well as problems of selecting optimum laws of movement of driven links are solved.

Synthesis of automats using photoelectronic devices is described in the articles of B. N. Sklyadnev et al.

The articles by L. B. Maisyuk, A. E. Kropp and V. S. Karelin describe the synthesis of complex cam-planetary-connecting rod and hinged-toothed mechanisms.

Nomographic methods of synthesis of hinged lever and cam mechanisms are covered in the articles of L. P. Storozhev and M. M. Gernet.

Mechanisms of certain machines and instruments, e.g. radial-piston multipath hydromotors, molding presses, pneumatic-hydraulic drives for stopcocks and electrical switches, are described in articles by A. S. Gel'man et al., D. M. Lukichev et al., M. S. Rozovskii et al. and A. V. Sinev et al.

CONTENTS

Foreword v

Kinematic Analysis of the Steering Linkage of an Automobile—*N. I. Aleksishvili* 1

New Methods of Synthesis of Mechanisms for Reproducing and Enveloping Curves—*E. G. Berger* 10

Determination of Momentum in Three-Link Mechanisms with a Higher Pair of the 4th Class—*L. N. Borisenko* 21

A Method of Calculating the Change in Primary Dimensions of Mechanisms Due to Wear for the Purpose of Estimating Their Reliability—*E. I. Vorob'ev* 31

Calculation of Kinematic Parameters of Radial-Piston Multipass Hydraulic Motors with Guide Block Profile Consisting of Arcs of Circles—*A. S. Gel'man, Yu. A. Danilov, L. V. Krymova* and *A. M. Makeev* 41

Nomographs for Selecting Optimal Laws of Motion of Driven Links of Cam Mechanisms—*M. M. Gernet* 52

Design of a Four-Link Mechanisms for Reproducing a Given Motion—*N. M. Guseinov* and *S. I. Gamrekeli* 60

Synthesis of Cam Lever Mechanisms for Different Types of Motions of Driven Links—*R. P. Dzhavakhyan* 71

Effects of Errors in the Working Profile of the Cam on Velocity and Acceleration of the Follower—*E. N. Dokuchaeva* .. 88

Kinematic Study of Spatial Mechanisms by the Technique of Vector Analysis—*Yu. M. Zingerman* 102

A Method of Analytical Synthesis of Plane Toothed Lever Mechanisms—*V. S. Karelin* 112

Two Simple Methods of Regulating Motion of the Driven Link in Three-Dimensional Single Contour Mechanisms—*A. A. Kasamanyan* 132

Synthesis of a Toothed Lever Transmission Mechanism—*A. E. Kropp* 143

Design of Three Dimensional Four-Link Mechanisms Conforming to the Travel of the Driven Link and Coefficient of Increase in Velocity of the Reverse Stroke—*V. I. Kulyugin* 152

Classification of Slotted Bar and Lever Mechanisms of Discontinuous Motion—*P. G. Kukharenko* 163

Peculiarities of the Lagrangian Method in the Synthesis of Mechanisms—*N. I. Levitskii* and *Yu. L. Sarkisyan* 180
Design of Cam Elements of Electrical Switches—*D. M. Lukichev, V. A. Nikonorov* and *Z. S. Gazizova* 188
Synthesis of Cam-Planetary-Connecting Rod Mechanism with Reverse Stroke and Stop—*L. B. Maisyuk* 196
Determination of the Zones of Existence of Slotted Lever Mechanisms—*V. A. Mamedov* 207
Three-Dimensional Five-Link Hinged Mechanisms—*P. G. Mudrov* .. 213
Kinematic Study of Three-Dimensional Three-Link Lever Mechanisms Using Analytical Methods—*Z. S. Natsvlishvili*.. .. 220
An Approximate Method for Synthesizing a Hinged Lever Amplifying Mechanisms of a Molding Press—*M. S. Rozovskii, E. N. Dokuchaeva* and *V. G. Lapteva* 233
Dynamic Force Analysis of Plane-Mechanisms in Three-Dimensional Space—*K. F. Sasskii* 246
Analysis of the Structural and Technical Errors of Six-Link Mechanisms in the Dwell Zone—*V. I. Sergeev, S. A. Cherkudinov* and *I. G. Oleinik* 262
Fundamentals of the Theory of Dynamic Synthesis of Cam Mechanisms—*P. V. Sergeev* 277
Kinematic and Force Analysis of Spatial Mechanism of Pneumatic and Hydraulic Drive for Stopcocks of Gas Mains of Type DU 1000—*A. V. Sinev, I. Z. Brodotskaya* and *I. S. Charnaya* .. 284
Design of Automats with Photoelectronic Devices for the Control and Measurement of Linear Dimensions and Areas—*B. N. Sklyadnev, B. N. Yurukhin, Yu. I. Evteev* and *E. I. Astakhov* .. 296
A Nomographical Method for the Synthesis of Multiple Contour Plane Hinged-Lever Mechanisms—*L. P. Storozhev* 309
Techniques for Synthesizing Adjustable Lever Mechanisms—*B. S. Sunkuev* 323
An Approximate Technique for the Synthesis of Disk Cam Mechanisms—*K. V. Tir* and *D. N. Senik* 334
The Problem of Existence of the Crank in the Spatial Four-Link Mechanism with Two Turning and Two Spherical Pairs —*K. A. Tonoyan* 349
Functions with Minimum Deviations from Zero in Problems of Synthesis of Cam Mechanisms—*Yu. V. Epshtein* and *V. A. Novgorodtsev* 366
Abstracts 378

N. I. Aleksishvili

KINEMATIC ANALYSIS OF THE STEERING LINKAGE OF AN AUTOMOBILE

The steering linkage installed on all existing models of automobiles with one-piece front axles is a spatial four-link mechanism [1].

Conforming to the generally accepted classification [2], such a mechanism has two rotating pairs of the 5th class (forked turning cams, connected to the shaft of the front axle with the help of steel cotter pins) and two spherical joints of the 3rd class. The latter are ball joints at the junction of turning cam levers with the transversal rod of the steering linkage. There are no common connections affecting the motion of links of such a mechanism and therefore, it belongs to the category of mechanisms of the zeroth family.

The degree of mobility of a mechanism of the zeroth family is in general expressed by the following equation:

$$\omega = 6n - 5p_5 - 4p_4 - 3p_3 - 2p_2 - p_1,$$

where n is the number of mobile links and p_i is the number of kinematic pairs whose class is indicated in the form of index $i = 1, 2, 3, 4$ and 5.

Using this equation, the degree of mobility of the steering linkage of an automobile is given by:

$$\omega = 6 \times 3 - 5 \times 2 - 4 \times 0 - 3 \times 2 - 2 \times 0 - 0 = 2,$$

i.e., there is a surplus degree of mobility due to the possibility of rotation of the transversal link AC of the linkage about its longitudinal axis (Fig. 1).

This motion however does not take part in the functioning of the linkage as a whole, i.e., actually the mechanism has one degree of mobility.

The presence of ball joints gives rise to a number of difficulties in the manufacturing process as well as during the operation of the steering linkage. Firstly, fabrication of spherical surfaces requires special tools and fixtures. Secondly, inevitable deviations of the ball joint from the drawing dimensions give rise to intensive wear and tear and an increase in the play between the mating surfaces.

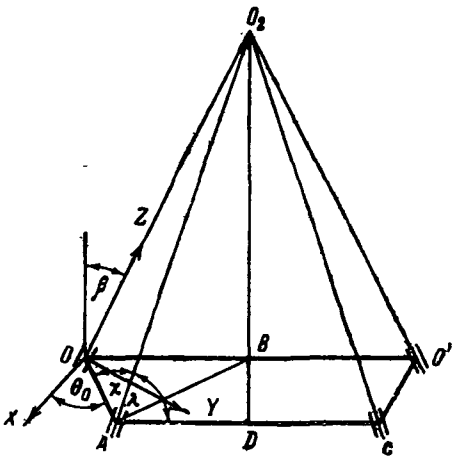

Fig. 1.

Attempts to compensate for this wear and tear with the help of adjustable spring inserts (automobiles MAZ-200, ZIL-164, UAZ-69, etc.), or the insertion of hemispherical pins (GAZ-51A, URAL-355M, etc.) complicate the design and operation of the ball joint.

The above problems initiated research into the possibility of replacing ball joints by spherical ones (for example, in automobiles GAZ-63 and others).

However, the necessary condition—intersection of the axes of all the pairs of steering linkages at one point—was not fulfilled for cylindrical pairs in any of the proposed designs of such joints. As a result, there was additional wear and tear of mating surfaces and other undesirable effects which forced designers to pursue a more complicated and expensive method of installing spherical joints.

It should be stated at this point that the condition for intersection of all cylindrical pairs at one point is a purely theoretical requirement. In practice, this point occupies a volume constrained by conical surfaces. These surfaces are obtained as a result of possible angular displacements of the axes of cylindrical pairs in clearances permissible between the mutually rotating elements of these kinematic pairs—sleeves and pins. Therefore, the farther the theoretical point of intersection of axes and the larger the permissible clearance, the greater will be the value of the above mentioned volume as well as the limits of possible deviations from drawing dimensions of the links of the steering linkage.

Let us examine closely the condition of substitution of spherical pairs of the steering linkage of an automobile by cylindrical (turning) pairs.

The steering linkage of an automobile is represented in Fig. 1 in the form of a four-link mechanism *ACO'O*. The following symbols refer to Fig. 1:

S—length of the transversal rod of the steering linkage, $AC=S$;

$R_l=R_r=R$—length of the lever of the rotating cam along a straight line perpendicular to the axis of the pin, $OA=R_l$; $O'C=R_r$;

d—distance between the projections of the ends of levers of turning cams on the pin axis, $OO'=d$;

O_2—point of intersection of the pin axis inclined at an angle of 2β;

θ_0—angle between the coordinate axis OX and lever of turning cam OA in the case of straight motion of the automobile;

θ_l—angle of rotation of the lever of turning cam, facing the internal side of the trajectory of the automobile on a turn;

θ_e—the same angle but toward the outer side of the automobile on a turn (in the case of straight motion of the automobile $\theta_e=\theta_l=0$);

β—angle of transversal inclination of the pin of the turning cam.

Cartesian coordinates $XY\zeta$ are selected in such a manner that the axis $O\zeta$ is directed along the pin axis, center O lies at the intersection of straight lever of the linkage with the axis of the corresponding pin and the axis OY lies in the plane, passing through points O and O' perpendicular to the plane of linkage in the case of neutral (straight) position of the wheels of the automobile.

Let us examine some of the kinematic problems of this mechanism. In $\triangle AOO_2$ and $\triangle CO'O_2$, the sides $CO'=R_r$ and $AO=R_l$ are equal in accordance with the requirement of similar kinematics of turning of the automobile toward left as well as toward right. The sides $OO_2=O'O_2$, since $\triangle OO'O_2$ is an isosceles triangle in view of the equality of angles at the base ($\angle OO'O_2=\angle O'OO_2=90°-\beta$).

Thus, in $\triangle AOO_2$ and $CO'O_2$, two sides and the angle between them ($\angle CO'O_2=\angle AOO_2=$const) are equal, i.e. $\triangle AOO_2=\triangle CO'O_2$.

The last equality leads to the conclusion that $O_2A=O_2C$. Since this expression is valid for an arbitrary position of the links of the steering linkage of an automobile, by taking point O_2 as the center of sphere of radius $r=O_2A=O_2C$, it can be shown that points A and C remain on the surface of this sphere in the case of motion of the elements of this four-link mechanism in any direction.

Thus, the steering linkage of an automobile is a spherical mechanism [3]. It also follows from the equality $O_2C=O_2A$ that $\triangle O_2AC$ is an isosceles triangle, i.e. angles at the base, $\angle O_2AC$ and $\angle O_2CA$ are equal. Since this equality is valid for all link positions of the linkage, the spherical pairs A and C can be replaced by cylindrical ones with axes intersecting at point O_2.

The position of the axes of rotating pairs with centers at points A and C is defined by the angles χ and λ (see Fig. 1).

From the right-angled $\triangle AOO_2$, $\tan \chi = OO_2/R$, while in right-angled $\triangle OBO_2$, hypotenuse $OO_2 = d/(2 \sin \beta)$. Substituting the last equality in the expression for χ, we get the following value for this angle:

$$\chi = \arctan \mathbf{d}/(2 \sin \beta), \tag{1}$$

where $\mathbf{d} = d/R$

Angle λ is determined from the right-angled $\triangle ADO_2$

$$\cos \lambda = AD/AO_2,$$

where $AD = S/2$; $AO_2 = R/\cos \chi$, the final expression for λ reduces to:

$$\lambda = \arccos \frac{\mathbf{S} \cos \chi}{2}, \tag{2}$$

where $\mathbf{S} = S/R$.

Because of symmetry of the steering linkage of an automobile, equations (1) and (2) are also valid for the rotating pair at point C.

It should be noted that the parameters $\mathbf{d}$ and $\mathbf{S}$ are mutually related by the requirement of optimum kinematics of the steering linkage of an automobile [1] and consequently, the angles χ and λ in the general case are functions of β, $\mathbf{d}$ (or $\mathbf{S}$) and P/L where P is the distance between the points of intersection of the axis of pins of turning cams with the plane of the track and L is the base of the automobile.

The relationship between $90° - \chi$ and the parameters $\mathbf{d}$ and β are graphically shown in Fig. 2.

As is obvious from these graphs, the angle χ deviates considerably from 90° as angle β increases and the deviation is significant at small values of $\mathbf{d}$. At $\beta = 0°$, angle $\chi = \lambda = 90°$, i.e., the steering linkage functions as a two-dimensional four-link mechanism.

The functional relation of angle $90° - \lambda$ with parameters $\mathbf{d}$ and β is shown in Fig. 3. Here, parameter $\mathbf{d}$ is related to $\mathbf{S}$ by the requirement of minimum deviation of the dependence of the actual angles of turning of the steering (front) wheels of the automobile [1] from the equation:

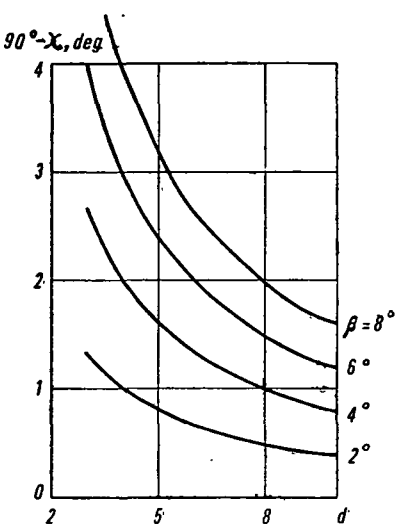

Fig. 2.

$$\cot \theta_e = \cot \theta_i + P/L.$$

Fig. 3 shows that the angle λ tends to 90° as β decreases and P/L increases. This rule holds strictly for decreasing d.

If the value of the angle of transversal inclination of the pin on the turning cam is reduced, these curves have a tendency to converge and thus, the effect of P/L ratio is insignificant at low values of β.

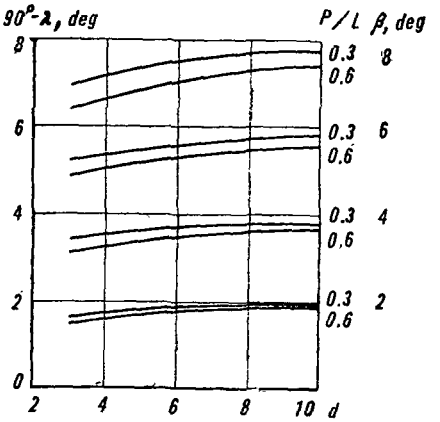

Fig. 3.

The above rule of substitution of spherical joints of the linkage by kinematic pairs of the 5th class is only theoretical. In practice, while constructing such a four-link mechanism, it often becomes necessary to deviate from the given geometrical dimensions of the links of the steering linkage and consequently, to deal with the deviations from the theoretical conditions of intersection of all axes at point O_2 (see Fig. 1).

The efficiency of this mechanism can, however, be retained by rationally selecting the permissible clearance between mutually rotating elements of cylindrical (rotating) pairs. This clearance aids in securing the angular displacements of the axes of these pairs.

Thus, the axis of a cylindrical pair occupies any position in the cone having the half angle at the vertex, determined from the plan of the joint under consideration (Fig. 4). In Fig. 4, a shaft, which constitutes one of the elements of the pair is represented in two positions: normal ($ACBE$) and inclined at an angle $\Delta(A'C'B'E')$.

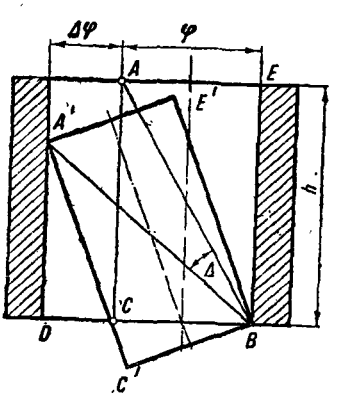

Fig. 4.

It follows from the figure that

$$\Delta = \angle ABC - \angle A'BD,$$

for right-angled $\triangle ACB$

$$\sin \angle ABC = h/\sqrt{h^2+\varphi^2},$$

for right-angled $\triangle A'DB$

$$\sin \angle A'BD = \sqrt{1-(\varphi+\Delta\varphi)^2/(h^2+\varphi^2)},$$

and finally, after simple transformations, the following expression for the angle is obtained:

$$\sin \Delta=[h(\varphi+\Delta\varphi)-\varphi\sqrt{h^2-2\varphi\Delta\varphi-\Delta\varphi^2}]/(h^2+\varphi^2), \qquad (3)$$

where h—height of the rotating pair;
φ—shaft diameter;
$\varphi+\Delta\varphi$—hole diameter;
$\Delta\varphi$—tolerance for fitting the shaft in the hole ($\Delta\varphi\geqslant 0$).

Because of the small value of angle $\Delta\leqslant 4°$, dividing the numerator and denominator of the right-hand side of equation (3) by φ^2, we obtain approximately:

$$\Delta=[\mathbf{h}(1+\Delta\varphi)-\sqrt{\mathbf{h}^2-2\Delta\varphi-\Delta\varphi^2}]/(1+\mathbf{h}^2), \qquad (3a)$$

where $\mathbf{h}=h/\varphi$ and $\Delta\varphi=\Delta\varphi/\varphi$.

Solving the equation (3a) with respect to $\Delta\varphi$, we obtain

$$\Delta\varphi=1/(1+\mathbf{h}^2)\{\Delta\mathbf{h}^3+\Delta\mathbf{h}-\mathbf{h}^2-1+\sqrt{(\Delta\mathbf{h}^3+\Delta\mathbf{h}-\mathbf{h}^2-1)^2-(\mathbf{h}^2+1)\cdot[(\mathbf{h}-\Delta-\Delta\mathbf{h}^2)^2-\mathbf{h}^2]}\}. \qquad (4)$$

To obtain a numerical expression for the efficiency of the steering linkage of an automobile, let us define the position of the axis of each of the four rotating pairs with the help of the equation of a straight line, passing through the center of the given pair parallel to the unit vector $j=(l, m, n)$ which is, for the time being, unknown. The direction of this vector, given by the directional cosines, facilitates intersection of the axis of all the pairs at one point in the presence of deviations in the link dimensions of the linkage.

Equation (4) permits us to determine the 3 cosines. Let us now determine the tolerance required for the contact surface of the rotating pair under consideration.

Here, it should be kept in mind that out of the three directional cosines, only one for the possible angular deviations of the shaft of the kinematic pair in its hole, defines the value of the tolerance. Specifying the remaining two cosines corresponds to the selection of the position of pair axis on the above mentioned conical surface.

We find the position of the centers of the rotating pairs in the XYZ coordinate system (see Fig. 1) in the following manner [1]:

1. Point O

$$x_0=0;\ y_0=0;\ z_0=0.$$

Guide vector $j_O(l_O; m_O; n_O)$.

2. Point A

$$x_A=R_1\cdot\cos(\theta_0+\theta_i);\quad y_A=R_1\cdot\sin(\theta_0+\theta_i);\quad z_A=0.$$

Guide vector $j_A(l_A; m_A; n_A)$.

3. Point C

$$x_C=R_T \cdot \cos(\theta_0-\theta_e); \quad y_C=d \cdot \cos\beta-R_T \cdot \cos 2\beta \cdot \sin(\theta_0-\theta_e);$$
$$z_C=d \cdot \sin\beta-R_T \cdot \sin 2\beta \cdot \sin(\theta_0-\theta_e).$$

Guide vector $j_C(l_C; m_C; n_C)$.

4. Point O'

$$x_{O'}=0; \quad y_{O'}=d \cdot \cos\beta; \quad z_{O'}=d \cdot \sin\beta.$$

Guide vector $j_{O'}(l_{O'}; m_{O'}; n_{O'})$, where l, m and n are directional cosines of the corresponding vectors and the dimensions R and d are estimated by considering the permissible deviations.

The conditions of intersection of the axes of these rotating pairs of an actual linkage expressed in the canonical form, is given by the following system of algebraic equations:

$$(x_A-x_0+\xi_0 \cdot y_0-\xi_A \cdot y_A)/(\xi_0-\xi_A)=(x_C-x_0+\xi_0 \cdot y_0-\xi_C \cdot y_C)/(\xi_0-\xi_C)$$
$$=(x_{O'}-x_0+\xi_0 y_0-\xi_{O'} y_{O'})/(\xi_0-\xi_{O'})=(x_C-x_A+\xi_A y_A-\xi_C y_C)/(\xi_A-\xi_C)$$
$$=(x_{O'}-x_{A'}+\xi_A \cdot y_A-\xi_{O'} \cdot y_{O'})/(\xi_A-\xi_{O'})=(x_{O'}-x_C+\xi_C \cdot y_C-\xi_{O'} \cdot y_{O'})/(\xi_C-\xi_{O'}),$$
$$(z_A-z_0+\psi_0 \cdot x_0-\psi_A \cdot x_A)/(\psi_0-\psi_A)=(z_C-z_0+\psi_0 \cdot x_0-\psi_C \cdot x_C)/(\psi_0-\psi_C)$$
$$=(z_{O'}-z_0+\psi_0 \cdot x_0-\psi_{O'} \cdot x_{O'})/(\psi_0-\psi_O)=(z_C-z_A+\psi_A \cdot x_A-\psi_C \cdot x_C)/(\psi_A-\psi_C)$$
$$=(z_{O'}-z_A+\psi_A \cdot x_A-\psi_{O'} x_{O'})/(\psi_A-\psi_{O'})=(z_{O'}-z_C+\psi_C \cdot x_C-\psi_{O'} x_{O'})/(\psi_C-\psi_{O'}),$$

where $\xi=l/m$; $\psi=n/l$; the index refers to the kinematic pair of the steering linkage.

Writing this system of equations in the form of individual equalities and keeping only linearly independent equations, we arrive at the system of equations given below, in matrix form for the sake of compactness:

$$\begin{pmatrix} x_A-x_C; & x_C-x_0; & x_0-x_A; & 0; & y_0-y_A; \\ x_A-x_{O'}; & x_{O'}-x_0; & 0; & x_0-x_{A'}; & y_0-y_A; \\ x_C-x_{O'}; & 0; & x_{O'}-x_0; & x_0-x_C; & 0; \end{pmatrix}$$

$$\begin{pmatrix} y_C-y_0; & 0; & y_A-y_C; & 0; & 0 \\ 0; & y_{O'}-y_0; & 0; & y_A-y_{O'}; & 0 \\ y_0-y_C & y_{O'}-y_0; & 0; & 0; & y_C-y_{O'} \end{pmatrix} \begin{pmatrix} u_1 \\ u_2 \\ u_3 \\ u_4 \\ u_5 \\ u_6 \\ u_7 \\ u_8 \\ u_9 \\ u_{10} \end{pmatrix} = (0), \qquad (5)$$

where (0) is the null matrix:

$$\begin{array}{lll} u_1 = \xi_0\,; & u_5 = \xi_0 \cdot \xi_A\,; & u_8 = \xi_A \cdot \xi_C\,; \\ u_2 = \xi_A\,; & u_6 = \xi_0 \cdot \xi_C\,; & u_9 = \xi_A \cdot \xi_{O'}\,; \\ u_3 = \xi_C\,; & u_7 = \xi_0 \cdot \xi_{O'}\,; & u_{10} = \xi_C \cdot \xi_{O'}\,. \\ u_4 = \xi_{O'}\,; & & \end{array}$$

Similarly for the second system of equations:

$$\begin{pmatrix} z_A - z_C\,; & z_C - z_0\,; & z_0 - z_A\,; & 0\,; & x_0 - x_A\,; \\ z_A - z_{O'}\,; & z_{O'} - z_0\,; & 0\,; & z_0 - z_A\,; & x_0 - x_A\,; \\ z_C - z_{O'}\,; & 0\,; & z_{O'} - z_0\,; & z_0 - z_C\,; & 0\,; \end{pmatrix}$$

$$\begin{pmatrix} x_C - x_0\,; & 0\,; & x_A - x_C\,; & 0\,; & 0 \\ 0\,; & x_{O'} - x_0\,; & 0\,; & x_A - x_{O'}\,; & 0 \\ x_0 - x_C\,; & x_{O'} - x_0\,; & 0\,; & 0\,; & x_C - x_{O'} \end{pmatrix} \begin{pmatrix} v_1 \\ v_2 \\ v_3 \\ v_4 \\ v_5 \\ v_6 \\ v_7 \\ v_8 \\ v_9 \\ v_{10} \end{pmatrix} = (0), \qquad (5a)$$

where (0) is the null matrix:

$$\begin{array}{lll} v_1 = \psi_0\,; & v_5 = \psi_0 \cdot \psi_A\,; & v_8 = \psi_A \cdot \psi_C\,; \\ v_2 = \psi_A\,; & v_6 = \psi_0 \cdot \psi_C\,; & v_9 = \psi_A \cdot \psi_{O'}\,; \\ v_3 = \psi_C\,; & v_7 = \psi_0 \cdot \psi_{O'}\,; & v_{10} = \psi_C \cdot \psi_{O'}\,. \\ v_4 = \psi_{O'}\,; & & \end{array}$$

As the rank of a matrix composed of the coefficients of the system of equation (5) [similarly for system (5a)] is less than the number of unknown variables, equations (5) and (5a) have several basic systems of solutions.

However, if the direction of axes of any two kinematic pairs of the linkage is specified, equations (5) and (5a) make it possible to determine the only one possible direction of the axes of all the four pairs at which this mechanism can function. Generally this solution does not give values of angles χ and λ which coincide with theoretical values calculated from equations (1) and (2). Varying the positions of the two given axes, it is easy to achieve minimum deviation of these angles from their theoretical values.

The direction cosines are related to each other by the equation:

$$l^2 + m^2 + n^2 = 1\,. \qquad (6)$$

The clearance Δ restricts the possible change of only one of the three directional cosines while the values of the remaining two should be selected in such a manner that the two selected axes intersect in space.

The permissible clearances, at which there will be minimum deviation of the values of angles χ and λ from theoretical values, will be the minimum possible required to retain the efficiency of the automobile steering linkage considered as a four-link spatial mechanism.

Since numerous calculations are possible, they should be done on high-speed electronic computers using standard programs for solving determinants. In this case, the results obtained serve as reference material for designers and can be drawn up in the form of tables or graphs.

References

1. Dvali, R. R. and N. I. Aleksishvili. Kinematika rulevoi trapetsii avtomobilya (Kinematics of the steering linkage of an automobile). *Soobshch. AN GruzSSR*, XLIV, No. 3, 1966.
2. Artobolevskii, I. I. Teoriya mashin i mekhanizmov (Theory of Machines and Mechanisms). Moscow—Leningrad, GITTL, 1952.
3. Tavkhelidze, D. S. K voprosu sinteza i kinematiki prostranstvennykh chetyrekhzvennykh mekhanizmov (Problems of Synthesis and Kinematics of Spatial Four-Link Mechanisms). Tbilisi, Izd-vo Tsodna, 1960.

E. G. Berger

NEW METHODS OF SYNTHESIS OF MECHANISMS FOR REPRODUCING AND ENVELOPING CURVES

Modern methods of synthesis of mechanisms, designed for reproducing and enveloping plane curves are based either on different geometrical transformations (projections, cissoidal, [*m-n*] marking, inversion, etc.) or on preliminary determination of the properties of curves leading to their construction [1-3].

However, the problem of determining the properties of a curve from its equations or of finding out transformations from which the curves can be obtained without using the general methods of solving the equation, is extremely time consuming and complicated.

The methods which follow are helpful in designing mechanisms for constructing curves directly from their equations without taking into account the properties of the given curves.

Mechanisms used in reproducing and enveloping curves are commonly found in subassemblies of various automatic machines and in precision instruments and calculators. Mechanisms whose rectilinear links are used in enveloping particular curves are of special importance as their working component, which can take the form of a rack, hobbing cutter or a wide cutter, facilitates machining of profile surfaces by the method of generation [4, 5].

1. Reproduction of Curves

1. Theory of the method: The method is based on the theory of plotting curves of the type:

$$F(x, y)=0 \tag{1.1}$$

as the geometrical location of intersection of corresponding curves belonging

to the design groups:

$$f_1(x, y, \lambda)=0, \ldots, \text{(a)} \quad \text{and} \quad f_2(x, y, \lambda)=0, \ldots, \text{(b)}. \qquad [6]$$

A technique of synthesizing mechanisms directly from the equations of the curves without going into the laborious examination of their properties is the main feature of this article.

The equivalence between the curves of groups (a) and (b) is determined in the following manner. Initially the equation of one of the groups, for example (a), is selected arbitrarily. Then, the equation of the second group (b) is found out by simultaneously solving the equations (1.1) and (a). Eliminating parameter λ from equations (a) and (b) results in the initial equation (1.1). Consequently, the points of intersection of curves (a) and (b) at $\lambda=\lambda_1, \lambda_2, \lambda_3, \ldots$, lie on the given curve (1.1).

Selecting different variables such as an angle or its trigonometric function, a segment of a straight line, etc. as λ, we define the method of plotting the curves (a) and (b) respectively. Sets of straight lines and circles can be taken as the design groups for curves of all orders [7] and in many cases this simplifies the process of plotting these curves.

Considering the structure of these graphical representations as the abstract geometrical drawing of the mechanism to be designed, we fabricate it by replacing the points by rollers or slide blocks and straight lines by rocker arms, linear guides or by cranks.

2. Let the conical sections be given by the equation

$$y^2=2px-(1-\varepsilon^2)x^2. \qquad (1.2)$$

To synthesize a conicograph, let us arbitrarily select the following group of straight lines passing through the origin as one of the design groups:

$$y=\lambda x. \qquad (1.3)$$

On simultaneously solving the expression (1.2) and (1.3) we get the equation of the second group:

$$(x+l)/(k+l)=(y-l/\lambda)/(-l/\lambda), \qquad (1.4)$$

where $l=2p/\varepsilon^2$; $k=2p/(1-\varepsilon^2)$.

Equation (1.4) represents a group of straight lines passing through two points with coordinates $(k, 0)$ and $(-l, l/\lambda)$.

On the basis, let us determine the method of plotting the groups of straight lines (1.3) and (1.4) at variable $\lambda=\tan\varphi$ (Fig. 1, a). The straight lines AN, passing through a fixed point $A(k, 0)$ and point N $(-l, l/\lambda)$ of intersection of straight line $BL(x=-l)$ with the line $ON \perp OM$, corresponds

to the arbitrary ray OM of group (1.3). The points of intersection of straight lines OM and AN lie on the conic sections (1.2).

A universal conicograph can be fabricated from this drawing.

For plotting ellipses, the slide block A of the rocker arm AN should be fixed on the right of the origin O at a distance k, since when $\varepsilon<1$, $k>0$. For drawing hyperbolas ($\varepsilon>1$, $k<0$), this slide block must be fixed on the left of 0 at the same distance k. For drawing parabolas ($\varepsilon=1$, $k=\infty$), the rocker arm AN is moved parallel to the x-axis. For this setting, the mechanism is similar to the well-known Antonov's parabolograph [8].

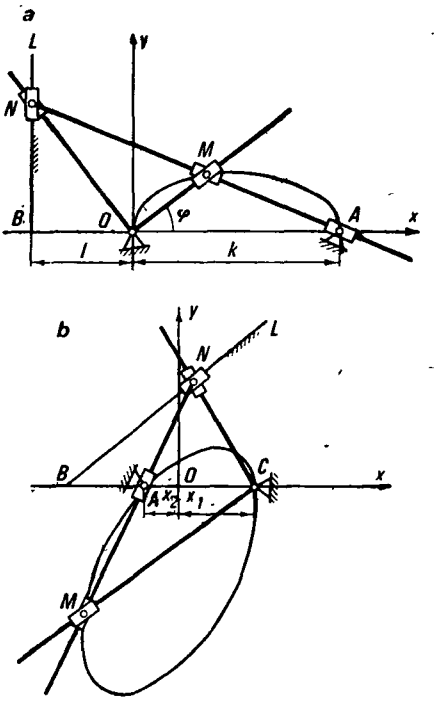

Fig. 1.

For drawing conic sections defined by the general equation

$$Ax^2+2Bxy+Cy^2+2Dx+2Ey+F=0 \tag{1.5}$$

supports of the rotating straight lever and of the rocker arm AN are made to coincide with the points of intersection C and A of curve (1.5) with the x-axis (Fig. 1, b). Abscissas X_1 and X_2 of these points are calculated from the equation $Ax^2+2Dx+F=0$. In this case, if the guide line BL is arranged arbitrarily (as a straight line $ax+by+f=0$) the point M of the mechanism describes a conic section of the type:

$$(ax_2+f)\,x^2+b\,(x_2-x_1)\,xy+(ax_1+f)\,y^2-(ax_2+f)\,(x_1+x_2)x+$$
$$bx_2(x_1-x_2)\,y+x_1x_2(ax_1+f)=0. \tag{1.6}$$

Comparing coefficients of equations (1.5) and (1.6), we determine the parameters a, b and f which define the required position of the guide line BL

$$a=(A-C)/(x_2-x_1);$$
$$b=2B/(x_2-x_1);$$
$$f=(Cx_2-Ax_1)/(x_2-x_1).$$

3. To construct a mechanism for producing Descartes sheet defined by the equation

$$x^3+y^3=3axy, \tag{1.7}$$

consider the same group of straight lines given by (1.3). Substituting expression (1.3) in (1.7), we get the equation of a family of straight lines

$$x/(b\lambda)+y/(b/\lambda)=1, \tag{1.8}$$

where $b=3a$, intercepting segments $OA=b\cdot\tan\varphi$ and $OB=b\cdot\cot\varphi$ (Fig. 2, a) on coordinate axis at variable $\lambda=\tan\varphi$. To plot OA and OB, let us draw $OK\perp OM$ and project the points K and L of intersection of OK with straight lines $x=-b$ and $y=-b$ on the coordinate axis. Descartes sheet is the locus of the points of intersection M of straight lines OM and AB.

On the basis of the graphical representation, we construct the mechanism which is adjusted by changing the length of levers AK and BL.

4. The mechanism obtained for producing Descartes sheet can also be adjusted for drawing Bernoulli's lemniscate

$$(x^2+y^2)^2=b^2xy. \tag{1.9}$$

The curve (1.9) is the locus of points of intersection of the group of straight lines

$$y=\lambda^2x \tag{1.10}$$

and the group of straight lines (1.8), which are plotted by this mechanism.

The group of straight lines (1.10) and (1.8) are mutually perpendicular. Therefore, if lever OM is hinged at support O and a cross-shaped slide block with mutually perpendicular guides is installed at the place of intersection of the lever with the rocker arm AB, we get a mechanism for generating Bernoulli's lemniscate (Fig. 2, b).

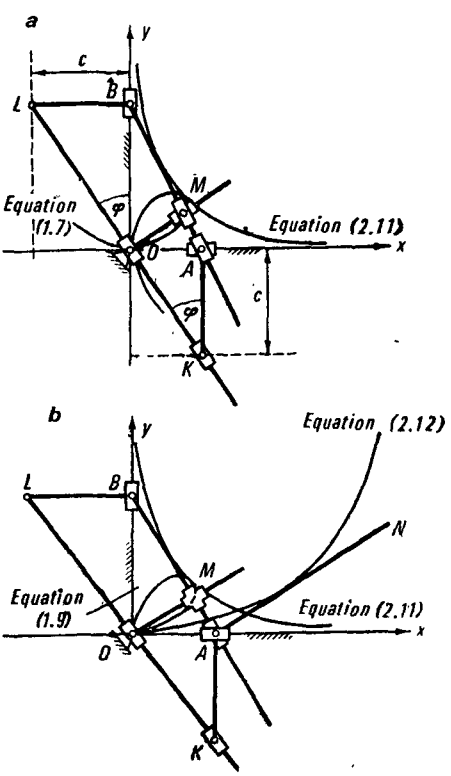

Fig. 2.

5. Let us examine the mechanism for generating curves of 4th order $(x-y+a)^2\ (b^2-y^2)=(b^2-y^2-xy)$ as investigated by Durer [9] (see Fig. 3).

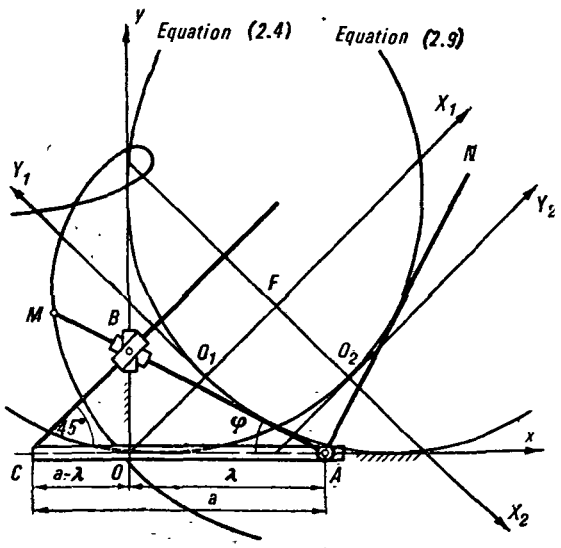

Fig. 3.

The following parametric equations are taken as the design groups

$$x=a/(1+\tan\varphi)-b\cdot\cos\varphi;\ y=b\cdot\sin\varphi. \tag{1.11}$$

As shown in Fig. 3, coordinates of point M are defined by equations (1.11). Consequently, this point lies on the given curve.

The mechanism defined in this manner is of interest since its connecting rods are not restricted and extend to ∞.

2. Enveloping of Curves

1. Theory of the method. The method is based on finding the curve which envelopes the group of straight lines

$$[x-f_1(\lambda)]/[f_2(\lambda)-f_1(\lambda)]=[y-\psi_1(\lambda)]/[\psi_2(\lambda)-\psi_1(\lambda)] \tag{2.1}$$

and satisfies certain geometrical conditions.

From the general theory of envelopes [10], the equation of the curve F enveloping this group, can be obtained by differentiating equation (2.1) with respect to λ and eliminating λ by substitution of this equation in (2.1).

Synthesis of mechanisms, whose rectilinear links envelop F, is facilitated by mechanically plotting straight lines (2.1). To simplify the task, let us assume that straight lines (2.1) pass through points (x_A, y_A) and (x_B, y_B) describing the curves F_A and F_B, on changing λ, having the following parametric equations:

$$x_A=f_1(\lambda); \qquad x_B=f_2(\lambda);$$
$$y_A=\psi_1(\lambda); \qquad y_B=\psi_2(\lambda),$$

when $\psi_1(\lambda)=0$ and $f_2(\lambda)=0$, equation (2.1) takes the form

$$x/f_1(\lambda)+y/\psi_2(\lambda)=1, \tag{2.2}$$

where F_A and F_B are straight lines coinciding with coordinate axis.

Thus, it is easy to plot straight lines (2.2) by putting segments $OA=f_1(\lambda)$ and $OB=\psi_2(\lambda)$ on axes.

Geometrical conditions imposed on straight line groups (2.1) and (2.2) are established by the specific selection of functions $f_1(\lambda)$, $f_2(\lambda)$, $\psi_1(\lambda)$, $\psi_2(\lambda)$. For the mechanisms analyzed in this article, this selection is made on the basis of the following theorems. The first and second theorems are from analytical geometry [11] and the rest have been derived for the first time.

Theorem 1. *Tangents to a hyperbola along with its asymptotes form isometric triangles.*

Theorem 2. *The segment of the tangent to the conical section included in between the tangents at the vertices make a right angle at the focus.*

Theorem 3. *Straight lines intercepting coordinate axes at points the algebraic sum of whose coordinates is constant envelop a parabola.*

Let the straight line AB (see Fig. 3) intercept the coordinate axes at points $(x_A, 0)$ and $(0, y_B)$ in such a manner that $x_A+y_B=a$. For determining the equation of the group of straight lines satisfying this condition, it is sufficient to put $f_1(\lambda)=\lambda$ and $\psi_2(\lambda)=a-\lambda$ in equation (2.2).

Differentiating the equation

$$x/\lambda+y/(a-\lambda)=1 \tag{2.3}$$

with respect to λ, we find $\lambda=1/2\cdot(a+x-y)$. Substitution of λ in equation (2.3) leads to the equation of a parabola

$$x^2+y^2-2xy-2ax-2ay+a^2=0 \tag{2.4}$$

with parameter $p=1/2\cdot 2^{1/2}\,a$.

Theorem 4. *Envelopes of polytropic curves*

$$x^p\cdot y^q=a \tag{2.5}$$

with respect to polytropic curves of the type

$$(y/q)^q=c(x/n)^n$$

and (2.6)

$$(x/p)^p=c(y/m)^m,$$

where $n=2q+p$, $m=2p+q$, $c=p^pq^q/a$ *are straight lines coinciding with* x *and* y *coordinate axes.*

As is well known, a right angle whose sides touch the curves will be the generalized conic envelope of two curves or the conic envelope of one of them with respect to the other.

The equation of the tangent to the curve (2.5) at an arbitrary point (x_1, y_1)

$$(x-x_1)\ p\cdot x_1^{p-1}y_1^q+(y-y_1)\ qx_1^py_1^{q-1}=0 \tag{2.7}$$

intersects one of the axes, for example $y=0$, at the point $[(p+q)/p\cdot x_1, 0]$.

Equation of the straight line perpendicular to the tangent and passing through this point will be:

$$y=qx_1/(py_1)\cdot[x-(p+q)x_1/p]. \tag{2.8}$$

To find the curve enveloping the group (2.8), substitute $x_1=\lambda$ and $y_1=a/\lambda$, as determined from equality (2.5) in formula (2.8).

Differentiating the single parameter group

$$a^{1/q}\cdot y=\frac{q}{p}\lambda^{1/p+1/q}x-q(p+q)/p^2\cdot\lambda^{2/p+1/q} \tag{2.8a}$$

with respect to λ, we get $\lambda=y^pp^p/(p+q)^p$. Substituting λ in formula (2.8a), we get the required equation of the enveloping curve in the form

$$(y/q)^q=p^pq^q/a\cdot[x/(2q+p)]^{2q+p}. \tag{2.6a}$$

Similarly we get the equation of the curve enveloping the group of straight lines, perpendicular to tangent (2.7) and passing through the point of its intersection with the other axis $x=0$, in the form

$$(x/p)^p=p^p\cdot q^q/a\cdot[y/(2p+q)]^{2p+q}. \tag{2.6b}$$

Corollary: Asymptotes $y=0$ and $x=0$ of hyperbolic curves (2.5) are their conic envelopes with respect to parabolic curves (2.6).

Thus, if the indices p and q in equation (2.5) have the same signs, the polytropic equation will represent hyperbolas with asymptotes $y=0$ and $x=0$. If the indices in equation (2.6) have the same sign, the polytropic equations will represent parabolic curves.

Theorem 5. *Generalized envelopes of two equal cofocal parabolas, whose axes are perpendicular to each other, is a straight line coinciding with their common tangent.*

Let us consider parabola (2.4). The equation of a parabola, rotated through 90° and having the same parameter and focus, is

$$x^2+y^2+2xy-4ay=0. \tag{2.9}$$

The straight line $y=0$ is the tangent common for these parabolas (see Fig. 3).

According to theorem 3, straight lines AM of group (2.3) become the tangents to parabola (2.4). It must be shown that straight lines $AN \perp AM$, passing through point A of intersection of curve (2.3) with $y=0$, envelope the parabola (2.9). The proof is obtained by differentiating the equation of the group of straight lines AN

$$y=(x-\lambda)\cdot\lambda/(a-\lambda) \tag{2.10}$$

with respect to λ and we get $\lambda=1/2\cdot(x+y)$. Substituting the value of λ in equation (2.10) we get equation (2.9).

2. Let us examine the family of straight lines, satisfying the requirements of the theorem 1. On putting $f_1(\lambda)=b\lambda$ and $\psi_2(\lambda)=b/\lambda$ in equation (2.2), we get the equation of the required group in the form of equation (1.8). According to theorem 1, a hyperbola is the enveloping curve for this group. Differentiating equation (1.8) with respect to λ and substituting the value of $\lambda=b/(2y)$, we obtain

$$xy=1/4\cdot b^2. \tag{2.11}$$

The straight lines of group (1.8) are plotted by the mechanism shown in Fig. 2. Hence, its rocker arm AB envelops an equilateral hyperbola (2.11).

On the basis of theorem 4 and its corollary, we find that asymptote $y=0$ of hyperbola (2.11) will be its envelope with respect to a cubic parabola

$$y=4/(27b^2)\cdot x^3. \tag{2.12}$$

Therefore, to obtain a mechanism enveloping a cubic parabola (2.12), it is sufficient to connect a lever $AN \perp AB$ to the slide block A of the rocker arm AB (Fig. 2, b). This results in a mechanism that can be set to draw Descartes sheet and Bernoulli's lemniscate by simultaneously enveloping a hyperbola and cubic parabola.

3. Graphical representation of straight lines of group (2.3), which according to theorem 3, envelop parabola (2.4), and can be plotted by the mechanism designed for plotting Durer curves (Fig. 3).

Actually, if $f_1(\lambda)=OA=\lambda$, then $\psi_2(\lambda)=OB=a-\lambda$ which on substitution in equation (2.2) results in equation (2.3). Thus, rocker arm AB of this mechanism envelops parabola (2.4).

On the basis of theorem 5, let us connect a lever $AN \perp AB$ to the rocker arm AB. In this case, the link AN describes the parabola (2.9).

To set the mechanism to envelop simultaneously two parabolas with a given parameter p, the length a of the slide block AC must be $a=2\frac{1}{2}p$.

4. On the basis of theorem 2, we take $f_1(\lambda)=b$, $f_2(\lambda)=m$; $\psi_1(\lambda)=-b/\lambda$; $\psi_2(\lambda)=m\lambda$. Substituting these expressions in equation (2.1), we get the equation of the family of straight lines

$$(x-l)/(m-l)=(y+l/\lambda)/(m\lambda+l/\lambda), \tag{2.13}$$

which are enveloped by the conic section

$$y^2(m-l)^2=4ml\,\{[x-(m+l)/2]^2-[(m-l)/2]^2\}. \tag{2.14}$$

Equation (2.14) represents:

hyperbola $[x-(m+l)/2]^2/[(m-l)/2]^2-y^2/(ml)=1$,
with semiaxes $a=(m-l)/2$, $b=(ml)^{\frac{1}{2}}$, when $l>0$;
an ellipse $[x+(m-l)/2]^2/[(m+b)/2]^2+y^2/(ml)=1$,
with semiaxes $a=(m+l)/2$, $b=(ml)^{\frac{1}{2}}$, when $l<0$;

a parabola $y^2=-4m(x-m)$ with parameter $p=2m$, when $l=\infty$.

The straight line (2.13) passes through points $(m, m\lambda)$ and $(l, -l/\lambda)$ which on changing λ move along straight lines $x=m$ and $x=l$.

On this basis, we determine the method of plotting straight line AB of group (2.13). The graph for enveloping an ellipse ($l=-l$) is shown in Fig. 4. Two mutually perpendicular lines OA and OB are drawn from center O till they intersect straight lines CA ($x=m$) and BD ($x=-l$) at points A and B. On putting $\lambda=\tan\varphi$, coordinates of these points will be $A(m, m\cdot\tan\varphi)$ and $B(-l, +l/\tan\varphi)$.

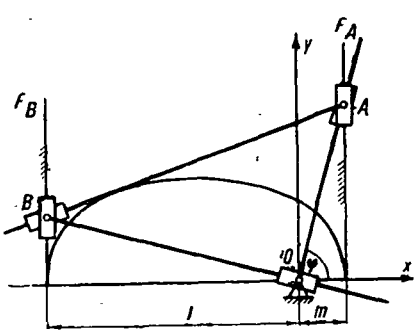

Fig. 4.

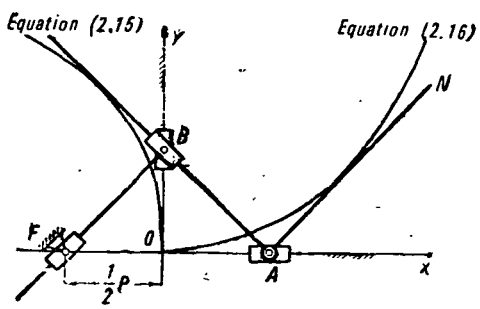

Fig. 5.

Hence, straight line AB belongs to the group (2.13) and on changing λ, envelops the curves (2.14).

A universal mechanism for enveloping conic sections can be constructed from these plottings. To set it for enveloping a hyperbola, the guide F_B is installed on the left of the origin ($l>0$). For enveloping a parabola, the rocker arm AB is fixed perpendicular to the link OA ($l=\infty$).

5. It follows from theorem 4 that the generalized envelope of a quadratic parabola

$$y^2=-2px \tag{2.15}$$

and semicubical parabola

$$y^2=8/(27p)\cdot x^3 \tag{2.16}$$

is a straight line coinciding with the abscissa.

On the basis of this, if a lever $AN \perp AB$ is connected to the mechanism designed for enveloping parabolas (Fig. 5) [4], we get a mechanism for simultaneously enveloping the curves (2.15) and (2.16). To set it for enveloping the semicubical parabola $y^2=cx^3$, it is necessary to take $OF=4/(27c)$.

In conclusion, it should be noted that mechanisms for reproducing and enveloping curves utilizing the above methods are synthesized in the following order:

1) a curve is constructed either in the form of the locus of the points of intersection of design groups or as the enveloping curve of the group of straight lines;

2) methods of graphical representation of these groups are defined; and then

3) mechanisms fabricated from these plottings are designed.

These methods point out new approaches to the theory and practice of synthesis of mechanisms.

References

1. Artobolevskii, I. I. Teoriya mekhanizmov dlya vosproizvedeniya ploskikh krivykh (Theory of Mechanisms for Reproduction of Plane Curves). Izd-vo AN SSSR, 1959.
2. Dobrovol'skii, V. V. Teoriya mekhanizmov dlya obrazovaniya ploskikh krivykh (Theory of Mechanisms for Formation of Plane Curves). Izd-vo AN SSSR, 1953.

3. MISHAGIN, V. N. Graficheskoe i mekhanicheskoe postroenie ploskikh krivykh (Graphical and Mechanical Plotting of Plane Curves). Kand. diss., Sverdlovsk, 1960.
4. ARTOBOLEVSKII, I. I. Mekhanizmy dlya ogibaniya konicheskikh sechenii (Mechanisms for enveloping conic sections). *Vestnik inzhenera i tekhnika,* No. 11, 12, 1946.
5. KAMINSKII, V. P. Novyi konikograph i ustroistvo dlya universal'noi obrabotki po sposobu "obkatki" poverkhnostei vrashcheniya i tsilindrov 2-go poryadka (A new conicograph and device for universal plotting of surfaces of revolution and cylinders of 2nd order). *Vestnik metallopromyshlennosti,* No. 8, 1939.
6. POLYNOVSKII, G. L. Novye sposoby graficheskogo i mekhanicheskogo postroeniya tekhnicheskikh krivykh (New Methods of Graphical and Mechanical Plotting of Technical Curves). Kand. diss., Moscow, 1947.
7. BERGER, E. G. O sinteze mekhanizmov dlya obrazovaniya ploskikh krivykh (Synthesis of mechanisms for formation of plane curves). Tezisy XVI nauchn. konf. Astrybvtuza. Astrakhan'. 1966.
8. DELONE, N. B. Peredacha vrashcheniya i mekhanicheskoe cherchenie krivykh sharnirno-rychazhnymi mekhanizmami (Transmission of Motion and Mechanical Drawing of Curves by Hinged Lever Mechanisms). St. Petersburg, 1894.
9. QUNTHER, S. Albrecht Durer einer der moderner Vurvenlehre. *Bibl. math.,* 1886.
10. RASHEVSKII, P. K. Kurs differentsial'noi geometrii (Textbook of Differential Geometry). Moscow, Fizmatgiz, 1950.
11. ADAMAR, ZH. Elementarnaya geometriya (Elementary Geometry). Moscow, Fizmatgiz, 1958.

L. N. Borisenko

DETERMINATION OF MOMENTUM IN THREE-LINK MECHANISMS WITH A HIGHER PAIR OF THE 4TH CLASS

The problem of determining the angular momentum of the driven link in a planar three-link mechanism possessing a higher element of the fourth class has been solved earlier in [1] by the method of substitution. Its solution also follows from the equation, obtained by Ya. L. Geronimus [2] which relates parameters of Burmester curves with the curvature of conjugating roulettes and their evolutes.

Through an inversion, consisting of converting the driving link into a support, an auxiliary plane is introduced below whose stationary centroid is the evolute of the profile of the driving link and whose movable centroid is selected on the basis that the profile of the driven link is the movable centroid during motion with respect to this plane. Determination of the motion of the driven link relative to this plane enables us to plot the momentum "diagram".

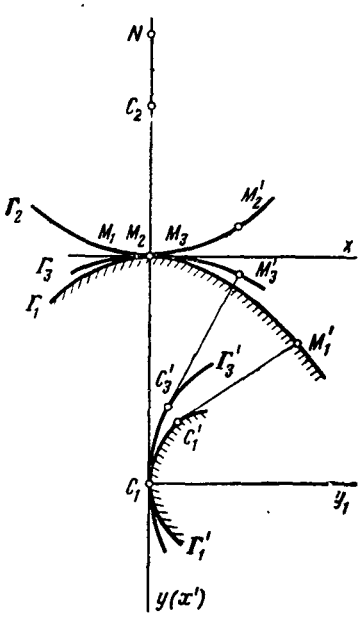

Fig. 1.

1. Let us consider the plane $\mathcal{P}_2$ (Fig. 1) whose motion is defined by the instantaneous center of rotation and the pair of conjugating roulettes Γ_1 and Γ_2 (with radii of curvature ρ_1 and ρ_2 at the point of conjugation and radii of curvature of their evolutes a_1 and a_2 at the corresponding points).

Let us introduce a new movable plane

$\mathcal{P}_3$. Let evolute Γ_1' of the stationary roulette be the stationary centroid of this plane (movable centroid Γ_3' being unknown). Then the polar tangent C_1x' to plane $\mathcal{P}_3$ coincides with the common normal My to the roulettes Γ_1 and Γ_2.

Consider rolling the polar tangent over each of the centroids without slipping. According to Kamyu's theorem [3], point M of this straight line, coincides with the point of conjugation of the roulettes at the given position and describes a pair of conjugating roulettes. The stationary one coincides with the given curve Γ_1 and the movable one coincides with Γ_3 at a point where the radius of curvature of the two are equal $\rho_3=\rho_1$.

Curves Γ_2 and Γ_3 touch each other at all positions since curve Γ_1 conjugates with each of the curves Γ_2 and Γ_3. Let us select the curvature of movable centroid Γ_3' of plane $\mathcal{P}_3$ in such a manner that there is no slipping between the curves Γ_2 and Γ_3, i.e. the corresponding arcs of these curves are equal $\Delta s_2=\Delta s_3$. Thus, both roulettes Γ_2 and Γ_3, while rolling on a curve with slip will have the same rate of slipping for conjugating points M_2 and M_3 at any position.

It has been previously shown that radii of curvature ρ_3 of curve Γ_3 and a_3 of its evolute Γ_3' are related to each other as follows:

$$a_3=\rho_3|d\rho_3/ds_3|\,.$$

Taking $\rho_1=\rho_3$ and $\Delta s_2=\Delta s_3$, we obtain:

$$a_3=\rho_1|d\rho_1/ds_2|\,.$$

Similarly for curve Γ_1 and its evolute Γ_1' we obtain:

$$a_1=\rho_1|d\rho_1/ds_1|,$$

and

$$a_3=a_1|ds_1/ds_2|\,.$$

Let us define the rate of displacement $u=ds_2/dt$ of the points of conjugation of roulettes on curve Γ_2 and $u'=ds_1/dt$ on curve Γ_1 and denote v_{rt} as the projection of the velocity of the point of conjugation of roulettes on tangent Mx to the roulettes as:

$$v_{rt}=pr_x\mathbf{v}_{M_2}\,.$$

Then $u'=u+v_{rt}$ and the ratio of differentials of the corresponding arcs will be:

$$ds_1/ds_2=(u+v_{rt})/u=1+v_{rt}/u\,.$$

Thus, the radius of curvature of movable centroid of plane $\mathcal{P}_3$ is

$$a_3=a_1\,(1+v_{rt}/u). \qquad (1)$$

To find the ratio v_{rt}/u, defining the geometry of motion, let us consider the motion of plane $\mathcal{P}_2$ relative to plane $\mathcal{P}_3$.

For this case, curves Γ_2 and Γ_3 will be centroids since the curvature of the stationary centroid $K_1=1/\rho_1$, and of the movable centroid $K=-1/\rho_2$ are known. The "minus" sign shows that the center of curvature of the movable centroid is on the negative side of the polar normal My.

The rate of displacement u of the point of conjugation of roulettes over Γ_2 for the motion under consideration equals the rate of rolling of the centroids and can be easily determined.

The diameter d of the rotating circle for the relative motion is given by:

$$d=1/(K-K_1)=-\rho_1\rho_2/(\rho_1+\rho_2). \tag{2}$$

If the rate of slipping is known, then the angular velocity of planes $\mathcal{P}_2$ and $\mathcal{P}_3$ will respectively be equal to

$$\omega_2=v_{rt}/(MN)=v_{rt}/p,\ \omega_3=-v_{rt}/(MC_1)=-v_{rt}/\rho_1,$$

where p is the distance between the conjugating point M of the roulettes and the instantaneous center of slipping (N) of plane $\mathcal{P}_2$.

Angular velocity ω for the relative motion is:

$$\omega=\omega_2-\omega_3=v_{rt}/(p+\rho_1)/p\rho_1,$$

while the rate of rolling of centroids is:

$$u=-d\omega=v_{rt}\rho_2/p\cdot(p+\rho_1)/(\rho_1+\rho_2).$$

Now from formula (1), we get the radius of curvature of the movable centroid of plane $\mathcal{P}_3$:

$$a_3=a_1[1+p/\rho_2\cdot(\rho_1+\rho_2)/(p+\rho_1)], \tag{3}$$

or by using the diagram:

$$a_3=a_1[1+(C_1C_2\cdot MN)/(MC_2\cdot C_1N)]. \tag{4}$$

Thus, curvatures K_1 and K of both the centroids ($K_1=1/a_1$ for the stationary centroid and $K=1/a_3$ for the movable centroid) are known for plane $\mathcal{P}_3$. The curvature K of the movable centroid is positive since the radius of curvature lies in the positive direction of the polar normal C_1y_1.

Let us calculate the diameter of the rotating circle for plane $\mathcal{P}_3$:

$$d=1/(K-K_1)=a_1a_3/(a_1-a_3) \tag{5}$$

and parameter l of the curve of cyclic points (see [4]):

$$l_3=3/(2K-K_1)=3a_1a_3/(2a_1-a_3). \tag{6}$$

Let us now analyze the motion of plane $\mathcal{P}_2$ relative to plane $\mathcal{P}_3$.

In this case the radii of curvature of centroids and the radii of curvature of their evolutes a_2 and a_3 are known and hence, it is possible to completely solvẽ the geometrical problem of the third order for this motion, i.e. to determine the parameters of Burmester's curves.

Let us determine the derivative of the curvature of the centroid from the arc of centroid having known radii of its curvature ρ_1 and a (of the evolute):

$$K'=dK/ds=d/ds(\pm 1/\rho)=\mp 1/\rho^2 \cdot d\rho/ds=\mp a/\rho^3.$$

The "minus" sign denotes simultaneous satisfaction of two conditions, namely curvature K of the curve is positive and the radius of curvature at the given point increases, i.e. both the radii of curvature $K'=a_2/\rho_2^3$, $K_1'=-a_3/\rho_1^3$ for the centroids Γ_2 and Γ_3 respectively increase.

Let us now determine the parameters m and l of the curve of cyclic points for the relative motion (see [4]) :

$$m=(3K-K_1)/(K'-K_1')=\rho_1^2\rho_2^2(3\rho_1+\rho_2)/(a_3\rho_2^3+a_2\rho_1^3),$$

$$l=3/(2K-K_1)=-3\rho_1\rho_2/(2\rho_1+\rho_2). \tag{7}$$

If the trajectory of some point is specified in addition to that of the conjugating roulettes (curvature at the given position and the curvature of the evolute of the point in the corresponding position) and also the first three derivatives $\dot{s}$, $\ddot{s}$, $\dddot{s}$, of the arc coordinate with respect to time, then to plot the jerk diagram in plane $\mathcal{P}_2$, will require the determination of ω and ε from the velocity and accelearation diagrams, the acceleration of the instantaneous center of slipping (M) in the relative motion and the projection of the acceleration of the instantaneous center of slipping of plane $\mathcal{P}_3$ on the polar normal.

Let us expand the coordinates x_p, y_p coinciding with the instantaneous center of slipping into a polynomial series of φ, the angle of rotation of the movable plane (see [4]):

$$x_p=A_3\varphi^3/3!+\ldots,$$

$$y_p=B_2\varphi^2/2!+B_3\varphi^3/3!+\ldots, \tag{8}$$

where

$$A_3=d^3x_p/d\varphi^3|_{\phi=0}\,;\quad B_n=d^ny_p/d\varphi^n|_{\phi=0},$$

while

$$x_p'''=3d^2/l,\quad y_p''=d,\quad y_p'''=3d^2/m.$$

Differentiating with respect to time and substituting from equation (8), we get the projection of angular displacement of instantaneous center of slipping on tangent R_x and normal R_y to centroids:

$$R_x = 3d^2\omega^3/l,$$

$$R_y = 3d\omega\varepsilon + 3d^2\omega^3/m. \qquad (9)$$

The technique of plotting the momentum diagram is shown below for the case of a three-link mechanism with a higher pair of the 4th class.

2. A planar three-link mechanism with a higher pair of the fourth class is given in Fig. 2, a. Let us denote centers of curvature of the profile of the driving link Γ_1 and the driven link Γ_2 by C_1 and C_2 respectively and the centers of curvature of evolutes of these curves by A_1 and A_2. The equation of motion of the driving link is known: $\varphi_1 = f(t)$.

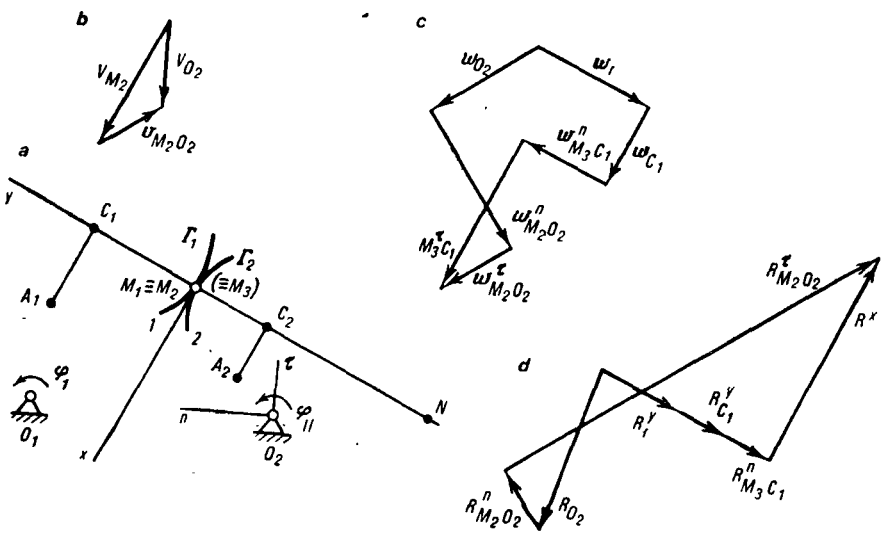

Fig. 2.

Let us perform an inversion in such a way that the driving link *1* becomes column. Then the profiles Γ_1 and Γ_2 of links *1* and *2* form conjugating roulettes. Angular velocity, acceleration and momentum of link O_1O_2 in this case will be $-\omega_1$, $-\varepsilon_1$ and $-\beta_1$ respectively while those of plane $\mathcal{P}_2$ associated with the driven link will be:

$$\omega_2 = \omega_{II} - \omega_1, \qquad \varepsilon_2 = \varepsilon_{II} - \varepsilon_1, \qquad \beta_2 = \beta_{II} - \beta_1.$$

Let us find out the projections of velocity, acceleration and jerk of hinge O_2 (which now moves along a circle of radius O_1O_2) on the tangent $O_2\tau$ and normal O_2n to the trajectory (see, for example, reference [5]):

$$
\begin{aligned}
&v_{O_2}=-\omega_1 O_1O_2;\\
&w^{\tau}_{O_2}=-\varepsilon_1 O_1O_2;\\
&w^{n}_{O_2}=\omega_1^2 O_1O_2;\\
&R^{\tau}_{O_2}=-(\beta_1-\omega_1^3)O_1O_2;\\
&R^{n}_{O_2}=3\omega_1\varepsilon_1 O_1O_2.
\end{aligned}
\tag{10}
$$

Let us draw the velocity diagram (Fig. 2, b):

$$\mathbf{v}_{M_2}=\mathbf{v}_{O_2}+\mathbf{v}_{M_2O_2}$$

and determine the angular velocity ω_2 of plane $\mathcal{P}_2$.

Let us introduce a plane $\mathcal{P}_3$ as described in Section 1 and relate the movable references system with this plane.

We find the radius of curvature a_3 of the movable centroid, diameter d of the rotating circle and parameter l_3 of the curve of cyclic points of plane $\mathcal{P}_3$ from formulas (3), (5) and (6) and the diameter d of rotating circle and parameter l of the curve of cyclic points during motion of plane $\mathcal{P}_2$ relative to $\mathcal{P}_3$ from formulas (2) and (7).

From the velocity diagram, we compute the angular velocity of the plane $\mathcal{P}_3$ as:

$$\omega_3=-v_{M_2}/\rho_1$$

and angular velocity for the relative motion as $\omega=\omega_2-\omega_3$.

To plot the acceleration diagram, we use the equality:

$$\mathbf{w}_{M_2}=\mathbf{w}_{O_2}+\mathbf{w}^{n}_{M_2O_2}+\mathbf{w}^{\tau}_{M_2O_2}=\mathbf{w}_r+\mathbf{w}_e+\mathbf{w}_{\mathrm{cor}}. \tag{11}$$

Here

$$w^{n}_{M_2O_2}=\omega^2 M_2O_2, \quad w_{\mathrm{cor}}=0$$

In relative motion, point M_2 is the instantaneous center of slipping, i.e., $v_r=0$ and the relative acceleration of the instantaneous center of slipping is equal to:

$$w_r=d\omega^2. \tag{12}$$

The relative[1] acceleration w_e i.e., the acceleration of point M_3 on the plane $\mathcal{P}_3$, will be:

$$\mathbf{w}_e=\mathbf{w}_{C_1}+\mathbf{w}^{n}_{M_3C_1}+\mathbf{w}^{\tau}_{M_3C_1}, \tag{13}$$

while the center of curvature C_1 of curve Γ_1 becomes the instantaneous center of slipping of plane $\mathcal{P}_3$ as a result of which:

$$
\begin{aligned}
&w_{C_1}=d\omega_3^2;\\
&w^{n}_{M_3C_1}=\rho_1\omega_3^2.
\end{aligned}
\tag{14}
$$

[1] This is the acceleration of the moving system of coordinates (associated with the point) with respect to the fixed coordinate system.

Thus, from equations (11) and (13) we get:

$$\mathbf{w}_{O_2}+\mathbf{w}^{n}_{M_2O_2}+\mathbf{w}^{\tau}_{M_2O_2}=\mathbf{w}_r+\mathbf{w}_{C_1}+\mathbf{w}^{n}_{M_3C_1}+\mathbf{w}^{\tau}_{M_3C_1}. \tag{15}$$

Let us plot the acceleration diagram (Fig. 2, c) and find angular accelerations ε_2 and ε_3 of planes $\mathcal{P}_2$ and $\mathcal{P}_3$ and relative angular acceleration $\varepsilon=\varepsilon_2-\varepsilon_3$:

$$\varepsilon_2=w^{\tau}_{M_2O_2}/(M_2O_2),\ \sqrt{\varepsilon_3}=\mathbf{w}^{\tau}_{M_3C_1}/\rho_1.$$

The projection on the tangent to the trajectory of point with respect to pole $w^{\tau}_{M_2O_2}$ will be positive if the vector $\mathbf{w}^{\tau}_{M_2O_2}$ is in the counter clockwise direction with respect to the pole O_2 for the present and succeeding cases.

To plot the momentum diagram, we shall use the principle of vector addition [5]:

$$\mathbf{R}_a=\mathbf{R}_r+\mathbf{R}_e+\mathbf{R}_g, \tag{16}$$

where

$$\mathbf{R}_g=3(\boldsymbol{\omega}_e\times\mathbf{w}_r+\varepsilon_e\times\mathbf{v}_r-w_e^2\mathbf{v}_r).$$

For a point, $M_2v_r=0$ and $\mathbf{R}_g=3\boldsymbol{\omega}_e\times\mathbf{w}_r$ and therefore, vector $\mathbf{R}_g$ is directed along the axis Mx, since the relative acceleration $\mathbf{w}_r$ of the instantaneous center of slipping M_2 is directed along the polar normal My.

Momentum of point M_2—the instantaneous center of slipping during relative motion, consists of two components:

$$\mathbf{R}_r=\mathbf{R}^x+\mathbf{R}^y.$$

From formula (9), let us determine its projection R_y on the polar normal (on the basis of the values of ω, ε, d and m calculated earlier).

The relative momentum, i.e., the momentum of point M_3 of plane $\mathcal{P}_3$ can be written in the form:

$$\mathbf{R}_e=\mathbf{R}_{C_1}+\mathbf{R}^{n}_{M_3C_1}+\mathbf{R}^{\tau}_{M_3C_1}. \tag{17}$$

We find

$$R^{n}_{M_3C_1}=3\omega_3\varepsilon_3\rho_1, \tag{18}$$

and since point C_1 is the instantaneous center of slipping of plane $\mathcal{P}_3$, on the basis of the values of ω_3, d_3, l_3 determined earlier and formulas (9), we calculate the projection of the momentum of point C_1 on the polar tangent C_1x' of plane $\mathcal{P}_3$, coinciding with My axis:

$$R^{x'}_{C_1}=R^{y}_{C_1}.$$

From equations (16) and (17), we get

$$\mathbf{R}_{M_2}=\mathbf{R}^x_r+\mathbf{R}^y_r+\mathbf{R}^x_{C_1}+\mathbf{R}^y_{C_1}+\mathbf{R}^{n}_{M_3C_1}+\mathbf{R}^{\tau}_{M_3C_1}+\mathbf{R}_g=\mathbf{R}^y_r+\mathbf{R}^y_{C1}+\mathbf{R}^{n}_{M_3C_1}+\mathbf{R}^x, \tag{19}$$

where the first three vectors are known in magnitude as well as direction and the last one is parallel to Mx-axis:

$$\mathbf{R}^x=\mathbf{R}^x_r+\mathbf{R}^x_{C1}+\mathbf{R}^\tau_{M_3C_1}+\mathbf{R}_g.$$

From the study of motion of plane $\mathcal{P}_3$, we have:

$$\mathbf{R}_{M_2}=\mathbf{R}_{O_2}+\mathbf{R}^n_{M_2O}+\mathbf{R}^\tau_{M_2O_2}, \tag{20}$$

where vector:

$$\mathbf{R}_{O_2}=\mathbf{R}^\tau_{O_2}+\mathbf{R}^n_{O_2},$$

has been determined earlier and:

$$R^n_{M_2O_2}=3\omega_2\varepsilon_2M_2O_2. \tag{21}$$

Finally, from equations (19) and (20), we get:

$$\mathbf{R}^y_r+\mathbf{R}^y_{C1}+\mathbf{R}^n_{M_3C_1}+\mathbf{R}^x=\mathbf{R}_{O_2}+\mathbf{R}^n_{M_2O_2}+\mathbf{R}^\tau_{M_2O_2}, \tag{22}$$

where lines of action of vectors $\mathbf{R}^x$ and $\mathbf{R}^\tau_{M_2O_2}$ are known and the remaining have been determined in magnitude as well as in direction.

From the momentum diagram (Fig. 2, d) we get the angular momentum of plane $\mathcal{P}_2$:

$$\beta_2=R^\tau_{M_2O_2}/(M_2O_2)-\omega^3_2, \tag{23}$$

where the projection of vector $\mathbf{R}^\tau_{M_2O_2}$ on the corresponding tangent is positive if this vector has counterclock-wise direction with respect to pole O_2.

Then, the angular momentum of the driven link will be:

$$\beta_{II}=\beta_2+\beta_1. \tag{24}$$

3. Let us consider the example of drawing the momentum diagram of a cam mechanism with plane rotating disk (Fig. 3, a). Let the cam be rotating uniformly $\omega_1=\text{const}$. Let us denote the profile of the cam by Γ_1 and the rectilinear profile of the disk by Γ_2. From Formulas (10), we get:

$$v_{O_2}=-\omega_1O_1O_2; \quad w^\tau_{O_2}=0; \quad w^n_{O_2}=\omega^2_1O_1O_2;$$
$$R^\tau_{O_2}=\omega^3_1O_1O_2; \quad R^n_{O_2}=0.$$

For plane $\mathcal{P}_3$ from equations (3), (5) and (6) we determine the values of a_3, d_3 and l_3:

$$a_3=a_1(\rho_1+2p)/(\rho_1+p);$$
$$d_3=-a_1(\rho_1+2p)/p;$$
$$l_3=3a_1(\rho_1+2p)/\rho_1; \tag{25}$$

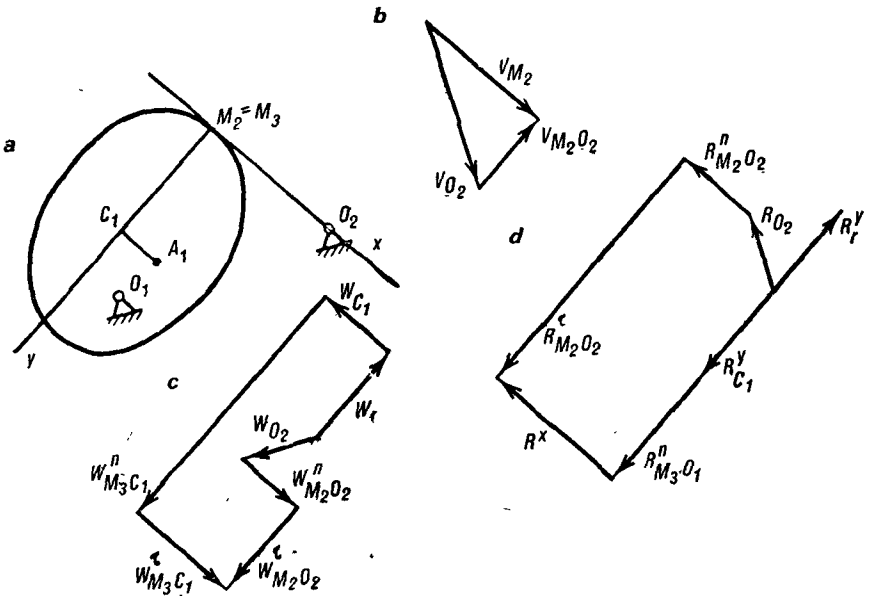

Fig. 3.

(in these equations $p=-MN$ since point N is located on the positive side of My-axis) and for the relative motion of plane $\mathcal{P}_2$, from equations (2) and (7), we get the values of d and m.

$$d=-\rho_1;$$
$$m=\rho_1^2/a_3. \tag{26}$$

Let us draw the velocity diagram (Fig. 3, b) and calculate angular velocities ω_2, ω_3 and $\omega=\omega_2-\omega_3$.

Let us calculate the modulii of vectors $\mathbf{w}_r$, $\mathbf{w}_{C_1}$ $\mathbf{w}^n_{M_3C_1}$ and $\mathbf{w}^n_{M_2O_2}$ from equations (12) and (14) and plot the acceleration diagram by using equation (15). Let us determine angular accelerations ε_2, ε_3 and ε.

For plotting the momentum diagram on the basis of equations (9), (25) and (26) we find that:

$$R^y_r=-3\omega\varepsilon\rho_1+3a_3\omega^3, \qquad R^y_{C_1}=-\rho_1 d_3/p\cdot\omega_3^3,$$

as well as we determine modulii of vectors $\mathbf{R}^n_{M_3C_1}$ and $\mathbf{R}^n_{M_2O_2}$ with the help of equations (18) and (21).

We plot the momentum diagram in accordance with equation (22) and find the angular momentum of the driven link from equations (23) and (24).

References

1. Borisenko, L. N. and Ya. L. Geronimus. O zameshchayushchikh mekhanizmakh razlichnykh poryadkov (Substituting mechanisms of different orders). Sb. *Mekhanika mashin*, vyp. 13-14, Izd-vo Nauka, 1968.
2. Geronimus Ya. L. Reshenie zadach 3-go poryadka pri pomoshchi analoga uravneniya Eilera-Savari (Solution of problems of 3rd order with the help of Euler-Savari equation analog). *Mezhvedomstv. nauchn. tekhn.*, sbornik *Teoriya mashin i mekhanizmov*, No. 1, Khar'kov, Izd-vo KhGU, 1966.
3. Stolyarov Ya. V. Teoriya mekhanizmov (Theory of Mechanisms). Khar'kov, Izd-vo Ukraina, 1926.
4. Gerominus Ya. L. Geometricheskii apparat teorii sinteza ploskikh mekhanizmov (Geometrical Techniques in the Theory of Synthesis of Plane Mechanisms). Fizmatgiz, 1962.
5. Meyer zur W. Capellen. Die Beschleunigungsanderung, *Ingr. Arch.*, **27**, No. 1-2, 1959.

E. I. Vorob'ev

A METHOD OF CALCULATING THE CHANGE IN PRIMARY DIMENSIONS OF MECHANISMS DUE TO WEAR FOR THE PURPOSE OF ESTIMATING THEIR RELIABILITY

1. Introduction

The problem of developing methods of evaluating reliability and durability of mechanisms and machines at the design stage is of great significance in machine building.

It has been shown in [1, 2] that reliability of mechanisms in the sense that they remain within design limits is related to the change in primary dimensions in kinematic pairs due to wear and tear.

Data concerning the change in primary errors dimensions can be obtained on the basis of operation or prolonged tests on machines and instruments. These tests and the collection of data on operating characteristics are time-consuming, expensive and sometimes practically impossible. Another possible solution, would be to develop methods of calculating wear and tear in the elements of kinematic pairs on the basis of empirical laws of wear and tear. This can be undertaken without eliminating the necessity of collecting data on the change in primary dimensions of mechanisms.

In the modern theory of machines the problem of defining the process of wear and tear is extremely complicated. However, significant progress has been achieved in this direction. The first investigation on the relationship between parameters of a cam mechanism and wear and tear of the profile, was undertaken by N. G. Bruevich [3]. Additional investigations by E. A. Chudakov [4] on calculations of wear and tear of gears, by B. Ya. Ginsburg [5] on wear and tear of piston rings and by N. I. Glagolev [6] on wear and tear of wheels, etc. may also be mentioned in this connection.

The hypothesis regarding the proportionality of wear and tear to the

specific work due to friction forms the basis of all these research investigations.

Further advances in the science of friction and wear in machines and the large number of theoretical and experimental investigations, undertaken primarily by M. M. Khrushchov, I. V. Kragel'skii and other authors, demonstrates that proportionality of wear and tear to specific work of friction is valid only in a special case, namely in the case of abrasive wear when microcutting is the mechanism of wear and tear.

The basic laws of wear and tear in a general case are given by equation [7, 8]:

$$\mathcal{J}=d\Delta/ds=cP; \tag{1}$$

$$\mathcal{J}_1=d\Delta/ds=c_1P^{\alpha}. \tag{2}$$

Here Δ—wear and tear;

$\mathcal{J}$—wear intensity;

P—specific pressure;

c and α—coefficients depending on the material and conditions of wear and tear.

The first equation reflects the basic law of wear and tear during microcutting while the second equation refers to the more general case of interaction of surfaces. The exponent can be greater or less than 1. The exponent is less than 1 using lubricants in the presence of abrasive, when an increase in pressure impedes the flow of abrasive to the working surface.

In most cases and for a wide range of materials, the exponent α is greater than 1 for dry and limiting friction which causes fatigue destruction of the surface [7].

It can be easily shown that equation (1) leads to the realization of the assumption about the proportionality of wear and tear to specific work of friction.

Exponential laws of wear and tear similar to equation (2) were investigated by A. S. Pronnikov [9] in the study of wear and durability of components of machine tools. However, only elements of lower kinematic pairs were taken into account in the calculations.

In references [10, 11], equations of normal wear, obtained on the basis of exponential laws of wear, were used for solving some problems of analysis and synthesis of cam mechanisms. A linear dependence between specific pressure on the elementary area and the sliding path was used to derive equations of normal wear for the general case of relative motion of cam and follower.

Equations of wear and tear of elements of kinematic pairs of mechanisms have been derived below for the general case on the basis of exponential laws similar to equation (2) but without the above limiting constraints. Mechanisms with linear contact in the higher pair have been considered. It is assumed that the reaction at the higher pair is a variable parameter.

2. Linear Wear of Elements of Kinematic Pairs

1. Higher pair. Let us assume that the elementary laws of wear and tear for the given material are known or can be obtained on the basis of the methods suggested in works [7, 8, 12] and by other authors. Let us study the zone of contact in the higher pair of a mechanism.

Let us assume the wear of an infinitesimal area ΔF, located on the working surface to represent the wear of the element of a kinematic pair. We will also assume that the rate of sliding is constant during time Δt of the passage of the zone of contact over the area ΔF (since it is small).

In this case:

$$\Delta t = 2a/w . \tag{3}$$

The total path of friction on area ΔF during 1 cycle will be:

$$s_m = 2a/w \cdot v_{\text{slid}} , \tag{4}$$

where v_{slid} is the rate of sliding on the contact surface and w is the rate of its displacement over the elements of the kinematic pair.

As the specific pressure changes with the sliding path, wear intensity will not be constant but will be a function of specific pressure.

In the case of variable specific pressure, the wear of area ΔF is determined from the expression:

$$\Delta = \int_0^{s_m} \mathcal{J}(s)\, ds , \tag{5}$$

where $\mathcal{J}(s)$ is the variable wear intensity, depending upon s, on area ΔF, as the specific pressure changes along the sliding path (Fig. 1).

Let us assume that the distribution of specific pressure in the contact zone is parabolic, i.e.

$$p = p_0 (1 - x_0^2/a^2) , \tag{6}$$

where p_0—maximum specific pressure in the contacting zone;
x_0—current coordinate;
a—semiwidth of the area of contact.

In the case of uniform displacement of the parabolic curve of specific pressure (Fig. 1) over the infinitesimal area, it can be shown that:

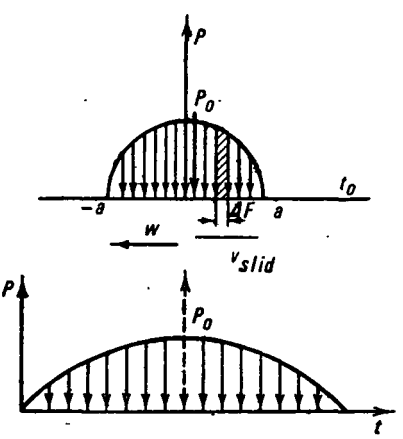

Fig. 1.

$$p=p_0\,[1-(t-a/w)^2/t_0^2]\,, \tag{7}$$

where t_0—the time of passage for half the curve:

$$t_0=a/w\,. \tag{7a}$$

Putting $(t-a/w)=t'$ and remembering that for the case of constant rate of sliding, the sliding path s is proportional to time, we have:

$$p=p_0[1-v_{\text{slid}}^2 s^2/t_0^2]=p_0(1-s^2/s_0^2)\,, \tag{8}$$

where

$$s_0=v_{\text{slid}}\cdot t_0=av_{\text{slid}}/w\,. \tag{8a}$$

We obtain an expression for the wear of the element of the higher pair by using equations (5) on the basis of which:

$$\Delta=\int_0^{s_m} c_1\,[p(s)]^{\alpha}ds\,. \tag{9}$$

Let us now introduce the notation:

$$\alpha=1+\gamma\,. \tag{9a}$$

Parameter γ can be represented in a different manner depending on the nature of the contact.

In the case of elastic contact [7]:

$$\gamma=\beta t\,, \tag{9b}$$

where $\beta=1/(2\nu+1)$;

ν—characteristic of surface finish in the process of wear;

t—exponent of the contact fatigue curve. In the case of plastic contact [7]:

$$\gamma=(1+t)/2\nu\,. \tag{9c}$$

The constants t and ν in this case differ in absolute value from those in the case of elastic contact.

Using equations (8) and (9), we obtain:

$$\Delta=\int_0^{s_m} c_1\,[p_0(1-s^2)/s_0^2]^{1+\gamma}ds=c_1p_0^{1+\gamma}s_m[(2+2\gamma)/(3+2\gamma)]\,. \tag{10}$$

Comparing equations (10) and (2), we can write:

$$\Delta = c_1 \mathcal{J}(p_0) s_m [(2+2\gamma)/(3+2\gamma)], \tag{11}$$

where $\mathcal{J}(p_0)$ is the wear intensity, corresponding to maximum specific pressure.

Considering equation (4) and expressing semiwidth of contact area and maximum specific pressure in terms of the specific load (force per unit length of the line of contact), we have:

$$\Delta_1 = c_2 f' \mathcal{N}^{(1+0.5\gamma)} \rho_{red}^{-(0.5\gamma)} \delta [(2+2\gamma)/(3+2\gamma)], \tag{12}$$

where $\delta = v_{slid}/w$;

$\rho_{red} = \rho_1\rho_2/(\rho_1+\rho_2)$ — reduced radius of curvature;

$c_2 = 2c_1(4/\pi \cdot \eta)^{0.5} \cdot 0.418^{1+\gamma} E_{red}^{0.5+0.5\gamma}$; $E_{red} = 2E_1E_2/(E_1+E_2)$;

Δ — wear and tear measured along the normal;

f — coefficient of friction:

$$\eta = (1-\mu_1)/E_1 + (1+\mu_2)/E_2; \tag{12a}$$

μ_1, μ_2, E_1, E_2 — Poisson's ratio and modulus of elasticity of the first and second bodies respectively.

To find the total wear during n cycles, we multiply equation (12) by the number of cycles.

This will be a general equation for estimating the wear and tear of the elements of higher kinematic pairs of mechanisms. The equation taking into account wear and tear is given below. In particular, for a cam mechanism with plane follower, we obtain:

$$\delta = v_{slid}/w = s/(s+s'') = (r_0+s)/(r_0+s+s'') = s/\rho; \tag{13}$$

$$\rho_{red} = \rho = (s+r_0+s''); \tag{13a}$$

then

$$\Delta = c_2 f' [2+2\gamma)/(3+2\gamma)] \cdot [\mathcal{N}^{1+\gamma}(s+r_0)/\rho^{1+\gamma}] n, \tag{14}$$

where n — number of cycles;

s — radius vector of the point of contact;

ρ — radius of curvature of the profile;

$$s'' = d^2s/d\varphi^2;$$

φ — angle of rotation of the cam;

r_0 — initial radius of the profile.

For a toothed mechanism

$$\mathcal{N} = P/(b \cos \beta), \tag{15}$$

where P—force applied to the tooth;

b—width of the wheel;

β—angle of obliquity.

The velocity of sliding for the higher pair of a toothed mechanism may be expressed in the following manner [4]:

$$v_{\text{slid}}=\lambda(\omega+\omega_1), \tag{16}$$

where ω, ω_1—angular velocity of the driven and driving wheels respectively;

λ—distance between the point of contact and pitch point.

Rate of displacement of the area of contact on the working surface of the tooth is determined by equation:

$$w=\omega\rho. \tag{17}$$

Substituting the expressions obtained above in equation (12), we obtain for the driving wheel:

$$\Delta=c_2 f^t[\rho_1\rho_2/(\rho_1+\rho_2)]^{-0.5\gamma}(\omega+\omega_1)/\omega_1\cdot(2+2\gamma)/(3+2\gamma)\lambda N^{1+0.5\gamma}\cdot 1/\rho. \tag{18}$$

The normal reaction N, in the equation for wear, depends on a large number of factors and is therefore a variable parameter. A general formula for calculating wear intensity in the case of variable load, is given in reference [12].

We may derive an expression for wear and tear in the higher pair of a mechanism by taking the normal reaction as a random variable.

Since a large number of factors affect the reaction N, and since they are usually independent, the mathematical expectation of N is expressed with the help of the normal distribution:

$$N=1/\sigma\sqrt{2\pi}\cdot e^{-(N-N)^2/2\sigma^2}, \tag{19}$$

where σ—mean square deviation;

$\boldsymbol{N}$—average load on the higher pair of the mechanism.

Then, under the conditions of a variable normal load, the equation for wear can be determined in the following manner

$$\Delta=\int_{-\infty}^{+\infty}\Delta N dN=\int_{-\infty}^{+\infty}k_0 N^{(1+0.5\gamma)}\frac{1}{\sigma\sqrt{2\pi}}\cdot e^{-(N-N)/2\sigma^2}dN$$

$$=k\boldsymbol{N}^{-(1+0.5\gamma)}\int_{-\infty}^{+\infty}\frac{(1+\theta v)^{(1+0.5\gamma)}}{\sqrt{2\pi}}e^{-\theta^2/2}d\theta=\Delta\lambda, \tag{20}$$

where $\theta=(\mathcal{N}-\mathbf{N})/\sigma$; $\lambda=(1+0.5\gamma)/\mathcal{N}^{(1+0.5\gamma)}$;

$v=\sigma/\mathbf{N}$—coefficient of variation;

$k_0=c_2 f^t \rho_{\text{red}}^{(-0.05\gamma)} \delta[(2+2\gamma)/(3+2\gamma)]$.

Statistical parameters of the normal reaction are determined by processing oscillograms measured of the driven link of the mechanism.

2. Sliding Pair. For example, let us consider the sliding pair of a cam mechanism. Assume that the specific pressure in the sliding pair is distributed linearly (Fig. 2).

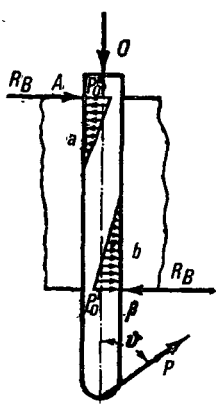

Fig. 2.

Considering the deformation of elements of a sliding pair to be elastic, we can write:

$$R_A=1/2\cdot p_0'' \qquad a=1/2\cdot p_0''^2 \tan\gamma; \tag{21}$$

$$R_B=1/2\cdot p_0' \qquad b=1/2\cdot p_0'^2 \tan\gamma, \tag{22}$$

where a and b—length of specific-pressure curves (see Fig. 2);

γ—inclination (misalignment) of the follower axis in the guide;

R_A, R_B—total reactions at points A and B;

p_0', and p_0''—maximum specific pressures.

Reactions R_A and R_B are easily determined from the equation of dynamic force analysis and pressure p_0' and p_0'' are determined from equations (21) and (22).

Due to friction between the elements of the kinematic pair, and consequent wear and tear, the follower gets rotated through a certain angle. Consider the wear and tear of the guide (Fig. 2).

Wear intensity of element of area ΔF may be written as:

$$d\Delta_1/ds=cp^\alpha, \tag{23}$$

$$\Delta_1=\int_0^s cp(s)^\alpha ds. \tag{24}$$

Since the area ΔF is small, specific pressure on it can be taken to be constant and the wear of the area in the path of friction will be:

$$\Delta_1=cp^\alpha s. \tag{25}$$

At point A:

$$\Delta_1'=cp'^\alpha s_0, \tag{26}$$

similarly at point B:

$$\Delta_1''=cp_0''^\alpha s_0, \tag{27}$$

where s_0—is the travel of the follower.

Wear of the mating surface of the follower rod in the zone will be:

$$\Delta_2^1 = \int_0^{s_0} p(s)^\alpha ds = \int_0^{s_0} (cs+d)^\alpha ds = (cs+d)^{\alpha+1}/(\alpha+1)c; \tag{28}$$

$$\Delta_2'' = \int_0^{s} (c_1 s+d_1)\, ds = (c_1 s+d_1)^{\alpha+1}/(\alpha+1)c\,. \tag{29}$$

Here c, d, c_1, d_1 are coefficients describing the linear law of pressure distribution in the guide.

3. Turning pair. Calculations relating to the wear of elements of a turning pair have been considered in reference [9].

Equations for the wear of sleeve and shaft have the form:

$$\Delta_1' = v_{w_1}\,(c+\sin\alpha_0)/(\alpha_0 c+\pi c_1)\cdot t\,; \tag{30}$$

$$\Delta_2' = v_{w_2} = [\cos\alpha - (c_1+\sin\alpha_0)/(\alpha_0 c+\pi c_1)]\cdot t\,; \tag{31}$$

where v_{w_1} and v_{w_2} are the rate of wear of the 1st and 2nd body respectively; the rate of wear is expressed in terms of intensity:

$$J = d\Delta/dt\cdot dt/ds = v_w/v_{slid}\,, \tag{32}$$

and α—angle of contact can be found from [13];

$$t = N/n\,. \tag{33}$$

Here N is the number of cycles and n is r.p.m.

3. Change in Primary Dimensions of Mechanisms

If the wear of elements of a kinematic pair is known we can calculate the change in primary dimensions of a mechanism due to wear, which makes it possible to study the reliability of the mechanism.

1. Higher pair. Since formulas (14) and (18) determine wear measured along the normal to the surface, we have:

$$\Delta_1 = \Delta\rho_1^n\,; \tag{34}$$

$$\Delta_2 = \Delta\rho_2^n\,, \tag{35}$$

where $\Delta\rho_1^n$ and $\Delta\rho_2^n$ are the errors in the dimensions of the elements of a kinematic pair, measured along normals.

2. Sliding pair. If wear of the guide at points A and B is known and if the wear of the follower has been determined, it is easy to find change in the angle of inclination of the axes of follower and guide

$$\text{displacement at point } A \qquad \Delta_A=\Delta_1'+\Delta_2'; \tag{36}$$

$$\text{at point } B \qquad \Delta_B=\Delta_1''+\Delta_2''. \tag{37}$$

Inclination of the follower due to wear will be

$$\Delta\gamma_w=L/(\Delta_A+\Delta_B), \tag{38}$$

where L is the length of guide.

The change in the clearance of a sliding pair is equal to the sum of the values of wear in the elements of kinematic pair, i.e.

$$\Delta g=\Delta_1+\Delta_2. \tag{38a}$$

The change of inclination in a sliding pair is observed even in the absence of initial inclination. In this case, the value of inclination is determined from equation

$$\Delta\gamma_w'=L/|\Delta_A-\Delta_B|. \tag{39}$$

Changes in other primary dimensions in kinematic pairs due to wear can be determined in a similar way [14].

References

1. Bruevich, N. G. O nadezhnosti i tochnosti avtomaticheskogo proizvodstva (Reliability and accuracy of automatic control). Sb. *Voprosy tochnosti i nadezhnosti v mashinostroenii*, izd-vo AN SSSR, 1962.
2. Bruevich, N. G. and V. I. Sergeev. Nekotorye obshchie voprosy tochnosti i nadezhnosti ustroistv (Some general problems of accuracy and reliability of devices). Sb. *Teoriya mekhanizmov i mashin*, Izd-vo Nauka, 1964.
3. Bruevich, N. G. Kinetika raspredelitel'nogo mekhanizma s kulachkom, deistvuyushchim na pryamolineino dvizhushcheesya zveno (Kinetics of distributing mechanism with cam acting on the rectilinear motion of the link). *Tekhnika vozdushnogo flota*, No. 1, 1931.
4. Chudakov, E. A. Raschet avtomobilya (Design of an Automobile). Mashgiz, 1947.

5. GINSBURG, B. YA. Teoriya i raschet porshnevykh kolets (Theory and Design of Piston Rings). Mashgiz, 1945.
6. GLAGOLEV, N. I. Rabota treniya i iznos perekatyvaemykh tel (Work of friction and wear of rolling bodies). Trudy III Vses. konf. po treniyu i iznosu v mashinakh. Izd-vo AN SSSR, 1960.
7. KRAGEL'SKII, I. V. Trenie i iznos (Friction and Wear). Mashgiz, 1962.
8. KHRUSHCHOV, M. M. and M. A. BABICHEV. Issledovanie iznashivaniya metallov (Study of Wear in Metals). Izd-vo AN SSSR, 1958.
9. PRONNIKOV, A. S. Iznos i dolgovechnost' stankov (Wear and Durability of Machine Tools). Mashgiz, 1957.
10. VOROB'EV, E. I. Ob iznosostoikosti i proektirovanii kulachkovykh mekhanizmov (Wear resistance and design of cam mechanisms). Sb. *Analiz i sintez mekhanizmov-avtomatov.* Izd-vo Nauka, 1964.
11. VOROB'EV, E. I. Vliyanie parametrov kulachkovogo mekhanizma na iznos pri plasticheskom kontakte (Effect of parameters of a cam mechanism on wear in the case of plastic contact). *Mashinovedenie,* No. 3, 1965.
12. KRAGEL'SKII, I. V., E. F. NEPOMNYASHCHII and G. M. KHARACH. Vliyanie neustanovivshikhsya rezhimov nagruzheniya na iznos (Effect of variable loading schedules on wear). Sb. *Teoriya treniya i iznosa,* Izd-vo Nauka, 1965.
13. BILIK, M. M. Pary treniya metall-plastmassa v mashinakh i mekhanizmakh (Metal-Plastic Friction Pair in Machines and Mechanisms). Izd-vo Mashinostroenie, 1964.
14. KRAGEL'SKII, I. V., E. F. NEPOMNYASHCHII and G. M. KHARACH. Osnovnye polozheniya i kratkaya metodika priblizhennogo rascheta poverkhnostei treniya na iznos pri skol'zhenii (Basic Aspects and Method of Approximate Calculation of Wear in Friction Surfaces during Sliding). Izd-vo Znanie, 1966.

A. S. Gel'man, Yu. A. Danilov,
L. V. Krymova and *A. M. Makeev*

CALCULATION OF KINEMATIC PARAMETERS OF RADIAL-PISTON MULTIPASS HYDRAULIC MOTORS WITH GUIDE BLOCK PROFILE CONSISTING OF ARCS OF CIRCLES

Basic operating characteristics of radial-piston multipass hydraulic motors can be obtained through the analysis of their kinematics. In hydromotors of this type complicated profiles are often substituted by conjugated arcs of circles and straight line segments to simplify and raise the accuracy of the guide block [1-6].

During motion of the roller over the guide block, the piston moves relative to the block of cylinders and undergoes relative motion along with the block. Absolute value of the velocity v and acceleration are determined from the equations (Fig. 1):

$$v = v_p + v_t; \tag{1}$$

$$a = a_p + a_s + a_c, \tag{2}$$

where v_p—relative velocity;
v_t—velocity of the moving system of coordinates;
a_p—relative acceleration;
a_s—acceleration of the moving system of coordinates;
a_c—Coriolis acceleration.

In the case of accelerated rotation of the cylinder block:

$$a_s = a_{sp} + a_{st}, \tag{3}$$

where a_{sp}—normal component of acceleration of the moving coordinate system;
a_{st}—tangential component of acceleration of the moving coordinate system.

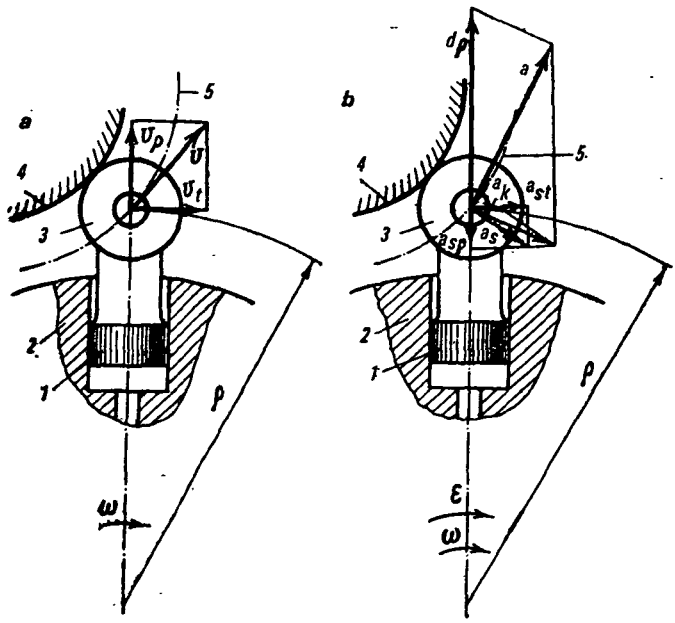

Fig. 1. Velocity and acceleration diagram of the piston:
a—*velocity diagram;* b—*acceleration diagram*: 1—*piston;* 2—*cylinder block;* 3—*roller;* 4—*guide-block profile;* 5—*trajectory of motion of the roller center.*

Thus absolute acceleration of the piston can be represented in the form:

$$\boldsymbol{a}=\boldsymbol{a}_n+\boldsymbol{a}_t\,, \tag{4}$$

where

$$a_n=a_{sp}+a_p; \tag{5}$$

$$a_t=a_{st}+a_c\,. \tag{6}$$

Since the profile of the guide block consists of arcs of circles and straight line segments, the path of motion of the roller center will also consist of arc segments and straight lines, conjugating each other. Hence the trajectory segments are of four types: concentric, convex, concave and rectilinear.

From now on we will consider the angular velocity and acceleration of the cylinder block to be positive in the clock-wise direction and the normal acceleration and velocity of the piston, to be positive in the radially outwards direction. Similarly, we will consider the tangential velocity and acceleration of the piston to be positive in the direction corresponding to positive angular velocity and acceleration.

1. Concentric Section of the Trajectory

For the concentric section of the trajectory:

$$v_\rho = 0; \tag{4a}$$

$$a_\rho = 0; \tag{5a}$$

$$a_c = 0; \tag{6a}$$

$$v_t = \omega\rho; \tag{7}$$

$$a_{s\rho} = -\omega^2\rho; \tag{8}$$

$$a_{st} = \varepsilon\rho, \tag{9}$$

where ω—angular velocity of the cylinder block;
ρ—radius vector of the roller center;
ε—angular acceleration of the cylinder block.

These equations for velocity and acceleration of a moving coordinate system are valid for any section of the trajectory.

2. Convex Section of the Trajectory

The radius vector of the trajectory of motion of the roller center is determined from $\triangle BOO_1$ and $\triangle AO_1B$ (Fig. 2):

$$\rho = R\cos\alpha - (r_g + r_r)\cos\gamma, \tag{10}$$

where R—distance between the center of cylinder block and the center of arc forming the guide-block profile;
r_g—radius of the arc forming guide-block profile;
α—angle between the radius vector of the trajectory of motion of roller center and line of centers of cylinder block and arc forming the guide-block profile;
r_r—radius of the piston roller;
γ—pressure angle.

Angle γ is found from $\triangle OO_1A$:

$$\sin\gamma = R/(r_g + r_r)\cdot\sin\alpha. \tag{11}$$

Substituting the value of $r_g + r_r$ from equation (11) in (10), we get a simpler equation for the radius vector of trajectory ρ:

$$\rho = R\sin(\gamma - a)/\sin\gamma. \tag{12}$$

If the distance of the roller from the concentric section is increased, the relative velocity of the piston is obtained by differentiating equation

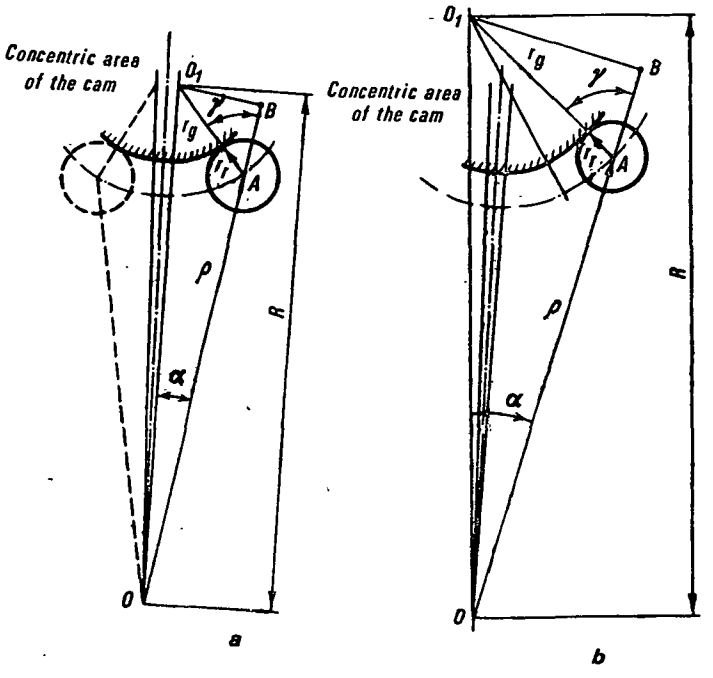

Fig. 2. Determination of radius vector of the trajectory of motion of roller center on the convex section of the trajectory:
a—*on the section conjugating the concentric part;* b—*on the section not conjugating with the concentric part.*

(10) with respect to time:

$$v_\rho = d\rho/dt = -R \sin \alpha \cdot d\alpha/dt + (r_g + r_r) \sin \gamma \cdot d\gamma/d\alpha \cdot d\alpha/dt$$
$$= \omega[-R \sin \alpha + (r_g + r_r) \sin \gamma \cdot d\gamma/d\alpha]. \qquad (13)$$

To calculate the derivative $d\gamma/d\alpha$ differentiate the left and right-hand sides of equation (11) with respect to α, i.e.

$$\cos \gamma d\gamma/d\alpha = R/(r_g + r_r) \cdot \cos \alpha,$$

from where:

$$d\gamma/d\alpha = R/(r_g + r_r) \cdot \cos \alpha/\cos \gamma. \qquad (14)$$

Substituting equation (14) and (12) in equation (13), we obtain:

$$v_\rho = \omega(-R \sin \alpha + R \sin \gamma \cdot \cos \alpha/\cos \gamma) = \omega R \cdot \sin (\gamma - \alpha)/\sin \gamma \cdot \tan \gamma.$$

Thus:

$$v_\rho = \omega\rho \tan \gamma. \qquad (15)$$

Relative acceleration of the piston is determined by differentiating equation(15) with respect to time, i.e.

$$a_p=dv_p/dt=d\omega/dt\cdot\rho\tan\gamma+\omega\cdot d\rho/dt\cdot\tan\gamma+\omega\rho\cdot d\tan\gamma/dt$$
$$=\varepsilon\rho\tan\gamma+\omega v_p\tan\gamma+\omega\rho\cdot 1/\cos^2\gamma\cdot d\gamma/d\alpha\cdot d\alpha/dt$$
$$=\varepsilon\rho\tan\gamma+\omega^2\rho\tan^2\gamma+\omega^2\rho\cdot R/(r_g+r_r)\cdot\cos\alpha/\cos^3\gamma.$$

Consequently:

$$a_p=\omega^2\rho\tan\gamma\,[\tan\gamma+1/(\tan\alpha\cdot\cos^2\gamma)]+\varepsilon\rho\tan\gamma. \tag{16}$$

Coriolis acceleration a_c is determined from the expression:

$$a_c=2v_p\omega=2\omega^2\rho\tan\gamma. \tag{17}$$

Substituting values of a_{sp}, a_p, a_{st} and a_c from equations (8), (16), (9) and (17) in equations (5) and (6), we obtain the values of normal and tangential components of absolute acceleration of the piston:

$$a_n=\omega^2\rho\{\tan\gamma\,[\tan\gamma+1/(\tan\alpha\cdot\cos^2\gamma)]-1\}+\varepsilon\rho\tan\gamma; \tag{18}$$
$$a_t=2\omega^2\rho\tan\gamma+\varepsilon\rho. \tag{19}$$

It is simple to show that when the roller approaches the concentric section of the projection cam, we have:

$$v_p=-\omega\rho\tan\gamma; \tag{15a}$$
$$a_p=\omega^2\rho\tan\gamma\,[\tan\gamma+1/(\tan\alpha\cdot\cos^2\gamma)]-\varepsilon\rho\tan\gamma; \tag{16a}$$
$$a_c=-2\omega^2\rho\tan\gamma; \tag{17a}$$
$$a_n=\omega^2\rho\{\tan\gamma\,[\tan\gamma+1/(\tan\alpha\cdot\cos^2\gamma)]-1\}-\varepsilon\rho\tan\gamma; \tag{18a}$$
$$a_t=-2\omega^2\rho\tan\gamma+\varepsilon\rho. \tag{19a}$$

3. Concave Section of the Trajectory

Similarly for the concave section of the trajectory we obtain:

$$\rho=R\cos\alpha+(r_g-r_r)\cos\gamma; \tag{20}$$
$$\sin\gamma=R/(r_g-r_r)\sin\alpha; \tag{21}$$
$$\rho=R\cdot\sin(\gamma+\alpha)/\sin\gamma; \tag{22}$$

a) on taking the roller away from the concentric section of the trough:

$$v_\rho = -\omega\rho \tan\gamma; \tag{23}$$

$$a_\rho = \omega^2\rho \tan\gamma \left[\tan\gamma - 1/(\tan\alpha \cdot \cos^2\gamma)\right] - \varepsilon\rho \tan\gamma; \tag{24}$$

$$a_c = -2\omega^2\rho \tan\gamma; \tag{25}$$

$$a_n = \omega^2\rho \left\{\tan\gamma \left[\tan\gamma - 1/(\tan\alpha \cdot \cos^2\gamma)\right] - 1\right\} - \varepsilon\rho \tan\gamma; \tag{26}$$

$$a_t = -2\omega^3\rho \tan\gamma + \varepsilon\rho; \tag{27}$$

b) on bringing the roller close to the concentric section of the trough:

$$v_\rho = \omega\rho \tan\gamma; \tag{23a}$$

$$a_\rho = \omega^2\rho \tan\gamma \left[\tan\gamma - 1/(\tan\alpha \cdot \cos^2\gamma)\right] + \varepsilon\rho \tan\gamma; \tag{24a}$$

$$a_c = 2\omega^2\rho \tan\gamma; \tag{25a}$$

$$a_n = \omega^2\rho \left\{\tan\gamma \left[\tan\gamma - 1/(\tan\alpha \cos^2\gamma)\right] - 1\right\} + \varepsilon\rho \tan\gamma; \tag{26a}$$

$$a_t = 2\omega^2\rho \tan\gamma + \varepsilon\rho. \tag{27a}$$

4. Rectilinear Section of the Trajectory

Radius vector of the trajectory of motion of roller center is determined from $\triangle OBA$ (Fig. 3):

$$\rho = L/\cos\gamma, \tag{28}$$

where L is the perpendicular distance from the center of rotation of the cylinder block to the rectilinear section of the trajectory.

This parameter is determined from $\triangle OBC$, i.e.

$$L = \rho_1 \cdot \cos\gamma_1. \tag{29}$$

Here ρ_1 is the length of the radius vector at the beginning of the rectilinear section and γ_1 is the pressure angle at the beginning of the rectilinear section.

As is obvious from Fig. 3:

$$\gamma = \gamma_1 + \alpha. \tag{30}$$

For the case, when the roller is moving away from the concentric section of the cam, the relative velocity of the piston is calculated by differentiating equation (28) with respect to time:

$$v_\rho = d\rho/dt = L \sin\gamma/\cos^2\gamma \cdot d\alpha/dt = \omega\rho \tan\gamma. \tag{31}$$

Relative acceleration of the piston is determined by differentiating equation (31) with respect to time:

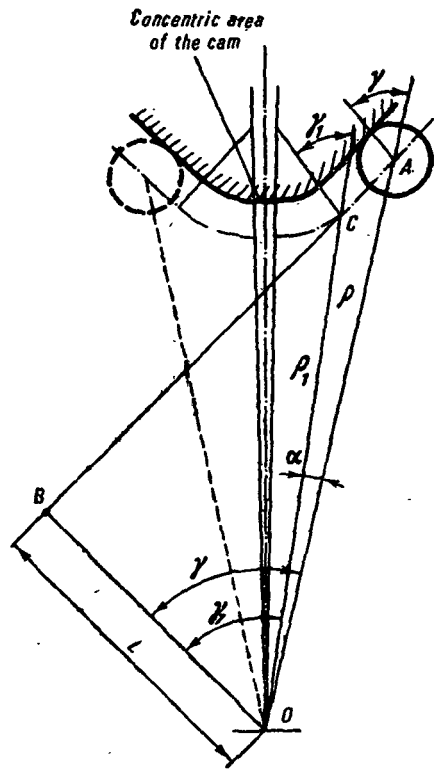

Fig. 3. Determination of radius vector of the trajectory of motion of roller center on the rectilinear section.

$$a_\rho = dv_\rho/dt = d\omega/dt \cdot \rho \tan\gamma + \omega \cdot d\rho/dt \cdot \tan\gamma + \omega\rho \cdot d \tan\gamma/dt$$
$$= \varepsilon\rho \tan\gamma + \omega^2\rho \tan^2\gamma + \omega^2\rho \cdot 1/\cos^2\gamma ,$$

from where:

$$a_\rho = \omega^2\rho (1 + 2\tan^2\gamma) + \varepsilon\rho \tan\gamma . \qquad (32)$$

Coriolis acceleration:

$$a_c = 2\omega^2\rho \tan\gamma . \qquad (33)$$

Normal and tangential components of absolute acceleration will respectively be:

$$a_n = 2\omega^2\rho \tan^2\gamma + \varepsilon\rho \tan\gamma ; \qquad (34)$$

$$a_t = 2\omega^2\rho \tan\gamma + \varepsilon\rho . \qquad (35)$$

For the case of the roller advancing close to the concentric section of the cam:

$$v_\rho = -\omega\rho \tan\gamma; \tag{31a}$$

$$a_\rho = \omega^2\rho\,(1+2\tan^2\gamma) - \varepsilon\rho\tan\gamma; \tag{32a}$$

$$a_c = -2\omega^2\rho\tan\gamma; \tag{33a}$$

$$a_n = 2\omega^2\rho\tan^2\gamma - \varepsilon\rho\tan\gamma; \tag{34a}$$

$$a_t = -2\omega^2\rho\tan\gamma + \varepsilon\rho. \tag{35a}$$

Equations derived for kinematic parameters of the group of pistons of the hydraulic motor for various sections of the trajectory are given in Table 1.

These equations are for calculating the normal and tangential components of absolute velocity and acceleration of the piston of a radial-piston multipass hydraulic motor guide-block which consists of arcs of circles.

To illustrate the analytical expressions, Fig. 4 shows the curves of velocity and acceleration components of the piston of a hydromotor whose

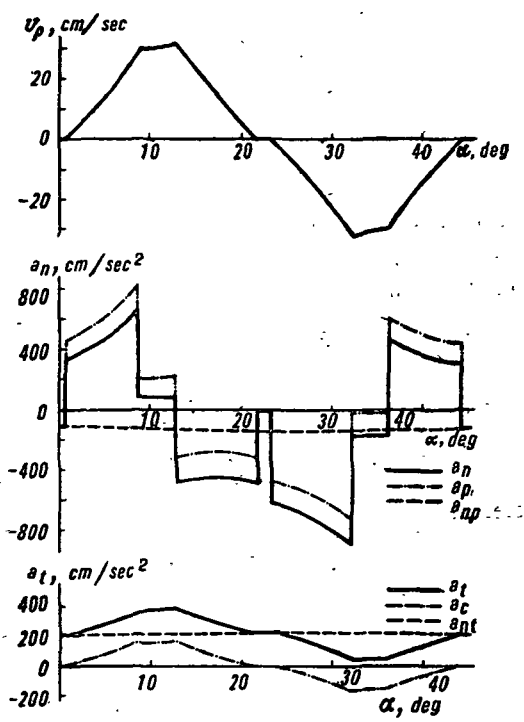

Fig. 4. Relative velocity and components of absolute acceleration.

Table 1. Kinematic parameters of a radial-piston multipass hydraulic motor with guide-block profile consisting of arcs of circles

Section of the trajectory of motion of the roller center*		Radius vector, ρ	Pressure angle, γ	Relative velocity, v_ρ	Normal component of absolute acceleration, a_n	Tangential component of absolute acceleration, a_t
Concentric		$r_g - r_r$	0	0	$-\omega^2\rho$	$\varepsilon\rho$
Convex	Case where the roller is far from the concentric section of the cam	$R\sin(\gamma-\alpha)/\sin\gamma$	$\arcsin R/(r_g+r_r)\sin\alpha$	$\omega\rho\tan\gamma$	$\omega^2\rho\,[\tan\gamma\,(\tan\gamma + 1/\tan\alpha\cdot\cos^2\gamma) - 1] + \varepsilon\rho\tan\gamma$	$2\omega^2\rho\tan\gamma+\varepsilon\rho$
	Case where the roller is close to the concentric section of the cam			$-\omega\rho\tan\gamma$	$\omega^2\rho\,[\tan\gamma\,(\tan\gamma + 1/\tan\alpha\cdot\cos^2\gamma) - 1] - \varepsilon\rho\tan\gamma$	$-2\omega^2\rho\tan\gamma+\varepsilon\rho$
Concave	Case where the roller is far from the concentric section of the trough	$R\sin(\gamma+\alpha)/\sin\gamma$	$\arcsin R/(r_g-r_r)\sin\alpha$	$-\omega\rho\tan\gamma$	$\omega^2\rho\,[\tan\gamma\,(\tan\gamma - 1/\tan\alpha\cdot\cos^2\gamma) - 1] - \varepsilon\rho\tan\gamma$	$-2\omega^2\rho\tan\gamma+\varepsilon\rho$
	Case where the roller is close to the concentric section of the trough			$\omega\rho\tan\gamma$	$\omega^2\rho\,[\tan\gamma\,(\tan\gamma - 1/\tan\alpha\cdot\cos^2\gamma) - 1] + \varepsilon\rho\tan\gamma$	$2\omega^2\rho\tan\gamma+\varepsilon\rho$
Rectilinear	Case where the roller is far from the concentric section of the cam	$L/\cos\gamma$	$\gamma_1+\alpha$	$\omega\rho\tan\gamma$	$2\omega^2\rho\tan^2\gamma+\varepsilon\rho\tan\gamma$	$2\omega^2\rho\tan\gamma+\varepsilon\rho$
	Case where the roller is close to the concentric section of the cam			$-\omega\rho\tan\gamma$	$2\omega^3\rho\tan^2\gamma-\varepsilon\rho\tan\gamma$	$-2\omega^2\rho\tan\gamma+\varepsilon\rho$

* For all the sections of trajectory of motion of the roller center $v(t)=\omega\rho$.

Table 2. Relationship between profile dimensions of a hydraulic motor piston and the type of section

Type of section	Angle between radius vector and line of center, α	Distances between the center of cylinder block and the center of arc forming the profile R, mm	Radius of arc forming profile of the guide-block r_g, mm
Concentric section of the projection	$0 < \alpha < 40'$	0	240
Concave section of the cam	$0 < \alpha < 8° 11' 47''$	290.5	50.5
First concave section	$110° 48' 30'' < \alpha < 114° 46' 43''$	163.587	353.085
Second concave section	$0 < \alpha < 9°$	171.6	92.9
Concentric section of the trough	$0 < \alpha < 40'$	0	264.5

profile dimensions are given in Table 2 and roller radius $r_r=3.75$ cm at $\omega=2.6$ *l*/sec and $\varepsilon=10$ *l*/sec^2.

References

1. Krymskii, A. N. Izuchenie neravnomernosti vrashcheniya vysokomomentnykh radial'no-plunzhernykh gidrodvigatelei so zvezdoobraznymi napravlyayushchimi (Study of non-uniform rotation of high-moment radial-piston hydraulic motors with star shaped guides). Sb. *Issledovanie gidroperedach i elementy rascheta,* vyp. XXII. Izd. VNII-Stroidormash, 1958.
2. Pluzhnikov, A. I. Novyi metod profilirovaniya napravlyayushchei radial'no-plunzhernykh gidromotorov mnogokratnogo deistviya (New method of determining profiles of the guides of radial-piston multi-action hydraulic motors). Sb. *Issledovaniya v oblasti metallorezhushchikh stankov,* vyp. 4, Mashgiz, 1961.
3. Ponomarenko, Yu. F. and A. Ya. Rogov. Radial'no-porshnevye vysokomomentnye gidromotory (Radial-Piston High-Moment Hydraulic Motors). Izd-vo Mashinostroenie, 1964.
4. Reshetov, L. N. Kulachkovye mekhanizmy (Cam Mechanisms). Mashgiz, 1953.
5. Rogov, A. Ya. and A. I. Khabarov. Profilirovanie napravlyayushchikh gidromotorov mnogokratnogo deistviya (Guide profiles of multi-action hydraulic motors). *Vestnik mashinostroeniya,* No. 1, 1965.
6. Khorin, V. N., S. N. Fateev and A. I. Chernyshev. Vysokomomentnye gidrodvigateli v gornom mashinostroenii (High-Moment Hydraulic Motors in Mine-Machine Building). Izd-vo Nedra, 1964.

M. M. Gernet

NOMOGRAPHS FOR SELECTING OPTIMAL LAWS OF MOTION OF DRIVEN LINKS OF CAM MECHANISMS

New techniques of calculating and designing automats are necessary if productivity of automatic machines is to be increased.

Increasing the velocities and accelerations of the driven links is one of the important methods of raising the productivity of a machine. However, an increase in velocities and accelerations of moving masses results in increased dynamic loads and loss due to friction. This also causes high torques on the cam shaft.

Due consideration should be given to the fact that different forces give rise to different types of acceleration in the driven links of automatic machines. Consequently, the driven link can attain the given velocity earlier or later depending on the state of motion.

The law of motion of driven links is based on the condition that the maximum values of acceleration a_{max} and velocity v_{max} should not exceed the design limits so that the productivity of the machine is increased without overloading.

On this basis equations for computing relative duration of movement u were obtained in [1] for the laws of motion with asymmetrical two-section :

$$u=[1/(\delta_{max})-(1-\lambda_2)]/(\lambda_2-\lambda_1) \tag{1}$$

and three-section tachograms:

$$u=[1/\delta_{max}-(1-\lambda_2+c\lambda_2)]/(\lambda_2-\lambda_1)\,, \tag{2}$$

where δ_{max}—coefficient of maximum velocity of the driven link; $\delta_{max}=v_{max}\cdot t_i/S_i$ (v_{max}—absolute value of the maximum velocity; S_i and t_i—path and duration of interval respectively);

λ_1—distance between the beginning of the interval and the center of gravity of the area of the positive acceleration diagram as a fraction of the run;

λ_2—distance between the end of the interval and the center of gravity of the area of the negative acceleration diagram as a fraction of the run;

c—relative duration of the section with constant velocity.

From these equations, let us determine the relative duration of run in the case of various laws of motion of the driven links and subsequently let us select the conditions under which the value of u is minimum.

To simplify the work of designers with regard to selecting the law of motion for the driven link and for comparing the laws, nomographs can be constructed from equations (1) and (2) (Fig. 1) for determining the value of u for a given value of δ_{max}.

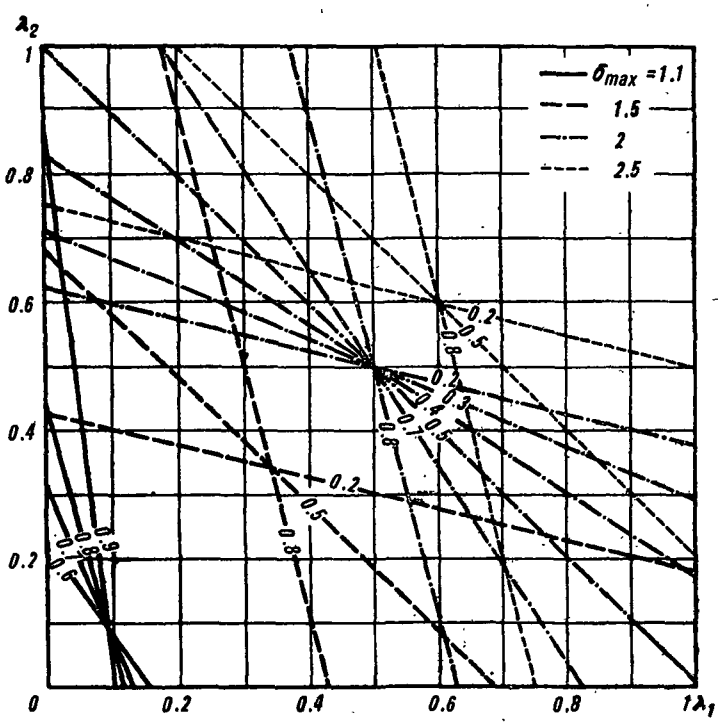

Fig. 1.

The nomographs are applicable at $\lambda_1 \neq \lambda_2$. Note that each value of δ_{max} corresponds to a group of straight lines of relative duration u for the run. The center of the group lies at the point $\lambda_1 = \lambda_2$. From equation (1) we observe that the relative duration of the run at this point does not have any

particular value. (The case $\lambda_1=\lambda_2$ has been discussed below).

Centers of the groups lie on the straight line $\lambda_1=\lambda_2$. The region, situated between this straight line and the ordinate, corresponds to the values $\lambda_2>\lambda_1$ while the region included between this straight line and the abscissa corresponds to the values $\lambda_2<\lambda_1$.

The straight lines representing equal relative durations of runs (for example, $u=0.2$ or 0.5) at various velocities are parallel to each other. It also follows from equation (1) that the slope of the straight lines is expressed by the ratio:

$$k=\Delta\lambda_2/\Delta\lambda_1=u/(u-1). \tag{3}$$

To simplify the nomographs, let us plot only a few groups corresponding to $\delta_{max}=1.1$; 1.5; 2 and 2.5. The value of u corresponding to intermediate values of δ_{max} can be easily determined by drawing straight lines parallel to the ones plotted earlier and passing through the point $\lambda_1=\lambda_2$.

It is obvious from the nomograph that δ_{max} increases on increasing λ_1 and λ_2. This confirms the law [2] that the center of gravity of the area of the positive acceleration diagram should be displaced towards the beginning of the interval in order to reduce the coefficient δ_{max}.

To simplify the procedure for selecting the appropriate law of motion of the driven link let us plot the nomographs of the dependence of relative durations of run on velocity at different values of λ_1 and λ_2. Let us denote the coefficients of maximum velocity δ_{max} in this case by 0.1 from $\delta_{max}=1.1$ to $\delta_{max}=2.5$ which corresponds to the usual velocities of the driven links in modern machines.

Let us examine the example of selecting the law of motion when it is necessary to obtain the maximum productivity of a machine and when the coefficient of maximum velocity should not go beyond 2.1. Nomograph (Fig. 2) helps in selecting the relative duration of run on the basis of given technological and kinematic characteristics. There are right and left branches on the nomograph. The right branch corresponds to the values $\lambda_1>\lambda_2$ while the left branch to $\lambda_1<\lambda_2$.

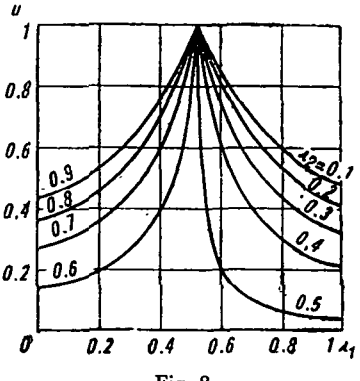

Fig. 2.

One point with coordinates $\lambda_1=0.7$ and $\lambda_2=0.5$ corresponds to the relative duration of run $u=0.1$ while four points ($\lambda_1=0.1$, $\lambda_2=0.7$; $\lambda_1=0.33$, $\lambda_2=0.6$; $\lambda_1=0.57$; $\lambda_2=0.5$; $\lambda_1=0.8$, $\lambda_2=0.4$) correspond to the relative duration $u=0.3$. The designer selects the optimum point keeping in mind the profile of the cam and its manufacturing process.

Other points for intermediate values

of λ_2 can be found out by interpolation.

Increased machine productivity is better achieved by use of the laws of motion of driven links having tachograms with three sections.

In fact, if, during the motion of the driven link utilizing the law of double-section tachogram the given path is covered and the maximum velocity at the end of the run is attained then (in the case of motion of the driven link according to the law of three-section tachogram) the maximum velocity is maintained until the required path is covered.

In the second case the driven link covers the positive distance earlier.

A nomograph (Fig. 3) has been plotted for the laws of motion with three-section tachogram. This nomograph helps to determine the relative duration of run and characteristics of the laws of motion providing that the coefficient δ_{max} of maximum velocity does not go beyond the permissible limit.

This nomograph is used in the same way as the nomograph for laws of motion with two-section tachograms. The following characteristics should be mentioned.

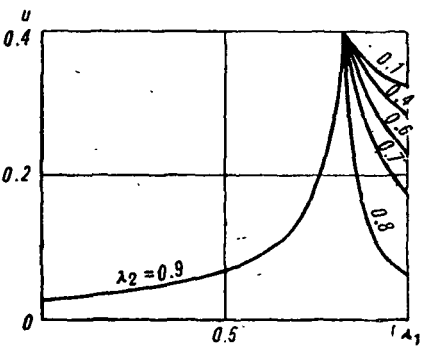

Fig. 3.

Since duration of the whole interval has been taken equal to one, the nomograph is included within the value of relative duration of run not exceeding $u=1-c$. As in the case of laws of motion with two-section tachograms the nomograph has right and left branches. The right branches correspond to the values $\lambda_1>\lambda_2$ while the left branches to $\lambda_1<\lambda_2$.

Other values of u corresponding to intermediate values of λ_2 are found by interpolation.

The question of the possibility of obtaining other values of relative duration of constant velocity (for example $c=0.7$) at the given value of maximum velocity coefficient (for example $\delta_{max}=1.5$) arises at this stage.

To show this, let us determine the coordinates of the center of the nomograph group plotted for the laws of motion with three-section tachogram. All the curves λ_2 intersect in this group having coordinates λ_1 and λ_2.

Then after selecting the curves λ_2' and λ_2'' and solving the system of equations:

$$u=[1/\delta_{max}-(1-\lambda_2'+c\lambda_1')]/(\lambda_2'-\lambda_1);$$

$$u=[1/\delta_{max}-(1-\lambda_2''+c\lambda_2'')]/(\lambda_2''-\lambda_1),$$

we get the coordinates of the center of the group:

$$u=1-c; \tag{4}$$

$$\lambda_1=(1-1/\delta_{max})/(1-c). \tag{5}$$

Using equation (5) let us plot the nomograph (Fig. 4) representing the dependence of the coefficient of maximum velocity on the value of relative duration of uniform motion and on the parameter λ_1 of the law of motion of the driven link. The center of the group of curves in this case lies at the point $\delta_{max}=1$ and $\lambda_1=0$ corresponding to uniform motion.

The nomograph shows that duration of uniform motion cannot be selected for every coefficient of maximum velocity.

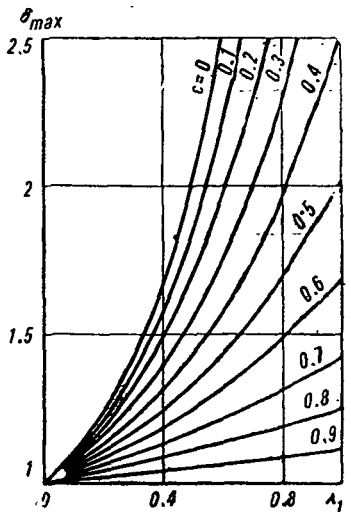

Fig. 4.

Therefore, when $\delta_{max}=1.5$, it is not possible to run the driven link according to the law in which the relative value of the duration of uniform motion $c=0.7$. In addition the greater the velocity of the driven link, the lesser will be the value of c for the given law of motion. It is not difficult to explain this dependence.

As a matter of fact, if the duration of uniform motion is large, there is little time for starting and running down the mechanism and at higher velocities, larger accelerations are required which may not be attainable at all times.

If it is necessary to select the law of motion with three-section tachogram from the premise that the velocity may not exceed the maximum permissible value, then employing this nomograph we establish the value of relative duration of uniform motion and utilizing the nomograph shown in Fig. 3 we determine the relative duration of starting u and the values of λ_1 and λ_2 for laws of motion with three-section tachograms.

In practice such laws of motion of driven links are often used for which $\lambda_1=\lambda_2=\lambda$. In this case, well-known equations (2) are used for determining the coefficient of maximum velocity. The first equation $\delta_{max}=1/(1-\lambda)$ is used in the case of laws of motion with two-section tachogram while the second equation $\delta_{max}=1/[(1-\lambda)\ (1-c)+c]$ is used in the case of laws of motion with three-section tachogram.

It is obvious from the equations that δ_{max} does not depend on the duration of starting, i.e. any value of velocity can be attained instantaneously.

However, this leads to very high accelerations which may not be desirable and therefore, we must keep within the permissible values of maximum acceleration.

Solving simultaneously the obtained equations with the relation:

$$\delta_{max}=\xi_{max}\cdot u/\alpha,$$

where ξ_{max}—coefficient of maximum accelerations of the driven link $\xi_{max}=a_{max}\cdot t_i^2/S_i$ (a_{max}—absolute value of the maximum accelerations; S_i and t_i path and duration of the interval respectively);

α—coefficient introduced by S. I. Artobolevskii [3] and denoting the ratio of maximum ordinate of acceleration curve on the starting section to the ordinate of such a constant acceleration at which the given velocity is achieved on the same section.

We obtain an expression relating the value of relative duration of starting with the coefficient of maximum acceleration:

$$u=\alpha/[\xi_{max}(1-\lambda)]. \tag{6}$$

For the laws of motion with two-section tachogram; and for the case of three-section tachogram, we have:

$$u=\alpha/\{\xi_{max}[(1-\lambda)\ (1-c)+c]\}. \tag{7}$$

The nomograph for fundamental laws of motion has been plotted on the basis of these formulas. For example, nomographs are given for motion with acceleration changing according to sine or cosine law ($\alpha=1.57$) for two-section (Fig. 5, a) and three-section (Fig. 5, b) tachograms. The curves demonstrate that the given velocity can be easily attained after a large interval of time but in the case of short duration of run, the acceleration sharply increases.

These nomograms can be utilized in the following manner.

The value of λ from the given value of the coefficient of maximum velocity may be determined:

$$\lambda=1-1/\delta_{max}. \tag{8}$$

The relative duration of start is then obtained from the nomograph (Fig. 5, a) or from some other nomograph (depending on the law of motion) based on the condition that the coefficient of maximum acceleration does not exceed the permissible value. Only one solution is possible. One relative duration of start corresponds to the obtained value of ξ_{max}.

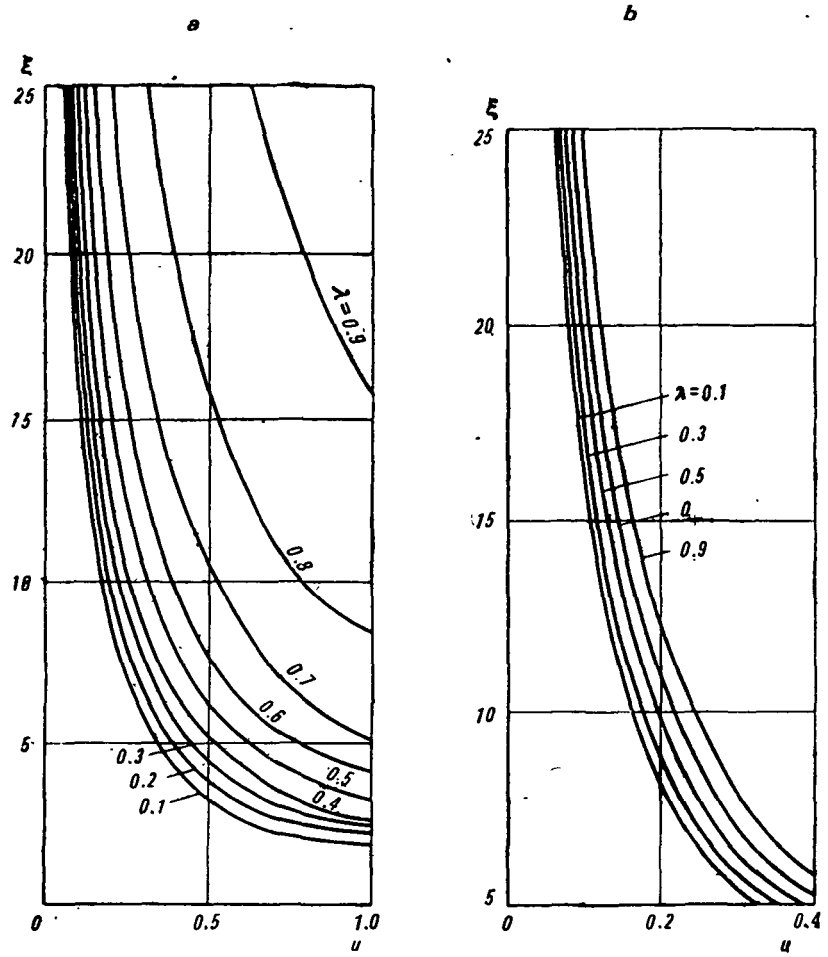

Fig. 5.

If it is necessary to select the law of motion of the driven link with three-section tachogram, depending on the coefficient of maximum velocity, parameters λ and c are calculated from the nomograph shown in Fig. 4. The relative duration of start is then determined from the nomograph shown in Fig. 5, b depending on the value of c.and α, from the given value of ξ_{max} and from the obtained value of λ.

As in the previous case, only one solution is possible.

Sometimes, in selecting the law, the designer restricts himself only to the maximum permissible acceleration. In this case, using equation:

$$\xi_{max}=\delta_{max}\cdot\alpha/u, \tag{9}$$

the author plotted nomographs for the most common laws of motion [constant acceleration $\alpha=1$ (Fig. 6); change of acceleration according to sine or cosine law ($\alpha=1.57$); acceleration increases or decreases along a straight line ($\alpha=2$)].

The nomograph and equation (9) demonstrate that the designer can operate with different laws and values of δ_{max} and u. Also at one and the same value of ξ_{max}, relative duration of start increases on increasing δ_{max}, i.e. at one, and the same acceleration, a longer interval of time is required to get higher velocity.

These nomographs permitted an interesting analysis of the existing laws of motion and confirmed certain prior assumptions. These nomographs considerably simplify the work of engineers designing mechanisms.

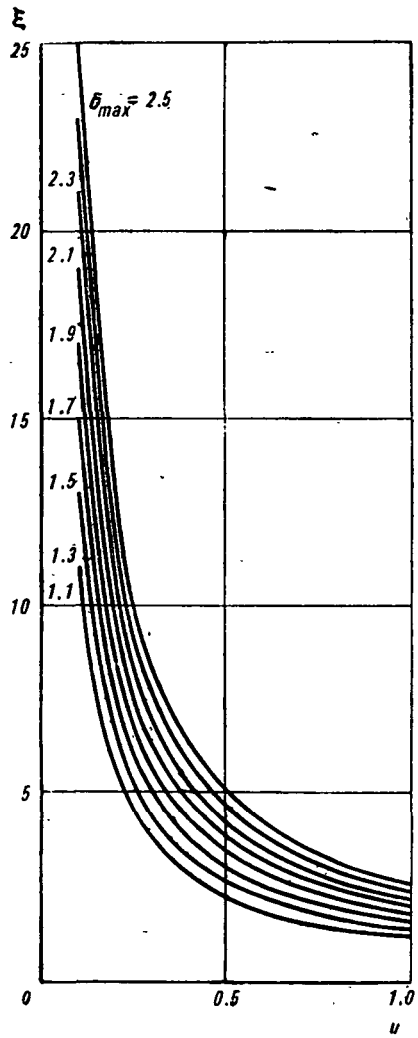

Fig. 6.

References

1. Gernet, M. M. O kinematicheskikh usloviyakh sovmestnoi roboty kulachkovykh mekhanizmov (Kinematic conditions for simultaneous operation of cam mechanisms). *Mashinovedenie,* No. 5, 1966.
2. Levitskii, N. I. Kulachkovye mekhanizmy (Cam Mechanisms). Izd-vo Mashinostroenie, 1964.
3. Artobolevskii, S. I. Mashiny-avtomaty (Automatic Machines). Mashgiz, 1949.

N. M. Guseinov and *S. I. Gamrekeli*

DESIGN OF A FOUR-LINK MECHANISM FOR REPRODUCING A GIVEN MOTION

Computer technology has made significant contribution to the development of methods of synthesis and analysis of mechanisms. At present, the most complicated problems on the theory of machines and mechanisms are being solved on high-speed digital computers and modeling devices which provide alternative design of mechanisms and aid in constructing functional charts, graphs, tables and nomographs for selecting (suitable) mechanisms [1-6].

As a result of the development of precision machines, instrumentation, orientation mechanisms and mechanisms of automatic control, the problem of reproducing a given function has attained great importance. The solution to this problem is of current interest since hinged four-link mechanisms, characterized by simplicity, high accuracy, relability and durability, are widely used in technology.

The problem of reproduction of a given motion is very important in designing computing mechanisms and various automatic machines. Solution of this problem is associated with significant mathematical difficulties.

Firstly, it is necessary to establish the given law of motion by taking into account the technological, kinematic and dynamic conditions. Secondly, the parameters of the hinged four-link mechanism which can approximately reproduce the given function, have to be determined. Determination of the parameters of a hinged four-link mechanism, for reproducing the given relation, namely determination of the length of links and initial values of the angles φ_0 and ψ_0, is an indeterminate problem and its solution mainly depends on the correct selection of the mechanism parameters and on the initial values of the angles of rotation of the crank and rocker arm.

As is well known, exact reproduction of a given law of motion in a hinged four-link mechanism is possible for only some exceptional cases.

It is difficult to find the law of motion of a mechanism correctly reproducing the given function during the whole time interval. Therefore, a solution is determined which gives the exact value of function at certain positions and an approximate value at the remaining positions. However, the deviation of the actual values from the theoretical values should not go beyond the stated limits for good results.

While discussing the reproduction of a given function, I. I. Artobolevskii states the following:

"The practical and simple method of determining the necessary parameters of the kinematic scheme lies in a rapid and systematic study of all the possible alternatives of the mechanism, which reproduces the given function within prescribed error limits with the aim of finding those alternatives which satisfy all the conditions required of the given mechanism."

Keeping this in mind a rapid method of modeling a mechanism is to determine all possible alternative positions of a hinged four-link mechanism.

Modeling based on the theory of similarity, is a general method of scientific investigations. This method explores the relationship between quantitative and qualitative aspects of similar physical phenomena which are of great importance during preliminary selection of the parameters of a mechanism.

The theoretical and practical problems associated with the design of plane hinged four-link mechanisms for a given law of motion, are described below.

Consider the reproduction of the function $y_1=f_1(x)$, which is defined by a graph (or a table) in coordinates φ and φ where φ is the angle of rotation of the crank, and ψ is the angle of rotation of the rocker arm

The functional dependence is approximately reproduced for certain interval of change in the value of argument x_i. Arbitrary values of the argument x_i are selected within the limit $x_0<x_i<x_m$.

Bounding values of the arguments x_0 and x_m are already known. After preliminary selection of the basic parameters of the mechanism, let us denote the functional dependence reproduced by the mechanism in terms of $y_m=f_2(x)$.

The main objectives of approximate calculation and mathematical analyses of the function are to compare these functions and calculate their maximum deviations. Deviation of the function can be expressed in terms of Δ_x, Δ_y and Δ_n. By the term deviation, we mean the difference of function $\Delta_y=y-y_m$.

In the same way, we calculate Δ_x, Δ_y and Δ_n depending on the direction of the change. It is obvious that the difference Δ_n correctly measures the deviations from the given function. The given motion is correctly reproduced at the points of intersection of the two-functional curves The form of the given function and the reproduction function determines the existence of a point of intersection.

The analytical expression for the difference Δ_x is extremely complicated even for the simplest four-link mechanism. Various mathematical techniques including the theory of functions, the method of interpolation, best approximation, uniform approximation and the method of quadratic approximation, are used for calculating these differences. Use of analytical methods depend on the correct specification of the deviation function. Various methods of variation, such as the method of iteration, method of selecting free parameters, etc. are used for approximate calculation of the parameters of a mechanism.

The parameters of a hinged four-link mechanism, approximately reproducing a given function, should be selected in such a manner that the maximum deviation should not exceed a limiting value.

It is known that the position of a hinged four-link mechanism, i.e. deviation of the rocker arm (angle ψ) is defined by independent parameters a, b, c, d and by the angle of rotation φ of the crank.

Various contours of four-link mechanisms are obtained directly by changing (variations of) the lengths of links a, b, c and d successively or simultaneously. Tentatively, internal and external variations of the contours of a four-link mechanism are differentiated. In the case of external variation of a four-link contour, the sum of the lengths of all the links is not constant, i.e. the condition $a+b+c+d \neq P_i \neq$ const is satisfied.

In the case of internal variation, the parameter of the contour of the four-link mechanism is $P_i = \text{const}$.

For the first case, the parameter of the four-link mechanism P_i changes due to variation in link i. In the second case, i.e. in the case of internal variation of the contour of four-link mechanism, the parameter remains constant and each link changes as a result of the change in another link.

Analytical relationships between increments in links and increments (deviations) in the rotation of the driven link, i.e. the deviations from the given function of the mechanism, are given below.

External variation of the links of a hinged four-link mechanism is shown in Fig. 1. A sliding pair is fixed at hinges, A, B, C, and O to change the links. In this case, the hinged four-link mechanism $OABC$ with one degree of freedom changes into a dummy five-link hinged mechanism $OABC$ with two degrees of freedom. Let us construct a four-link hinged mechanism ABC with one sliding pair from the dummy five-link, hinged mechanism $OABC$ by constraining the length of any two links and angle φ to be constant. In the case of Fig. 1, a, d, we have a usual slider-crank mechanism, and a slotted lever mechanism for Fig. 1, b, c.

The crank a is varied in Fig. 1, a. For a deviation Δ_a, the driven link of the rocker arm c is rotated through angle Δ_ψ. Since the value of deviation Δ_a is small, we use the method of small displacements to determine the changes as a result of Δ_ψ.

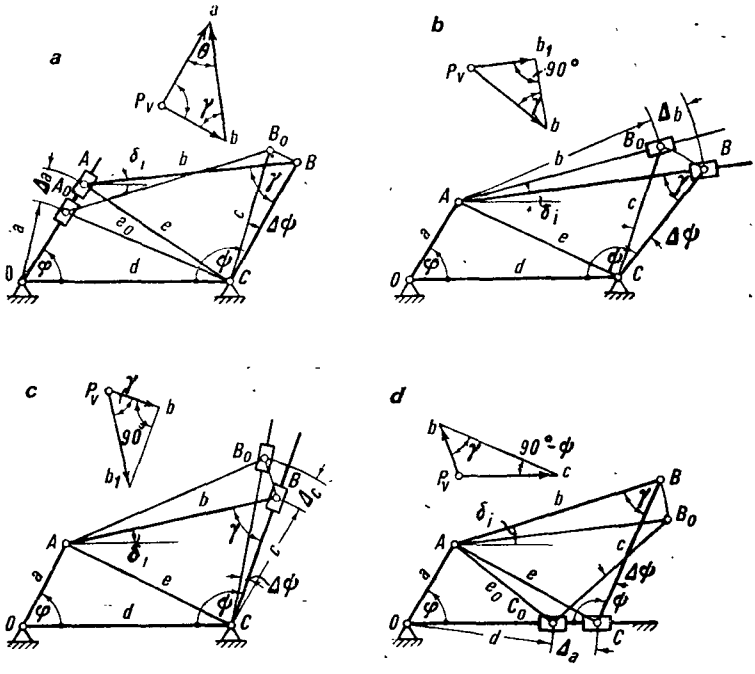

Fig. 1.

Assume that infinitesimal displacements of the points of a mechanism are proportional to their velocities. Displacing point A_0 to point A, the point B_0 also moves to B. Thus a deviation Δ_ψ is formed between the two positions of the rocker arm.. Assuming a value for the velocity of point A, we can construct the velocity diagram P_v from which the deviation Δ_ψ can be obtained.

From the velocity diagram, we get the proportion:

$$v_a/\sin\gamma = v'_b \sin\theta\,. \tag{1}$$

On taking $v_a=\Delta_a/\Delta t$ and $v_b=c\Delta_\psi/\Delta t$, we determine deviation from the following formula:

$$\Delta\psi_a=\Delta_a \sin\theta/(c\sin\gamma)\,, \tag{2}$$

where γ is the angle of transmission in the hinged four-link mechanism and $\theta=\varphi-\delta_i$ is the angle previously defined.

Fig. 1, b shows that a change Δ_b in the length of the connecting rod in the driven link, moves the rocker arm through an angle Δ_ψ. Assuming

that point B moves relative to point C with a specific velocity, we draw the velocity diagram P_v and derive the equation showing the relation between increments Δ_b and Δ_ψ:

$$\Delta\psi_b=\Delta_b/(c\sin\gamma)\ . \tag{3}$$

Fig. 1, c shows the effect of change in the length of the rocker arm. If point B moves with respect to point A with specific velocity, we can plot the velocity diagram P_v and obtain relation between parameters Δ_c and Δ_{ψ_c}:

$$\Delta\psi_c=\Delta_c/c\cdot\cot\gamma\ . \tag{4}$$

Fig. 1, d shows the effect of change in link d. Assuming that point C moves with a specified velocity, we plot the velocity diagram P_v. From the velocity diagram, the functional relation between deviations Δ_d and Δ_{ψ_d} can easily be determined:

$$\Delta\psi_d=\Delta_d\sin(90^\circ+\psi+\gamma)/(c\sin\gamma)\ . \tag{5}$$

The case of internal variation of the links of a hinged four-link mechanism is considered in Figs. 2-4. In this case the angle of rotation of the crank $\varphi=$const. In Fig. 2, crank a and support d are invariant in addition to the angle φ. The lengths of the connecting rod b and of the rocker arm c are changed in such a manner that the sum of these links remains constant.

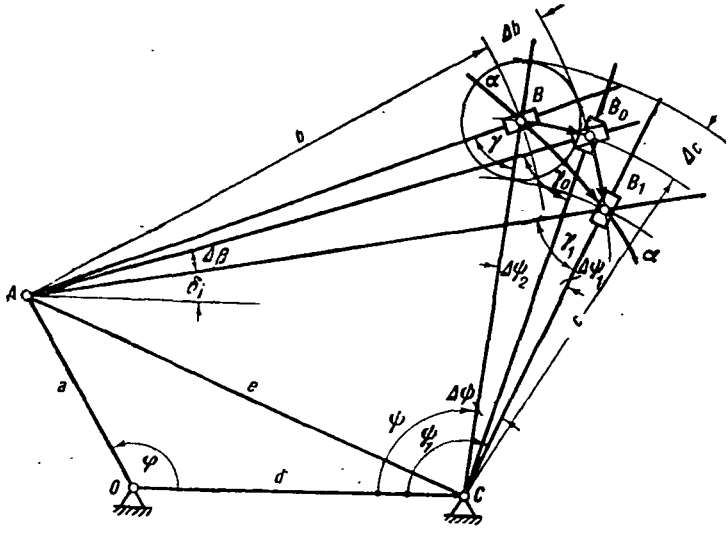

Fig. 2.

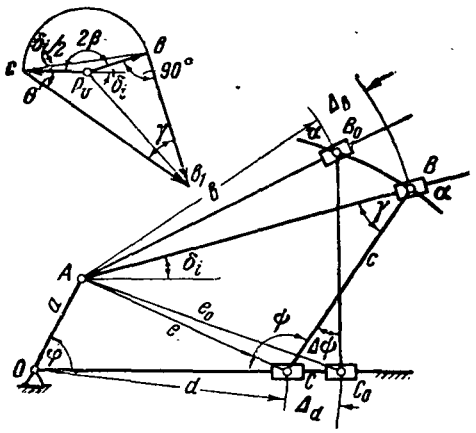

Fig. 3.

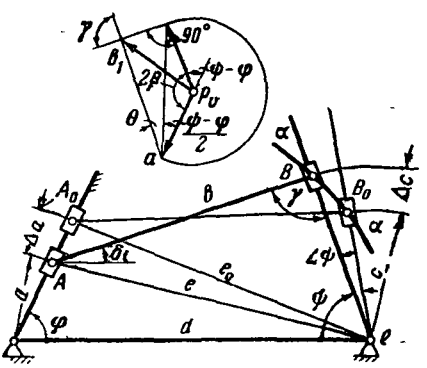

Fig. 4.

In this case, the following condition is satisfied:

$$(b+\Delta_b)+(c-\Delta_c)=P_i=\text{const}\,, \tag{6}$$

where $\Delta_b=\Delta_c$ and takes an arbitrary value.

For the case of internal variation, we find that the length of the first link increases on decreasing the length of the second link. In this case, hinges A and C are fixed points and the variable links b and c are connected to them.

It may be noted that the movable point B which moves along an elliptical curve $\alpha-\alpha$ with focal points at hinges A and C, is the locus of variation of links b and c.

The procedure for determining the variation Δ_ψ, due to variations of links b and c is as follows [Fig. 2]: A circle of radius Δ_b is drawn with center at point B (point of intersection of links b and c). With points A and C as centers, draw circles of radii $b+\Delta_b$ and $c-\Delta_c$ respectively, the intersection of which gives point B_1. Angle $BCB_1=\Delta_\psi$ which is the angle of displacement or deviation.

Similarly, draw circles of radii $b+\Delta_b$ and C from points A and C respectively, whose intersection gives point B_0. Connect point B_0 with points A and C.

It is obvious from the Fig. that:

$$\Delta_\psi=\Delta_{\psi_1}+\Delta_{\psi_2}\,. \tag{7}$$

From the slotted lever mechanisms ABC and AB_1C (see Fig. 3) and equations (3) and (4) derived for the case of external variations of links of hinged four-link mechanism, we obtain:

$$\Delta_{\psi_1}=\Delta_c\cos\gamma_1/(C\sin\gamma_1)\;; \tag{8}$$

$$\Delta_{\psi_2}=\Delta_b/(C\sin\gamma_0)\,. \tag{9}$$

If $\Delta_c=\Delta_b$, we determine the total deviation from the formula:

$$\Delta_\varphi=\Delta_b/C\ (1/\sin\gamma_0+\cot\gamma_1)\ . \tag{10}$$

Links b and d in the contour of hinged four-link mechanism $OABC$ are changed in Fig. 3. Here φ, a and c are constant. To consider the change in links b and d simultaneously, let us change the hinged four-link mechanism $OABC$ into a dummy five-link mechanism ABC with two sliding pairs. For this purpose, let us fix slide blocks, installed at free ends of connecting rod b and support d, at points B and C of rocker arm c. For the case of internal variation, the displacement of point B_0 to B causes the displacement of point C_0 to point C.

Here it is assumed that $v_b=v_c$.

Let us draw the velocity diagram for the dummy five-link mechanism ABC. From the velocity diagram, we get the proportion:

$$cb/\sin\gamma=cb_1/\sin(90°+\delta_i/2)\ . \tag{11}$$

If it is taken that $cb=2\Delta_b\sin\beta/\Delta t$ and $cb_1=c\Delta\psi/\Delta t$, then after substituting these values in formula (11), we get the deviation:

$$\Delta_\varphi=2\Delta_b\sin\beta\cos(\delta_i/2)/(c\sin\gamma)\ , \tag{12}$$

where $\beta=90°-\delta_i/2$.

It may be concluded that upon varying the links b and d, the curve $\alpha-\alpha$ representing a distorted ellipse of second order becomes the locus of displacement of point B.

In Fig. 4, b and d are considered as constant parameters. To vary the links a and c, the four-link mechanism $OABC$ is changed into a dummy five-link mechanism ABC with two sliding pairs. These slide blocks freely move at the free ends of the links a and c and are hinged to points A and B on the connecting rod b. Considering internal variation of links a and c, displacement of point A_0 to point A causes the point B_0 to move the point B along a distorted ellipse, i.e. a curve of second order, which is the locus of displacement of point B.

In the case of displacement of slide blocks in the opposite direction we assume that the velocity $v_a=v_b$. Let us plot the velocity diagram P_v. From the velocity diagram, we get the proportion:

$$bb_1/\sin\theta=ab/\sin\gamma\ . \tag{13}$$

Taking into account that $bb_1=c\Delta_\psi/\Delta t$ and $ab=2\Delta_a\sin\beta/\Delta t$ and after putting these values, we get the deviation:

$$\Delta_\varphi=2\Delta_a\sin\beta\cdot\sin\theta/(c\sin\gamma)\ . \tag{14}$$

where $\beta=90°+0.5(\varphi-\psi)$ and $\theta=90°+\psi+\varphi-(\gamma-\delta_i)$.

Fig. 5 shows the basic features of the modeling device with the help of which it is possible to simulate and study all the possible variants of the contours of a hinged four-link mechanism. These devices consist of vector contours of the four-link mechanism, arranged in parallel planes and made of flexible inextensible threads. The vector contours of four-link mechanisms are supported by two rigid systems of cranks and rocker arms S_1 and S_2.

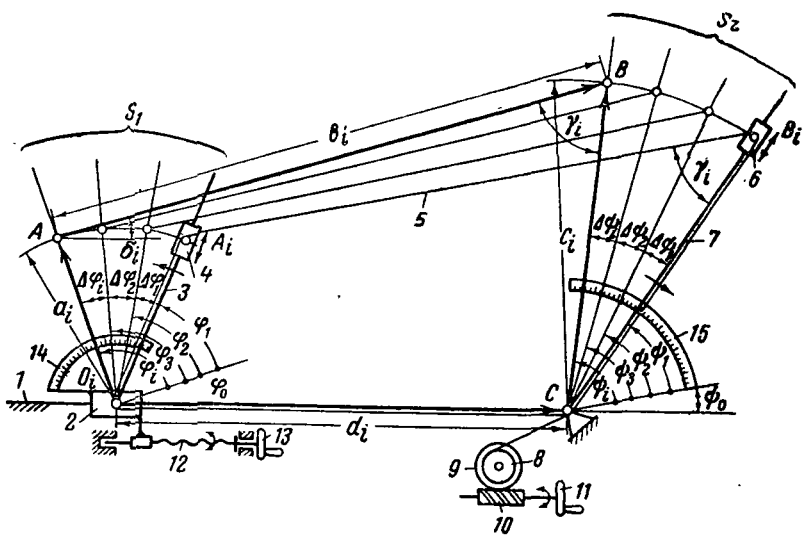

Fig. 5.

The slide block *2* is freely installed on guide *1*. The cranks *3* with slide blocks *4* sit freely on slide block *2*. A screw *12* and flywheel *13* which help in regulating the length of support d_i are connected to slide block *2*. Slide blocks *4* having pins on cranks are arranged along the circle of crank a_i. There are two handles at point O_i. With the help of a worm gear one of the handles changes the length of cranks a_i and the other rotates the system S_1 by increasing or decreasing the initial angle φ_0.

Angles φ_1, φ_2, φ_3 and φ_i of the rotation of cranks are set and fixed manually. Values of the angles are measured on scale *14*.

The rocker arm *7* is hinged at the stationary point C and the slide blocks *6* with pins B_i are installed on the arm. Pins B_i of rocker arm *7* are arranged along the circle of radius C_i. There is a handle at point C which changes the length of rocker arm C_i simultaneously with the help of worm gear. The system S_2 is fixed by the second handle and the initial angle φ_0 is set. Deviation of the angles $\Delta\varphi_1$, $\Delta\varphi_2$, $\Delta\varphi_i$ between the rods is measured on scale *15*. The flexible cord is fixed to point C and is

passed through hinges (pins) O_i, A_i, B_i and C_i and is wound round the free ends of shaft *8*. Vector contours of four-link mechanisms $O_iA_iB_iC_i$ with equal lengths P_i are obtained.

It is a necessary condition that the total length of vector contour of cords *5* is the same for every four-link mechanism.

External variation of the links of the hinged four-link mechanism is provided by handle *11* which is connected to shaft *8* through a worm gear drive *9* and *10*. Position of the connecting rod b_i can be changed by rotating handle *11*. Springs stretching the flexible cord *5* between points A_i and B_i are installed on rocker arm *7* to keep the flexible cord of connecting rod b_i rigid, i.e. stretched.

Kinematic scheme of the device is shown in Fig. 6. Slide block *2* which moves freely in guide *1* has a hole *0*. The shaft *O* moves freely in the hole. Washers *27* sit freely in the shaft *O* and conical gears *31* are kept in place by the force of friction. Washers *27* are connected to hollow rods *3* which have slide blocks *4* in the longitudinal grooves. Slide blocks *4* are moved with the help of screw *33*, conical gears *31*, *32* and handle *16* which regulate the length of cranks a_i. Pins A_i with incisions, playing the role of hinges, are fixed to the slide blocks. Handle *17* connected to washers *27* through link *26* sits freely on shaft *O*. Washers *27* along with the cranks *3* try to rotate in the counterclock-wise direction due to spring *29* and flexible

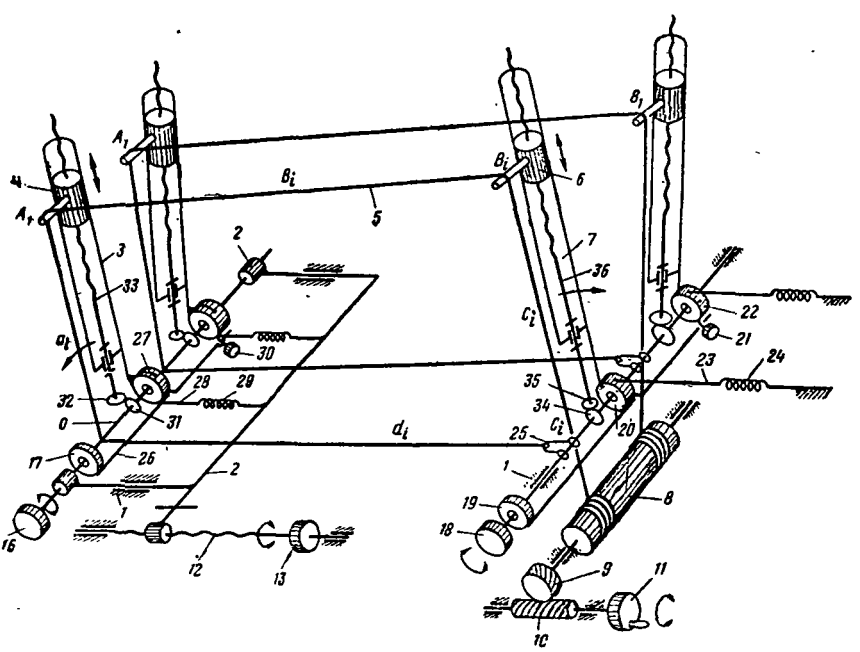

Fig. 6.

links *28*. A screw-stop (not shown in Figure) stops this movement. Angle of rotation of the crank is measured on the scale and is fixed by screw *30*. Slide block *2* along with the system of cranks *3* is put into motion by the screw *12* and handle *13*. Length of the support d_i is changed with the help of handle *13*.

There exists a similar design for the system of rocker arm. Handle *18*, conical gears *35* and freely-fitted washers *20* and *22* sit rigidly on shaft *C* which freely rotates in the casing *1*. Hollow rocker arms *7* are connected to washers *20*. The angle of deviation $\Delta\psi_i$ between the rocker arms is measured on the scale and, if necessary, is fixed by the screw *21*. The rocker arms *7* are rotated in the clockwise direction by the flexible link *23* and spring *24*. This rotation helps in stretching the vector contour of four-link mechanisms, made of flexible cords. The system of rocker arms can be rotated through angle ψ by handle *19*.

The length of rocker arms c_i is changed by handle *18*. Pins B_i fixed to slide blocks *6* simultaneously move along rocker arms *7* through a pair of conical gears *34*, *35* and screw *36* which is kinematically connected to slide block *6*. Pins B_i have incisions and play the role of hinges B_i. The free end of the flexible cord *5* is fixed to catch *25* passed through points O_i, A_i, B_i and C_i and is wound on shaft *8*. Shaft *8* is kinematically connected to handle *11* through a worm gear drive *9* and *10*. Total perimeter P_i of the hinged four-link mechanism *OABC* is changed with the help of handle *11*.

Thus, the main parameters (a_i, b_i, c_i, d_i, φ and ψ) of a hinged four-link mechanism can be changed successively or simultaneously with the help of handles *16*, *11*, *18*, *13*, *17* and *19* respectively.

The device operates in the following manner: All the given parameters are fixed, and the remaining parameters are determined by mechanically changing the free parameters. The additional condition of rotation of cranks or angles of transmission in hinged four-link mechanisms is observed in this case.

The deviations are simultaneously recorded by changing the parameters and by comparing them with the given function. Thus the errors of the mechanism are determined.

Application of modeling methods is one of the practical means of solving various problems of the synthesis of hinged four-link mechanisms. Modeling four-link hinged mechanisms makes it possible to successively form various alternative contours of four-link mechanisms, for the purpose of studying the change in the values of the parameters of mechanisms.

Modeling permits us to study the effect of change in mechanism parameter values.

While changing the parameters of a mechanism, the parameter to be determined is considered as the expected value of the result of some arbitrary process. A large number of values for the parameters of the

four-link mechanisms, enable us to define easily the function under consideration.

References

1. Artobolevskii, I. I. Teoriya mekhanizmov i mashin (Theory of Mechanisms and Machines). Moscow-Leningrad, GITTL, 1954.
2. Artobolevskii, I. I. Osnovnye problemy teorii mashin i mekhanizmov (Basic Problems of the Theory of Machines and Mechanisms). Izd-vo AN SSSR, 1956.
3. Levitskii, N. I. Proektirovanie ploskikh mekhanizmov s nizshimi parami (Design of Two Plane Mechanisms with Lower Pairs). Izd-vo AN SSSR, 1950.
4. Zinov'ev, V. A. Analiticheskie metody rascheta ploskikh mekhanizmov (Analytical Methods of Calculating Plane Mechanisms). Moscow-Leningrad, Gostekhizdat, 1949.
5. Guseinov, N. M. and S. I. Gamrekeli. Ob odnom sposobe modelirovaniya prostranstvennykh chetyrekhzvennykh mekhanizmov (A method of modeling spatial four-link mechanisms). Sb. *Sovremennye problemy teorii mashin i mekhanizmov*, Izd-vo AN SSSR, 1965.
6. Gamrekeli, S. I. and R. S. Natsvlishvili. Ob odnom sposobe modelirovaniya ploskikh chetyrekhzvennykh mekhanizmov (A method of modeling plane four-link mechanisms). *Trudy GPI*, No. 1 (94), 1964.

R. P. Dzhavakhyan

SYNTHESIS OF CAM LEVER MECHANISMS FOR DIFFERENT TYPES OF MOTIONS OF DRIVEN LINKS

In practice, it is often required to vary the operating parameters of a machine. Research studies have been undertaken on adjustable four-link and six-link lever mechanisms used for this purpose. Some adjustable multilink cam mechanisms are also considered in references [1-5].

Adjustable cam mechanisms are commonly used in steam engine for controlling admission, in internal combustion engines for establishing the required lift of exhaust valves, for changing distribution phases in an experimental engine, in machine tools for changing the travel, velocity and direction of motion of the carriage, etc.

In such cases, the mechanisms have an uniformly rotating cam with a fixed axis of rotation. Moreover, adjustments are carried out by changing or resetting (along, or around the axis of rotation) the cam or by changing the gear ratio between the roller and the working link. However, it is not possible to get a different motion for the driven link without changing the cam, in such mechanisms, whereas this is possible with lever-cam mechanisms.

In cam mechanisms, it is often required to control the travel s_i or phase φ_i of motion of the driven link independently or to control both the parameters according to a given functional relationships $s_i=s_i(\varphi_i)$. For example, the latter condition is associated with medical equipment used for artificial blood circulation and respiration as well as for mechanical massage of heart when the working link moves according to the law "raising-lowering" and it is required that the quantity of blood (air or liquid) pumped in by the piston during one cycle should change according to the given functional relationship in the case of deviation in the ratio of durations of the forward and reverse travels of the piston during the cycle.

Depending on the method, the following two types of control can be distinguished:

1) control during the working of the machine, i.e. in the case of continuous rotation of the driving link, and

2) control carried out only in the case of the stationary state of the mechanism. Control when the mechanism is in operation, has many advantages since in this case, it is possible to trace the process of control and to set the required parameters.

To convert a nonadjustable cam lever mechanism with one degree of mobility, into an adjustable one an additional (adjustable) link is introduced, which forms a kinematic pair with the links forming the original pair. In this case, the number of links and kinematic pairs increases by one and the original mechanism gets two degrees of mobility.

The adjustable link is constructed in the form of a block which can move in a groove in the slide plate in the links forming a kinematic pair. During operation of the mechanism, the block is fixed in the groove by imposing a rigid joint on the kinematic pair. The process of control lies in changing the position of the block relative to the groove of the rocker arm. If the groove is located on the moving link, the block is adjusted when the mechanism is stationary. If the groove is on the support, it is adjusted during the operation of the mechanism.

Cam lever mechanisms (Fig. 1) in which travel of the driven link 6 is

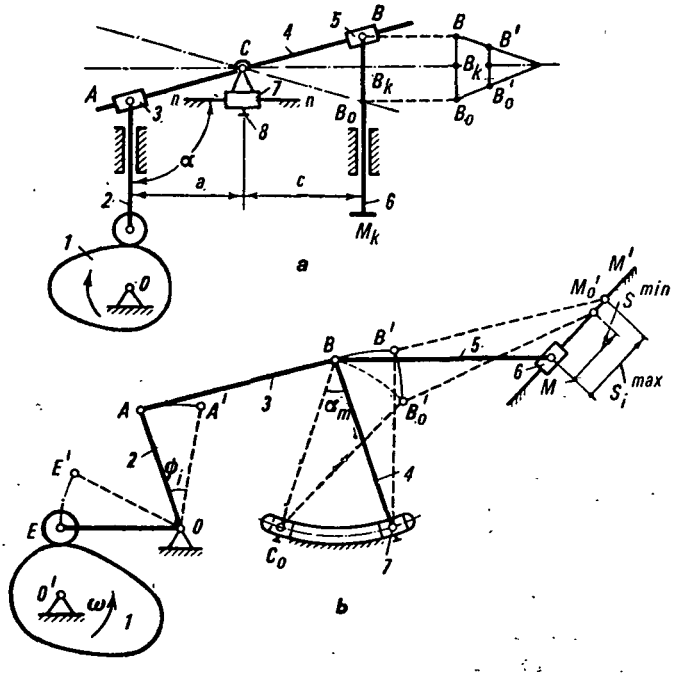

Fig. 1. Regulation of travel of the driven link in the case of invariable motion.

regulated by changing the gear ratio between the follower *2* and driven link *6* by rearranging the adjustable link *7*, are used for controlling the travel of the driven link for a particular phase of its motion.

In cam lever mechanisms in which the cam moves nonuniformly, it is possible to regulate the phases as well as travel of the driven link in the following two ways depending on the phase of motion:

1) by changing any one parameter of the four link lever mechanism putting the cam in nonuniform motion; and

2) by changing the relative position of the cam and the link on which the cam is installed.

The problem of synthesis of plane multilink adjustable cam mechanisms is considered below for changing the travel and phases of motion of the driven link independently or according to a given functional relationship for both the stationary and operational states.

1. Regulation of the Travel of Driven Link

Multilink adjustable mechanisms, constructed by connecting cam and lever mechanisms in series, are widely used nowadays for changing the travel of the driven link for the case of constant phases of its motion. In these designs, the starting link (which gets uniform motion from the cam) is equipped with control elements and regulation is carried out by changing the parameters of the lever mechanism.

If the lever mechanism has four links, its travel can be regulated only in the case of stationary state of the mechanism by changing the dimensions of one of the moving links of the four link lever mechanism. Travel of the driven link during operation is regulated with the help of a mechanism (see Fig. 1) in which motion is transmitted from the cam to the driven link by a six link lever mechanism and the regulation is carried out by resetting the link *7* possessing hinge *C*. If the link *7* moves, the mechanism gets two degrees of mobility and it can be regulated during continuous rotation of the driven cam. To regulate the travel of the driven link with respect to its arbitrary position B_k (see Fig. 1a) it is necessary to change the ratio of arms *a* and *b* in such a manner that hinge *C* during regulation may move along line CB_k, representing the position of link *4* corresponding to the position M_kB_k of the driven link. For this purpose, a slide block *7* with guide $nn \,||\, CB_k$ is introduced in the mechanism. Slide block *7* is fixed at the required position by screw *8*. On displacing the slide block *7* toward right, we get $s_i'=B'B_0'$; moreover, $BB_k : B_kB_0=B'B_k : B_kB_0'$, while phases and law of motion of the driven link do not change. If the travel is regulated with respect to the lower (or upper) position of link *6*, the condition $nn \,||\, CB_0$ (or $nn \,||\, CB$) must be observed.

Fig. 1, b shows a cam lever mechanism in which travel of the driven

slide block *6* is regulated on one side with respect to its extreme left position. Regulation is carried out by changing the position of hinge *C* about which link *4* oscillates. The circular groove CC_0 made in the support has its center at point *B* and represents invariable extreme left position of the hinge which connects the connecting rod *5* with rocker arm *4*. If the center of groove CC_0 is selected properly, the mechanism can also be used for regulating the travel of slide block *6* on both the sides. Mechanisms shown in Fig. 1 are designed in the following manner: an unadjustable cam lever mechanism (with stationary hinge *C*) meant for reproduction of maximum travel of the driven link *6*, is designed by taking into account the permissible transmission angles in accordance with the given law of motion (or other conditions).

Thus the position of guides *nn* (Fig. 1, a), the center of groove CC_0 and the value of regulating angles α_m (Fig. 1, b), are determined according to the nature and limits of regulations.

Regulation of the second mechanism causes a change in the motion of the driven link *6*.

2. Regulation of the Phases of Motion of the Driven Link

While regulating the phases of motion of the driven link, it is often required to get the constant position of the driving link corresponding to the beginning of motion of the driven link and invariable travel of the latter for all phases of regulation.

Adjustable cam lever mechanisms are considered below in which it is possible to obtain variable phases of the motion of driven link by adhering to the requirement that the profile of the nonuniformly moving cam is constant.

1. Motion of the driven link without dwell. To get a motion of the driven link of the type "Raising-lowering", an eccentric mechanism is often used in conjunction with uniformly rotating cam.

Fig. 2, a shows an adjustable rocker plate eccentric mechanism with cam rotating about hinge *C*. Rotation of the eccentric through an angle $0 \leqslant \varphi \leqslant \pi$ corresponds to the rotation of crank through $0 \leqslant \psi \leqslant \pi$ in a rocker mechanism with central rotating eccentric.

If the point $\varphi=0$ corresponds to the beginning of the outstroke of the follower, we get equal phases of motion of the follower (curve *1*). A circular groove C_2C_3 of radius $O'C=OC$, center O' of which coincides with the geometrical center of the eccentric, is made on the eccentric to change the phases of motion of the follower in the case of constant travel. Screw *6* aids in connecting the eccentric to block *5* which rotates about the stationary hinge *C*. Regulation is carried out by setting the eccentric relative to block *5*.

Position of the crank shown in Fig. 2, c by dotted line corresponds to

the end of the outstroke of the follower. Let us fix the crank OA_0 to the eccentric in this position and after loosening the screw *6*, rotate them about point O through an angle α; the follower in this case remains at its upper extreme position. Now if the eccentric is fixed to block *5*, the eccentric on rotating the crank OA will rotate above its new point C_2, and the rocker mechanism will be displaced. In order to lower the follower from its upper position, it is necessary to rotate the eccentric through 180° (from position C_1B_1 to position $C_1'B_1'$ of the groove). The angle of rotation of the crank (phase) in this case depends on the position of point A_i, the intersection of the trajectory of hinge A of the crank with the axis of groove $C_1'B_1'$. Position OA_i of the crank will correspond to the beginning of the outstroke of the follower.

It follows from Fig. 2, c that, if the relative dimension of crank (in the case of column $OC=1$) r equals 2, point A_i will lie on the extension of support OC irrespective of the value of angle α and the invariable position OA_i of the driving crank will correspond to the beginning of follower motion under all regulations. In this case, we get $\varphi_i=\pi+\alpha$ and $\varphi_i^0=\pi-\alpha$.

Consequently, rotation of the eccentric with respect to the block in the direction of rotation of the crank causes an increase in the raising phase and a decrease in the lowering phase by the same angle α. Curve *2* (see Fig. 2, a) of follower displacement corresponds to this case. If the eccentric (during regulation) is rotated in the opposite direction, we get $\varphi_i=\pi-\alpha$ and $\varphi_i^0=\pi+\alpha$ (curve *3*). Thus, phases of the motion of follower can be regulated within the limits $\Delta\varphi_i=2\alpha$ where $2\alpha=\angle C_2O'C_3$ is the central angle of the circular groove C_2C_3 of the eccentric.

If the follower is set as shown in Fig. 2, c by dotted line, the invariable position OA_i of the driving crank will correspond to the end of follower raising in all regulations, i.e. vertices E_1, E_2, and E_3 of displacement graphs of the follower will coincide.

Dimensions of the mechanism are determined from the equations:

$$OC=0.5\cdot s_i$$

and

$$OA=r\cdot OC=s_i, \tag{1}$$

where s_i is the total displacement of the follower.

In the case of an eccentric with central follower, the maximum pressure angle ϑ_m in the cam pair is obtained at point B_m of the profile for which $CB_m\perp OC$.

At the given maximum value ϑ_m of pressure angle, radius r_e of the eccentric is calculated from equation:

$$r_e=0.5\cdot s_i\operatorname{cosec}\vartheta_m, \tag{2}$$

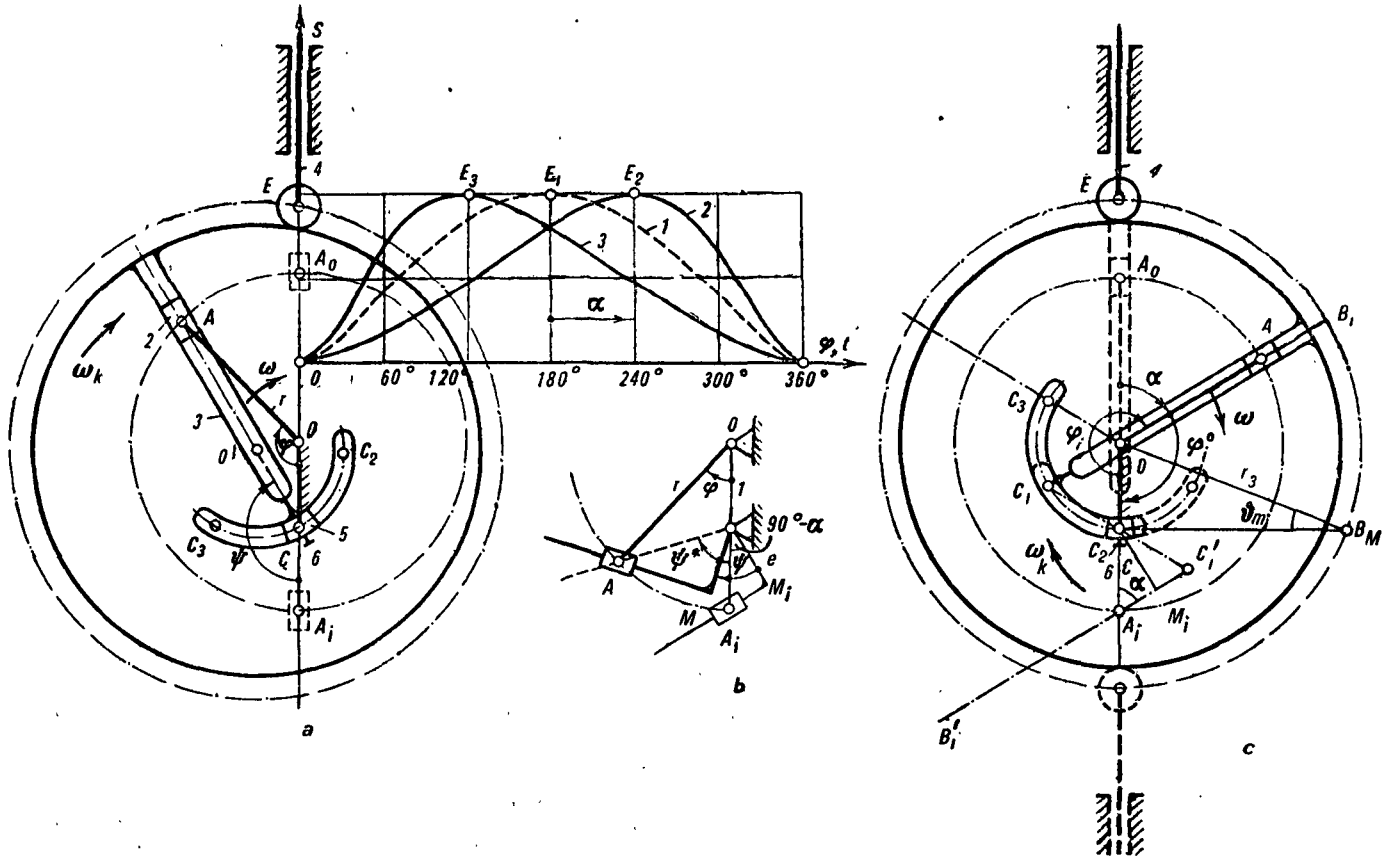

Fig. 2. Rocker cam mechanism with adjustable phases of motion of the driven link.

obtained from $\triangle OCB_M$ by taking into account equation (1).

Displacement function $s=s(\varphi)$ of an eccentric rocker mechanism can be determined by eliminating the angle ψ of rotation of the rocker from the displacement function $s=s(\psi)$ of the eccentric mechanism [1] by considering equations (1) and (2) and can be written as:

$$s=0.5\,s_i\,(1-\operatorname{cosec}\vartheta_m-\cos\psi+\sqrt{\operatorname{cosec}^2\vartheta_m-\sin^2\psi})$$

and from the displacement function $\psi=\psi(\varphi)$ of the rocker mechanism.

In the case of the complex rocker mechanism (Fig. 2, b) if angles φ and ψ are measured from the position of mechanism (OA_iM_iC) corresponding to the rise stroke of the follower, from $\triangle ACM$ we have:

$$\cos(90^\circ-\alpha+\psi^*-\psi)=e/AC,$$

where ψ^* is the angle of rotation of the rocker when $e=0$ and α is the angle of regulation.

Taking into account that:

$$\tan\psi^*=r\sin\varphi/(r\cos\varphi-1)\text{ and }AC=\sqrt{1+r^2-2r\cos\varphi}\,,$$

we get[1]

$$\psi=\arctan r\sin\varphi/(r\cos\varphi-1)+\arcsin e/\sqrt{1+r^2-2r\cos\varphi}-\alpha. \qquad (3)$$

For the slide plate mechanism (see Fig. 2, c) $r=2$, $e=\sin\alpha$ and formula (3) becomes:

$$\psi=\arctan\sin\varphi/(\cos\varphi-0.5)+\arcsin\alpha/\sqrt{5-4\cos\varphi}-\alpha.$$

2. Motion of the driven link with one dwell. In practice, it often becomes necessary to regulate the idling time of the working link in one of its extreme positions.

Fig. 3, a shows a cam lever mechanism with an adjustable stop in the driving link *4* in which cam *3* and yoke *3'* are connected rigidly. Phases of motion of the follower *4* are regulated by changing the length and orientation of support *OC* of the yoke of the four-link mechanism OA_iBC_1 which increases or decreases the angle of swing of the cam.

Position OA_i of the crank and extreme right position of the cam correspond to the beginning of the outstroke of the follower. When the invariable position OA_i of the driving crank corresponds to the beginning of the outstroke of the follower for all regulations, length of the column *OC* should be changed in such a manner that the position of hinge *B* remains

[1] This equation differs from that suggested by V. V. Dobrovol'skii [6] as the angle of rotation of the rocker has been defined differently.

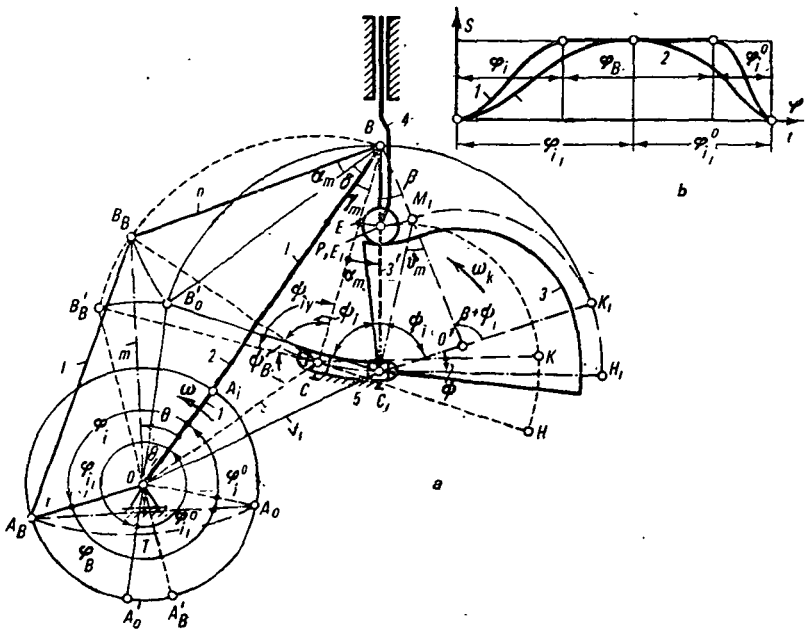

Fig. 3. Cam lever mechanism with adjustable dwell in the driven link.

unchanged at all the extreme right positions of yoke BC since in this position of the yoke, crank OA_i and connecting rod A_iB form one straight line.

Rotation (during regulation) of hinge C about the support point coinciding with the extreme right position of hinge B, satisfies this condition. A circular groove CC_1 with center at point B and of radius equal to the length of the yoke is made on the support.

The process of regulation includes the arrangement of block *5* forming a turning pair with the yoke-cam in circular groove.[2] During motion of links, the mechanism has two degrees of mobility and can be regulated during operation.

Suppose it is desired to produce motion of the type "rise-dwell-fall" with given phase angles φ_i, φ_B and φ_i^0 of the motion of follower (Fig. 3b, curve *1*) and to have the follower move with stop φ_{Bi} within the limits through one mechanism. In the case of motion without dwell ($\varphi_{Bi}=0$) the follower must have the given phase angles of motion (curve *2*). Travel of the follower at all the values of φ_{Bi} remains unchanged.

Let the axis of the follower be directed along line BC_1 (Fig. 3, a). If the maximum radius vector C_1K_1 of the cam profile is equal to the length of

[2] Hinge C is also made to rotate about point B by introducing a link in the mechanism which forms turning pairs with the support and the points B and C respectively [7].

the yoke BC_1, and independent of the position of hinge C on arc CC_1, profile K_1H_1 of the cam corresponding to the specified dwell of the follower passes through the point B, and under all adjustments we obtain an unchanged upper position of the follower.

If yoke BC_1 is rotated around hinge B, when crank OA_i, connecting rod A_iB and follower are stationary, point P at the extreme lower position of the roller axis describes arc E_1M_1, with center at point B, on the plane of the cam. If the initial section of the profile of a rotating cam is prepared corresponding to this arc, we get an unchanged lower position of the follower under all regulations. In this case the condition $\beta \geqslant \alpha_m$ must be observed. Here β is the central angle of the arc E_1M_1 and $\alpha_m = \angle CBC_1$ is the central angle of circular groove CC_1.

When block *5* is fixed at point C (cam is shown by dotted lines), on rotating the crank through an angle φ_i from position OA_i to position OA_B, the yoke gets rotated through angle $\psi_i = \angle BCB_B$. If $\angle BCK = \angle BCB_B = \psi_i$, the section of profile PK of the cam raises the follower from the lower position to the upper position. On rotating the crank further through an angle $\varphi_B = \angle A_BOA_0$ the yoke rotates (through angle ψ_B) from position CB_B to position CB_B and returns to the initial position CB_B. If $\angle KCH = \angle B_BCB'_B = \psi_B$, section KH of the cam profile during its direct and reverse runs, makes the follower dwell at the upper position. Phase of the upper dwell of the follower decreases on displacing point C of block to point C_1.

When block *5* is fixed at point C_1 and the follower does not have the upper dwell, it is necessary to satisfy the condition $\angle BC_1K_1 = \angle BCK = \angle BC_1B'_0 = \angle BCB_B = \psi_i$ from which it follows that $\triangle BC_1B'_0 = \triangle BCB_B$ and $BB'_0 = BB_B$.

Let us denote the relative dimensions (if length of yoke $BC = 1$) of the crank, connecting rod and support of the four link mechanism OA_iBC by r, l and f respectively and the dimensions of chords BB_B and OB_B by n and m.

To solve this problem it is necessary to design an auxiliary four-link mechanism OA_BB_BB with column OB along the given directions of rays $A_0OB'_0$, OA_B, OB_B and OB on which hinges of the four-link mechanism must be placed in the intermediate (OA_BB_BB) and extreme ($OA'_0B'_0B$) positions by observing the condition $OB = OA_B + A_BB_B = r + l$. Direction of the rays OB'_0 and OB_B relative to column OB is defined by the angles[3] $\theta_1 = 0.5\,(\varphi_{il} - \varphi^0_{il})$ and $\theta = 0.5\,(\varphi_i - \varphi^0_i)$. From $\triangle OB'_0B$ and $\triangle OB_BB$

$$(l-r)^2 - 2(l^2-r^2)\cos\theta_1 = m^2 - 2m(l+r)\cos\theta$$

[3] The mechanism can be designed at $\theta_1 < \theta$, which is obvious from Fig. 3, a.

or, putting the value:

$$m=\sqrt{l^2-r^2\sin^2\varphi_B/2}-r\cos\varphi_B/2\,, \tag{4}$$

found from $\triangle TA_BB_B$ and putting:

$$\lambda=l/r\,, \tag{5}$$

we get:

$$p_4\lambda^4+p_3\lambda^3+p_2\lambda^2+p_1\lambda+p_0=0\,, \tag{6}$$

where:

$p_4=\cos^2\theta_1-\cos^2\theta$;
$p_3=2\{\cos\theta_1-\cos\theta[\cos\theta+\cos(\varphi_B/2)-\cos\theta_1\cdot\cos(\varphi_B/2)]\}$;
$p_2=(1-2\cos\theta_1)\cdot\sin^2(\varphi_B/2)+2\cdot\cos\theta_1[\cos\theta\cdot\cos(\varphi_B/2)-\cos\theta_1]$;
$p_1=2\{\cos^2\theta-\sin^2(\varphi_B/2)-\cos\theta_1+(1-\cos\theta_1)\cdot\cos(\varphi_B/2)\cdot\cos\theta\}$;
$p_0=\cos^2\theta_1+\cos^2\theta+\sin^2(\varphi_B/2)+2\cos\theta_1[\sin^2(\varphi_B/2)-\cos(\varphi_B/2)\cdot\cos\theta]$.

If boundary phase angles of the follower are known, from equation (6) we obtain the value of parameter λ, representing the ratio of the lengths of connecting rod A_iB and crank OA_i of the four-link mechanism OA_iBC. To determine the values of parameters r, l, and f of the four-link mechanism OA_iBC, it is necessary to take into consideration the angle of transmission from connecting rod A_iB to yoke BC as well as the acceleration of yoke-cam at its extreme right position [8].

For the extreme right position of yoke, we have [8].

$$\xi_m=[\varphi_{iy}^2\, r(r+l)]/(\psi_{iy}\, l\sin\gamma_m)\,, \tag{7}$$

where ξ_m—coefficient of acceleration of yoke BC;

$\gamma_m=\angle OBC$—angle of transmission from connecting rod to cam.

The angle of swing ψ_{iy} of the yoke and the corresponding angle φ_{iy} of rotation of crank are related to each other as follows [7]:

$$\sin\psi_{iy}/2=1/\sqrt{2}\cdot\sqrt{l^2+r^2-(l^2-r^2)\cos\varphi_{iy}}\,. \tag{8}$$

If the extreme right positions of the yoke under various regulations are considered, it follows from Fig. 3, a and equation (7) that the minimum value of the angle of transmission γ_m and the maximum value of the coefficient of acceleration ξ_m is obtained when block *5* is fixed at point *C*. For this position of block $\psi_{iy}=\psi_i$ and taking into consideration equation (5), from equalities (7) and (8), we obtain:

$$r=1/\varphi_{iy}^2\cdot\xi_m\psi_i\sin\gamma_m/(1+\lambda)\,,$$

$$r=\sqrt{2}\cdot\sin\frac{\psi_i}{2}/\sqrt{1+\lambda^2+(\lambda^2-1)\cos\varphi_{iy}}\,. \tag{9}$$

At given values of ξ_m and γ_m, after determining the values of λ from equation (7) and selecting the value of angle ψ_i, we obtain the relative dimension r of the crank by solving the system of equations (9). Relative dimensions l of the connecting rod and f of the support are calculated from formulas (5) and:

$$f=\sqrt{1+(r+l)^2-2(r+l)\cos\gamma_m},$$

$$f_1=\sqrt{1+(r+l)^2-2(r+l)\cos(\gamma_m+\alpha_m)}, \tag{10}$$

where α_m is the central angle of groove CC_1 value of which can be determined from the formula:

$$\alpha_m=2\arcsin[\sqrt{(l-r)^2+m^2-2m(l-r)\cos(\theta-\theta_1)}/4\sin(\psi_i/2)],$$

obtained from $\triangle OB_BB'_0$, $\triangle BB_BB'_0$ and $\triangle BC_1B'_0$ by taking into account equation (5).

From Fig. 3, a we have $\varphi_B=2\pi-(\varphi_i+\varphi_i^0)=2(\pi-\angle A_BOB_B)$. Substituting the value of $\angle OA_BB_B$ found from $\triangle OA_BB_B$ and rewriting the expressions for an arbitrary angle α of regulation, we get a relation between the adjustable φ_{Bi} and adjusting α parameters:

$$\varphi_{Bi}=2(\pi-\arccos\{n^2+2(r+l)[r-n\cos(\delta+\alpha)]\}/2r \times\sqrt{n^2+(r+l)^2-2n(r+l)\cos(\delta+\alpha)}),$$

where

$$n=\sqrt{2[l^2+r^2-(l^2-r^2)\cos\theta_1]},$$

and

$$\delta=[\arcsin(l-r)\sin\theta/n],$$

which is obvious from $\triangle OBB'_0$.

To calculate the absolute dimensions of the four-link mechanism OA_iBC, it is necessary to know the dimension $BC=c$ of the yoke which was taken as equal to the maximum radius of the cam. Section E_1K_1 of the profile of cam with central angle ψ_i, corresponding to rise of the follower, can be described by arcs E_1M_1 and M_1K_1 of the circles with centers at points B and O_1.

In this case, the maximum pressure angle ϑ_m in the cam pair is obtained at transient point M_1. Radius of the arc E_1M_1 is equal to travel s_i of the follower while radius of arc M_1K_1 is determined from equation:

$$R=[2c^2[(1-\cos\psi_i)]-s_i^2]/\{2[c(1-\cos\psi_i)]+s_i\}, \tag{11}$$

obtained from $\triangle C_1BO_1$.

Let us determine the value of angle ϑ_m. From $\triangle C_1BM_1$, we have:

$$\cot\vartheta_m=(\cos\beta-s_i/c)/\sin\beta,$$

or, substituting the value:

$$\sin\beta=[(c-R)/(s_i+R)]\sin\psi_i \text{ and } \cos\beta=[c/(s_i+c)]-\cot\psi_i\sin\beta,$$

determined from $\triangle C_1BO_1$ by the sine law we have:

$$\cot\vartheta_m=[2c^3(1-\cos\psi_i)-cs_i^2(2-\cos\psi_i)-s_i^3]/[cs_i(2c+s_i)\sin\psi_i], \quad (12)$$

where $c=R_{\max}$ is the maximum radius of the pitch profile of the cam.

Denoting:

$$p=R_{\max}/s_i=1+R_0/s_i \quad (13)$$

and solving equation (12) with respect to p, we get:

$$2(1-\cos\psi_i)p^3-2\sin\psi_i\cot\vartheta_m\cdot p^2-(2-\cos\psi_i-\sin\psi_i\cdot\cot\vartheta_m)p-1=0. \quad (14)$$

Graph in Fig. 4 plotted from equation (14) shows the parameter p as a function of the polar angle ψ_i of the cam, for different values of the maximum pressure angle ϑ_m in the cam pair. At given angles ψ_i and ϑ_m, we find the value of parameter p from these graphs and the value of minimum radius R_0 of the pitch profile of the cam and length c of the yoke from equation (13).

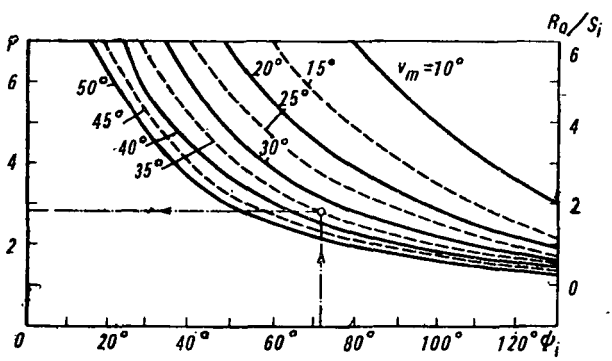

Fig. 4. Graphs for determining the minimum radius of cam at the given minimum angle of transmission and angle of motion of the cam.

3. Motion of follower with two dwells. Sketch of a cam lever mechanism with adjustable dwells of the driven link at its extreme lower and upper positions is shown in Fig. 5.

Adjustments are made by rotating cam *3* with respect to block *5*. With the help of this mechanism it is possible to get the motion of follower with

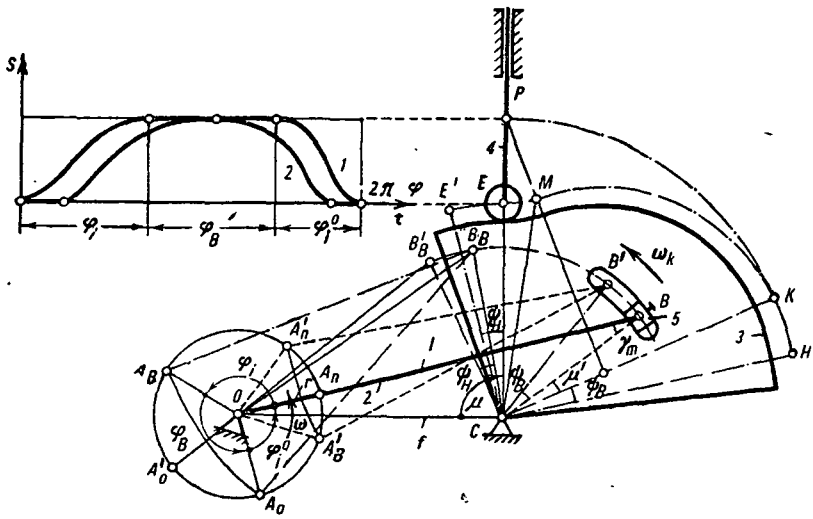

Fig. 5. Cam lever mechanism with adjustable dwells of the driven link.

lower φ_{Hi} and upper φ_{Bi} dwells, only with upper dwell (φ_B, $\varphi_{Hi}=0$, curve *1*) and only with lower stop ($\varphi_H<\varphi_B$, $\varphi_B=0$). If block *5* is fixed at point *B*, section *EMKH* of the cam profile will produce motion of the follower with upper dwell and if the block is fixed at point *B'*, then section *E'EMK* will generate motion of the follower with lower dwell.

At intermediate positions of the block, the follower moves with upper and lower dwells. The cam is profiled in such a manner that arcs *EE'* and *KH* corresponding to the lower and upper dwells of the follower, have equal central angles $\psi_H=\psi_B$ from which it follows that angles of rotation of the cam must be equal for the lower and upper dwells of the follower, i.e. $\angle B'CB=\angle B_BCB'_B$.

At known values of the phase angles φ_i, φ_B and φ_i^0 of the limiting law of motion of the follower with upper dwell, coefficient of acceleration ξ_m of the cam at its extreme right position and at known value of the minimum angle γ_m of transmission, parameters r, l and f of the yoke of four-link mechanism OA_iBC can be determined from equations (6), (9) and (10) by taking the values $\theta_1<\theta=0.5\ (\varphi_i-\varphi_i^0)$ and swing angle of the cam $\psi_{iK}=\psi_i+\psi_H$.

Section *EMK* of the profile corresponding to follower rise is profiled just like section $E_1M_1K_1$ (see Fig. 3, a). In that case, we get the value of parameter p of cam from equation (14) or from graphs of Fig. 4 by assuming that $\psi_i=\psi_{iK}-\psi_H$. Value of angle ψ_H is determined from formula:

$$\sin\psi_H/2=0.5\sqrt{m^2+(l-r)^2+2m(l-r)\cos(\varphi_{iK}-\theta)},$$

obtained from $\triangle OB_BB_B$ and $\triangle CB_BB_B$ (see Fig. 5) taking into account equation (5).

Absolute dimensions of the four-link mechanism and angles μ and μ' are calculated on the basis of design considerations.

3. Regulation of Travel and Phases of Motion of the Driven Link

In cases where it is simultaneously required to regulate travel and phase of motion of the driven link, a combined regulating mechanism [3] with two adjustments is often used. This combined mechanism consists of two adjustable mechanisms one of which is designed for changing the travel and the other for adjusting the phases of motion of the driven link.

Fig. 6 shows an adjustable cam lever mechanism in which two parameters of the motion of the driven link (travel s_i and phases φ_B of upper stop) can be changed in accordance with the given functional relationship $s_i=s_i(\varphi_B)$ with the help of only one adjustment.[4]

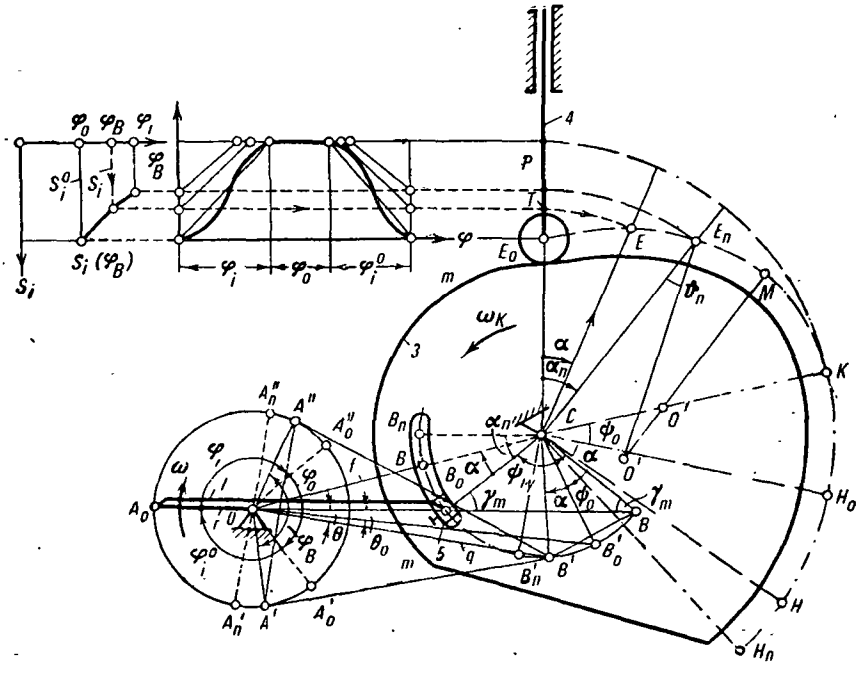

Fig. 6. Cam lever mechanism for regulation of the travel of the driven link on one side depending on the phase of its dwell.

[4] The function $s_i=s_i(\varphi_B)$ must be monotonic in the given interval $\varphi_0 \leqslant \varphi_B \leqslant \varphi_n$ of regulation. The case of regulation according to relation $s_i=s_i(\varphi_i)$ has been considered in work [7].

The cam is put into swinging motion by the symmetrical yoke-four-link mechanism OA_0B_0C the dimensions of which are related as follows [8]:

$$f^2-l^2=1-r^2, \tag{15}$$

while the angle of swing of the yoke and relative dimensions of the crank are determined from equations $\psi_{iy}=180°-2\gamma_m$ where γ_m is the angle of transmission of the four-link mechanism corresponding to extreme position of the yoke, and

$$r=\cos\gamma_m . \tag{16}$$

Adjustments are made by arranging cam *3* with respect to block *5*. If the block is fixed at point B_0, on rotating the driving crank from position OA_0'' to OA_0' (through angle φ_0 corresponding to upper top of the follower), the yoke gets rotated through angle ψ_0 from position CB_0' to the extreme position CB_k and back to position CB_0'. In this case, section KH_0 of the cam profile produces the motion.

If the block is fixed at point B, by rotating the cam through angle α, point E of the profile will correspond to the beginning of follower raising, and arc KH ($\angle HCH_0=\alpha$) to its stop.

While designing a yoke four-link mechanism, it is necessary to keep in mind that ray OB_0', whose inclination with respect to line OB is defined by the angle $\theta_0=0.5(\varphi_i-\varphi_i^0)$ must intersect the trajectory B_kB_0 of hinge B (limitation on dimension l from above). Moreover, to prepare the crank in the form of a circular disk, trajectory of hinges A_0 and B_0 should not intersect[5] (limitation on dimension l from below).

To provide these requirements, the following condition must be satisfied:

$$2\cos\gamma_m<l<\operatorname{cosec}\theta_0-\cot\theta_0\cos\gamma_m . \tag{17}$$

If the phase angles φ_i, φ_0 and φ_i^0 of the limiting law of motion of follower with maximum travel s_i^0 and the angle of transmission γ_m of the four-link mechanism are known, relative dimensions l, r and f are found from relation (17) and equations (15) and (16).

The relation between phase φ_B of the upper stop of the follower and regulation angle α is determined from equation:

$$\cos\varphi_B/2=(r^2+q^2-l^2)/2rq;$$
$$q=\sqrt{(l+r)^2+4\sin^2\left(\frac{\psi_0+\alpha}{2}\right)-4(l+r)\sin\left(\frac{\psi_0+\alpha}{2}\right)\sin\left(\gamma_m+\frac{\psi_0+\alpha}{2}\right)}, \tag{18}$$

obtained from $\triangle OA'B'$, $\triangle OB'B_k$ and $\triangle CB'B_k$.

[5] Strictly speaking arc *mm* and circle of the crank disk do not intersect.

Section E_0E_p of the cam profile for regulation angle $0 \leqslant \alpha \leqslant \alpha_p$ is profiled on the basis of the given relationship $s_i = s_i(\varphi_B)$.

Taking into account Fig. 6, we have $CE = CE_0 + E_0P - PT$ or

$$R = R_0 + s_i^0 - s_i(\varphi_B), \tag{19}$$

where R_0 is the minimum radius of the cam profile.

Polar coordinates R and α of the section E_0E_p of the profile are determined from formulas (18) and (19). Minimum radius R_0 of the cam is determined from the condition of limiting minimum angle of transmission in the cam pair on the section E_0E_p of the profile at known function of position $s = s(\alpha) = s_i^0 - s_i$.

Section E_nK of the cam profile can be described by two arcs (E_nM and MK) of circles with centers at points O'' and O'. For this purpose, it is necessary to know the value of angle ϑ_n between the normal and radius vector at transition point E_n.

We have:

$$\tan \vartheta_n = (1/R_n) \cdot (dR/d\alpha)_{\alpha=\alpha_n} = -[1/(R_0 + s_i^0 - s_i^n)] \cdot (ds_i/d\varphi_B \cdot d\varphi_B/d\alpha)_{\phi_B=\phi_n}.$$

Absolute dimensions of the four link mechanism OA_0B_0C are determined on the basis of design conditions of the mechanism.

This method can be used for the synthesis of the cam lever mechanism for regulating the travel of follower (with respect to its extreme lower position) depending on the phase of the lower dwell.

References

1. Dzhavakhyan, R. P. K sintezu ploskikh kulachkovykh mekhanizmov s neravnomerno vrashchayushchimisya kulachkami (Synthesis of plane cam mechanisms with nonuniform rotation of cams). *Mashinovedenie*, No. 5, 1967.
2. Eremeev, N. V. K sintezu ploskikh mekhanizmov s izmenyaemym zakonom dvizheniya rabochego zvena (Synthesis of plane mechanisms with variable motion of the working link). Sb. *Analiz i sintez mekhanizmov*. Izd-vo Mashinostroenie, 1966.
3. Orlikov, M. L. Kulachkovye mekhanizmy mashin-avtomatov (Cam Mechanisms of Automatic Machines). Mashgiz, 1955.
4. Reshetov, L. N. Kulachkovye mekhanizmy (Cam Mechanisms). Mashgiz, 1953.
5. Rotbart, G. A. Kulachkovye mekhanizmy (Cam Mechanisms). Moscow, Sudpromgiz, 1960.

6. DOBROVOL'SKII, V. V. Teoriya mekhanizmov (Theory of Mechanisms). Mashgiz, 1953.
7. DZHAVAKHYAN, R. P. K sintezu rychazhno-kulachkovykh mekhanizmov po zadannomu zakonu izmeneniya khoda vedomogo zvena v zavisimosti ot fazy ego udaleniya (Synthesis of cam lever mechanisms according to the law of change in travel of the driven link depending upon the phase of its motion). *Mashinovedenie,* No. 4, 1967.
8. DZHAVAKHYAN, R. P. K sintezu ploskikh kulachkovykh mekhanizmov s kachayushchimisya kulachkami (Synthesis of two-dimensional cam mechanisms with swinging cams). *Izv. AN ArmSSR, seriya tekhnicheskikh nauk,* No 3, 1967.

E. N. Dokuchaeva

EFFECTS OF ERRORS IN THE WORKING PROFILE OF THE CAM ON VELOCITY AND ACCELERATION OF THE FOLLOWER

Until now the effect of cam accuracy on the operation of a follower has not been studied in sufficient detail.

The effect of errors in the theoretical profile (trajectory of the axis of the follower roller relative to a cam) on the value of velocity and acceleration of the follower has been studied in a few cases. Reference [1-5].

Such a study of errors is possible only to the first approximation. Errors in the design profile (profile of the cam) are the main errors. It is more correct to start with the consideration of these errors. For example, the design and theoretical profiles will not be identical when there are sharp tansitions or concave sections with radius of curvature less than the roller radius on the working surface of the cam.

The effect of errors in the design profile on the law of motion of the roller follower (without taking into account its elasticity) has been studied in this article. Analytical expressions have been obtained for additional velocity and acceleration of the follower resulting from errors in the geometric form of the design profile and the roller radius. For simplicity the motion of roller over the uneven surface of the plane is considered first and then for unevenness of the cam profile.

Analytical equations derived here, describe the motion of the absolutely rigid follower but knowledge of these relations is also necessary for solving the problem pertaining to the effect of these errors on the motion of an elastic follower.

1. Motion of a Roller over a Single Bump in a Plane

This is the first step toward solving the problem of determining the effect of manufacturing errors of the cam on the operation of the follower.

In this and following sections, we will consider unevenness of two types:

1) the uneven surface changes smoothly, i.e. at every point, the derivative of the height of bumps or unevenness with respect to a coordinate directed along it (unevenness with differentiable surface) exists,

2) there are sharp transitions (discontinuities in the uneven surface).

1. Unevenness with differentiable surface. Bumps with smooth transitions are shown in Fig. 1. x and y are the current coordinates of the unevenness. The relation $y=f(x)$ is known and it is required to determine the coordinates of roller axis $X=f(x)$ and $Y=f(x)$ during motion of the roller over the uneven surface.

The problem is solved in one plane since it is considered that the function $y=f(x)$ does not change in the plane perpendicular to the drawing.

Equation of the roller surface is:

$$(Y-y)^2+(X-x)^2-R_r^2=0. \tag{1}$$

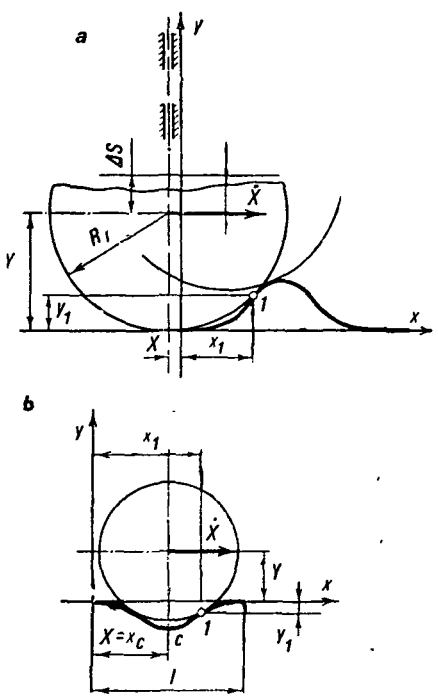

Fig. 1.

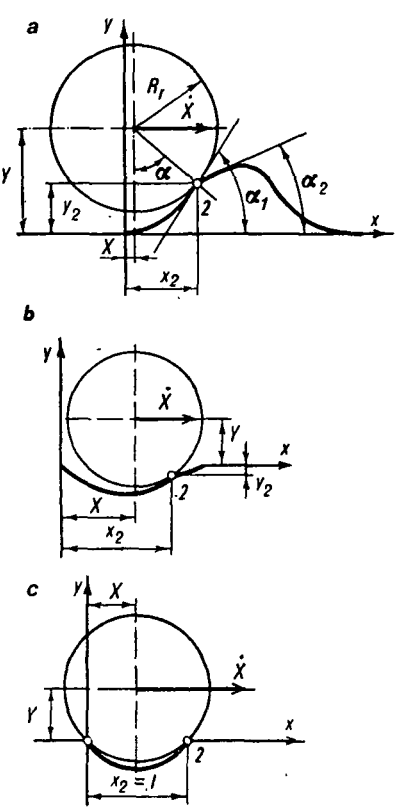

Fig. 2.

Expression (1) is the equation of a complete group of circles. A bump over which the roller rolls is the enveloping curve of this group.

To get the equation of motion of roller center during displacement of the roller along the enveloping curve, it is necessary to differentiate equation (1) of the group of curves with respect to the independent parameter x and to solve the equation obtained simultaneously with the initial equation:

$$(Y-y)\cdot dy/dx+(X-x)=0.$$

Solving the equation obtained above, simultaneously with expression (1), we have:

$$Y=R_r/\sqrt{1+(dy/dx)^2}+y; \tag{2}$$

$$X=x-R_r\cdot dy/dx/\sqrt{1+(dy/dx)^2}. \tag{3}$$

Thus, displacement of the roller axis as it moves over the bump at point (x_1, y_1) will be described by equations (2) and (3) which are valid for the unevenness shown in Fig. 1, a as well as for unevenness shown in Fig. 1, b.

2. Unevenness with sharp transitions (Fig. 2). The relationship $y=f(x)$ with sharp transition at point (x_2, y_2) is known. It is obvious that when angle α during the displacement of the roller axis, lies within the limits $\alpha_1>\alpha>\alpha_2$, coordinates x and y remain unchanged and are equal to x_2 and y_2 respectively, on changing Y and X.

Value of Y can be determined from equation (1):

$$Y=\sqrt{R_r^2-(X-x_2)^2}+y_2. \tag{4}$$

This relation is valid for all the bumps shown in Fig. 2 from the moment of start of rolling of the roller over points of inflection *2*.

2. Velocity and Acceleration of the Roller during its Motion over a Single Discontinuity (Unevenness)

Let us denote the vertical displacement of roller by ΔS. Obviously:

$$\Delta S=Y-R_r. \tag{5}$$

Let us determine $d\Delta S/dt$ and $d^2\Delta S/dt^2$ for the case when the velocity $\dot{X}=\text{const}$ (see Figs. 1 and 2) is known. This case is similar to calculation scheme of a cam mechanism. Differentiating equation (5), we get:

$$d\Delta s/dt=dY/dt=\dot{X}dY/dX; \tag{6}$$

and

$$d^2\Delta S/dt^2=\dot{X}^2d^2Y/dX^2. \tag{7}$$

Let us determine $d\Upsilon/dX$ and $d^2\Upsilon/dX^2$ for two types of unevennesses:

(1) Unevenness with differentiable surface (see Fig. 1, a). We get the values of $d\Upsilon/dX$ and $d^2\Upsilon/dX^2$ by differentiating equations (2) and (3):

$$d\Upsilon/dX=d\Upsilon/dx\cdot dx/dX; \tag{8}$$

$$d^2\Upsilon/dX^2=d\Upsilon/dx\cdot d^2x/dX^2+d^2\Upsilon/dx^2\cdot(dx/dX)^2. \tag{9}$$

To facilitate differentiation, we substitute:

$$u=R_r/\sqrt{1+(dy/dx)^2}. \tag{10}$$

Then:

$$d\Upsilon/dx=du/dx+dy/dx;$$

$$d^2\Upsilon/dx^2=d^2u/dx^2+d^2y/dx^2;$$

$$dx/dX=1/\{-(du/dx\cdot dy/dx+u\cdot d^2y/dx^2)\};$$

$$d^2x/dX^2=(du/dx\cdot d^2y/dx^2+dy/dx\cdot d^2u/dx^2+ud^3y/dx^3$$
$$+du/dx\cdot d^2y/dx^2)/\{1-[du/dx\cdot dy/dx+u\cdot d^2y/dx^2]\},$$

where du/dx and d^2u/dx^2 are determined by successively differentiating equation (10).

Taking comparatively small values of bumps into account, i.e. taking $(dy/dx)^2\ll 1$, for calculating values of derivatives du/dx and d^2u/dx^2 and for value of u we assume that

$$1+(dy/dx)^2\approx 1.$$

Then:

$$u=R_r;$$

$$du/dx=-R_r\cdot dy/dx\cdot d^2y/dx^2;$$

$$d^2u/dx^2=-R_r[dy/dx\cdot d^3y/dx^3+(d^2y/dx^2)^2-3(dy/dx)^2\cdot(d^2y/dx^2)^2].$$

Replacing these derivatives in equations for $d\Upsilon/dx$, $d^2\Upsilon/dx^2$; dx/dX and d^2x/dX^2 and substituting them in equations (8) and (9), we get:

$$d\Upsilon/dX=dy/dx; \tag{8a}$$

$$d^2\Upsilon/dX^2=d^2y/dx^2/(1-R_r\cdot d^2y/dx^2). \tag{9a}$$

Substituting expressions (8a) and (9a) in formulas (6) and (7), we get the velocity and acceleration of additional displacement of roller during its motion over unevenness on the plane with constant velocity in the direction parallel to this plane:

$$d\Delta S/dt = \dot{X}dy/dx; \tag{11}$$

$$d^2\Delta S/dt^2 = \dot{X}^2 d^2y/dx^2 \Big/ \left(1 - R_r \frac{d^2y}{dx^2}\right). \tag{12}$$

Equations (11) and (12) are valid for rolling of the roller over bumps from the moment the roller comes across the unevenness at point *1* (see Fig. 1, a, b).

2. Unevenness with sharp transition. In this case, vertical displacement ΔS of the roller axis is determined from formula (5) where Y is found from equation (4) and dY/dX and d^2Y/dX^2, by successively differentiating equation (4).

In accordance with this, velocity and acceleration of vertical displacement of the roller will be:

$$d\Delta S/dt = [(x_2 - X)/\sqrt{R_r^2 - (x_2 - X)^2}]\dot{X}; \tag{13}$$

$$d^2\Delta S/dt^2 = \{-R_r^2/[R_r^2 - (x_2 - X)^2]^{3/2}\}\dot{X}^2. \tag{14}$$

Formulas (13) and (14) are valid for all types of bumps shown in Fig. 2, from the moment of starting of rolling of the roller over the point of inflection *2*.

It is obvious that maximum values of $d\Delta S/dt$ and $d^2\Delta S/dt^2$ will be at $(x_2 - X)_{max}$, i.e. at the time when the roller moves over the sharp discontinuity.

3. Velocity and Acceleration of Vertical Displacement of a Roller for Motion over Periodically Repeating Discontinuities (Bumps)

1. Unevenness with differentiable surface. If the radius of roller is more than the radius of curvature of the concave sections, the nature of change in the values of S; $d\Delta S/dt$; $d^2\Delta S/dt^2$ will be similar to the one shown in Fig. 3, a.

For sections a-b values of $d\Delta S/dt$ and $d^2\Delta S/dt^2$ during rolling of roller over bumps are determined from formulas (11) and (12).

If the radius of the roller is less than the radius of concave sections, formulas (11) and (12) are also applicable to the case of passage of the roller over the whole length of the unevenness.

2. Unevenness with sharp transition. Let us consider the case when the roller rests on the peaks of the bumps. In this case, the values of ΔS; $d\Delta S/dt$ and $d^2\Delta S/dt^2$ change in the manner shown in Fig. 3, b.

The roller will move with jerks. Velocity and acceleration during roller over the uneven peaks are determined from equations (13) and (14) where

$$(x_2 - X)_{max} = l/2.$$

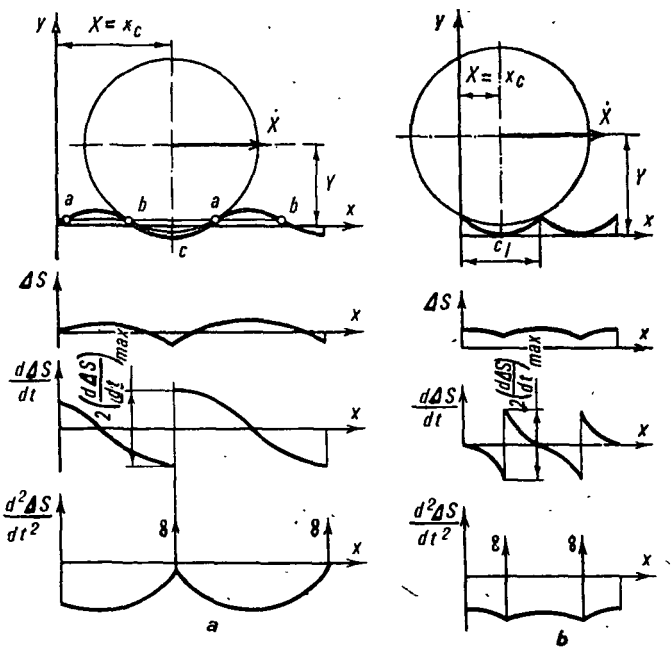

Fig. 3.

Here l is the distance between the peaks of the bumps.

The above example can also be used for studying the relationship between surface finish and the motion of the roller. If the radius of the roller is less than the radius of curvature of the unevenness preceding the trough, the roller will move without any jerks. Equations (11) and (12) are valid for the case of rolling over the crest and equations (13) and (14) for the case of rolling over the trough.

4. Effect of Roller Radius on Roller Motion over Discontinuities (Bumps)

We can evaluate the smoothness of motion of the roller from the value of acceleration $d^2\Delta S/dt^2$ and if $(d^2\Delta S/dt^2)_{max} = \infty$, from the difference of velocities $2(d\Delta S/dt)_{max}$ at point c with minimum radius of curvature (see Fig. 3), the value of which can be determined approximately from the ratio $1/(d^2y/dx^2)_c$, where $(d^2y/dx^2)_c$ is the second derivative of the uneven curve at point c.

The smaller the value of $2(\Delta S/dt)_{max}$, the smaller are the number of jerks which will be experienced by the roller during its motion.

Fig. 4 shows the graph of drop in velocity $2(d\Delta S/dt)_{\max}$ for different values of the radius of the roller. If the radius lies within the limits

$$0 \leqslant R_r < 1/d^2y/dx^2$$

the roller rolls over the concave section of the bump and its velocity $d\Delta S/dt$ is determined from equation (11) and since $(dy/dx)_c=0$ at point c, $(d\Delta S/dt)_c=0$.

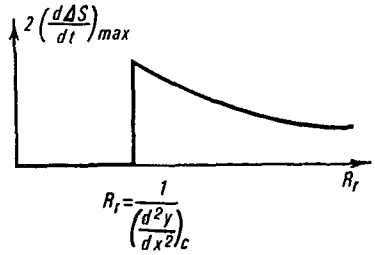

Fig. 4.

When $R_r=1/d^2y/dx^2$, the acceleration according to equation (12), becomes equal to ∞, while the velocity $d\Delta S/dt$ instantaneously attains some value $(d\Delta S/dt)_{\max}$.

On further increasing the radius, the roller rests on the peaks of the discontinuities and the velocity $(d\Delta S/dt)_{\max}$ decreases which is confirmed by equations (11) and (13). The analysis of this graph shows that if it is not possible to design a roller of radius:

$$R_r < 1/(d^2y/dx^2)_c,$$

then the radius should be increased to get smoother motion of the roller.

If this inequality is observed, the roller radius can have an optimum value so as to reduce the maximum values of acceleration, which is analyzed below.

To determine the maximum absolute value of acceleration $|d^2\Delta S/dt^2|_{\max}$, let us write equation (12) in the form:

$$d^2\Delta S/dt^2 = X^2/(1/d^2y/dx^2 - R_r). \tag{12a}$$

If

$$(d^2y/dx^2)_{\max} \gg |(d^2y/dx^2)_{\min}|,$$

where $(d^2y/dx^2)_{\max}>0$—maximum positive value of the second derivative;
$(d^2y/dx^2)_{\min}<0$—maximum modulus of the negative value of the second derivative,

then:

$$(d^2\Delta S/dt^2)_{\max} = X^2/(1/(d^2y/dx^2)_{\max} - R_r)\ . \tag{12b}$$

In this case, a decrease in the value of R_r makes the motion of roller smoother.

If $(d^2y/dx^2)_{max} < |(d^2y/dx^2)_{min}|$, the value of $|d^2\Delta S/dt|_{max}$ should be determined from equation (12b):

$$(d^2\Delta S/dt^2)_{max} = X^2/(1/(d^2y/dx^2)_{min} - R_r) \tag{12c}$$

and maximum of the calculated values should be selected.

To reduce the maximum values of accelerations, the optimum value $R_{r_{opt}}$ should be selected in such a manner that:

$$(d^2\Delta S/dt^2)_{max} = |(d^2\Delta S/dt^2)_{min}|,$$

from where:

$$R_{r_{opt}} = 1/2 \cdot [1/(d^2y/dx^2)_{max} - 1/|(d^2y/dx^2)_{min}|] . \tag{15}$$

Let us put

$$\lambda = |(d^2y/dx^2)_{min}|/(d^2y/dx^2)_{max}.$$

On the basis of equality (15):

$$R_{r_{opt}} = (1 - 1/\lambda)/[2(d^2y/dx^2)_{max}]$$

or

$$[R_r(d^2y/dx^2)_{max}]_{opt} = 1/2 \cdot (1 - 1/\lambda) . \tag{16}$$

The change in the maximum positive and negative values of d^2Y/dX^2 is shown in Fig. 5 depending on the product $R_r(d^2y/dx^2)_{max}$ for two values of λ.

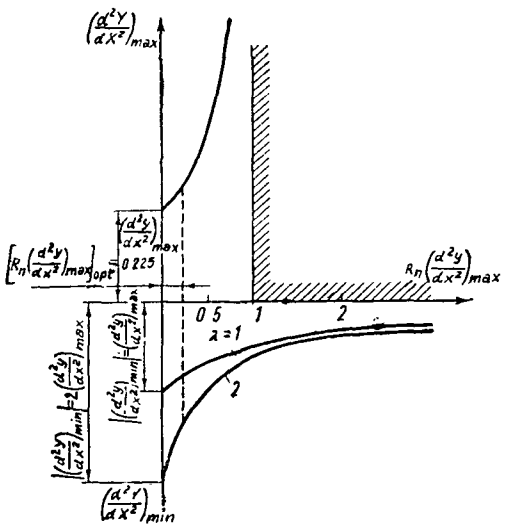

Fig. 5.

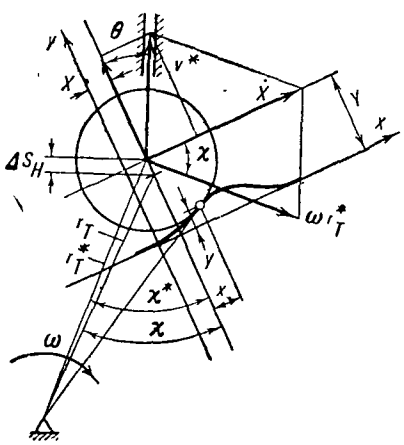

Fig. 6.

As an example, it is shown by dotted line that at $\lambda=2$.

$$[R_r(d^2y/dx^2)_{\max}]_{\text{opt}}=0.225\ .$$

From this result and a knowledge of (d^2y/dx^2), we can determine the optimum value of the radius of the roller.

5. Additional Velocity and Acceleration of Roller Follower due to Errors in the Design Profile of the Cam

1. Unevenness with differentiable surface. Let us consider the inverse motion of the follower relative to a cam (Fig. 6). Here the surface of the cam in the region of a single bump is taken to be plane (i.e. curvature is not taken into account) while the position of the follower guide and radius vector is changed in such a manner that pressure angle θ and angle of action of the cam for the outstroke χ correspond to the values of these angles at the mutual position of the follower and cam.

It is known that in the case of inverse motion, the roller axis rotates about the cam center with an angular velocity ωr_T^* and moves along the guide with a velocity of v^*.

Here r_T^* is the actual radius vector of the theoretical profile of the cam and v^* is the actual velocity of the follower.

If velocities ωr_T^* and v^* are known, it is possible to determine velocity $\dot{X}$ in the direction of tangent to the surface of the design profile of the cam:

$$\dot{X}=\omega r_T^* \cos\varkappa^* + v^* \sin\Theta\ . \tag{17}$$

For small amplitudes and for the case of a single bump we make the following assumptions:

1. $r_T^* \approx r_T=\text{const}$;
2. $v^* \approx v=\text{const}$;
3. $\Theta=\text{const}$;
4. $\chi^*=\chi=\text{const}$.

Similar assumptions were made by B. I. Sandler and V. F. Krasnikov for studying the errors in the theoretical profile of a central follower. This follows from a comparison of the equations for the additional velocities Δv and accelerations Δw of a central follower ($\chi=\Theta$) and theoretical profile $R_r=0$), obtained in this study with similar equations obtained by V. F. Krasnikov and B. I. Sandler.

For these assumptions we obtain:

$$\dot{X}=\omega\cdot r_T \cos\chi + v\sin\Theta$$

or

$$\dot{X}=(r_T\cos\chi + dS/d\varphi \sin\Theta)\cdot\omega\ . \tag{18}$$

Let us denote the displacement of the roller axis along follower guides for motion over a bump by ΔS_H.

Then according to Fig. 6, we have:

$$\Delta S_H = \Delta S/\cos\Theta = (Y - R_r)/\cos\Theta\,, \tag{19}$$

where ΔS is the displacement along the normal to the profile determined from equation (5).

Under these assumptions, the additional velocity of the follower due to bumps will be:

$$\Delta v = d\Delta S_H/dt = d\Delta S/dt\,1/\cos\Theta\,, \tag{20}$$

while the additional acceleration of the follower due to bumps is:

$$\Delta w = d^2\Delta S_H/dt^2 = d^2\Delta S/dt^2\,1/\cos\Theta\,. \tag{21}$$

In equations (20) and (21), depending on the nature of the bumps, the values of $d\Delta S/dt$ and $d^2\Delta S/dt^2$ are determined in the same manner as explained in previous sections by substituting the value of $\dot{X}$ from equation (18).

Values of r_T, χ, Θ, $dS/d\varphi$ are calculated with the help of well-known equations.

These relations are valid for all configurations of cam-roller-follower mechanisms.

Example. Let the working profile of a cam have following parameters: $r_{OT}=50$ mm; $S_{max}=20$ mm; $\varphi_S=\pi/2$ where r_{OT} is the initial radius of the theoretical profile of the cam; S_{max} is the maximum displacement of the follower and φ_s is the angle of rotation of the cam corresponding to maximum displacement of the follower.

It obeys a simple harmonic law, i.e.

$$S = S_{max}(1-\cos\pi\varphi/\varphi_s)/2\,.$$

The follower is made in the form of a central roller and consequently $\chi=\Theta$. The profile has been machined by the method of small divisions through every 2°, i.e. $\Delta\psi_c=2°$.

In accordance with reference [3], let us assume that the profile has undulations of the type:

$$y = y_{max}\cdot\sin x\cdot 2\pi/L,$$

where $L=2\Delta\psi_C r_C$;

r_C—radius vector of the design profile of the cam (elements of the cam).

Let us consider two alternatives: $y_{max}=0.05$ mm and $y_{max}=0.01$ mm. We have to determine:

1. Radius of the roller for which there will be no hard impacts.
2. Ratio $\Delta w_{max}/w_{max}$.

1) In accordance with equation (12), $R_r(d^2y/dx^2)_{max}<1$ is the condition for the absence of hard impacts ($d^2\Delta S/dt^2 \neq \infty$).

For the case of undulations considered above:

$$d^2y/dx^2=-(2\pi/L)^2 \cdot y_{max} \cdot \sin x\, 2\pi/L;$$

$$(d^2y/dx^2)_{max}=(2\pi/L)^2\, y_{max}.$$

Then

$$R_r<1/[(2\pi/L)^2\, y_{max}].$$

To simplify the calculations we take $r_C \approx r_T - R_r$, where r_T is the radius vector of the theoretical cam profile.

Let us put the values of L and r_C in the inequality

$$R_r<1/[\pi/\Delta\psi_C(r_T-R_r)]^2\, y_{max}.$$

To determine the maximum permissible value of radius R_r, we solve the equations:

$$\pi^2 y_{max} \cdot R_{r_{max}}/(r_T-R_{r_{max}})^2\Delta\psi_C^2=1;$$

$$R^2_{r_{max}}-(2r_T+\pi^2 y_{max}/\Delta\psi_C^2)R_{r_{max}}+r_T^2=0.$$

The maximum permissible value R_{rmax} should lie on the minimum cam radius where there is maximum curvature of the bump.

Then at $r_T=r_{OT}=50$ mm and $y_{max}=0.05$ mm, we have:

$\pi^2 y_{max}/\Delta\psi_C^2=3.14^2\times 0.05/(0.035)^2=9.86\times 0.05/0\cdot 00122=405$ mm;

$$R^2_{r_{max}}-505\, R_{r_{max}}+2500=0;$$

$$R_{r_{max}}=505/2\pm\sqrt{63800-2500}=252.5-248=4.5 \text{ mm}.$$

From stress considerations, the roller axle radius should not be less than 10 mm. Consequently, we cannot have impact less operation of a rigid follower by selecting roller diameter in the presence of the above mentioned errors of the profile.

Let us consider the case when $y_{max}=0.01$ mm,

$$\pi^2 y_{max}/\Delta\psi_C^2=9.86\times 0.01/0\cdot 00122=88 \text{ mm};$$

$$R^2_{r_{max}}-188\, R_{r_{max}}+2500=0;$$

$$R_{r_{max}}=94\pm\sqrt{8840-2500}=94-79.6=14.4 \text{ mm}.$$

Here, at $R_r=10$ mm, impactless operation of the follower is provided.

2) We will determine the ratio $\Delta w_{max}/w_{max}$ for the case when $y_{max}=0.01$ mm and $R_r=10$ mm.

The value of Δw is measured within the limits of one bump and along the length of cam profile. Therefore, to get Δw_{max} along the length of profile we get the value of this parameter at three points:

a) at minimum radius of the cam where there is maximum curvature of the bump;

b) at the middle of the profile where velocity is maximum and the pressure angle is close to the maximum value; and

c) at the maximum radius of cam where peripheral velocity is maximum.

Maximum value of Δw within the limits of one bump is determined from equation (21) where the maximum value of $d^2\Delta S/dt^2$ is calculated from equation (12b). Since in this example:

$$(d^2y/dx^2)_{max}=|(d^2y/dx^2)_{min}|,$$

then

$$(d^2\Delta S/dt^2)_{max}=[1/(d^2y/dx^2)_{max}-R_r]\dot{X}^2.$$

a) $\Theta=0$; $r_T=r_{OT}$

$$(d^2y/dx^2)_{max}=(\pi/\Delta\psi_C(r_T-R_r))^2\cdot y_{max}-(\pi/(0.035\times 40))^2\times 0.01=0.05/\text{mm};$$

$$\dot{X}=r_T\cdot\omega=0.05\omega \text{ m/sec};$$

$$\Delta w=(d^2\Delta S/dt^2)_{max}=50^2\cdot\omega^2/0.05-10$$

$$=0.1\times 2500\,\omega^2 \text{ mm/sec}^2=0.250\,\omega^2 \text{ m/sec}^2.$$

b) $r_T=60$; $\tan\Theta=dS/d\varphi/(r_{OT}+0.5S_{max})=S_{max}\cdot\pi/2/(r_{OT}+0.5\,S_{max})$

$$=10\pi/60=0.524,$$

where $dS/d\varphi$ is the first transmission function of the law of simple harmonic motion:

$$(d^2y/dx^2)_{max}=[\pi/[\Delta\psi_C(r_T-R_r)]]^2\cdot y_{max}=\pi/(0.035\times 50)^2\cdot y_{max}=0\cdot 0322 \text{ 1/mm};$$

$$\dot{X}=(r_T\cdot\cos\Theta+dS/d\varphi\sin\Theta)\omega=(60\times 0.886+31.4\times 0.464)\omega=67.7\omega \text{ mm/sec};$$

$$\Delta w=(d^2\Delta S/dt^2)_{max}\cdot 1/\cos\Theta;$$

$$\Delta w=(67.7)^2\omega^2\cdot 1/0.886\left(\frac{1}{0.0322}-10\right)=1.13\times 0.0477\times 4580\times\omega^2 \text{ mm/sec}^2$$

$$=0.246\cdot\omega^2 \text{ m/sec}^2.$$

c) $\Theta=0$; $r_T=70$ mm

$$d^2y/dt^2=(\pi/0.035\times 60)^2\cdot y_{max}=0.015 \text{ 1/mm};$$

$$\dot{X}=r_T\cdot\omega=70\cdot\omega \text{ mm/sec};$$

$$\Delta w=(d^2\Delta S/dt^2)_{max}=(70)^2\cdot\omega^2/(1/0.015-10)=0.0177\times 4900=$$

$$0.087\cdot\omega^2 \text{ m/sec}^2.$$

Thus the maximum value of Δw will be at the beginning of the profile and is equal to:

$$\Delta w_{max} = 0.250 \cdot \omega^2 \text{ m/sec}^2.$$

Maximum acceleration of the follower is determined from the formula:

$$w_{max} = S_{max}/\varphi_S^2 \cdot \pi^2/2 \cdot \omega^2 = 0.02/2.46 \times 4.935 \cdot \omega^2 = 0.04\omega^2 \text{ m/sec}^2.$$

Let us determine the ratio $\Delta w_{max}/w_{max}$

$$\Delta w_{max}/w_{max} = 0.25 \cdot \omega^2/0.04 \cdot \omega^2 = 6.25.$$

On the basis of this example, we arrive at the conclusion that undulations of small amplitude $y_{max} = 0.01$ mm and of wave length corresponding to two pitches can give rise to significant overloading.

Conclusions

1. In that case when the working surface of a cam represents a wavy surface (see Fig. 3, a) or a surface with sharp transition as shown in Fig. 3, b due to errors, acceleration of the follower depends on the ratio of the radius of its roller to the parameters of the bumps.

In this case, when

$$R_r \geqslant 1/d^2y/dx^2,$$

where d^2y/dx^2 is the second derivative of the height of the bump with respect to the length of its concave section, the motion of the follower will be accompanied by hard impacts ($\Delta w = \infty$).

The larger the radius of the roller, the lesser will be the impacts.

If $R_r < 1/d^2y/dx^2$, the roller will roll over the bumps smoothly. Maximum additional acceleration of the follower can be determined from formulas (21) where $d^2\Delta S/dt^2$, is determined from equations (12b) or (12c).

If $|d^2y/dx^2|_{max} \geqslant |(d^2y/dx^2)|_{min}$, a decrease in the roller radius makes motion of the follower smoother. If $|d^2y/dx^2|_{max} < |(d^2y/dx^2)|_{min}$, value of the roller radius optimum for additional acceleration is calculated from formula (16).

2. The law of motion of the follower has a weaker effect on additional velocity and acceleration than the ratio of the roller radius to the dimensions of the bumps. The effect of the law is related to its effect on the value of velocity $\dot{X}$ of roller in a direction tangent to the cam profile. The law for which the values of $\dot{X}_{max}$ are large, has a stronger effect on nonuniformity of motion of the follower due to uneven surface of the cam.

3. Calculations show (see example) that significant accelerations appear even at small amplitudes (0.01 mm) in the case of undulations of wave length corresponding to two pitches. In the case of an actual follower, these accelerations are less due to its elasticity. The obtained analytical

relationships of motion of the roller center over bumps are also necessary for determining additional velocities and accelerations of the follower by taking its elasticity into account.

4. There is insufficient data available about the nature of errors originating during machining of cams. The contradictory requirements, imposed on the roller radius in Section 1, demonstrate the necessity of studying the surface of the working profile of a cam from the point of view of establishing the predominant type of errors originating at the time of cam machining.

References

1. Krasnikov, V. F. K vyboru dopuskov na rabochii profil' kulachkov s uchetom kinematicheskikh i dinamicheskikh uslovii (Selection of tolerance on working profile of cams taking into account the kinematic and dynamic conditions). Sb. *Analiz i sintez mashin-avtomatov*, Izd-vo Nauka, 1965.
2. Krasnikov, V. F. Teoreticheskoe i eksperimental'noe issledovanie raboty kulachkovogo mekhanizma s uchetom tochnosti ego izgotovleniya (Theoretical and experimental study of operation of a cam mechanism by taking into account its manufacturing accuracy). *Mashinovedenie,* No. 1, 1965.
3. Krasnikov, V. F. Nekotorye voprosy analiza i sinteza kulachkovykh mekhanizmov s uchetom tochnosti ikh izgotovleniya (Some problems of the analysis and synthesis of cam mechanisms by taking into account their manufacturing accuracy). Sb. *Analiz i sintez mekhanizmov i teoriya peredach,* Izd-vo Nauka, 1965.
4. Sandler, B. I. Nekotorye voprosy tochnosti v svyazi s profilirovaniem kulachkov (Some problems of accuracy of cam profiles). Sb. *Avtomatizatsiya proizvodstvennykh protsessov v mashinostroenii i priborostroenii*, vyp. 2, Riga, RPI, 1963.
5. Sandler, B. I. K opredeleniyu dinamicheskikh oshibok kulachkovykh mekhanizmov bez ucheta uprugosti tolkatelya (Determination of dynamic errors of cam mechanisms without considering elasticity of the follower). Sb. *Avtomatizatsiya proizvodstvennykh protsessov v mashinostroeni i priborostroenii*, vyp. 3, Riga, RPI, 1964.
6. Baranov, G. G. Kurs teorii mekhanizmov i mashin (Textbook of Theory of Mechanisms and Machines). Mashgiz, 1959.

Yu. M. Zingerman

KINEMATIC STUDY OF SPATIAL MECHANISMS BY THE TECHNIQUE OF VECTOR ANALYSIS

1. Kinematic Pairs and their Properties

This article examines the properties of kinematic pairs using the technique of vector-projections [1, 2] and applies the results to kinematic analysis of spatial mechanisms.

Of the numerous possible types of kinematic pairs, we will consider only eight pairs which are commonly in use (see Table 1); sliding, turning, screw (helical), cylindrical, spherical with pin in the sphere, spherical with pin in the cylinder, spherical and spherical in cylinder.

To solve the problem of studying the relative motion of two links *1* and *2* forming some kinematic pair (Fig. 1), we will state the problem as follows: to establish common kinematic elements of the two links by taking these elements as vector projections of kinematic parameters. The law of motion of one of the links, for example of link *1*, is known. This means that six vector projections of kinematic parameters of the link are given. For link *2*, the number of these vector projections must be less by the degrees of freedom f in the relative motion of the group of links *1* and *2*. Here, number f is apparently equal to the difference between *6* and number N of the class of kinematic pair.

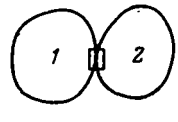

Fig. 1.

Thus the number of vector projections lost during transition from one link to another is $f=6-N$.

Table 1.

Class of the pair	Name of the pair	Notation	Schematic representation	Figurative representation
V	Sliding	V^{slid}		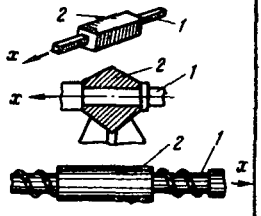
	Turning	V^{turn}		
	Screw	V^{screw}		
IV	Cylindrical	IV^{cyl}		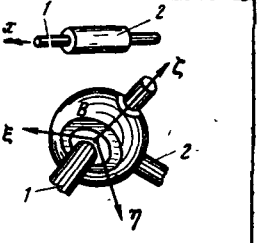
	Spherical with pin in the sphere	IV^{spher}		
III	Spherical	III^{spher}		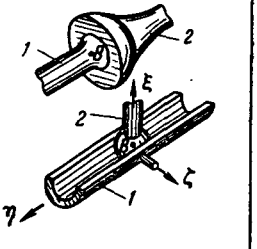
	Spherical with pin in the cylinder	$III^{spher-cyl}$		
II	Sphere in cylinder	II		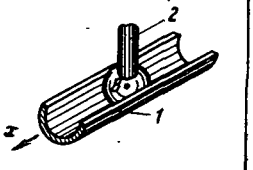

Vector projections insufficient for the kinematic analysis of link 2 should be determined from the conditions of the remaining kinematic chain.

Let us denote the kinematic parameters as follows:

ω_i—angular velocity of link i relative to the support of the mechanism;

ω_{ij}—angular velocity of link i in its motion relative to link j;

v_{B_i}—velocity of point B of link i relative to the support;

$v_{B_{ij}}$—velocity of point B of link i in its motion relative to link j;

$\mathbf{r}_{B_{ij}}$—radius vector of point B drawn from same point on the axis of kinematic pair $(i; j)$, connecting links i and j;

$\mathbf{v}_{ij}$—velocity of rectilinear motion of link i relative to link j;

$\mathbf{w}^C$—Coriolis acceleration;

$\mathbf{w}_{B_i}$—absolute acceleration of point B of link i;

$\mathbf{w}_{ij}$—acceleration of rectilinear motion of link i relative to link j;

ε_i—absolute angular acceleration of link i;

ε_{ij}—angular acceleration of the relative motion of link i.

Let us consider the kinematic properties of various pairs.

1. Sliding pair ($f=1$). Let links *1* and *2* be connected into a sliding pair (1;2). In this case, velocity of an arbitrary point M of link *2* is written as:

$$\mathbf{v}_{M_2}=\mathbf{v}_{M_1}+\mathbf{v}_{21}. \tag{1}$$

If vector $\mathbf{v}_{21}$ is directed along the axis of the pair (1; 2), it follows from equation (1) that projection of this velocity on a plane perpendicular to the axis of the pair is the common kinematic element of point M of the two links.

In other words, we do not compute the total velocity but its projection on the plane for point M of link *2* and it means a loss of one vector projection.

Similar phenomena are observed in the case of accelerations as well.

Acceleration of point M of link *2* can be written as:

$$\mathbf{w}_{M_2}=\mathbf{w}_{M_1}+\mathbf{w}_{21}+\mathbf{w}^C. \tag{2}$$

Since $\mathbf{w}^C$ is a known parameter after calculating velocities, and projecting the sum of known vectors of the right hand side of equation (2) on the same plane perpendicular to the axis of the pair, we obtain the projection of the vector $\mathbf{w}_{M_2}$ on this plane.

2. Turning pair ($f=1$). Let us write the basic vector equations defining the velocity and acceleration of an arbitrary point M of link *2*.

$$\mathbf{v}_{M_2}=\mathbf{v}_{M_1}+\omega_{21}\times\mathbf{r}_{M_{12}}, \tag{3}$$

$$\mathbf{w}_{M_2}=\mathbf{w}_{M_1}+\varepsilon_{21}\times\mathbf{r}_{M_{12}}+\bar{\omega}_{21}\times(\omega_{21}\times\mathbf{r}_{M_{12}})+2\omega_1\times\mathbf{v}_{M_{21}}. \tag{4}$$

If the vectors $\omega_{21}\times\mathbf{r}_{M_{12}}$ and $\varepsilon_{21}\times\mathbf{r}_{M_{12}}$, whose moduli are not known, are directed along the perpendicular to the plane passing through point M and axis (1; 2), it follows from equations (3) and (4) that projections of its velocity and acceleration on this plane will be the common kinematic elements of point M of the two links.

3. Cylindrical pair ($f=2$). It follows from the analysis of basic vector equations:

$$\mathbf{v}_{M_2}=\mathbf{v}_{M_1}+\mathbf{v}_{21}+\omega_{21}\times\mathbf{r}_{M_{12}}; \tag{5}$$

$$\mathbf{w}_{M_2}=\mathbf{w}_{M_1}+\mathbf{w}_{21}+\omega_{21}\times(\mathbf{w}_{21}\times\mathbf{r}_{M_{12}})+\varepsilon_{21}\times\mathbf{r}_{M_{12}}+2\omega_1\times\mathbf{v}_{M_{21}} \tag{6}$$

that vector projections of velocity and acceleration of the radial direction, i.e. on the direction of the perpendicular drawn from point M on axis (1; 2) are the common kinematic elements of point M of the two links.

4. Screw pair ($f=1$). Let parameter p of the screw be given: In the basic vector equation:

$$\mathbf{v}_{M_2}=\mathbf{v}_{M_1}+\mathbf{v}_{21}+\mathbf{v}_{21}^{rot}, \tag{7}$$

axial and angular velocity of point M situated at a distance d from the axis (1; 2) is determined from equations:

$$v_{21}=\omega_{21}p;\ v_{21}^{rot}=\omega_{21}d,$$

we obtain:

$$v_{21}/v_{21}^{rot}=p/d\,. \tag{8}$$

Equation (8) shows that some straight line $\beta-\beta$ representing the vector of total relative velocity of point M can be drawn through this point. Projecting equation (7) on a plane perpendicular to the straight line $\beta-\beta$, we get the common kinematic elements of velocity of point M of the two links, i.e. projection on this plane. This means that assignment of screw parameter is equivalent to assignment of two vectors projections and loss of one vector projection.

In the second vector equation:

$$\mathbf{w}_{M_2}=\mathbf{w}_{M_1}+\mathbf{w}_{21}+\mathbf{w}_{21}^{n}+\mathbf{w}_{21}^{\tau}+2\omega_1\times\mathbf{v}_{M_{21}} \tag{9}$$

numerically unknown vectors $\mathbf{w}_{21}$ and $\mathbf{w}_{21}^{\tau}$ are also related to each other as follows:

$$w_{21}/w_{21}^{\tau}=p/d\,. \tag{10}$$

Thus the straight line $\beta-\beta$ can also be used for calculating accelerations.

5. Sphere with pin in the sphere ($f=2$). A pin in the slot helps link *2* (see Table 1) to have relative motion of rotation in two mutually perpendicular planes, one of which is perpendicular to axis of the pin ζ while the other passes through the middle plane of the slot (axis ξ is the normal to it).

In this way, there is no possibility of rotation about η-axis lying in the plane of the slot and perpendicular to two other axis ζ and ξ.

The equation relating angular velocities of the two links is written as:

$$\omega_2=\omega_1+\omega_{21}\,. \tag{11}$$

Considering that projection of vector ω_{21} on η-axis is equal to zero, we get the first common kinematic element of links *1* and *2*, namely vector projection of absolute angular velocity on η-axis. Moreover, taking point B in the center of the spherical joint, we have

$$\mathbf{v}_{B_1}=\mathbf{v}_{B_2}.$$

This is equivalent to assigning three more vector-projections for link *2*.

Thus pair IV$^{\text{spher}}$ transfers from link *1* to link *2* four vector projections of kinematic parameters: three vector projections of the velocity and one vector projection of the angular velocity. A similar result is obtained from calculating accelerations. Firstly $\mathbf{w}_{B_1}=\mathbf{w}_{B_2}$ and secondly $\varepsilon_{21\eta}=0$.

6. Spherical pair ($f=3$). Center B of the pair is the center of relative rotation of links *1* and *2*. Therefore:

$$\mathbf{v}_{B_1}=\mathbf{v}_{B_2};\qquad \mathbf{w}_{B_1}=\mathbf{w}_{B_2}.$$

Thus, the spherical pair helps in determining the velocity and acceleration of the first point of link *2*, which is equivalent to the assignment of three vector projections of each kinematic parameter for link *2* and consequently, means loss of three vector projections out of the six known for link *1*.

7. Sphere with pin in the cylinder ($f=3$). The pair makes it possible for link *2* to have the three simplest types of motion relative to link *1*: rectilinear motion along η-axis and rotary motion about ζ and ξ axes (see Table 1). Existence of the pin makes relative rotation about η-axis impossible.

It follows from the vector equation:

$$\omega_2=\omega_1+\omega_{21}. \tag{12}$$

that vector projection of the angular velocity on η-axis will be the first kinematic element for link *1* and *2*.

Let us take point K on plane Q, passing through center B of the sphere and perpendicular to η-axis. We have:

$$\mathbf{v}_{K_2}=\mathbf{v}_{K_1}+\mathbf{v}_{21}+\boldsymbol{\omega}_{21}\times\mathbf{BK}. \tag{13}$$

If vectors $\mathbf{v}_{21}$ and $\boldsymbol{\omega}_{21}\times\mathbf{BK}$ are perpendicular to plane Q, it follows from equation (13) that projection of velocity of point K on plane Q is the second kinematic element of the links.

A similar result is obtained from the calculation of accelerations. In this case, it is necessary to derive and solve the basic vector equation once again for point K:

$$\mathbf{w}_{K_2}=\mathbf{w}_{K_1}+\mathbf{w}_{21}+\boldsymbol{\omega}_{21}\times(\boldsymbol{\omega}_{21}\times\mathbf{BK})+\boldsymbol{\varepsilon}_{21}\times\mathbf{BK}+2\boldsymbol{\omega}_1\times\mathbf{v}_{K21}. \tag{14}$$

8. Sphere in cylinder ($f=4$). Center B of the sphere is the center of relative rotation of links *1* and *2* (see Table 1). Moreover, the pair permits relative rectilinear motion along x-axis. The projections of the velocity and acceleration of point B on a plane passing through the point B and perpendicular to x-axis, become the common kinematic elements of links.

2. Examples of Kinematic Analysis of Spatial Mechanisms

Let us apply the principle of vector projections in determining velocities and accelerations in spatial mechanisms.

Example 1. Five-link mechanism $V^{turn}-V^{turn}-III^{spher}-V^{turn}-V^{turn}$. This mechanism (Fig. 2)[1] was suggested by many authors who solved the problem of determining velocities and accelerations analytically (P. A. Lebedev [3]) as well as graphically (G. D. Ananov [4]). Chzhan Tsy-syan' [5] used the method of matrix calculations.

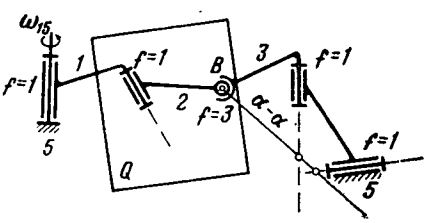

Fig. 2.

The mechanism transmits rotary motion between two skew axes (5; 1) and (4; 5) in the case of arbitrary position of the axes of two internal turning pairs (1; 2) and (3; 4).

Although this kinematic scheme has been the subject of numerous investigations, it does not cover the diversity of spatial mechanisms which can be obtained by combining various kinematic pairs and by changing their number, assuming that the degree of mobility of the mechanism remains equal to one. This led the author to attempt to find a general kinematic method of analyzing all spatial mechanisms. The method of vector projections was selected for achieving this purpose.

Let us describe the method of determining velocities in the five-link mechanism. Let us impose number f of vector projections lost on each kinematic pair ($\Sigma f=7$ for the whole mechanism) and take center B of spherical pair (2; 3), i.e. common point of links *2* and *3*, as the calculation point.

Let us determine the absolute velocity of point B. It is obvious from

[1] For Figs. 2-4, $\Sigma f=7$.

the arrangement of f, that projection of vector $\mathbf{v}_B$ on the plane can be found from the left and vector projection on the direction from the right hand side. It is easily determined from these data that $\mathbf{v}_{B_2}=\mathbf{v}_{B_3}$.

We may proceed in the following manner.

1. Calculate velocity of point B of link *1* whose angular velocity ω_{15} is given.

2. By projecting $\mathbf{v}_{B_1}$ on plane Q passing through point B and axis (1; 2), we determine the projection $\mathbf{v}_{B_Q}$ of vector $\mathbf{v}_{B_2}$ on this plane.

3. Let us draw a straight line $\alpha-\alpha$ through point B simultaneously intersecting axes (4; 5) and (3; 4). The vector $\mathbf{v}_{B_3}$ has zero projection on this straight line.

4. By reprojecting, we determine $\mathbf{v}_{B_2}=\mathbf{v}_{B_3}$ from the projection of $\mathbf{v}_{B_Q}$ on plane Q and from zero vector projection on straight line $\alpha-\alpha$.

We calculate accelerations of the points and angular accelerations of all the links of the mechanism in the same manner by taking center B of the pair (2; 3) as the calculation point.

Example 2. Four-link mechanism $V^{\text{turn}}-V^{\text{turn}}-IV^{\text{cyl}}-III^{\text{spher-cyl}}$ (Fig. 3). Let us again define the calculation point. This point should be found on link *3* since Σf for the point of link *2* toward right is $2+3=5$, while the number of lost vector projections must be $\leqslant 2$ for determining the total velocity of any point. We get $\Sigma f=3$ for an arbitrary point M of link *3* toward left on coming from the driving link and toward right on coming from the support.

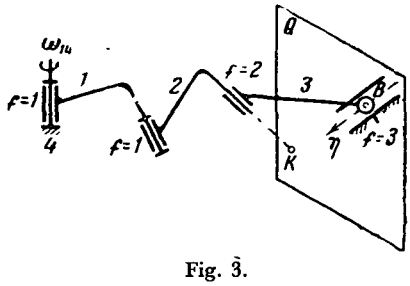

Fig. 3.

It is not possible to find velocity of an arbitrary point M of link *3*. Taking into account the methods described in Section 1, we will search for the calculation point in plane Q drawn through center B and perpendicular to η-axis of the pair (3; 4).

Let us consider a part of the kinematic chain situated between the driving link and link *3*. To reduce Σf from 3 to 2, let us take the point of link *3* on the axis of cylindrical pair (2; 3). This helps in eliminating relative velocity of rotation $\mathbf{v}_{32}$.

Consequently, the calculation point K should be taken at the intersection of axis (2; 3) with plane Q. For this

point K of link *3*, we have: vector projection of its velocity on the line of intersection of two planes passing through the point K, one of which passes through axis (1; 2) and the second is perpendicular to axis (2; 3), toward left and vector v_{K_3} perpendicular to plane Q toward right.

Utilizing this data, we determine v_{K_3} by reprojecting. Further from vector v_{K_3}, we determine the vectors ω_{21} and v_{32} by the method of arranging them according to the known directions and then by the method of reprojection we solve the vector equation:

$$\omega_{14}+\omega_{21}+\omega_{32}+\omega_{43}=0$$

relative to vectors ω_{32} and ω_{43}.

We calculate accelerations in the same manner by considering point K.

Example 3. Seven-link mechanism with turning pairs. A seven-link mechanism with rotating pairs was the subject of kinematic analysis by a number of authors: N. I. Mertsalov [6], G. G. Baranov [7] and many others who adopted various means of investigation, mainly the method of decomposition of the given angular velocity of the driving link of the mechanism along six arbitrary directions in space.

Let us demonstrate the method of determining velocities in a seven-link mechanism using vector projection with subsequent restoration (reprojection) of kinematic vectors according to the other vector projections.

Fig. 4 shows the kinematic scheme of a spatial seven-link mechanism with arbitrarily arranged turning pairs. It must be clarified in the very beginning that in this case it is not possible to determine total velocity of any point of the driven section of the mechanism since Σf is always more than three at least on one side of the chain.

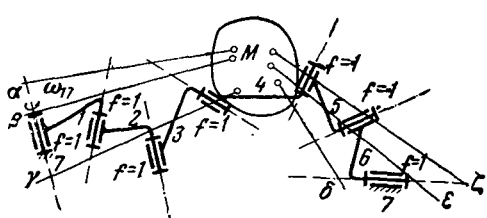

Fig. 4.

Thus, there is not even a single "special" point in a seven-link mechanism. This factor makes kinematic analysis of a seven-link mechanism more complex as compared to any other type of spatial mechanism made of simple chains. Velocities can be calculated by the method of vector projections in the following manner. Let us take link *4* separated from the driving link *1* and from the support by three kinematic pairs.

As is well-known from line geometry, three skew straight lines can always be intersected by an infinite number of other straight lines. In this case, a single pole hyperboloid which is unambiguously defined by only three straight lines intersecting three given straight lines is formed. Taking this into consideration, let us intersect axes (4; 5), (5; 6) and (6; 7) by three straight lines δ, ε and ζ. Along these directions we have zero projections of velocities for points of link *4*. Let us intersect axes (1; 2), (2; 3) and (3; 4) by three straight lines α, β and γ along these directions. Thus, we may determine vector projections of velocities for points of link *4* by knowing the given angular velocity ω_{17} of the driving link of the mechanism.

Thus, six vector projections of velocities along six directions α, β, γ, δ, ε and ζ will be known for link *4*. But as shown in reference [1], this is sufficient for the determination of angular velocity ω_{47} of link *4* as well as for determination of the velocity of an arbitrary point *M*. Then angular velocities of all the remaining links of the mechanism can be calculated without any major difficulties.

The advantages of this method lie in the fact that they confirm the universality of the method of vector projections which is suitable for kinematic analysis of even very complicated spatial mechanisms.

References

1. Zingerman, Yu. M. Opredelenie peremeshchenii uzlov prostranstvennoi sterzhnevoi sistemy metodami nachertatel'noi geometrii (Determination of displacements of the components of a spatial system by geometrical methods). *Trudy Khabarovskogo in-ta inzh. zh.-d. transporta*, vyp. 7, Moscow, 1954.
2. Zingerman, Yu. M. Primenenie metoda proektsii k kinematicheskomu analizu prostranstvennykh mekhanizmov s nizshimi parami (Application of the projection method to kinematic analysis of spatial mechanisms with lower pairs). *Trudy Khabarovskogo in-ta inzh. zh.-d. transporta*, vyp 10, Moscow, 1959.
3. Lebedev, P. A. Kinematika prostranstvennogo pyatizvennogo krivoshipno-koromyslovogo mekhanizma (Kinematics of a spatial five-link crank-yoke mechanism). *Izv. vuzov. Priborostroenie*, **4**, No. 1, 1961.
4. Ananov, G. D. Issledovanie kinematiki prostranstvennogo pyatizvennogo mekhanizma obshchego vida (Study of kinematics of a general spatial five-link mechanism). *Izv. vuzov. Priborostroenie*, **5**, No. 2, 1962.
5. Chzhan Tsy-syan'. Kineticheskii analiz prostranstvennykh pyatizvennykh mekhanizmov metodom matrits (Kinematic analysis of spatial

five-link mechanisms by the matrix method). *Izv. vuzov. Mashinostroenie*, No. 2, 1962.

6. MERTSALOV, N. I. Teoriya prostranstvennykh mekhanizmov (Theory of Spatial Mechanisms). Mashgiz, 1951.
7. BARANOV, G. G. Kinematika prostranstvennykh mekhanizmov (Kinematics of spatial mechanisms). *Trudy VVA im. N. E. Zhukovskogo*, No. 18, 1937.

V. S. Karelin

A METHOD OF ANALYTICAL SYNTHESIS OF PLANE TOOTHED LEVER MECHANISMS

Each year an increasing number of mechanisms are used in the design of components for automatic machines.

Complicated mechanisms with higher and lower kinematic pairs, are among these new mechanisms. They include toothed lever mechanisms designed on the basis of planetary mechanisms. These are planetary mechanisms with Assur-Artobolevskii kinematic groups connected to the planet wheel and column.

In a planetary mechanism, a point on the planet wheel or on the plane of the planet wheel, reproduces a cyclic curve on a fixed plane. Depending on the sign of gear ratio between the central wheel and the planet-wheel plane, these curves are usually classified into elongated and shortened epi- and hypotrochoids which in the general case will be termed as p l a n e t - w h e e l c u r v e s.

For specific values of the parameters of the planetary mechanism, a part of the planet-wheel curve reproduced can be approximated as a straight line, part of a conical section, etc.

If a section of the curve reproduced by a mechanism varies from a straight line or from an arc of a circle, the driven link of the connected kinematic group can have a dwell. Depending on the initial position of the point on the planet wheel and position of the point of connection of the kinematic group to the column of the mechanism, we get mechanisms having no dwell, one dwell (Fig. 1, a) two (Fig. 1, b) or many dwells in the kinematic cycle. By rotating the central wheel relative to the reference system, we can obtain all these types of motion.

Synthesis of such a mechanism leads to the following two problems:

a) synthesis of a planetary mechanism, section of the planet-wheel curve of which does not differ much from the given curve

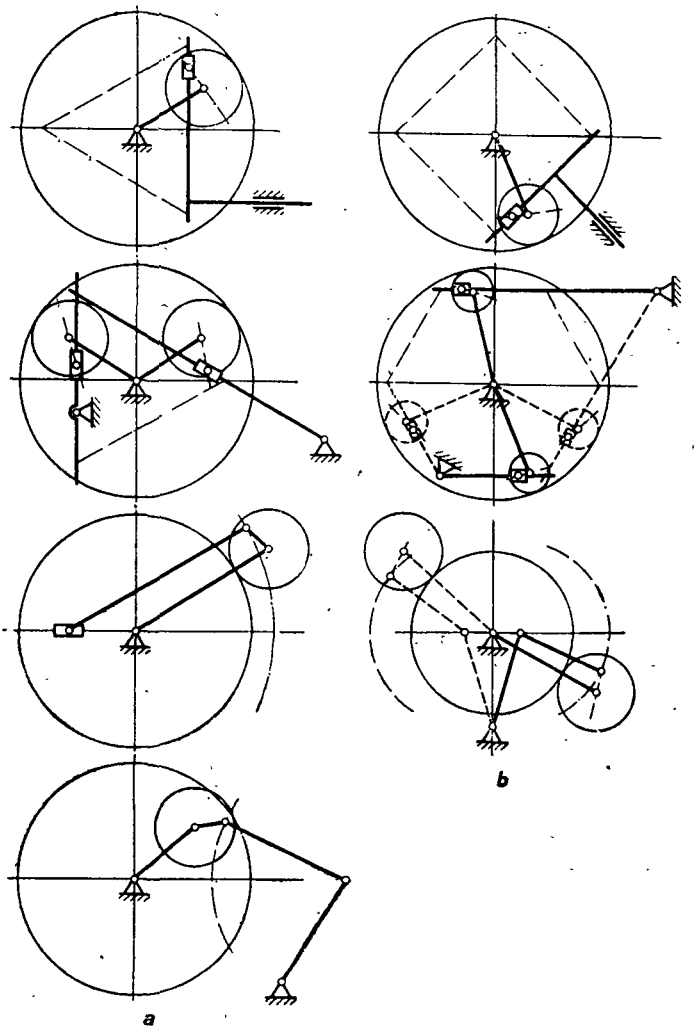

Fig. 1.

(straight line or arc of a circle); and

b) synthesis of the connected kinematic group.

Mechanisms, the planet-wheel curve of which does not differ much from a straight line or arc of a circle, are of maximum interest since only they help in getting mechanisms with dwell of the driven link of the connected kinematic group.

Only the first part of the problem, i.e. synthesis of planetary mechanisms with planet-wheel curve not differing from a straight line or arc of a circle is examined in this article.

Synthesis of mechanisms having lower pairs and directed along a straight line or an arc of a circle was studied by P. L. Chebyshev and due to the research of his followers, it has become an engineering method in the form of various alternatives of the method of best approximation [1-3]. Recently, this method was applied to the synthesis of planetary lever mechanisms, obtained by transforming lever-toothed mechanisms [4].

Usually the function of deviation of the curve reproduced by the mechanism from the given curve is considered in the case of best approximation according to Chebyshev's method.

While plotting a deviation curve according to Chebyshev's method, it is assumed that the kinematic scheme of the mechanism is already known.

Consequently, it is necessary to derive the deviation function and to study it for every mechanism. Simple as well as multiple interpolation points can be given. This imposes additional requirements in the form of multiple roots on the deviation function. The problem of synthesis becomes complicated and requires extensive calculations.

An effort is made here to study the problems of synthesis of plane mechanisms guiding along a straight line or arc of a circle between coordinates of the points of the given curve. Then parametric equations of the selected mechanism are put in this dependence and parameters of the mechanism are determined as a function of the position of common points of the given curve and of the curve reproduced by the mechanism.

In this case, there is no difference in the methods of assigning common points and simple as well as multiple common points can be assigned without any limitations. This facilitates study of the kinematic schemes of various mechanisms and selection of schemes which can best satisfy the conditions formulated earlier.

1. Mathematical Basis of the Method of Synthesis

The method of synthesis suggested here is the interpolation method for which the determinant:

$$\Delta(\varphi_1, \ldots, \varphi_m) = \begin{vmatrix} \varphi_1(x_1)\, \varphi_2(x_1), \ldots, \varphi_m(x_1) \\ \cdots\cdots\cdots\cdots\cdots\cdots \\ \varphi_1(x_m)\, \varphi_2(x_m), \ldots, \varphi_m(x_m) \end{vmatrix} \tag{1}$$

differs from zero when all its elements $\varphi_1, \varphi_2, \ldots, \varphi_m$ differ in pairs. It also corresponds to the condition when the polynomial:

$$\varphi(x) = \lambda_1\varphi_1(x) + \lambda_2\varphi_2(x) + , \ldots, + \lambda_m\varphi_m(x) \tag{2}$$

becomes equal to zero at not more than $m-1$ points.

As known, such systems are called Chebyshev systems [5].

The interpolation problem in this case is known as interpolational approximation with simple units [5].

If $k+1$ simple interpolation points within the selected interval of approximation are moved towards each other till their fusion, then in the limiting case, we get interpolation point of multiplicity factor k.

Condition (1) in this case is written as follows:

$$\Delta(\varphi_1, \ldots, \varphi_1^{(k)}) = \begin{vmatrix} \varphi_1(x_1)\, \varphi_2(x_1), \ldots, \varphi_m(x_1) \\ \cdots\cdots\cdots\cdots\cdots\cdots \\ \varphi_1^{(k)}(x_1)\varphi_2^{(k)}(x_1), \ldots, \varphi_m^{(k)}(x_1) \end{vmatrix}, \tag{3}$$

where determinant Δ is not equal to zero and $\varphi', \ldots, \varphi^{(k)}$ are derivatives of φ from first to k-th order.

The interpolation problem in this case is known as interpolation approximation with multiple units or multiple interpolation [5].

Interpolation approximation according to the above mentioned method is extremely tedious especially in the case of a large number of interpolation points since it is related to the calculation of determinants of higher orders.

If the approximation function is represented in the general form by the polynomial:

$$\varphi(x) = ax + bx^k = cx^t + , \ldots, + dx^s,\ 3 \leqslant k < t < s,\ k < t+1,\ s > t+1, \tag{4}$$

parameters $a, b, \ldots, d$ can be determined by solving Kramer equations.

The determinants of these equations become:

$$\Delta a = \begin{vmatrix} \varphi(x_1) & x_1^k, \ldots, x_1^s \\ \varphi(x_2) & x_2^k, \ldots, x_2^s \\ \cdots\cdots & \cdots\cdots\cdots \\ \varphi(x_m) & x_m^k, \ldots, x_m^s \end{vmatrix}, \ldots, \Delta d = \begin{vmatrix} x_1\, x_1^k, & \ldots, \varphi(x_1) \\ x_2\, x_2^k, & \ldots, \varphi(x_2) \\ \cdots\cdots & \cdots\cdots\cdots \\ x_m\, x_m^k, & \ldots, \varphi(x_m) \end{vmatrix} \tag{5}$$

and are known as Vandermond type determinants in contrast to the Vandermond determinants which are written as [6]:

$$D = \begin{vmatrix} 1\ x_1\ x_1^2, & \ldots, x_1^m \\ 1\ x_2\ x_2^2, & \ldots, x_2^m \\ \cdots\cdots & \cdots\cdots\cdots \\ 1\ x_m\, x_m^2, & \ldots, x_m^m \end{vmatrix} = \Pi(x_i - x_j) \quad 1 \leqslant i < j \leqslant m. \tag{6}$$

If angle α of the rotation of the driving link is taken as the parameter of the system and x-axis as the one coinciding with the axis of symmetry of the planet-wheel curve, the function describing the planet-wheel curve can be written in the parametric form for planetary mechanisms:

$$x=a\cos\alpha-b\cos\beta\pm c\cos\gamma-,\ \ldots,\ \pm d\cos\delta;$$
$$y=a\sin\alpha-b\sin\beta+c\sin\gamma\pm,\ \ldots,\ +d\sin\delta, \tag{7}$$

where $\beta=\varphi_1(\alpha)$, $\gamma=\varphi_2(\alpha)$, $\delta=\varphi_m(\alpha)$.

In the case of planetary mechanisms with spur gears, the relationships $\varphi_1,\ldots,\varphi_m$ are linear functions of the type:

$$\varphi_i=n_i\alpha \quad 1\leqslant i\leqslant m, \tag{8}$$

and equation (7) in this case can be written as:

$$x=a\cos\alpha-b\cos n_1\alpha\pm c\cos n_2\alpha-,\ \ldots,\ \pm d\cos n_m\alpha;$$
$$y=a\sin\alpha\pm b\sin n_1\alpha+c\sin n_2\alpha-\ \ldots\ +d\sin n_m\alpha, \tag{9}$$

where $n_1<n_2<,\ \ldots,\ <n_m$.

In these equations, the upper sign corresponds to a "plus" sign of the gear ratio between the central wheel and the planet wheel while the lower sign corresponds to a "minus" sign of the gear ratio between these elements of the mechanisms.

Thus, the planet-wheel curve of a planetary mechanism can be represented as the geometrical sum of several cyclic vectors. This peculiarity of planetary mechanisms was recognized earlier by V. V. Dobrovol'skii [7] and M. V. Semenov [8].

In general, equation of the planet-wheel curve:

$$F=\Sigma\bar{\varphi}_i(\alpha)\ 1<i<m \tag{10}$$

and the determinant expressing the solution of the system of equations obtained in this case will be the Vandermond type determinants [2].

Vandermond type determinants have the same properties as all other determinants. Moreover, Vandermond type determinants are related to Vandermond determinants. These relations are defined by the following theorems.

Theorem 1. *Vandermond type of determinant is the product of Vandermond determinant of the same order as Vandermond type determinant, and a polynom.*

Both these determinants can be written as polynomials by expanding them according to the elements of their rows and columns. The functions described by the determinants pass through the same common points after every interval of approximation. It is equivalent to the fact that both the polynomials have the same roots. Their maximum common denominator is written in the form:

$$(x_1-x_2)(x_1-x_3),\ \ldots,\ (x_{m-1}-x_m)=\Pi(x_i-x_j)\ \ 1\leqslant i<j\leqslant m. \tag{11}$$

But this is the Vandermond determinant [9] which is the maximum common denominator of these determinants.

Theorem 1 can be written in the following manner:

$$\Delta = MD, \tag{12}$$

where Δ—Vandermond type determinant;

D—Vandermond determinant;

M—Polynomial obtained as the result of transformation of the Vandermond type determinant.

Theorem 2. *Polynomials obtained as a result of expansion of Vandermond type determinants into Vandermond determinant and polynomial are uniform and symmetrical.*

Homogeneity of polynomials directly follows from the properties of Vandermond type determinants and Vandermond determinant which are homogeneous. Let us show the symmetry of the polynomials obtained by changing the places of two rows or two columns in the Vandermond type determinant. The Vandermond determinant will correspond to the new Vandermond type determinant only if the corresponding rows or columns are changed in it. The polynomial obtained in this way does not change its sign.

An extremely important conclusion is obtained from this theory.

Conclusion. If the position of elements with similar indices in the matrices coincide in the Vandermond type determinant and in the Vandermond determinant corresponding to it, then the polynomial obtained as a result of expansion in accordance with theorem 1 is positive, i.e. all its terms have positive sign.

Theorem 3. *The order of the polynomial obtained as a result of expansion of the Vandermond type determinant in accordance with theorem* 1, *is equal to the difference of the sum of the indices of all elements of some row in the Vandermond type determinants and the corresponding sum of the Vandermond determinant of the same order.*

On expanding the Vandermond type determinant into elements of the row or column, we get a homogeneous and symmetrical polynomial. The sum of the indices of every member of this polynomial θ is constant. Similarly in the case of Vandermond determinant, the index q of every term of the polynomial is equal to the sum of indices of all the elements of same row. Dividing these polynomials by each other, on the basis of the Bezu theorem, we get a polynomial with index η defined by the expression:

$$\eta = \theta - q. \tag{13}$$

For example, let us consider the solution of the system of equations formed by the following system of functions:

$$\begin{aligned} &1+a\cos\alpha_1+b\cos^2\alpha_1+c\cos^3\alpha_1+d\cos^4\alpha_1=0;\\ &\cdots\cdots\cdots\cdots\cdots\cdots\cdots\cdots\cdots\cdots\\ &1+a\cos\alpha_4+b\cos^2\alpha_4+c\cos^3\alpha_4+d\cos^4\alpha_4=0. \end{aligned} \tag{14}$$

Parameters a, b, c and d of this system can be determined from the solution of the following Kramer equations:

$$a=\Delta_a/\Delta;\quad b=\Delta_b/\Delta;\quad c=\Delta_c/\Delta;\quad d=\Delta_d/\Delta. \tag{15}$$

The determinant of the system Δ and the algebraic complements of the system in parameters a, b, c and d are expressed by the following determinants:

$$\begin{aligned} \Delta a&=\begin{vmatrix} 1 & \cos^2\alpha_1 & \cos^3\alpha_1 & \cos^4\alpha_1\\ \cdots & \cdots & \cdots & \cdots\\ 1 & \cos^2\alpha_4 & \cos^3\alpha_4 & \cos^4\alpha_4 \end{vmatrix};\quad \Delta b=-\begin{vmatrix} 1 & \cos\alpha_1 & \cos^3\alpha_1 & \cos^4\alpha_1\\ \cdots & \cdots & \cdots & \cdots\\ 1 & \cos\alpha_4 & \cos^3\alpha_4 & \cos^4\alpha_4 \end{vmatrix};\\ \Delta c&=\begin{vmatrix} 1 & \cos\alpha_1 & \cos^2\alpha_1 & \cos^4\alpha_1\\ \cdots & \cdots & \cdots & \cdots\\ 1 & \cos\alpha_4 & \cos^2\alpha_4 & \cos^4\alpha_4 \end{vmatrix};\quad \Delta d=-\begin{vmatrix} 1 & \cos\alpha_1 & \cos^2\alpha_1 & \cos^3\alpha_1\\ \cdots & \cdots & \cdots & \cdots\\ 1 & \cos\alpha_4 & \cos^2\alpha_4 & \cos^3\alpha_4 \end{vmatrix};\\ \Delta&=\begin{vmatrix} \cos\alpha_1 & \cos^2\alpha_1 & \cos^3\alpha_1 & \cos^4\alpha_1\\ \cdots & \cdots & \cdots & \cdots\\ \cos\alpha_4 & \cos^2\alpha_4 & \cos^3\alpha_4 & \cos^4\alpha_4 \end{vmatrix}. \end{aligned} \tag{16}$$

These are Vandermond type determinants. On the basis of theorem 1, they can be written as products:

$$\begin{aligned} \Delta a&=D\,(\cos\alpha_1\cos\alpha_2\cos\alpha_3+\cos\alpha_1\cos\alpha_2\cos\alpha_4+\cos\alpha_1\cos\alpha_3\cos\alpha_4+\\ &\quad\cos\alpha_2\cos\alpha_3\cos\alpha_4);\\ \Delta b&=-D\,(\cos\alpha_1\cos\alpha_2+\cos\alpha_1\cos\alpha_3+\cos\alpha_1\cos\alpha_4+\cos\alpha_2\cos\alpha_3+\\ &\quad\cos\alpha_2\cos\alpha_4+\cos\alpha_3\cos\alpha_4);\\ \Delta c&=D\,(\cos\alpha_1+\cos\alpha_2+\cos\alpha_3+\cos\alpha_4);\\ \Delta d&=-D;\\ \Delta&=D\cos\alpha_1\cos\alpha_2\cos\alpha_3\cos\alpha_4 \end{aligned} \tag{17}$$

where D is the Vandermond determinant of the fourth order:

$$D=\begin{vmatrix} 1 & \cos\alpha_1 & \cos^2\alpha_1 & \cos^3\alpha_1\\ 1 & \cos\alpha_2 & \cos^2\alpha_2 & \cos^3\alpha_2\\ 1 & \cos\alpha_3 & \cos^2\alpha_3 & \cos^3\alpha_3\\ 1 & \cos\alpha_4 & \cos^2\alpha_4 & \cos^3\alpha_4 \end{vmatrix}. \tag{18}$$

After this transformation, equation (15) can be written as:

$$\begin{aligned} a&=(\cos\alpha_1\cos\alpha_2\cos\alpha_3+\cos\alpha_1\cos\alpha_2\cos\alpha_4+\cos\alpha_1\cos\alpha_3\cos\alpha_4+\\ &\quad\cos\alpha_2\cos\alpha_3\cos\alpha_4)/\cos\alpha_1\cos\alpha_2\cos\alpha_3\cos\alpha_4;\\ b&=-(\cos\alpha_1\cos\alpha_2+\cos\alpha_1\cos\alpha_3+\cos\alpha_1\cos\alpha_4+\cos\alpha_2\cos\alpha_3+\cos\alpha_2\cos\alpha_4+\\ &\quad\cos\alpha_3\cos\alpha_4)/\cos\alpha_1\cos\alpha_2\cos\alpha_3\cos\alpha_4;\\ c&=(\cos\alpha_1+\cos\alpha_2+\cos\alpha_3+\cos\alpha_4)/\cos\alpha_1\cos\alpha_2\cos\alpha_3\cos\alpha_4;\\ d&=-1/\cos\alpha_1\cos\alpha_2\cos\alpha_3\cos\alpha_4. \end{aligned} \tag{19}$$

The above transformation helps in using simple as well as multiple interpolation points. In this case, there is no difference in the methods of simple and multiple interpolation but the mathematical expressions of the functions and other calculation are simplified.

2. Synthesis of Straight-line Mechanisms

A straight line of a plane in the rectilinear system of coordinates is described by the parametric equations [9]:

$$x'=\varphi(\alpha');$$
$$y'=\psi(\alpha'). \tag{20}$$

By turning the system of coordinates, they can be so arranged that one of the axis is parallel to the given straight line. Then in the new system of coordinates, parametric equation of the straight line takes the following form (see Fig. 2, a where *1* is the turned system and *2* is the initial system):

$$x=\varphi(\alpha). \tag{21}$$

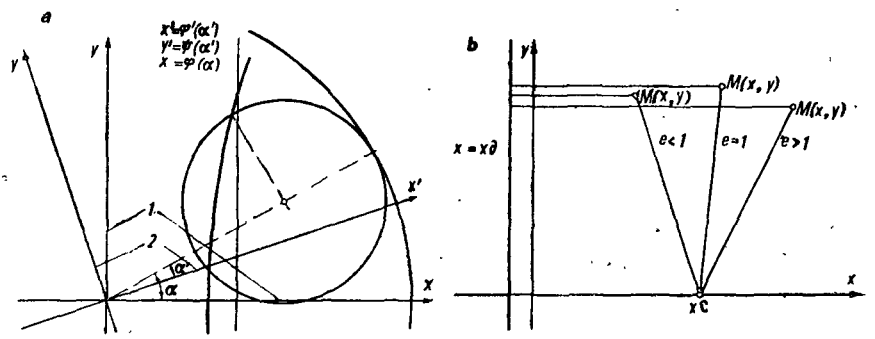

Fig. 2.

Substituting equation (9) in the equation (21), we get the following system of equations for interpolation points:

$$x=a\cos\alpha_1-b\cos n_1\alpha_1+c\cos n_2\alpha_1-,\ \ldots,\ +d\cos n_m\alpha_1;$$
$$x=a\cos\alpha_m-b\cos n_1\alpha_m+c\cos n_2\alpha_m-,\ \ldots,\ +d\cos n_m\alpha_m. \tag{22}$$

Parameters of the mechanism are determined from equations (15) which after transformation on the basis of theorem 1 become:

$$a=M_a/M;\qquad b=M_b/M;\qquad c=M_c/M,\ \cdots,\qquad d=M_d/M. \tag{23}$$

where M, M_a, $M_b,\ldots,$ M_d are polynomials of expression of Vandermond type determinants on the basis of theorem 1.

The number of interpolation points in this case is not limited and simple as well as multiple points can be assigned.

3. Synthesis of Mechanisms Directing along Conical Sections

Let us derive the equation of the relation between coordinates of the interpolation points for conical sections. On the basis of the directorial properties of conical sections [9], we obtain the following equation of relation between coordinates of the points of a conical section:

$$e(x-x_d)=\sqrt{(x-x_c)^2+y^2}, \tag{24}$$

where e—eccentricity of the conical section;

$x=x_d$—equation of the directrix;

x_c—abscissa of the focus of conical section (see Fig. 2, b).

Only symmetrical curves are considered in this paper and therefore focus of the conic section lies on the abscissa axis and its ordinate $y=0$.

Eliminating x_c and x_d from equation (24) forming a system for the case of several interpolation points, after transformation we get the equation:

$$\Delta^2\{e^4[Bc+Ad+4cd(1-e^2)x_1]^2-2e^2[c^2(B^2-b)+d^2(A^2-a)]+\Delta^2\}=0, \tag{25}$$

where coefficients:

$$\begin{aligned}
&a=4c(1-e^2)[y_1^2x_2-y_2^2x_1+(1-e^2)x_1x_2c];\\
&b=4d(1-e^2)[y_1^2x_3-y_3^2x_1+(1-e^2)x_1x_3d];\\
&A=y_1^2-y_2^2+(1-e^2)(x_1^2-x_2^2);\\
&B=y_1^2-y_3^2+(1-e^2)(x_1^2-x_3^2);\\
&c=x_1-x_2,\ d=x_1-x_3;\\
&\Delta=\begin{vmatrix} 1 & x_1 & (1-e^2)x_1^2+y_1^2\\ 1 & x_2 & (1-e^2)x_2^2+y_2^2\\ 1 & x_3 & (1-e^2)x_3^2+y_3^2 \end{vmatrix}.
\end{aligned} \tag{26}$$

In the case of even a single multiple interpolation point, from equation (25) we get:

$$\Delta=0. \tag{27}$$

If all the interpolation points are simple, then $\Delta\neq 0$ and equation (25) can be written as:

$$e^4(Bc+Ad+4cd(1-e^2)x_1)^2-2e^2(c^2(B^2-b)+d^2(A^2-a))+\Delta^2=0. \tag{28}$$

Equations (27) and (28) help in determining the parameters of the mechanism by putting parametric equations of the planet-wheel curve of the selected planetary mechanism in place of x and y.

For conical sections with $e<1$, i.e. ellipses and with $e>1$, i.e. hyperbolas, equations (27) or (28) can be used directly depending on the selection of simple or multiple interpolation points for the synthesis.

For parabolas $e=1$, equations (27) and (28) take the following form, when there is at least one multiple point:

$$\Delta=\begin{vmatrix} 1 & x_1 & y_1^2 \\ 1 & x_2 & y_2^2 \\ 1 & x_3 & y_3^2 \end{vmatrix}=0 \tag{29}$$

and if all the interpolation points are simple:

$$(y_1^2-y_2^2)\,(y_1^2-y_3^2)+4(x_1-x_2)\,(x_1-x_3)\,y_1^2=0. \tag{30}$$

For a circle $e=0$, equations (27) and (28) change into one expression suitable for simple as well as multiple interpolation points:

$$\begin{vmatrix} 1 & x_1 & x_1^2+y_1^2 \\ 1 & x_2 & x_2^2+y_2^2 \\ 1 & x_3 & x_3^2+y_3^2 \end{vmatrix}=0. \tag{31}$$

For multiple interpolation points, the value of parameter $k=a/b$ is determined in the final form only when it is single, i.e. in the case of three-link planetary mechanism. For polyplanetary mechanisms [10], we get $m+1$ equations of relation between parameters k, k_1, ..., k_m and it is necessary to assign m parameters.

In the case of simple interpolation points, if the number of parameters k is more than one, we have the following system of nonlinear equations:

$$\begin{aligned} &M_1k_1k_2+M_2k_2k_3+,\ \ldots,\ +M_mk_{m-1}k_m=0; \\ &\ldots\ldots\ldots\ldots\ldots\ldots\ldots\ldots\ldots\ldots \\ &M_1'k_1k_2+M_2'k_2k_3+,\ \ldots,\ +M_m'k_{m-1}k_m=0. \end{aligned} \tag{32}$$

Coordinates of the focus of the conical section are determined from the equation:

$$x_c=\{[y_1^2-y_2^2+(1-e^2)\,(x_1^2-x_2^2)]\pm e\sqrt{[(y_1-y_2)^2+(1-e^2)\,(x_1-x_2)^2]\,[(y_1+y_2)^2+(1-e^2)\,(x_1-x_2)^2]}\}/2\times (1-e^2)\,(x_1-x_2). \tag{33}$$

In certain cases, we get for a parabola:

$$x_c=\begin{vmatrix} 1 & y_1^2 \\ 1 & y_2^2 \end{vmatrix}\Big/4\begin{vmatrix} 1 & x_1 \\ 1 & x_2 \end{vmatrix}+\begin{vmatrix} x_1 & y_1^2 \\ x_2 & y_2^2 \end{vmatrix}\Big/\begin{vmatrix} 1 & y_1^2 \\ 1 & y_2^2 \end{vmatrix} \tag{34}$$

and for a circle:

$$x_c = \begin{vmatrix} 1 & x_1^2+y_1^2 \\ 1 & x_2^2+y_2^2 \end{vmatrix} \Big/ 2 \begin{vmatrix} 1 & x_1 \\ 1 & x_2 \end{vmatrix}. \tag{35}$$

Radius vector of the conical section can be calculated from an expression of the following type [9]:

$$\rho = \sqrt{(x_1-x_c)^2+y_1^2}. \tag{36}$$

Boundary Conditions in the Synthesis of Toothed Lever Planetary Mechanisms

The above relations can be used at arbitrary values of simple as well as multiple interpolation points. However, mechanisms obtained in this way have only a completely defined point of the curve reproduced by them and of the given curve and do not have arbitrarily assigned points. These are mechanisms in which the common points of planet-wheel curves and of given curves lie only at the ends of the approximation interval and at the ends of the semi-interval of approximation in the case of symmetrical curves. In the future, we will call such mechanisms as b o u n d a r y m e c h a n i s m s and the curves reproduced by them as b o u n d a r y c u r v e s. For the whole approximation interval, there is only one boundary mechanism while there are $m-1$ boundary mechanisms for the semi-interval of approximation where m is the number of parameters.

The following theorem can be suggested by considering the properties of boundary curves drawn by boundary mechanisms.

T h e o r e m. *Planet-wheel curves reproduced by boundary mechanisms have a deviation from the given curve more than the planet-wheel curves of similar mechanisms but have common points with the given curve within the approximation interval.*

Let us consider a planetary mechanism, the planet wheel curve of which can be described by the following parametric equations:

$$\begin{aligned} x &= a\cos\alpha \pm b\cos n_1\alpha \pm c\cos n_2\alpha \pm, \cdots, \\ y &= a\sin\alpha \mp b\sin n_1\alpha \mp c\sin n_2\alpha \mp, \cdots. \end{aligned} \tag{37}$$

On considering the case of rectilinearly directing mechanism, we get only one parametric equation on the basis of equation (21). Parameters of this mechanism in a general case are the functions of the position of a mechanism. The parametric equation of the planet-wheel curve of such a mechanism becomes:

$$x = M_a\cos\alpha \pm M_b\cos n_1\alpha \pm M_c\cos n_2\alpha \pm, \cdots. \tag{38}$$

Taking the first derivative of the obtained equation with respect to x and making it equal to zero, we get the equation for determination of the extreme value of the interpolation point at which the deviation of the curve reproduced by the mechanism from the given curve is maximum:

$$dx/d\alpha = M_a \sin\alpha + M_a' \cos\alpha + M_b n_1 \sin n_1\alpha + M_b' \cos n_1\alpha + , \cdots , = 0. \quad (39)$$

This equation can be written in the form of the sum:

$$M_a \sin\alpha + M_b n_1 \sin n_1\alpha + , \ldots , + M_a' \cos\alpha + M_b' \cos n_1\alpha + , \ldots , = 0. \quad (40)$$

From the first half of equation (40), we get:

$$\sin\alpha = 0;$$
$$\alpha = 0°. \quad (41)$$

In the second half, the coefficients are cosine functions and their derivatives are:

$$M_a' (\cos\alpha) = T_a (\sin\alpha),$$
$$M_b' (\cos\alpha) = T_b (\sin\alpha). \quad (42)$$

From here just like equation (41), we get:

$$\sin\alpha = 0;$$
$$\alpha = 0°. \quad (43)$$

Thus, the deviation of the curve reproduced by the mechanism from a straight line will be maximum when all interpolation points lie at the end of the semi-interval of approximation at $\alpha = 0°$.

Let us now turn the system of coordinates through an angle $\mu = 180°/n$. Then the parametric equation of the system can be written as:

$$x = M_a \cos(\alpha + 180°/n) \pm M_b \cos n_1 (\alpha + 180°/n) \pm M_c \cos n_2 (\alpha + 180°/n) \pm , \ldots . \quad (44)$$

By comparing equations (38) and (44), we notice that they differ from each other only in signs before the parameters. It can be further shown that equation (44) has maximum deviation from a straight line at $\alpha = \mu = 180°/n$.

Consequently, the curves reproduced by the mechanism have maximum deviation from the given curve when all the interpolation points lie at the boundaries of the interval or semi-interval of approximation and when there are no such points within the interval. This condition corresponds to boundary curves and boundary mechanisms.

As an example of substantiation of this method of synthesis, let us consider the synthesis of a toothed lever planetary mechanism meant for

reproduction of a straight line and curves of conical section. Let us take a biplanetary mechanism, the planet-wheel curve of which is described by the following parametric equations as the base of rectilinearly directing mechanism:

$$x=a\cos\alpha-b\cos 2\alpha+c\cos 4\alpha;$$
$$y=a\sin\alpha+b\sin 2\alpha+c\sin 4\alpha. \tag{45}$$

For the synthesis of an approximate rectilinearly directing mechanism, we use equation (21). Substituting parametric equations (45) in place of x, we obtain the following system of equations:

$$\begin{aligned} x&=a\cos\alpha_1-b\cos 2\alpha_1+c\cos 4\alpha_1;\\ x&=a\cos\alpha_2-b\cos 2\alpha_2+c\cos 4\alpha_2;\\ x&=a\cos\alpha_3-b\cos 2\alpha_3+c\cos 4\alpha_3. \end{aligned} \tag{46}$$

After solving the system of equations (46) and its transformation in accordance with theorem 1, we obtain equations for the determination of the parameters of the mechanism:

$$a=M_a/M; \qquad b=M_b/M; \qquad c=M_c/M, \tag{47}$$

where polynomials M_a, M_b, M_c and M are determined from expressions:

$$\begin{aligned} M_a&=8(\cos\alpha_1+\cos\alpha_2)(\cos\alpha_1+\cos\alpha_3)(\cos\alpha_2+\cos\alpha_3)R;\\ M_b&=4(\cos^2\alpha_1+\cos^2\alpha_2+\cos^2\alpha_3+\cos\alpha_1\cos\alpha_2+\cos\alpha_1\cos\alpha_3+\\ &\quad\cos\alpha_2\cos\alpha_3)R-4R;\\ M_c&=R;\\ M&=[8(\cos^2\alpha_1+\cos^2\alpha_2+\cos^2\alpha_3)+8(\cos\alpha_1\cos\alpha_2+\cos\alpha_1\cos\alpha_3+\\ &\quad\cos\alpha_2\cos\alpha_3)+16\cos\alpha_1\cos\alpha_2\cos\alpha_3(\cos\alpha_1+\cos\alpha_2+\cos\alpha_3)-6]. \end{aligned} \tag{48}$$

For this mechanism, the following boundary mechanisms are possible at the semi-interval of approximation (since the planet wheel curve is symmetrical about x axis).

Mechanism 1. Multiple interpolation point with tangent of first order at $\alpha_1=0°$ and multiple interpolation point with tangent of the third order at $\alpha_2=\alpha_3=60°$.

Mechanism 2. Multiple interpolation point with a tangent of third order at $\alpha_1=\alpha_3=0°$ and multiple interpolation point with a tangent of first order at $\alpha_2=60°$.

The parameters of these mechanisms follow:

For mechanism 1: $a=3/4R$, $b=14/48R$, $c=2/48R$; (49)

For mechanism 2: $a=3/4R$, $b=13/48R$, $c=1/48R$. (50)

Parametric equations of abscissa of the planet-wheel curves of these mechanisms are written as:

$$\begin{aligned} &1.\quad x=(36\cos\alpha-14\cos 2\alpha+2\cos 4\alpha)\,R/48;\\ &2.\quad x=(36\cos\alpha-13\cos 2\alpha+\cos 4\alpha)\,R/48. \end{aligned} \tag{51}$$

Making the first derivative of the angle of rotation of the pole, i.e. of parameter α, equal to zero and solving the equations obtained, we may determine the extreme values of α at which maximum deviations of the curve reproduced by the mechanism, from a straight line are observed:

$$\begin{aligned} &1.\quad 9\sin\alpha-7\sin 2\alpha+4\sin 4\alpha=0;\ \alpha=32°54';\\ &2.\quad 18\sin\alpha-13\sin 2\alpha+2\sin 4\alpha=0;\ \alpha=47°44'. \end{aligned} \tag{52}$$

The abscissa of the planet-wheel curve at the obtained values of α and its deviations from a straight line are given by:

$$\begin{aligned} &1.\quad x=0.48255\,R;\ \delta=-0.01745\,R;\\ &2.\quad x=0.50980\,R;\ \delta=0.01\,R. \end{aligned} \tag{53}$$

For comparison, let us state the characteristics of the mechanism, the planet-wheel curve of which has a straight line having multiple points with tangent of the first order on the boundaries of the semi-interval of approximation and one simple interpolation point within the approximation interval at $\alpha=40°$. The parametric equation of the abscissa of the planet-wheel curve will be:

$$x=(0.75\cos\alpha-0.27796\cos 2\alpha+0.02796\cos 4\alpha)\,R. \tag{54}$$

Maximum deviation of the planet-wheel curve from the straight line is obtained at the following values of α:

$$\left.\begin{aligned} \alpha'&=25°50';\\ \alpha''&=52°05'. \end{aligned}\right\} \tag{55}$$

Deviation of the planet-wheel curve from a straight line at these points will be:

$$\begin{aligned} \delta'&=-0.00379\,R;\\ \delta''&=+0.00426\,R. \end{aligned} \tag{56}$$

The planet wheel curves reproduced by mechanisms are shown in Fig. 3 ($OO'=a$; $O'B=b$; $BD=c$).[1]

[1]Figure on the right-hand side has been magnified along x-axis by 18.5 times.

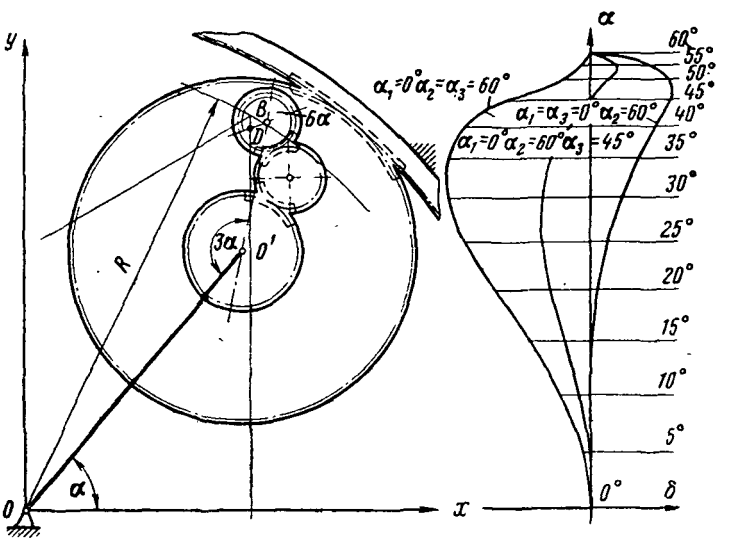

Fig. 3.

As an example of the mechanism guiding along conic sections, let us consider the mechanisms, the planet-wheel curve of which is described by the parametric equations of the type:

$$\begin{aligned} x &= a\cos\alpha - b\cos 2\alpha; \\ y &= a\sin\alpha + b\sin 2\alpha. \end{aligned} \tag{57}$$

Dividing all the terms of equation (57) by parameter b, we obtain:

$$\begin{aligned} x' &= k\cos\alpha - \cos 2\alpha; \\ y' &= k\sin\alpha + \sin 2\alpha. \end{aligned} \tag{58}$$

For a mechanism, approximately guiding along the arc of a circle, we obtain:

$$\begin{vmatrix} 1 & k\cos\alpha_1 - \cos 2\alpha_1 & 1+k^2-2k\cos 3\alpha_1 \\ 1 & k\cos\alpha_2 - \cos 2\alpha_2 & 1+k^2-2k\cos 3\alpha_2 \\ 1 & k\cos\alpha_3 - \cos 2\alpha_3 & 1+k^2-2k\cos 3\alpha_3 \end{vmatrix} = 0. \tag{59}$$

After transformation on the basis of theorem 1, we obtain an equation for the determination of parameter k:

$$k = [4(\cos\alpha_1\cos\alpha_2 + \cos\alpha_1\cos\alpha_3 + \cos\alpha_2\cos\alpha_3) + 3]/2(\cos\alpha_1 + \cos\alpha_2 + \cos\alpha_3). \tag{60}$$

Parameters a and b of the mechanism are determined from the relations:

$$\begin{aligned} a&=kR/(1+k);\\ b&=R/(1+k). \end{aligned} \tag{61}$$

where R is the radius of the circle on which cyclic points of the planet-wheel curve lie.

On reproducing conic sections with the help of this mechanism at the semi-interval of approximation 0-60°, there is a possibility of two boundary mechanisms under boundary conditions similar to equation (45).

The parameters of mechanisms and geometrical characteristics of circles whose arcs are reproduced approximately are as follows:

$$\begin{aligned} &1.\quad x=R/3(2\cos\alpha-\cos 2\alpha), && y=R/3(2\sin\alpha+\sin 2\alpha),\\ &\quad k=2, \quad x_c=8/3\,R, && \rho=7/3\,R;\\ &2.\quad x=R/6(11\cos\alpha-5\cos 2\alpha), && y=R/16\,(11\sin\alpha+5\sin 2\alpha)\\ &\quad k=11/3, \quad x_c=55/16\,R, && \rho=49/16\,R. \end{aligned} \tag{62}$$

Radius vector of the planet-wheel curves of boundary mechanisms is equal to:

$$\begin{aligned} &1.\quad \rho=R/3\,\sqrt{69-32\cos\alpha+16\cos 2\alpha-4\cos 3\alpha};\\ &2.\quad \rho=R/16\,\sqrt{3171-1210\cos\alpha+550\cos 2\alpha-110\cos 3\alpha}. \end{aligned} \tag{63}$$

Putting the first derivative of the angle of rotation of the pole equal to zero, we get values of α at which there will be maximum deviation of the planet-wheel curve from an arc of a circle:

$$\begin{aligned} &1.\quad \alpha=33°\,33';\\ &2.\quad \alpha=48°\,12'. \end{aligned} \tag{64}$$

Absolute value of deviation at these points will be:

$$\begin{aligned} &1.\quad \delta=+0.00704\,R;\\ &2.\quad \delta=-0.00500\,R. \end{aligned} \tag{65}$$

For comparison, let us describe the characteristics of a mechanism the planet-wheel curve of which has multiple points of the first order at the ends of these semi-interval of approximation and a simple point at $\alpha_3=45°$.

$$\begin{aligned} &x=(0.67829\cos\alpha-0.32171\cos 2\alpha)\,R;\\ &y=(0.67829\sin\alpha+0.32171\sin 2\alpha)\,R;\\ &k=2.10838;\\ &a=0.67829\,R;\\ &b=0.32171\,R;\\ &x_c=3.04265\,R;\\ &\rho=2.68607\,R. \end{aligned} \tag{66}$$

Maximum deviations of this curve from an arc of a circle are observed at $\alpha=27°$ and $52°50'$; which are respectively equal to:

$$\begin{aligned}\delta' &= +0.00003\,R;\\ \delta'' &= -0.00002\,R.\end{aligned} \tag{67}$$

The planet-wheel curves of these mechanisms are shown in Fig. 4 ($OO'=a$; $OD=b$).[1]

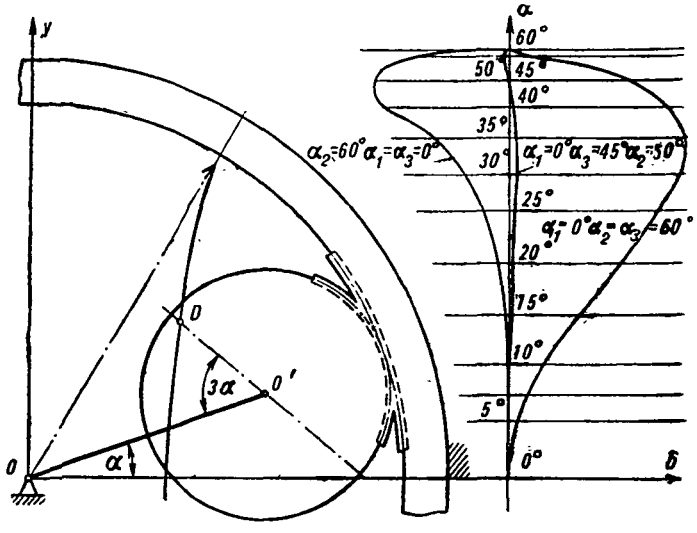

Fig. 4.

Let us consider the synthesis of boundary mechanisms approximately guiding along the arc of a parabola.

Substituting the parametric equations of the planet-wheel curve (57) reproduced by the mechanism, in equation (29), we obtain the following matrix equation:

$$\begin{vmatrix} 1\;k\cos\alpha_1-\cos 2\alpha_1\;k^2\sin^2\alpha_1+2k\sin\alpha_1\sin 2\alpha_1+\sin^2 2\alpha_1 \\ 1\;k\cos\alpha_2-\cos 2\alpha_2\;k^2\sin^2\alpha_2+2k\sin\alpha_2\sin 2\alpha_2+\sin^2 2\alpha_2 \\ 1\;k\cos\alpha_3-\cos 2\alpha_3\;k^2\sin^2\alpha_3+2k\sin\alpha_3\sin 2\alpha_3+\sin^2 2\alpha_3 \end{vmatrix} = 0. \tag{68}$$

After transformation on the basis of theorem 1, we write the equation of third order for determining parameter k of the mechanism:

$$\begin{aligned} k^3+4k^2(\cos\alpha_1+\cos\alpha_2+\cos\alpha_3)+4k(\cos^2\alpha_1+\cos^2\alpha_2+\cos^2\alpha_3-\\ \cos\alpha_1\cos\alpha_2-\cos\alpha_1\cos\alpha_3-\cos\alpha_2\cos\alpha_3-12)+8(\cos\alpha_1+\cos\alpha_2)\times\\ (\cos\alpha_1+\cos\alpha_3)(\cos\alpha_2+\cos\alpha_3)=0. \end{aligned} \tag{69}$$

[1] Figure on the right hand side has been magnified along x-axis by 58 times.

The parameters of the boundary mechanisms and geometrical characteristics of parabolas which have been approximated by the mechanism, follow:

1. $k=-9$; $a=9/8\,R$; $b=-1/8\,R$; $x_c=0.7638\,R$; $x_d=1.5\,R$;
2. $k=-10.7$ $a=1.103\,R$; $b=-0.103\,R$; $x_c=0.6992\,R$; $x_d=1.4548\,R$. (70)

Boundary planet-wheel curves reproduced by these mechanisms and the parabolas which they approximate are shown in Fig. 5 ($OO'=a$; $OD=b$).

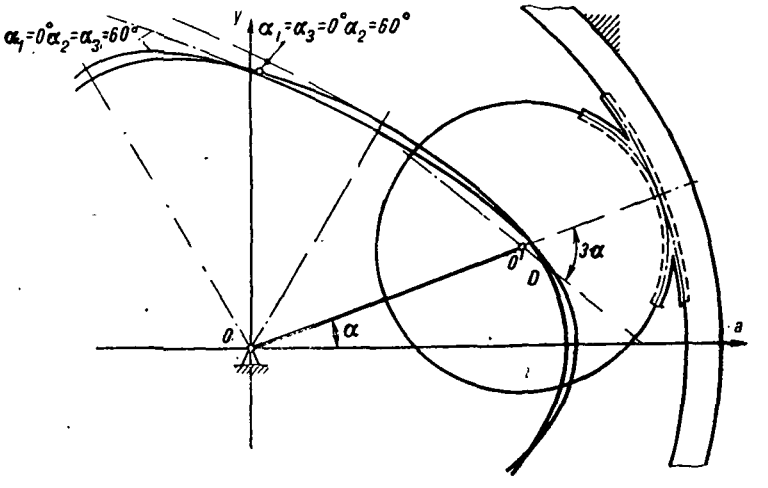

Fig. 5.

Let us consider the synthesis of boundary mechanisms approximately guiding along the arc of an ellipse and hyperbola.

Substituting the parametric equations of the planet-wheel curve reproduced by the mechanism in the basic equation (27), we obtain:

$$\begin{vmatrix} 1 & k\cos\alpha_1-\cos 2\alpha_1 & (1-e^2) & (k\cos\alpha_1-\cos 2\alpha_1)^2+(k\sin\alpha_1+\sin 2\alpha_1)^2 \\ 1 & k\cos\alpha_2-\cos 2\alpha_2 & (1-e^2) & (k\cos\alpha_2-\cos 2\alpha_2)^2+(k\sin\alpha_2+\sin 2\alpha_2)^2 \\ 1 & k\cos\alpha_3-\cos 2\alpha_3 & (1-e^2) & (k\cos\alpha_3-\cos 2\alpha_3)^2+(k\sin\alpha_3+\sin 2\alpha_3)^2 \end{vmatrix}=0. \tag{71}$$

After transformation on the basis of theorem 1 and simplification, we obtain an equation of third order for determining the parameter k:

$$e^2k^3+4k\,(2k-ke^2+2)\,(\cos\alpha_1+\cos\alpha_2+\cos\alpha_3)-12k+4ke^2\times (\cos^2\alpha_1+\cos^2\alpha_2+\cos^2\alpha_3)-8k\,(1-1.5e^2)\,(\cos\alpha_1\cos\alpha_2+\cos\alpha_1\cos\alpha_3+\cos\alpha_2\cos\alpha_3)-8\,(\cos\alpha_1+\cos\alpha_2)\,(\cos\alpha_1+\cos\alpha_3)\,(\cos\alpha_2+\cos\alpha_3)=0. \tag{72}$$

To obtain a numerical solution, it is necessary to assign the value of eccentricity e. Let us take $e=0.5$ for an ellipse and $e=2$ for a hyperbola. From equation (72), we obtain for an ellipse and hyperbola respectively:

$$\begin{array}{lll} 1. & k=-72.2; & k=-2.44; \\ 2. & k=-58.24; & k=2.36. \end{array} \tag{73}$$

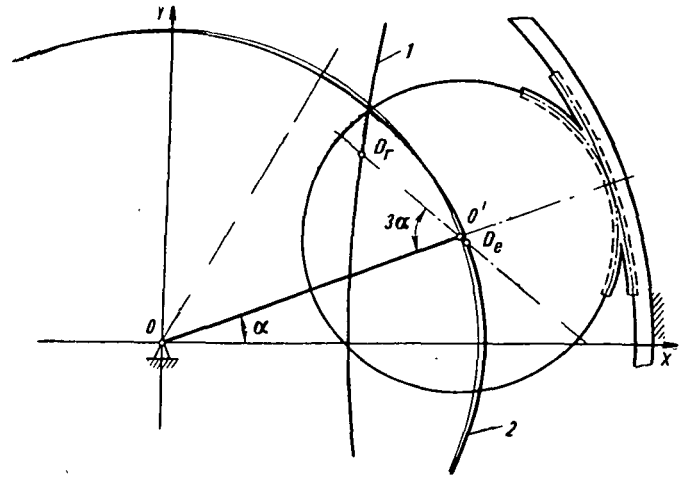

Fig. 6.

Parameters of the mechanism and its geometrical characteristics for the case when the planet-wheel curve approaches an ellipse will be:

$$\begin{array}{lll} 1. & k=-72.2; & a=1.014\,R; \quad b=-0.014\,R; \\ 2. & k=-58.24; & a=1.01747\,R; \quad b=-0.01747\,R; \end{array} \tag{74}$$

and for the case when the planet-wheel curve approaches a hyperbola:

$$\begin{array}{lll} 1. & k=2.44; & a=0.7093\,R; \quad b=0.2907\,R; \\ 2. & k=2.36; & a=0.70238\,R; \quad b=0.29762\,R. \end{array} \tag{75}$$

The curves reproduced by these mechanisms are shown in Fig. 6 where 1—hyperbola at $k=2.44$; 2—ellipse at $k=-72.2$; and $OO'=a$; $O'D=b$.

Conclusions

The method of synthesis of plane toothed lever mechanisms discussed in this article generalizes two popular methods of interpolation synthesis. The suggested transformations help in simplifying the calculations during

the process of synthesis while the results establish the limits of the mechanism by determining the parameters of the boundary mechanism.

Parameters of mechanisms which are not boundary mechanisms can be selected arbitrarily within the region of the existence of this type of mechanisms.

References

1. Artobolevskii, I. I., N. I. Levitskii and S. A. Cherkudinov. Sintez ploskikh mekhanizmov (Synthesis of Plane Mechanisms). Fizmatgiz, 1959.
2. Levitskii, N. I. Sintez mekhanizmov po Chebyshevu (Chebyshev Method of Synthesis of Mechanisms). Izd-vo AN SSSR, 1946.
3. Levitskii, N. I. Proektirovanie mekhanizmov s nizshimi parami (Design of Plane Mechanisms with Lower Pairs). Izd-vo AN SSSR, 1950.
4. Shcherba, I. I. Kinematicheskoe proektirovanie semizvennogo rychazhnogo mekhanizma s krugovym preryvistym dvizheniem vedomogo zvena (Kinematic design of seven-link mechanism with cyclic discontinuous motion of the driven link). Sb. *Teoriya mekhanizmov i mashin*, Izd-vo Mashinostroenie, 1965.
5. Goncharov, V. L. Teoriya interpolirovaniya i priblizheniya funktsii (Theory of Interpolation and Approximation of Functions). ONTI-GTTI, 1934.
6. Kurosh, A. G. Kurs vyshei algebry (Textbook of Higher Algebra). Fizmatgiz, 1959.
7. Dobrovol'skii, V. V. Teoriya mekhanizmov dlya obrazovaniya ploskikh krivykh (Theory of Mechanisms for Formation of Plane Curves). Izd-vo AN SSSR, 1953.
8. Semenov, M. V. Issledovanie dvizheniya satellitov planetarnykh mekhanizmov (Study of motion of planet-wheels of planetary mechanisms). *Trudy seminara po teorii mashin i mekhanizmov*, XV, vyp. 60, Izd-vo AN SSSR, 1956.
9. Muskhelishvili, N. I. Kurs analiticheskoi geometrii (Textbook of Analytical Geometry). Moscow, GTTI, 1947.
10. Tsyplakov, Yu. S. Biplanetarnye mekhanizmy (Biplanetary Mechanisms). Izd-vo Mashinostroenie, 1966.

A. A. Kasamanyan

TWO SIMPLE METHODS OF REGULATING MOTION OF THE DRIVEN LINK IN THREE-DIMENSIONAL SINGLE CONTOUR MECHANISMS

Adjustable mechanisms are used in machines in various branches of industry for regulating the feed of components being processed or for controlling working organs of machines, in pulse variable-ratio transformers in the capacity of converting mechanisms, in piston pumps, efficiency of which is regulated by changing the stroke of the piston, etc.

In the past they were used to regulate the distribution of steam in steam engines.

Stepless adjustable mechanisms in which adjustments can be made during operation are of interest in modern technology because of the rapid transition time of the driven link from one motion to another and the high degree of accuracy of the required type of motion they provide. They can be controlled manually as well as automatically.

Most of the adjustable mechanisms discussed in technical literature and in practical use are plane mechanisms. However, three-dimensional mechanisms offer more versatility. Plane mechanisms can carry out only part of the functions of the three-dimensional mechanisms.

The greater suitability of materialization of three-dimensional mechanism over a plane mechanism will be demonstrated using examples of three-dimensional and plane sine-tangent adjustable mechanism.

Since, as in the case of three-dimensional unadjustable mechanisms, study of three-dimensional adjustable mechanisms is much more complicated than that of plane mechanisms, they have not been widely used.

Here we will consider the possibility of controlling a simple, i.e. single contour, three-dimensional mechanism as the most popular type of three-dimensional mechanisms met in practice and we will analyze its operation by switching over to the particular case, i.e. plane mechanism.

In a single contour mechanism, each link forms two kinematic pairs with other links. In practice, the stationary link usually forms turning sliding and screw pairs with the moving links. The links belonging to the support are usually driving and driven links. It is known that motion of the driven link is defined by its displacement function and by the law of motion of the driving link. The possibility of changing the motion of the driven link in the case of unchanged law of motion of the driving link is considered in this paper, since it is assumed that change in the motion of the latter is provided by some other mechanism. Displacement function, i.e. relation between displacements of the driving and driven links, includes parameters of the mechanism by changing which, it is possible to get various types of motion of the driven link.

In general, a change in some parameter of the mechanism leads to simultaneous change in the law, travel, phase and other characteristics of the motion of the driven link. Therefore, by change in motion of driven link we mean all types of changes in the graph of its motion (change in the law, travel, phase, etc.).

Devices can be provided in the mechanism which help in changing the parameters of the mechanism only during its stationary state or during its operation. We will describe here only the mechanisms of the second type.

All mechánisms with two degrees of mobility and with two driving links, and thus having two independent input motions serve as the model for mechanisms which are adjusted during operation. One of the driving links, known as the driving link of the adjustable mechanism, moves constantly and imparts the main, i.e. working motion to the driven link while the second driving link known as the regulating link moves only during the process of regulation and imparts additional motion or the motion of regulation to the driven link: it remains stationary at a fixed position for the rest of the period.

By fixing the regulating link at various positions, we can obtain different types of motion of the driven link.

It is clear from this that the mechanism which is regulated during operation can be taken as a mechanism with one degree of mobility during the process of accomplishment of a specific operation and as a mechanism with two degrees of mobility during the process of regulation.

Fixing one of the driving links of a mechanism with two degrees of mobility at various positions is equivalent to changing parameters of the mechanism with one degree of mobility during operation. Thus single contour three-dimensional mechanisms which are adjusted during operation, can be obtained from single-contour mechanism with one degree of mobility only by increasing their mobility. To accomplish this, kinematic pairs of the mechanism must be replaced by other pairs by reducing the number of constraints in them.

For example if we replace every turning or sliding pair by the cylindrical pair the degree of freedom of the pair increases by one, leading to an increase in the mobility of the mechanism. If necessary, we may replace every cylindrical pair by one turning and sliding pair by introducing one additional link D in the mechanism (Fig. 1).

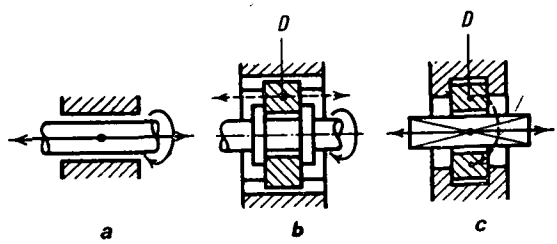

Fig. 1.

Let us explain the meaning of the term parameters of a mechanism.[1] The term kinematic dimensions of a given link of a mechanism signifies the shortest distance and angle between the fixed axes of its kinematic elements; let us call them linear and angular dimensions of the link respectively. If the elements of a given link are cylindrical surfaces, i.e. if the link forms with other two links cylindrical pairs whose axes in the general case do not intersect, such a link simultaneously possesses linear and angular dimensions.

When these axes are parallel or intersecting the link has only linear or angular dimensions respectively.

Obviously, if the linear and angular dimensions of a link are simultaneously equal to zero, it will not have any effect on the kinematics of the mechanism. The link, whose elements have spherical and cylindrical or two spherical surfaces, also possesses linear dimensions. In the first case, the distance between the center of the sphere and axis of the cylinder is the dimension of the link while in the second case, dimension of the link represents the distance between the centers of the two spheres. Linear and angular dimensions of the link are known as linear and angular parameters of the link.

By the term distance and angle between the links forming a kinematic pair, we mean the shortest distance and angle between the segments representing linear parameters of these links.

The distance and angle between the links of a cylindrical pair absolutely define their elative position. If the position of the links along or about the axis of the pair remains unchanged, i.e. fixed, we have the turning or sliding pair in place of cylindrical pair. We will call the unchanged distance between links along the axis, the parameter of a turning pair and

[1] Here, we mean constant parameters of the mechanism.

the constant angle about the axis, the parameter of a sliding pair. This means that the turning pair has linear parameter and the sliding pair angular parameter.

The ratio of the displacements of one link relative to the other along and about the axis of the pair is taken as the parameter of a screw pair.

Thus turning, sliding and screw pairs are the particular cases of a cylindrical pair. Cylindrical and spherical pairs do not have any parameter.

Number of parameters of a mechanism denotes the sum of parameters of all the links and pairs constituting the mechanism. For example, the seven-link mechanism with only turning pairs has in the general case 21 parameters. Of them, 14 are linear and angular parameters of the links while the remaining seven are linear parameters of the turning pairs.

It is not necessary that all the parameters of the mechanism should have an effect on the law of motion of its driven link. Consequently, it should be clarified in the given mechanism and the parameter to be regulated should be selected only afterwards. It should also be noted that it is relatively easy to change certain parameters of the mechanism during operation while it is more complicated to change some other parameters.

While the mechanism is under operation it is more difficult to change the parameters of moving links or parameters of the pairs whose axes continuously change their position in space than the parameters of a fixed link of pairs whose axis remains stationary since only the latter links and pairs have a free approach. In most cases, it is more appropriate to regulate the motion of the driven link in such a manner that kinematic dimensions of the stationary link remain unchanged. The driving or driven link can be rearranged with respect to support (change of parameters of the pairs with fixed axes) for regulating the motion of the driven link. Then it will be the simplest method of regulating three-dimensional single-contour mechanisms.

In this article, the driving and driven links of the mechanism form cylindrical pairs with the stationary link since the turning and sliding pairs can always be obtained as a particular case of cylindrical pair. Let us consider two methods of regulating single-contour mechanisms.

1. Regulation by Rearranging the Driving or Driven Link along its Fixed Axis

This method is used in three-dimensional cam mechanisms [1] but can be applied to other lever mechanisms as well. It is used in that case when the main motion of the link being adjusted is rotary motion while the regulating motion is rectilinear. If the driving link is rearranged, then it is assumed that the motor shaft and driving shaft of the mechanism are connected by the help of couplings which allow axial displacement of one

shaft relative to the other, for example by splined joint, clutch coupling, etc. Similar coupling is provided between the driven shaft of the mechanism and driving shaft of the operating machine on rearranging the driven link.

2. Regulation by Rearranging the Driving or Driven Link about its Fixed Axis

Such a method was tried by the author of this paper [2] in one of the three-dimensional lever mechanisms shown in Fig. 2. It is used in that case when the main motion of the adjustable link is rectilinear and the regulating motion is rotary.

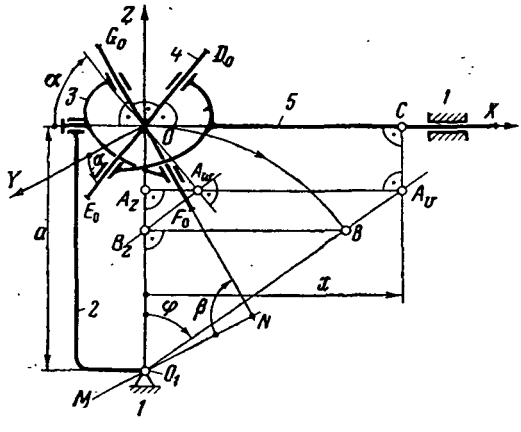

Fig. 2.

The adjustable link forms with the support a cylindrical pair which if necessary can be replaced by turning and sliding pairs in the case of the first method of regulation according to Fig. 1, b and according to Fig. 1, c in the case of the second method. It is obvious from Fig. 1 that the kinematic pair formed by the additional link *D* with the stationary link can be made as a screw pair in place of a turning or sliding pair. Kinematics of the mechanism does not change in this.

Let us demonstrate these two methods using simple three-dimensional mechanism as examples.

Example 1. Fig. 2 shows the kinematic scheme of a three-dimensional five-link mechanism with one turning (*2-3*) and four cylindrical (*1-2, 3-4, 4-5, 1-5*) pairs which has been studied in article [2]. This mechanism has three degrees of mobility. Displacement of the driven link *5* along *x*-axis is expressed by the equation:

$$x = a\sin^2\alpha\sin\varphi + (a\cos^2\alpha - b\sin\alpha\cos\alpha)\tan\varphi, \qquad (1)$$

where α—angle between links *5* and *1* defined by the angle between axis D_0E_0 of pair *4-5* and axis OY;

φ—angle of rotation of the driven link *2* about fixed axis $MN \parallel OY$;

a—linear dimension of links *1* and *2*;

b—distance of link *2* relative to link *1* when link *2* is displaced along axis MN in the positive direction of axis OY.

The mechanism shown in Fig. 2 was studied in article [2] in the position when $b=\text{const}=0$. The angle β between links *3* and *2* is defined by the angle between axes MN and G_0F_0. The relation between angles α and β is expressed by the formula:

$$\cot \alpha = \tan \beta \cos \varphi. \qquad (2)$$

As in article [2], expressions (1) and (2) are obtained on projecting the mechanism on $\angle OX$ and $\angle OY$ planes.

Motion of link *5* along *X*-axis is regulated in the case of the given law of change of φ by rearranging link *2* along axis *MN*, i.e. by changing the distance b and by rearranging link *5* about *X*-axis (by changing angle α).

If the distance b is fixed and the cylindrical pair of links *1* and *2* is changed into a turning pair, we get a mechanism with two degrees of mobility. after fixing angle α, we change the cylindrical pair of links *1-5* into a sliding pair and we get a mechanism with one degree of mobility.

Thus the mechanism (see Fig. 2) has two parameters b and α which can be regulated during operation and the mechanism serves for converting the oscillating rotary motion of link *2* with a given angle of oscillation into oscillating rectilinear motion of link *5* with variable travel.

Fig. 3 shows the kinematic scheme of a plane mechanism with adjustable parameter α which facilitates the same motion of driven link *5* as the three-dimensional mechanism at $b=\text{const}=0$ (see Fig. 2). The two-dimensional mechanism kinematically equivalent to the three-dimensional mechanism was obtained in the following way. In the beginning, points O_1, O, C, A_v, A_w, A_z, B_z, B (see Fig. 2) were found by superposing Fig. 2 over Fig. 1 in such a manner that the similar points O, A_z and B_z coincided on the two figures [2]. Then the plane mechanism was designed which could reproduce exactly the same motion of points C, A_v, A_w, A_z, B_z, B as the three-dimensional mechanism.

Let us compare the plane mechanism obtained (see Fig. 3) with the three-dimensional mechanism (Fig. 2).

If they are taken as mechanisms with two degrees of mobility (φ and α change), then the plane mechanism will have ten moving links, six turning and eight sliding pairs while the three-dimensional mechanism after substituting its cylindrical pairs (*3-4*, *4-5*, *5-1*) in accordance with Fig. 1 by turning and sliding pairs, will have seven moving links, five turning and three sliding pairs.

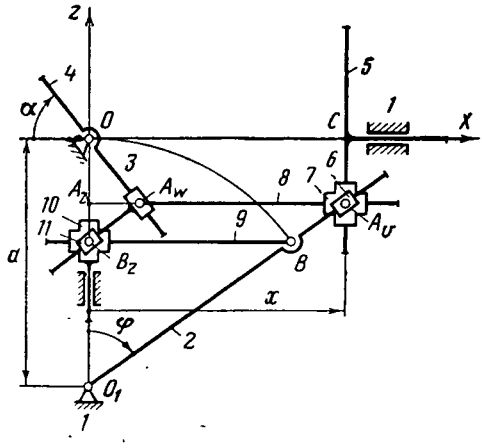

Fig. 3.

If we consider them as mechanisms with one degree of mobility (α is fixed) we have nine moving links, five turning and eight sliding pairs for the plane mechanism and six moving links, four turning and three sliding pairs for the three-dimensional mechanism.

This data confirms the suitability of three-dimensional adjustable mechanisms in place of plane adjustable mechanism, in this case.

Consequently, study and application of three-dimensional adjustable mechanisms deserves special attention.

If link *3* is fixed to link *2* (see Fig. 2), i.e. if angle β is fixed at various positions, as shown by L. N. Reshetov [3], we again get link *5* in various motions.

It follows from formulas (1) and (2) that at a given value of angle β, distance x and angle α are variables at the same time, i.e. in order for the mechanism to have one degree of mobility, pair *1-5* must be cylindrical.

Thus, we have a four-link mechanism with one turning (*1-2*) and three cylindrical (*3-4*, *4-5*, *5-1*) pairs.

It should be kept in mind that it is easy to fix angle β at various positions in a stationary mechanism and it should be used in that case when in addition to the regulation of motion of link *5* along *X*-axis, it is necessary to change its oscillation about this axis.

It is seen from equation (2) that α does not depend on *b*. Therefore, if it is necessary to regulate the motion of link *5* only along *X*-axis, link *2* should be rearranged along *MN* axis, i.e. *b* should be changed during the stationary or moving state of the mechanism.

At $\alpha=90$ and 0°, according to expressions (2) and (1), pair *2-3* no longer exists and we get a plane mechanism whose driven link moves independent of parameter *b*.

Thus, when a three-dimensional mechanism is converted to a plane one, motion of the driven link is not regulated by rearranging the driving link along the stationary axis of its rotation.

Example 2. In contrast to the single Carden joint in the mechanism schematically shown in Fig. 4, all the pairs are cylindrical and axes of the pairs *1-4* and *3-4* skew at that place where the verticle segment $OM=a_4$ is the shortest distance; the driving fork *1* is displaced from point *M* along the axis of the pair *1-4* by S_{14}. The *X*, *Y*, *Z* axes form a rectangular system of coordinates on the right hand side.

If pair *1-4* is made turning ($S_{14}=\text{const}$) and fork *1* is rotated, the links of pairs *1-2*, *2-3* and *3-4* move along a spiral. This mechanism is a particular case of the mechanism considered in article [4].

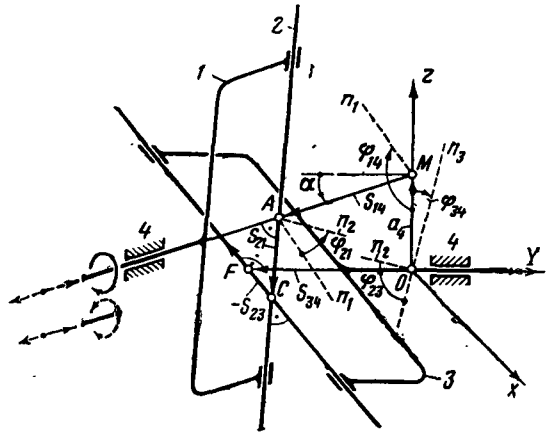

Fig. 4.

According to data [4], the relative motion of links of the mechanisms (see Fig. 4) is expressed by the following equations:

$$\tan\varphi_{34}=-\cos\alpha\cot\varphi_{14}; \tag{3}$$

$$\cos\varphi_{23}=\sin\alpha\cos\varphi_{14}; \tag{4}$$

$$\sin\varphi_{21}=\lambda\cos\alpha; \tag{5}$$

$$S_{34}=-a_4\lambda^2\sin\alpha\sin\varphi_{14}\cos\varphi_{14}+S_{14}\lambda^2\cos\alpha; \tag{6}$$

$$S_{23}=-a_4\lambda\cos\alpha\cos\varphi_{14}-S_{14}\lambda\sin\alpha\sin\varphi_{14}; \tag{7}$$

$$S_{21}=a_4\lambda^2\sin\varphi_{14}-S_{14}\lambda^2\sin\alpha\cos\alpha\cos\varphi_{14}, \tag{8}$$

where $\lambda=1/\sqrt{1-\sin^2\alpha\cos^2\varphi_{14}}$,

φ_{14}—angle of rotation of the driving link *1* about fixed axis *AM*, defined by the angle between segment *MO* and normal Mn_1 to the plane of the fork *1*;

α—angular dimension of the stationary link *4*;

φ_{34}—angle between links *3* and *4* corresponding to the angle between the segment *OM* and normal On_3 to the plane of the fork *3*;

φ_{23}—angle between links *2* and *3* defined by the angle between normals On_2 and n_3O to planes of the cross *2* and fork *3*;

φ_{21}—angle between links *2* and *1* which is determined with the help of the angle between normals An_1 and An_2 to planes of the fork *1* and cross-shaped link *2*;

$S_{34}=OF$—segment representing the position (displacement) of link *3* relative to link *4* along the axis of the pair *3-4*;

$S_{23}=CF$—segment showing the displacement of link *2* relative to link *3* along the axis of the pair *2-3*;

$S_{21}=AC$—segment corresponding to displacement of link *2* relative to link *1* along axis of the pair *2-1*.

Reference points for angles and segments are shown by arrows in Fig. 4.

If the main motion of the driving link *1* is rotary, then to change the law of motion of the driven link *3*, it is possible to apply the first method of regulation, i.e. rearrange the driving link *1* along the axis *AM* (change of parameter S_{14}).

It is obvious from expressions (3)-(8) that only linear displacements (S_{34}, S_{23} and S_{21}) will be regulated in this case.

Fig. 5 shows graphs of motion of link *3* along *OF* axis depending on angle of rotation φ_{14} of the driving link *1* but at various values of the regulated parameter S_{14}. In this figure curve *4* corresponds to the value $S_{14}=60$ mm,

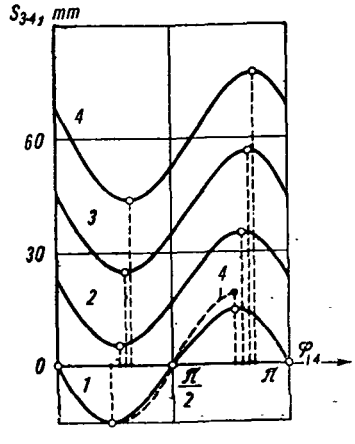

Fig. 5.

curve *3* to 40 mm, curve *2* to 20 mm and curve *1* to 0 mm.

Thus, in the case of the first method of regulation, the four-link mechanism with four cylindrical pairs helps in converting the given rotary motion into spiral motion by changing the travel of the driven link along the axis of its rotation.

This mechanism is changed into a plane mechanism at $\alpha=0$ and 90°.

In the first case ($\alpha=0$), the driven link *3* is capable of rotary motion only and this cannot be regulated by changing S_{14} since φ_{34}, in accordance with expression (3), does not depend on S_{14} while in the second case ($\alpha=90°$), the driven link accomplishes only rectilinear motion which also does not depend on S_{14}.

If the main motion of the driving link *1* is rectilinear, then by changing the law of motion of the driven link *3*, it is possible to use the above mentioned second method of regulation, i.e. by the rearrangement of the driving link *1* about the axis *AM* (change of parameter φ_{14}).

It is obvious from equation (3)-(8) that if $\varphi_{14}=\text{const}$ and if S_{14} changes according to the given law, then there can be only rectilinear relative motion of the links in all the pairs, i.e. we have a three-dimensional four-link mechanism with four sliding pairs.

In the particular case, when $\varphi_{14}=0$, the condition $S_{23}=-a_4=\text{const}$ is satisfied, i.e. there is no sliding pair *2-3* and the links *2* and *3* are taken as one link while at $\varphi_{14}=90°$, $S_{21}=a_4=\text{const}$. In this case, the sliding pair *1-2* does not exist and the links *1* and *2* are taken as one link.

Consequently, the three-dimensional four-link mechanism with four sliding pairs gets converted at $\varphi_{14}=0$ and 90° into a plane three-link mechanism with three sliding pairs.

At a given displacement of the driving link *1*, we get various displacements of the driven link *3* (see Fig. 6) by fixing the link *1* about axis *AM* at various positions.

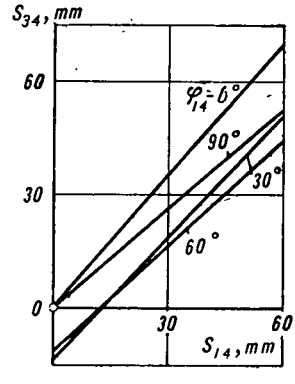

Fig. 6.

Thus, in the case of the second method of regulation, the four-link mechanism with four cylindrical pairs converts the reciprocating motion into reciprocating motion with adjustable displacement.

References

1. Reshetov, L. N. Kulachkovye mekhanizmy (Cam Mechanisms). Mashgiz, 1953.
2. Kasamanyan, A. A. Mekhanizm s reguliruemoi kharakteristikoi (Mechanism with controllable characteristic). *Izv. vuzov. Mashinostroenie,* No. 9, 1966.
3. Reshetov, L. N. Konstruktirovanie ratsional'nykh mekhanizmov (Design of Rational Mechanisms). Mashgiz, Moscow, 1967.
4. Kasamanyan, A. A. Opredelenie otnositel'nykh peremeshchenii zven'ev odinarnogo sharnira Kardana s bol'shimi lineinymi otkloneniyami (Determination of relative displacements of links of a single Kardan joint with linear deviations). *Izv. vuzov. Mashinostroenie,* No. 10, 1966.

A. E. Kropp

SYNTHESIS OF A TOOTHED LEVER TRANSMISSION MECHANISM

The gear box described in article [1] is often used in a mechanism which provides stepless regulation of torque and velocity of the shaft of the operating machine without use of any frictional devices. The design of one of the possible mechanisms (Fig. 1) consisting of body *1*, *2* and *3* with pressed rims *4* on the inner surface of which sufficiently small triangular teeth are cut is described below. The pole along with body *5* and cover *6* is mounted in the body of the mechanism on bearings *7*. The body of the pole *5* is connected to the driven shaft *8* by a key. A sun wheel consisting of two semihelicals *10* and *11* is mounted on the splines of shaft *9* which is the driving shaft of the mechanism. The pole is provided with three axes of planet wheel *12*. Planet wheel *13* and *14* are installed on each axis and the planet wheel *14* is geared with semihelical *10* and sits freely on the axis *12*. The axis *12* has two eccentric journals on which eccentric sleeves *15* are installed.

Grooves are made on the faces of sleeves *15*, facing the planet wheel *14*. Similar grooves are made on the faces of naves of the planet wheel *14*. Sleeves *15* are connected to planet wheel *14* with the help of floating disks *16* having projections which fit into the corresponding grooves of the faces of planet wheel *14* and sleeves *15*.

Fig. 1 shows that catches (projections) on the left face of the floating disk *16* are made perpendicular to the similar projections on the right face. Thus, the joint of sleeve *15* with planet wheel *14* forms Oldham's coupling.

Levers *23* on bearings *22* are mounted on sleeves *15*. At the other end of the lever, there is a hole for pin *24* on which shoe *25* is installed. Surface of the shoe *25* conjugating with rim *4* is provided with small triangular teeth of pitch and profile equal to the corresponding parameters of teeth on rim *4*. Position of shoe *25* is restricted by stop *26*. Shoe *25*

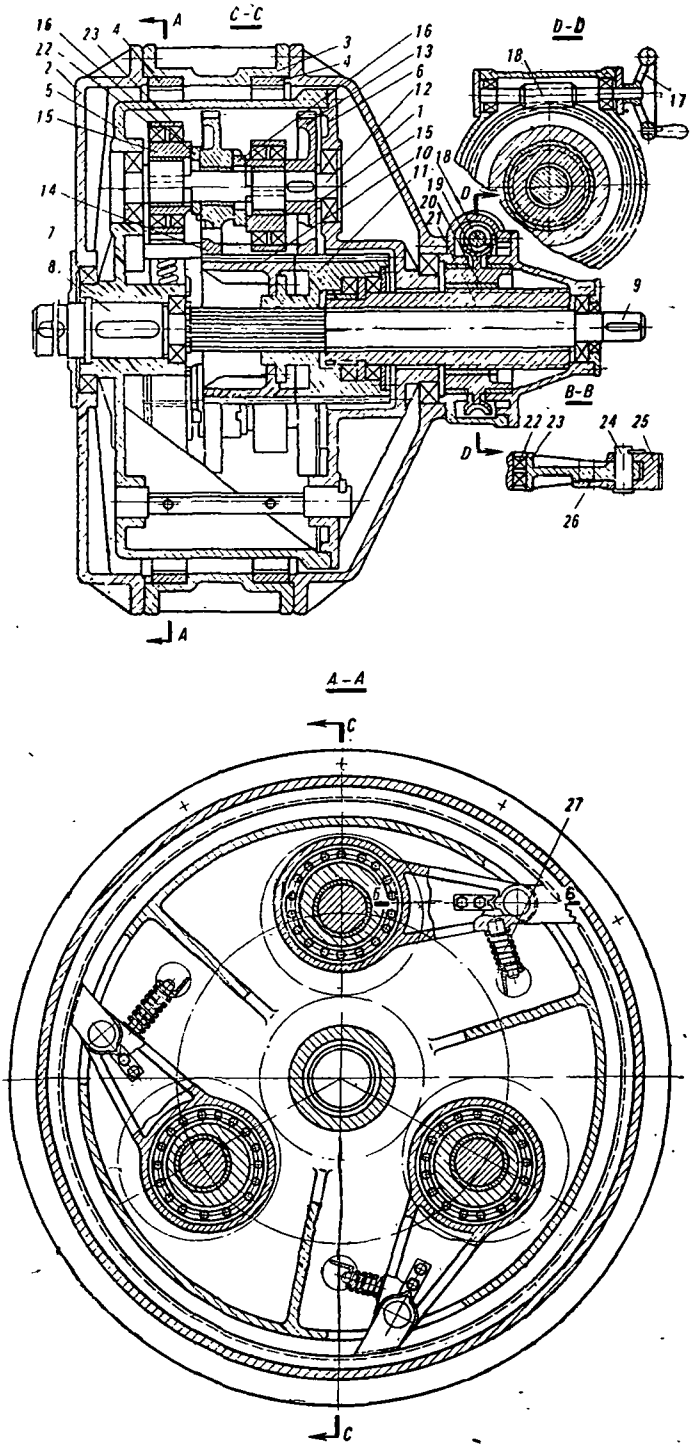
C-C
D-D
B-B
A-A
A
C
D
16
23
4
22
2
5
15
14
7
8
3
4
16
13
6
12
1
15
10
11
18
19
20
21
18
17
9
22
23
24
25
26
27
6

Fig. 1.

is pressed to rim *4* by the spring *27*. The sun wheel consisting of semihelicals *10* and *11* can move along splines of driving wheel *9* with the help of flywheel *17*, worm gears *18* and *19*, screw and nut *20* and *21*.

Let us differentiate between the two mechanisms described in the design: the main mechanism consisting of a system of four-link mechanisms and transmitting motion from the driving shaft to the driven link, and the regulating mechanism regulating the speed of rotation of the driven link.

The gear ratio is regulated by changing the radius of total eccentricity of the position of levers *23* on the axis of planet wheels *12*. For this purpose, two screw pairs with opposite directions of helix angles of the screw threads are used. One of the semihelicals forms a screw pair with planet-wheel, for example, with the right hand direction of the helix angle while the other two similar components form the screw pair with the left hand direction of the helix angle of the teeth. Therefore, axial displacement of semihelicals in one direction gives rise to rotation of planet wheels in different directions.

Relative rotation of the planet wheels changes mutual position of the radii of eccentricity of the planet-wheel shaft journal, and of the eccentric sleeve *15* which changes the total eccentricity of levers *23*.

The ratio of radii of the eccentrics on shaft *12* and sleeve *15* determines the dependence of gear ratio of the mechanism on the position of the regulating device.

As a matter of fact, total eccentricity of lever (Fig. 2a):

$$r^2=\rho_1^2(1+k_1^2+2k_1\cos\alpha),$$

where $k_1=\rho_2/\rho_1$ is the ratio of radii of eccentrics ρ_2 and ρ_1 and α is the angle of their relative rotation.

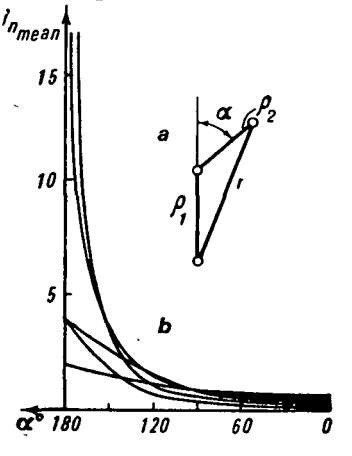

Fig. 2.

Then, in the case of incomplete rotation of the driving link, the average gear ratio of the four-link mechanism will be:

$$i_{n_{av}}=R/r,$$

where R is some constant.

The relationships:

$$i_{n_{av}}=f(\alpha, k_1)$$

are shown in Fig. 2, b for $R/\rho_1^2=1$.

This property of a transmission mechanism can be useful in the drive of various types of machines.

For example, in the case of a transport vehicle, it is very important to get traction characteristics similar to rectangular hyperbolas. It may be observed that when $k_1=1$, hyperbola and curves similar to it ($k_1=0.75$) and shown in Fig. 2, b provide traction characteristics suitable for transport vehicles.

Let us examine the operation of four-links of the main mechanism. The angle of rotation of the driving link to which the pole moves under the effect of the four-link mechanism under reference, will be known as the active travel and the given four-link mechanism of the angle of rotation of the driving link to which the pole rotates under the action of other four-link mechanisms will be known as the idle travel.

Every four-link mechanism (see Fig. 3) during active travel represents a double yoke mechanism with a driving connecting rod in which:

1) driven link *OA* is equal to the distance between centers of the wheel and driven wheel;

2) driving link *AB* corresponds to the total radius of eccentric position of the lever on the planet wheel axis;

3) link *BC* is equal to the length of lever (as applicable to this mechanism—distance from the center of the bore for bearing *22* to the axis to the hole for pin *24*, see Fig. 1);

4) link *OC* (support) is equal to the distance between the centers of the sun wheel and end of the lever (axis of the hole for pin *24*).

Periodic fluctuations in the velocity of the driving link are observed in toothed lever transmission mechanisms. The period of these fluctuations is equal to the active travel of one of the four-link mechanisms while the dependence of the velocity of the driven link on the angle of rotation of the driving link during active travel is represented by the curve having single maxima [2].

Accomplishment of active travel by the four-link mechanism under examination (for example $OA_2B_2C_2$) is defined by the property of this mecha-

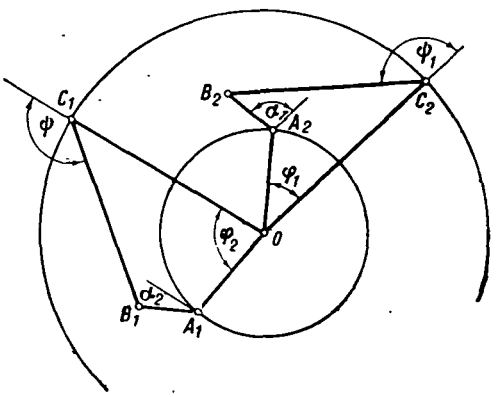

Fig. 3.

nism to impart a velocity more than that which can be imparted to the driven link by any other four-link mechanism during active travel.

Thus, operation of the main mechanism includes successive materialization of active travel by every four-link mechanism. In the design examined here, there are 6 four-link mechanisms with phase differences in the operation equal to 60°. From the point of view of design this phase difference is provided in the following way: phase difference between cranks situated on one shaft of the planet wheel is equal to 180° while the phase difference between cranks on neighboring shafts is equal to 120°.

It may be observed from the previously mentioned facts that if k is the number of four-link mechanisms in the main mechanism, then rotation of the driving link through an angle:

$$\Delta\alpha_a = 2\pi/k = \alpha_2 - \alpha_1 \tag{1}$$

during active travel, leads to a rotation of the driven link OA through:

$$\Delta\varphi_a = \varphi_2 - \varphi_1. \tag{2}$$

During the idle travel, i.e. during rotation of the driven link through an angle:

$$\alpha_z = 2\pi - 2\pi/k, \tag{3}$$

the four-link mechanism under reference represents a crank yoke mechanism with column OA in the motion relative to the pole.

Let us call the positions of two four-link mechanisms at which the active travel comes to an end in one (for example in four-link mechanism $OA_1B_1C_1$) while its starts in the other [four-link mechanism $OA_2B_2C_2$ (see Fig. 3)] as moment of conjugation.

It is known that during operation of toothed lever and other similar mechanisms, the phenomenon of run down (see for example [2, 3]) may arise when velocity of the driven link at some sections of active travel is greater than that expected from kinematic relations which do not take into account the dynamic properties of the system motor-transmission mechanism-operating machine.

The run down shifts the beginning and end of the active travel by keeping its duration unchanged during steady motion and displaces the moment of conjugation towards velocities greater than those expected in the absence of run down.

Since all four-link mechanisms of the main mechanism have the same dimensions, diagrams of velocity of the driven link in the absence of run down during active travel due to the action of various four-link mechanisms are identical. The diagrams of velocity of the driven link due to various four-link mechanisms are also identical in the case of steady motion and in the presence of run down.

The possibility of providing moment of conjugation at equal angular velocities of the driven link at the beginning ω_{A_1} and the end ω_{A_2} of the active travel, i.e. at

$$\omega_{A_1}=\omega_{A_2} \tag{4}$$

is the consequence of this.

Satisfaction of condition (4) is very important for operation of a mechanism since it greatly reduces impact at the moment of conjugation. Equation (4) is satisfied if:

$$\Delta\varphi_a=zt_y, \tag{5}$$

where z is the number of teeth on the rim; and t_y is the angular pitch of teeth.

It is not difficult to see that condition (5) can be easily satisfied for some calculation schedule (for example, in the absence of run down). In the presence of run down, the deviation $\Delta\varphi_a$ from the calculated value appears.

Thus, equation (5) is not satisfied in the presence of run down and active travel starts at:

$$\omega_{A_2}>\omega_{A_1}.$$

To reduce the difference:

$$\omega_{A_2}-\omega_{A_1}=\Delta\omega, \tag{6}$$

it is necessary to decrease the pitch of the teeth on the rim and one should try to get accelerations of the driven links of both the four-link mechanisms at the moment of conjugation close to zero if possible.

It is not difficult to point out (see Fig. 3) that direction of rotation of the driven link is defined by the position of point C of the four-link mechanism relative to the driving link and does not depend on the direction of its rotation.

To obtain reverse for the driven link, the lever must have two arms. Only one arm should be put into operation with the help of a special device which should act depending upon the direction of rotation of the driving link. It was, for example, done in article [4].

If their number is known and if $\Delta\varphi_a$ is given, synthesis of four-link mechanisms of the main mechanism leads to the problem of synthesis according to positions by taking into account some additional conditions.

Let us put (see Fig. 3)

$$OC/OC=1; \quad OA/OC=c; \quad AB/OC=a; \quad BC/OC=b.$$

Considering the links as vectors and eliminating angle ψ, we get the equation in a form similar to that described in article [5]:

$$b^2-c^2-a^2-1=2[ac\cos(\alpha-\varphi)-c\cos\varphi-a\cos\alpha]. \tag{7}$$

Equation (7) is written for two positions, i.e. for the beginning and end of the active run. After solving the equations simultaneously and after transformations, we get:

$$a=c\sin\varphi_{aver}\cdot\sin\Delta\varphi_a/2/(c\sin\gamma\cdot\sin\theta-\sin\alpha_{aver}\cdot\sin\Delta\alpha_a/2); \tag{8}$$

$$b=\sqrt{1+c^2+a^2+2[ac\cos(\gamma-\theta)-c\cos(\varphi_{aver}-\Delta\varphi_a/2)-a\cos(\alpha_{aver}-\Delta\alpha/2)]}, \tag{9}$$

where $\alpha_{aver}=(\alpha_2+\alpha_1)/2$ and $\varphi_{aver}=(\varphi_2+\varphi_1)/2$; $\gamma=\alpha_{aver}-\varphi_{aver}$ and $\theta=\Delta\alpha_a/2-\Delta\varphi_a/2$; α_1, φ_1 and α_2, φ_2 are the angles in the four-link mechanism (see Fig. 3) referring to the beginning and end of the active run respectively.

Let us take equation (4) in the absence of run down as one of the additional conditions. Since:

$$\omega_A=d\varphi/d\alpha\cdot\omega_B,$$

where ω_B is the angular velocity of the driving link, equation (4) takes the form:

$$(d\varphi/d\alpha)_1=(d\varphi/d\alpha)_2, \tag{10}$$

where indices 1 and 2 correspond to the beginning and end of the active run.

Differentiating equation (7), we get:

$$d\varphi/d\alpha=a/c[(c\sin(\alpha-\varphi)-\sin\alpha)/(a\cdot\sin(\alpha-\varphi)+\sin\varphi)]. \tag{11}$$

Then after transforming equation (10) and keeping in mind the notations used in formulas (8) and (9), we get:

$$c[\sin(\gamma-\theta)\sin(\varphi_{aver}+\Delta\varphi_a/2)-\sin(\gamma+\theta)\sin(\varphi_{aver}-\Delta\varphi_a/2)]$$
$$-a[\sin(\gamma+\theta)\cdot\sin(\alpha_{aver}-\Delta\alpha_a/2)-\sin(\gamma-\theta)\sin(\alpha_{aver}+\Delta\alpha_a/2)]$$
$$-[\sin(\alpha_{aver}-\Delta\alpha_a/2)\sin(\varphi_{aver}+\Delta\varphi_a/2)-\sin(\alpha_{aver}+\Delta\alpha_a/2)$$
$$\times\sin(\varphi_{aver}-\Delta\varphi_a/2)=0. \tag{12}$$

It may be readily discerned that it is not possible to synthesize four-link mechanisms according to relationships (8), (9) and (12) since no conditions have been imposed on the selection of angles α_{aver} and φ_{aver}.

While regulating the gear ratio of a toothed lever mechanism, dimensions of the driving link change at constant parameters of the remaining links. We will take value of the angles $\Delta\varphi_a$ at which synthesis of four-link mechanisms of main mechanism is possible as the optimum value and denote it by $\Delta\varphi_{a_0}$. The driving link corresponding to $\Delta\varphi_{a_0}$ will be denoted by a_0.

Let us determine $a\neq a_0$ in the absence of run down and in the case of known values of b, c, k, $\Delta\varphi_a\neq\Delta\varphi_{a_0}$.

Solving equation (7) with respect to a and writing it for the initial position of the active run, we get:

$$a=[\cos\alpha_1-c\cos(\alpha_1-\varphi_1)]+$$
$$\sqrt{[\cos\alpha_1-c\cos(\alpha_1-\varphi_1)]^2+2(c\cos\varphi_1+H)}, \tag{13}$$

where $H=(b^2-c^2-1)/2$.

Writing equation (13) for the end position of the active run, we have:

$$[\cos\alpha_1-c\cos(\alpha_1-\varphi_1)]+\sqrt{[\cos\alpha_1-c\cos(\alpha_1-\varphi_1)]^2+2(c\cos\varphi_1+H)}$$
$$=[\cos\alpha_2-c\cos(\alpha_2-\varphi_2)]+\sqrt{[\cos\alpha_2-c\cos(\alpha_2-\varphi_2)]^2+2(c\cos\varphi_2+H)}, \tag{14}$$

where α_2 and φ_2 are determined from formulas (1) and (2).

Finally, condition (4) gives:

$$(c\sin(\alpha_1-\varphi_1)-\sin\alpha_1)/(a\sin(\alpha_1-\varphi_1)+\sin\varphi_1)=\{c\sin[(\alpha_1-\varphi_1)$$
$$+(\Delta\alpha_a-\Delta\varphi_a)]-\sin(\alpha_1+\Delta\alpha_a)\}/\{a\sin[(\alpha_1-\varphi_1)+(\Delta\alpha_a-\Delta\varphi_a)]$$
$$+\sin(\varphi_1+\Delta\varphi_a)\}. \tag{15}$$

It should be noted that in the absence of run down, condition (4) is satisfied only if equation (5) is valid. While analyzing the operation of a toothed lever mechanism, it is necessary to know the value of $\varphi=f(\alpha)$ for every four-link mechanism. This is obtained from equation (7) at known parameters of the links and at the given initial position in the form

$$\varphi=\arcsin[D/(1+T^2)+\sqrt{D^2/(1+T^2)^2-(D^2-T^2)/(1+T^2)}], \tag{16}$$

where

$$D=[ac\cdot\cos(\alpha_1-\varphi_1)-c\cdot\cos\cdot\varphi_1+a(\cos\alpha-\cos\alpha_1)]/ac\cdot\sin\alpha;$$
$$T=(a\cdot\cos\alpha-1)/a\sin\alpha.$$

From equation (11), after transformation, we get:

$$d^2\varphi/d\alpha^2 = a/\{c[a\cdot\sin(\alpha-\varphi)+\sin\varphi]^2\}\{\sin\varphi[a+c\cos(\alpha-\varphi)-\cos\alpha] - d\varphi/d\alpha\cdot\sin\alpha[a\cdot\cos(\alpha-\varphi)+c-\cos\varphi]\}. \quad (17)$$

Conclusions

1. The article describes a toothed lever transmission mechanism which assists in the alteration of the velocity and torque on the driving shaft of the operating machine without using any frictional devices.

2. It has been shown that the required dependence of gear ratio of the mechanisms on the position of the regulating organ can be obtained within wide limits. In particular, use is made of this property of the mechanism for getting the regulated traction characteristic of transport vehicles.

3. Calculation equations are given for the synthesis of four-link mechanisms of the main mechanism at the given average value of gear ratio for the case of operation of the transmission mechanism without run down.

4. In the case of operation of the transmission mechanism without run down, relationships have been calculated for the synthesis of four-link mechanisms of the main mechanism at given parameters of some links and at variable average gear ratio.

5. Relations of velocities and accelerations of the driven link are given for these schedules of operation of the transmission mechanism.

References

1. Kropp, A. E. Kinematika vzaimodeistviya khrapovika s khrapovym ventsom v impul'snykh planetarnykh reduktorakh i variatorakh (Kinematics of interaction between ratchet and ratchet wheel in pulse planetary gear boxes and variators). Sb. *Peredatochnye mekhanizmy*, Izd-vo Mashinostroenie, 1966.
2. Mal'tsev, V. F. Impul'snye variatory (Pulse Variators). Mashgiz, 1963.
3. Pilipenko, M. N. Mekhanizmy svobodnogo khoda (Free Motion Mechanisms). Izd-vo Mashinostroenie, 1966.
4. Kropp, A. E. Impul'snyi planetarnyi reduktor. Avt. svid. No. 151538 (Impulse planetary gear box. Author's patent No. 151538). *Byull. izobretenii,* No. 21, 1962.
5. Artobolevskii, I. I. Teoriya mekhanizmov i mashin (Theory of Mechanisms and Machines). Mashgiz, 1952.

V. I. Kulyugin

DESIGN OF THREE DIMENSIONAL FOUR-LINK MECHANISMS CONFORMING TO THE TRAVEL OF THE DRIVEN LINK AND COEFFICIENT OF INCREASE IN VELOCITY OF THE REVERSE STROKE

This article is concerned with graphical and analytical techniques based on G. G. Baranov's [1] method of solving problems of synthesis of a three-dimensional crank yoke mechanism in accordance with the travel of the driven link and coefficient of increase in velocity of the reverse stroke. It also suggests the method of plotting zones of possible position of the hinge center, connecting crank with the support. This method facilitates geometrical as well as kinematic satisfaction of the conditions formulated in the problem.

The problem of the synthesis of plane hinged four-link mechanisms was solved by H. Alt [2] and G. G. Baranov [1]. The solution suggested by H. Alt is based on the application of the curve of centers and the curve of cyclic points.

Solution of the problem [1] based on the application of the theorem of elementary geometry concerning equality of angles included by one and the same chord in a circle is described in detail in Soviet literature.

This solution is simple and clear.

Further development of the theory of plane hinged four-link mechanisms led to differentiation of the possible position of center of hinge C, which connects crank to the support, on a circle; this provides geometrical satisfaction of the requirements formulated in the problem as well as differentiation of the arcs of a possible position of hinge C which assists in kinematic satisfaction of these conditions in addition to geometrical satisfaction. This fact is reflected in the ability of the driven link to move through a given value at the selected position of the hinge center C.

As was previously mentioned, G. G. Baranov's [1] method forms the

basis for all the known methods of solving the problem of synthesis of three-dimensional four-link mechanisms [3-5].

Graphical and analytical solution of the problem of synthesis is discussed in article [3], depending on the angle of oscillation of the yoke and the coefficient of increase in velocity of the reverse stroke of a hinged four-link mechanism in which the links directly connected to the support are arranged in mutually perpendicular planes. Graphical and analytical solution of one of the problems of synthesis of a general type of three-dimensional crank yoke mechanism is given in article [4] while graphical solution of the problem for a general type of crank gear rod under the same conditions is given in article [5].

In these articles [3-5], by utilizing Monzh projections the authors limited themselves to the study of geometrical satisfaction of these conditions.

Application of the concept of two-dimensional similarity of plane mechanism with a three-dimensional mechanism [6] leads to the solution of problems of synthesis according to the given travel of the driven link and coefficient of increase in the velocity of reverse stroke of three-dimensional mechanisms. Wide application of nomographs as well as inversion of motion helps in eliminating analytical calculations while solving the problems and makes the design more compact and clear.

Fig. 1 shows a kinematic scheme of a three-dimensional crank yoke mechanism[1] at those moments when the yoke OA exists at the extreme positions OA' and OA''.

It can be seen that:

$$\alpha_{swing}=\alpha''-\alpha', \tag{1}$$

where α_{swing}—swing angle of the yoke;

α'—angle describing the extreme position OA' of the yoke;

α''—angle corresponding to extreme position OA'' of the yoke.

It is known that the yoke exists at the extreme position if the direction of the projection of connecting rod on plane P of the rotation of crank coincides with the corresponding position of the crank.

The minimum angle ϑ between projections $A_p'B'$ and $A_p''B''$ of the connecting rod is equal to:

$$\vartheta=(\gamma_{dir}-\gamma_{rev})/2, \tag{2}$$

where γ_{dir}—angle of direct stroke of the crank (during direct stroke the crank moves from position CB' to CB'' and the yoke from OA' to OA'');

[1] Arrangement of the kinematic scheme of a three-dimensional hinged four-link mechanism adopted in this paper is the same as in article [6]. Parameters describing the kinematic scheme of the mechanism are also the same.

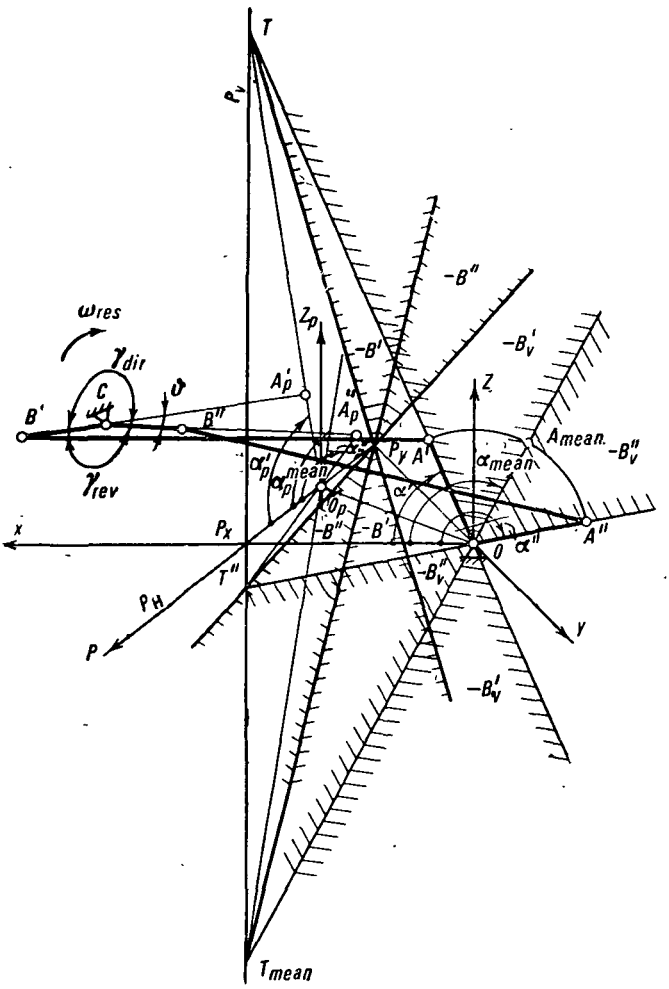

Fig. 1.

γ_{rev}—angle of reverse stroke of the crank (during reverse stroke, the crank moves from position CB'' to CB' and the yoke from OA'' to OA'). (Direction of rotation of the crank is shown in Fig. 1 by an arrow).

The coefficient k of increase in the velocity of reverse stroke denotes the ratio:

$$k=\omega_{rev}/\omega_{dir}, \tag{3}$$

where $\omega_{rev}=\alpha_{swing}/t_{rev}$—average angular velocity of rotation of the yoke during reverse stroke;

$\omega_{dir}=\alpha_{swing}/t_{dir}$—average angular velocity of rotation of the yoke during direct stroke;

t_{dir} and t_{rev}—time taken by the direct and reverse strokes of the yoke respectively.

In the case of uniform rotation of the crank BC, the coefficient k is expressed by the equation:

$$k=(180°+\vartheta)/(180°-\vartheta). \tag{4}$$

From this, the value of angle ϑ at the given value of k can be determined from the equation:

$$\vartheta=180°\cdot(k-1)/(k+1). \tag{5}$$

Let us state the first problem of synthesis of the mechanism under consideration according to the angle of oscillation of yoke and coefficient k as follows. The design for three dimensional crank-yoke four-link mechanism is required on the basis of the following data: swing sector (angle α_{swing} and length of yoke OA), plane of rotation of the crank (angle Q and parameter e) and coefficient k.

Assuming that the length of the yoke is unit values of parameters b, c, d, α' and η have to be determined. Selecting angle α', let us assign the positions of the swing sector of the yoke in the $Oxyz$ system of the coordinates. After this, we get the value of angle α'' from equation (1). Let us replace the three-dimensional mechanism under reference at positions α' and α'' by two-dimensional similar mechanisms $O_pA'_pB'C$ and $O_pA''_pB''C$ values a'_p, a''_p, α'_p, and α''_p of which are either determined from formulas or are taken from nomographs given in reference [6].

Let us begin the plotting from the drawing of projections of the swing sector of the yoke on plane P by drawing lines $O_pA'_p$ and $O_pA''_p$ in the plane of coordinates Oz_pP at angles of α'_p and α''_p and to O_pP axis and by selecting segments a'_p and a''_p on these lines (Fig. 2). Taking into account that straight lines A'_pC and A''_pC intersect at angle ϑ which can be determined from equation (5), we get the center of hinge C on the circle passing through points A'_p and A''_p making an angle equal to ϑ [1].

There will be two such circles $\lambda\lambda$ and $\beta\beta$ situated symmetrically with respect to segment $A'_pA''_p$. The point of intersection C of one of these circles with the straight line passing through point O_p at an angle η with O_pp-axis defines the location of the center of hinge C (see Fig. 2).

The length of segment O_pC will be the required value of parameter d. To determine the values of b and c, let us make use of the inversion of motion by fixing crank BC at the position $B''C$. Let us plot the relative position α' of the analog by rotating it about point C through angle γ_{rev}

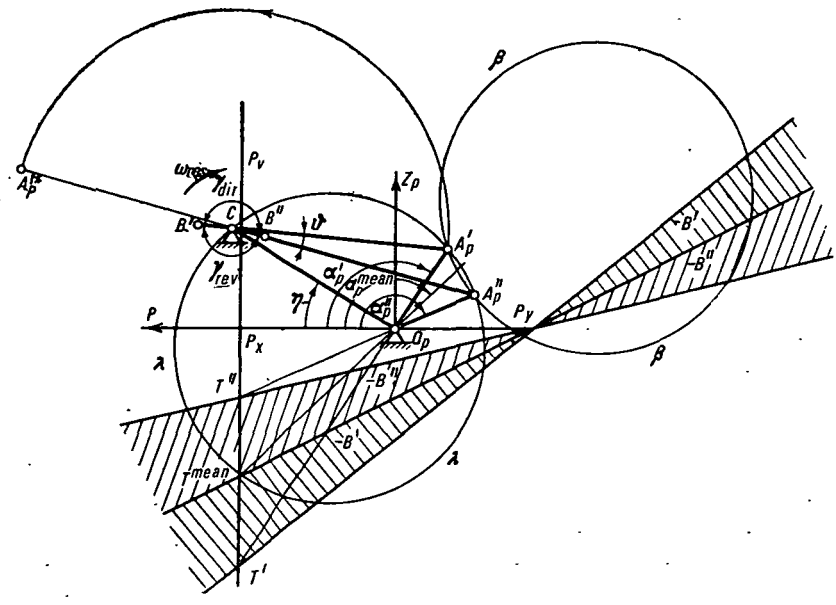

Fig. 2.

in the direction opposite to the rotation of crank. Let us denote the relative position of point A_p' by A_p^*.

Consequently, segment $CA_p'^*$ lies on segment CA_p^*. Assigning an arbitrary value to parameter b, we may draw a straight line BB'' at possible positions of the center of hinge B [6]. Point of intersection B'' of straight lines BB'' and $A_p^*A_p'^*$, becomes the center of hinge B at position B''.

We select the required value of parameter $c=CB$ and $b_p^*=B''A_p^*$ directly from the drawing (see Fig. 2). We determine the required value of parameter b from the known values of α'', Q, b_p^* and e [6].

The second problem of synthesis of the mechanism under reference according to the angle of swing of the yoke and coefficient k may be stated in the following manner.

The design for the three-dimensional crank-yoke four-link mechanism on the basis of the following data is required: swing sector of the yoke (angle α_{swing} and length of the yoke OA) plane of rotation of the crank (angle Q and parameter e), length of connecting rod AB and coefficient k.

Values of the parameters c, d, α' and η are to be determined (length of the yoke is taken equal to one).

This problem can be solved by using: a) geometrical plotting; and b) tracing paper.

The second problem is solved by using geometrical plottings in the following manner. Similar to the first problem of synthesis, from the angle

of swing of the yoke and coefficient k, projection of the sector of swing of the yoke on plane P at the selected value of angle α', circles $\lambda\lambda$ and $\beta\beta$ of the possible position of the center of hinge C are drawn in the $O_p z_p p$ system of coordinates.

With points A_p' and A_p'' as centers, let us draw circles m' and m'' of radii b_p' and b_p'' respectively. The values of b_p' and b_p'' are either determined from an equation or are taken from nomographs [6].

The center of hinge C must lie on one of the circles $\lambda\lambda$ and $\beta\beta$ in the region included between arcs of circles m' and m''. Moreover, the length of the crank BC is selected in such a manner that the trajectory of the center of hinge B touches both the circles m' and m''.

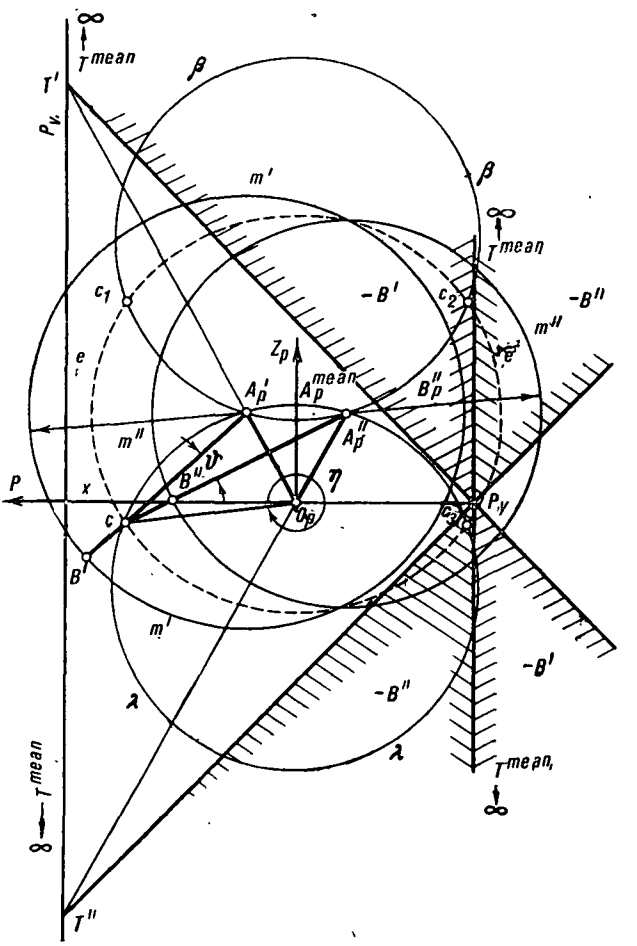

Fig. 3.

The latter condition can be satisfied only when point C lies on the ellipse ee with foci A_p' and A_p'', passing through the points of intersection of circles m' and m''. It is not difficult to verify this since sum of distances from points A_p' and A_p'' to C is always the same at the given value of B and at the selected position of the sector of swing of the yoke.

As a matter of fact, under these conditions:

$$(A_p'C+A_p''C)/OA=b_p'-a+b_p''+a=b_p'+b_p''=\text{const.}$$

The points of intersection of the ellipse ee with circles $\lambda\lambda$ and $\beta\beta$ are the places of possible locations for the center of hinge C. Let us place the center of hinge C at one of these points (Fig. 3). Connecting point C to points O_p and A_p' (or A_p'') by straight lines, directly from the drawing (Fig. 3) we get $c=CB'$ (or $c=CB''$), $d=O_pC$ and $\eta=\angle pO_pC$.

The second problem is solved by using the tracing paper in the follow-

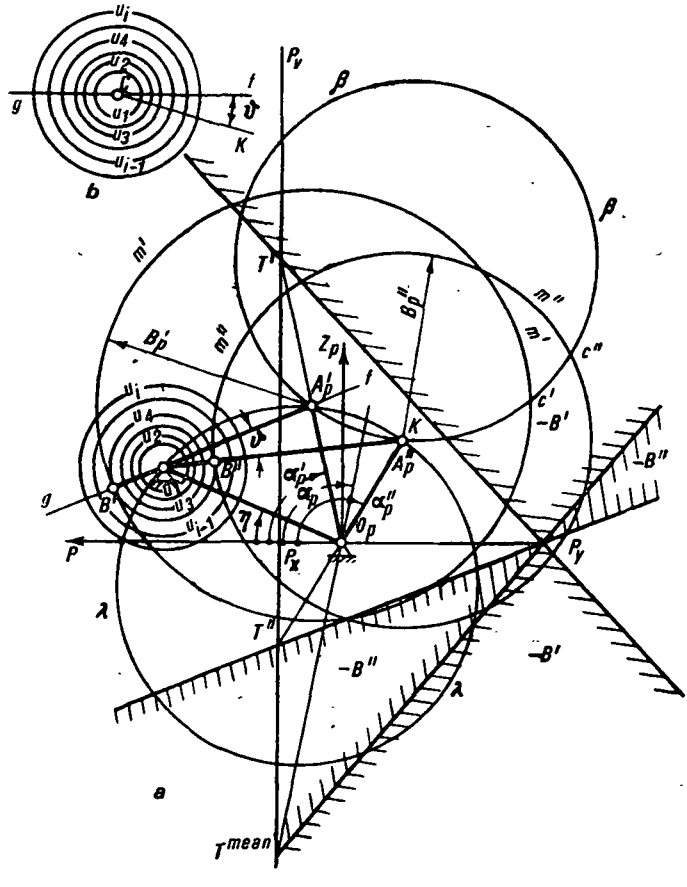

Fig. 4.

ing manner. Projection of the sector of swing of yoke on plane P at the selected value of angle α' and circles $\lambda\lambda$ and $\beta\beta$ of the possible position of the center of hinge C are drawn in the $O_p zp$ system of coordinates.

These plottings are done in the same way as those used in solving the first problem of synthesis from the angle of swing of the yoke and coefficient k. From points A_p' and A_p'' as centers, let us draw circles m' and m'' exactly in the same way as solving the second problem by using the method of plottings.

After this, let us follow the procedure suggested in article [5]. A gauge representing the angle ϑ and its conjugating angle fCk included between concentric circles u_i of center C is drawn on the tracing paper (see Fig. 4, b).

The essence of the method lies in the determination of such a position of the gauge on the drawing, at which point C will lie on the arc of circle $\lambda\lambda$ or $\beta\beta$ included between circles m' and m'', the straight line Cf will pass through point A_p' and the straight line Ck through point A_p'' and at the same time, one of the circles u_i will be simultaneously tangent to circles m' and m'' (see Fig. 4, a).

Connecting the point C obtained in this manner to points O_p and A_p' (or A_p''), directly from the drawing we get the required values $c=CB'$ (or $c=CB''$), $d=CO_p$ and $\eta=<CO_p p$ where B' (or B'') is the point of intersection of circle $\lambda\lambda$ with the straight line CA_p' (or CA_p'').

The parameters, obtained while solving the first and second problems of synthesis of three dimensional crank-yoke four-link mechanisms from the angle of swing of the yoke and coefficient k, provide geometrical satisfaction of the conditions formulated above since the center of hinge C is taken on circle $\lambda\lambda$ or $\beta\beta$. But it does not mean that it will always provide satisfaction[2] of the kinematic conditions.

For satisfaction of the kinematic conditions, it is necessary that the yoke should be able to move through the given angle α_{swing}, i.e. there should be no intermediate extreme positions of the center of hinge A on arc $A'A''$. In the presence of these positions, it will be impossible to complete the swing of the yoke of the mechanisms designed and to move the yoke from position OA' to position OA'' since the yoke on its path falls into the intermediate extreme position from where the yoke cannot be moved further to position OA'' without disturbing the integrity of the mechanism. For these reasons, it is not possible to move yoke from position OA'' to position OA'.

Analyzing the mutual situation of the sector of swing of the yoke and when possible, from the point of view of the absence of intermediate extreme positions of the yoke, and position of the projections of center of hinge B on the plane of swing of the yoke, it is not difficult to notice that these projections of B at position:

[2] The term is taken from the article by S. A. Cherkudinov [7].

a) B'' should not lie within the vertical angles $\alpha''-\alpha^{aver}$ (in the region "$-B_v''$");

b) B' should not lie within the vertical angles $\alpha^{aver}-\alpha'$ (in the region "$-B'$") of Oxz system of coordinates. [Here $\alpha^{aver}=(\alpha'+\alpha'')/2$].

Let us call the regions "$-B'$" and "$-B''$" as the regions of impossible position of the projection of center of hinge B on Oxz plane at positions B' and B''.

Let us denote the regions "$-B'$" and "$-B''$" as the regions for the inadmissible position of the projection of center of hinge B on Oxz plane at $T'O_p$ and $T^{aver}O_p$ will be the boundaries of region "$-B_v'$" and straight lines $T^{aver}O_p$ and $T''O_p$ will be the boundaries of region "$-B_v''$".

It is not difficult to notice that the region "$-B'$", i.e. the region for the inadmissible position of the center of hinge B at position B', is the region within the vertical angle $T'P_yT^{aver}$ whose projection on Oxz plane gives the vertical angle $T'OT^{aver}$ while the region "$-B''$" i.e. the region for the inadmissible position of the center of hinge B at position B'', becomes the region within vertical angle $T^{aver}P_yT''$ whose projection on Oxz plane gives the vertical angle $T^{aver}O_pT''$. (Here P_y is the point of intersection of trace P_H with Oy axis of the system of coordinates). Regions "$-B'$" and "$-B''$" lie in plane P.

Regions "$-B'$" and "$-B''$" can easily be plotted by finding the points T', T^{aver} and T'' as points of intersection of straight lines drawn through point O_p at angles α_p', α^{aver} and α_p'' with O_pp axis with the straight line $p=e\tan Q$.

The last equation is the equation of trace P_v in the O_pz_pp system of coordinates.

Let us plot the regions "$-B'$" and "$-B''$" by drawing straight lines through points T', T^{aver}, T'' and $P_y=P_y(0,-e/\tan Q)$ (see Figs. 1-4).

It is not difficult to derive the equations of straight lines $T'P_y$, $T^{aver}P_y$ and $T''P_y$ defining the boundaries of regions "$-B'$" and "$-B''$". Let us write the equation of the straight line passing through points P_y and $T(T', T^{aver}$ or $T'')$:

$$(P_{P_y}-P)/(P_{P_y}-P_T)=(\mathcal{Z}_{P_y}-\mathcal{Z})/(\mathcal{Z}_{P_y}-\mathcal{Z}_T), \tag{6}$$

where PP_y, $\mathcal{Z}P_y$, P_T and $\mathcal{Z}_T$ are coordinates of points P_y and T in the O_pz_pp system of coordinates respectively.

Using Fig. 1, we have in relative units of length:

$$\begin{aligned} P_{P_y}&=-e/\tan Q;\\ \mathcal{Z}_{P_y}&=0;\\ P_T&=e\tan Q;\\ \mathcal{Z}_T&=e\cdot\tan\alpha/\cos Q. \end{aligned} \tag{7}$$

Taking into consideration equation (7), equation (6) can be written as:

$$\mathcal{Z}=p\sin Q\tan\alpha+e\cos Q\tan\alpha. \tag{8}$$

Let us plot the regions "$-B'$" and "$-B''$" by either using the graphical determination of points T', T^{aver}, T'' or equations (8). Simultaneous study of the regions "$-B'$" and "$-B''$" and plottings, necessary for geometrical satisfaction of the above formulated conditions, assists in selecting the values of the required parameters, simultaneously satisfying geometrical and kinematic requirements of the problem.

Analyzing the above mentioned solutions of the problems (see Figs. 2-4), we may confirm that the selected positions of the center of hinge C are correct from the point of view of simultaneous geometrical and kinematic satisfaction of the conditions.

This is explained by the fact that:

1) point C is either situated on circle $\lambda\lambda$ or on circle $\beta\beta$;

2) positions B' and B'' of the center of hinge B do not fall in the regions "$-B'$" and "$-B''$" in any of the solutions.

If the center of the hinge C is displaced to point c_2 (see Fig. 3) or is selected on arc $c'c''$ (see Fig. 4), in these cases, the solution will give only geometrical satisfaction of the conditions because, in the first case, point B' will be in the region "$-B'$" and point B'' in region "$-B''$" while in the second case, point B' will be in the region "$-B''$".

The methods suggested for solving the problems of synthesis of three-dimensional crank-yoke mechanisms from the angle of swing of the yoke and coefficient k of increase in the velocity of reverse stroke, are most general since they can be used for solving similar problems of synthesis of crank-yoke mechanisms which are particular types of three-dimensional crank-yoke mechanisms.

Summary

Location of the sector of swing in the Oxz system of coordinates is of great importance in solving the problems formulated above. It should be particularly noted that situation of the sector of swing of mechanisms at $Q=0°$ where points A_p' and A_p'' coincide, makes the solution of these problems impossible from the angle of swing of the yoke and coefficient k differing from 1.

References

1. Baranov, G. G. Kinematika i dinamika mekhanizmov (Kinematics and Dynamics of Mechanisms). Part 1, Gosenergoizdat, 1932.

2. ALT, H. Über die Totlagen des Gelenkvierecks. Zeitschrift für angewandte Mathematik und Mechanik, V, 1925, S, 337.
3. KOZHEVNIKOV, S. N. K voprosu o kinematike i sinteze prostranstevennykh krivoshipno-koromyslovykh mekhanizmov (Kinematics and synthesis of three-dimensional crank-yoke mechanisms). *Trudy seminara po teorii mashin i mekhanizmov,* IV, vyp. 14, Izd-vo AN SSSR, 1947.
4. POPLAVSKII, A. M. Proektirovanie sharnirno-prostranstvennogo chetyrekhzvennika po zadannomu koeffitsientu izmeneniya skorosti khoda (Design of a hinged three-dimensional four-link mechanism from the given coefficient of change in the velocity of stroke). *Nauchnye trudy MTILP,* No. 5, 1955.
5. TSVIYAK, P. B. Graficheskii metod proektirovaniya prostranstvennogo krivoshipno-shatunnogo mekhanizma po zadannomu koeffitsientu uvelicheniya skorosti obratnogo khoda (Graphical method of designing a three-dimensional crank-yoke mechanisms from the given coefficient of increase in the velocity of reverse stroke). *Dokl. PI,* VI. L'vov, 1962.
6. KULYUGIN, V. I. Reshenie nekotorykh zadach sinteza prostranstvennogo sharnirnogo chetyrekhzvennogo mekhanizma grafo-analiticheskimi metodami (Solution of some problems of synthesis of three-dimensional hinged four-link mechanisms by graphical and analytical methods). *Mashinovedenie,* No. 5, 1966.
7. ARTOBOLEVSKII, I. I., N. I. LEVITSKII and S. A. CHERKUDINOV. Sintez ploskikh mekhanizmov (Synthesis of Plane Mechanisms). Fizmatgiz, 1959.

P. G. Kukharenko

CLASSIFICATION OF SLOTTED BAR AND LEVER MECHANISMS OF DISCONTINUOUS MOTION

Automatic machines of discontinuous and continuous operation are in wide use in machine building, electronics, polygraphic, chemical and food industries as well as other branches of the national economy.

The latter type of machine provides maximum productivity but cannot always be used because of certain difficulties. Most of the multi-operation automatic machines belong to the category of machines of discontinuous operation in which the discontinuous technological process is carried out during continuous or periodic transportation of the objects being processed.

Each type of machine has its advantages and disadvantages which depend on the scale of the industry, peculiarities of the technological processes and objects being processed. The correct type of machine can be selected only after careful and accurate analysis of their characteristic features. This necessitates accumulation of reference data on the design of operating, transmitting and transporting mechanisms of technological automatic machines [1].

Discontinuous motion of links in automatic machines is provided with the help of various mechanisms: Maltese mechanism, ratchet, spiders, cam mechanisms, cogging cam mechanism, toothed-lever mechanism, combined mechanisms, as well as mechanisms with hydraulic, pneumatic, electrical and other types of devices. Two-dimensional Maltese mechanisms (Fig. 1, *a-l*) are widely used in rotating-cum-fixing devices of automatic machines. The disadvantage of Maltese mechanisms lies in the fact that they do not provide arbitrary selection of the ratio of duration of motion to the duration of stop. With a small number of grooves, their duration is characterized by significant inertia loads while with a large number of grooves, there are significant losses of time on idle run which decrease the productivity of the automatic machines.

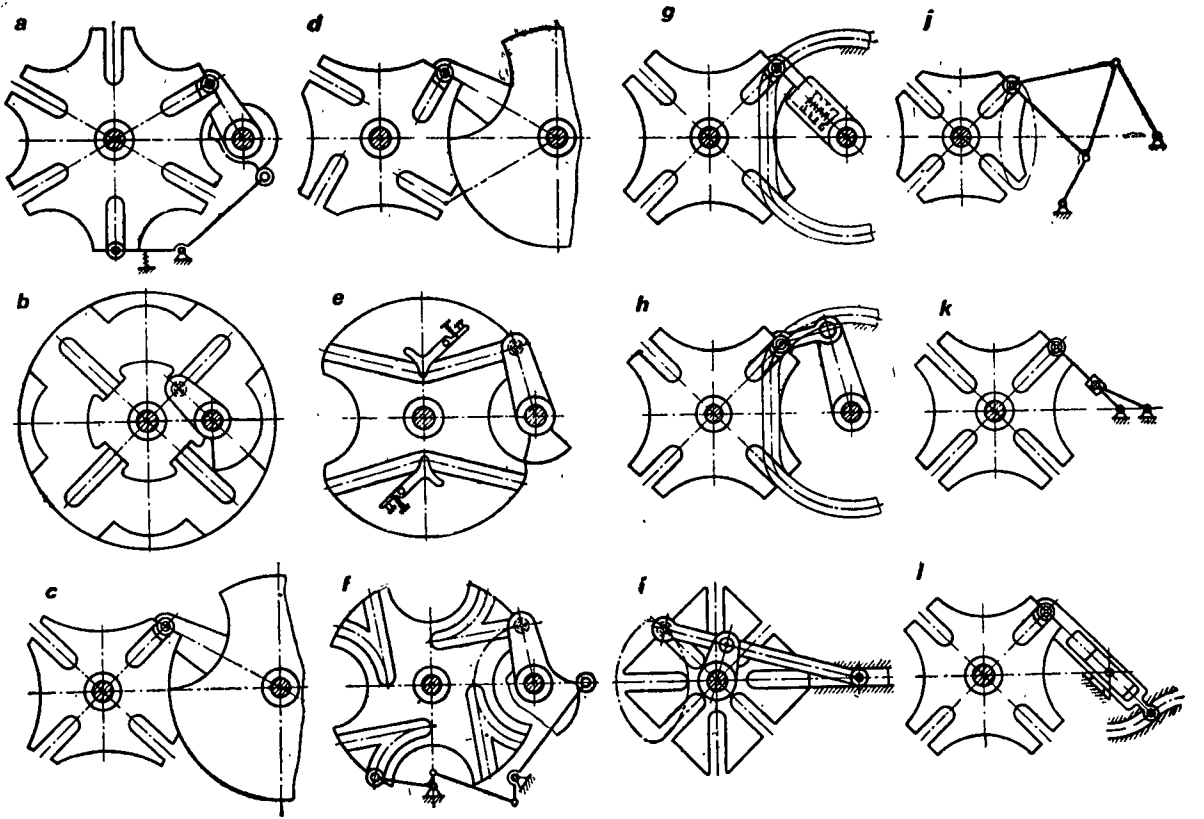

Fig. 1. Basic types of two-dimensional Maltese mechanisms.

Smoother rotation can be achieved by using spherical Maltese mechanisms which at $z \leqslant 10$ have minimum values of dimensionless positional coefficients of accelerations. Irrespective of the number of grooves, these mechanisms have a constant ratio of the period of rest to that of motion of the driven link which imposes serious limitation on cyclograms and often leads to artificial decrease in the productivity of automatic machines.

The following methods are suggested to improve the basic characteristics of Maltese mechanisms:

1) utilization of multi-link drives for periodic rotation of the usual Maltese cross; and

2) use of curvilinear grooves on the driven link.

In the second case, there is a possibility of wider selection of the required laws of motion and of the ratio of duration of rotation to that of stop.

To study the kinematic characteristics of lever mechanisms with curvilinear profile of the driven link (including Maltese mechanisms with curvilinear grooves), let us consider the general conditions of motion, instantaneous stop and idling of links in these mechanisms.

1. Condition of Motion of Driving Link in a Three Link Mechanism

To get continuous motion of the driving crank in a three-link mechanism with curvilinear profile of the driven link, let us derive the vector equation relating velocities of various points for an arbitrary position of links of this mechanism (Fig. 2, a).

$$\mathbf{v}_{A_1O} = \mathbf{v}_{A_2B} + \mathbf{v}_{A_1A_2}. \tag{1}$$

If motion of the crank is not possible, velocity of every point of this link will be equal to zero, i.e. $\mathbf{v}_{A_1O} = 0$.

Then it follows from equation (1) that:

$$\mathbf{v}_{A_2B} = -\mathbf{v}_{A_1A_2}. \tag{2}$$

In equation (2), it is assumed that the tangents T_{a13} and T_{a23} coincide[1] and the common normal N_{a12} (N_{a23}) passes through the absolute instantaneous center of rotation of the driven link (point B).

Consequently in order to secure continuous motion of the driving crank the central profile of the driven link must be designed in such a manner that the normal to the profile drawn through the center of the driving roller does not coincide with the absolute instantaneous center of the driven link at any position of the mechanism.

[1] In Fig. 2, a, segments between points A and T_{a13} and T_{a23} are not shown.

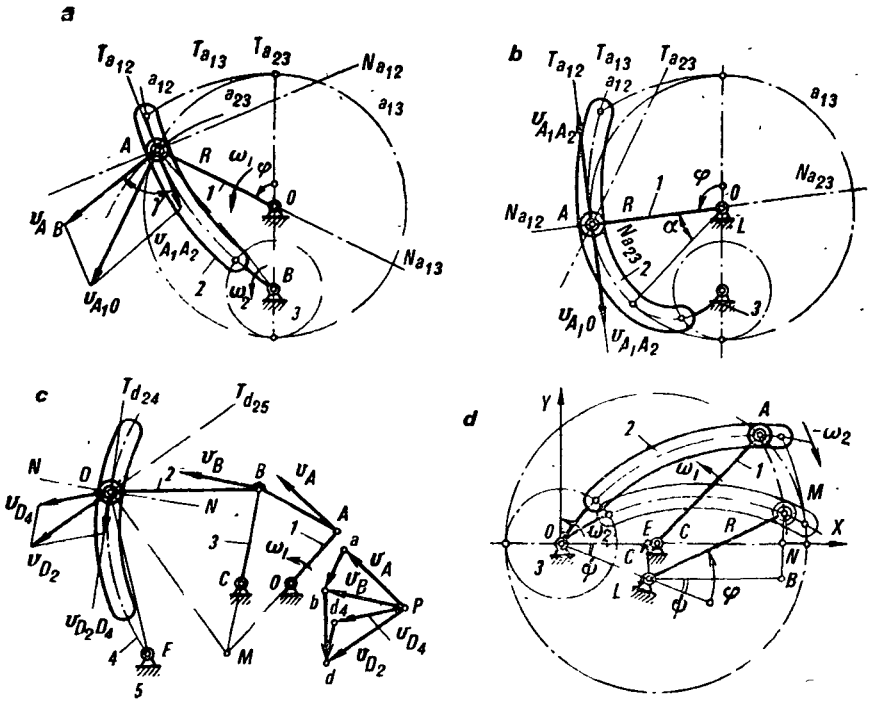

Fig. 2. To the derivation of conditions of motion, instantaneous stop and dwell in slotted bar and lever mechanisms.

This condition is for example, satisfied by the central crank and slotted lever mechanism with straight slotted lever transmission, the functions of which are defined by the position of the driven link and by the geometrical characteristic λ representing the ratio of the radius of driving link to the distance between two centers of the mechanism.

2. Condition of Motion of the Driven Link

If the slotted lever has curvilinear profile, the law of motion of the mechanism depends not only on the parameter λ but also on configuration of the profile. The angle of transmission γ determined from the following formula has an effect on the operation of the mechanism:

$$\gamma = \text{arc tan}\, \lambda \sin\varphi / [\lambda(\lambda + \cos\varphi) - k_\omega (1 + \lambda^2 + 2\lambda\cos\varphi)], \qquad (3)$$

where $k_\omega = d\psi/d\varphi$ is the first transmission function of the mechanism [2].

At certain values of angle γ, motion of the curvilinear roller becomes impossible due to blocking of the mechanism. To avoid the appearance

of large reactions at the hinges and overloads on links, the angle of transmission at all positions of the mechanism should exceed:

$$\gamma \geqslant \gamma_{min}. \tag{4}$$

Dynamic condition (4) has to be satisfied while designing power transmission as well as kinematic transmission and mechanisms of instruments since the errors of position and displacement of the driven link continuously increase when the value of the angle of transmission approaches zero at the same values of the primary errors in the dimensions of links and the clearances in the kinematic pairs [1].

Equation (3) makes it possible to verify the observance of dynamic condition (4) in the case of all types of configuration of the profile of driven link in a three-link mechanism. It should, however, be noted that condition (4) is necessary but not sufficient to provide motion of the driven link at permissible values of reactions in kinematic pairs.

In some cases, even when condition (4) is satisfied the driven link may not be in motion but in the state of dwell (prolonged stop). These cases are considered below.

3. Condition of Dwell of the Driven Link

Let us determine the condition under which a mechanism with a completely rotating rocker can be designed to provide regular stops of the driven link in the case of a continuously moving driving crank. If rocker *2* (see Fig. 2) is at rest, then the absolute velocity of all points of its profile is equal to zero.

Then at $v_{A_2B}=0$ from equation (1) we get:

$$v_{A_1O}=v_{A_1A_2}=-v_{A_2A_1}. \tag{5}$$

But it is possible only if the tangents T_{a12} and T_{a13} (see Fig. 2, b) coincide. It is obvious that the common normal N_{a12} (N_{a13}) will pass through point *O* representing the absolute instantaneous center of rotation of the crank.

Consequently, instantaneous stop of the driven link is possible at that point of the mechanism where the normal drawn from the center of the driving roller to the profile of slotted lever coincides with the absolute instantaneous center of rotation of the driving link. Stop (or prolonged stop of the slotted lever) is provided at a particular section of the profile along the length of which this condition is satisfied.

In a central crank and slotted lever mechanism with completely rotating straight slotted lever, neither the condition of instantaneous stop nor the condition of prolonged stop can be fulfilled. Only the condition of instantaneous stop at two extreme positions of the driven link is satisfied in the mechanism with swinging straight slotted lever.

It is shown in Fig. 2, b that the common normal N_{a12} (N_{a13}) can pass through absolute instantaneous center of the crank only during an interval of its motion when the central profile of the rocker coincides with the trajectory of the center of crank pin.

Thus, we can formulate the condition of dwell of the driven link in the following manner: dwell of the slotted lever is provided within the limits of such an interval of motion of the crank when the axial line of the slot of the slotted lever (central profile) coincides with the trajectory of the center of a driving roller. In the case of a driving crank of constant length, the slotted lever of a three-link mechanism will have regular periodic dwells if a part of its central profile is made along the arc of a circle whose radius is equal to the radius of the driving crank. It follows from Fig. 2, b that the completely rotating slotted lever has a prolonged stop at an angle α of the rotation of crank [1, 2].

This condition of dwell is applicable to two dimensional slotted bar and lever and cam-lever mechanisms of any complexity. For example, let the slotted lever be put into motion by pin D belonging to the connecting rod of a hinged four-link mechanism (see Fig. 2, c). By plotting the velocity diagram, we may determine the velocity of all the points of links and the absolute instantaneous center M of the connecting rod directly putting the slotted lever into motion.

On the basis of the theorem of addition of velocities:

$$\mathbf{v}_{D_2}=\mathbf{v}_{D_4}+\mathbf{v}_{D_2D_4}. \tag{6}$$

Slide plate *4* will have an instantaneous stop if the condition $\mathbf{v}_{D_4}=\bar{0}$ is satisfied at the given position of the mechanism.

Then equation (6) becomes:

$$\mathbf{v}_{D_2}=\mathbf{v}_{D_2D_4}. \tag{7}$$

Coincidence of tangents T_{d24} and T_{d25} is a necessary condition for equation (7) and therefore, the common normal N to the slotted lever profile drawn from the point of contact of the profile with the center of the driving roller must pass through the absolute instantaneous center M at the given moment of time.

As in the case considered earlier, this condition must be satisfied to get prolonged stop on some interval of motion of the driving link, i.e. the profile of the driven link during this interval of motion coincides with the trajectory of the center of the driving roller.

Thus, for all types of two-dimensional mechanisms having a slotted lever (or cam) as the driven link, in the same way we arrive at the following conclusion: dwell of the driven link is provided during that interval of motion of the driving link when the central profile of the driven link coincides with the trajectory of the center of a driving roller, since only in this case,

the normal to the profile drawn from the point of contact of the profile with the center of the driving roller, passes through the absolute instantaneous center of the link directly putting the slotted lever (or cam) into motion at every instance of the interval of motion under reference.

It should be pointed out that this conclusion is applicable not only to rotating driven links but also to links which have oscillating rectilinear motion when their absolute instantaneous center tends to infinity.

On the basis of the conditions for dwell as formulated above, Figs. 3-5 show kinematic schemes of mechanisms in which regular stops of the driven link are used in the case of various types of motion [1-17].

Fig. 3 shows the schemes of mechanisms with discontinuous reciprocating motion. Mechanism *a* provides prolonged and instantaneous stops at extreme positions of the driven link. Mechanism *b* and *c* have two prolonged stops. Using straight line mechanisms, we get prolonged stops of the driven link with rectilinear profile (*d-l*).

Fig. 4 shows the scheme for mechanisms with prolonged stops of swinging slotted lever. The three-link mechanism *a* has a prolonged stop of the curvilinear slotted lever at the extreme left position and instantaneous stop at the extreme right position. Mechanisms *b* and *c* also have one prolonged and one instantaneous stop of swinging curvilinear slotted lever. Using straight line mechanisms, we may synthesize a six-link slotted bar and lever mechanism with prolonged stops of swinging slotted lever with rectilinear profile (*d-l*).

Schemes of mechanisms with prolonged stops of a completely rotating slotted lever are shown in Fig. 5. In the three-link mechanisms *a* and *b*, the completely rotating slide plates have one prolonged stop during each rotation of the crank, while in the first case, each rotation of the crank corresponds to one complete rotation of the slide plate. In the second case, the slide plate accomplishes one complete rotation only during two rotations of the crank. The driven link of mechanisms *c* has prolonged stops during alternate rotation of the crank and not during rotation of the driving link.

It should be noted that the mechanisms *b* and *c* are characterized by the uncertain position of the driven link, and under certain conditions, characterized by dynamic factors, they can change into two-link mechanisms. Practical application of these mechanisms is governed by the necessity of using additional devices guaranteeing transmission of the driven link through the uncertain position.

Completely rotating slide plates of mechanisms (*d-l*) have one prolonged stop during each rotation of the driving crank and they do not require any special fixing devices. Double crank hinged mechanisms, slotted-lever mechanisms, circular guiding and other types of hinged lever mechanisms are used to provide discontinuous rotary motion of slotted levers in these

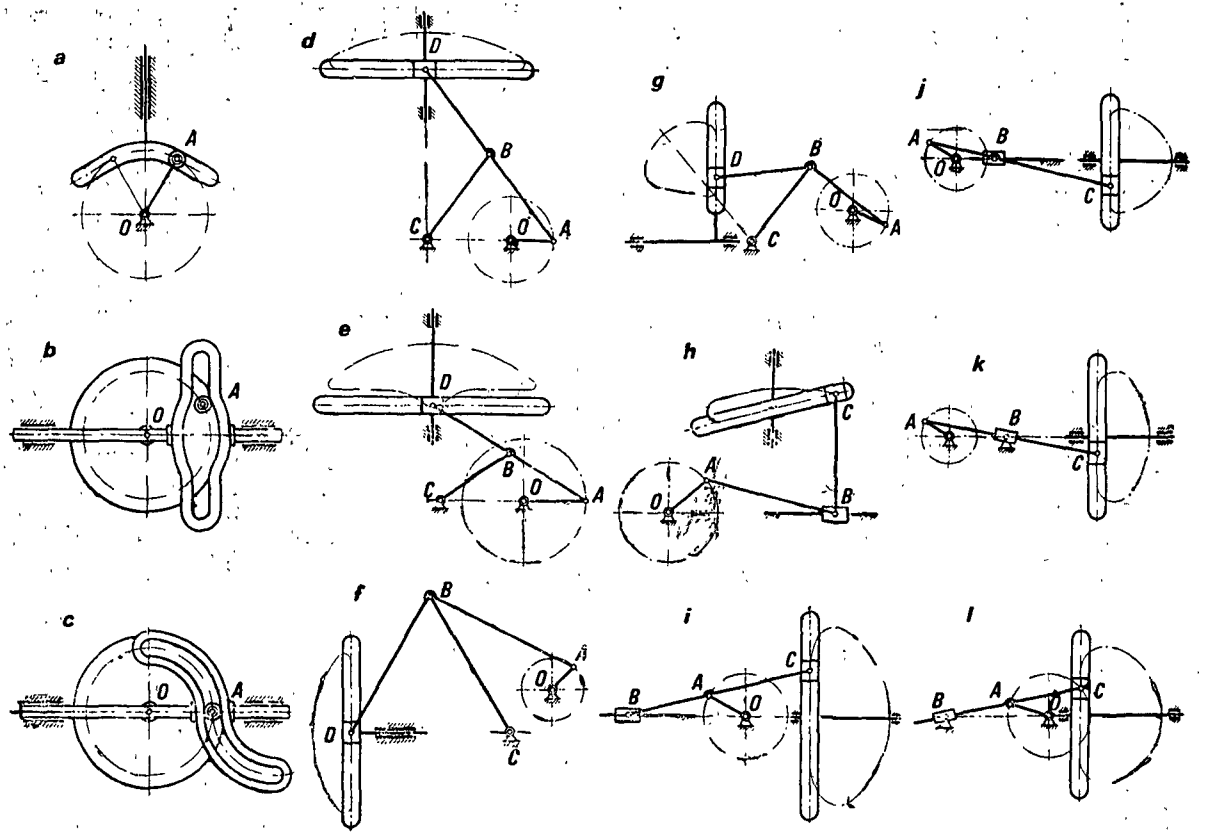

Fig. 3. Mechanisms with prolonged stops of the driven link in the case of reciprocating motion.

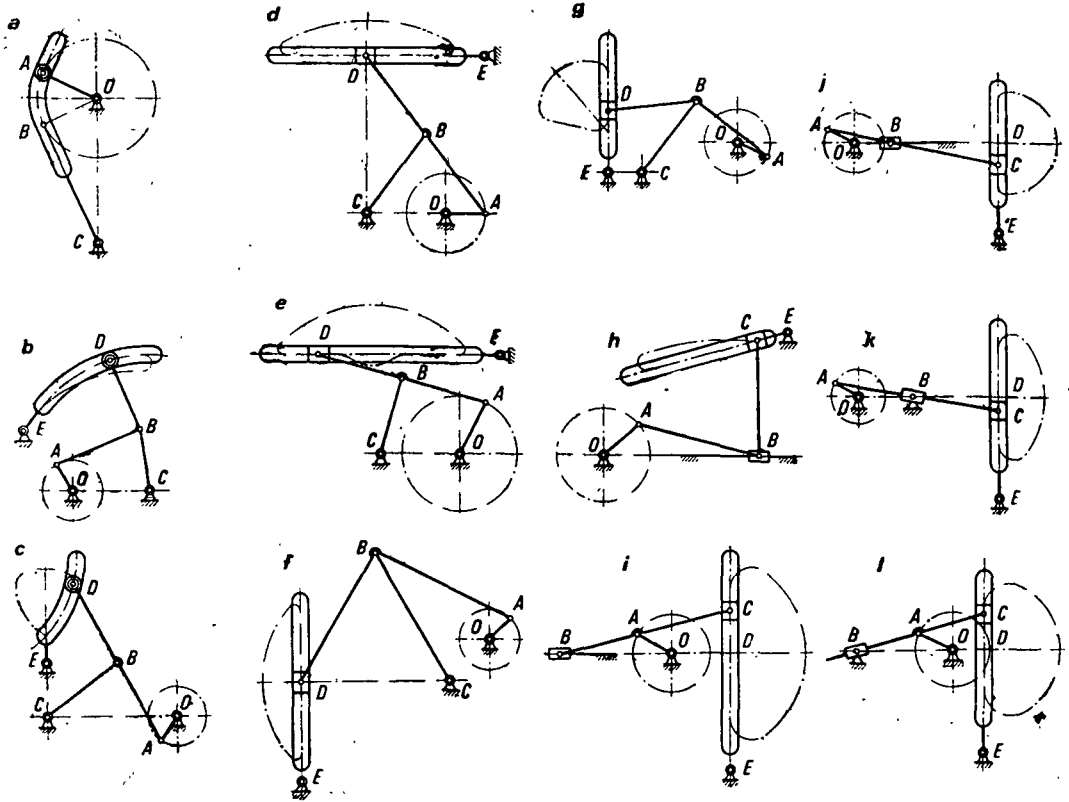

Fig. 4. Mechanisms with prolonged stops of swinging slotted lever.

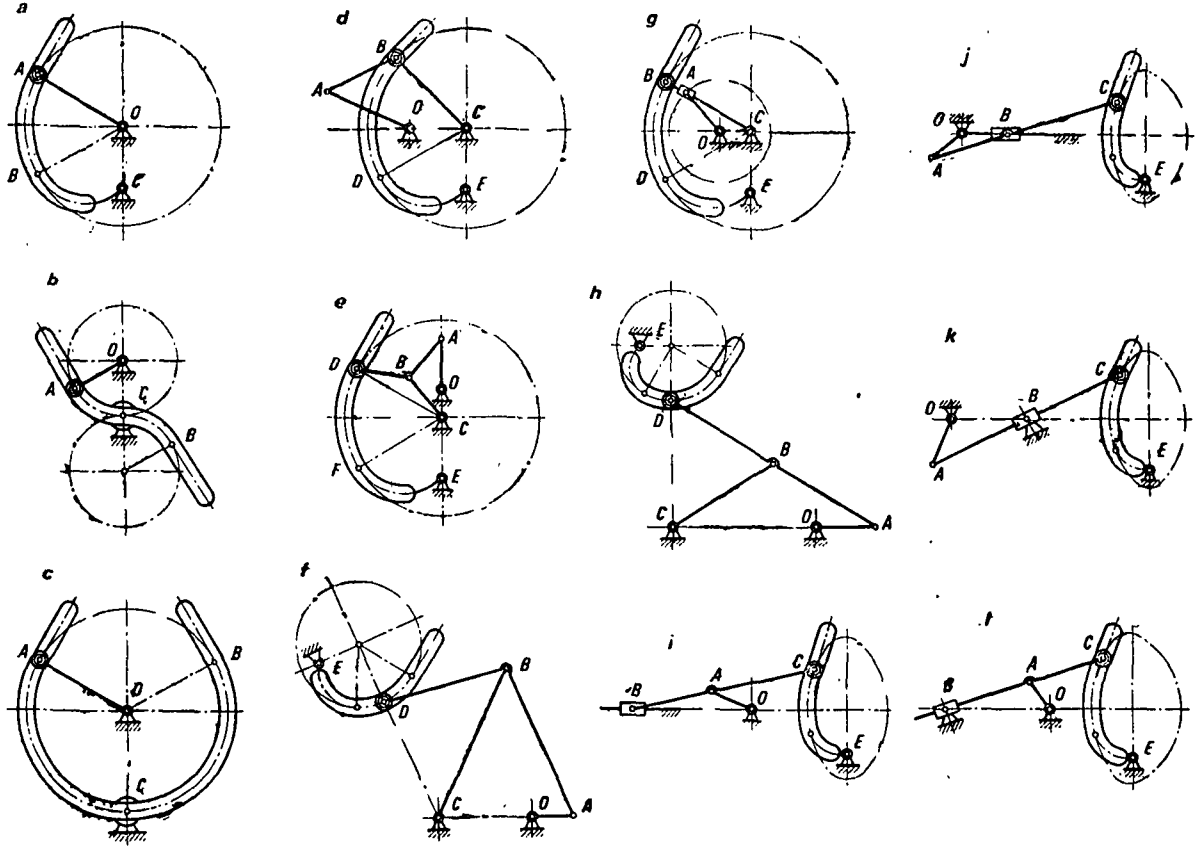

Fig. 5. Mechanisms with prolonged stops of completely rotating slide plates.

mechanisms. The center of rotation of the slotted levers in each of these mechanisms must be within the closed trajectory described by the center of the driving roller.

Some advantages of these mechanisms of discontinuous motion are that they assist in securing the desired law of motion of the driven link, facilitate selection of the ratio of duration of motion to that of stop within wide limits and can be designed with adjustable stop of the driven link.

The disadvantages of such mechanisms include difficulty in the preparation of the curvilinear profiles and the relatively large dimensions of some of the mechanisms. Three-link mechanisms do not have large dimensions.

It should be pointed out that the profiles for the dwell section are simple if the driven link is put into motion directly by the driving crank or by the straight line and circular guiding mechanisms.

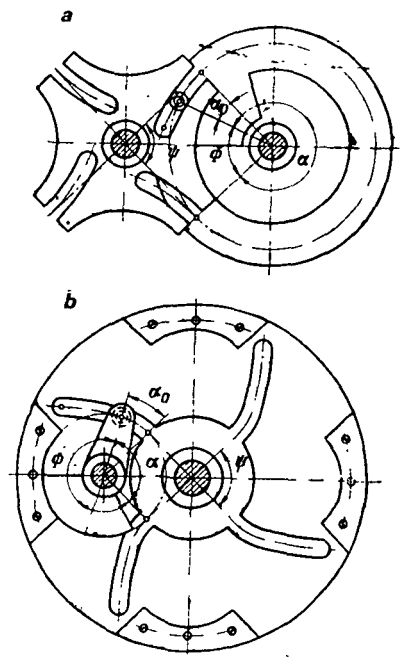

Fig. 6. Maltese mechanisms with increased angles of dwell.

On the basis of the conditions of dwell of links described above, Maltese mechanisms are designed with increased angles of dwell [3]. As a result of application of curvilinear grooves of simple configuration (Fig. 6), these mechanisms help in varying the ratio of the duration of motion to that of stop for a given number of grooves, reduce inertia loads and make it possible to increase the productivity of multiposition automatic machines without introducing multilink drives [4] by decreasing the duration of the idle runs.

4. Functions of Position of Some Mechanisms of Discontinuous Motion

In order to determine the function of position of the driven link in mechanisms of discontinuous motion, it is advisable to use the method of closed vector contour suggested by V. A. Zinov'ev [8].

Formulas for calculation purposes for some mechanisms are presented in Tables 1-4. Indices in the legends of the function of the position show the radii of curvature and the profile on corresponding intervals of motions. If there is no index in the legends of the function of position, the calculation

Table 1. Functions of position of the driven link in the case of reciprocating motion (see Fig. 3)

Mechanisms	Functions of position of the driven link	Geometrical conditions
a	$x_\rho = a\cos\varphi_0 + r\cos\varphi + \sqrt{(a\cos\varphi_0 + r\cos\varphi)^2 + 2ar[1-\cos(\varphi-\varphi_0)]}$; $x_r = 2r\cos\varphi$; $x = [\cos(\varphi-\varphi_0)-1]r/\cos\varphi_0$	$OA=r$; $\rho=r+a$; $[\varphi_0 \leqslant \varphi \leqslant 360^\circ - \varphi_0]$
b	$x = r\cos\varphi$	$OA=r$; $[-\varphi_0 \leqslant \varphi \leqslant \varphi_0]$; $[180^\circ - \varphi_0 \leqslant \varphi \leqslant 180^\circ + \varphi_0]$
c	$x_r = r(2\cos\varphi - 1)$	$OA=r$; $[0^\circ \leqslant \varphi \leqslant 90^\circ]$; $[180^\circ \leqslant \varphi \leqslant 270^\circ]$
d	$y = r(5\sin\xi - \sin\varphi)$; $\xi = \arctan\sin\varphi/(2+\cos\varphi) + \text{arc}\cos{}^1/_5 \cdot \sqrt{1+4(1+\cos\varphi)}$	$OA=r$; $OC=l=2r$; $y_0=4r$; $AB=BD=BC=b=2.5r$; $[-90^\circ \leqslant \varphi \leqslant 90^\circ]$
e	$y = 2b\sin\xi - r\sin\varphi$; $\xi = \arctan r\sin\varphi/(l+r\cos\varphi) + \text{arc}\cos{}^1/_2 b \cdot \sqrt{r^2+l^2+2rl\cos\varphi}$	$OA=r$; $OC=l=1.394r$; $AB=BD=BC=b=1.409r$; $[90^\circ \leqslant \varphi \leqslant 128^\circ]$; $[232^\circ \leqslant \varphi \leqslant 270^\circ]$
h	$y = a/b(r\cos\delta\sin\varphi + \sin\delta\sqrt{b^2 - r^2\sin^2\varphi})$	$OA=r$; $AB=b=3r$; $BC=a=2.47r$; $\angle ABC=\delta=75^\circ$; $[-60^\circ \leqslant \varphi \leqslant 60^\circ]$
i	$x = r\cos\varphi + a/b \cdot \sqrt{b^2 - r^2\sin^2\varphi}$	$OA=r$; $AB=b$; $AC=a$; $BC=l$; $x > b^2\sin^2\varphi/b\sqrt{b^2-r^2\sin^2\varphi}$; $[110^\circ \leqslant \varphi \leqslant 250^\circ]$
j	$x = r\cos\varphi + l/b \cdot \sqrt{b^2 - r^2\sin^2\varphi}$	$OA=r$; $AB=b$; $AC=l$; $rl>b^2$; $r<b<l$; $b=2.1786r$; $l=6r$; $[120^\circ \leqslant \varphi \leqslant 240^\circ]$
k	$x = r\cos\varphi + l(L - r\cos\varphi)/\sqrt{r^2+L^2-2rL\cos\varphi}$	$OA=r$; $AC=l=6.8r$; $OB=L=2.1r$ $[110^\circ \leqslant \varphi \leqslant 250^\circ]$
l	$x = r\cos\varphi + a(L + r\cos\varphi)/\sqrt{r^2+L^2+2rL\cos\varphi}$	$OA=r$; $OB=L=2.27r$; $AC=a=1.6r$; $[-30^\circ \leqslant \varphi \leqslant 30^\circ]$

REMARKS:

Angles φ and φ_0 in the mechanisms shown in Fig. 3, a are counted from X-axis directed vertically downward.

Mechanism *f* and *g* have not been considered in this case.

Table 2. Functions of position of mechanisms with prolonged and instantaneous stops of swinging slide plates (see Fig. 4)

Mechanisms	Functions of position of the driven link	Geometrical conditions
a	$\psi r = 2 \arctan \lambda \sin \varphi/(1+\lambda \cos \varphi)$; $\psi_\rho = \psi = \arctan(y/z) + \arccos(x/\sqrt{y^2+z})^2$; $x_\rho = 1+\lambda \cos \varphi - \tau(\lambda+\cos \varphi_0)$; $x = \lambda + \cos \varphi_0$; $y_\rho = \lambda \sin \varphi + \tau [\sin \varphi_0 - \lambda \sin (\varphi - \varphi_0)]$; $y = \lambda \sin (\varphi - \varphi_0) - \sin \varphi_0$; $z_\rho = 1+\lambda \cos \lambda - \tau [\cos \varphi_0 + \lambda \cos (\varphi - \varphi_0)]$; $z = \lambda \cos (\varphi - \varphi_0) + \cos \varphi_0$	$\lambda = r/L < 1$; $\tau = a/L$; $OA = r$; $\rho = r+a$; $\angle OAB = \alpha = \varphi_0 -$ $\alpha_0 \leqslant 150°$; $[\alpha_0 \leqslant \varphi \leqslant \varphi_0]$. X-axis is pointed upwards
d	$\psi = \arctan[(5 \sin \xi - \sin \varphi - 4)/(6 - 5\cos \xi + \cos \varphi)]$; $\xi = \arctan[\sin \varphi/(2+\cos \varphi)] +$ $\arccos {}^1/_5 \cdot \sqrt{1+4(1+\cos \varphi)}$	$OA = r$; $OC = l = 2r$; $Y_E = 4r$; $X_E = 2r$; $AB = BC = BD = 22.5r$; $[-90° \leqslant \varphi \leqslant 90°]$
e	$\psi = \arctan\{(2b \sin \xi - r \sin \varphi - h)/[L + r \cos \varphi +$ $2(l - b \cos \xi)]\}$; $\xi = \arctan[r \sin \varphi/(l + r \cos \varphi)] +$ $\arccos {}^1/_2 b \cdot \sqrt{r^2+l^2+2rl \cos \varphi}$	$OA = r$; $OC = l = 1.394\,r$; $AB = BC = BD = b = 1.409\,r$; $X_E = L = 1.5\,r$; $Y_E = h =$ $1.818\,r$; $[90° \leqslant \varphi \leqslant 128°]$; $[232° \leqslant \varphi \leqslant 270°]$
h	$\psi = \arctan\{[a(r \cos \delta \sin \varphi +$ $\sin \delta \sqrt{b^2 - r^2 \sin^2 \varphi} - bh)]/[b(L - r \cos \varphi) -$ $\arcsin \delta \cdot \sin \varphi + (a \cos \delta + b)\sqrt{b^2 - r^2 \sin^2 \varphi}]\}$.	$OA = r$; $AB = b = 2.7\,r$; $BC =$ $a = 2.4\,r$; $\angle ABC = \delta = 75°$; $X_E = L$; $Y_E = h$; $[-60° \leqslant$ $\varphi \leqslant 60°]$
i	$\psi = \arctan\{[br(1+\cos \varphi) +$ $a(\sqrt{b^2 - r^2 \sin^2 \varphi} - b)]/[(a+b)\, r \sin \varphi + bh]\}$	$OA = r$; $AB = b$; $AC = a$; $BC = l$; $BD > lr^2 \sin^2 \varphi/b$. $\sqrt{b^2 - r^2 \sin^2 \varphi}$; $[110° \leqslant \varphi \leqslant$ $250°]$
j	$\psi = \arctan\{[br(1+\cos \varphi) +$ $l(\sqrt{b^2 - r^2 \sin^2 \varphi} - b)]/(bh - ar \sin \varphi)$	$OA = r$; $AB = b = 2.1786\,r$; $AC = l = 6\,r$; $r < b < l$; $rl > b^2$; $[120° \leqslant \varphi \leqslant 240°]$
k	$\psi = \arctan\{\{r(1+\cos \varphi) -$ $b[1 - (l - r \cos \varphi)/\sqrt{r^2+l^2-2rl \cos \varphi}]\}/$ $[h + r \sin \varphi (1 - b/\sqrt{r^2+l^2-2rl \cos \varphi})]\}$	$OA = r$; $AC = l = 6.8\,r$; $OB = L = 2.1\,r$; $Y_E = h$; $[110° \leqslant \varphi \leqslant 250°]$
l	$\psi = \arctan\{\{r(1+\cos \varphi) -$ $a[1 - (l + r \cos \varphi)/\sqrt{r^2+l^2+2rl \cos \varphi}]\}/$ $[h + r \sin \varphi (1 + a/\sqrt{r^2+l^2+2rl \cos \varphi})]\}$	$OA = r$; $OB = L = 2.27\,r$; $AC = a = 1.6\,r$; $Y_E = h$; $[-30° \leqslant \varphi \leqslant 30°]$

REMARKS: Mechanisms *b*, *c*, *f* and *g* are not described here.

Table 3. Functions of position of mechanisms with prolonged stops of completely rotating slide plates (see Fig. 5)

Mechanisms	Functions of position of the driven link	Geometrical conditions
a	$\psi_r=2 \arctan [\lambda \sin \varphi/(1+\lambda \cos \varphi)]$; $\psi_\rho=\psi=\arctan (y/z)+\arccos (x/\sqrt{y^2+z^2})$; $x_\rho=1+\lambda \cos \varphi-\tau (\lambda+\cos \varphi_0)$; $y_\rho=\lambda \sin \varphi+\tau [\sin \varphi_0-\lambda \sin (\varphi-\varphi_0)]$; $z_\rho=1+\lambda \cos \varphi-\tau [\cos \varphi_0+\lambda \cos (\varphi-\varphi_0)]$; $x=\lambda+\cos \varphi_0$; $y=\lambda \sin (\varphi-\varphi_0)-\sin \varphi_0$; $z=\lambda \cos (\varphi-\varphi_0)+\cos \varphi_0$	$OA=r$; $\rho=r+a$; $\lambda=r/L>1$; $\tau=a/L$; $\angle AOB=\alpha=\varphi_0-\alpha_0 \leqslant 100°$; $[\alpha_0 \leqslant \varphi \leqslant \varphi_0]$. X-axis is pointed upward
b	Formulas of mechanism *a* (Fig. 5) hold good at $\lambda=1$	$\angle AOC=\alpha=180°-\varphi_0 \leqslant 150°$; $[\varphi_0 \leqslant \varphi \leqslant 150°]$; $\lambda=1$
c	Formulas of mechanisms *a* (Fig. 5) hold good at $\lambda=1$. The mechanism stabilizes after one rotation of the crank shaft	$[\varphi_0 \leqslant \varphi \leqslant 360°-\varphi_0]$; $\lambda=1$
d	$\psi_\rho=\arctan (y/z)+\arccos (x/\sqrt{y^2+z^2})$; $x_\rho=1+\lambda \cos \xi-\tau (\lambda+\cos \xi_0)$; $y_\rho=\lambda \sin \xi+\tau [\sin \xi_0-\lambda \sin (\xi-\xi_0)]$; $z_\rho=1+\lambda \cos \xi-\tau [\cos \xi_0+\lambda \cos (\xi-\xi_0)]$; $\xi_\rho=\arctan [(l+r \sin \varphi)/(r \cos \varphi)]+$ $\arccos [(r^2+R^2+l^2-b^2+2rl \sin \varphi)/2R\sqrt{r^2+l^2+2rl \sin \varphi}]$ $\psi_R=\psi_\rho$ for $\tau=0$	$OA=r$; $AB=b$; $BC=R$; $OC=l$; $CE=L<R$; $\lambda=R/L>1$; $\tau=a/L$; $\rho=R+a$; $l+r<b+R$; $l+b<r+R$; $l+R<r+b$; $60° \leqslant \xi_0 \leqslant 90$; $[\xi_0 \leqslant \varphi \leqslant 180°-\xi_0]$
g	Formulas of mechanism *d* (Fig. 5) hold good at $\xi=\arctan [(l+r \sin \varphi)/r \cos \varphi]$	$OC=l<r$; $\lambda=R/L>1$; $30° \leqslant \xi_0 \leqslant 90°$; $[\xi_0 \leqslant \varphi \leqslant 180°-\xi_0]$

REMARKS: Mechanisms *e* and *f* have not been described here.

equation corresponds to the period of interaction of the driven roller with the rectilinear section of the profile.

The limits of change in the angle of rotation of crank during prolonged stop of the driven link are shown in square brackets.

5. Peculiarities of Synthesis of Mechanisms with Curvilinear Profile of the Driven Link

Graphical methods of designing mechanisms with curvilinear slotted levers are considered in article [1]. Accuracy in the preparation of components is of great significance in the modern machine building industry

Table 4. Functions of position of Maltese mechanisms with curvilinear grooves in the case of a reference system of usual Maltese mechanisms (see Fig. 6)

Mechanisms	Functions of position of the driven link	Geometrical conditions
a	$\psi_r=2\arctan[\lambda\sin\varphi/(1-\lambda\cos\varphi)]-\pi/Z$;	$\rho=r$; $\tau=0$; $\lambda=r/L$;
	$\psi_\rho=-(\arctan(y/z)+\arccos(x/\sqrt{y^2+z^2})+\pi/z)$;	$\rho=r+a$; $\tau=a/L$;
	$x=1-\lambda\cos\varphi-\tau(\lambda-\sin\beta)$;	$\beta=\pi/Z+\alpha_0$;
	$y=-\lambda\sin\varphi+\tau[\cos\beta-\lambda\cos(\varphi-\beta)]$;	$\alpha=\pi(Z+2)/Z+\alpha_0$;
	$z=1-\lambda\cos\varphi+\tau[\sin\beta+\lambda\sin(\varphi-\beta)]$;	$\alpha_0<\pi(Z-2)/2Z$
	$\psi=\arctan[\lambda\sin\varphi/(1-\lambda\cos\varphi)]-$ $\arcsin[(\lambda-\sin\beta)/\sqrt{1+\lambda^2-2\lambda\cos\varphi}]+\alpha_0$	
b	$\psi_r=2\arctan[\lambda\sin\varphi/(1+\lambda\cos\varphi)]+\pi/Z$;	$\rho=r$; $\tau=0$; $\lambda=r/L$;
	$\psi_\rho=\arctan(y/z)+\arccos(x/\sqrt{y^2+z^2})+\pi/Z$;	$\rho=r+a$; $\tau=a/L$;
	$x=1+\lambda\cos\varphi-\tau(\lambda-\sin\beta)$;	$\beta=\pi/Z-\alpha_0$;
	$y=\lambda\sin\varphi+\tau[\cos\beta+\lambda\cos(\varphi-\beta)]$;	$\alpha=\pi(Z-2)/Z+\alpha_0$;
	$z=1+\lambda\cos\varphi+\tau[\sin\beta-\lambda\sin(\varphi-\beta)]$;	$\alpha_0<\pi(Z+2)/2Z$
	$\psi=\arctan[\lambda\sin\varphi/(1+\lambda\cos\varphi)]-$ $\arcsin[(\lambda-\sin\beta)/\sqrt{1+\lambda^2+2\lambda\cos\varphi}]+\alpha_0$	

especially in the design of high-speed machines. It necessitates the use of analytical methods of calculation and the application of progressive methods of machining curvilinear profiles. These requirements are of special significance in the design of mechanisms of discontinuous motion.

Let us derive the equations for determining the coordinates of the profile of a curvilinear slotted lever in three-link mechanism using the method of inversion of motion (see Fig. 2, d). We will stop the slotted lever and after releasing the support, rotate it along with the crank through an angle ψ in the opposite direction of the rotation of the driven link. In this case the central line of the mechanism occupies position OC'. Let us put φ, the corresponding angle of rotation of crank in the inverse mechanism and mark the position of the center of roller from the condition $MC'=R$. Then:

$$X=OE+EN=OE+BC'=L\cos\psi+R\cos(\varphi-\psi), \tag{8}$$

$$Y=MB-NB=MB-EC'=R\sin(\varphi-\psi)-L\sin\psi; \tag{9}$$

or

$$X=L[\lambda\cos(\varphi-\psi)+\cos\psi], \tag{10}$$

$$Y=L[\lambda\sin(\varphi-\psi)-\sin\psi]. \tag{11}$$

Equations (10) and (11) facilitate determination of the required coordinates of profile for any laws of motion. Calculations show that in all cases excepting that of the law of motion of a usual slotted-lever mechanism

with symmetrical tachograms, the configuration of the profile is obtained in the form of a closed loop with sharp edges while in some cases (for example, in the case of change of acceleration according to the sine law), the profile has mutually intersecting sections which cannot be accepted in practice.

To simplify the configuration of the profile, it is necessary to assign two or three paths of motion only during the first interval ($0 \leqslant \varphi \leqslant \pi$) by assuming that the driving roller interacts with the same profile during the second interval ($\pi \leqslant \varphi \leqslant 2\pi$) just as during the first interval.

After synthesizing several alternatives for the profile for the first interval, we will carry out comparative analysis of the main kinematic characteristics during the second interval and finally, on the basis of the results of synthesis and analysis, select the most suitable variant for given conditions.

In the design of mechanisms of discontinuous motion, use of the laws of motion with asymmetrical tachograms in which the extreme value of positive acceleration is 1.5 to 3 times the extremes value of negative acceleration [16] is recommended.

Summary

1. The necessary and sufficient conditions of motion, instantaneous stop and dwell of the links of slide plate lever mechanisms have been obtained in this work.

2. Calculation equations for determining coordinates of the profile of a rotating curvilinear slotted lever have been derived and the peculiarities of the method of synthesis of mechanisms with curvilinear profile of the driven link are shown.

3. Classification of 38 single position and multiposition mechanisms of discontinuous motion are given and the functions of position of some mechanisms have been found out for the case of reciprocating, swinging and rotating motions of the driven link. These mechanisms assist in obtaining the required law of motion, make it possible to change the ratio of the duration of motion to the duration of stop within wide limits and can be synthesized for regulating the dwell of the driven link.

4. The reference data given here can be employed in the design of mechanisms of discontinuous motion of automatic machines in engineering design.

References

1. Artobolevskii, I. I., N. I. Levitskii and S. A. Cherkudinov. Sintez ploskikh mekhanizmov (Synthesis of Plane Mechanisms). Fizmatgiz, 1959.

2. KUKHARENKO, P. G. Trekhzvennyi mekhanizm s vystoem polnooborotnoi kulisy (Three-link mechanisms with stop of completely rotating slotted lever). Sb. *Teoriya mekhanizmov i mashin*, Izd-vo Mashinostroenie, 1965.
3. KUKHARENKO, P. G. Mal'tiiskii mekhanizm s uvelichennymi uglami vystoya. Avt. svid. No. 167721 (Klass F 06 h; 47 h, 5) [Maltese mechanism with increased angles of dwell. Authors Patent No. 167721 (Class F 06 h; 47h, 5)]. *Byull. izobretenii*, No. 2, 1965.
4. KUKHARENKO, P. G. Mal'tiiskie mekhanizmy dlya snizheniya inertsionnykh nagruzok v avtomatakh s privodami preryvistogo dvizheniya (Maltese mechanisms with drives of discontinuous motion for reducing inertia loads in automatic machines). *Mashinovedenie*, No. 4, 1965.
5. ARTOBOLEVSKII, I. I. Mekhanizmy, I-IV (Mechanisms, I-IV). Izd-vo AN SSSR, 1947-1951.
6. BEIER, R. Kinematicheskii sintez mekhanizmov (Kinematic Synthesis of Mechanisms). Mashgiz, 1959.
7. EREMEEV, N. V. Sharnirnye mekhanizmy so mnozhestvom zakonov dvizheniya rabochego zvena (Hinged mechanisms with many laws of motion of the working link). Sb. *Analiz i sintez mekhanizmov*, Mashgiz, 1963.
8. ZINOV'EV, V. A. Kurs teorii mekhanizmov i mashin (Textbook of Theory of Mechanisms and Machines). Fizmatgiz, 1960.
9. KOZHEVNIKOV, S. N., YA. I. ESIPENKO and YA. M. RASKIN. Mekhanizmy (Mechanisms). Izd-vo Mashinostroenie, 1965.
10. LIKHTENKHEL'D, V. Sintez mekhanizmov (Synthesis of Mechanisms). Izd-vo Nauka, 1964.
11. SPERANSKII, N. V. Proektirovanie mal'tiiskikh mekhanizmov (Design of Maltese Mechanisms). Izd-vo AN SSSR, 1960.
12. YUDIN, V. A. Mekhanizmy priborov (Mechanisms of Instruments). **1**, Mashgiz, 1949.
13. Nauchnoe nasledie P. L. Chebysheva. Teoriya mekhanizmov (Scientific Inheritance of P. L. Chebyshev. Theory of Mechanisms). Izd-vo AN SSSR, 1945.
14. BOCK, A. Der Systematische Aufbau der Schaltgetriebe. *Maschinenbautechnik*, No. 3, 1955.
15. KIPER, G. Möglichkeiten und Grenzen des einfachen Kurvengetriebes mit umlaufenden Gliedern für Antrieb und Abtrieb. *Maschinenbautechnik*, No. 11, 1956.
16. ROTBART, H. Cams, New York, 1956.
17. HAIN, K. Systematik mehrgliedriger Kurvengetriebe und ihre Anwendungsmöglichkeiten. *Maschinenbautechnik*, No. 12, 1960.

N. I. Levitskii and *Yu. L. Sarkisyan*

PECULIARITIES OF THE LAGRANGIAN METHOD IN THE SYNTHESIS OF MECHANISMS

If the expression of the weighed difference cannot be expressed in the form of a generalized polynom, the conditions of minimum mean square deviation lead to nonlinear systems of equations.

Some peculiarities of the Lagrangian method leading to linearization of nonlinear systems in the quadratic synthesis of mechanisms are considered in this article.

In solving design problems of mechanism, one often encounters an approximating function of the following type:

$$\Delta_q = A\,[F(\alpha) - p_0 f_0(\alpha) \cdot - p_1 f_1(\alpha) -, \ldots, \; p_4 f \;\; (\alpha)], \tag{1}$$

where coefficient p_4 conforms to the condition:

$$p_4 - p_0 p_1 = 0\,. \tag{2}$$

The necessary expression of the relative minimum of integral:

$$I = \int_{\alpha_0}^{\alpha_m} [\Delta_q(\alpha)]^2\, d\alpha \tag{3}$$

in accordance with the invariant form of the first differential can be written as:

$$\sum_{i=0}^{4} (\partial I / \partial p_i)\, dp_i = 0. \tag{4}$$

But it should not be concluded from expression (4) that the coefficients $\partial I/\partial p_i$ of differentials are equal to zero, since the differential dp_4 is not arbitrary.

Formulating the auxiliary function:

$$\Phi=I+\lambda(p_0p_1-p_4) \tag{5}$$

and following the well-known Lagrangian method, we find the necessary conditions of converting the mean square integral into relative minimum:

$$\partial\Phi/\partial p_i=0; \quad i=0,\ 1,\ 2,\ 3 \text{ and } 4. \tag{6}$$

System (6) can be written as:

$$\begin{aligned}
&c_{00}p_0+c_{01}p_1+c_{02}p_2+c_{03}p_3+c_{04}p_4+\lambda p_1=\gamma_0;\\
&c_{10}p_0+c_{11}p_1+c_{12}p_2+c_{13}p_3+c_{14}p_4+\lambda p_0=\gamma_1;\\
&c_{20}p_0+c_{21}p_1+c_{22}p_2+c_{23}p_3+c_{24}p_4=\gamma_2;\\
&c_{30}p_0+c_{31}p_1+c_{32}p_2+c_{33}p_3+c_{34}p_4=\gamma_3;\\
&c_{40}p_0+c_{41}p_1+c_{42}p_2+c_{43}p_3+c_{44}p_4-\lambda=\gamma_4,
\end{aligned} \tag{7}$$

where

$$\begin{aligned}
c_{kl}&=\int_{\alpha_0}^{\alpha_m} f_k(\alpha)f_l(\alpha)\,d\alpha; \qquad k=0,\ 1,\ 2,\ 3 \text{ and } 4;\\
\gamma_k&=\int_{\alpha_0}^{\alpha_m} F(\alpha)f_k(\alpha)\,d\alpha; \qquad l=0,\ 1,\ 2,\ 3 \text{ and } 4.
\end{aligned} \tag{8}$$

Correct solution of the systems of equations (7) and (2) requires solution of the equation of the fifth order [1].

From the fifth equation of system (7), we have:

$$\lambda=1/A\cdot\int_{\alpha_0}^{\alpha_m}\Delta_q(\alpha)f_4(\alpha)d\alpha. \tag{9}$$

If the function $f_4(\alpha)$ does not change its sign during the approximation interval $[\alpha_0, \alpha_m]$ in accordance with the first theorem about the means, we have:

$$\lambda=1/A\cdot\Delta_q(\alpha_k)\int_{\alpha_0}^{\alpha_m} f_4(\alpha)\,d\alpha, \tag{10}$$

where α_k is some value of angle α belonging to the interval $[\alpha_0, \alpha_m]$. When the function $f_4(\alpha)$ to be integrated, changes its sign on the approximation section, the segment $[\alpha_0, \alpha_m]$ should be divided into intervals of constant sign and the theorem of means should be used.

For example, if the function changes sign only once:

$$\lambda=1/A\cdot\left[\Delta_q(\alpha_{k_1})\int_{\alpha_0}^{\alpha'_m}f_4(\alpha)d\alpha+\Delta_q(\alpha_{k_2})\int_{\alpha'_m}^{\alpha_m}f_4(\alpha)\,d\alpha\right], \tag{11}$$

where α_{k_1} and α_{k_2} are some values of angle α from intervals $[\alpha_0, \alpha'_m]$ and $[\alpha'_m, \alpha_m]$ within which the function $f_4(\alpha)$ retains constant sign.

The second theorem of means,

$$\lambda=1/A\cdot\left[f_4(\alpha_0)\int_{\alpha_0}^{\alpha_k}\Delta_q(\alpha)\,d\alpha+f_4(\alpha_m)\int_{\alpha_k}^{\alpha_m}\Delta_q(\alpha)d\alpha\right] \tag{12}$$

where $\alpha_0\leqslant\alpha_k\leqslant\alpha_m$, can be applied to the integral expression of polynom λ in the case of a monotonously changing function $f_4(\alpha)$ on the approximation section.

In the case of an arbitrary change in function $f_4(\alpha)$, the approximation segment $[\alpha_0, \alpha_m]$ can be divided into intervals of monotonic nature and we obtain the corresponding equation for estimating the value of λ.

By analyzing expressions (10)-(12), we can prove that the value of λ on the section of approximation is sufficiently small. Either sin α or cos α represents function $f_4(\alpha)$ in the problems of synthesis of mechanisms.

Then for every interval $[\alpha_0, \alpha_m]$, the following inequality is valid:

$$\left|\int_{\alpha_0}^{\alpha_m}f_4(\alpha)\,d\alpha\right|\leqslant 2,$$

and on the basis of equation (10), we have:

$$|\lambda|\leqslant 2/A\cdot|\Delta_q(\alpha_k)|. \tag{13}$$

It should be expected from the formulation of the problem of approximate synthesis that, at all values of α_k on the approximation section, the value of weighted difference will be sufficiently close to zero. In the case of correct approximation in equation (13), the values of integrals are sufficiently small since Δ_q frequently changes its sign.

Consequently, the Lagrangian polynom can be put equal to zero in some approximation on the basis of equations (10)-(13).

Putting $\lambda=0$, system (7) can be written as:

$$\sum_{l=0}^{4}c_{kl}p_k=\gamma_k; \qquad k=0,\ 1,\ 2,\ 3 \text{ and } 4. \tag{14}$$

It is not difficult to prove that linear equations (14) represent the conditions of minimum mean square integral (1) when the parameters p_i and consequently, differentials dp_i in sum (14) are independent, i.e.

$$\partial I/dp_i=0; \qquad i=0,\ 1,\ 2,\ 3 \text{ and } 4. \tag{15}$$

As mentioned earlier, this conclusion does not follow from equation (4) but is valid only where $\lambda=0$.

As we demonstrated above, usually $\lambda\approx 0$ in the problems of synthesis of mechanisms. Therefore, in some approximation, the conditions of minimum mean square integral require that its derivatives with respect to independent parameters p_i should be equal to zero.

This conclusion is based on the properties of quadratic approximation in the synthesis of mechanisms. The conditions of minimum (15) do not depend on equation (2) which is only approximately satisfied in the case of values of the required parameters determined from the linear system (15).

In general, determination of approximate values of $n+1+m$ unknown coefficients of the approximate function:

$$\begin{aligned}\Delta_q=A\,[\,F(\alpha)-p_0 f_0(\alpha)-,\ \ldots,\ -p_n f_n(\alpha)-p_{n+1}f_{n+1}(\alpha)-,\ \ldots,\\ -p_{n+m}f_{n+m}(\alpha)\,]\end{aligned} \tag{16}$$

we approximately have the simultaneous (redetermined) system of equations:

$$\begin{aligned}p_i&=\varphi_i(p_0, p_1, \ldots, p_n)\\ i&=n+1, n+2, \ldots, n+m.\end{aligned} \tag{17}$$

and $n+1+m$ linear heterogeneous equations:

$$\sum_{l=0}^{n+m} c_{kl}p_k=\gamma_k; \qquad k=0,\ 1,\ 2,\ \ldots,\ n+m. \tag{18}$$

The unknown parameters p_k should be calculated from the linear system (18). In addition, the approximate satisfaction of equations (17) should be verified and if necessary the values of parameters p_k should be corrected by using the method of iteration or linear correction.

Approximate values of the required parameters can also be determined from the system of $n+1$ linear equations and m equations of constraints.

In this case, the unknown parameters are determined by solving the equation of the higher order (second, third, etc.) and are verified in accordance with the unused linear equations [1].

Other alternatives of solving the above mentioned redetermined system are also possible.

The total number of such methods is equal to the combination of one out of $1+2$ elements.

If the matrix of heterogeneous linear system (18) is symmetrical, it is easier to use the method of quadratic roots for the purpose of reducing the calculations.

For example, let us calculate four parameters of a four-link digital-calculating mechanism meant for the reproduction of logarithmic function $y=\log x$ within limits from $x=1$ to $x=10$ in the case of given values of the input and output angles:

$$\varphi_m=55°,\ \psi_m=-90°.$$

Solution of this problem with the help of the quadratic equation is given in article [2]. Assuming $\lambda=0$, the conditions of minimum square value of the given weighted difference are written as the following linear system:

$$\begin{aligned}
&11p_3+7.19867p_2-3.34302p_1-7.25870p_0-6.42196p_4=9.96784;\\
&7.19867p_3+5.694236p_2-2.613900p_1-5.624414p_0-3.572215p_4\\
&\qquad=6.441909;\\
&-3.34302p_3-2.613900p_2+1.777937p_1+3.008803p_0+0.934039p_4\\
&\qquad=-2.671287;\\
&-7.25870p_3-5.624414p_2+3.008803p_1+5.884735p_0+3.133354p_4\\
&\qquad=-6.264517;\\
&-6.42196p_3-3.512215p_2+0.934039p_1+3.133354p_0+5.115289p_4\\
&\qquad=-6.286323.
\end{aligned}$$

Solving the system, we get the approximate values of parameters $p_0=0.748208$; $p_1=-0.483908$; $p_2=0.604942$ and $p_3=0.645565$.

Values of the required parameters, corrected by the method of iteration are $p_0=0.76805$; $p_1=-0.51134$; $p_2=0.63037$ and $p_3=0.61578$.

In some cases, nonlinear systems of quadratic synthesis lead to homogeneous systems after linearization in the above mentioned way.

We often come across an approximate function of the following type in problems of the design of mechanisms:

$$\Delta_q=p_0f_0(\alpha)+p_1f_1(\alpha)+p_2f_2(\alpha)+,\ \ldots,+p_5f_5(\alpha)+p_6f_6(\alpha), \tag{19}$$

in which coefficients p_5 and p_6 are given by the equations:

$$p_5=-(p_0p_2+p_1p_3); \tag{20}$$

$$p_6=p_1p_2-p_0p_3. \tag{21}$$

The conditions of relative minimum of the mean square integral are expressed in the form of the wellknown nonlinear system (1). If the Lagrangian factors are taken equal to zero, we get the following linear system:

$$\sum_{l=0}^{6} c_{kl} p_k = 0; \qquad k=0, 1, 2, 3, 4, 5 \text{ and } 6. \tag{22}$$

In order that the homogeneous linear system (22) may not have zero solution, it is a necessary and sufficient condition that the following determinant is equal to zero:

$$D = \begin{vmatrix} c_{00} & \cdots & c_{06} \\ \cdots & \cdots & \cdots \\ \cdots & \cdots & \cdots \\ c_{60} & \cdots & c_{66} \end{vmatrix} = 0. \tag{23}$$

The general solution of system (22) can be found from the first six equations.

Thus, expressing all the unknown parameters through p_0, we have:

$$p_i = k_i p_0, \qquad i=1, 2, \ldots, 6, \tag{24}$$

where k_i are some known numerical coefficients.

To fulfill the conditions (23), the seventh equation of the system (22) after putting equation (24) becomes an identity.

Putting equation (24) in the constraint equations (20) and (21), we get the following equations for determining the approximate value of p_0:

$$p_0 = -k_5/(k_2 + k_1 k_3); \tag{25}$$

$$p_0 = -k_5/(k_1 k_2 - k_3). \tag{26}$$

After determining p_0 from either equation (25) or (26), we get the value of the remaining parameters from relations (24). With these values of the parameters the unused expression for p_0 is satisfied identically. Thus, on fulfilling the condition (23), we have an approximately simultaneous system of nine equations (20), (21) and (22) with seven unknown parameters. For example, let us consider five parameters of the above mentioned digital-calculating mechanisms for the same initial data.

Solution of this problem using a cubic equation is given in article [1].

On assuming $\lambda = \lambda_1 = 0$ the conditions of minimum mean square deviation of the weighted difference have the form:

$$\begin{aligned}
&11 p_4 + 3.71084 p_5 - 6.98502 p_6 + 6.85312 p_2 - 6.85312 p_3 \\
&\qquad + 3.34302 p_1 + 9.96784 p_0 = 0; \\
&3.71084 p_4 - 5.438359 p_5 - 1.09038 p_6 + 4.57992 p_2 - 0.292962 p_3 \\
&\qquad - 0.655802 p_1 + 4.194198 p_0 = 0; \\
&-6.98502 p_4 - 1.09038 p_5 + 5.561608 p_6 - 3.635997 p_2 + 5.38794 p_3 \\
&\qquad - 2.658872 p_1 - 6.197281 p_0 = 0; \\
&6.85312 p_4 + 4.57992 p_5 - 3.635997 p_6 + 5.500031 p_2 - 3.156895 p_3 \\
&\qquad + 1.115981 p_1 + 6.657043 p_0 = 0;
\end{aligned}$$

$$-6.85312\,p_4-0.292962\,p_5+5.38794\,p_6-3.156895\,p_2+5.500031\,p_3$$
$$-2.946175\,p_1-5.86907\,p_0=0;$$
$$-3.34302\,p_4-0.655802\,p_5-2.658872\,p_6+1.115981\,p_2-2.946175\,p_3$$
$$+1.777937\,p_1+2.671286\,p_0=0;$$
$$9.96784\,p_4+4.194198\,p_5-6.197281\,p_6+6.657043\,p_2-5.86907\,p_3$$
$$+2.671286\,p_1+9.222036\,p_0=0.$$

Following the procedure outlined in article [1], we reduce the approximate solution of this system to the solution of the cubic equation with respect to the ratio p_1/p_0 by using the first four equations of the system and relations (20) and (21).

Let us solve this system according to the above described method. From the first six equations, we get the relations (24), i.e.

$$p_1=-0.473451\,p_0; \qquad p_4=-0.599102\,p_0;$$
$$p_2=-0.400013\,p_0; \qquad p_5=-0.000006\,p_0;$$
$$p_3=-0.76850\,p_0; \qquad p_6=-0.618752\,p_0.$$

Substituting these values in the sixth equation of the system changes it into an identity (with the accuracy up to five decimal places).

Consequently, the homogeneous system is approximately simultaneous and condition (23) is satisfied.

Putting the expressions for the coefficients p_1, p_2, p_3 and p_6 in the equation (21), we get the approximate value of the coefficient:

$$p_0=0.645785\,.$$

Further, we calculate the approximate values of the remaining coefficients:

$$p_1=-0.305747;$$
$$p_2=-0.258322;$$
$$p_3=-0.496449;$$
$$p_4=-0.386891;$$
$$p_5=0.000004;$$
$$p_6=0.399581.$$

Verification shows that these values of the coefficients approximately satisfy the equation (20).

The required parameters of the mechanism are calculated from equations given in article [1].

$$a=0.714446; \quad b=1.024619; \quad c=0.559638; \quad \alpha=25°30'30'';$$
$$\beta=62°3'035''.$$

The mechanism obtained is shown in Fig. a. Further, the values of the weighted difference have been calculated for all the selected points. The graph of change in Δ_q is shown in Fig. b where Δ_q attains maximum value at $i=3$.

These peculiarities of the Lagrangian method in the synthesis of mechanisms provide a base for optimum selection of approximation method. In many cases, especially while calculating a large number of parameters when sufficiently small value of the weighted difference is expected, the method of minimum squares should be assumed to be the most rational method since the solution can be obtained from linear systems.

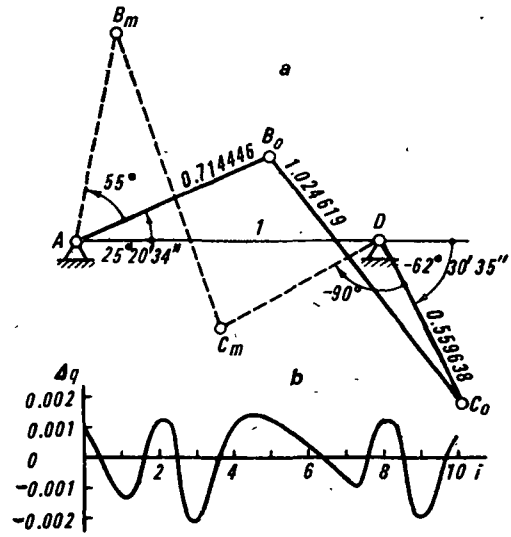

Fig.

In a discussion of the analytical methods of synthesis F. Freudenstein [3] points out the general nature and simplicity of the N. I. Levitskii's method of calculating a small number of parameters as well as the complications of this method in the calculation of a large number of parameters due to nonlinear equations present in the expression for the approximate function. The quadratic synthesis should however be considered equally effective in the case of small and large number of parameters since these complications can be absolutely eliminated on using the above suggested method of linearization.

References

1. Artobolevskii, I. I., N. I. Levitskii and S. A. Cherkudinov. Sintez ploskikh mekhanizmov (Synthesis of Plane Mechanisms). Fizmatgiz, 1959.
2. Levitskii, N. I. Proektirovanie ploskikh mekhanizmov s nizshimi parami (Design of Plane Mechanisms Having Lower Pairs). Izd-vo AN SSSR, 1950.
3. Freudenstein, F. Structural error analysis in plane kinematic synthesis. *Journal of Engineering for Industry*, **21**, 1959.

D. M. Lukichev, V. A. Nikonorov and *Z. S. Gazizova*

DESIGN OF CAM ELEMENTS OF ELECTRICAL SWITCHES

Studies on existing designs of cam elements and fixing mechanisms of electrical switches were undertaken by the Department of Theory of Mechanisms at the Bauman Moscow Higher Technical School (MVTU). Recommendations concerning designs for reliable operation have been worked out.

Schemes of cam elements with swinging lever and translatory followers were studied. The scheme for one of the cam elements is shown in Fig. 1.

For normal operation of the cam contactor, provision must be made for the following:

1) sufficient contact pressure which should be maintained during use in spite of wear and tear of components;

2) optimum aperture (opening) of contacts which should be constant in spite of wear and tear;

(3) sufficient velocity of the contact during breaking, but this condition contradicts the smooth operation of the mechanism, with the aim of reducing the wear, therefore, the initial velocity of breaking of the contact must be selected on the basis of electrical parameters;

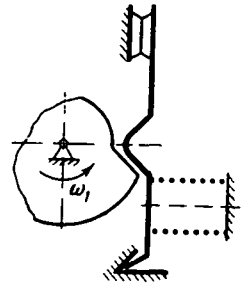

Fig. 1.

4) certain value of the instantaneous efficiency of the mechanism to avoid self breaking or large forces, which is particularly important in the case of manual control of power cam elements;

5) self cleaning of contacts by their slipping provided by the clearance in the kinematic pairs and by the elasticity of the components;

6) cam profile satisfactory from the point of view of its simplicity, maximum pressure angle, and minimum radius of curvature of the profile as defined by the value of the permissible stresses in the material; and

7) correct selection of material taking into account the coefficients of friction and wear of various kinematic pairs to fulfill condition (2) and to secure the required number of cycles of contact operation.

Determination of optimum geometrical dimensions of the mechanism links, forces in the spring and rational location of the axis of the latter are related to the above mentioned conditions.

A comparative analysis of the designs of cam elements with swinging lever and translatory follower showed the advantages of the former in terms of (higher) instantaneous efficiency and slipping of contacts for their self cleaning. Therefore, problems of designing only lever schemes are considered below.

1. Calculation of Profiles of Plate Cam and Lever

The basic parameters for calculation purposes follow: aperture of contacts along the normal to the surface S_{cs} (see Fig. 2 where *1* is the design profile and *2* is the pitch profile), angle of inclination β of the contact with the line of the lever, length of lever l_k, distance up to the center of the profile l_B, working angle of rotation of the cam φ_p, maximum permissible pressure angle α.

In order to obtain symmetrical law of motion of the lever for both directions of rotation of the plate cam, it is necessary to place the lever at its middle position at an angle of 90° with the radius O_1B. Total symmetry of the law of motion would have been for the case of rectilinear motion of point B and therefore, in actual practice, this symmetry is the best approximation.

If the center of rotation O_2 of the lever is displaced, the asymmetry of the law of motion and pressure angles will be intensified. On the basis of the given aperture of contacts, we find the design arc of displacement of point K from the equation:

$$S_k = S_{cs}/\cos\beta, \qquad (1)$$

by approximately taking $\triangle K_1K_2K'$ as a straight line. Then, we determine the displacement of the center of

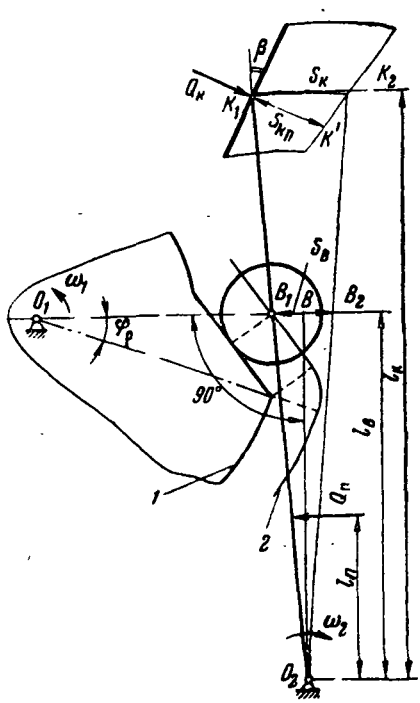

Fig. 2.

rounding B of the working profile of the lever:

$$S_B=h=S_k \cdot l_B/l_k. \tag{2}$$

The larger the angle β, the larger will be the displacement S_B and (at the given value of maximum permissible pressure angle α) the dimensions of the plate cam; therefore, from this point of view, it is advantageous to take $\beta=0$.

First the pitch profile (equidistance) of cam should be drawn, then, the lever can be replaced by a follower sharpened at point B and if the angles of rotation of the lever are not large as usually happens in practice, the motion of point B is considered rectilinear. The corresponding calculation scheme is shown in Fig. 3.

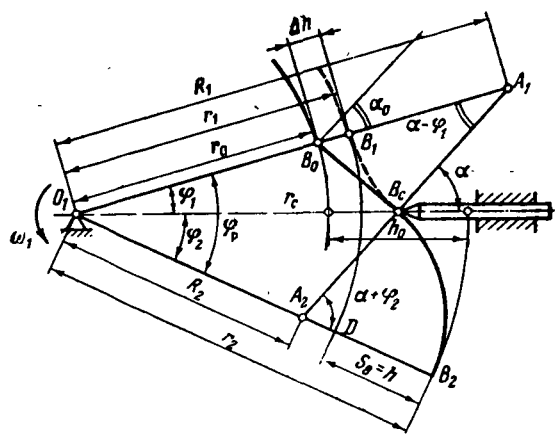

Fig. 3.

Let us calculate the convex section of the profile according to L. N. Reshetov's method [1, 2] by assuming the smooth operation of the mechanism. In order to do this as demonstrated in article [3], let us determine the maximum and minimum radius vectors of the pitch profile from $\triangle O_1B_1B_c$ and $\triangle O_1B_cB_2$:

$$r_1=r_c \cos[(\alpha+\varphi_1)/2]:\cos[(\alpha-\varphi_1)/2]; \tag{3}$$

$$r_2=r_c \cos[(\alpha-\varphi_2)/2]:\cos[(\alpha+\varphi_2)/2]; \tag{4}$$

where profile angles:

$$\varphi_1=\varphi_p/(1+\nu); \tag{5}$$

$$\varphi_2=\varphi_p\nu/(1+\nu) \tag{6}$$

and radius vector of the profile at the transition point:

$$r_c=O_1B_c=h \cos[(\alpha-\varphi_1)/2] \cdot \cos[(\alpha+\varphi_2)/2]:\sin\alpha \cdot \sin(\varphi_w/2). \tag{7}$$

The ratio of the average accelerations will be:

$$\nu = a_1/a_2 = \varphi_2/\varphi_1 . \tag{8}$$

Parameter ν is selected by taking into account that the lever is taken away from the cam center during breaking of the contacts by the plate cam and brought close to the cam center on closing the contacts by the spring. To avoid separation of the lever from the cam (and the resulting jerk), the spring must overcome the reduced force of inertia of the lever with some safety factor ψ.

Reference [1] at $\psi=2.2$ gave the optimum value $\nu=1.5$. Thus the permissible pressure angle α for cam-lever mechanisms is between 50-60°.

From $\triangle O_1B_cA_1$ and $\triangle O_1B_cA_2$, the distance up to the centers of arcs B_1B_c and B_2B_c will be:

$$R_1 = O_1A_1 = r_c \sin\alpha/\sin(\alpha-\varphi_1) = h/2 \cdot \cos[(\alpha+\varphi_2)/2] : \{\sin[(\alpha-\varphi_1)/2]\sin(\varphi_2/2)\} \tag{9}$$

and

$$R_2 = O_1A_2 = r_c \sin\alpha/\sin(\alpha+\varphi_2) = h/2 \cdot \cos[(\alpha-\varphi_1)/2] : \{(\sin[(\alpha+\varphi_2)/2]\sin(\varphi_2/2)\}. \tag{10}$$

Graphical solution is also possible [2]. However, the resulting concave section of the profile B_1B_c, calculated by taking into account the smooth operation and indicated by the dotted line, does not produce the necessary initial velocity for closing the contacts, which may get burnt.

Therefore, it is necessary to replace the concave section of the profile by a straight line and to design a tangential cam with jerk of plate cam against lever at point B_0 (see Fig. 3).

As a result, the possible travel of point B of the lever increases by $\Delta h = B_0B_1$, i.e. from h to

$$h_0 = h + \Delta h. \tag{11}$$

The additional displacement is determined from the drawing with the help of the equations:

$$\Delta h = B_0B_1 = A_1B_c/\cos(\alpha-\varphi_1) - A_1B_1 = (R_1-r_1)/\cos(\alpha-\varphi_1) - (R_1-r_1);$$

or

$$\Delta h = (R_1-r_1)\{[1/\cos(\alpha-\varphi_1)]-1\}. \tag{12}$$

To avoid sharp points in the design profile, the radius of rounding of the working profile of lever (see Fig. 4 where *1* is the design profile and *2* is the pitch profile) must be:

$$r_r < A_2B_2 = r_2 - R_2 . \tag{13}$$

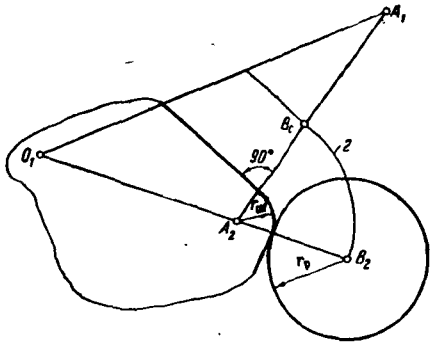

Fig. 4.

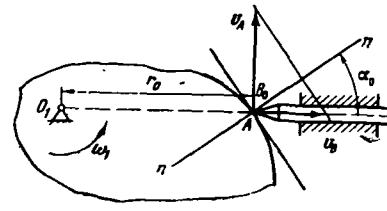

Fig. 5.

In this case, it is necessary to take into account the elasticity of the material and to satisfy the condition:

$$r_r \geqslant r_{r\,\min}, \tag{14}$$

where $r_{p\min}$ is the minimum permissible value taken depending on technological considerations. The maximum radius of design profile of the plate cam is calculated from equation:

$$R_w = r_2 - r_p. \tag{15}$$

The initial radius vector of the pitch profile is:

$$r_0 = r_1 - \Delta h = O_1 B_0. \tag{16}$$

The distance between the axes of rotation of the plate cam and lever is calculated from the right angled $\triangle O_1 B O_2$ for the middle position of lever from the equation:

$$A = O_1 O_2 = \sqrt{(r_2 - h_0/2)^2 + l_B^2}. \tag{17}$$

The initial velocity of separation of contacts v_C can be determined from Fig. 5.

If point A lies on the cam profile then:

$$\tan \alpha_0 = \mathbf{v}_B / \mathrm{v}_A = \underline{\mathbf{v}}_B / (\omega_1 \cdot r_0),$$

but $\underline{\mathbf{v}}_C = \underline{\mathbf{v}}_B l_k / l_B$, consequently:

$$v_c = \tan \alpha_0 \cdot \omega_1 \cdot r_0 l_k / l_B. \tag{18}$$

This value for the velocity of breaking of contacts must be comparable with the value of minimum permissible velocity $v_{k\vartheta} = f$ (electrical parameters) obtained experimentally:

$$v_C \geqslant v_{k\vartheta}. \tag{19}$$

If this velocity is low, it can be increased by increasing the pressure angle α_0 or by redistributing angles φ_1 and φ_2. The velocity can be reduced by introducing an intermediate section of concave profile, i.e. by introducing a combined profile consisting of a rectilinear section, concave and convex arcs of the circle.

It should, however, be kept in mind that an increase in pressure angles reduces the efficiency of the mechanism and at a given force on the control handle, the actual velocity of breaking of contacts can increase as well as decrease.

2. Calculation of Spring Tension

The spring must be able to overcome the reduced force of inertia of the lever $m_l^{\text{red}} \cdot a_2$, equal to the product of the reduced mass of the lever and acceleration with some safety factor ψ.

The spring force $Q_{s \cdot p} = \psi m_l^{\text{red}} \cdot a_2$ is necessary to avoid separation of lever from the disc cam during closing of contacts. Moreover, in the case of closed contacts, the spring must provide required force to the contacts Q_c and consequently, the force in the spring in the case of closed contacts must be:

$$Q_{s1} = Q_k \frac{l_k \cdot \cos\beta}{l_s \eta_s}, \tag{20}$$

where η_s is the efficiency of the lever with spring (tentatively it can be taken that $\eta_s = 0.95$).

It is expedient to start calculation of spring from formula (20) and later on, to verify the value of spring force $Q_{s.c}$ for the transition point B_c from formula:

$$Q_{s \cdot c} \geqslant Q_{s \cdot p} = \psi \cdot m_l^{\text{red}} a_2, \tag{21}$$

by assigning the maximum possible value of angular velocity ω_1 of plate cam since the acceleration a_2 of point B of the lever is proportional to the square of angular velocity ω_1.

The reduced mass at point B of the lever is determined from the equation:

$$m_l^{\text{red}} = I_l / l^2, \tag{22}$$

where I_l is the moment of inertia of the lever about the axis of rotation.

If the spring force Q_{s1} obtained under the given conditions with closed contacts is much more than the value $Q_{s \cdot p}$ obtained from dynamic calculations, while drawing the pitch profile of the plate cam (if it is advisable from the point of view of other reasons, for example, technological considera-

tions for selecting the radius of rounding of the lever profile), it is possible to take $\nu > 1.5$ and consequently, to increase the safety factor of the spring in the dynamic calculations.

3. Consideration of Wear of Contacts and Kinematic Pairs while Drawing Pitch Profile of the Plate Cam

With reference to Fig. 2, the wear of contacts directly increases their aperture $S_{c.s}$ by some value λ_k and in individual cases maximum value attained is equal to twice the thickness of the contact metal. On the other hand, wear of the profiles of plate cam λ_w and lever λ_l reduces the aperture of contacts by $(\lambda_w+\lambda_l)l_k/l_B \cos\beta$.

In the case of wear λ_0 of fulcrum O_2 of the lever, the separation of contacts increases by $\lambda_0=(l_k-l_B)/l_B \times \cos\beta$. The condition of constant separation will be:

$$\lambda=\lambda_k-(\lambda_w+\lambda_l)l_k/l_B \cdot \cos\beta+\lambda_0(l_k-l_B)/l_B \cos\beta=0. \qquad (23)$$

If for example, $\lambda_k=2$; $\lambda_w=\lambda_l=0.25$; $\lambda_0=0.25$; $l_k=30$; $l_B=16$ are taken in millimeters and β is taken equal to 30°, then the maximum change in the separation of contacts will be

$$\Delta S_k=\lambda=2-(0.25+0.25)30/16\times 0.866+0.25\times 14/16\times 0.866=1.38 \text{(increase)}.$$

Since this increase in the separation of contacts causes a change in the main calculation parameter (the displacement of point $B(S_B=h_0)$ and it is not possible to increase the angle φ_p of the cam, the pitch profile should be designed in accordance with the parameter $S_{c.s}+\Delta S_k$, i.e. by orienting upon the cam element with total wear, and not in accordance with the displacements $S_{c.s}$.

Then the actual working angle of rotation of the cam φ_r becomes slightly less than that given by the number of positions for a new mechanism and equal to it for a completely worn-out mechanism. This is important since if a new cam element is designed with reference to angle φ_p, then due to wear, the actual angle φ_p becomes more than the value given by the number of positions and the contacts may open and burn.

Problems concerning rational location of lever fulcrum, spring axis and sliding contacts are also taken into account in the design of the optimum version of the kinematic scheme of a cam element.

References

1. Reshetov, L. N. Kulachkovye mekhanizmy (Cam Mechanisms). Mashgiz, 1953.

2. RESHETOV, L. N. Proektirovanie diskovykh kulachkov naimen'shikh gabaritov (Design of disk cams of minimum dimensions). Sb. *Voprosy teorii mekhanizmov i mashin*, Mashgiz, 1955.
3. RESHETOV, L. N. and D. M. LUKICHEV. Novyi metod rascheta profilya kulachkov, ocherchennykh dugami okruzhnostei (A new method of calculating profile of circular arc cams). *Trudy seminara po teorii mashin i mekhanizmov*, vyp. 74, Izd-vo AN SSSR, 1959.

L. B. Maisyuk

SYNTHESIS OF CAM-PLANETARY-CONNECTING ROD MECHANISM WITH REVERSE STROKE AND STOP

Designs of modern industrial process machinery often call for the reproduction of complicated one-sided motion. For example, in an automatic sugar refining line "Shambon" [1], the horizontal conveyor of the drier has a reverse stroke motion.

The nature of this motion is shown in Fig. 1, a by the curve $\psi=f(\varphi)$. The angles of rotation of the driving and driven links of the mechanism which run the operating unit, are taken along the abscissa and ordinate axes of the graph respectively. A more complicated case of one-sided motion occurs in the driving mechanism of flying shears used for cutting the ends of rolled strips [2]. Fig. 1, b shows the graph of the displacement function $\psi=f(\varphi)$ of this mechanism.

In some cases, substitution of the law of two-sided motion by a more complex law of one-sided motion can give positive results. As an example, let us consider the process of bending thimbles on a circular bending semi-automatic machine [2].

The displacement function $\psi=f_t(t)$ corresponding to the two-sided motion with stop (curve *1*) is shown in Fig. 1, c (t is time and ψ is the angle of rotation of the driven link). The displacement function $\psi=f_0(t)$ corresponding to the proposed one-sided motion with reverse

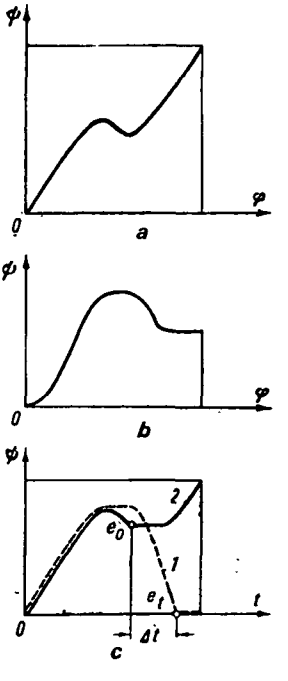

Fig. 1.

stroke and stop (curve *2*) is shown by the continuous curve. The points e_t (for two-sided motion) and e_0 (for one-sided motion) denote the angles corresponding to the beginning of feed of the next blank to the bending die.

The improvement in efficiency:

$$t_{e_t} - t_{e_0} = \Delta t$$

is obvious from Fig. 1, c in the case of the more complex one-sided motion for the bending semi-automatic machine.

The laws of motion shown in Fig. 1, a can be reproduced by the simplest toothed lever mechanisms. However, they are not always suitable for reproducing the laws of motion shown in Figs. 1, b and 1, c. This results from the fact that toothed lever mechanisms only approximately reproduce the complicated laws of one-sided motion. Cam toothed lever mechanisms including cam-planetary-connecting rod mechanisms do not have this deficiency because they do not possess any higher pairs.

Fig. 2 is the schematic diagram of a cam-planetary-connecting rod mechanism consisting of hinged four-link mechanism *lbcd*, three toothed gears z_1, z_2, z_3 and higher pair *lef* with fixed cam. Link *d* is the support. The crank *l* to which the toothed gear z_1 is attached represents the driving link of the mechanism. The toothed gear z_3 is the driven link. For uniform rotation of the driving crank, the driven link of the mechanism generates complicated one-sided motion.

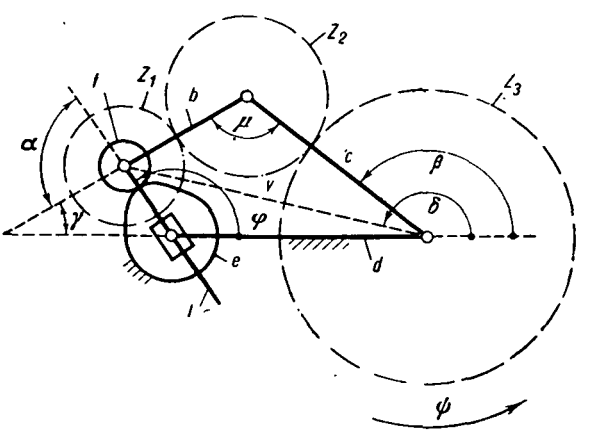

Fig. 2.

Let us define the problem of reproduction of the displacement function shown by continuous curve in Fig. 3, a with the aid of this mechanism where $1-\psi=f_2(\varphi)$; $2-\psi=f_3(\varphi)$; $3-\psi=\text{const}$. The angles of rotation φ of the driving crank-follower *l* are taken along the abscissa axis and the angles of rotation ψ of the driven toothed gear z_3, along the ordinate axis. The curve

shown by dotted line [$\psi=f_1(\varphi)$] can be reproduced by the toothed lever mechanism. If the design conditions require stop of the driven link in addition to the reverse stroke, the corresponding motion shown in Fig. 3, a by continuous curve, can be provided by the cam-planetary-connecting rod mechanism.

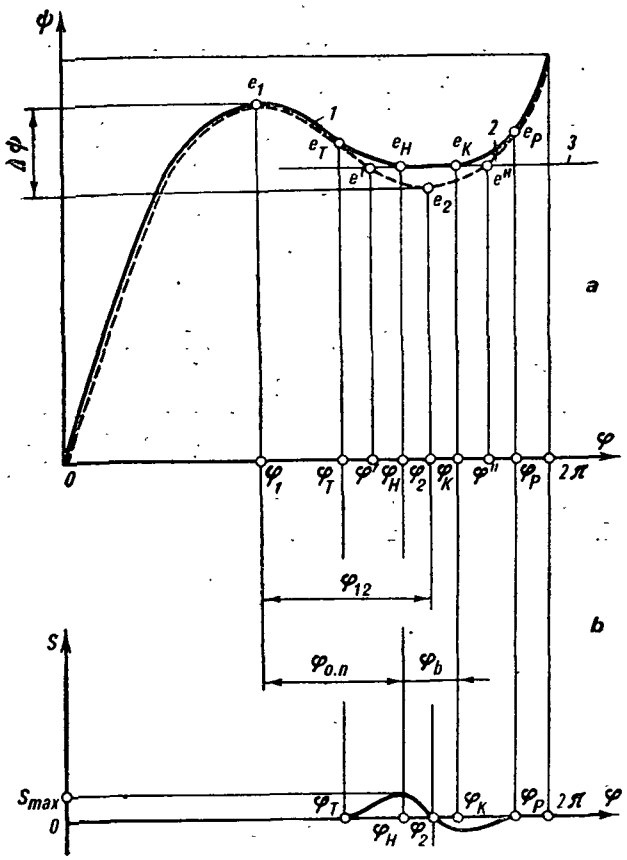

Fig. 3.

Rotation of the driving link through an angle $0-\varphi_1$ causes the driven link to rotate in one direction. In the case of rotation of the crank through an angle $\varphi_1-\varphi_H$ the driven toothed gear z_3 rotates in the reverse direction. The driven link has a dwell at the angle of rotation $\varphi_H-\varphi_k$ of the driving link. Further, at section $\varphi_k-2\pi$, the driven link rotates in the initial direction.

Let us call the angles of rotation of the crank:

$$\varphi_H-\varphi_1=\varphi_{r\cdot r}; \qquad (1)$$

$$\varphi_k-\varphi_H=\varphi_a, \qquad (2)$$

as the angle of reverse rotation and the angle of dwell.

The conditions of dwell of the driven link of the cam-planetary-connecting rod mechanism are given in reference [3].

$$\begin{aligned} &\psi=f(\varphi);\\ &\psi=\text{const}=C;\\ &l\neq\text{const}. \end{aligned} \tag{3}$$

Corresponding to conditions (3), the straight line $\psi=\text{const}$, intersects the curve of the displacement function of the toothed lever mechanism, shown by dotted lines, at points e' and e''. If the driven link is stopped at the angle of rotation $\varphi'\varphi''$ of the crank, then abrupt motions at the beginning and end of the stop are inevitable. To eliminate these it is necessary to introduce transient sections of smooth curves in the functional position of the mechanism during the intervals from motion to stop e_Te_H and from stop to motion, e_ke_p.

Thus, the required displacement function will consist of four different functions:

$$\psi=f_1(\varphi);\ \psi=f_2(\varphi);\ \psi=f_3(\varphi);\ \psi=\text{const}.$$

The function $\psi=f_1(\varphi)$ is considered to be known [3], since it is reproduced by this mechanism under the conditions:

$$\psi\neq\text{const};\qquad l=\text{const}=a, \tag{4}$$

and the function:

$$\psi=f_2(\varphi);\ \psi=\text{const};\ \psi=f_3(\varphi) \tag{5}$$

is reproduced under conditions (3).

Consequently, to generate the motion shown in Fig. 3, a by the dotted curve, it is necessary to determine the change in the length of link l, which is taken as the follower and the cam profile for which equation (5) will be satisfied.

If the curves $\psi=f_2(\varphi)$ and $\psi=f_3(\varphi)$ are selected arbitrarily then the condition at which these curves will touch the curve $\psi=f_1(\varphi)$ can be written as:

$$\begin{aligned} &f_2(\varphi_{T_1})=0;\\ &f_2'(\varphi_{T_1})=0;\\ &\cdots\cdots\cdots\\ &f_2^n(\varphi_{T_1})=0; \end{aligned} \tag{6}$$

$$\begin{aligned} &f_3(\varphi_{P_1})=0;\\ &f_3'(\varphi_{P_1})=0;\\ &\cdots\cdots\cdots\\ &f_3^n(\varphi_{P_1})=0. \end{aligned} \tag{7}$$

These conditions are obtained by assuming that the coordinates φ, ψ in the equations of curves $\psi=f_2(\varphi)$, $\psi=f_3(\varphi)$ have been replaced by the coordinates of the points of the curve $\psi=f_1(\varphi)$.

The relative displacement of the follower is determined from the equation:

$$s=l_i-l, \tag{8}$$

where l_i is the instantaneous length of link l.

The displacement curve $s=f(\varphi, \psi)$ providing the given law of motion of the driven link of the mechanism is plotted in Fig. 3, b in coordinates: abscissa φ and ordinate s.

While synthesizing a mechanism, we assume that the torque is to be maximum on the driving shaft [4].

In this case [3] the minimum value of the coefficient of maximum follower velocity δ_{max} will be observed when:

$$\mu_{min}=\pi-\mu_{max}, \tag{9}$$

where μ_{min} and μ_{max} are the extreme transmission angles of the four-link mechanism constituting the cam-planetary-connecting rod mechanism.

Equation (9) differentiates a small family from the whole complex of mechanisms. Let us consider the synthesis of one of the mechanisms satisfying the constraint (9) and conditions:

$$\left.\begin{aligned} i_{13}&=1;\\ b&=c, \end{aligned}\right\} \tag{10}$$

where i_{13}—gear ratio of the mechanism;

b, c—connecting rod and yoke of the four-link mechanism.

From Fig. 2 we get:

$$\mu=\beta-\gamma;$$

$$\alpha=\gamma-\varphi+\pi;$$

$$y=\sqrt{l^2+1-2l\cos\varphi}=-2b\cos(\delta-\gamma)=2b\cos(\delta-\beta);$$

$$\psi=-\alpha+i_{23}\mu+\beta,$$

where i_{23} is the gear ratio of toothed gears z_2z_3.

After transformations, the driving crank considered to be the follower, is determined from the expression

$$l=\cos\varphi\pm\sqrt{4b^2\cos^2\rho/2-\sin^2\varphi}, \tag{11}$$

where $\rho=(\psi+\pi-\varphi)/(i_{23}+1)$.

After differentiating equation (11), we get analogs of velocity and acceleration of the follower:

$$ds/d\varphi = -\sin\varphi \pm [2b^2 \sin\rho - (i_{23}+1)\sin 2\varphi]/[2(i_{23}+1)\sqrt{n}];$$

$$d^2s/d\varphi^2 = -\cos\varphi \pm \{(n_1 \sin 2\varphi - 2\sqrt{n}\cos 2\varphi)/2n - b^2[\sqrt{n}\cos\rho + n_1(1+i_{23})\cdot\sin\rho]/[n(1+i_{23})^2]\},$$

where $n = 4b^2\cos^2\rho/2 - \sin^2\varphi;$

$$n_1 = [2b^2\sin\rho - (1+i_{23})\sin 2\varphi]/[2(1+i_{23})\sqrt{n}].$$

Coordinates of points e_1, e_2 lying on the displacement function $\psi = f_1(\varphi)$ of the toothed lever mechanism are determined from equations:

$$\varphi = \arccos \pm \sqrt{l^2(\lambda^2-1)[l^2\lambda^2 + 0.25(1+l^2)(1+l^2-4b^2)]}/[l^2(\lambda^2-1)]; \quad (12)$$

$$\psi = \varphi + \lambda[\arcsin(\cos\mu_{\min}\cdot\cos\varphi) - \arcsin(\cos\mu_{\min})]; \quad (13)$$

$$\lambda = b/r_1, \quad (14)$$

where $\mu_{\min}$ is the minimum value of transmission angle μ.

Let us consider the section of the displacement function of the mechanism in the coordinates φ, ψ included by the angles $\varphi_1 - \varphi_{II}$ of rotation of the crank (see Fig. 4).

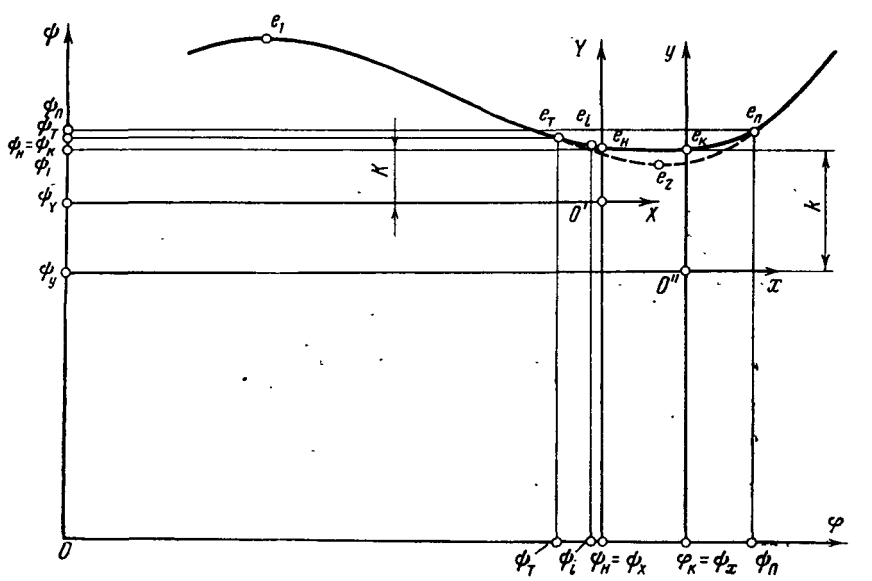

Fig. 4.

Let us introduce new Cartesian coordinates XY. The origin of these coordinates O' is defined by the coordinates φ_X, ψ_Y.

Let us take that $\varphi_H=\varphi_X$.

In the same manner, let us draw the coordinates xy whose origin O'' is determined with the help of coordinates $\varphi_x=\varphi_k$, ψ_y.

Let us select the curves of conic section, for example equilateral hyperbolas for the transition sections e_Te_H and e_Ke_Π.

For section e_Te_H:

$$-X^2+Y^2=K^2, \tag{15}$$

and section e_Ke_Π:

$$-x^2+y^2=k^2. \tag{16}$$

The equations of hyperbolas (15) and (16) rewritten in φ, ψ coordinates are:

$$-(\varphi_H-\varphi_T)^2+(\psi_T-\psi_Y)^2=(\psi_H-\psi_Y)^2; \tag{17}$$

$$-(\varphi_K-\varphi_\Pi)^2+(\psi_\Pi-\psi_y)^2=(\psi_K-\psi_y)^2. \tag{18}$$

The conditions at which the curve $\psi=f_1(\varphi)$ touches the hyperbolas by taking into account equations (6) and (7) are:

at point e_T

$$-(\varphi_H-\varphi_T)^2+(\psi_T-\psi_Y)^2=(\psi_H-\psi_Y)^2; \tag{19}$$

$$\varphi_T-\varphi_H+(\psi_T-\psi_Y)\,\psi_T'=0; \tag{20}$$

$$1+(\psi_T-\psi_Y)\,\psi_T''+(\psi_T')^2=0, \tag{21}$$

and at point e_Π

$$-(\varphi_K-\varphi_\Pi)^2+(\psi_\Pi-\psi_y)^2=(\psi_K-\psi_y)^2; \tag{22}$$

$$\varphi_\Pi-\varphi_K+(\psi_\Pi-\psi_y)\psi_\Pi'=0; \tag{23}$$

$$1+(\psi_\Pi-\psi_y)\,\psi_\Pi''+(\psi\ )^2=0. \tag{24}$$

Solving the system of equations (19)-(21) with respect to unknown parameters ψ_Y, φ_H and ψ_H:

$$\psi_Y=\psi_T\pm[(\psi_T')^2+1]/\psi_T''; \tag{25}$$

$$\varphi_H=\varphi_T+(\psi_T-\psi_Y)\,\psi_T'; \tag{26}$$

$$\psi_H=\psi_Y\pm\sqrt{(\psi_T-\psi_Y)^2-(\varphi_H-\varphi_T)^2}, \tag{27}$$

where

$$\psi_T'=\pm\,[1\pm 2l\lambda\sin\varphi/\sqrt{n_2}]; \tag{28}$$

$$\psi_T''=\pm\,[2l\lambda\,(1-l^2)^2\cos\varphi]/n_2\sqrt{n_2}; \tag{29}$$

$$n_2=(1+l^2)^2-4l^2\cos^2\varphi.$$

Equations (28) and (29) have been obtained by differentiating the displacement function $\psi=f_1(\varphi)$ on satisfying the conditions (9) and (10)

Taking into consideration the equation $\psi_H=\psi_K$ from the system of equations (22) and (23), we get:

$$\psi_Y=(\psi_H-\psi_\Pi\sqrt{1+(\psi'_\Pi)^2})/(1-\sqrt{1+(\psi'_\Pi)^2}); \quad (30)$$

$$\varphi_K=\varphi_\Pi+(\psi_\Pi-\psi_v)\,\psi'_\Pi, \quad (31)$$

where ψ'_Π is determined from equation (28) by substituting angle φ_Π corresponding to point e_Π.

Coordinates of the points of transition sections of the curves are calculated with the help of equations (15) and (16). Relative displacement s of the follower at angle of rotation $\varphi_T-\varphi_H$ is calculated in the following manner.

Firstly, coordinates of points e_i (see Fig. 4) lying on curve $\psi=f_2(\varphi)$ are determined from equation (17).

Then, the instantaneous length of follower l_i is determined by substituting the obtained coordinates φ_i; ψ_i in equation (11) and the relative displacement s is determined from equation (8).

The relative displacement of the follower at angle of rotation $\varphi_K-\varphi_\Pi$ is determined in a similar manner except that coordinates of the points of curve $\psi=f_3(\varphi)$ are determined from equation (18) in place of the coordinates of points of the curve $\psi=f_2(\varphi)$.

The instantaneous length of the follower at angle of rotation $\varphi_H-\varphi_K$ is calculated by substituting the constant $\psi=\psi_H$ and the instantaneous value of angle φ_i from the interval $\varphi_H-\varphi_K$ in equation (11).

It is recommended that the cam should be profiled in accordance with the known formulas and laws [4] at the minimum value of the coefficient of maximum follower velocity δ_{max}. While developing the profile of the cam, if there is the necessity for correcting the displacement function of the mechanism $\psi=f_1(\varphi)$ on the section e'_T-e_Π (see Fig. 3, a) as a result of the selection of one or the other law of motion of the follower, this should be accomplished with the help of the method of successive approximations by changing the angles φ_T, φ_Π, φ_{12} at constant values of the given parameters φ_B and $\varphi_{r..r}$.

To explain this procedure a numerical example of determining the coordinates of characteristic points of the displacement function of the driven link of a cam-planetary-connecting rod mechanism and the value of maximum displacement of the follower is given below.

Given that:

$$\varphi_B=\Delta\psi=25°-30°;$$

$$\varphi_{r..r}\approx\varphi_{12}=90°;$$

$$\mu_{min}=45°,$$

it is necessary to find the coordinates of characteristic points of the displacement function of the mechanism e_1, e_2, e_H, e_K and displacement s_{max}.

All the dimensions are given in relative numbers. The support of the four-link mechanism is taken as the unit of length.

Let us determine parameters of the mechanism by satisfying equations (4);

$$l=1/\cos\mu_{min}\pm\sqrt{1/\cos^2\mu_{min}-1}. \tag{32}$$

Equation (32) and some subsequent expressions are taken from reference [5].

$$l=1/0.7071\pm\sqrt{1/(0.7071)^2-1}=0.4142;$$
$$\lambda=(\Delta\psi+\varphi_{12})/[2\arcsin(\cos\mu_{min}\cdot\sin\varphi_{12}/2)];$$
$$\lambda=(30°+90°)/[2\arcsin(0.7071\times0.7071)]=2;$$
$$b=\sqrt{l/\cos\mu}=\sqrt{0.4142/0.7071}=0.7654.$$

The radius of toothed gear is calculated from equation (14)

$$r=0.7654/2=0.3827.$$

Let us now determine the coordinates of characteristic points of the displacement function $\psi=f_1(\varphi)$.

Angles φ_1 and φ_2 are determined from equation (12) and the angles ψ_1 and ψ_2 from expressions (13)

$$\varphi=\arccos\times\sqrt{0.1716\times3[0.176\times4+0.25\times1.1716\,(1.1716-4\times0.5858)]}/(0.1716\times3)=+35°42';$$
$$\varphi_1=180°+35°42'=215°42';$$
$$\varphi_2=360°-35°42'=324°18';$$
$$\psi_1=215°42'+2\,[180°+35°18'-(180°-45°)]=376°18';$$
$$\psi_2=324°18'+2\,[180°-35°18'-(180°-45°)]=343°42'.$$

The ordinate ψ_Y of the origin O' of the coordinate system is calculated from equation (25) before calculating the coordinates of point e_H. The instantaneous value of angle ψ_T is calculated from equation (13) and the derivatives ψ_T', ψ_T'' are obtained from expressions (28) and (29) beforehand.

After selecting the angle $\varphi_T=300°$, we have:

$$\psi_T=300°+2[180°-20°40'-(180°-45°)]=348°40';$$
$$\psi_T'=\pm[1-2\times0.4142\times2\times0.866/\sqrt{(1.1716)^2-4\times0.1716\times0.25}]=0.3093;$$
$$\psi_T''=(2\times0.4142\times2\,(1-0.1716)^2\times0.5)/(1.0959\sqrt{1.0959})=0.4319;$$
$$\psi_Y=348°40'-[(0.3093\times57°.3)^2+57°.3]/(0.4319\times57°.3)=333°40'.$$

Let us determine the coordinates of point e_H from equations (26) and (27)

$$\varphi_H=300°+(348°40'-333°40')\,0.3093=304°38',$$

$$\psi_H=333°40'+\sqrt{(348°40'-333°40')^2-(304°38'-300°00')^2}=347°56'.$$

Before calculating the abscissa of point e_K, let us determine the instantaneous value of angle ψ_Π from equation (13), derivative ψ'_Π from expression (28) and ordinate ψ_v of the origin O'' of the coordinate system from formula (30).

Taking angle $\psi_\Pi=350°$, we have:

$$\psi_\Pi=350°+2\,[180°-43°20'-(180°-45°)]=353°20',$$

$$\psi'_\Pi=\pm[1-2\times0.4142\times2\times0.1736/\sqrt{(1.1716)^2-4\times0.1716\times0.9698}]$$
$$=0.6579,$$

$$\psi_v=(347°56'-353°20'\sqrt{1+(0.6579)^2})/(1-\sqrt{1+(0.6579)^2}=381°00'.$$

Abscissa of point e_K is calculated from expression (31), i.e.

$$\varphi_K=350°+(353°20'-381°00')\times0.6579=331°46'.$$

From formulas (1) and (2), we determine the angles:

$$\varphi_{r.r}=88°56',\ \varphi_B=27°08'.$$

Maximum displacement of follower $s_{\max}$ is calculated from equations (11) and (8):

$$\varphi_{s\max}=304°38',\ \psi_{s\max}=347°56';$$

$$l_{i\min}=0.5682\pm\sqrt{4\times0.58\times0.3159-0.6765}=0.3310,$$

where:

$$\rho/2=(347°56'+180°-304°38')/4=55°49';$$

$$s_{\max}=0.4142-0.3310=0.0832.$$

References

1. Lobusov, V. M. Issledovanie kulisno-rychazhnogo mekhanizma s obratnym khodom v avtomaticheskoi linii sakhara-rafinada (Study of slotted bar and lever mechanism with reverse stroke in sugar-refining automatic line). *Izv. vuzov. Pishchevaya tekhnologiya,* No. 2, 1965.

2. Mashinostroenie. Konstruktirovanie mashin (Machine building. Design of machines). *Entsikl. spr.*, 8, pp. 621-628, 972-982, Mashgiz, 1949.
3. Maisyuk, L. B. Nekotorye voprosy kinematiki kulachkovo zubchatorychazhnykh mekhanizmov (Some problems of kinematics of cam-toothed lever mechanisms). Sb. *Mekhanika mashin*, vyp. 11-12, Izd-vo Nauka, 1967.
4. Levitskii, N. I. Kulachkovye mekhanizmy (Cam Mechanisms). Izd-vo Mashinostroenie, 1964.
5. Maisyuk, L. B. Sintez sharnirno-zubchatogo mekhanizma s pomosh-ch'yu elektronnykh tsifrovykh mashin (Synthesis of hinged toothed mechanisms with the help of digital computers). Sb. *Teoriya mashin i mekhanizmov* vyp. 100, Izd-vo Nauka, 1964.

V. A. Mamedov

DETERMINATION OF THE ZONES OF EXISTENCE OF SLOTTED LEVER MECHANISMS

Reference charts showing the zones of existence of optimum alternatives of one of the schemes of mechanism aid in the application of existing methods of approximate synthesis. Determination of the zones of existence and the method of plotting reference charts for obtaining rational design schemes of a slotted lever mechanism utilizing the digital computer "Ural-1" have been described in article [1].

The above mentioned article proves that the extreme points of materialization of this slotted lever mechanism are determined by the minimum angle of transmission of the mechanism which should not be less than some given value and by equating the discriminant of the biquadratic equation occurring in the calculation of the length of yoke to zero.

Another method for determining the boundary of the zone of existence of the slotted lever mechanism corresponding to the condition that the discriminant of the biquadratic equation is equal to zero, is given below. A flow chart and computer program for the calculations have been written in ALGOL-60 which is becoming increasingly popular [2, 3].

As shown in reference [2], ALGOL-60 has found worldwide acceptance as a programming language. However, ALGOL-60 has rarely been used in research on synthesis and analysis of mechanisms.

The points mentioned in article [1] are applicable in determining the boundary values of the minimum angle of transmission. Formulation of the problem, basic equations for calculating the parameters, value of these parameters and their notations are given in references [1, 4].

Length r of the yoke is determined from the following equation:

$$r=\sqrt{(-b\pm\sqrt{b^2-4ac})/2a} \qquad (1)$$

Coefficients a, b and c are calculated from equations:

$$a=2(1-\cos\alpha); \tag{2}$$

$$b=-a[(S_0+S_1)^2+S_0^2]+2a-4\sin^2\alpha; \tag{3}$$

$$c=[(S_0+S_1)^2-1]^2+(S_0^2-1)^2+2(1-S_0^2)\cos\alpha[(S_0+S_1)^2-1], \tag{4}$$

where S_0—initial value of the parameter characterizing displacement of the connecting rod;

S_1—displacement of the connecting rod;

α—angle rotation of the driven link.

The application of interpolation for determining the limiting value of the angle of rotation α of the yoke corresponding to $D=0$ has been described in earlier investigations by the author [1]. In this case, coefficients a, b and c were also calculated for those values of the angle of rotation α at which the discriminant D is negative.

Obviously, this procedure is time consuming. There is another method of calculating the limiting value of α corresponding to $D=0$. In this method the discriminant D of the biquadratic equation (1) is set equal to zero, i.e.

$$D=b^2-4ac=0. \tag{5}$$

Keeping the parameters S_0 and S_1 constant, let us separate out coefficients independent of α in equation (5). Substituting

$$\begin{aligned} &A=-2;\ B=+2;\ C=4;\\ &D=2[(S_0+S_1)^2+S_0^2]-4;\\ &E=-2[(S_0+S_1)^2+S_0^2];\\ &F=2(1-S_0^2)[(S_0+S_1)^2-1];\\ &G=[(S_0+S_1)^2-1]^2(S_0^2-1)^2 \end{aligned} \tag{6}$$

in accordance with equations (2), (3) and (4) for calculating the values of coefficients a, b and c, we get:

$$a=A\cos\alpha+B; \tag{7}$$

$$b=c\cos^2\alpha+D\cos\alpha+E; \tag{8}$$

$$c=F\cos\alpha+G. \tag{9}$$

Substituting equations (7), (8) and (9) in equation (5), we get the following equations of 4th order with respect to $\cos\alpha$:

$$k_4\cos^4\alpha+k_3\cos^3\alpha+k_2\cos^2\alpha+k_1\cos\alpha+k_0=0; \tag{10}$$

$$k_4=C^2;\ k_3=2CD;\ k_2=D^2+2EC-4AF; \tag{11}$$

$$k_1=2DE-4AG-4BF;\ k_0=E^2-4BG.$$

Since the value of D at $\alpha=0$ is equal to zero, we can reduce the order of equation (10) to three at $\cos\alpha=1$. Dividing equation (10) by $\cos\alpha-1$ in accordance with the notations adopted in equation (11), we get the following cubic equation with respect to $\cos\alpha$;

$$k_4\cos^3\alpha+(k_4+k_3)\cos^2\alpha+(k_4+k_3+k_2)\cos\alpha+(k_4+k_3+k_2+k_1)=0. \quad (12)$$

Let us write equation (12) in the following general form:

$$a_1x^3+b_1x^2+c_1x+d_1=0, \quad (13)$$

where $$x=\cos\alpha;\ a_1=k_4;\quad b_1=k_4+k_3;$$

$$c_1=k_4+k_3+k_2;\quad d_1=k_4+k_3+k_2+k_1. \quad (14)$$

Dividing equation (13) by a_1 and introducing new variable $y=x+b_1/3a_1$, in place of x, we finally get:

$$y^3+3py+2q=0, \quad (15)$$

where $$2q=2b_1^3/27a_1^3-b_1c_1/3a_1^2+d_1/a_1; \quad (16)$$

$$3p=3a_1c_1-b_1^2/3a_1^2. \quad (17)$$

The number of actual solutions of equation (15) depends on the sign of discriminant D_1, i.e. on the sign of:

$$D_1=q^2+p^3. \quad (18)$$

Let us determine the sign of discriminant D_1. For this, we determine the values of q and p from equations (16) and (17). To calculate the values of q and p the values of coefficients a_1, b_1, c_1 and d_1 must be determined successively from equations (14):

$$a_1=16;$$

$$b_1=a_1+16\{[(S_0+S_1)^2+S_0^2]-4\}; \quad (19)$$

$$c_1=b_1+\{2[(S_0+S_1)^2]-4\}^2-16[(S_0+S_1)^2+S_0^2]+16(1-S_0^2)[(S_0+S_1)^2-1]; \quad (20)$$

$$d_1=c_1+2\{2[(S_0+S_1)^2+S_0^2]-4\}\{-2[(S_0+S_1)^2+S_0^2]\}+8\{[(S_0+S_1)^2-1]^2+(S_0^2-1)^2\}-16(1-S_0^2)\times[(S_0+S_1)^2-1]. \quad (21)$$

Thus, by solving the resulting cubic equation (13), we get those values of $\alpha=f(S_0;\ S_1)$ at which $D=0$.

The flow chart of the program used for calculating equation (13) is given in the Figure. As stated earlier, the initial parameters S_0 and S_1 are

introduced and printed first. It is followed by the solution of cubic equation after which the value of r^2 is determined from the simplified equation:

$$r^2 = -b/2a. \tag{22}$$

Operator r^2 is the operator of the block diagram. If r^2 is positive, we get the values of β, μ_1, μ_2 and $\mu_{\min}$. When $\mu_{\min} > 10°$ the values of r, β, $\mu_{\min}$, $\alpha_{(3)}$ and the roots of cubic equation (13) are printed and the value of α, multiple of 5° and more than $\alpha_{(3)}$ is separated and the block scheme sends α to the input from which the subsequent calculation is started.

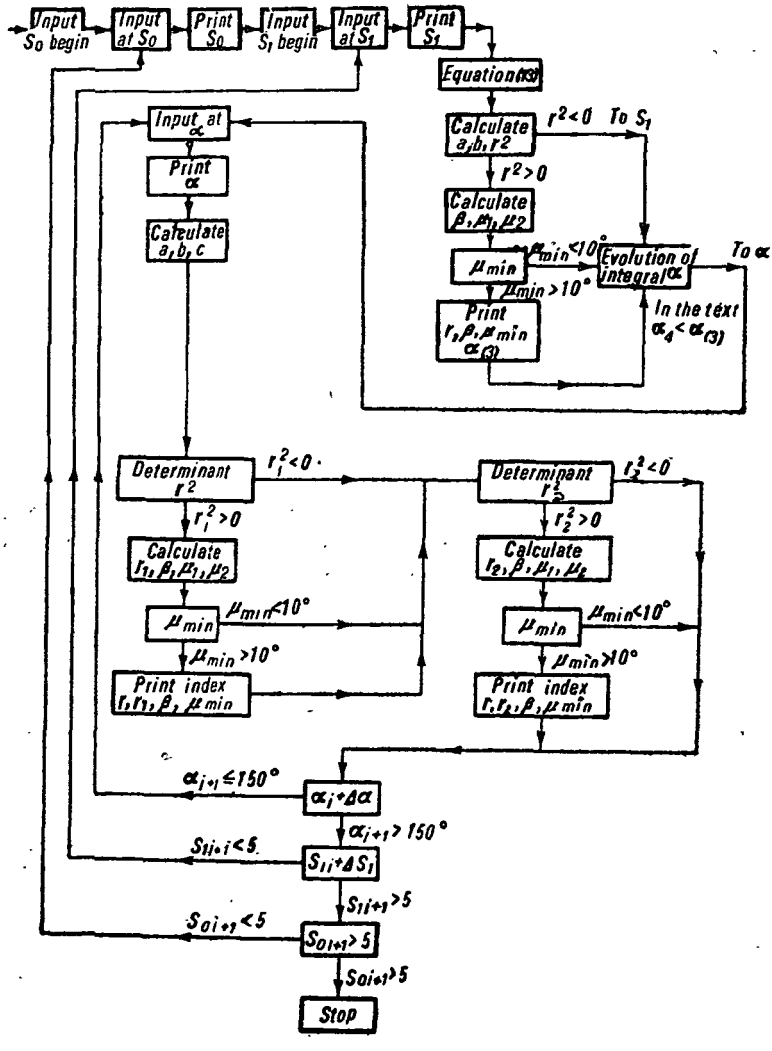

If it is found that $r^2<0$ or $\mu_{min}<10°$, then, in both the cases, the parameters are not printed and direct changeover to operator "separation of integral α" takes place after which α is sent to the input. The new value of α is printed, coefficients a, b and c are determined and the subsequent calculations are carried out in the same way as described in the flow chart with interpolation [1].

While programming in ALGOL-60, the author considered it appropriate not to write the whole program but to translate into this language only the main calculations for determining the parameters of slotted lever mechanism which could be used for solving other problems of synthesis of these mechanisms.

The subprogram for calculating the coefficients a, b and c of the biquadratic equation (1) and discriminant D from the given values of the angle of rotation α of yoke, initial distance S_0 and displacement S_1 is

```
begin real S[0], S[1], alfa;
insert (S[0], S [1], alfa);
h:=sin (alfa); g:=cos (alfa);
a:=2×(1−g); e:=(S[0]+S[1])↑2+S[0]↑2;
f:=(S[0]+S[1])↑2−1;
b:=−a×e+2×a−4×(h↑2);
c:=f↑2+(S[0]↑2−1)↑2+2×(1−S[0]↑2)×g×f;
d:=b↑2−4×a×c;
end result (a; b; c; d).
```

The symbols "begin" and "end" are known as operational brackets. They combine descriptions and operators into a one block-sequence.

As is obvious from this ALGOL-program, the block starts with the symbol "begin" and is followed by a description. The descriptions point out the type of variables, switches, massives and equipment used in the block. In this ALGOL-program, the discriminant D is denoted by d. This part of the program, is separated since the logic of subsequent calculations in the main program depends on the sign of D.

The ALGOL-subprogram for determining the parameters of the diagram is drawn after this. Moreover, the values of a, b and c are already known and D is positive

```
begin real a, b, c, alfa, S[0], S[1], beta, mu;
insert (a, b, c, alfa, S[0], S[1]);
d:=b↑2−4×a×c; e:=Sqrt(d);
f:=(−b±e)/(2×a).
```

One of the signs in this equation is taken as "comment" depending on the roots calculated:

```
                    if f < 0 then go to M;
          also begin r:=sqrt(f);
                    x:=(1+r↑2−S[0]↑2)/(2×r);
                    y:=sqrt(1−x↑2); z=y/x;
                beta:=arc tan (z);
                    g:=sin (beta); h:=sin (beta+alfa);
                    l:=g/S [0]; n:=h/(S[0]+S[1]);
                   m:=sqrt (1−l↑2); p:=sqrt (1−n↑2);
                    k:=l/m; t:=n/p;
            mu [1]:=arc tan (k); mu [2]:=arc tan (t);
            result (r, beta, mu [1]; mu [2]);
                        end
                        M: result (f)
                            end
```

Symbol "go to M" is called the transition operator which changes the natural sequence of operations [5].

References

1. Mamedov, V. A. Oblasti sushchestvovaniya kulisnogo mekhanizma s vedushchim shatunom (Zone of existence of slotted-lever mechanism with driving connecting rod). Sb. *Mekhanika mashin*, vyp. 3-4, Izd-vo Nauka, 1966.
2. Algoritmicheskii yazyk ALGOL-60 (Algorithmic Language ALGOL-60). Translation from English. Editors A. P. Ershov, S. S. Lavrov and M. R. Shura-Bura. Izd-vo Mir, 1965.
3. Speranskii, N. V. and I. G. Oleinik. Nekotorye voprosy programmirovaniya zadach sinteza sharnirnykh mekhanizmov (Some questions regarding the programming of the problems on synthesis of hinged mechanisms). Sb. *Mekhanika mashin*, vyp. 3-4, Izd-vo Nauka, 1966.
4. Mamedov, V. A. K sintezu sharnirnykh mekhanizmov s vedushchim shatunom (Synthesis of hinged mechanisms with driving connecting rod). Sb. *Analiz i sintez mashin-avtomatov*, Izd-vo Nauka, 1965.
5. Kagan, B. M. and T. M. Ter-Mikaelyan. Reshenie inzhenernykh zadach na tsifrovykh vychislitel'nykh mashinakh (Solving Engineering Problems on Digital Computers). Izd-vo Energiya, 1964.

P. G. Mudrov

THREE-DIMENSIONAL FIVE-LINK HINGED MECHANISMS

In most Soviet literature concerning three-dimensional hinged lever mechanisms, very little attention has been given to the study of three-dimensional hinged five-link mechanisms consisting of only turning pairs (pairs of the 5th class).

Moreover, some scientists refute the existence of such a mechanism. However, this mechanism does in fact exist.

As early as 1931, the French scientist M. Moard reference [1] considered a three-dimensional hinged five-link mechanism consisting of two Bennett mechanisms [2] in which the angles between the axes of the hinges of the connecting links are equal to 90°.

In 1943, the American scientist M. Goldberg published an article [3] in which he also demonstrated the possibility of obtaining a three-dimensional hinged five-link mechanism by joining two Bennett mechanisms. He considers the formation of the five-link mechanism for a specific example when the connecting links lie along one straight line.

Independent of the research works of these authors, a similar five-link mechanism of a more general nature was developed in the (USSR) by B. V. Shitikov.

As shown by models, a three-dimensional hinged five-link mechanism possesses sufficient rigidity and can be of interest to research workers as well as to designers.

This mechanism is of two types: a five-link mechanism with two cranks and a five-link mechanism with crank and reciprocating lever. In the latter case, a five-link mechanism can be obtained in which the angle of rotation (travel) of the reciprocating lever is more than 180°.

The structure and kinematics of a three-dimensional hinged five-link mechanism are considered as follow.

1. Structure of a Five-link Mechanism

The three-dimensional hinged five-link mechanism consists of two Bennett mechanisms. To produce it, it is necessary to take two Bennett mechanisms *ABCF* and *KCDE* (Fig. 1, a) with similar links *CF* and *CK* and to connect them in such a manner that similar links *CF* and *CK* coincide.

Then, rejecting these links and connecting the columns (joining the hinges *A* and *E* by link *AE*), we get a five-link mechanism *ABCDE* with one degree of mobility (Fig. 1, b).

A model of such a mechanism is shown in Fig. 2. Based on the properties of a Bennett mechanism, the parameters of the resulting five-link mechanism will be related as follows:

$$l_1/\sin\alpha_1 = l_2/\sin\alpha_2 = l_3/\sin\alpha_3, \tag{1}$$

where l_1, l_2 and l_3 are the lengths (shortest distances between the hinge axis) of the links *1(AB)*, *2(BC)* and *3(CD)* and α_1, α_2 and α_3 are the angles between the geometrical axes of the hinges of these links.

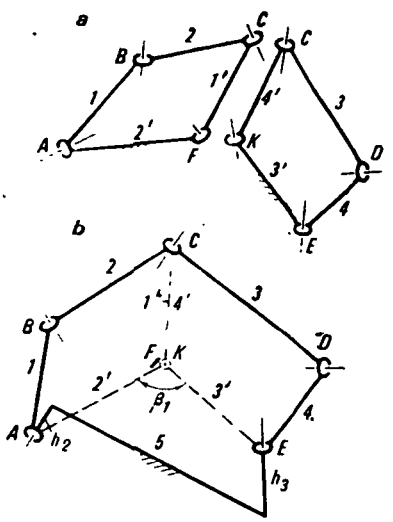

Fig. 1.

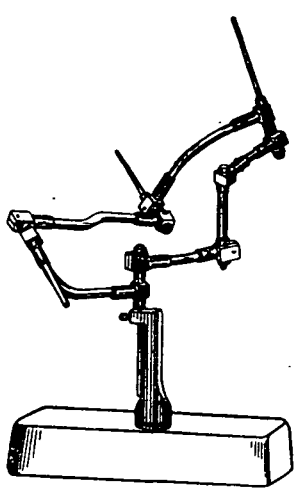

Fig. 2.

Link *4(DE)* does not differ from link *1*, i.e. $l_4 = l_1$ and $\alpha_4 = \alpha_1$. Parameters of the combined link *5(AE)* depend on the parameters of links *2* and *3*, and are determined from relations:

$$l_5 = -\sin\alpha_5 \,(l_2\,[\sin\alpha_3\cdot\cos\alpha_2\cdot\cos\beta_1 - \sin\alpha_2\cdot\cos\alpha_3) + l_3\,(\sin\alpha_2\cdot\cos\alpha_3\cdot\cos\beta_1 - \sin\alpha_3\cdot\cos\alpha_2)]/[(\sin\alpha_2\cdot\cos\alpha_3 - \sin\alpha_3\cdot\cos\alpha_2\cdot\cos\beta_1)^2 + \sin^2\alpha_3\cdot\sin^2\beta_1], \tag{2}$$

$$\alpha_5 = \arccos\,(\cos\alpha_2\cdot\cos\alpha_3 + \sin\alpha_2\cdot\sin\alpha_3\cdot\cos\beta_1), \tag{3}$$

$$h_2 = \sin\beta_1\,(l_3\cdot\sin\alpha_2 - l_2\cdot\sin\alpha_3\cdot\cos\alpha_5)/[(\sin\alpha_2\cdot\cos\alpha_3 - \sin\alpha_3\cdot\cos\alpha_2\cdot\cos\beta_1)^2 + \sin^2\alpha_3\cdot\sin^2\beta_1], \tag{4}$$

$$h_3=\sin\beta_1\,(l_2\cdot\sin\alpha_3-l_3\cdot\sin\alpha_2\cdot\cos\alpha_5)/[(\sin\alpha_2\cdot\cos\alpha_3-\sin\alpha_3\cdot\cos\alpha_2\cdot\cos\beta_1)^2+\sin^2\alpha_3\cdot\sin^2\beta_1]. \quad (5)$$

In general, axes of hinges *A* and *E* of link *5* are not parallel and do not intersect. In the particular case, when similar Bennett mechanisms are connected, they can be parallel ($\beta_1=180°$) or can intersect (at $\beta_1=0°$)[1].

2. Kinematics of the Driven Link of the Five-link Mechanisms

Case 1. Fig. 3 shows the scheme of a five-link mechanism *ABCDE* based on link *2* (*BC*). Let link *1* be the driving link and link *3*, the driven link. Let φ be the angle of rotation of the driving link and ψ_3—angle of rotation of the driven link of the five-link mechanism; further let β, γ_1 and γ_2 be the angles of rotation of the driving link and driven cranks *CF* of the Bennett mechanism *ABCF* and the angle of rotation of the driven crank *CD* of the Bennett mechanism *CDEF* respectively.

Angles β, β_1 and angle $AFC=\varphi$ lie in one plane perpendicular to the geometrical axis of hinge *F*.

It may be seen from Fig. 3 that:

$$\psi_3=\gamma_1+\gamma_2-180°. \quad (6)$$

Using the relations known for Bennett mechanism, between the angles of rotation of the driven and driving cranks [4], we obtain the values of γ_1, and γ_2:

$$\gamma_1=\arcsin\,[c_1\cdot\sin\varphi/(a_1-b_1\cdot\cos\varphi)];$$
$$\gamma_2=\arcsin\,[c_2\cdot\sin\beta/(a_2-b_2\cdot\cos\beta)], \quad (7)$$

or taking that $\beta=\beta_1+\varphi$ (see Fig. 4) we have:

$$\gamma_2=\arcsin\,\{c_2\cdot\sin(\beta_1+\varphi)/[a_2-b_2\cdot\cos(\beta_1+\varphi)]\}. \quad (8)$$

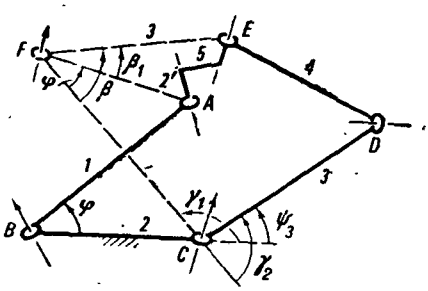

Fig. 3.

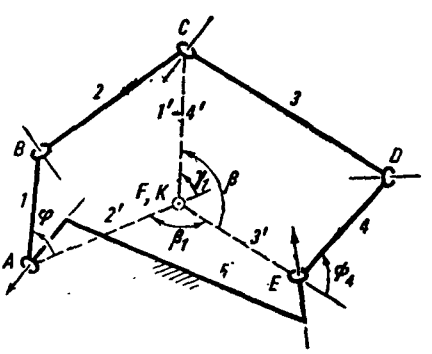

Fig. 4.

[1] In the case of connection of two similar Bennett mechanisms ($\beta_1=0°$), the five-link mechanism can be obtained by connecting parallelograms with antiparallelograms. In the opposite case, the five-link mechanism is changed into a Bennett mechanism.

Substituting expressions (7) and (8) in equation (6), we finally get:

$$\psi_3=\arcsin\left[c_1\cdot\sin\varphi/(a_1-b_1\cdot\cos\varphi)\right]+\arcsin\left\{c_2\cdot\sin(\beta_1+\varphi)/[a_2-b_2\cdot\cos(\beta_1+\varphi)]\right\}-180^\circ, \tag{9}$$

where

$$a_1=1-\cos\alpha_1\cdot\cos\alpha_2; \tag{10a}$$

$$b_1=\sin\alpha_1\cdot\sin\alpha_2; \tag{10b}$$

$$c_1=\cos\alpha_2-\cos\alpha_1; \tag{10c}$$

$$a_2=1-\cos\alpha_1\cdot\cos\alpha_3; \tag{10d}$$

$$b_2=\sin\alpha_1\cdot\sin\alpha_3; \tag{10e}$$

$$c_2=\cos\alpha_1-\cos\alpha_3\,. \tag{10f}$$

Differentiating expression (9) with respect to time, we obtain the angular velocity of the driven link:

$$\omega_3=\{c_1/(a_1-b_1\cdot\cos\varphi)+c_2/[a_2-b_2\cdot\cos(\beta_1+\varphi)]\}\,\omega_1, \tag{11}$$

where ω_1 is the angular velocity of the driving link.

The angular acceleration of the driven link of a five-link mechanism in the case of constant angular velocity of the driving link will be:

$$\varepsilon_3=-\{b_1\cdot c_1\cdot\sin\varphi/[(a_1-b_1\cdot\cos\varphi)]^2+b_2c_2\cdot\sin(\beta_1+\varphi)/[a_2-b_2\cdot\cos(\beta_1+\varphi)]^2\}\,\omega_1^2\,. \tag{12}$$

3. Conditions under which a Five-link Mechanism has either Two Cranks or One Crank and One Reciprocating Lever

Expression (11) shows that the angular velocity of the driven link *3* (*CD*) of the five-link mechanism is equal to the algebraic sum of the angular velocity ω_{CF} of link *CF* (angular velocity of the driven link *CF* of the Bennett mechanism *BAFC*) and angular velocity $\omega_{CD/CF}$ of link *CD* relative to the link *CF* (angular velocity of driven crank *CD* of the Bennett mechanism *CFED* when link *CF* is stationary).

In this case, equation (11) can be written as:

$$\omega_3=\omega_{CF}+\omega_{CD/CF}\,.$$

It is known that average angular velocities of cranks in a Bennett mechanism are equal. Therefore, when the driving cranks connected in five-link Bennett mechanisms rotate with average angular velocity ω_1, the average angular velocity of link *CD* (when the directions of angular velocities ω_{CF} and $\omega_{CD/CF}$ are same, i.e. links *CF* and *CD* rotate in one direction), is equal to $2\omega_1$, i.e. $\omega_3=2\omega_1$.

In this case, the driven link *CD* of the five-link mechanism is a crank making two rotations during one rotation of the driving link.

If the angular velocities ω_{CF} and $\omega_{CD/CF}$ have opposite signs (links *CF* and *CD* rotate in different directions), then $\omega_3=0$. The driven link of the five-link mechanism accomplishes oscillatory motion, i.e. it will be a reciprocating lever.

Direction of angular velocities ω_{CF} and $\omega_{CD/CF}$ is determined from the sign of coefficients c_1 and c_2 [expressions (10c) and (10f)] since $a_{1(2)}-b_{1(2)}\cos\varphi$ is always positive.

From here, assigning the values of c_1 and c_2 from expressions (10c) and (10f), we obtain the conditions under which either crank or reciprocating lever is possible.

Link *CD* will be a crank if ω_{CF} and $\omega_{CD/CF}$ have the same signs and it is possible in two cases.

First if $c_1>0$ and $c_2>0$, i.e. in the first Bennett mechanism $\alpha_1>\alpha_2$ which follows from expression $\cos\alpha_2-\cos\alpha_1=c_1>0$ and in the second Bennett mechanism, $\alpha_1<\alpha_3$ which follows from the equality $\cos\alpha_1-\cos\alpha_3=c_2>0$.

Thus, a five-link mechanism has angles satisfying the inequality:

$$\alpha_2<\alpha_1<\alpha_3\,. \tag{13}$$

Secondly, if $c_1<0$ and $c_2<0$, i.e. the first Bennett mechanism must have $\alpha_1<\alpha_2$ and the second, $\alpha_1>\alpha_3$. Thus, angles in a five-link mechanism satisfy the inequality:

$$\alpha_2>\alpha_1>\alpha_3\,. \tag{14}$$

In this case, as shown by expressions (9) and (11), the angle of rotation and angular velocity of the driven crank will be negative.

Link *CD* becomes the reciprocating lever if ω_{CF} and $\omega_{CD/CF}$, i.e. the first and second terms in expression (11), have opposite directions and it is also possible only in two cases.

1. If $c_1>0$ and $c_2<0$, i.e. $\alpha_1>\alpha_2$ in the first Bennett mechanism and $\alpha_1>\alpha_3$ in the second.

From here:

$$\alpha_2<\alpha_1>\alpha_3\,. \tag{15}$$

2. When $c_1<0$ and $c_2>0$, i.e. the condition $\alpha_1<\alpha_2$ is satisfied in the first Bennett mechanism and $\alpha_1<\alpha_3$ in the second. From here:

$$\alpha_2>\alpha_1<\alpha_3\,. \tag{16}$$

In the last two cases, there can be an arbitrary relation between angles α_2 and α_3. In the particular case, $\alpha_2=\alpha_3$.

Thus, the five-link mechanism (see Fig. 3) in which the angles between geometrical axes of link hinges satisfy the inequality (13) or (14) will

always have two cranks; moreover, the driven crank makes two rotations during one rotation of the driving crank. A five-link mechanism with angles satisfying expression (15) or (16) always has a crank and a reciprocation lever.

4. Kinematics of the Driven Link of a Five-link Mechanism

Case 2. The scheme of a five-link mechanism considered above but with stationary link *5* is shown in Fig. 4. In this case, the five-link mechanism, like Bennett mechanism always has two cranks, but the driven crank makes one rotation for one rotation of the driving crank.

Let link *1* be the driving link and link *4*, the driven link. Applying the obtained relationship between the angles of rotation of the driving and driven links of a Bennett mechanism, we have:

$$\sin \psi_4 = c_2' \cdot \sin \beta / (a_2 - b_2 \cdot \cos \beta), \tag{17}$$

where $c_2' = \cos \alpha_3 - \cos \alpha_1$;
and

$$\beta = 180° - (\beta_1 - \gamma_1), \tag{18}$$

(see Fig. 4).

Putting the values of β and γ_1 [see expression (7)] in equation (17), we finally get:

$$\sin \psi_4 = c' \cdot \sin \{\beta_1 - \text{arc sin} [c_1 \cdot \sin \varphi / (a_1 - b_1 \cdot \cos \varphi)]\} / \{a_2 + b_2 \cdot \cos [\beta_1 - \text{arc sin} [c_1 \cdot \sin \varphi / (a_1 - b_1 \cdot \cos \varphi)]]\}. \tag{19}$$

Angular velocity of the driven link:

$$\omega_4 = c_1 \cdot c_2' \omega_1 / (a_1 - b_1 \cdot \cos \varphi) \cdot \{a_2 + b_2 \cdot \cos [\beta_1 - \text{arc sin} [c_1 \cdot \sin \varphi / (a_1 - b_1 \cdot \cos \varphi)]]\}, \tag{20}$$

and angular acceleration under the condition that the driving link has constant angular velocity:

$$\varepsilon_4 = -c_1 \cdot c_2' \cdot \omega_1^2 \{b_1 \cdot \sin \varphi \cdot \{a_2 + b_2 \cdot \cos [\beta_1 - \text{arc sin} [c_1 \cdot \sin \varphi / (a_1 - b_1 \cos \varphi)]]\} + b_2 \cdot c_1 \cdot \sin [\beta_1 - \text{arc sin} [c_1 \cdot \sin \varphi / (a_1 - b_1 \cdot \cos \varphi)]]\} / \{(a_1 - b_1 \cos \varphi)^2 \cdot \{a_2 + b_2 \sin [\beta_1 - \text{arc sin} [c_1 \sin \varphi / (a_1 - b_1 \cos \varphi)]]\}\}. \tag{21}$$

If the link *AB* or *DE* becomes the column in the five-link mechanism (see Fig. 1), then the motion of links connected to the column does not differ from the motion of the corresponding links of the Bennett mechanism.

References

1. Myard, M. E. E. Chaine fermee a cinq couples rotoides, deformable au premier degre de *Comptes Rendus*, **192**, 1931, pp. 1352-1354.
2. Bennett, G. T. A new mechanism. *Engineering*, **76**, 1903, pp. 777, 778.
3. Goldberg, M. New five-bar and six-bar linkages in three dimensions. *Transactions of the ASME*, Aug., 1943, pp. 649-655.
4. Mudrov, P. G. Kinematicheskii analiz mekhanizma Bennetta (Kinematic analysis of Bennett mechanism). *Trudy Kazansk. s. kh. in-ta*, vyp. 47, 1965.

Z. S. Natsvlishvili

KINEMATIC STUDY OF THREE-DIMENSIONAL THREE-LINK LEVER MECHANISMS USING ANALYTICAL METHODS

In recent years, three-link mechanisms of the zero group (1-7) are becoming more and more popular in machine construction and in instrumentation along with four-link and five-link three-dimensional lever mechanisms.

Kinematic study of three-dimensional lever mechanisms is usually carried out graphically as in analytical study difficulties are caused by lengthy calculations. But the analytical method as applicable to three-link mechanisms is simpler and easier and, therefore, calculation equations are fully acceptable.

The relation between kinematic parameters of common three-link three-dimensional mechanisms which can be successfully used in practice, is considered in this article. The author has compiled tables and plotted corresponding diagrams by deriving equations for determining the values of kinematic parameters of mechanisms described below.

Let us consider the mechanism (Fig. 1) in which link O_1A is the driving link *1* which is connected to the support by a cylindrical kinematic pair of

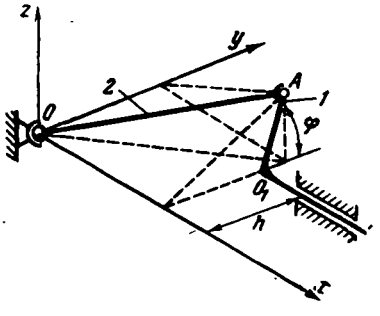

Fig. 1.

the 4th class and to the driven link *2* by a spherical kinematic pair of the 3rd class. In its own turn, the driven link forms a spherical, kinematic pair of the 4th class with the support.

In spite of the fact that this mechanism has one degree of mobility, its driving link accomplishes rotary as well as forward motion.

The constant kinematic parameters of the mechanism follow:

r—length of driving link *1* between point O_1 (x_1, y_1, z_1) and point A;

h—shortest distance between the center of spherical kinematic pair $O(O, O, O)$ and axis of rotation of the driving link;

l—length of the driven link AO.

Variable kinematic parameters of the mechanisms are:

φ—angle of rotation of the driving link O_1A, measured from the horizontal plane in the counter clock-wise direction;

x_1—abscissa of the center of rotation O_1 of the driving link *1*;

α, β, γ—angles formed by projections of driven link on the coordinate planes with the axes Ox, Oy, Oz.

The axis of rotation of the driving link lies in the xOy plane parallel to Ox axis. Therefore, $y_1=h$, $z_1=0$ and $x_1=x_2$.

It is obvious from Fig. 1, that:

$$y_2=h+r\cos\varphi;$$
$$z_2=r\sin\varphi. \tag{1}$$

If

$$l^2=(x_2-0)^2+(y_2-0)^2+(z_2-0)^2,$$

we have:

$$x_2^2=l^2-y_2^2-z_2^2. \tag{2}$$

Substituting the values of y_2 and z_2 from expressions (1) and after carrying out corresponding transformations, we get:

$$x_1=x_2=\sqrt{A-2rh\cos\varphi}, \tag{3}$$

where $A=l^2-h^2-r^2$.

Differentiating expression (3) with respect to time, we get velocity of displacement of the center of rotation of the driving link along the axis of rotation:

$$v_1=dx_1/dt=\omega_1 rh\sin\varphi/\sqrt{A-2rh\cos\varphi}. \tag{4}$$

Differentiating expression (4) with respect to time, we get the acceleration of the center of rotation:

$$w_1=d^2x_1/dt^2=\omega_1^2 rh\,(A\cos\varphi-rh\cos^2\varphi-rh)/[(A-2rh\cos\varphi)^{3/2}]. \tag{5}$$

Velocity of point A is determined from the equation:

$$v_A=\sqrt{(dx_2/dt)^2+(dy_2/dt)^2+(dz_2/dt)^2}. \tag{6}$$

After differentiating x_2, y_2 and z_2 with respect to time we substitute the values thus obtained in expression (6) and after corresponding transformations we have:

$$v_A=\omega_1 r\sqrt{[l^2-(r+h\cos\varphi)^2]/(A-2rh\cos\varphi)}. \tag{7}$$

Acceleration is determined from the equation:

$$w_A=\sqrt{(d^2x_2/dt^2)^2+(d^2y_2/dt^3)^2+(d^2z_2/dt^2)^2}=$$
$$\omega_1^2 r\sqrt{(r^2h^4\cos^4\varphi-B\cos^3\varphi+C\cos^2\varphi-D\cos\varphi+E)/(A-2rh\cos\varphi)^3}, \tag{8}$$

where $B=2Arh^3+8r^3d^3$; $C=A^2h^2+2r^2h^4+12r^2h^2A$;
$D=2Arh^3+6A^2rh$; $E=A^3+r^2h^4$.

Let us determine the angles formed by projections of the driven link on coordinate planes with Ox, Oy, Oz axes:

$$\begin{aligned}
&\alpha=\operatorname{arc\,tan}(z_2/y_2)=\operatorname{arc\,tan}[r\sin\varphi/(h+r\cos\varphi)];\\
&\beta=\operatorname{arc\,tan}(x_2/z_2)=\operatorname{arc\,tan}[\sqrt{A-2rh\cos\varphi}/r\sin\varphi];\\
&\gamma=\operatorname{arc\,tan}(y_2/x_2)=\operatorname{arc\,tan}[(h+r\cos\varphi)/\sqrt{A-2rh\cos\varphi}].
\end{aligned} \tag{9}$$

First and second derivatives of these angles with respect to time give the components of angular velocities and angular acceleration of the driven link.

$$\begin{aligned}
&d\alpha/dt=\omega_1 r\,(r+h\cos\varphi)/(h^2+r^2+2rh\cos\varphi);\\
&d\beta/dt=\omega_1 r\,(rh-A\cos\varphi+rh\cos^2\varphi)/[\sqrt{A-2rh\cos\varphi}\,(A+r^2\sin^2\varphi-\\
&\qquad 2rh\cos\varphi)];\\
&d\gamma/dt=-\omega_1 r\sin\varphi\,(l^2-r^2-rh\cos\varphi)/[\sqrt{A-2rh\cos\varphi}\,(l^2-r^2\sin^2\varphi)];\\
&\omega_2=\sqrt{(d\alpha/dt)^2+(d\beta/dt)^2+(d\gamma/dt)^2};\\
&d^2\alpha/dt^2=\omega_1^2 rh\sin\varphi\,(r^2-h^2)/[(h^2+r^2+2rh\cos\varphi)^2];\\
&d^2\beta/dt^2=\omega_1^2 r\sin\varphi\,(r^4h^2\sin^4\varphi+B_1\cos^3\varphi+C_1\sin^2\varphi+D_1\cos\varphi+E_1)/\\
&\qquad [(A-2rh\cos\varphi)^{3/2}\,(A+r^2\sin^2\varphi-2rh\cos\varphi)^2];\\
&d^2\gamma/dt^2=-\omega_1^2 r\,(B_2\cos^4\varphi+C_2\cos^3\varphi+D_2\cos^2\varphi+E_2\cos\varphi+F_2)/\\
&\qquad [(A-2rh\cos\varphi)^{3/2}\,(l^2-r^2\sin^2\varphi)^2];
\end{aligned} \tag{10, 11}$$

where

$$\varepsilon_2=\sqrt{(d^2\alpha/dt^2)^2+(d^2\beta/dt^2)^2+(d^2\gamma/dt^2)^2}\ ;$$

$$B_1=-3Ar^3h-2r^3h^3; \qquad C_1=-r^2A^2-3Ar^2h^2-10r^4h^2;$$

$$D_1=6r^3h^3-3A^2rh-5Ar^3h; \qquad E_1=3A^2r^2+A^3+8r^4h^2;$$

$$B_2=3l^2r^3h-3r^5h; \qquad C_2=3l^2r^2h^2+Ar^4-Al^2r^2-r^4h^2;$$

$$D_2=4r^5h+Ar^3h-2Arhl^2-l^4rh-3l^2r^3h;$$

$$E_2=Al^4-Ar^4-l^2r^2h^2+r^2h^4;$$

$$F_2=Arhl^2-Ar^3h-l^4rh+2l^2r^3h-r^5h.$$

($r=30$, $l=80$, $h=20$, see Table 1 and Fig. 2).

In the mechanism, shown in Fig. 3, the links are connected to each other by the following kinematic pairs:

1) support with the driving link *1*—cylindrical pair of 4th class;
2) driving link with the driven link *2*—spherical pair of 3rd class;
3) driven link with support-cylindrical pair of 4th class.

Axes of kinematic pairs *I—I* and *II—II* are skew.

The constant kinematic parameters of this mechanism follow:

r—length of the driving link *1* from point $O_1(x_1, y_1, z_1)$ to point A (x_2, y_2, z_2);

l—length of the driven link *2* from point A to point $B(x_3, y_3, z_3)$;

γ—angle of crossing of axes *I—I* and *II—II*;

h—shortest distance between axes *I—I* and *II—II*.

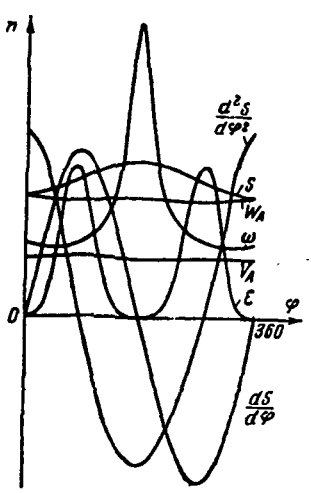

Fig. 2.

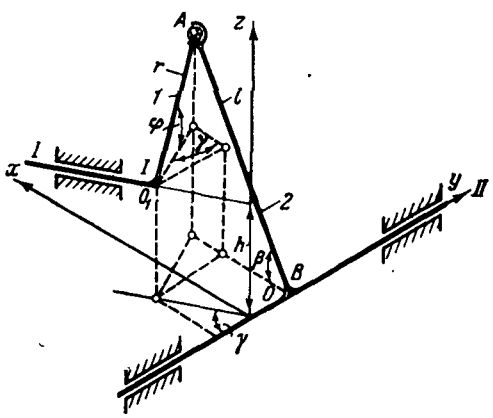

Fig. 3.

Table 1. Relations of velocities, accelerations and other parameters of driven link with φ°

φ°	S	$dS/d\varphi$	$d^2S/d\varphi^2$	v_A	w_A	α	β	γ	w	ε
0	65.450	0	9.608	30	3.147	0	1.570	0.675	0.678	0.048
15	62.777	2.473	9.134	30.102	3.133	0.157	1,448	0.662	0.757	0.311
30	63.724	4.708	7.806	30.367	3.098	0.315	1.339	0.625	0.735	6.427
45	65.203	6.507	5.857	30.697	3.056	0.475	1.256	0.563	0.726	28.084
60	67.082	7.746	3.578	30.984	3.021	0.638	1.201	0.481	0.739	58.611
75	69.206	8.374	1.230	31.147	3.002	0.807	1.174	0.381	0.771	77.855
90	71.414	8.402	−0.988	31.154	3.002	0.983	1.173	0.273	0.811	74.167
105	73.557	7.879	−2.955	31.017	3.014	1.171	1.195	0.165	0.862	52.599
120	75.498	6.882	−4.601	30.780	3.035	1.381	1.239	0.066	0.948	27.102
135	77.127	5.501	−5.893	30.500	3.057	−1.514	1.302	−0.015	1.123	92.130
150	78.353	3.829	−6.819	30.243	3.076	−1.191	1.382	−0.076	1.507	2.712
165	79.114	1.963	−7.374	30.064	3.089	−0.713	1.473	−0.113	2.305	3.912
180	79.372	0	−7.559	30	3.093	0	−1.571	−0.125	3.024	0.041
195	79.114	−1.963	−7.374	30.064	3.088	0.713	−1.473	−0.113	2.305	3.912
210	78.353	−3.829	−6.819	30.243	3.076	1.191	−1.382	−0.076	1.507	2.712
225	77.127	−5.501	−5.893	30.500	3.057	1.514	−1.302	−0.015	1.122	9.231
240	75.498	−6.882	−4.601	30.779	3.035	−1.381	−1.239	0.661	0.948	27.107
255	73.557	−7.879	−2.955	31.017	3.014	−1.171	−1.195	0.165	0.862	52.599
270	71.414	−8.402	−0.988	31.154	3.001	−0.983	−1.173	0.273	0.811	74.167
285	69.206	−8.374	1.230	31.147	3.002	−8.068	−1.174	0.381	0.771	77.855
300	67.082	−7.746	3.577	30.984	3.021	−0.636	−1.201	0.481	0.739	58.612
315	65.203	−6.507	5.857	30.697	3.056	−4.753	−1.256	0.564	0.726	28.084
330	63.724	−4.708	7.806	30.367	3.098	−3.153	−1.339	0.625	0.736	6.427
345	62.776	−2.474	9.134	30.102	3.133	−0.157	−1.448	0.662	0.757	0.311
360	62.450	0	9.608	30	3.147	0	1.571	0.675	0.769	0.048

Variable kinematic parameters of the mechanism are:

φ—angle of rotation of the driving link measured from horizontal plane in the counter clock-wise direction;

β—angle of rotation of the driven link, measured from the horizontal;

S_1—displacement of driving link *1* along *I—I* axis measured from point $O(O, O, O)$ of intersection of this axis with h;

S_2—displacement of driven link *2* along *II—II* axis measured from point O.

The coordinate system xyz is selected in such a manner that Oy axis coincides with *II—II* axis, Oz axis with h and xOy plane passes through *II—II* axis and parallel to *I—I* axis.

It is obvious from Fig. 3 that:

$$x_1/-y_1=\tan\gamma;\ z_1=h\,.$$

Therefore:

$$\begin{aligned} x_2&=-y_1\tan\gamma+r\cos\gamma\cos\varphi;\\ y_2&=y_1+r\sin\varphi\cos\varphi;\\ z_2&=h+r\sin\varphi;\\ x_3&=0;\\ y_3&=S_2;\\ z_3&=0. \end{aligned} \tag{12}$$

If the projection of driven link AB on xOy plane is parallel to Ox axis, then ordinate $y_2=y_3=S_2$, and abscissa x_2 is determined from the relation:

$$x_2=\sqrt{l^2-z_2^2}\,. \tag{13}$$

On the other hand:

$$x_2=-y_1\tan\gamma+r\cos\gamma\cos\varphi\,.$$

Equating these values, we get the value of y_1

$$y_1=r\cos\gamma\cot\gamma\cos\varphi-\cot\gamma\sqrt{l^2-(h+r\sin\varphi)^2}\,. \tag{14}$$

Then:

$$x_1=-r\cos\gamma\cos\varphi+\sqrt{l^2-(h+r\sin\varphi)^2}\,, \tag{15}$$

and the displacement of the driving link along I—I axis is calculated from the equation:

$$S_1=\pm\sqrt{x_1^2+y_1^2}=\pm\left[r\cot\gamma\cos\varphi-1/\sin\gamma\sqrt{l^2-(h+r\sin\varphi)^2}\right]. \tag{16}$$

Velocity of the center of rotation of the driving link can be obtained from the expression:

$$\begin{aligned} v_1=dS_1/dt=\pm\omega_1 r/\sin\gamma\,[&-\cos\gamma\sin\varphi+(h+r\sin\varphi)\cos\varphi\times\\ &\sqrt{l^2-(h+r\sin\varphi)^2}]\,. \end{aligned} \tag{17}$$

Differentiating equation (17) with respect to time, we get the acceleration of the center of rotation of driving link along I—I axis:

$$\begin{aligned} w_1=\pm\omega_1^2\, r/\sin\gamma\,\{&-\cos\gamma\cos\varphi+(r^3\sin^4\varphi+3r^2h\sin^3\varphi+A\sin^2\varphi\\ &+B\sin\varphi+rl^2)/[l^2-(h+r\sin\varphi)^2]^{3/2}\}\,, \end{aligned} \tag{18}$$

where

$$A=3rh^2-2rl^2;\qquad B=-hl^2-h^3\,.$$

To determine S_2, let us put the value of y_1, in expression of y_2:

$$S_2=r\cos\varphi/\sin\gamma-\sqrt{l^2-(h+r\sin\varphi)^2}\cot\gamma. \tag{19}$$

Velocity and acceleration of driven link *2* along *II—II* axis are determined from equations:

$$v_2=dS_2/dt=\omega_1 r/\sin\gamma\,[(h+r\sin\varphi)\cos\gamma\cos\varphi/\sqrt{l^2-(h+r\sin\varphi)^2}-\sin\varphi]; \tag{20}$$

$$w_2=dV_2/dt=\omega_1^2 r/\sin\gamma\,\{-\cos\varphi+(rl^2+B\sin\varphi+A\sin^2\varphi+3r^2h\sin^3\varphi +r^3\sin^4\varphi)/[l^2-(h+r\sin\varphi)^2]^{3/2}\cos\gamma\}, \tag{21}$$

where values of A and B have been given above.

Angle of rotation of driven link *2* about *II—II* axis is calculated from equation:

$$\beta=\arcsin z_2/l=\arcsin(h+r\sin\varphi)/l. \tag{22}$$

Angular velocity and angular acceleration of the driven link will be:

$$\omega_2=d\beta/dt=\omega_1 r\cos\varphi/\sqrt{l^2-(h+r\sin\varphi)^2};$$
$$\varepsilon_2=d^2\beta/dt^2=\omega_1^2 r\,(rh\sin^2\varphi+C\sin\varphi+rh)/[l^2-(h+r\sin\varphi)^2]^{3/2}, \tag{23}$$

where

$$C=h^2-l^2+r^2.$$

To determine extreme values of β, we equate the value of $d\beta/d\varphi$ to zero and by solving the equation, we get the corresponding values of φ on putting which in expression (22) we get the required values.

We get, that at $\varphi=270°$, $\beta_{min}=\arcsin(h-r)/l$ if $h>r$ and at $\varphi=90°$ — $\beta_{max}=\arcsin(h+r)/l$.

These values of β will be valid at $l\neq(h\pm r)$, i.e. at $r=30$, $\gamma=60°$, $h=20$, $l=60$ (see Table 2 and Fig. 4),

where $1-d\beta/d\varphi=d\beta/d\varphi\,(\varphi)$; $2-\beta=\beta\,(\varphi)$; $3-dS/d\varphi=dS/d\varphi\,(\varphi)$; $4-S_1=S_1\,(\varphi)$; $5-d^2S_1/d\varphi^2=d^2S/d\varphi\,(\varphi)$; $6-dS_2/d\varphi=dS_2/d\varphi\,(\varphi)$; $7-S_2=S_2\,(\varphi)$; $8-d^2S_2/d\varphi^2=d^2S_2/d\varphi^2\,(\varphi)$; $9-d^2\beta/d\varphi^2=d^2\beta/d\varphi^2\,(\varphi)$.

In the three-dimensional three-link mechanism shown in Fig. 5, the links form the following kinematic pairs:

1) support with driving link *1*—cylindrical pair of the 4th class;
2) driving link with driven link *2*—cylindrical pair of 4th class;
3) driven link with support-spherical pair of 3rd class.

The driving link consists of two skew shafts *1—1* and *I—I*. On rotating the driving link, every point on the driven link moves along a spherical surface and the driving link itself gets displacement along *I—I* axis.

Table 2. Relations of accelerations, velocities and other parameters of driving link with φ°

φ°	S_1	v_1	w_1	S_2	v_2	w_2	β	ω_2	ε_2
0	47.999	−12.247	−3.347	1.981	6.124	−24.307	0.339	0.530	0.099
15	44.688	−12.983	−15.917	2.752	−0.233	−17.137	0.481	0.545	0.009
30	41.273	−12.885	−45.289	1.863	−6.548	0.623	0.623	0.533	−0.104
45	38.104	−10.903	−104.905	−0.681	−12.919	34.081	0.757	0.486	−0.263
60	35.848	−5.661	−210.632	−4.934	−19.669	92.326	0.873	0.389	−0.493
75	35.537	4.060	−349.484	−11.044	−27.126	168.018	0.955	0.224	−0.765
90	38.297	17.320	−426.332	−19.148	−34.641	213.166	0.985	0	−0.904
105	44.502	29.400	−358.450	−28.975	−39.796	185.949	0.955	−0.224	−0.765
120	53.169	35.661	−227.953	−39.575	−40.331	126.967	0.873	−0.389	−0.493
135	62.599	35.398	−129.399	−49.671	−36.070	83.071	0.757	−0.486	−0.263
150	71.273	30.206	−75.289	−58.166	−28.093	60.144	0.623	−0.533	−0.104
165	78.148	21.949	−49.378	−64.170	−17.699	49.784	0.481	−0.544	0.089
180	82.640	12.247	−37.988	−67.301	−6.124	44.975	0.339	−0.530	0.099
195	84.556	2.487	−33.573	−67.374	5.481	41.882	0.205	−0.493	0.183
210	84.041	−6.151	−32.492	−64.520	16.066	38.746	0.083	−0.434	0.266
225	81.515	−12.743	−32.963	−59.129	24.742	34.853	−0.020	−0.354	0.351
240	77.597	−16.735	−33.703	−51.789	30.868	29.842	−0.099	−0.251	0.429
255	72.985	−18.087	−33.270	−43.217	34.139	23.359	−0.150	−0.131	0.486
270	68.313	−17.321	−30.281	−34.156	34.641	15.140	−0.167	0	0.507
285	54.019	−153.735	−24.305	−25.285	32.782	5.428	−0.150	0.131	0.486
300	60.277	−13.265	−16.383	−17.148	29.132	−4.799	−0.099	0.251	0.429
315	57.020	−11.752	−8.468	−10.139	24.247	−14.137	−0.020	0.353	0.351
330	54.041	−11.169	−2.492	−4.521	18.575	−21.254	0.083	0.434	0.266
345	51.096	−11.453	−0.112	−0.452	12.451	−25.039	0.205	0.493	0.183
360	47.999	−12.247	−3.347	1.981	6.124	−24.307	0.339	0.530	0.099

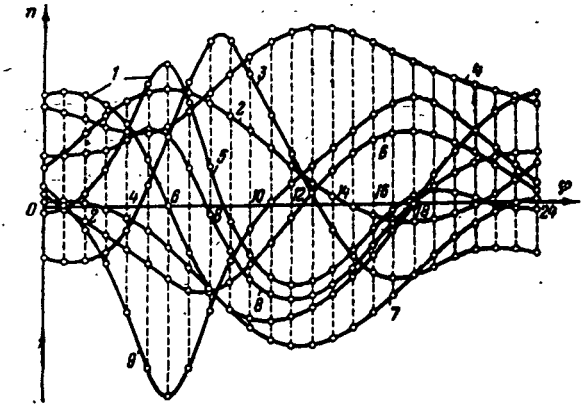

Fig. 4.

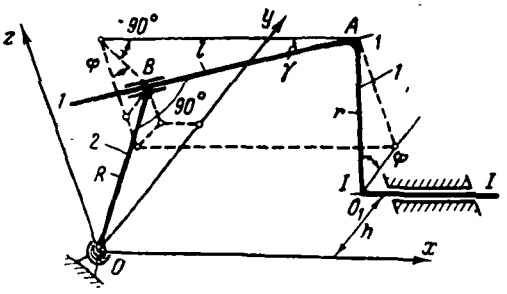

Fig. 5.

Following are the constant kinematic parameters of this mechanism:

γ—angle of crossing of the axes *1—1* and *I—I*;

r—shortest distance between axes *1—1* and *I—I* distance between points $O(x_0, y_0, z_0)$ and $A(x_1, y_1, z_1)$;

R—length of driven link *2*;

h—shortest distance between point O and *I—I* axis.

The variable kinematic parameters of the mechanism are:

φ—angle of rotation of the driving link *1*, measured from the horizontal in the counter clock-wise direction;

S_1—displacement of the driving link along *1—1* axis;

l—distance between points A and B.

x_2, y_2, z_2—coordinates of point B of the driven link *2*.

The system of coordinates xOz is selected in such a manner that the origin of coordinates O, coincides with the center of the spherical pair and plane xOy passes through *I—I* axis.

Axis Ox is taken parallel to *I—I* axis.

It is seen from Fig. 5 that:

$$x_0=S_1; \quad x_1=x_0; \quad x_2=x_1-l\cos\gamma;$$
$$y_0=h; \quad y_1=h+r\cos\varphi; \quad y_2=y_1+l\sin\gamma\sin\varphi;$$
$$z_0=0; \quad z_1=r\sin\varphi; \quad z_2=z_1-l\sin\gamma\cos\varphi.$$

The distance between a given point $A(x_1, y_1, z_1)$ and the origin of coordinates is:

$$OA=\sqrt{x_1^2+y_1^2+z_1^2}\,. \tag{24}$$

Since angle OBA is constant and equal to 90° for the given mechanism, then:

$$l=AB=\sqrt{x_1^2+y_1^2+z_1^2-R^2}\,, \tag{25}$$

and on the other hand, length of the segment, coordinates of the ends of which are known, is determined from the equation:

$$l=\sqrt{(x_1-x_2)^2+(y_1-y_2)^2+(z_1-z_2)^2}\,. \tag{26}$$

Equating expressions (25) and (26) and taking into account that:

$$x_2^2+y_2^2+z_2^2=R^2\,,$$

we get the expression:

$$x_1x_2+y_1y_2+z_1z_2=R^2\,. \tag{27}$$

Substituting values of x_2, y_2, and z_2 from expressions (24) in formula (27) and after transformation, we get:

$$x_1=x_0=S_1=1/\sin\gamma\,[-h\cos\gamma\sin\varphi\pm\sqrt{R^2-(h\cos\varphi+r)^2}]; \tag{28}$$

$$v_1=dS_1/dt=\omega_1 l/\sin\gamma\,[-\cos\gamma\cos\varphi\pm(h\cos\varphi+r)\sin\varphi/$$

$$\sqrt{R^2-(h\cos\varphi+r)^2}]\;; \tag{29}$$

$$w_1=d^2S_1/dt^2=\omega_1^2 h/\sin\gamma\,\{\cos\gamma\sin\varphi\pm(-h^3\cos^4\varphi-3rh^2\cos^3\varphi+A\cos^2\varphi+$$

$$B\cos\varphi-R^2h)/[R^2-(h\cos\varphi+r)^2]^{3/2}, \tag{30}$$

where

$$A=2hR^2-3hr^2;\qquad B=rR^2-r^3.$$

Let us put the value of x_1, obtained earlier, in equation (25):

$$l=1/\sin\gamma\,[\sqrt{R^2-(h\cos\varphi+r)^2}\cos\gamma-h\sin\varphi]. \tag{31}$$

Differentiating equation (31) with respect to time, we get the velocity of the driving link relative to the driven link:

$$dl/dt=\omega_1 h/\sin\gamma\,[(h\cos\varphi+r)\cos\gamma\cos\varphi/\sqrt{R^2-(h\cos\varphi+r)^2}-\cos\varphi]. \tag{32}$$

Substituting the values of x_1, y_1, and z_1 in (24) and knowing l, we get the coordinates of a point on the driven link:

$$\begin{aligned} x_2&=\sin\gamma\sqrt{R^2-(h\cos\varphi-r)^2};\\ y_2&=\cos\gamma\sin\varphi\sqrt{R^2-(h\cos\varphi-r)^2};\\ z_2&=(h\cos\varphi+r)\sin\varphi-\sqrt{R^2-(h\cos\varphi+r)^2}\cdot\cos\gamma\cos\varphi. \end{aligned} \tag{33}$$

Differentiating these expressions with respect to time, we determine the components of velocities of a point of driven link along Ox, Oy and Oz axes:

$$v_{2x}=\omega_1 h \sin\gamma \sin\varphi\,(h\cos\varphi+r)/\sqrt{R^2-(h\cos\varphi+r)^2};$$

$$v_{2y}=\omega_1\{[-2h^2\cos^3\varphi-3rh\cos^2\varphi+(R^2-r^2+h^2)\cos\varphi+rh]$$

$$\cos\gamma/\sqrt{R^2-(h\cos\varphi+r)^2}-\sin\varphi\,(2h\cos\varphi+r)\}; \tag{34}$$

$$v_{2z}=\omega_1\{[R^2-r^2-3rh\cos\varphi-2R^2\cos^2\varphi\cos\gamma\sin\varphi\sqrt{R^2-(h\cos\varphi+r)^2}$$

$$+(2h\cos\varphi+r)]\cos\varphi-h\}.$$

Velocity of point B will be:

$$v_2=\sqrt{(v_{2x})^2+(v_{2y})^2+(v_{2z})^2}, \tag{35}$$

$r=30$, $\gamma=20$, $h=20$, $R=80$, see Table 3 and Fig. 6, where curve

$1-S_1=S_1(\varphi)$; $2-l=l(\varphi)$; $3-V_2=V_2(\varphi)$; $4-dl/d\varphi=dl/d\varphi(\varphi)$;

$5-d^2S_1/d\varphi^2=d^2S_1/d\varphi^2(\varphi)$; $6-dS_1/d\varphi=dS_1/d\varphi(\varphi)$.

Thus, the relationships suggested in this work simplify solution of problems of kinematic analysis and synthesis of three-link mechanisms of zero group and facilitate wider application of these mechanisms in machine building and instrumentation.

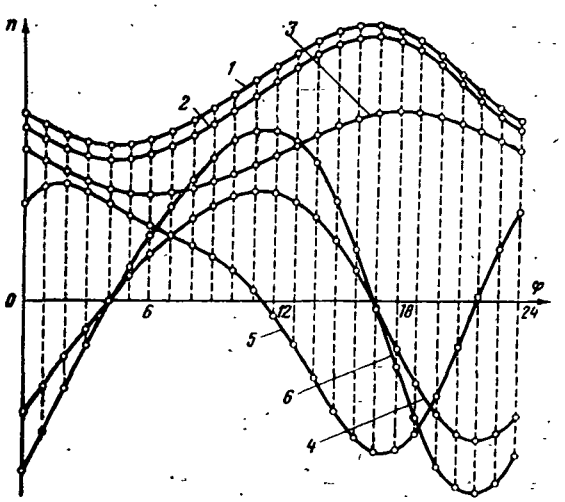

Fig. 6.

Table 3. Relations of displacement, velocities and other parameters of driven link with φ°

φ°	S_1	$dS_1/d\varphi$	$d^2S_1/d\varphi^2$	l	$dl/d\varphi$	v_2	x_2	y_2	z_2
0	182.354	−54.954	46.821	171.354	−58.562	77.053	21.359	50.000	−58.603
15	169.726	−41.230	56.444	157.720	−45.108	70.531	21.544	62.938	−44.338
30	160.912	−26.141	57.658	147.790	−29.964	64.644	22.062	71.253	−28.772
45	156.016	−11.500	53.615	141.773	−14.982	59.928	22.819	75.498	−13.072
50	154.777	1.763	47.591	139.523	−1.165	56.649	23.696	76.324	2.122
75	156.798	13.432	41.664	140.739	11.210	54.861	24.575	74.257	16.520
90	161.674	23.656	36.602	145.089	22.260	54.504	25.365	69.620	30.300
105	169.061	32.263	32.263	152.263	32.188	55.444	26.011	62.535	42.455
120	178.656	40.553	27.962	161.962	41.068	57.674	26.493	52.970	53.676
135	190.160	47.221	22.732	173.858	48.722	60.902	26.819	40.831	63.257
150	203.208	52.285	15.550	187.534	54.686	65.129	27.016	26.088	70.544
165	217.305	55.120	5.607	202.429	58.246	69.961	27.117	8.940	74.636
180	231.768	54.954	−7.368	217.788	58.562	75.148	27.147	−10.000	74.483
195	245.712	51.042	−22.839	232.659	54.856	80.361	27.117	−29.572	69.094
210	258.086	42.898	−39.404	245.935	46.641	85.281	27.016	−48.036	57.841
225	267.770	30.495	−54.984	256.449	33.918	89.626	26.819	−63.230	40.804
240	273.708	14.400	−67.220	263.116	17.295	93.172	26.493	−72.930	19.012
255	275.078	−4.215	−73.899	265.085	−2.010	95.740	26.011	−75.335	−55.513
270	271.431	−23.656	−73.305	261.892	−22.260	97.182	25.365	−69.567	−29.300
285	262.815	−41.878	−64.499	253.562	−41.370	97.354	24.575	−55.999	−51.422
300	249.830	−56.717	−47.591	240.677	−57.144	96.116	23.696	−36.284	−67.137
315	233.625	−66.217	−24.101	224.365	−67.586	93.359	22.819	−13.045	−75.471
330	215.791	−69.042	2.704	206.191	−71.308	89.075	22.062	10.722	−76.070
345	198.133	−64.932	27.998	187.950	−67.976	83.475	21.544	32.544	−69.853

References

1. Artobolevskii, I. I. Teoriya prostranstvennykh mekhanizmov (Theory of Three-dimensional Mechanisms). ONTI, 1937.
2. Tavkhelidze, D. S. Issledovanie prostranstvennykh mekhanizmov (Study of Three-dimensional Mechanisms). Gruz. industr. in-t im. Kirova, Tbilisi, 1945.

3. PANTELEEV, S. I. Opredelenie polozhenii prostranstvennykh trekhzvennykh mekhanizmov graficheskim metodom (Graphical determination of positions of three-dimensional three-link mechanisms). *Izv. vuzov, Mashinostroenie,* No. 7, 8, 1958.
4. PARTENSKII, B. M. Rychazhnye mekhanizmy (Lever Mechanisms). Izd-vo Mashinostroenie, 1964.
5. ROTINJAN, L. A. and I. VOLMER. Legenkonstruktionen bei raümlichen dreigliedrigen Getrieben. *Maschinenbautechnik,* **6**, 1957.
6. ALTMANN, F. G. Raumgetriebe. *Feinwerktechnik,* **60**, 1956, S. 83, 92.
7. BEYER, R. and E. SCHÖRNER. Raumkinematische Grundlagen. *J. A. Barth, München,* 1953, S. 56.

M. S. Rozovskii, E. N. Dokuchaeva and *V. G. Lapteva*

AN APPROXIMATE METHOD FOR SYNTHESIZING A HINGED LEVER AMPLIFYING MECHANISM OF A MOLDING PRESS

1. Lever Mechanism of the Press

Let us consider an approximate method of synthesis for a complicated plane hinged-lever amplifying mechanism of a molding press utilizing high pressure compression.[1]

The scheme and design of the press have been developed at NII-Traktorosel'khozmash (Tractor and Agricultural Machinery Research Institute).

The lever mechanism of the press consists of two coupled six-link mechanisms (Fig. 1,a). Piston *4* of the pneumatic cylinder is the driving

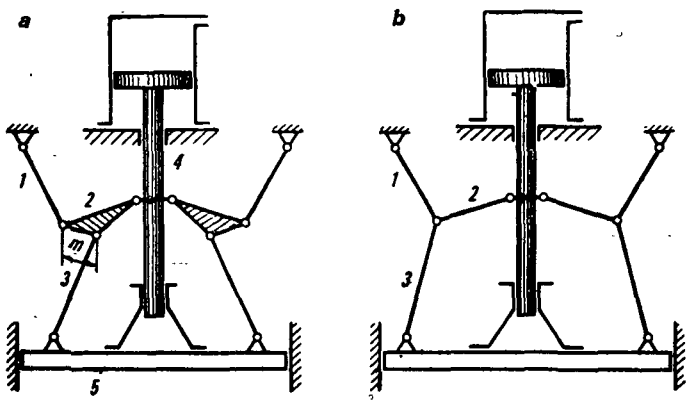

Fig. 1.

[1] Artobolevskii, I. I., N. I. Lavitskii and S. A. Cherkudinov. Sintez ploskikh mekhanizmov (Synthesis of Plane Mechanisms). Fizmatgiz, 1959.

element of the mechanism. The force from the piston is transmitted to the driven link i.e. plate *5* through the system of levers and the force from driving link to the driven link is increased by i times. The parameters i is the transmission ratio of the lever mechanism (amplification factor).

In contrast to most lever mechanisms of presses (Fig. 1,b) with breaking lever, levers *1* and *3* in the mechanism of Fig. 1,a are connected to lever *2* at different points due to eccentricity m. As a result of such a change, the scheme provides almost constant transmission ratio during the working stroke of plate *5* (i.e. while pressing).

Fig. 2 shows the relations between transmission ratio and the travel h of the press plate (curve *1*—for scheme of Fig. 1,a; curve *2*—for scheme of Fig. 1,b). It is clear from Fig. 2 that the scheme of Fig. 1,a provides almost constant transmission ratio $i \approx A$ in the pressing region Δh.

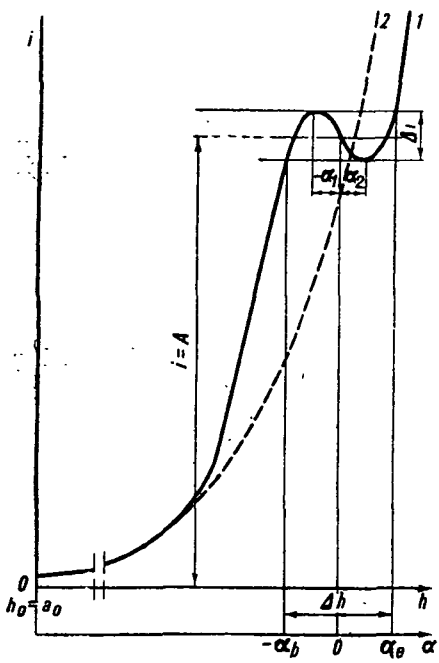

Fig. 2.

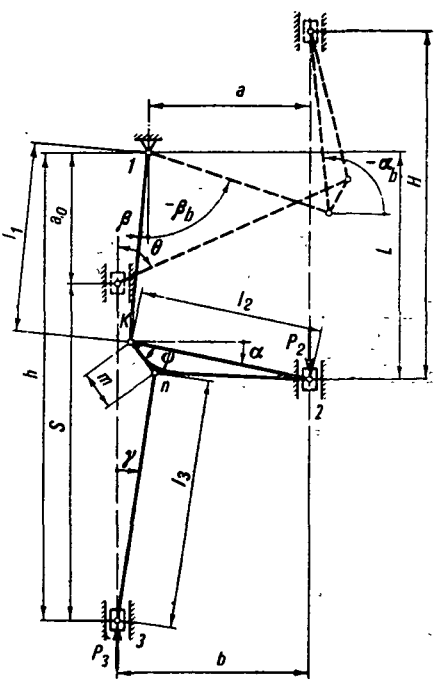

Fig. 3.

Since both six-link mechanisms of Fig. 1,a work in the same way, we will consider only one of these six-link mechanisms in our analysis (see Fig. 3). In this figure the mechanism is shown at two positions: at the upper position of the driven link (dotted, slide-block *3*) as well as at the lower position of the same link (continuous lines). Slide-block *2* is the driving link in Fig. 3.

2. Determination of Transmission Ratio of the Mechanism

Transmission ratio (amplification factor) of the mechanism is:

$$i=P_3/P_2. \tag{1}$$

Here P_2 is the vertical force applied to the driving link of the mechanism (at hinge *2*), and P_3 is the vertical force applied to the driven link of the mechanism (at hinge *3*).

Let us consider the lower position of the mechanism. Assuming that the possible displacement of hinge *2* is δL and of hinge *3*—δh, we get from the principle of possible displacements (see Fig. 3):

$$i=\delta L/\delta h. \tag{2}$$

Projecting the broken line *1k2* on the vertical axis, we have:

$$L=l_1 \cos \beta+l_2 \sin \alpha. \tag{3}$$

Then, projecting broken line *1kn3* on the vertical axis and broken lines *1k2* and *3nk2* on horizontal axis we get:

$$h=l_1 \cos \beta+m \sin (\alpha+\psi)+l_3 \cos \gamma; \tag{4}$$

$$a=l_2 \cos \alpha-l_1 \sin \beta; \tag{5}$$

$$b=l_3 \sin \gamma-m \cos (\alpha+\psi)+l_2 \cos \alpha. \tag{6}$$

After differentiating, from equation (3), we get:

$$\delta L=-l_1 \sin \beta \delta \beta+l_2 \cos \alpha \delta \alpha. \tag{7}$$

Here $\delta\beta$ and $\delta\alpha$ are increases of angles β and α for possible displacement δL.

On differentiating and after simplification, from equation (5) we get:

$$\delta \beta=-l_2/l_1 \cdot \sin \alpha/\cos \beta \cdot \delta \alpha. \tag{8}$$

Differentiating both sides of equation (4), we get:

$$\delta h=-l_1 \sin \beta \delta \beta+m \cos (\alpha+\psi) \delta \alpha-l_3 \sin \gamma \delta \gamma, \tag{9}$$

($\delta\gamma$ is the increase in angle γ for the possible displacement δL).

On differentiating equation (6), we have:

$$\delta \gamma=[l_2 \sin \alpha-m \sin (\alpha+\psi)] \cdot \delta \alpha / l_3 \cos \gamma. \tag{10}$$

From equations (2), (7), (8), (9) and (10), we arrive at the following relationship after simple transformations:

$$i=l_2 \cos(\alpha-\beta)\cos\gamma/[l_2 \sin\alpha \cdot \sin(\beta-\gamma)+m\cos\beta \cdot \cos(\alpha+\psi-\gamma)]. \quad (11)$$

Equation (11) helps in calculating the transmission ratio of the mechanisms.

Here angles α, β and γ change depending on the position of links of the mechanisms:

$$\sin\beta=(l_2\cos\alpha-a)/l_1; \quad (12)$$

$$\sin\gamma=(b+m\cos(\alpha+\psi)-l_2\cos\alpha)/l_3. \quad (13)$$

3. Formulation of the Problem of Synthesis

Parameters providing the required value of the transmission ratio $i\pm\Delta i/2$ within the given range of travel of the press plate Δh (see Fig. 2) are determined while synthesizing a mechanism.

The following parameters are given for the pressing operation on the basis of technological considerations (see Fig. 2):

i—average value of transmission ratio during pressing;

Δh—travel of the plate during pressing;

Δi—fluctuations of transmission ratio for plate travel Δh.

The following parameters are selected on the basis of the designs of the mechanism (see Fig. 3):

S—total travel of the plate (link *3*);

a_0—distance between the stationary hinge of lever l_1 (support *1*) and upper position of the plate.

It is necessary to determine (see Fig. 3):

l_1, l_2, l_3—lengths of levers of the mechanism;

a—distance between support *1* of lever l_1 and direction of link *2*;

b—distance between directions of motion of links *2* and *3*;

m—eccentricity, i.e. distance between hinges of levers l_1 and l_3;

ψ—angle of location of the eccentric with respect to lever l_2.

4. An Approximate Equation for Determining Transmission Ratio *i*

In order to solve the given problem, it is necessary to study the effect of various parameters on transmission ratio. Such a study utilizing equation (11) is extremely complicated. Therefore, we will make certain assumptions, which simplify the study.

Since angles β and γ are small in the pressing interval and α within this period hardly differ from 0° (in both the directions) we take:

$$\cos\beta\simeq 1; \qquad \sin\beta\simeq\beta; \qquad \cos\alpha\simeq 1-\alpha^2/2;$$

$$\cos\gamma\simeq 1; \qquad \sin\gamma\simeq\gamma; \qquad \sin\alpha\simeq\alpha-\alpha^3/6\,.$$

These assumptions help in replacing equation (11) by the approximate relationship:

$$i=[1+A_1\alpha-{}^1/_2\alpha^2-(C_1+A_1/6)\alpha^3]/(A_2+B_2\alpha+C_2\alpha^2+D_2\alpha^3)\,, \tag{14}$$

where coefficients A_1, C_1, A_2, B_2, C_2, D_2 are expressed in terms of the parameters of the lever mechanisms.

Let us rewrite equation (14) in the form:

$$i=(1-\mu)/(A_2+\lambda)\,, \tag{15}$$

where

$$\mu=-A_1\alpha+{}^1/_2\alpha^2+(C_1+A_1/6)\alpha^3; \qquad \lambda=B_2\alpha+C_2\alpha^2+D_2\alpha^3\,.$$

As shown by investigations, value of λ is small as compared to A_2 and therefore, expression (15) can be expanded into a series of powers of λ, neglecting terms of the series with powers of λ more than 3;

$$i=(1-\mu)(1-\lambda/A_2+\lambda^2/A_2^2-\lambda^3/A_2^3)/A_2\,. \tag{16}$$

Putting their values in place of μ, λ and A_2 in equation (16), after simplification we get:

$$i=A+B\alpha+C\alpha^2+D\alpha^3\,, \tag{17}$$

where coefficients A, B, C, and D expressed by parameters of the lever mechanism are determined from equations:

$$A=l_2l_3/\{m[l_3\cos\psi+(b+m\cos\psi-l_2)\sin\psi]\}; \tag{18}$$

$$B=(l_2-a)\cdot A(A-1)/l_1-A^2\cdot[(b+m\cos\psi-l_2)(m\cos\psi-l_2)- m\sin\psi(m\sin\psi+l_3)]/l_2l_3\,; \tag{19}$$

$$C=B^2/A-(l_2-a)B/l_1-3A^2m\sin\psi\cdot(l_2-m\cos\psi)/2l_2l_3\,; \tag{20}$$

$$D=(l_2-a)[A^3-A^2+6B^2-6AC]/6l_1A+ Al_2(A-1)/2l_1+B[A^2-2B^2+4AC]/2A^2- A^2[-4(l_2-m\cos\psi)^2+b(l_2-m\cos\psi)+ m\sin\psi(4m\sin\psi+l_3)]/6l_2l_3\,. \tag{21}$$

To find out the degree of approximation of equation (17), it was compared with the accurate equation (11).

The calculations of transmission ratio i in accordance with the approximate and accurate equations for various dimensions of the mechanism showed that the values of Δi, calculated with the help of approximate equation, on the humpshaped sections of the curve, hardly differ from the values of Δi calculated by the accurate equation.

Therefore, expression (17) can also be used for determining the dimensions of a lever mechanism.

Let us study the effect of coefficients B, C and D on transmission ratio i. It may be noted by examining equation (17) that $i=A$ at $\alpha=0°$. Coefficient A is approximately equal to the mean value of i within the pressing interval (see Fig. 2).

Fig. 2 shows the relation between the transmission ratio i and travel h of the driven link as well as α-angle of rotation of lever $k2$ relative to the horizontal position (see Fig. 3).

It will be demonstrated that increases in the values of h and α are approximately proportional to each other within the pressing interval. The pressing interval is determined on the basis of the following considerations. Two horizontal straight lines, corresponding to the maximum and minimum of curve on the graph of Fig. 2 are drawn. The abscissa of the point of intersection of the lower straight line with the left descending branch of curve i shows the beginning of pressing. Let us denote angle α at the beginning of pressing by α_b. Abscissa of the point of intersection of the upper straight line with the right (ascending) branch of curve i defines the end of pressing.

Denote angle α corresponding to end of pressing by α_e.

Let us examine the variable part of the right-hand side of equation (17) after denoting it by u:

$$u=B\alpha+C\alpha^2+D\alpha^3. \tag{22}$$

Taking the first derivative and equating it to zero, we get the values of angle α at which function (22) has maximum and minimum values (see angles α_1 and α_2 in Fig. 2).

$$du/d\alpha=B+2C\alpha+3D\alpha^2=0;$$
$$\alpha=(-C\pm\sqrt{C^2-3BD})/3D.$$

At $\alpha_1=(-C+\sqrt{C^2-3BD})/3D$, u will be minimum, and it will be maximum at $\alpha_2=(-C-\sqrt{C^2-3BD})/3D$.

Analysis of equations (19) and (21) showed that B is always less and D more than zero at all dimensions of mechanisms which can be materialized in practice.

If C differs from zero, which is obvious from the last 2 equations $|\alpha_1|\neq|\alpha_2|$, the middle of the interval $|\alpha_1|+|\alpha_2|$ is slightly displaced

relative to point $\alpha=0°$; here, positive values of C displace the middle of the interval toward negative values of α and the negative values toward positive. The higher the value of C, the larger will be the displacement.

To determine the effect of coefficients B and D, let us determine the sum of angles:

$$|\alpha_1|+|\alpha_2|=2\sqrt{C^2-3BD}/3D\,.$$

Calculations have shown that $C^2 \ll |3BD|$ and therefore, we obtain approximately

$$|\alpha|_1+|\alpha_2|=2\sqrt{-B/3D}\,. \tag{23}$$

Consequently, ratio of coefficients B and D defines the interval of change in angle α at which value of i changes from minimum to maximum.

Let us calculate the value of this change Δi.

$$\Delta i=B(\alpha_2-\alpha_1)+C(\alpha_2^2-\alpha_1^2)+D(\alpha_2^3-\alpha_1^3)\,.$$

Putting the values of α_1 and α_2 in the last equation and simplifying we get:

$$\Delta i=-2B\sqrt{C^2-3BD}/3D+2C^2\sqrt{C^2-3BD}/9D^2-2\sqrt{(C^2-3BD)^3}/27D^2\,.$$

Calculations have shown that the second term and parameters C^2 in the remaining terms of this equation can be neglected and then:

$$\Delta i=-{}^4/_3\cdot B\sqrt{-B/3D}\,. \tag{24}$$

It is clear from equation (24) that fluctuations in the value of transmission ratio depend on coefficient B and ratio B/D. Here, the lesser the coefficient B, the lesser will be Δi.

As it is shown later, the value of Δh is directly proportional to the value of $|\alpha_1|+|\alpha_2|$. It is obvious from equations (23) and (24) that in order to reduce Δi by keeping value $|\alpha_1|+|\alpha_2|$ constant, it is necessary to reduce B simultaneously with D in such a manner that B/D remains constant.

5. Approximate Method of Synthesis

It follows from section 3 that during the synthesis of mechanism it is necessary to determine seven parameters, namely: l_1, l_2, l_3, a, b, m and ψ.

Let us derive the relations which help in determining these parameters:

a) relation between m, l_1, l_2 and ψ. Since angle γ is small within the pressing interval, we assume that travel of the plate Δh (Fig. 4, link *3*) on this section is approximately equal to the vertical displacement of hinge a.

We determine the vertical displacement of hinge a from $\Delta aa'c$ (see Fig. 4).

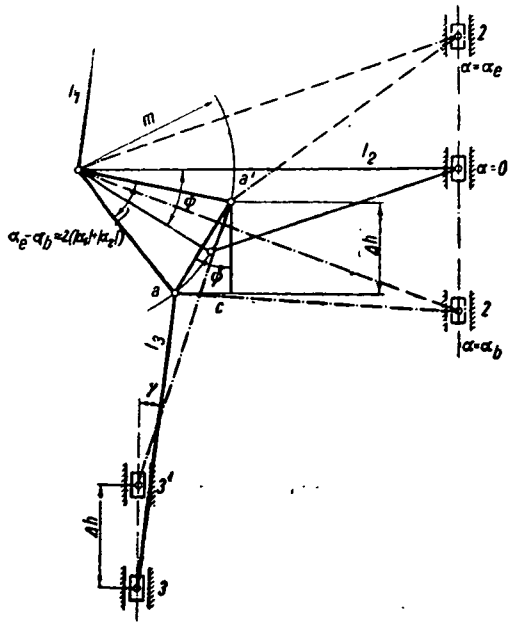

Fig. 4.

Since angle $(\alpha_e-\alpha_b)$ is small in this triangle, we take side aa' equal to arc aa' of rotation of hinge a through angle $(\alpha_e-\alpha_b)$.

The calculations have shown that with a sufficient degree of accuracy, it can be taken that:

$$\alpha_e-\alpha_b\approx 2(|\alpha_1|+|\alpha_2|)\,,$$

then:

$$aa'\approx 2(|\alpha_1|+|\alpha_2|)m\,,$$

$$\Delta h\approx 2(|\alpha_1|+|\alpha_2|)m\cos\psi\,.$$

Hence:

$$m=\Delta h/[2(|\alpha_1|+|\alpha_2|)\cos\psi]. \tag{25}$$

From equations (23) and (24) we get:

$$|\alpha_1|+|\alpha_2|=\sqrt[3]{2\Delta i/D}\,. \tag{26}$$

Coefficient D is determined from equation (21).

Let us simplify this equation by making the following assumptions which slightly alter the value of D:

1) The first and third terms of equation (21) as well as the term $m\sin\psi\,(4m\sin\psi+l_3)$ can be neglected since they are small;

2) Let us take $A \simeq i$;

3) Let us equate $b \approx l_2$, $l_1 \approx l_3$;

4) Taking $b \approx l_2$ and neglecting the term $m \cos \psi \cdot \sin \psi$ which is small as compared to other terms constituting this equation, we get from equation (18):

$$A \approx i \approx l_2/(m \cos \psi),$$

from where we get:

$$m \cos \psi \approx l_2/i. \tag{26a}$$

Introducing these assumptions in equation (21), and after subsequent simplifications we get:

$$D \simeq i(i-1)l_2(2+{}^4/_3 i)/2l_1 \simeq i(i-1)l_2/l_1. \tag{27}$$

Putting D from equation (27) in equation (26) we find that:

$$|\alpha_1|+|\alpha_2| \approx \sqrt[3]{2\Delta l_1/i(i-1)l_2}. \tag{28}$$

The effect of these assumptions was verified in numerous calculations which showed that equation (28) can be used for selecting the parameters of lever-mechanism of a press with a sufficient degree of accuracy.

Using equation (28) let us rewrite equation (25) for the eccentricity in the form:

$$m = \Delta h/2 \cos \psi \sqrt[3]{2\Delta i l_1/[i(i-1)l_2]}. \tag{29}$$

b) Relation between l_2, l_3, b, m and ψ. Equation (18), when $A \approx i$ gives:

$$l_2 = m \cos \psi \cdot i[1+(b+m \cos \psi) \tan \psi/l_3)]/(1+im \sin \psi/l_3). \tag{30}$$

c) Relation between a, l_1, l_2, m, ψ, b and α_B.

Let us project the lengths of the links of the mechanism at its upper positions on vertical axis (see Fig. 3). For this case:

$$a_0 = l_1 \cos \beta_B + l_3 \cos \gamma_B + m \sin (\alpha_B - \psi).$$

Let us express angle β_B in this equation through parameters of the mechanism:

$$\sin \beta_B = -(l_2 \cos \alpha_B - a)/l_1.$$

Then

$$a_0 = l_1 \cdot \sqrt{1-[(l_2 \cos \alpha_B - a)/l_1]^2} + l_3 \cos \gamma_B + m \sin (\alpha_B - \psi).$$

Therefore:

$$a = l_2 \cos \alpha_B + \sqrt{l_1^2 - [a_0 - l_3 \cos \gamma_B - m \sin(\alpha_B - \psi)]^2}. \tag{31}$$

"Plus" sign is taken before the square root since at $|\alpha_B| > 90°$ the value of $l_2 \cos\alpha$ is less than zero and the value of α can only be positive

$$\sin\gamma_B = (b - l_2\cos\alpha_B + m\cos\alpha_B)/l_3 .$$

d) Relation between b, m, l_1, l_2, l_3, and ψ.

From equations (23), (24) and (25) we get:

$$B = -3\Delta i m\cos\psi/\Delta h .$$

Putting this value of B in equation (19) and assuming $A = i$, we express b in the form:

$$b = 3\Delta i m\cos\psi l_2 l_3/[\Delta h i^2(m\cos\psi - l_2) + (l_2 - a)(1-i)l_2 l_3/[l_1 i(m\cos\psi - l_2)] - (m\cos\psi - l_2) + [m\sin\psi(m\sin\psi + l_3)]/(m\cos\psi - l_2) . \quad (32)$$

e) Relation between l_1, l_3, m and ψ. Considering the small values of angles β and γ we get from Fig. 3 for the extreme lower position of hinge *3*:

$$l_1 + l_3 = a_0 + S + m\sin(\alpha + \psi) . \quad (33)$$

Thus five equations (29)-(33) have been obtained above, which relate eight geometrical parameters of the lever mechanism (l_1, l_2, l_3, a, b, m, ψ and α_B) at given initial values.

Thus, some of the parameters can be selected arbitrarily and used for optimizing some other parameters of the mechanism. For example it is necessary to get the value of eccentricity m as small as possible.

It is obvious from equation (29) that this is possible at $\psi = 0$[2].

Putting $\psi = 0$ we get five equations for seven parameters to be determined.

Stroke of piston H (see Fig. 3) will be the second important parameter. The smaller the stroke of the piston, the more economical will be the press.

Let us study the effect of ratio l_1/l_3 on the ratio of stroke H of the piston to the total travel S of the plate. Values of H and S can be easily expressed in terms of parameters of the mechanism.

A number of mechanism at $X = 0.5$; 0.7; 0.8; 0.9; 1.1 and 1.5 were studied to find the effect of the value of $X = l_1/l_3$ on the ratio H/S.

Fig. 5 shows the results of investigations for mechanisms with the following initial data:

$S = 640$ mm; $i = 10$; $\Delta h = 24$ mm; $\Delta i = 1$; $a_0 = 390$ mm; $\gamma_B = 75°$. It is seen from Fig. 5 that the ratio H/S decreases on decreasing $X = l_1/l_3$.

[2] The ratio l_2/l_1 present in this equation has a comparatively weaker effect on the value of m.

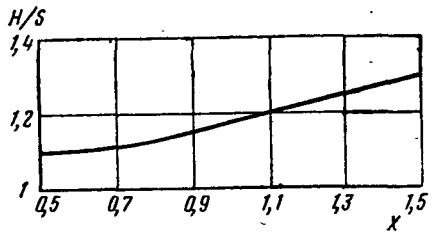

Fig. 5.

However, at $X<0.9$ this ratio changes insignificantly on decreasing the value of X. For example H/S ratio decreases only from 1.15 to 1.1 on changing the value of X from 0.9 to 0.5.

The above method is not applicable at small values of X since in this case angles β and γ increase in the pressing interval as a result of which the above assumptions are not valid.

Therefore we take $l_1/l_3=X=0.9$.

It can be shown that a decrease in the value of a and an increase in the value of b reduce the transmission ratio i_B at the upper position of levers of the plate. In accordance with this the value of a should be selected as low as possible but in such a manner that angle β is small in the pressing interval, otherwise this method will not be applicable. After this the value of transmission ratio i_B should be verified in order to facilitate return of the mechanism to the upper position.

In the subsequent discussion we assume that at $\alpha=0$, $\beta=10°$ and from equation (12) we have:

$$a=l_2-0.17\,l_1. \tag{34}$$

If the thrust of the piston is insufficient for the return of the mechanism to the upper position (low value of i_B) at the value of a determined from expression (34) then the corresponding value of i_B should be selected by increasing the value of a.

Putting $\psi=0$ and $X=l_1/l_3=0.9$ in equations (29), (30) and (32), (33) and using equation (34), we get simple equations for calculating the parameters of the mechanism:

a) Eccentricity m from equations (25), (26a), (28) and (33)

$$m=\Delta hi/4\sqrt{[\Delta h(i-1)]/[0.47\Delta i(S+a_0)]}\,;$$

b) Lengths of levers l_1, l_2 and l_3

$$l_1=0.47(S+a_0),\ l_2=im,\ l_3=S+a_0-l_1\,;$$

c) Values of a and b

$$a=l_2-0.17\,l_1\,;$$
$$b=l_2(2.13-{}^1/_2)-1.13a-3\Delta iml_3/[1.06\Delta hi(i-1)];^3$$

d) Value of i_B is determined from expressions (11), (12) and (13) by putting the value $\alpha=\alpha_B$ corresponding to the upper position of the mechanism. This position can be easily determined graphically by drawing the mechanism at the upper position of the plate.

The method helps in calculating the parameters of press providing the value of Δi on the pressing interval, differing from the given value within the limits of 10%. However, it should be kept in mind that this accuracy is observed when angle α does not exceed 30° in the pressing interval which corresponds to the condition:

$$\sqrt{[0.47\Delta i(S+a_0)]/\Delta hi^2(i-1)}\leqslant 0.25,$$

derived by simultaneously solving the equations (26a), (28), (29) and (33).

6. Example of Selecting Basic Parameters of a Lever Mechanism

The initial data are:

$S=640$ mm ; $i=10$; $\Delta h=24$ mm ; $\Delta i=1$; $a_0=390$ mm.

Solution:

1) Determination of the value of eccentricity

$$m=24\times 10\times\sqrt{24\times 9/0.47\times 1\times[(640+390)]}/4=40\text{ mm}.$$

2) Determination of the length of levers

$$l_1=0.47(640+390)=484\text{ mm};$$
$$l_2=10\times 40=400\text{ mm};\ l_3=640+390-484=542\text{ mm}.$$

3) Calculation of the values of a and b

$$a=400-0.17\times 484\approx 318\text{ mm};$$
$$b=400(2.13-0.1)-1.13\times 318-3\times 1\times 40\times 546/$$
$$(1.06\times 24\times 10\times 9)\approx 424\text{ mm}.$$

[3] The coefficient 1.06 introduced in the last equation takes into consideration the assumptions made while deriving the equations for this method. This coefficient is empirical and has been obtained as a result of many calculations. The value of b must be calculated with an accuracy of 1 mm.

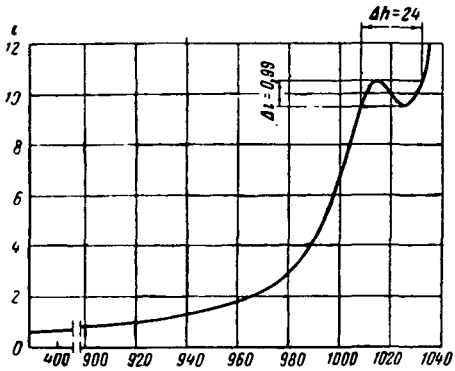

Fig. 6.

The graph of the relation between the transmission ratio and the travel of the pressing plate for the given mechanism is drawn in Fig. 6 in accordance with the accurate equations. In this example the error in the actual value of Δi is not more than 1% of the given value.

K. F. Sasskii

DYNAMIC FORCE ANALYSIS OF PLANE-MECHANISMS IN THREE-DIMENSIONAL SPACE

Kinematic chain with links, which move parallel to one and the same plane is termed a plane-kinematic chain in the theory of machines and mechanisms. However, because of design peculiarities, kinematic pairs joining the links of a plane chain have dimensions in the direction perpendicular to the plane of motion of the chain.

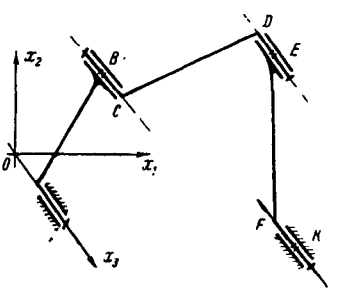

Fig. 1.

Because of this any chain is a spatial kinematic chain.

This concept is illustrated in Fig. 1.

In the kinematic analysis of a chain, these conditions do not create any complications and it is necessary to approach the problem of statics of such a chain in an altogether different way.

In considering the group *BCDEFK* as a plane-kinematic chain, it is assumed that the group is statically determinate. If the chain is considered as a spatial one then the chain is statically indeterminate, because in general there are three unknown components of reaction force and two unknown components of moment of reaction couple in kinematic pair of 5th class.

Consequently, there are 15 unknowns in the static calculations while only 12 equations of statics can be formed for two-links of the above mentioned group.

In the present paper an attempt has been made to consider the statics of Assur's "plane" groups in space.

1. Derivations of Fundamental Relationships

Let us consider any spatial bar-type linkage in which bars can be connected rigidly or with hinged joints.

If the cross section of any one of the links is not constant and varies along its axis, such a link will be considered as representing a number of coaxial rods, and along the length of each such link, the cross section is constant. Each of the links of the linkage is loaded with any arbitrary system of external force, which is applied to its axis. If a concentrated force is applied to the link q at a point B, then it may be considered to be made up either of two parallel forces applied at the ends of the link and whose magnitude is inversely proportional to the distances of the point B from the ends of the link or it may be considered that two rigidly fixed coaxial links meet at point B.

If the link is loaded with distributed force then the resultant force is determined and we proceed further as described above.

The points of connection of the rods are known as joints. It follows accordingly that the number of links of calculated diagram may be more than the actual number of links which form the linkage. Let us designate the joints connecting the k-th rod, by numbers K-1 and K and its length as S_k.

Since the problem of determination of reactions in the kinematic pairs of the groups cannot rely on the static method alone, for its solution we must consider the linear and angular displacements of cross sections of the link. Internal forces in the cross sections of each link must be calculated and linear displacements of the center of gravity of any section and components of angle of rotation of any cross section of the link must be determined.

Let us combine the fixed rectangular system of coordinate axes x_1, x_2, x_3 (see Fig. 1) with the linkage under consideration. We need to combine the rectangular system of coordinate axes ξ_{1j}, ξ_{2j}, ξ_{3j} with each j-th portion (of link) of the design diagram, placing its origin in the joint j-1 and directing the axes ξ_{1j} along the axis of the corresponding portion and axes ξ_{2j} and ξ_{3j} in the direction of the main central axes of inertia of the cross section containing the origin of coordinates.

Cosines of angles between the axes of these two systems form the matrix;

$$\Lambda_j=\begin{Vmatrix}\cos(x_1\xi_{1j}) & \cos(x_2\xi_{1j}) & \cos(x_3\xi_{1j})\\ \cos(x_1\xi_{2j}) & \cos(x_2\xi_{2j}) & \cos(x_3\xi_{2j})\\ \cos(x_1\xi_{3j}) & \cos(x_2\xi_{3j}) & \cos(x_3\xi_{3j})\end{Vmatrix}=\begin{Vmatrix}l_{1j} & m_{1j} & n_{1j}\\ l_{2j} & m_{2j} & n_{2j}\\ l_{3j} & m_{3j} & n_{3j}\end{Vmatrix}.$$

Under the action of external forces, internal forces and moments appear in any cross section (portion) j, and linear displacement of the center of gravity of the section as well as the rotation of this cross section take place. Components u_{1j}, u_{2j}, u_{3j}, of linear displacement of the center of gravity of the cross section in the system of coordinates x_1, x_2, x_3; components of internal moments M_{x1j}, M_{x2j}, M_{x3j} and internal forces P_{x1j}, P_{x2j}, P_{x3j} in the same system, and also components α_{1j}, α_{2j}, α_{3j} of angles of rotation of the cross section form the line matrix.

$$W_{xj}=\|u_{1j}u_{2j}u_{3j}\alpha_{1j}\alpha_{2j}\alpha_{3j}M_{x1j}M_{x2j}M_{x3j}P_{x1j}P_{x2j}P_{x3j}\|=\|\mathbf{u}_j\alpha_j\mathbf{M}_{xj}\mathbf{P}_{xj}\|.$$

We will call the above matrix as the matrix of parameters of cross section j in the system x. These elements form the line-matrix, if the components of internal moments and forces are considered in the system ξ:

$$W_{\xi j}=\|u_{1j}u_{2j}u_{3j}\alpha_{1j}\alpha_{2j}\alpha_{3j}M_{\xi 1j}M_{\xi 2j}M_{\xi 3j}P_{\xi 1j}P_{\xi 2j}P_{\xi 3j}\|=\|\mathbf{u}_j\alpha_j\mathbf{M}_{\xi j}\mathbf{P}_{\xi j}\|.$$

Designate this matrix as the matrix of parameters of cross section j in the system ξ. The relationship between the components of moments and forces in different systems is given below:

$$\begin{aligned}\mathbf{M}_{\xi j}&=\Lambda_j\mathbf{M}_{xj}\,;\\ \mathbf{P}_{\xi j}&=\Lambda_j\mathbf{P}_{xj}\,.\end{aligned}\tag{1}$$

Considering expression (1), we get the equation:

$$W_{\xi j}=\left\|\begin{matrix}E & 0 & 0 & 0\\ 0 & E & 0 & 0\\ 0 & 0 & \Lambda_j & 0\\ 0 & 0 & 0 & \Lambda_j\end{matrix}\right\| W_{xj}\,.\tag{2}$$

Here E is a binary matrix of 3rd order. Designate the line matrix which consists of 12 values (under consideration) for the cross section, that passes through the beginning of the 1st portion, as the matrix of initial parameters.

$$W_{xo}=\|u_{10}u_{20}u_{30}\alpha_{10}\alpha_{20}\alpha_{30}M_{x10}M_{x20}M_{x30}P_{x10}P_{x20}P_{x30}\|.$$

External force (P^* and moment M^*) and kinematic (u^* and α^*) reactions, applied to the joint K, form line matrix:

$$V_k=\|u^*_{1k}u^*_{2k}u^*_{3k}\alpha^*_{1k}\alpha^*_{2k}\alpha^*_{3k}M^*_{1k}M^*_{2k}M^*_{3k}P^*_{1k}P^*_{2k}P^*_{3k}\|\,,$$

and let us term it as the matrix of external forces in the system x.

Matrix of parameters of joint j can be expressed in terms of the matrix of initial parameters and also in terms of all the matrices of external forces applied at the joints from 1 to j-1:

$$W_{xj}=W_{xj(0)}+\sum_{k=1}^{j-1}W_{xj(k)}. \tag{3}$$

The first part of equation (3) expresses the effect of initial parameters and the last part shows the effect of external forces on the elements of the matrix W_{xj}.

Let us express the effect of each of the initial parameters on each of the parameters of matrix $W_{\xi j}$. Each of the 12 elements of this matrix is the sum of 12 components which depend on one of the 12 initial parameters.

For linear displacements, we represent this symbolically as:

$$u_{i1}=f_{i1}(u_{10})+f_{i2}(u_{20})+f_{i3}(u_{30})+f_{i4}(\alpha_{10})+f_{i5}(\alpha_{20})+f_{i6}(\alpha_{30})+$$
$$f_{i7}(M_{\xi 10})+f_{i8}(M_{\xi 20})+f_{i9}(M_{\xi 30})+f_{i10}(P_{\xi 10})+f_{i11}(P_{\xi 20})+f_{i12}(P_{\xi 30}). \tag{4}$$

Similarly, we represent the remaining elements of the matrix $W_{\xi j}$. In the first six terms of expression (4), displacements of the j-th link are considered as a rigid body and in the remaining 6 terms, displacements are because of the elasticity of the link.

Let us express the elements of the matrix $W_{\xi 1}$ in terms of the elements of the matrix W_{x0}.

The cross section, for which matrix $W_{\xi 1}$ is calculated, is taken at an infinitesimally small distance from the joint 1.

1. Calculation of linear displacements. Matrix of linear displacements of joint 1 can be represented in terms of the initial parameters in the following way:

$$\mathbf{u}_1=\begin{Vmatrix}u_{11}\\u_{21}\\u_{31}\end{Vmatrix}=\|F_1\|\begin{Vmatrix}u_{10}\\u_{20}\\u_{30}\end{Vmatrix}+\|F_2\|\begin{Vmatrix}\alpha_{10}\\\alpha_{20}\\\alpha_{30}\end{Vmatrix}+\|F_3\|\begin{Vmatrix}M_{\xi 10}\\M_{\xi 20}\\M_{\xi 30}\end{Vmatrix}+\|F_4\|\begin{Vmatrix}P_{\xi 10}\\P_{\xi 20}\\P_{\xi 30}\end{Vmatrix}. \tag{5}$$

Let us determine all the four matrices of the effects $\|F_i\|$.

Point O in the joint of the first link has linear displacements u_{10} u_{20} u_{30} (see Fig. 2). Linear displacements at point 1 will be the same as at point O.

Consequently:

$$\|F_1\|\begin{Vmatrix}u_{10}\\u_{20}\\u_{30}\end{Vmatrix}=\begin{Vmatrix}1&0&0\\0&1&0\\0&0&1\end{Vmatrix}\begin{Vmatrix}u_{10}\\u_{20}\\u_{30}\end{Vmatrix}=E\begin{Vmatrix}u_{10}\\u_{20}\\u_{30}\end{Vmatrix}=E\mathbf{u}_0.$$

2. Calculation of the angular displacements. During the rotation of the initial cross section, the end of the link is linearly

displaced. Let us calculate them (see Fig. 2). Rotation of the initial cross section can be represented by the vector α_0, which can be resolved along fixed axes into α_{10}, α_{20}, α_{30}.

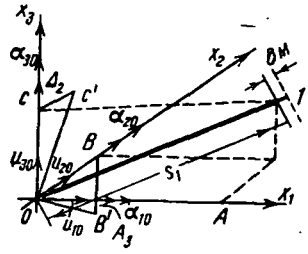

Fig. 2.

Let us assume that at $\alpha_{ik}>0$, rotation of the cross section takes place in the plane perpendicular to the vector α_{ik}, in a counter-clockwise direction. Components α_{10} rotates the cross section around the axis x_1, in the plane x_2x_3, points C and B occupy new positions as C' and B'. Linear displacements Δ_1, Δ_2 and Δ_3, parallel to the axes x_1, x_2, x_3 will be respectively equal to:

$$\Delta_1=0;$$

$$\Delta_2=\mathbf{OC}\alpha_{10}=s_1n_{11}\alpha_{10};$$

$$\Delta_3=-\mathbf{OB}\alpha_{10}=-s_1m_{11}\alpha_{10}.$$

Similarly linear displacements due to rotations α_{20} and α_{30} are calculated. If the link is considered to be rigid then the displacements will also be at the end of the link at the point I and:

$$\|F_2\|\begin{Vmatrix}\alpha_{10}\\ \alpha_{20}\\ \alpha_{30}\end{Vmatrix}=\begin{Vmatrix}0 & -s_1n_{11} & s_1m_{11}\\ s_1n_{11} & 0 & -s_1l_{11}\\ -s_1m_{11} & s_1l_{11} & 0\end{Vmatrix}\begin{Vmatrix}\alpha_{10}\\ \alpha_{20}\\ \alpha_{30}\end{Vmatrix}=A_{11}\begin{Vmatrix}\alpha_{10}\\ \alpha_{20}\\ \alpha_{30}\end{Vmatrix}=A_{11}\alpha_0.$$

3. Calculation of the effect of moments $M_{\xi 10}$, $M_{\xi 2}{}^0$ and $M_{\xi 30}$ on the linear displacements of the end of the link (Fig. 3). Moments $M_{\xi 10}$, acting in the plane $\xi_2\xi_3$ twists the link and therefore it does not produce any linear displacements of its ends.

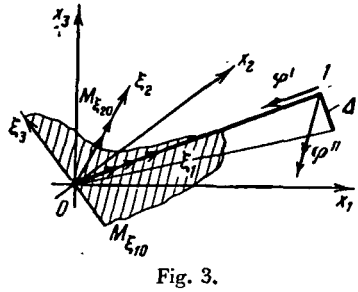

Fig. 3.

Moment $M_{\xi 20}$ (if moment is positive, it rotates the link in the clockwise direction) bends the link in the plane $\xi_1\xi_3$. Displacement Δ of the end *1* parallel to axis ξ_3 is equal to:

$$\Delta = -s_1^2 M_{\xi 20}/2E\mathcal{J}_{\xi 21},$$

where E—Modulus of elasticity;

$\mathcal{J}_{\xi 21}$—moment of inertia with respect to the axis ξ_1 see [1].

Components of this displacement along fixed axes will be:

$$\Delta_{x1}=\Delta l_{31}; \qquad \Delta_{x2}=\Delta m_{31}; \qquad \Delta_{x3}=\Delta n_{31}.$$

Similarly, displacements along fixed axes due to action of $M_{\xi 30}$ are calculated. These will be equal to:

$$\delta x_1=\delta l_{21}; \qquad \delta x_2=\delta m_{21}; \qquad \delta x_3=\delta n_{21},$$

where $\delta=s_1^2 M_{\xi 30}/2E\mathcal{J}_{\xi 31}$.

Taking into consideration the above mentioned facts we write:

$$\|F_3\| \begin{Vmatrix} M_{\xi 10} \\ M_{\xi 20} \\ M_{\xi 30} \end{Vmatrix} = \begin{Vmatrix} l_{11} & l_{21} & l_{31} \\ m_{11} & m_{21} & m_{31} \\ n_{11} & n_{21} & n_{31} \end{Vmatrix} \begin{Vmatrix} 0 & 0 & 0 \\ 0 & 0 & s_1^2/2E\mathcal{J}_{31} \\ 0 & -s_1^2/2E\mathcal{J}_{21} & 0 \end{Vmatrix} \begin{Vmatrix} M_{\xi 10} \\ M_{\xi 20} \\ M_{\xi 30} \end{Vmatrix} = \Lambda_1' L_{11} \mathbf{M}_{\xi 0}.$$

here Λ_1' and Λ_1—mutually transposed matrices.

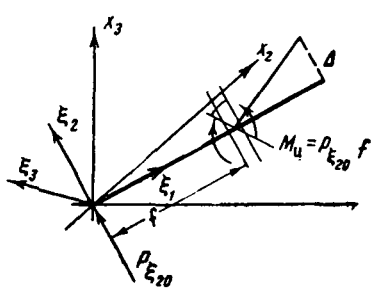

Fig. 4.

4. Linear displacements of the end of the link caused by the forces $P_{\xi 10}$, $P_{\xi 20}$, $P_{\xi 30}$. Force $P_{\xi 10}$ directed along the axis of the link produces compression of the axis by an amount $|\Delta l| = s_1 P_{\xi 10}/EF$, see Ref. [1].

Here F—area of the cross section of the link. Components of this displacement along the fixed axes will be equal to:

$$\Delta lx_1=-\Delta l l_{11}; \qquad \Delta lx_2=-\Delta l m_{11}; \qquad \Delta lx_3=-\Delta l n_{11}.$$

Force $P_{\xi 20}$ bends the link in the plane $\xi_1\xi_2$. Displacement Δ (Fig. 4) of the end of the rod will be parallel to the axis ξ_2 and its magnitude is equal to Reference [1].

$$\Delta = s_1^3 P_{\xi 20}/6EJ_{31}.$$

Components of such displacement along fixed axes will be equal to:

$$\Delta x_1 = \Delta l_{21}; \qquad \Delta x_2 = \Delta m_{21}; \qquad \Delta x_3 = \Delta n_{21}.$$

Values of displacement of the link are neglected. Components of the displacement due to the action of force $P_{\xi 30}$ are calculated in a similar manner:

$$\delta x_1 = \delta l_{31}; \qquad \delta x_2 = \delta m_{31}; \qquad \delta x_3 = \delta n_{31},$$

where $\delta = s_1^3 P_{\xi 30}/EJ_{21}$.

Considering the above stated facts, let us write

$$\|F_4\| \begin{Vmatrix} P_{\xi 10} \\ P_{\xi 20} \\ P_{\xi 30} \end{Vmatrix} = \begin{Vmatrix} l_{11} & l_{21} & l_{31} \\ m_{11} & m_{21} & m_{31} \\ n_{11} & n_{21} & n_{31} \end{Vmatrix} \begin{Vmatrix} -s_1/EF & 0 & 0 \\ 0 & s_1^3/6EJ_{31} & 0 \\ 0 & 0 & s_1^3/6EJ_{21} \end{Vmatrix} \begin{Vmatrix} P_{\xi 10} \\ P_{\xi 20} \\ P_{\xi 30} \end{Vmatrix} = \Lambda_1' L_{21} \mathbf{P}_{\xi 0}.$$

Let us determine the angular displacements of the end of the link, depending on the initial parameters. In accordance with the above, matrix of angular displacements of the joint *1* can be represented in terms of the initial parameters, as given below:

$$\alpha_1 = \begin{Vmatrix} \alpha_{11} \\ \alpha_{21} \\ \alpha_{31} \end{Vmatrix} + \|H_1\| \begin{Vmatrix} u_{10} \\ u_{20} \\ u_{30} \end{Vmatrix} + \|H_2\| \begin{Vmatrix} \alpha_{10} \\ \alpha_{20} \\ \alpha_{30} \end{Vmatrix} + \|H_3\| \begin{Vmatrix} M_{\xi 10} \\ M_{\xi 20} \\ M_{\xi 30} \end{Vmatrix} + \|H_4\| \begin{Vmatrix} P_{\xi 10} \\ P_{\xi 20} \\ P_{\xi 30} \end{Vmatrix}.$$

Let us determine all four matrices of effects $\|H_i\|$.

1) It is evident that $\|H_i\|$ is the zero matrix, since linear displacements of one end of the link cannot produce angular displacements of its other end.

2) If the link is considered to be rigid, then it is easy to understand that rotation of initial cross section produces the same rotation of its cross section at other end, therefore:

$$\|H_2\| \begin{Vmatrix} \alpha_{10} \\ \alpha_{20} \\ \alpha_{30} \end{Vmatrix} = \begin{Vmatrix} 1 & 0 & 0 \\ 0 & 1 & 0 \\ 0 & 0 & 1 \end{Vmatrix} \begin{Vmatrix} \alpha_{10} \\ \alpha_{20} \\ \alpha_{30} \end{Vmatrix} = E\alpha_0.$$

3) Moment $M_{\xi 10}$, acting on the initial cross section and the reaction moment acting in the cross section *1*, cause twisting of the link. Magnitude of the angle of twist is equal to:

$$\varphi' = M_{\xi 10} s_1/GJ_d \text{ (see Ref. [1])}.$$

If this angle is considered as vector φ' (see Fig. 3) directed similarly as the vector of the reaction moment along the axis of the rod, then components of the angular displacements of the cross section *1* due to the initial parameter $M_{\xi 10}$ along the fixed axes will be:

$$\varphi'_{x1}=\varphi' l_{11}; \qquad \varphi'_{x2}=\varphi' m_{11}; \qquad \varphi'_{x3}=\varphi' n_{11}.$$

Moment $M_{\xi 20}$ forms a couple acting in the plane $\xi_1\xi_3$ and it bends this plane. Designate the angle of rotation of the cross section *1* during bending by the vector φ'' (see Fig. 3) which should be directed in a similar way to the reaction moment in the cross section *1*, i.e. parallel to axis ξ_2 in the direction opposite to the direction of $M_{\xi 20}$.

Then angular displacement of the cross section *1* due to the parameter $M_{\xi 20}$ is written as:

$$\varphi''_{x1}=\varphi'' l_{21}; \qquad \varphi''_{x2}=\varphi'' m_{21}; \qquad \varphi''_{x3}=\varphi'' n_{21},$$

where $\varphi''=-s_1 M_{\xi 20}/EJ_{21}$.

Angular displacements of the cross section *1* due to parameter $M_{\xi 30}$ are calculated similarly and they are equal to

$$\varphi'''_{x1}=\varphi''' l_{31}; \quad \varphi'''_{x2}=\varphi''' m_{31}; \quad \varphi'''_{x3}=\varphi''' n_{31},$$

where $\varphi'''=-s_1 M_{\xi 30}/EJ_{31}$.

Considering the above statement, we have:

$$\|H_3\| \begin{Vmatrix} M_{\xi 10} \\ M_{\xi 20} \\ M_{\xi 30} \end{Vmatrix} = \begin{Vmatrix} l_{11} & l_{21} & l_{31} \\ m_{11} & m_{21} & m_{31} \\ n_{11} & n_{21} & n_{31} \end{Vmatrix} \begin{Vmatrix} -s_1/GJ_d & 0 & 0 \\ 0 & -s_1/EJ_{21} & 0 \\ 0 & 0 & -s_1/EJ_{31} \end{Vmatrix} \begin{Vmatrix} M_{\xi 10} \\ M_{\xi 20} \\ M_{\xi 30} \end{Vmatrix} = \Lambda'_1 L_{31} \mathbf{M}_{\xi 0}.$$

4) Force $P_{\xi 10}$ causes compression of the link and cannot produce the angular displacement of its end (see Fig. 5). Force $P_{\xi 20}$ bends the link in the plane $\xi_1\xi_2$. Direct moment with $P_{\xi 20}>0$ causes the rotation of the cross section in the clockwise direction, and the reaction moment in anti-

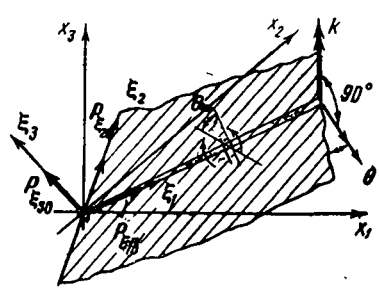

Fig. 5.

clockwise direction. Then vector angle of rotation Θ should be directed parallel and in the negative direction of axis ξ_3 that is:

$$\Theta=-s_1^2 P_{\xi 20}/2E\mathcal{J}_{31}\,.$$

Projection of the vector Θ on the fixed axis should be:

$$\Theta_{x1}=\Theta l_{31}; \qquad \Theta_{x2}=\Theta m_{31}; \qquad \Theta_{x3}=\Theta n_{31}.$$

It is easy to understand that at $P_{\xi 30}>0$ the rotation of the cross section *1* is expressed by the vector k, parallel to axis ξ_2 and its projections on the fixed axes will be:

$$k_{x1}=kl_{21}; \qquad k_{x2}=km_{21}; \qquad k_{x3}=kn_{21}\,,$$

where $k=s_1^2 P_{\xi 30}/2E\mathcal{J}_{21}$.

Effect of all three parameters of $P_{\xi i0}$ on the angular displacements of the cross section *1* is expressed as:

$$\|H_4\|\begin{Vmatrix}P_{\xi 10}\\P_{\xi 20}\\P_{\xi 30}\end{Vmatrix}=\begin{Vmatrix}l_{11} & l_{21} & l_{31}\\ m_{11} & m_{21} & m_{31}\\ n_{11} & n_{21} & n_{31}\end{Vmatrix}\begin{Vmatrix}0 & 0 & 0\\ 0 & 0 & -s_1^2/2E\mathcal{J}_{21}\\ 0 & -s_1^2/2E\mathcal{J}_{31} & 0\end{Vmatrix}\begin{Vmatrix}P_{\xi 10}\\P_{\xi 20}\\P_{\xi 30}\end{Vmatrix}=\Lambda_1'(-L_{11}')\,\mathbf{P}_{\xi 0}.$$

Here, L_{11}'—transposed matrix with respect to L_{11}. Shifting the forces $P_{\xi 10}$, $P_{\xi 20}$, $P_{\xi 30}$ to the center of gravity of the cross section *1* we get:

$$P_{\xi 10}=P_{\xi 11}; \qquad P_{\xi 20}=P_{\xi 21}; \qquad P_{\xi 30}=P_{\xi 31}.$$

This shifting generates two moments which are:

$$M_1=P_{\xi 21}s_1 \text{ and } M_2=-P_{\xi 31}s_1.$$

The relationship between the parameters $M_{\xi 10}$, $M_{\xi 20}$, $M_{\xi 30}$, $M_{\xi 11}$, $M_{\xi 21}$, $M_{\xi 31}$ are given below:

$$\mathbf{M}_{\xi 1}=\begin{Vmatrix}M_{\xi 11}\\M_{\xi 21}\\M_{\xi 31}\end{Vmatrix}=\begin{Vmatrix}1 & 0 & 0\\0 & 1 & 0\\0 & 0 & 1\end{Vmatrix}\begin{Vmatrix}M_{\xi 10}\\M_{\xi 20}\\M_{\xi 30}\end{Vmatrix}+\begin{Vmatrix}0 & 0 & 0\\0 & 0 & -s_1\\0 & s_1 & 0\end{Vmatrix}\begin{Vmatrix}P_{\xi 10}\\P_{\xi 20}\\P_{\xi 30}\end{Vmatrix}=E\mathbf{M}_{\xi 0}+L_{41}P_{\xi 0}; \tag{6}$$

$$\mathbf{P}_{\xi 1}=\begin{Vmatrix}P_{\xi 10}\\P_{\xi 21}\\P_{\xi 31}\end{Vmatrix}=\begin{Vmatrix}1 & 0 & 0\\0 & 1 & 0\\0 & 0 & 1\end{Vmatrix}\begin{Vmatrix}P_{\xi 10}\\P_{\xi 20}\\P_{\xi 30}\end{Vmatrix}=E\mathbf{P}_{\xi 0}. \tag{7}$$

If matrix Λ_1 is orthogonal, then $\Lambda_1'=(\Lambda_1)^{-1}$ and besides,

$$(\Lambda_1)_1^{-1}E\Lambda_1=E;$$

and

$$\Lambda_1'L_{41}\Lambda_1=A_{11}. \tag{8}$$

Let us rearrange expressions (5)-(8) and represent these in the form given below:

$$W_{x1(0)}=\begin{Vmatrix}\mathbf{u}_1\\ \boldsymbol{\alpha}_1\\ \mathbf{M}_{x1}\\ \mathbf{P}_{x1}\end{Vmatrix}=\begin{Vmatrix}E & A_{11} & A_{21} & A_{31}\\ 0 & E & A_{41} & A_{51}\\ 0 & 0 & E & A_{11}\\ 0 & 0 & 0 & E\end{Vmatrix}\begin{Vmatrix}\mathbf{u}_0\\ \boldsymbol{\alpha}_0\\ M_{x0}\\ P_{x0}\end{Vmatrix}=k_1W_{x0}. \tag{9}$$

Index (0) with W_{x1}, indicates the effect of initial parameters only. The following symbols have been used in the expression (9):

$$A_{21}=\Lambda_1'L_{11}\Lambda_1, \qquad A_{31}=\Lambda_1'L_{21}\Lambda_1,$$
$$A_{41}=\Lambda_1'L_{31}\Lambda_1, \qquad A_{51}=-\Lambda_1'L_{11}\Lambda_1.$$

Equation (1) has been taken into consideration. The second index of each block-matrix from the quasimatrix k_1 denotes the number of section of the link. Every subsequent matrix is expressed in terms of the previous one, just as W_{x1} was expressed in terms of W_{x0}.

Now let us express the matrix W_{xj} in terms of the matrix W_{xj-1} and finally in terms of the matrix W_{x0} [Matrices k_j, A_{ij}, L_{ij} ($i=1, 2, 3, 4, 5$) are obtained from matrices k_1, A_{i1}, L_{i1} by replacing 1 by i in each element of the matrix].

Then the general expression will be:

$$W_{xj(0)}=\prod_{n=j}^{1}k_nW_{x0}. \tag{10}$$

5. Let us consider the effect of external forces. If the external forces u^*, α^*, M^*, P^* are applied to the joint r, then these influence parameters of the matrix W_{xj}, i.e.

$$W_{xj}=\Gamma V_r,$$

where V_r—matrix of external forces which can be represented as below:

$$V_r=\|u^*\alpha^*M^*P^*\|=\|u_{1r}^*u_{2r}^*u_{3r}^*\alpha_{1r}^*\alpha_{2r}^*\alpha_{3r}^*M_{1r}^*M_{2r}^*M_{3r}^*P_{1r}^*P_{2r}^*P_{3r}^*\|;$$

Γ—function of effect (influence) which must be determined. If matrix V_r is considered as the matrix of initial parameters then its effect on the matrix W_{xj} (at $r<j$) may be written similar to the expression (10) i.e.

$$W_{xj(r)}=k_jk_{j-1}k_{j-2},\ldots,\ k_{r+1}V_r=\prod_{n=j}^{r+1}k_nV_r.$$

If a number of external forces are acting on different joints ($r=1, 2, 3,\ldots, j-1$) then the matrix $W_{xj}(r)$ is determined as a sum in the following form:

$$W_{xj(r)}=\sum_{r=1}^{j-1} W_{xj(r)}=\sum_{r=1}^{j-1}\left(\prod_{n=j}^{r+1} k_n\right)v_r.$$

Now matrix W_{xj} is expressed in terms of the matrix of initial parameters and all matrices of external forces will be expressed in the following forms:

$$W_{xj}=\left(\prod_{n=i}^{1} k_n\right)W_{x0}+\sum_{r=1}^{j-1}\left(\prod_{n=j}^{r+1} k_n\right)v_r. \tag{11}$$

These equations were first of all shown by A. P. Filin in Ref. 2.

2. Static Calculation of the Assur Double-link Group

Let us use the above stated method for the determination of 15 components of reaction in the three turning pairs of the double-link group shown in Fig. 6. On each link of the group either a plane (or spatial) system of forces acts, which for the sake of convenience is resolved into two forces, parallel to the axes x_1 and x_2 and a couple of forces with the moment, the vector of which is parallel to the axis x_3.

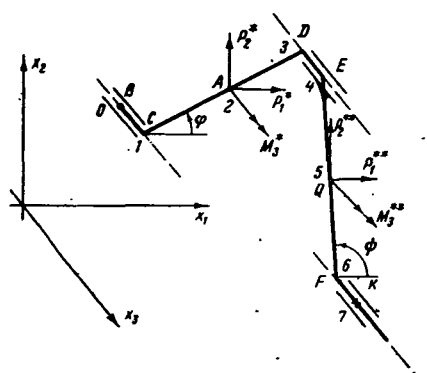

Fig. 6.

The calculation scheme for the group consists of seven parts. Angle φ and ψ which determine the position of the group are known.

Let us write the matrix of the directional cosines for the 7 parts.

$$\Lambda_1=\Lambda_4=\Lambda_7=\begin{Vmatrix}0&0&1\\1&0&0\\0&1&0\end{Vmatrix};\qquad \Lambda_2=\Lambda_3=\begin{Vmatrix}\cos\varphi&\sin\varphi&0\\0&0&-1\\-\sin\varphi&\cos\varphi&0\end{Vmatrix};$$

$$\Lambda_5=\Lambda_6=\begin{Vmatrix}-\cos\psi&-\sin\psi&0\\\cos\psi&-\sin\psi&0\\0&0&1\end{Vmatrix}.$$

Then we write the matrices A_{1j}, L_{1j}, L_{2j}, L_{3j}, A_{2j}, A_{3j}, A_{4j}, A_{5j};

1) $j=1$, $\mathcal{J}_{21}=\mathcal{J}_{31}=\mathcal{J}_1$, since the first link is a pin of round cross section,

$$A_{11}=\begin{Vmatrix}0&-s_1&0\\s_1&0&0\\0&0&0\end{Vmatrix};\quad L_{11}=\begin{Vmatrix}0&0&0\\0&0&s_1^2/2E\mathcal{J}_1\\0&-s_1^2/2E\mathcal{J}_1&0\end{Vmatrix};\quad L_{21}=\begin{Vmatrix}0&0&0\\0&s_1^3/6E\mathcal{J}_1&0\\0&0&s_1^3/6E\mathcal{J}_1\end{Vmatrix};$$

$$\Lambda_1=\begin{Vmatrix}0&1&0\\0&0&1\\1&0&0\end{Vmatrix};\quad L_{31}=\begin{Vmatrix}-s_1/G\mathcal{J}_d&0&0\\0&-s_1/E\mathcal{J}_1&0\\0&0&-s_1/E\mathcal{J}_1\end{Vmatrix};$$

$$A_{21}=\Lambda_1L_{11}\Lambda_1;\quad A_{31}=\Lambda_1'L_{21}\Lambda_1;\quad A_{41}=\Lambda_1'L_{31}\Lambda_1;\quad A_{51}=-A_{21}.$$

2) $j=2$, second part is the connecting link to the point of application of external forces:

$$A_{12}=\begin{Vmatrix}0&0&s_2\sin\varphi\\0&0&-s_2\cos\varphi\\-s_2\sin\varphi&s_2\cos\varphi&0\end{Vmatrix};\qquad L_{12}=\begin{Vmatrix}0&0&0\\0&0&s_2^2/2E\mathcal{J}_{22}\\0&-s_2^2/2E\mathcal{J}_{22}&0\end{Vmatrix};$$

$$\Lambda_2'=\begin{Vmatrix}\cos\varphi&0&-\sin\varphi\\\sin\varphi&0&\cos\varphi\\0&-1&0\end{Vmatrix};$$

$$L_{22}=\begin{Vmatrix}0&0&0\\0&s_2^3/6E\mathcal{J}_{32}&0\\0&0&s_2^3/6E\mathcal{J}_{22}\end{Vmatrix};\quad L_{32}=\begin{Vmatrix}-s_2/G\mathcal{J}_d&0&0\\0&-s_2/E\mathcal{J}_{22}&0\\0&0&-s_2/E\mathcal{J}_{32}\end{Vmatrix};$$

$$A_{22}=-A_{52}=\Lambda_2'L_{12}\Lambda_2;\quad A_{32}=\Lambda_2'L_{22}\Lambda_2;\quad A_{42}=\Lambda_2'L_{32}\Lambda_2.$$

3) $j=3$. All the matrices have the same form as for $j=2$, if s_2 is replaced by s_3.

4) $j=4$. The pin of the joint is of circular cross section:

$$L_{14}=\begin{Vmatrix}0&0&0\\0&0&s_4^2/2E\mathcal{J}_4\\0&-s_4^2/2E\mathcal{J}_4&0\end{Vmatrix};\qquad L_{24}=\begin{Vmatrix}0&0&0\\0&s_4^3/6E\mathcal{J}_4&0\\0&0&s_4^3/6E\mathcal{J}_4\end{Vmatrix};$$

$$L_{34}=\begin{Vmatrix} -s_4/G\mathcal{J}_d & 0 & 0 \\ 0 & -s_4/F\mathcal{J}_4 & 0 \\ 0 & 0 & -s_4/E\mathcal{J}_4 \end{Vmatrix};$$

$$A_{14}=\begin{Vmatrix} 0 & -s_4 & 0 \\ s_4 & 0 & 0 \\ 0 & 0 & 0 \end{Vmatrix};\quad \Lambda_4'=\Lambda_1';\quad A_{34}=\Lambda_4'L_{24}\Lambda_4;\quad A_{54}=-A_{24}.$$
$$A_{24}=\Lambda_4'L_{14}\Lambda_4;\quad A_{44}=\Lambda_4'L_{34}\Lambda_4.$$

5) $j=5$. Part 5-rocker to the point of application of external forces.

$$A_{15}=\begin{Vmatrix} 0 & 0 & -s_5\sin\psi \\ 0 & 0 & s_5\cos\psi \\ s_5\sin\psi & -s_5\cos\psi & 0 \end{Vmatrix};\quad L_{15}=\begin{Vmatrix} 0 & 0 & 0 \\ 0 & 0 & s_5^2/2E\mathcal{J}_{35} \\ 0 & -s_5^2/2E\mathcal{J}_{25} & 0 \end{Vmatrix};$$

$$\Lambda_5'=\begin{Vmatrix} -\cos\psi & \cos\psi & 0 \\ -\sin\psi & -\sin\psi & 0 \\ 0 & 0 & 1 \end{Vmatrix};$$

$$L_{25}=\begin{Vmatrix} 0 & 0 & 0 \\ 0 & s_5^3/6F\mathcal{J}_{35} & 0 \\ 0 & 0 & s_5^3/6E\mathcal{J}_{35} \end{Vmatrix};\quad L_{35}=\begin{Vmatrix} -s_5/G\mathcal{J}_d & 0 & 0 \\ 0 & -s_5/E\mathcal{J}_{25} & 0 \\ 0 & 0 & -s_5/E\mathcal{J}_{35} \end{Vmatrix};$$

$$A_{25}=-A_{55}=\Lambda_5'L_{15}\Lambda_5;\qquad A_{35}=\Lambda_5'L_{25}\Lambda_5;\qquad A_{45}=\Lambda_5'L_{35}\Lambda_5.$$

6) $j=6$. All matrices for part 6 are obtained by replacing s_5 by s_6 in the matrices for part 5.

7) $j=7$. Part 7-rod of round cross section.

$$L_{17}=\begin{Vmatrix} 0 & 0 & 0 \\ 0 & 0 & s_7^2/2E\mathcal{J}_7 \\ 0 & -s_7^2/2E\mathcal{J}_7 & 0 \end{Vmatrix};\quad L_{27}=\begin{Vmatrix} 0 & 0 & 0 \\ 0 & s_7^3/6E\mathcal{J}_7 & 0 \\ 0 & 0 & s_7^3/6E\mathcal{J}_7 \end{Vmatrix};$$

$$L_{37}=\begin{Vmatrix} -s_7/G\mathcal{J}_d & 0 & 0 \\ 0 & -s_7/E\mathcal{J}_7 & 0 \\ 0 & 0 & s_7/E\mathcal{J}_7 \end{Vmatrix};$$

$$A_{17}=\begin{Vmatrix} 0 & -s_7 & 0 \\ s_7 & 0 & 0 \\ 0 & 0 & 0 \end{Vmatrix};\quad \Lambda_7'=\Lambda_1';\quad A_{37}=\Lambda_7'L_{27}\Lambda_7;\quad A_{57}=-A_{27},$$
$$A_{27}=\Lambda_7'L_{17}\Lambda_7;\quad A_{47}=\Lambda_7'L_{37}\Lambda_7.$$

Now we write quasimatrices k_j and their product:

$$k_nk_{n-1},\ldots,k_2k_1=\begin{Vmatrix} E & a_{1n} & a_{2n} & a_{3n} \\ 0 & E & a_{4n} & a_{5n} \\ 0 & 0 & E & a_{1n} \\ 0 & 0 & 0 & E \end{Vmatrix},$$

where

$$a_{1n}=\sum_{i=1}^{n}A_{1i};\quad a_{2n}=\sum_{i=1}^{n}A_{2i}+\sum_{i=2}^{n}A_{1i}\sum_{j=1}^{i-1}A_{4j};\quad a_{4n}=\sum_{i=1}^{n}A_{4i};$$

$$a_{3n}=\sum_{i=1}^{n}A_{3i}+\sum_{i=2}^{n}A_{1i}\Big[\sum_{j=1}^{i-1}A_{5j}+\sum_{j=2}^{i-1}A_{4j}\sum_{k=1}^{j-1}A_{1k}\Big]+\sum_{i=2}^{n}A_{2i}\Big[\sum_{j=1}^{i-1}A_{1j}\Big];$$

$$a_{5n}=\sum_{i=1}^{n}A_{5i}+\sum_{i=2}^{n}A_{4i}\sum_{j=1}^{i-1}A_{1j}.$$

Matrices of external reactions on the joints *2* and *5* (see Fig. 6) will be:

$$V_2=\|0\,0\,0\,0\,0\,0\,0\,0\,M_3^*\;P_1^*\;P_2^*\;0\|;$$
$$V_5=\|0\,0\,0\,0\,0\,0\,0\,0\,M_3^{**}P_1^{**}P_2^{**}0\|.$$

If relative rotation α_E is possible between the links *CD* and *EF*, then the matrix of external forces for joint *4* has the following form:

$$V_4=\|00000\alpha_E000000\|.$$

Matrix of initial parameters (matrix of reaction in the joint 0) for the scheme under consideration is written as:

$$W_0=\|00000\alpha_{30}M_{10}M_{20}0P_{10}P_{20}P_{30}\|.$$

Matrix of parameters of the joints n ($n=1, 2, 3, 4, 5, 6, 7$) in the general form is represented as:

$$W_n=\|u_{n1}u_{n2}u_{n3}\alpha_{n1}\alpha_{n2}\alpha_{n3}M_{n1}M_{n2}M_{n3}P_{n1}P_{n2}P_{n3}\|.$$

Write the matrices of parameters of all joints W_n in terms of matrices of initial parameters W_0 and matrices of external forces V_2, V_4, V_5:

$$(s)\begin{cases}W_1=k_1W_0,\\ W_2=k_2k_1W_0,\\ W_3=k_3k_2k_1W_0+k_3V_2,\\ W_4=k_4k_3k_2k_1W_0+k_4k_3V_2,\\ W_5=k_5k_4k_3k_2k_1W_0+k_5k_4k_3V_2+k_5V_4,\\ W_6=k_6k_5k_4k_3k_2k_1W_0+k_6k_5k_4k_3V_2+k_6k_5V_4+k_6V_5,\\ W_7=k_7k_6k_5k_4k_3k_2k_1W_0+k_7k_6k_5k_4k_3V_2+k_7k_6k_5V_4+k_7k_6V_5.\end{cases}$$

Each one of the matrices k_j is the diagonal of quasimatrix of the 12th order.

Let us write equation for W_7 as:

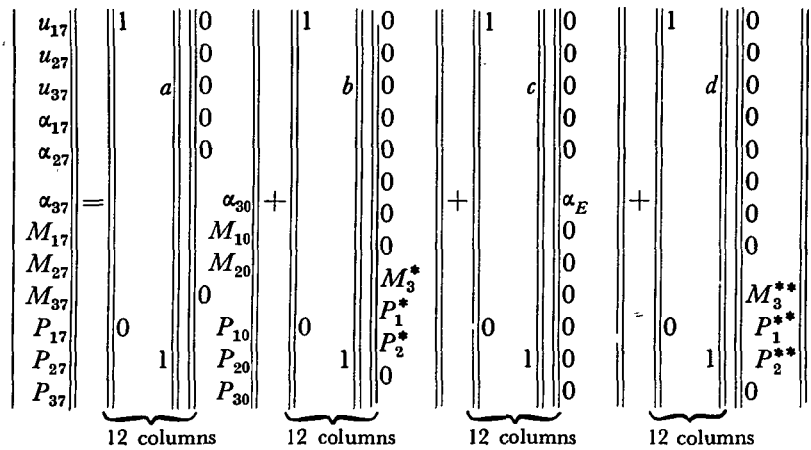

From the last equation, we may determine u_{17}, which will be equal to the sum of the products of the first row of matrices a, b, c, d with the matrix column W_0, V_2, V_4, V_5 respectively, i.e.

$$u_{17}=a'_{13}\alpha_{30}+a'_{11}M_0+a''_{12}M_{20}+a'''_{11}P_{10}+a'''_{12}P_{20}+a'''_{13}P_{30}+b'''_{13}M^*_3+$$
$$b'''_{11}P^*_1+b''_{12}P^*_2+c'_{13}\alpha_E+d''_{13}M^{**}_3+d'''_{11}P^{**}_1+d'''_{12}P^{**}_2 .$$

Similarly equation for u_{27}, u_{37}, α_{17}, α_{27}, M_{37} are written. Since in the kinematic pair, connecting the link EF with the support:

$$u_{17}=0,\ u_{27}=0,\ u_{37}=0,\ \alpha_{17}=0,\ \alpha_{27}=0,\ M_{37}=0,$$

then we shall have 6 equations with seven unknowns, i.e. α_{30}, M_{10}, M_{20}, P_{10}, P_{20}, P_{30}, α_E.

The 7th equation which is unknown, is obtained from the condition that the moment in the kinematic pair connecting links CD and EF with respect to axis of the pair is equal to zero. This equation is obtained from the relationship for W_4 [see system (s)].

In fact:

$$\begin{Vmatrix} u_{14} \\ u_{24} \\ u_{34} \\ \alpha_{14} \\ \alpha_{24} \\ \alpha_{34} \\ M_{14} \\ M_{24} \\ M_{34} \\ P_{14} \\ P_{24} \\ P_{34} \end{Vmatrix} = \underbrace{\begin{Vmatrix} 1 & & \\ & & \\ & & \\ & f & \\ & & \\ & & \\ & & \\ & & \\ 0 & & \\ & & \\ & & \\ & & 1 \end{Vmatrix}}_{12\text{ columns}} \begin{Vmatrix} 0 & & \\ 0 & & \\ 0 & & \\ 0 & & \\ 0 & & \\ & & \alpha_{30} \\ & & M_{10} \\ & & M_{10} \\ 0 & & \\ & & P_{10} \\ & & P_{20} \\ & & P_{30} \end{Vmatrix} + \underbrace{\begin{Vmatrix} 1 & & \\ & & \\ & & \\ & h & \\ & & \\ & & \\ & & \\ & & \\ 0 & & \\ & & \\ & & \\ & & 1 \end{Vmatrix}}_{12\text{ columns}} \begin{Vmatrix} 0 & & \\ 0 & & \\ 0 & & \\ 0 & & \\ 0 & & \\ 0 & & \\ 0 & & \\ 0 & & \\ & & M_3^* \\ & & P_1^* \\ & & P_2^* \\ & & 0 \end{Vmatrix}$$

From where:

$$M_{34}=f'_{31}P_{10}+f'_{32}P_{20}+f'_{33}P_{30}+M_3^*+h'_{31}P_1^*+h'_{32}P_2'=0.$$

After the determination of 7 unknowns, we shall know the value of matrix W_0 as all matrices k_j are known; then from equation (s) we find matrix W_n. Each equation from (s) gives 12 equations for the determination of 12 components of the matrix W_n.

If only factors are required, then we use only the equations which contain these factors.

It is understood from the above facts that the problem about errors in the position of the group under consideration is simultaneously solved by taking into consideration the elasticity of its links.

References

1. Pakarin, N. Ya. and I. I. Tarasenko. Soprotivlenie materialov (Strength of Materials). Mashgiz, 1962.
2. Filin, A. P. Raschet prostranstvennykh sterzhnevykh konstruktsii tipa sistemy perekrestnykh svyazei i ego primenenie k obolochkam pri ispol'zovanii elektronnykh vychislitel'nykh mashin (Calculation of Spatial Bar Linkages of Cross Links System and Its Application in an Electronic Computer). Sbornik "Issledovaniya po stroitel'noi mekhanike", Leningrad, 1962.

V. I. Sergeev, S. A. Cherkudinov and *I. G. Oleinik*

ANALYSIS OF THE STRUCTURAL AND TECHNICAL ERRORS OF SIX-LINK MECHANISMS IN THE DWELL ZONE

It is well known that a hinged six-link mechanism *ABCDEFG* (Fig. 1), formed by connecting two four-link mechanisms *ABCD* and *DEFG* in series has a sufficiently accurate stop of the driven link *GF* in one of its extreme positions for large angles of rotation of the driving link *AB*. This mechanism is widely used in different automatic machines in the light engineering and food industries.

The purpose of the present article is to minimise the structural errors of position of the driven link of a six-link mechanism during its dwell, and also to compare these errors with the possible technical errors of position for the same link during the dwell period for different manufacturing tolerances of the mechanism.

One of the necessary conditions for minimising the structural deviations will be the correct selection of the angle of jamming δ of the driven link *CD* of the first mechanism and of the driving link *DE* of the second mechanism [1]. Angle δ should have such a value so that during dwell, the driven link of the six-link mechanism will have 5 extreme deviations equal in magnitude but alternately positive and negative in sign, from the mean dwelling position marked by points e_0; e_1, e_2; e_1', e_0' (Fig. 2) on the graph of the displacement function of this mechanism.

These five extreme deviations are obtained because of the fact that extreme positions of the driven link of first mechanism nearly coincide in phase with the extreme positions of the driven link of the second mechanism.

For the selection of the jamming angle, structural errors for the dwell portion may be determined according to the following approximate equation [2]:

$$\Delta\psi=(\Delta\gamma)^2\cdot\varepsilon/8, \qquad (1)$$

where, $\Delta\gamma = \angle C_0DC_2$—it is the angle made by the driven link of first mechanism during the rotation of driving link for a given angle of dwell $\varphi_{00} = \angle B_0AB_0'$ (see Fig. 1); ε—angular acceleration of the driven link of second mechanism in the extreme position DE_1F_1G.

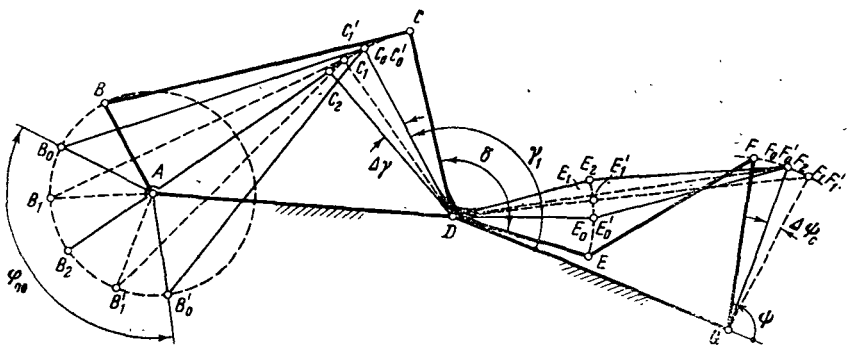

Fig. 1. Diagram of the six-link mechanism formed by the series connection of two four-link mechanisms.

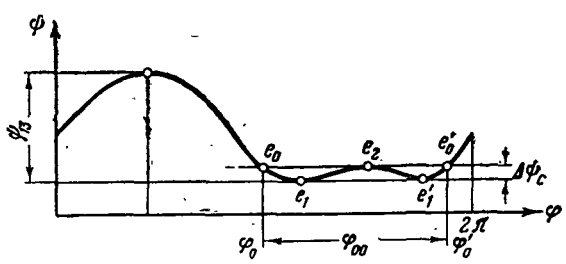

Fig. 2. Graph of the displacement function of driven link $\psi = f(\varphi)$ where ψ—coordinate of the driven link GF, and φ—coordinate of the driving link AB.

In Fig. 3, a six-link mechanism is shown in two such positions, for which the driven link occupies extreme positions GF_1, and GF_3. We shall consider, that for the design of the six-bar mechanism, the following data are given: Total angle of swing of the driven link ψ_{13} (see Figs. 2 and 3) and angle of rotation of the driving link φ_{00} (see Figs. 1 and 2) at which it is necessary to obtain the approximate dwell. It is required to obtain the parameters of the diagram of both the serially connected four-bar mechanism and the angle of total swing $\gamma_{23} = \angle C_2DC_3$ of the driven link of the first mechanism.

Table 1. Parameters of synthesized mechanisms for values of Δ varying from 0.1 to 0.4

γ_{23}, deg	Δ=0.1			Δ=0.2			Δ=0.3			Δ=0.4		
	μ_{min}, deg	a	c	μ_{min}, deg	a	c	μ_{min}, deg	a	c	μ_{min}, deg	a	c
20	43	0.173092	1.005387	51	0.172049	1.009963	53	0.171133	1.022081	53	0.170002	1.037062
22	42	0.189841	1.001997	49	0.188992	1.011210	51	0.188028	1.025079	51	0.186885	1.042493
24	40	0.206886	1.003279	47	0.205934	1.013327	50	0.204189	1.019891	50	0.202870	1.037238
26	38	0.223934	1.005266	46	0.222239	1.009314	48	0.221069	1.024525	49	0.218665	1.032363
28	37	0.240508	1.003265	44	0.239168	1.012903	47	0.237021	1.020377	47	0.235549	1.040353
30	36	0.256996	1.001573	43	0.255318	1.009848	45	0.253919	1.026680	46	0.251166	4.036588
32	34	0.274030	1.005272	41	0.272252	1.014916	44	0.269713	1.023575	44	0.268126	1.046502
34	33	0.290430	1.004400	40	0.288277	1.012824	43	0.285364	1.020840	43	0.283610	1.043886
36	32	0.306749	1.003833	39	0.304185	1.011086	41	0.302340	1.029544	42	0.298949	1.041667
38	31	0.322997	1.003570	38	0.319988	1.009697	40	0.317895	1.027880	41	0.314153	1.039848
40	30	0.339163	1.003614	36	0.337011	1.017479	39	0.333326	1.026603	40	0.329224	1.038438
42				35	0.352741	1.017075	38	0.348654	1.025705	39	0.344182	1.037431
44				34	0.368392	1.017025	37	0.363875	1.025200	38	0.359018	1.036852
46				33	0.383957	1.017341	36	0.379001	1.025090	37	0.373758	1.036688
48				32	0.399446	1.018023	35	0.394035	1.025383	36	0.388395	1.036967
50				31	0.414859	1.019079	34	0.408983	1.026090	35	0.402940	1.037699
52				30	0.428159	1.009959	33	0.423859	1.027212	34	0.417408	1.038885
54							32	0.438656	1.028772	33	0.431800	1.040556
56							31	0.453390	1.030772	32	0.446132	1.042711
58							30	0.468076	1.033217	31	0.460407	1.045383
60										30	0.474634	1.048594

NOTE: $a=AB$—length of the driving link of first mechanism; $b=BC$—length of its connecting rod; $c=CD$—length of the driven link, $\Delta=b-a$ for the length of the support $d=AD=1$.

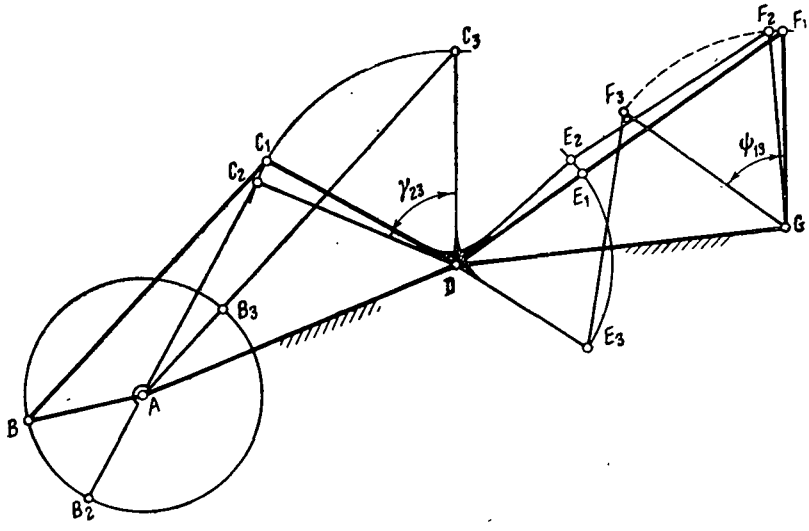

Fig. 3. AB_2C_2D and AB_3C_3D, illustrate the extreme positions of the driven link DC of the first four-link mechanism, while AB_1C_1D and AB_3C_3D—determine the extreme positions of the driven link GF of the six-link mechanism.

If the values $\Delta\gamma$ and ε were independent of each other, the minimization of the structural error $\Delta\psi_c$ under given conditions would have led to the minimization of values $\Delta\gamma$ and ε separately. However, values $\Delta\gamma$ and ε are functions of total angle of swing γ_{23} of the driven link of first mechanism, which simultaneously is the angle of swing of driving link of the second mechanism. This creates specific difficulties while finding out the parameters of six-link mechanisms with minimum values of structural error $\Delta\psi_c$ for the given values of φ_{00} and ψ_{13}.

Hence it is necessary to find out the solution of the above mentioned problem in two stages. In the first stage, a hinged six-link mechanism with the minimum structural error at selected constant value of the angle γ_{23} is found out. In this case, values $\Delta\gamma$ and ε, from formula (1) may be considered as independent. Thus the six-link mechanism with the minimum structural error $\Delta\psi_c$ will be the synthesis of two serially connected four-link mechanisms, in which the first one has the minimum value of angle of small swing $\Delta\gamma$ and the second has the minimum values of angular acceleration of the driven link ε in the extreme position.

The next stage of the problem involves finding the value of angle γ_{23} which will provide an absolute minimum value of the structural error $\Delta\psi_c$ for given values of φ_{00} and ψ_{13}.

For this sequence of solution, the problem involves determining a parameter of the first mechanism in the first stage which satisfy the following three conditions:

1) Angle of swing of the driven link γ_{23} must be equal to the given one;
2) Angle $\Delta\gamma$, for the given angle of rotation of driving link φ_{00} must be minimum;
3) Angle of transmission of the mechanism $\mu \geqslant \mu_0$.

A corresponding algorithm for synthesis of the first mechanism was developed according to these conditions, on a digital computer [3].

This analysis enables one to determine the parameters of mechanisms which satisfy the above mentioned conditions. During this, angle γ_{23} was varied in increments of 2° through the range 30° to 60° and angle of dwell φ_{00} was varied in increments of 10° through the range 20° to 180°.

Parameters of the synthesized mechanisms and the corresponding values of angles $\Delta\gamma$ are given in Tables 1 and 2.

It is interesting to note that minimum value of $\Delta\gamma$ for the given angles φ_{00} and γ_{23} was very often obtained in the region of large values of minimum angles of transmission μ.

With angle γ_{23} defined, the problem of synthesis of the second mechanism leads to the determination of parameters according to the following conditions [3, 4]:

1) In the first position of the mechanism, its driven link occupies the extreme position;

2) Angles of swing of the driven link must equal the given value of angle ψ_{13};

3) Corresponding angle of rotation of the driving link is equal to [2]:

$$\gamma'_{23}=\gamma_{23}-\Delta\gamma/2, \tag{2}$$

where γ_{23}—selected angle of total swing of the driven link of the first mechanism;

$\Delta\gamma$—minimum angle of small swing of the driven link of the first mechanism, corresponding to the rotation of its driving link on the dwell angle φ_{00} (see Fig. 1).

4) Angle of transmission of the mechanism must not be less than the value of μ_0, which is selected before hand.

The algorithm programmed, for a digital computer produced a table of parameters for the two mechanisms, which satisfy the above mentioned conditions. During this, angle was varied in increments of 2° through the range 30° to 60°, and the angle of swing of the driven link ψ_{13} was varied from 30° to 120° in steps of 10°.

Tables of parameters of the synthesized mechanisms are given in [3], where minimum values of ε at the extreme position of the driven link are also given.

While calculating first and second mechanisms their design limitations were taken into consideration. In designing the first mechanism, only those

Table 2. Parameters of synthesized mechanisms for values of Δ from 0.5 to 0.8

γ_{23}, deg	Δ=0.5			Δ=0.6			Δ=0.7			Δ=0.8		
	$\mu\Delta_{\gamma min}$, deg	a	c	$\mu\Delta_{\gamma min}$, deg	a	c	$\mu\Delta_{\gamma min}$, deg	a	c	$\mu\Delta_{\gamma min}$, deg	a	c
20	52	0.168650	1.054718	51	0.166428	1.065490	49	0.164672	1.088738	47	0.162413	1.110381
22	51	0.184484	1.048907	49	0.183318	1.077360	48	0.179981	1.083575	46	0.177458	1.105844
24	49	0.201362	1.058167	48	0.198830	1.072539	46	0.197026	1.101041	45	0.192295	1.101743
26	*48*	*0.216980*	*1.053536*	*47*	*0.214150*	*1.068109*	*45*	*0.212187*	*1.097353*	*44*	*0.206925*	*1.098107*
28	47	0.232407	1.049303	45	0.231248	1.083308	44	0.227157	1.094118	42	0.224486	1.123962
30	45	0.249402	1.061508	44	0.246402	1,080348	43	0.241954	1.091325	41	0.239110	1.122187
32	44	0.264691	1.058511	43	0.261419	1.077623	42	0.256581	1.089000	40	0.253574	1.120966
34	43	0.279824	1.055923	42	0.276276	1.075441	41	0.271049	1.087147	39	0.267904	1.120281
36	42	0.294810	1.053746	41	0.290988	1.073701	40	0.285364	1.085795	38	0.282107	1.120170
38	41	0.309650	1.051999	40	0.305554	1.072430	39	0.299546	1.084938	37	0.296201	1.120653
40	39	0.327064	1.069289	39	0.319988	1.071636	37	0.317887	1.112963	36	0.310170	1.121876
42	38	0.341890	1.068949	38	0.334302	1.071328	36	0.332201	1.114094	35	0.324087	1.123669
44	37	0.356603	1.069085	37	0.348509	1.071517	36	0.341383	1.085600	34	0.337923	1.126261
46	36	0.371213	1.069711	36	0.362611	1.072240	35	0.355115	1.087064	33	0.351719	1.129616
48	35	0.385736	1.070832	35	0.376635	1.073487	34	0.368811	1.089034			
50	34	0.400176	1.072478	34	0.390580	1.075315	33	0.382435	1.091744			
52	33	0.414545	1.074665	33	0.404444	1.077797	32	0.396024	1.095171			
54	33	0.424304	1.054474	32	0.418282	1.080852	31	0.409601	1.099345			
56	32	0.438275	1.057077	31	0.432081	1.084601						
58	30			30	0.445878	1.089017						
60	30	0.466100	1.064066	30	0.452450	1.062767						

NOTE: a, b, c and Δ are the same parameters as given in Table 1.

mechanisms were considered in which the difference between the length of the connecting rod and the length of the driving link was equal to or more than $0.2d$ (d—length of the stationary link).

During the design of the second mechanism, it was discovered that for similar conditions the value of ε approached its minimum value as the length of the driven link approached zero. This is the reason why mechanisms with absolute minimum value of ε were not investigated, and only those mechanisms with the minimum value of ε for which the length of the driven link was $c \geqslant 0.2d$ (where d—length of the stationary link of this mechanism [3]), were investigated.

This analysis established that for constant angle φ_{00}, minimum values of $\Delta\gamma$ monotonically increased with the increase of intermediate angle γ_{23}. Minimum values of the angular acceleration ε of the driven link of the second mechanism in its extreme position monotonically decrease with the increase of the angle γ_{23}. If value of the structural error is determined by equation (1), it may be presumed that the graph of error $\Delta\psi_c$ as a function of angle of swing γ_{23} will have the extreme point at a few intermediate values of this angle. Results have confirmed this hypothesis.

Graphs of optimum values of the intermediate angle γ_{23} as a function of the angle of the dwell φ_{00} are given in Fig. 4. It is clear from the graph that intermediate angle of swing γ_{23} increases with an increase of the angle of dwell φ_{00}, but in all cases this optimum angle does not exceed the limits of $\gamma_{23}=48°$-$60°$.

Graphs of the value of structural error $\Delta\psi_c$ as a function of the angle of swing ψ_{13} of the driven link of the six-link mechanism are given in Fig. 5. For different angles of the dwell φ_{00} for the case, when, the difference between the length of connecting rod, b, and the length of the driving link, a, in first mechanism is equal to $\Delta=0.4d$. The structural error $\Delta\psi_c$ considerably increases with an increase in the value of Δ.

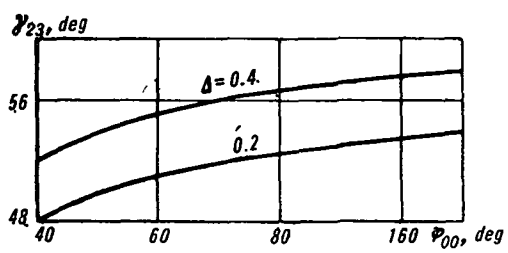

Fig. 4. Graphs, showing those values of the angle γ, at which structural error $\Delta\varphi_c$ is minimum for the given value of the angle of the dwell φ_{00}. Here, $\Delta=b-a$ is a design variable and it is the difference between the lengths of the connecting rod $b=BC$ (see Fig. 1) and of the driving link $a=AB$ in the first mechanism. These graphs are also true for the second mechanism where the driving and driven links rotate in different directions and at the dead center position, the connecting rod is the continuation of the driving link.

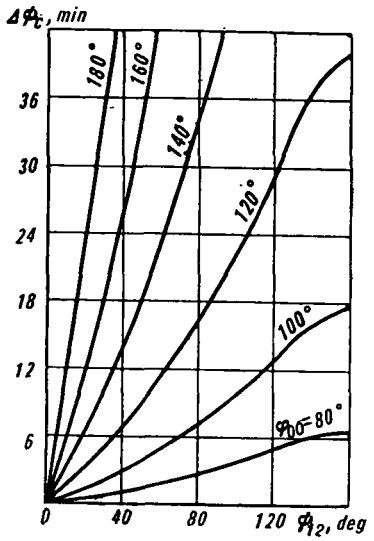

Fig. 5. Graphs of structural deviations $\Delta\psi_c$ as a function of the angle of swing of the driven link of the six-bar mechanism at different angles of the dwell $\varphi_{00}(\Delta=b-a=0.4;\ \mu_{min}=40°)$.

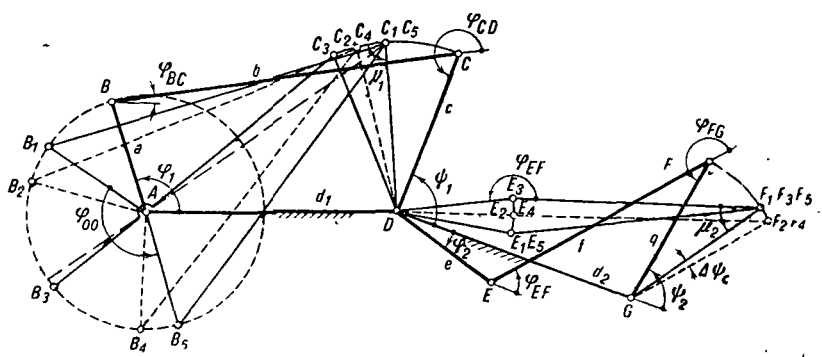

Fig. 6. Diagram of the six-link mechanism with the designations of angles which determine positions of the links.

Let us now consider the problem of the technical errors of position of the six-link mechanism (shown in the Fig. 1) at the dwell position of its driven link. In contrast to Reference [5], errors in the lengths of the links and the presence of small gaps in the kinematic pairs will be considered simultaneously, i.e. we consider the whole complex of the basically effective primary errors which are characteristic of the hinged mechanism.

Similar simultaneous solutions of the problems, connected with geometrical and precision analysis, make it possible to explain the extent to

which it is possible to deviate, during kinematic synthesis, from optimal design conditions, taking into account manufacturing tolerances. This is quite important during the design process, when it becomes necessary to depart from the optimum dimensions of the mechanism.

In this way, the overall index of accuracy of the mechanism will be determined by the structural and technical components.

In order to simplify subsequent calculations connected with the accuracy of six-link mechanism, let us assume that (Fig. 6):

$$AB=a;\quad BC=b;\quad CD=c,\quad AD=d_1;$$
$$DE=e;\quad EF=f;\quad FG=q;\quad DG=d_2,^{1}$$

where φ_1—angle determining the position of the driving link of the first mechanism;

φ_{BC}—angle of inclination of the connecting rod of the first mechanism;

ψ_1—angle of position of the driven link of second mechanism;

ψ_2—angle of position of the driving link of the second mechanism; these three angles are measured from the direction of the stationary link AD;

φ_{EF}—angle of inclination of the connecting rod of the second mechanism;

ψ_2—angle of position of the driven link of the second mechanism; these two angles are measured from the direction of the stationary link DG;

$\Delta\varphi_1$—error of position of the driving link of the first mechanism;

$\Delta\varphi_2$—error of position of the driving link of the second mechanism;

$\Delta\psi_1'$—error of position of the driven link of the first mechanism due to errors in the lengths of its links;

$\Delta\psi_2'$—error of position of the driven link of the second mechanism due to the errors in the lengths of its links;

$\Delta\psi'$—error of position of the six-link mechanism due to errors of the lengths of its links;

ψ_0—angle of position of the driven link of the ideal mechanism;

ψ_0'—angle determining the position of the driven link of the mechanism, which has ideal dimensions of all its links and has some difference in its diagram from the theoretical one; Δa, Δb, Δc, Δe, Δf, Δq and Δd are primary errors in the dimensions of the lengths of the corresponding links of the mechanism; Δ_A, Δ_B, Δ_C, Δ_D, Δ_E, Δ_F and Δ_G are the corresponding plays in the hinges A, B, C, D, E, F and G.

[1] For the case under consideration $d_1=d_2=d$.

$\Delta\psi_1''$—error of position of the driven link of the first mechanism due to plays in the pairs;

$\Delta\psi_2''$—error of position of the driven link of the second mechanism due to plays in the pairs;

$\Delta\psi''$—error of position of the driven link of the six-link mechanism due to play in the couples;

$\alpha_{AB},\ldots,$—angles of directions, along which displacements in the vicinity of gaps of elements of the kinematic pairs take place.

According to (6), equations for determining the accuracy of the hinge joint having error in the lengths of the links and plays in the kinematic pairs have the following forms:

$$\Delta\psi=\psi_0'-\psi_0+\sum_s(\partial\psi/\partial q_s)_0\Delta q_s+\sum_k(\partial\psi/\partial q_{uk})_0\Delta_{uk}, \tag{3}$$

where Δq_s—primary errors in the lengths of the links of the mechanism;

Δ_{uk}—errors which characterize the gaps in the kinematic pairs.

During a study of a set of mechanisms manufactured according to the same design for equation (3) a probabilistic statement is required to which under the conditions of statistical independence of all the primary errors Δq_s and Δ_{uk}, we have:

$$M[\Delta\psi]=\psi_0'-\psi_0+M\left[\sum_s(\partial\psi/\partial q_s)_0\Delta q_s\right]+M\left[\sum_k(\partial\psi/\partial q_{uk})_0\Delta_{uk}\right]; \tag{4}$$

$$\sigma^2[\Delta\psi]=\sigma^2\left[\sum_s(\partial\psi/\partial q_s)_0\Delta q_s\right]+\sigma^2\left[\sum_k(\partial\psi/\partial q_{uk})_0\Delta_{uk}\right], \tag{5}$$

where M and σ^2 are symbols for expected value and variance respectively.

While investigating the accuracy of the six-link mechanism, let us attribute the error of position of its driving link to the error of the drive, i.e. in the case under consideration, it is equal to zero and the error of position of the driven link of the first mechanism is equal to the error of position of the driving link of second mechanism, then:

$$\Delta\psi_1=\Delta\varphi_2.$$

Considering the above statement and on the basis of equation (3), we obtain the following expressions which determine the errors of the position of the mechanism due to the presence of errors in the lengths in its kinematic chain and due to plays in the kinematic pairs respectively:

$$\Delta\psi'=1/(q\sin\mu_2)\cdot[\cos\mu_2\Delta q+\cos\varphi_{EF}\Delta d-\cos\alpha_2\Delta e-\Delta f]+$$
$$e\sin d_2/(c\sin\mu_1)[(\cos\mu_1\Delta c+\cos\varphi_{BC}\Delta d-\Delta b-\cos\alpha_1\Delta a)]; \tag{6}$$

$$\Delta\psi''=1/(q\cdot\sin\mu_2)\cdot[-\cos\alpha_{FE}\Delta_E-\cos\alpha_{EF}\Delta_F+\cos\alpha_{GF}\Delta_G+ e\cdot\sin\alpha_2/(c\cdot\sin\mu_1)(-\cos\alpha_{CB}\Delta_B-\cos\alpha_{BC}\cdot\Delta_C+\cos\alpha_D\Delta_D)], \quad (7)$$

where $\mu_1=\psi_1-\varphi_{BC}$ and $\mu_2=\psi_2-\varphi_{EF}$.

The mechanism under consideration is designed for providing the dwell, specified by the operating conditions of the automat. That is why it is useful to carry out the calculation of the accuracy of the mechanism proceeding from its working conditions, i.e. for the angle of rotation of the driving link φ_{00}.

In this case, value of α_2 is very small, and because of this second order term in the equation (6) and (7) it becomes negligible, and we get:

$$\Delta\psi'\approx 1/(q\cdot\sin\mu_2)\cdot(\cos\mu_2\Delta q+\cos\alpha_{EF}\Delta d-\cos\alpha_2\Delta e-\Delta f); \quad (8)$$

$$\Delta\psi''\approx 1/(q\cdot\sin\mu_2)\cdot(-\cos\alpha_{FE}\Delta_E-\cos\alpha_{EF}\Delta_F+\cos\alpha_{GF}\Delta_G). \quad (9)$$

For the case of investigation of the accuracy of a set of similar mechanisms, equations (8) and (9) can be transformed in the following form, taking into consideration equations (4) and (5)

$$M[\Delta\psi']=1/(q\cdot\sin\mu_2)\cdot(\cos\mu_2 M[\Delta q]+\cos\varphi_{EF}M[\Delta d]-\cos\alpha_2 M[\Delta e]-M[\Delta f]; \quad (10)$$

$$\sigma^2[\Delta\psi']=1/(q\cdot\sin\mu_2)^2\cdot(\cos^2\mu_2\sigma^2[\Delta q]+\cos\varphi_{EF}\sigma^2[\Delta d]+\cos^2\alpha_2\sigma^2[\Delta e]+\sigma^2[\Delta f]); \quad (11)$$

$$M[\Delta\psi'']=1/(q\cdot\sin\mu_2)\cdot(-\cos\alpha_{FE}M[\Delta_E]-\cos\alpha_{EF}M[\Delta_F]-\cos\alpha_{GF}M[\Delta_G]); \quad (12)$$

$$\sigma^2[\Delta\psi'']=1/(q\cdot\sin\mu_2)^2\cdot(\cos^2\alpha_{FE}\sigma^2[\Delta_E]+\cos^2\alpha_{EF}\sigma^2[\Delta_F]+\cos^2\alpha_{GF}\sigma^2[\Delta_G]). \quad (13)$$

In the general case, when the distribution of primary errors differs substantially from the normal, the expected value and variance, contained in the equations (10)-(13) are connected with the quantities which characterize the tolerance field, with the help of the following equations [7]:

$$M[\Delta q_s]=\Delta_{0,s}+\alpha_s\delta_s; \quad (14)$$

$$\sigma^2[\Delta q_s]=1/9k_s^2\delta_s^2, \quad (15)$$

where $\Delta_{0,s}$—distance from the center of the tolerance field up to the nominal dimension;
α_s—coefficient of relative asymmetry;
k_s—coefficient of relative dispersion;
δ_s—half of the tolerance field.

Where the different elements of kinematic pairs of the six-link mechanism are manufactured through the same process, we shall assume that all primary errors are distributed, according to the Gauss's law, i.e. symmetrically distributed with respect to the mean error.

In this case, according to equation (14) and (15), we have:

a) For primary errors in the lengths of the links,

$$M[\Delta q_s]=0;\ \sigma^2[\Delta q_s]=\delta_s^2/9; \tag{16}$$

b) For primary errors, which lead to play (in the joints)

$$M[\Delta_{0,uk}]=M[\Delta^0_{0,u}]-M[\Delta^b_{0,k}],\ \sigma^2[\Delta_{0,uk}]=[(\delta^0_u)^2+(\delta^b_k)^2]/9, \tag{17}$$

where, $\Delta^0_{0,u}$; $\Delta^b_{0,k}$; δ^0_u; δ^b_k are respectively coordinates of the centers of the tolerance field and half of the tolerances for the female and male elements of the kinematic pair (here, tolerance of the female element is on the positive side and tolerance of the male element is on the negative side).

Considering equations (16) and (17) the equations (10) to (13) can be written in the following way:

$$M[\Delta\psi']=0; \tag{18}$$

$$9\sigma^2[\Delta\psi']=1/(q\cdot\sin\mu_2)^2\cdot(\cos^2\mu_2\delta^2_{\Delta q}+\cos^2\varphi_{EF}\delta^2_{\Delta d}+\cos^2\alpha_2\delta^2_{\Delta e}+\delta^2_{\Delta f}); \tag{19}$$

$$M[\Delta\psi'']=1/(q\cdot\sin\mu_2)\cdot\{-\cos\alpha_{FE}(M[\Delta^0_E]-M[\Delta^b_E])-\cos\alpha_{EF}(M[\Delta^0_F]-M[\Delta^b_F]-\cos\alpha_{GF}(M[\Delta^0_G]-M[\Delta^b_G]\}; \tag{20}$$

$$9\sigma^2[\Delta\psi'']=1/(q\cdot\sin\mu_2)^2\cdot\{\cos^2\alpha_{EF}[(\delta^0_E)^2+(\delta^0_E)^2]+\cos^2\alpha_{FE}[(\delta^0_F)^2+\delta^b_F)^2]+\cos^2\alpha_{GF}[(\delta^0_G)^2+(\delta^b_G)^2]\}. \tag{21}$$

On the basis of equations (1) and (18) to (21), the equation for the practical limiting errors of the position of a set of mechanisms is:

$$\Delta\psi_{P.L.}=|\Delta\psi_c+M[\Delta\psi'']|+3\sqrt{\sigma^2[\Delta\psi']+\sigma^2[\Delta\psi'']}\,. \tag{22}$$

Values of the practical limiting errors of position can be calculated according to equation (22), for a set of six-link hinged mechanisms for the entire range of the variation of angle φ_{00}, and a zone has been defined which characterizes the precision capabilities of the mechanisms. Within this zone, we carry out a comparison of the deviations in the value of angle φ_{00} due to manufacturing errors in the links of the mechanisms, with the deviations which are determined by its kinematic diagrams.

A similar comparison will provide the criteria for correctly formulating the general conditions of kinematic synthesis of the mechanism taking into account manufacturing errors.

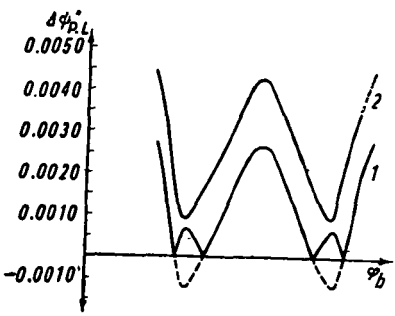

Fig. 7. Graphs of the functional relationship of practical limiting error of position of a set of mechanisms ($\psi_{12}=70°$; $\varphi_{00}=100°$): 1—($\Delta\psi°_{P.L.}$) *II class*; 2—($\Delta\psi°_{P.L.}$) *III class*.

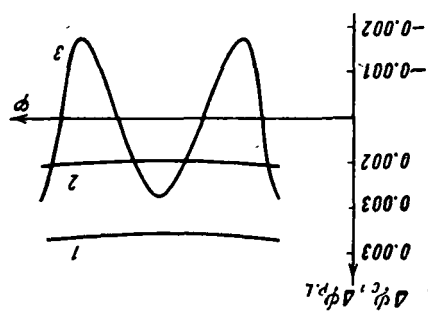

Fig. 8. Graphs of the structural and technical components of practical limiting error of position ($\psi_{12}=70°$; $\varphi_{00}=100°$): 1—($\Delta\psi_{P.L.}$) *III class*; 2—($\Delta\psi_{P.L.}$) *II class*; 3—$\Delta\psi_c$.

For example, if deviations due to production errors are significantly larger than the deviations determined by the kinematic diagram of the mechanism, then while designing the mechanism, special attention must be paid to the selection of tolerance limits while selecting the technological process of manufacturing the mechanism. And similarly in the reverse case, when deviations determined by the kinematic diagram of the mechanism considerably surpass the deviations resulting from the production errors, then design must lead to the correct selection of the diagram, i.e. for improving the diagram, which is based on the solution of the problem of kinematic synthesis.

From the above statement, it follows that it is more expeditious to design the mechanism, in general, in such a way that basic components of the practical limiting error (22) must be values of first order in the whole of the interval in which the independent variable changes its value.

Note one more important factor observed in the specific conditions of working of the mechanism under consideration at the dwell of the driven link, where high accuracy of the mechanism is required. Technological errors of the first bar mechanism have negligible effect on the error of position of the mechanism. In case when it is necessary to reduce the value of the practical limiting error of position, it is advisable to accomplish this by decreasing the tolerance for the connected second four-link mechanism alone.

The above stated facts allow us to make the following general conclusions: on the basis of equation (22), it is possible to compare the accuracy of the structural and technical components of the total error of position and thus to find out for the mechanism a rational relationship of these components during its design which is obtained proceeding from the requirements

of the synthesis on the one hand and from the effectiveness of the design of the mechanism on the other hand.

As an example, to illustrate the above mentioned points of precision analysis, consider a six bar mechanism with the intermediate angle of swing $\gamma_{23}=40°$ and the minimum angle of transmission $\mu=40°$. Parameters of the mechanism are:

$$a=0.32922\,; \quad b=0.72922\,; \quad c=1.03844; \quad d=1\,;$$

$$e=0.67694\,; \quad f=0.48332 \quad \text{and} \quad q=0.45886.$$

Angle of swing of the driven link of the mechanism $\psi_{13}=-60°$.

An investigation was carried out at angles of dwell equal to $\varphi_{00}=60°$, 80°, 100°, 120°, 140°, 160° and 180°. In accordance with Fig. 2, at angle of dwell φ_{00}, function $\psi=F(\varphi)$ uniformly approaches some constant value and has five extreme deviations (points e_0, e_1, e_2, e_1', and e_0').

Calculation of accuracy was carried out for the same five positions of the mechanism.

Tolerances on the distances between the axes of kinematic pairs were selected according to 2nd and 3rd class of accuracy (GOST. 1021, 1022 and 1023) and tolerance on the clearances (OST. 1012, 1042, 1044, 1022, 1069, 1013 and 1023) corresponding to the sliding fit for nominal value of the diameter, equal to 12 mm.

Characteristic results of the calculations, carried out according to equation (22), are given in the form of graphs in Fig. 7. Different components of the total (practical limiting) error: structural $\Delta\psi_c$ and technological $\Delta\psi_T$ are shown in Fig. 8.

Since values of errors $\Delta\psi_c$ and $\Delta\psi_T$ have the same order, then it may be assumed that mechanism is of satisfactory design according to the selected criteria of accuracy.

References

1. Cherkudinov, S. A. Sharnirno-rychazhnye mekhanizmy moshchnykh vytyazhnykh pressov (Hinged-lever Mechanisms of Power Presses). 2. Sbornik *Avtomatizatsiya mashinostroitel'nykh protsessov*, Izd-vo AN SSSR, 1959.
2. Cherkudinov, S. A., L. B. Maisyuk, I. G. Oleinik, M. K. Uskov and N. V. Speranskii. Sostavlenie spravochnykh kart po sintezu mekhanizmov mashin-avtomatov s ispol'zovaniem EVTsM (Compilation of Reference Charts for Synthesis of Mechanisms of Automatic Machines

Using Digital Computer). Sbornik *Analiz i sintez mekhanizmov.* Mashgiz, 1963.

3. Cherkudinov, S. A., N. V. Speranskii and N. G. Oleinik. K sintezu sharnirnogo shestizvennogo mekhanizma s ostanovkoi (Synthesis of Hinged Six-link Mechanism with Stop). Sbornik *Analiz i sintez mashin-avtomatov.* Izd-vo Nauka, 1964.
4. Oleinik, I. G. K sintezu sharnirnogo chetyrekhzvennika, u kotorogo odno iz polozhenii dolzhno byt' mertvym (Synthesis of Hinged Four-link Mechanisms in which One of the Positions should be "Dead"). Sbornik *Analiz i sintez mashin-avtomatov.* Izd-vo Nauka, 1964.
5. Sergeev, V. I. and M. K. Uskov. Sravnitel'nyi analiz strukturnykh i tekhnologicheskikh oshibok v peredatochnykh sharnirnykh mekhanizmakh (Comparative Analysis of Structural and Technological Errors in Hinged Transmission Mechanisms). Sbornik *Mekhanika Mashin,* vyp. 4. Izd-vo Nauka, 1966.
6. Bruevich, N. G. Tochnost' mekhanizmov (Accuracy of Mechanisms). Moscow-Leningrad, GITTL, 1946.
7. Borodachev, N. A. Obosnovanie rascheta dopuskov i oshibok razmernykh i kinematicheskikh tsepei (Basis for the Calculation of Tolerances and Errors of Dimensional and Kinematic Chains). Izd-vo AN SSSR, 1943.

P. V. Sergeev

FUNDAMENTALS OF THE THEORY OF DYNAMIC SYNTHESIS OF CAM MECHANISMS

One of the fields of development of synthesis of cam mechanisms is the processing of methods of determination of design parameters of diagrams of mechanisms according to given conditions.

At the same time it is assumed that the law of transformation of motion is known and the diagram and conditions, which must be satisfied by the parameters have been determined in accordance with the specifications of the mechanism being designed.[1]

Since we know that in the theory of machines and mechanisms such a problem is usually termed as one of dynamic synthesis of cam mechanisms, because the conditions under which synthsis is carried out are known as dynamic conditions.

Limitations on pressure angle, curvature of the profile, contact stresses in higher pair, wear out of the profile etc. are termed as dynamic conditions.

Depending on the requirements to be fulfilled by the mechanism, dynamic synthesis is carried out for one condition and also for a complex of dynamic conditions. Various scientific investigations have been devoted to solving problems of dynamic synthesis of cam mechanisms of which the following may be given special mention. The work of N. G. Bruevich, V. V. Dobrovol'skii, V. T. Kostitsin, N. I. Levitskii, L. N. Reshetov, L. P. Riftin, K. V. Tir and of V. A. Yudin.

In addition there is no general theoretical method in the theory of machines and mechanisms that can combine all the existing methods of solving the problems of dynamic synthesis of cam mechanisms. In fact, in a number of cases, there is no direct method for solving these problems.

Levitskii, N. I. Razvitie sinteza mekhanizmov (Development of synthesis of mechanisms). *Vestnik-AN SSSR*, No. 2, 1962.

A study of the different correlations of the given problem reveals that there is a possibility of finding general methods which can form the basis of the theory of dynamic synthesis of cam mechanisms. It is not difficult to be convinced of this if we reveal the mathematical aspects of the solution of typical problems of dynamic synthesis.

The effect of pressure angle ϑ on the working capacities of the cam mechanism is known. With an increase in the value of this angle, pressure and friction forces increase very sharply in the support of the driven link, which results in a decrease of efficiency and, at certain critical values of pressure angle, in a possible jamming of the mechanism.

In order to create favorable conditions for the transmission of forces and eliminate jamming of the mechanism, design parameters of the cam mechanism are determined from the conditions of limiting values of the pressure angle.

Effect of the design parameters on the pressure angle in the cam mechanism with the rocker follower is shown in Fig. 1, from where it is clear that at the ratio $l/l_0=0.6$, maximum values of the pressure angle in both intervals of motion coincide with the imposed limitation, equal to 45° ($\psi_0=\text{const}$).

In the design of cam mechanisms with roller followers, it is equally important, to prevent the possibility of undercutting and sharpening of the working profile. To create this condition, design parameters are so selected

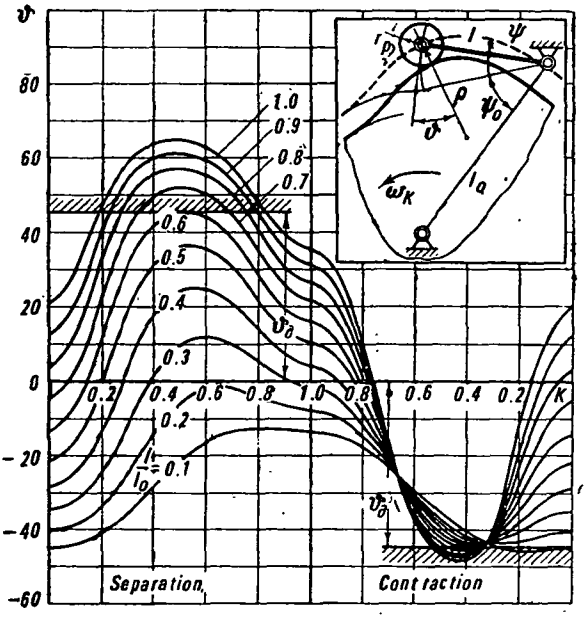

Fig. 1.

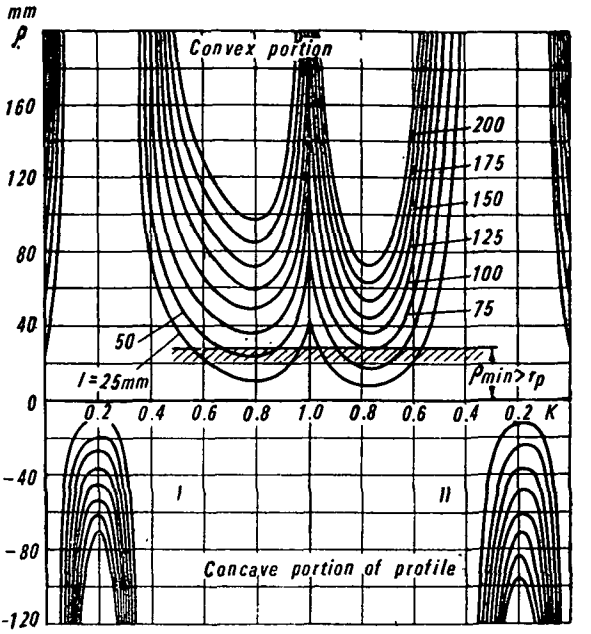
mm
ρ
Convex portion
160
120
80
40
0
-40
-80
-120
200
175
150
125
100
75
50
l=25mm
ρmin>rp
0.2 0.4 0.6 0.8 1.0 0.8 0.6 0.4 0.2 K
I
II
Concave portion of profile

Fig. 2.

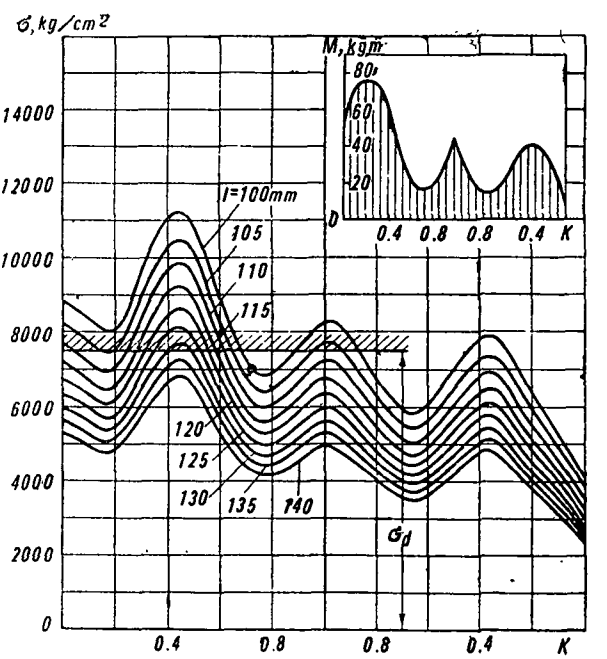
σ, kg/cm²
M, kg m
80
60
40
20
0
0.4 0.8 0.8 0.4 K
14000
12000
10000
8000
6000
4000
2000
0
l=100mm
105
110
115
120
125
130
135
140
σd
0.4 0.8 0.8 0.4 K

Fig. 3.

that the minimum radius of curvature ρ_{min} of the pitch curve of the cam at its convex portion must be more than the radius of the roller r_r (see Fig. 2, where $\psi_0=\text{const}$; II—$l/l_0=\text{const}$).

In this way, limitations are imposed on the maximum curvature of the concave portion of the pitch surface.

To prevent the occurrence and development of the fatigue failure of the elements of the higher pair, design parameters of a cam mechanism are selected from the limiting condition of contact stresses σ, which is fixed by taking into consideration the working life of the mechanism.

In Fig. 3 is shown ($\psi_0=\text{const}$; $l/l_0=\text{const}$) the effect of one of the design dimensions l on the contact stresses in the kinematic pair for the mechanism with rocker follower having a roller at its end.

A similar problem arises in the case of the design of a cam mechanism for limiting permissible wear of the profile.

The above mentioned discussions and analysis of the diagram confirm the fact that the solution of the problem of dynamic synthesis always leads to the determination of design parameters of the cam mechanism for which extreme values and limitations for the given dynamic conditions will coincide.

On the basis of this it may be determined that the problem of dynamic synthesis of cam mechanisms for any limitations is the problem of synthesis of parameters of functions at their extreme points, which may be considered similar to the classical problem of analysis of function for its extreme values. As, in general case, the problem under consideration is interesting not only for mechanisms with single degree of freedom, but also for cam mechanisms with two degrees of freedom of the conoid type. Thus the problem of synthesis of parameters of function as per their extreme points is formulated in the following manner:

Some function of variables x, y with parameter c is given:

$$z=F(x, y, c),$$

and it is required to find such value of the parameters c^*, at which function $F(x, y, c^*)$ should have the required extreme value z^*.

For solving a problem of this type, it is necessary to use an "auxiliary" function[2], whose characteristic is given in the following theorem.

Theorem: Let us have a differentiable function of variables x, y with parameter c,

$$z=F(x, y, c),$$

whose extreme value z^* is known. If this function is solvable with respect to the parameter, then the "auxiliary" function may be formed (by solving the original expression with respect to c)

[2] The first use of "auxiliary" function is seen in the papers of E. M. Gut'yar and A. G. Ovakimov.

$$c=f(x, y, z^*),$$

whose extreme value is equal to the value of parameter c^*, at which original function $F(x, y, c^*)$ has the given value of extreme z^*.

Proof.

If in the equation,

$$z=F(x, y, c), \tag{1}$$

the value of z is fixed and is equal to z^*, we get the equation of surface:

$$z^*=F(x, y, c). \tag{2}$$

Function c, given by the expression (2) is implicit, and will attain the extreme value c^* at certain values of $x=x^*$ and $y=y^*$ which satisfy the conditions:

$$\begin{aligned} &\partial c/\partial x=-\partial F/\partial x:\partial F/\partial c=0, \\ \text{and} \quad &\partial c/\partial y=-\partial F/\partial y:\partial F/\partial c=0, \end{aligned} \tag{3}$$

from where,

$$\begin{aligned} &\partial F(x^*, y^*, c^*)/\partial x=0, \\ &\partial F(x^*, y^*, c^*)/\partial y=0. \end{aligned} \tag{4}$$

At the same time, it is necessary that the condition, given below is also fulfilled:

$$\Delta=\left|\begin{matrix} \partial^2F/\partial x^2 & \partial^2F/\partial x\,\partial y \\ \partial^2F/\partial x\,\partial y & \partial^2F/\partial y^2 \end{matrix}\right|_{\substack{x=x^* \\ y=y^*}}>0. \tag{5}$$

If c is fixed in the expression (1), and put equal to the extreme value of function (2) c^*, we get the equation of the surface:

$$z=F(x, y, c^*). \tag{6}$$

Function (6) will attain its extreme values at x and y which satisfy the condition:

$$\begin{aligned} &\partial z/\partial x=\partial F/\partial x=0; \\ &\partial z/\partial y=\partial F/\partial y=0, \end{aligned} \tag{7}$$

from where,

$$\begin{aligned} &\partial F(x, y, c^*)/\partial x=0; \\ &\partial F(x, y, c^*)/\partial y=0. \end{aligned} \tag{8}$$

From a comparison of the equations (8) and (4), it follows that their roots will be similar, i.e. $x=x^*$ and $y=y^*$. As in the case of expression (5), determinant will also be more than 0.

In this way, extreme value of function (6), determined by taking $c=c^*$, coincides with the value z^* of the expression (2), by extreme value of whose quantity c^* was determined.

Inference. Quantities x^*, y^*, z^* and c^*, which determine the extreme points of original and "auxiliary" functions, coincide. It is not difficult to prove that the above considered theorem is also true for the parametric assignment of the function of two variables.

Utilizing the geometric proof of the formulated theorem for the function of one variable, the geometrical relationship between the original and "auxiliary" function may be shown.

In fact if its surface $y=F(x, c)$, shown in Fig. 4 is intersected by two mutually perpendicular planes $y=y^*$ and $c=c^*$ where y^* and c^* are selected in such a way that line of intersection of these planes touches the surface $F(x, c)$ at some point K, then equations of the lines of intersection of the surface with planes will have the form $y^*=F(x, c)$ and $y=F(x, c^*)$ respectively. The line of intersection of planes $y=y^*$ and $c=c^*$ touches the above mentioned curves in the common point K with coordinates x^*, y^* and c^*, where these coordinates determine the extremes of the original function $y=F(x, c^*)$ and extremes of the "auxiliary" function $y^*=F(x, c)$ written in the implicit form.

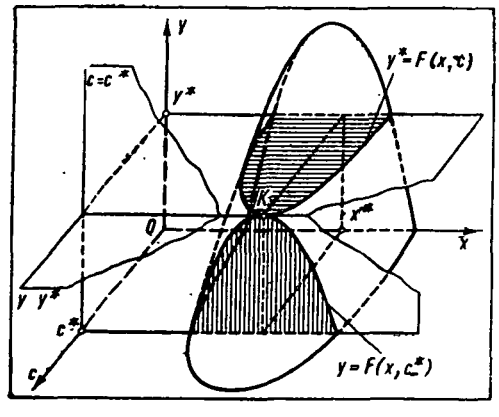

Fig. 4.

In this way, determination of the parameter of the original function from the given value of its extreme leads to the calculation of extreme value of the "auxiliary" function.

As has been demonstrated design parameters of different types of cam mechanisms with followers, having rollers at the ends and with the following limitations on the extremes, can be synthesized by the above method:

1) limitation on the pressure angle ϑ_p:

$$c_\vartheta = f_\vartheta(k, \vartheta_p),$$

where k—dimensionless time;

2) limitation on the pressure angle ϑ_p and on the permissible curvature of the profile ρ_p:

$$c_\vartheta = f_\vartheta(k, \vartheta_p); \qquad c_\rho = f_\rho(k, \rho_p);$$

3) limitation on the pressure angle ϑ_p and on the permissible contact stresses in the higher pair σ_p:

$$c_\vartheta = f_\vartheta(k, \vartheta_p); \qquad c_\sigma = f_\sigma(k, \sigma_p);$$

4) limitation on the pressure angle ϑ_p and on the permissible wear of the profile of the cam Δ_p:

$$c_\vartheta = f_\vartheta(k, \vartheta_p); \qquad c_\Delta = f_\Delta(k, \Delta_p);$$

5) limitation on the pressure angle ϑ_p and on the permissible contact stresses in the higher pair σ_p and on the permissible wear of the profile of the cam Δ_p:

$$c_\vartheta = f_\vartheta(k, \vartheta_p); \qquad c_\sigma = f_\sigma(k, \sigma_p); \qquad c_\Delta = f_\Delta(k, \Delta_p).$$

For mechanisms with flat followers, the problem of dynamic synthesis is similarly solved with the help of "auxiliary" functions.

In that case, when synthesis of the mechanism is carried out for one dynamic condition, design parameter or the parametric complex is determined from the extreme value of one auxiliary function. If the synthesis is carried out for a complex of dynamic conditions, then the complex of design parameters may be determined by solving the system of auxiliary functions.

The approach for solving the problem of dynamic synthesis, independent of the conditions, for which the design is carried out, is common for any design diagrams of plane and spatial cam mechanisms with one and two degrees of freedom.

Practical application of this method, permits solution of many problems of synthesis, for which there was no direct method of solution in the past.

A. V. Sinev, I. Z. Brodotskaya and *I. S. Charnaya*

KINEMATIC AND FORCE ANALYSIS OF SPATIAL MECHANISM OF PNEUMATIC AND HYDRAULIC DRIVE FOR STOPCOCKS OF GAS MAINS OF TYPE DU 1000

The construction of big pipe lines in the USSR like Bukhara-Ural and Central Asia-Center etc., with diameters of 1000-1200 mm, has necessitated the development of powerful drives to control the stopcocks fitted on the Se gas pipe lines.

A torque of about $6 \cdot 10^6$ kg · cm is necessary to turn the plug of a spherical valve with conditional passage of DU 1000 at a pressure of gas equal to 64 kg/cm^2.

However, for creating such moment with plane mechanisms, the dimensions become too large and thus a compact spatial mechanism of pneumatic hydraulic drive was devised.

The problem under investigation is the determination of forces occurring in the mechanism, taking into account friction, since the forces of friction might become so large in the kinematic pairs that the mechanism would not produce the required torque or would become jammed.

To determine forces, the position of links of the mechanism in space in different working positions must be known, which is determined by kinematic analysis.

A simplified diagram of the mechanism of the pneumatic and hydraulic drive is shown in Fig. 1. The drive contains the following links:

1) Piston *1* has reciprocating motion along the guides inside the cylinder;

2) Rotor *3*, rotating around the vertical axis;

3) Two tie rods *2*;

4) Bearings *4* in pairs, each on the piston and on the rotor;

5) Bearing bushes *5* in pairs, each on the piston and rotor.

Bearing bush and bearing are two mutually perpendicular cylinders.

Tie rod *2* is connected with the bearing *4* by screw joint and turns inside the thread.

In this way, the bush-bearing unit provides the rotation of the tie rod around three axes: axes of the bearing, of the bushing and around the longitudinal axis of the tie rod. During the opening of the valve, the piston moves up under pressure of the oil that enters the cylinder on the lower side of the piston from a special reservoir. Oil is fed by the pressure of the gas which is being transported in the pipe line. During this the rotor rotates which in turn rotates the plug of the valve connected to it by 90°. During the down stroke of the piston, pressure of the gas is formed in the upper portion of the cylinder and the motion of the plug is brought about in the reverse direction.

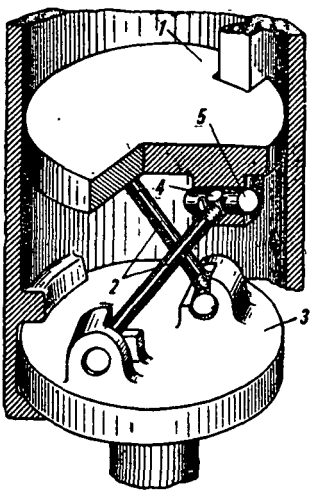

Fig. 1. Diagram of the mechanism of pneumatic and hydraulic drive: 1—*Piston;* 2—*Tie rod;* 3—*Rotor;* 4—*Bearings;* 5—*Bearing bush.*

1. Kinematic Analysis

The method of finite screw displacements is utilized [1-3] for the kinematic analysis. Let us select the initial position of the mechanism, in which axes of the connecting rods are parallel to the axis of the cylinder. As origin of the coordinates, let us take the point of intersection of the axis of the cylinder with the surface that passes through the point of the intersection of axes of hinges. Let us represent the axes by the in-pair-orthogonal vectors (unit vector) e_1, e_2 and e_3. Unit vector e_1 is directed along the axis of the cylinder, e_2 is parallel to the axis of the bearing *4* on the rotor and e_3 is along the axis of the bushing *5* on the rotor in the initial position of the mechanism. Axes of bearings, bushings and connecting rod are symbolically expressed by the unit vectors E_1, E_2, E_3, E_4, E_5 (Fig. 2,a).

By means of subsequent rotations and screw displacements let us bring all the links in position corresponding to any working position of the mechanism. Let us express all the vectors in terms of the unit vectors of the basic system of coordinates e_1, e_2, e_3 in the form of complex vectors.

$$\mathbf{E}_1=\mathbf{e}_1-\omega r(\mathbf{e}_2\cos\alpha_0-\mathbf{e}_3\sin\alpha_0);$$

$$\mathbf{E}_2=\mathbf{e}_2+\omega r\cos\alpha_0\,\mathbf{e}_1;\quad \mathbf{E}_3=\mathbf{e}_3-\omega r\sin\alpha_0\,\mathbf{e}_1;$$

$$\mathbf{E}_4=\mathbf{e}_3\sin 2\alpha_0-\mathbf{e}_2\cos 2\alpha_0-\omega r\mathbf{e}_1\cos\alpha_0-\omega l(\mathbf{e}_2\sin 2\alpha_0+\mathbf{e}_3\cos 2\alpha_0);$$

$$\mathbf{E}_5=\mathbf{e}_2\sin 2\alpha_0+\mathbf{e}_3\cos 2\alpha_0+\omega r\mathbf{e}_1\sin\alpha_0+\omega l_0(\mathbf{e}_3\sin 2\alpha_0-\mathbf{e}_2\cos 2\alpha_0),$$

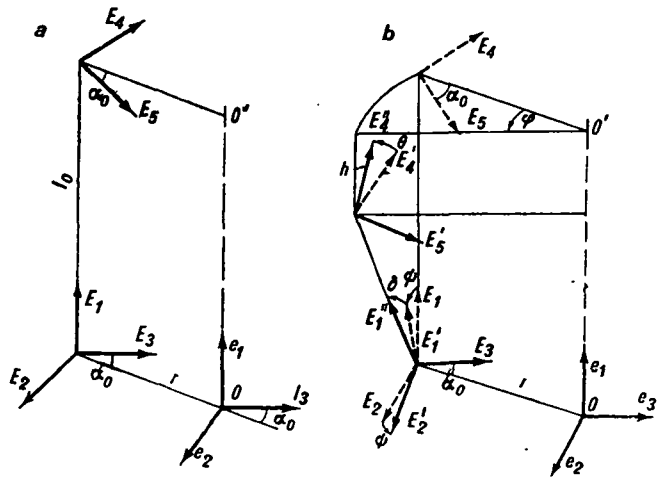

Fig. 2. Locations of vector at the initial moment (*a*) and in the working position of the mechanism (*b*):
E—vector of tie rod; E_r—vector of the bearing of the rotor; E_3—vector of the bushing of the rotor; E_4—vector of the bearing of the piston; E_5—vector of the bushing of the piston; e_1, e_2, e_3—unit vectors of the basic system of coordinates.

where r—distance from the center of rotor to the center of the bush-bearing unit (points of intersection of the axes of the hinges);

l_0—length of the tie rod (distance between the centers of the hinges);

α_0—angle between the axis of the bushing and radius r, joining the center of the rotor with the center of the hinge;

ω—Clifford factor.

Let us follow the sequence of displacements of links of the mechanism.

1. Let us rotate the vector $\boldsymbol{E}_1$ and $\boldsymbol{E}_2$ by an angle ψ with respect to the axis $\boldsymbol{E}_3$. Vector of finite rotation is equal to $\Psi=\Psi_3$, where $\Psi=\tan\Psi/2$, and finite values of vectors $\boldsymbol{E}_1'$ and $\boldsymbol{E}_2'$ are:

$$\boldsymbol{E}_1'=\boldsymbol{E}_1+2\Psi/(1+\Psi^2)\cdot(\boldsymbol{E}_1+\Psi\cdot\boldsymbol{E}_1);$$
$$\boldsymbol{E}_2'=\boldsymbol{E}_2+2\Psi/(1+\Psi^2)\cdot(\boldsymbol{E}_2+\Psi\cdot\boldsymbol{E}_2).$$

2. Rotate vector $\boldsymbol{E}_1'$ by an angle δ with respect to the vector $\boldsymbol{E}_2'$. Vector of finite rotation is equal to $\Delta=\Delta\boldsymbol{E}_2'$ where $\Delta=\tan\delta/2$, and finite value of vector $\boldsymbol{E}_1''$ is:

$$\boldsymbol{E}_1''=\boldsymbol{E}_1'+2\Delta/(1+\Delta^2)\cdot(\boldsymbol{E}_1'+\Delta\cdot\boldsymbol{E}_1').$$

3. Rotate vectors $\boldsymbol{E}_4$ and $\boldsymbol{E}_5$ through the complex angle $\Phi=\varphi+\omega h$ with respect to the axis of the rotor. Complex vector of finite screw

displacement is equal to $\boldsymbol{F}=F\mathbf{e}_1$, where $F=\tan \Phi/2$, and finite values of vectors $\boldsymbol{E}_4'$ and $\boldsymbol{E}_5'$ are:

$$\boldsymbol{E}_4'=\boldsymbol{E}_4+2F/(1+F^2)\cdot(\boldsymbol{E}_4+\boldsymbol{F}\cdot\boldsymbol{E}_4);$$
$$\boldsymbol{E}_5'=\boldsymbol{E}_5+2F/(1+F^2)\cdot(\boldsymbol{E}_5+\boldsymbol{F}\cdot\boldsymbol{E}_5).$$

4. Rotate vector $\boldsymbol{E}_4'$ by angle Θ with respect to the vector $\boldsymbol{E}_5'$. Vector of finite rotation is equal to $\boldsymbol{\Theta}=\Theta\,\boldsymbol{E}_5'$ where $\Theta=\tan \Theta/2$, and finite value of vector $\boldsymbol{E}_4''$ is:

$$\boldsymbol{E}_4''=\boldsymbol{E}_4'+2\boldsymbol{\Theta}/(1+\Theta^2)\cdot(\boldsymbol{E}_4'+\boldsymbol{\Theta}\cdot\boldsymbol{E}_4').$$

The mechanism works in such a way (see Fig. 1) so that the angle of rotation of the bushing on the rotor remains equal to the angle of rotation of the bushing on the piston, i.e. $\Theta=\psi$.

From the condition of perpendicularity of vectors $\boldsymbol{E}'$ and $\boldsymbol{E}_4''$, it follows:

$$\boldsymbol{E}_1''\cdot\boldsymbol{E}_4''=0, \tag{1}$$

and from the condition of intersection of vectors $\boldsymbol{E}_1''$ and $\boldsymbol{E}_5'$ we get:

$$\mathcal{J}m\,(\boldsymbol{E}_1''\cdot\boldsymbol{E}_5')=0, \tag{2}$$

complex angle between the vectors $\boldsymbol{E}_2'$ and $\boldsymbol{E}_4''$ is equal to:

$$\Gamma=\gamma+\omega[l_0+k(180^\circ-2\alpha_0-\gamma)],$$

where, γ—angle of rotation of the vector $\boldsymbol{E}_2'$ with respect to the vector $\boldsymbol{E}_4''$ in the plane, perpendicular to the tie rod;

k—coefficient, which takes into consideration the variation of the length of the tie rod during its turning in the threads through an angle $180^\circ-2\alpha_0-\gamma$.

Scalar product of vectors $\boldsymbol{E}_4''$ and $\boldsymbol{E}_2'$ will be:

$$\boldsymbol{E}_4''\cdot\boldsymbol{E}_2'=\cos\Gamma=\cos\gamma-\omega[l_0+k(180^\circ-2\alpha_0-\gamma)]\sin\gamma. \tag{3}$$

Expanding equations (1)-(3) in terms of the unit vectors $\mathbf{e}_1$, $\mathbf{e}_2$, $\mathbf{e}_3$, and separating the real parts of the equations from the complex parts, we get the following system of transcendental equations with respect to the unknowns φ, h, ψ, δ and γ:

$$-\cos\psi\,[\cos\delta\cdot\sin\psi-\cos\delta\cdot\sin\psi(\sin 2\alpha_0\cdot\sin\varphi+\cos 2\alpha_0\cdot\cos\varphi)-$$
$$\sin\delta(\sin 2\alpha_0\cdot\cos\varphi-\cos 2\alpha_0\cdot\sin\varphi)]=0; \tag{1}$$

$$r\cdot\cos^2\psi\cdot\cos\delta(\cos\alpha_0\cdot\cos\varphi-\cos\alpha_0+\sin\alpha_0\cdot\sin\varphi)-r\cdot\sin^2\psi\times$$
$$\cos\delta(\cos\alpha_0\cdot\cos\varphi-\cos\alpha_0+\sin\alpha_0\cdot\sin\varphi)+r\cdot\sin\psi\sin\delta\times$$
$$(\sin\alpha_0-\sin\alpha_0\cdot\cos\varphi+\cos\alpha_0\cdot\sin\varphi)+(l_0-h)\sin\delta\cdot\cos\psi\times$$
$$\cos(2\alpha_0-\varphi)-(l_0-h)\sin\psi\cdot\cos\psi\cdot\cos\delta\cdot\sin(2\alpha_0-\varphi);\qquad(2)$$

$$\sin^2\psi+\cos^2\psi\cdot\cos(2\alpha_0-\varphi)+\cos\gamma=0;\qquad(3)$$

$$2r\cdot\sin\psi\cdot\cos\psi(\cos\alpha_0\cdot\cos\varphi-\cos\alpha_0+\sin\alpha_0\cdot\sin\varphi)+(l_0-h)\times$$
$$\cos^2\psi\sin(2\alpha_0-\varphi)-\sin\gamma[l_0+k(180^\circ-2\alpha_0-\gamma)]=0;\qquad(4)$$

$$r\cdot\cos\psi\cdot\cos\delta(\sin\alpha_0+\sin\alpha_0\cos\varphi+\cos\alpha_0\cdot\sin\varphi)-$$
$$(l_0-h)\sin\delta\cdot\sin(2\alpha_0-\varphi)-$$
$$(l_0-h)\cdot\sin\psi\times\cos\delta\cdot\cos(2\alpha_0-\varphi)=0.\qquad(5)$$

Calculation for the concrete values of l_0, α_0 and r, on digital computer, gives the relationship of unknowns ψ, δ, h and γ with respect to the angle of rotation φ, as shown in the Fig. 3.

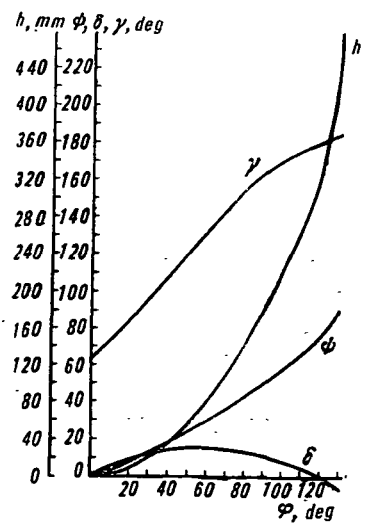

Fig. 3. Graph of relationship of parameters h, ψ, δ and of γ with the angle of rotation of the rotor φ.

2. Force Analysis of the Mechanism

Using the results of the kinematic analysis, let us carry out the force analysis of the mechanism. Consider separately the conditions of equili-

brium for each one of the following links: tie rod with the bearing (Fig. 4), bushing of the piston (Fig. 5), the piston (Fig. 6), bearings and bushings of the rotor, and rotor.

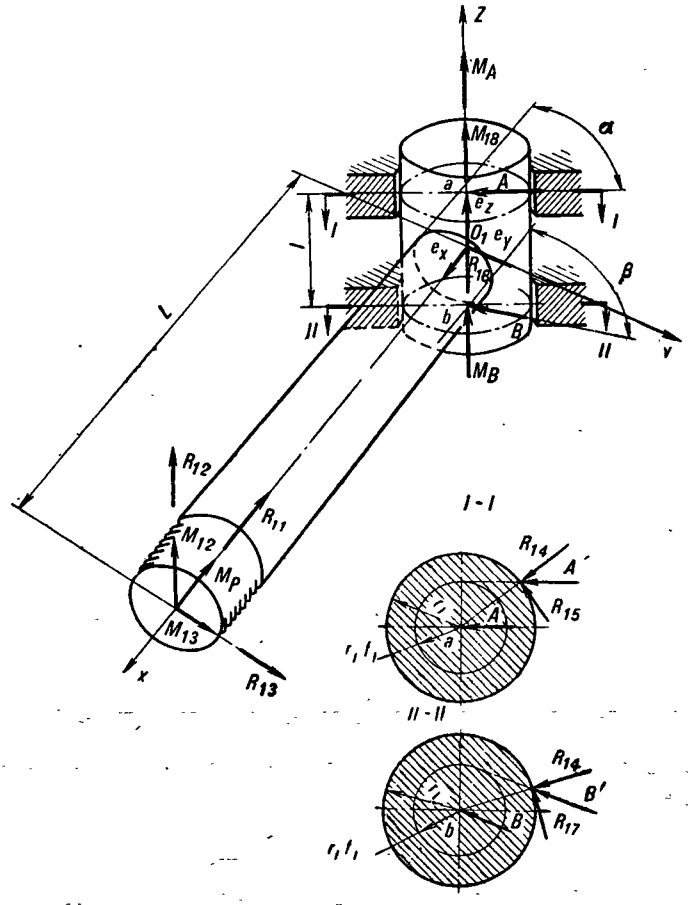

Fig. 4. Diagram of forces acting on the tie rod with bearings on the piston: $\mathbf{R}_{11}$, $\mathbf{R}_{12}$, $\mathbf{R}_{13}$, $\mathbf{M}_{12}$, $\mathbf{M}_{13}$—*reactions from the side of the bearing of the rotor;* **A**, **B**, $\mathbf{R}_{18}$—*reactions from the side of the bushing of the piston;* $\mathbf{M}_A$, $\mathbf{M}_B$—*moments of friction of bearing with the bushing in the supports a and b;* $\mathbf{M}_{18}$—*end force moment of friction of the bearing;* $\mathbf{M}_p$—*moment of friction in the thread of the tie rod;* $r_1 f_1$—*radius of the circle of friction.*

In view of the difficulty of exact determination of forces of friction in the kinematic pairs of spatial mechanisms, let us use Kulon's model of dry friction. Considering the small velocity of displacement of links (let us take time of one stroke of the piston from 20 seconds to two minutes). We

neglect inertia forces in the calculations, as these are small as compared to the applied external forces. Forces and couples are represented in the form of complex vectors. Conditions of equilibrium of each link are written in the form of a unit spiral equation.

Let us consider each link separately.

1) Tie rod and bearing on the rotor (see Fig. 4). Let us choose the system of coordinates with the center at the point O_1, x-axis (along axis of tie rod), y-axis (along axis of bearing) and z-axis. Reaction $\boldsymbol{A}(\boldsymbol{B})$ is the sum of the reactions of the bearing $\boldsymbol{R}_{14}$ ($\boldsymbol{R}_{16}$) acting from the side of the bushing *5* (see Fig. 1) and of the forces of friction $\boldsymbol{R}_{15}$ ($\boldsymbol{R}_{17}$) caused by this reaction.

Upon the transfer of reaction $\boldsymbol{A}(\boldsymbol{B})$ to the center of the cross section of the bearing, moment $\boldsymbol{M}_A(\boldsymbol{M}_B)$ appears:

$$R_{15}=f_1R_{14};\quad R_{17}=f_1R_{16};\qquad A=\sqrt{R_{14}^2+R_{15}^2}=R_{14}\sqrt{1+f_1^2};$$

$$B=\sqrt{R_{16}^2+R_{17}^2}=R_{16}\sqrt{1+f_1^2};\qquad M_A=r_1f_1A;\quad M_B=Br_1f_1;$$

$$M_{18}={}^2/_3r_1f_1R_{18};\qquad M_p=r_{\text{thread}}f_{\text{thread}}R_{11},$$

where, f_1—coefficient of friction between the bearing and the bush;

f_{thread}—coefficient of friction in the threads;

r_1—radius of cross section of the bearing;

r_{thread}—radius of the cross section of the thread.

From the condition of equilibrium we take the main vector and main couple equal to zero:

$$\boldsymbol{R}_{11}+\boldsymbol{R}_{12}+\boldsymbol{R}_{13}-\boldsymbol{A}+\boldsymbol{B}+\boldsymbol{M}_p+\boldsymbol{M}_{12}+\boldsymbol{M}_{13}+\boldsymbol{M}_{18}+\boldsymbol{M}_A+\boldsymbol{M}_B=0. \qquad (1)$$

Let us express all the forces and couples, acting on the bearing, in terms of the unit vectors $\mathbf{e}_x$, $\mathbf{e}_y$ and $\mathbf{e}_z$:

$$\boldsymbol{A}=A[\mathbf{e}_x(\cos\alpha+\omega l/2\sin\alpha)-\mathbf{e}_y(\sin\alpha-\omega l/2\cos\alpha)];$$

$$\boldsymbol{B}=B[\mathbf{e}_x(\cos\beta-\omega l/2\sin\beta)-\mathbf{e}_y(\sin\beta+\omega l/2\cos\beta)];\qquad \boldsymbol{R}_{18}=-R_{18}\mathbf{e}_z;$$

$$\boldsymbol{R}_{11}=R_{11}\mathbf{e}_x;\qquad \boldsymbol{R}_{12}=R_{12}(\mathbf{e}_z-\omega l_0/2\mathbf{e}_y);\qquad \boldsymbol{R}_{13}=R_{13}\,(\mathbf{e}_y+\omega l_0/2\mathbf{e}_z);$$

$$\boldsymbol{M}_A=\omega M_A\mathbf{e}_z=\omega r_1f_1A\mathbf{e}_z;\qquad \boldsymbol{M}_B=\omega M_B\mathbf{e}_z=\omega r_1f_1B\mathbf{e}_z;$$

$$\boldsymbol{M}_{12}=\omega M_{12}\mathbf{e}_z;\qquad \boldsymbol{M}_{13}=\omega M_{13}\mathbf{e}_y;\qquad \boldsymbol{M}_{18}=\omega M_{18}\mathbf{e}_z=\omega^2/_3r_1f_2R_{18}\mathbf{e}_z;$$

$$\boldsymbol{M}_p=-\omega M_p\mathbf{e}_x=-r_{\text{thread}}f_{\text{thread}}R_{11}\mathbf{e}_x.$$

Let us substitute the values of forces and moments in equation (1). Taking the real and complex parts of the equation equal to zero and resolving them along the axes of coordinates, we get a system of six equations with respect to the unknowns: R_{11}, R_{12}, R_{13}, R_{18}, A, B, M_{12}, M_{13}, α and β.

$$R_{11}-A\cos\alpha-B\cos\beta=0; \tag{1a}$$

$$R_{13}-A\sin\alpha-B\sin\beta=0; \tag{2a}$$

$$R_{12}-R_{18}=0; \tag{3a}$$

$$(A\sin\alpha-B\sin\beta)l/2-M_p=0; \tag{4a}$$

$$(A\cos\alpha-B\cos\beta)l/2+M_{13}-R_{12}l_0/2=0; \tag{5a}$$

$$M_{12}+R_{13}l/2+r_1f_1(A+B+{}^2/_3\,R_{18})=0. \tag{6a}$$

2) Bushing on the Piston (see Fig. 5). Let us use the same system of coordinates, as chosen for the case 1. Reactions shown in Fig. 5, are equal to:

$$R_{22}=R_{21}f_2; \qquad C=\sqrt{R_{21}^2+R_{22}^2}=R_{21}\sqrt{1+f_2^2},$$

$$R_{24}=R_{23}f_2; \qquad D=\sqrt{R_{23}^2+R_{24}^2}=R_{23}\sqrt{1+f_2^2};$$

$$M_D=Dr_2f_2; \qquad M_C=Cr_2f_2; \quad M_{25}={}^2/_3\,r_2f_2R_{25},$$

where f_2—coefficients of friction between the bushing and the piston.

Let us express all forces and moments, acting on the bushing in terms of the unit vectors $\mathbf{e}_x$, $\mathbf{e}_y$ and $\mathbf{e}_z$. From the condition of equilibrium of the system, we put main vector and main moment of the system equal to zero:

$$\mathbf{R}_{18}+\mathbf{R}_{25}+\mathbf{A}''+\mathbf{B}''+\mathbf{C}+\mathbf{D}+\mathbf{M}_A'+\mathbf{M}_B'+\mathbf{M}_{18}'+\mathbf{M}_C+\mathbf{M}_D+\mathbf{M}_{25}=0. \tag{2}$$

Substituting the values of forces and moments in equation (2), by expressing them in terms of the unit vectors $\mathbf{e}_x$, $\mathbf{e}_y$, $\mathbf{e}_z$ and setting the real and complex parts of the equation so obtained equal to zero and resolving them along the axes of coordinates, we get six equations with respect to the unknowns, C, D, R_{25}, A, B, R_{18}, ε, ξ, α, β, i.e.:

$$C\sin\varepsilon\cdot\cos\omega-D\sin\xi\sin\omega+A\cos\alpha+B\cos\beta-R_{25}\cos\omega=0; \tag{7a}$$

$$C\sin\varepsilon\cdot\sin\omega-D\sin\xi\cos\omega-A\sin\alpha-B\sin\beta+R_{25}\sin\omega=0; \tag{8a}$$

$$C\cos\varepsilon-D\cos\xi-R_{18}=0; \tag{9'}$$

$$Cl_1/2\cos\varepsilon\cdot\sin w+Dl_1/2\cos\xi\sin w-Al/2\sin\alpha+Bl/2\sin\beta+r_2f_2\cos w(C-D+2/3\,R_{25})=0; \tag{10a}$$

$$Cl_1/2\cos\varepsilon\cdot\cos w+Dl_1/2\cos\xi\cos w-Al/2\cos\alpha+Bl/2\cos\beta-r_2f_2\sin w(C-D+2/3\,R_{25})=0; \tag{11a}$$

$$Cl_1/2\sin\varepsilon\cdot\sin 2w+Dl_1/2\sin\xi+r_1f_1(A+B+2/3R_{18})=0. \tag{12a}$$

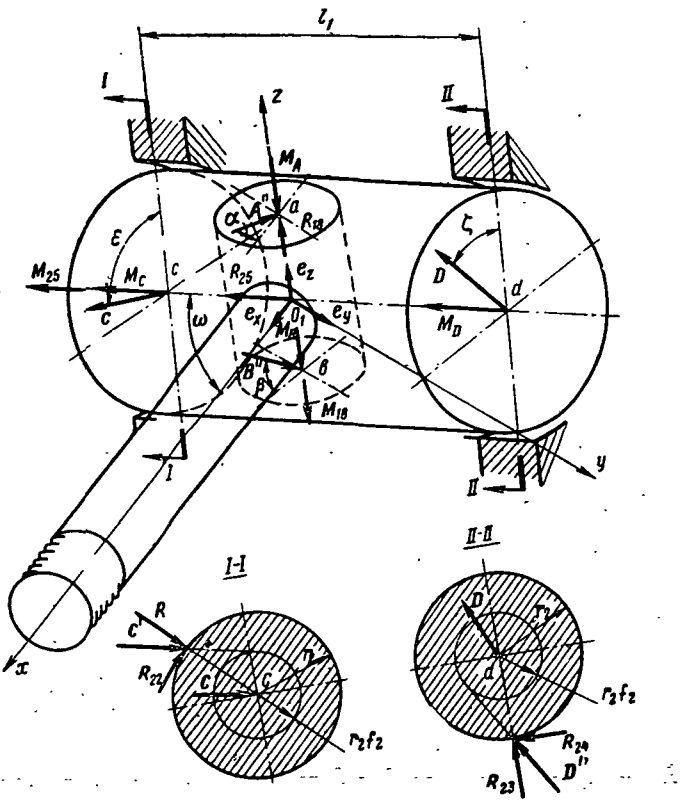

Fig. 5. System of forces, acting on the bushing of the piston:
$\mathbf{R}_{18}$, $\mathbf{A}'$, $\mathbf{B}'$—*reactions from side of the bearing;* $\mathbf{M}_A$, $\mathbf{M}_B$, $\mathbf{M}_{18}$—*moments of friction of the bushing with the bearing;* $\mathbf{C}$, $\mathbf{D}$, $\mathbf{R}_{25}$—*reactions from the side of piston;* M_C, M_D, M_{25}—*moments of the bushing with the piston.*

3) Piston (see Fig. 6). Let us use the same system of coordinates as in case 1, and the following symbols:

$\mathbf{P}$—force due to pressure of the gas on the piston (during down stroke);

$\mathbf{R}_{31}$, $\mathbf{R}_{32}$, $\mathbf{R}_{34}$—reactions of the guides and of the bearing assembly of the second tie rod, resolved along three mutually perpendicular directions.

$\mathbf{M}_{31}$, $\mathbf{M}_{32}$, $\mathbf{M}_{33}$—reactive moments, acting from the sides of the second bearing assembly and of guides on the piston;

$\mathbf{R}_{33}$—reactions in the guides;

$R_{34}=f_2 R_{33}$—force of friction in the guides, where

f_3—coefficient of friction between the guides and the piston;

$M_{33}=r_3 R_{33}$.

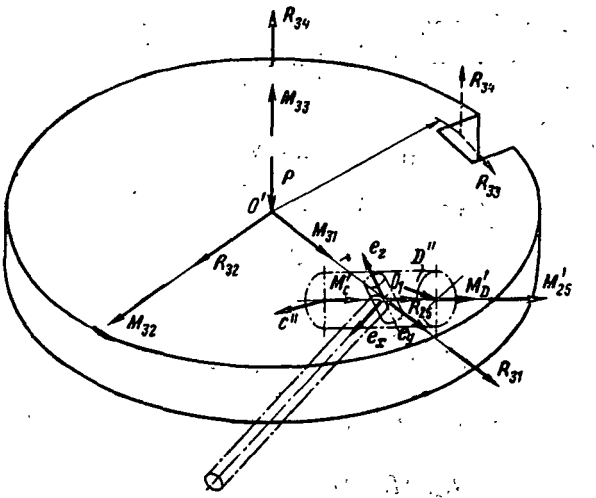

Fig. 6. System of forces, acting on the piston:
$\mathbf{R}_{31}$, $\mathbf{R}_{32}$, $\mathbf{R}_{34}$, M_{31}, M_{32}, M_{33}—*reactions on the piston;* P—*force due to gas pressure on the piston;* $\mathbf{P}_{33}$—*reaction in the guides;* $\mathbf{R}_{34}$—*force of friction in the guides.*

At the condition of equilibrium of the piston, main vector and main moment of all the forces and of the moments, applied to the piston are equal to zero, i.e.

$$\mathbf{P}+\mathbf{R}_{31}+\mathbf{R}_{32}+\mathbf{R}_{34}+\mathbf{C}''+\mathbf{D}''+\mathbf{R}_{25}'+\mathbf{M}_{31}+\mathbf{M}_{32}+\mathbf{M}_{33}+\mathbf{M}_C'+\mathbf{M}_D'+\mathbf{M}_{25}=0. \tag{13}$$

Substitute the values of forces and moments in the equation (13). Taking real and complex parts of the equation separately equal to zero and resolving them along the coordinate axes, we get 6 equations with respect to the unknowns: R_{31}, R_{32}, R_{33}, M_{31}, M_{32}, C, D, R_{25}, ε and ξ, that is:

$$R_{32}\sin\psi-R_{33}f_3\cos\psi+C\sin\varepsilon\cdot\cos w-D\sin\xi\cdot\sin w-R_{25}\cos w=0. \tag{13a}$$

$$R_{31}+C\sin\varepsilon\cdot\sin w-D\sin\xi\cdot\cos w+R_{25}\sin w=0; \tag{14a}$$

$$R_{32}\cos\psi+R_{33}f_3\sin\psi+C\cos\varepsilon-D\cos\xi-P\sin\psi=0; \tag{15a}$$

$$R_{32}r\cos\psi+R_{33}f_3r\sin\psi+l_1/2\sin w(C\cos\varepsilon+D\cos\xi)-Pr\sin\psi-M_{32}\sin\psi+R_{33}r_3\cos\psi+r_2f_2\cos w(C-D+{}^2/_3R_{25})=0; \tag{16a}$$

$$-l_1/2\cos w(C\cos\varepsilon-D\cos\xi)+M_{31}+r_2f_2\sin w(C-D+{}^2/_3R_{25})=0; \tag{17a}$$

$$R_{32}r\sin\psi-R_{33}f_3r_3\cos\psi+C\sin\varepsilon\sin(2wl_1/2)+Pr\cos\psi+Dl_1/2\sin\xi+M_{32}\cos\psi-r_3R_{33}\sin\psi=0. \tag{18a}$$

Similarly considering tie rod with the bearing on the rotor, bushing on the rotor and also rotor itself we get six equations:

Equations for the tie rod with the bearing are:

$$R_{11}+K\cos\lambda+N\cos\nu=0; \tag{19a}$$

$$R_{13}+K\sin\lambda\cos\Gamma+N\sin\nu\cos\Gamma=0; \tag{20a}$$

$$R_{45}\cos\Gamma-R_{12}=0; \tag{21a}$$

$$K\sin(\lambda l/2)+N\sin(\nu l/2)+r_{\text{thread}}f_{\text{thread}}R_{11}=0; \tag{22a}$$

$$R_{12}l_0/2+l/2\cos\Gamma(K\cos\lambda-N\cos\nu)-M_{13}=0; \tag{23a}$$

$$r_1f_1\cos\Gamma(K+N+{}^2/_3R_{45})-R_{13}l_0/2-M_{12}=0. \tag{24a}$$

Unknowns: R_{11}, R_{12}, R_{13}, M_{12}, M_{13}, K, N, R_{45}, λ, ν.

Equations for the bushing are:

$$K\cos\lambda+N\cos\nu+R_{55}\cos\eta-Q\sin\xi-V\sin\mu=0; \tag{25a}$$

$$K\sin\lambda\cos\Gamma+N\sin\nu\cos\Gamma+R_{55}\sin\eta=0; \tag{26a}$$

$$R_{45}\cos\Gamma+Q\cos\xi+V\cos\mu=0; \tag{27a}$$

$$K\sin(\lambda l/2)-N\sin(\nu l/2)+Q\cos(\xi l_1/2)-V\cos(\mu l_1/2)+r_2f_2\cos\eta(Q+V+{}^2/_3R_{55})=0; \tag{28a}$$

$$r_2f_2\sin\eta(Q+V+{}^2/_3R_{55})-l/2\cos\Gamma(K\cos\lambda+N\cos\nu)+\sqrt{2l_0h-h^2}(V\cos\mu-Q\cos\xi)=0; \tag{29a}$$

$$R_{55}\sin\eta\sqrt{2l_0h-h^2}-Q\sin(\xi l_1/2)-V\sin(\mu l_1/2)-r_1f_1\cos\Gamma(K+N+{}^2/_3R_{45})=0. \tag{30a}$$

Unknowns: R_{45}, K, N, R_{55}, Q, V, λ, ν, μ and ξ.

Equations for the rotor are:

$$Q\sin\xi+V\sin\mu-R_{55}\cos\eta-R_{63}\cos\rho\cdot\cos\tau\cdot\cos\sigma-R_{62}\cos\chi+R_{61}\cos\sigma=0; \tag{31a}$$

$$R_{61}\cos\tau-R_{62}\cos\tau\cdot\cos\sigma\cdot\cos\chi-R_{63}\cos\rho+R_{55}\sin\eta=0; \tag{32a}$$

$$Q\cos\xi+V\cos\mu+R_{63}\cos\rho\cdot\cos\tau\cdot\cos\psi+R_{62}\cos\chi\cdot\cos\sigma\cdot\cos\psi-R_{61}\cos\psi=0; \tag{33a}$$

$$Q\cos(\xi l_1/2)+Qr_2f_2\cos\eta-V\cos(\mu l_1/2)+Vr_2f_2\cos\eta+{}^2/_3r_2f_2R_{55}\cos\eta+M_{61}\cdot\cos\chi+M_{62}\cos\rho\cdot\cos\tau\cdot\cos\sigma+M_{\text{resist}}\cos\sigma=0; \tag{34a}$$

$$2\sqrt{2l_0h-h^2}\,(Q\cos\xi+V\cos\mu)+r_2f_2\sin\eta(Q+V)-r\cdot R_{61}\cdot\cos\psi+$$
$$r\cdot R_{62}\cos\chi\cdot\cos\sigma\cdot\cos\psi+rR_{63}\cos\psi\cdot\cos\tau\cos\rho+{}^2/_3r_2f_2\sin\eta\cdot R_{55}+$$
$$M_{62}\cos\rho+M_{61}\cdot\cos\chi\cos\tau\cos\sigma+M_{\text{resist}}\cos\tau=0; \qquad (35a)$$

$$Q\sin(\xi l_1/2)+V\sin(\mu l_1/2)-\sqrt{2l_0h-h^2}\,R_{55}\cdot\sin\eta+rR_{61}(\cos\sigma-\cos\tau)+$$
$$rR_{62}\cos\chi(\cos\sigma\cdot\cos\tau-1)-R_{63}\cdot\cos\rho\cdot r(\cos\tau\cos\sigma-1)+$$
$$\cos\psi(M_{61}\cos\chi\cos\sigma+M_{62}\cos\rho\cos\tau+M_{\text{resist}})=0. \qquad (36a)$$

Unknowns: Q, V, R_{55}, R_{61}, R_{62}, R_{63}, M_{61}, M_{62}, M_{resist}, ξ and μ.

The results make it possible to carry out strength calculations for the components of the drive; determine losses due to friction in the kinematic pairs, the efficiency of the mechanism, and to determine the mechanical characteristic of the drive and optimum parameters of the links.

References

1. Dimentberg, F. M. Opredelenie polozhenii prostranstvennykh mekhanizmov (Determination of the Positions of Spatial Mechanisms). Izd-vo AN SSSR, 1950.
2. Dimentberg, F. M. Vintovoe ischislenie i ego prilozheniya v mekhanike (Screw Calculation and Its Application in Mechanics). Izd-vo Nauka, 1965.
3. Lebedev, P. A. Kinematika prostranstvennykh mekhanizmov (Kinematics of Spatial Mechanisms). Moscow-Leningrad, Izd-vo Mashinostroenie, 1966.

B. N. Sklyadnev, B. N. Yurukhin, Yu. I. Evteev and *E. I. Astakhov*

DESIGN OF AUTOMATS WITH PHOTOELECTRONIC DEVICES FOR THE CONTROL AND MEASUREMENT OF LINEAR DIMENSIONS AND AREAS

Modern industrial automats have hydraulic, pneumatic, electrical and electronic components besides mechanical linkages.

This is connected with the increase in the number of functions, performed by the automats, which are automatically controlled through feedback systems.

Among the control systems of automats, photoelectronic control systems are common. In a number of gaging machines, such as IL and FEI-O etc., photoelectronic devices constitute the basic elements which determine the nature of their work [1]. These automats have proved themselves efficient in practical use.

Automats designed for measuring small diameters and for producing diagrams and experimental curves are based on photoelectronic systems. A basic design problem is the selection of the basic parameters of the automats for the conditions under which they have to function.

Selection of optimum parameters of automats with photoelectronic devices for prescribed efficiency and range of measurement or for control and measurement accuracy is discussed below.

1. Efficiency of the Automat for Measuring Linear Dimensions and Selection of the Kinematic Diagram

As shown in [2], photoelectronic numerical impulsive devices meant for the determination of different geometrical parameters of the figure are based on one or a number of related measurements of linear dimensions. Hence results for automats which check the linear dimensions will be used during the analysis of other more complex automats with photoelectronic devices.

As is well known, the photoelectronic numerical impulsive method of measurement may be described in short as that parameter to be measured is checked elementwise with the light ray (emitter) and measurement leads to the registration of the number of impulses emitted by a special generator during checking, on an electronic counter of impulses (ECI). Frequency of the impulses of the generator is kinematically synchronized with the velocity of the light control. The beginning and end of the measurements are automatically fixed by a command device which governs ECI.

One possible design for the automats for checking jobs of small diameters and based on the above mentioned principle of measurement is shown in Fig. 1,a. The automat is based on the schematic diagram of the device, given in Ref. [2], with minor changes.

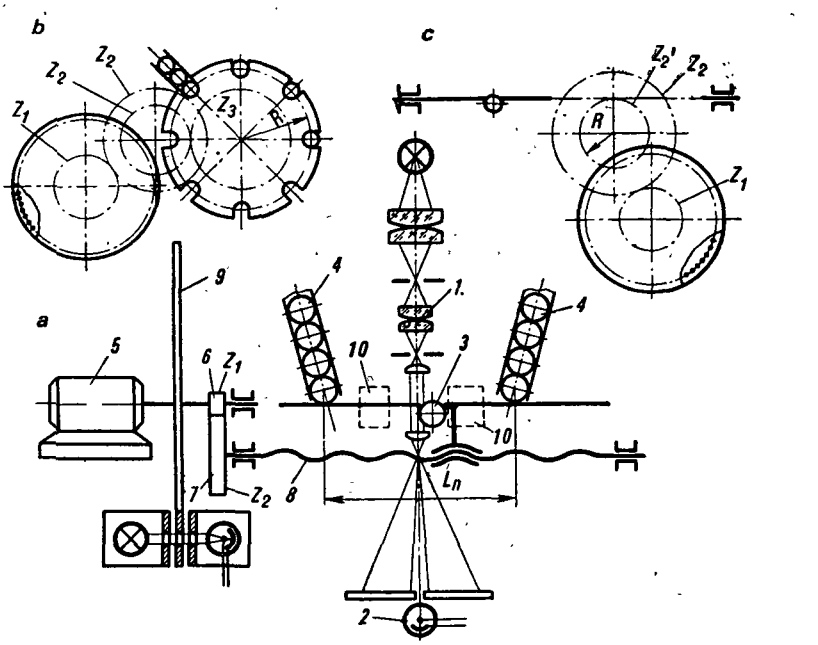

Fig. 1. Principle diagram of the photoelectronic automat for measuring linear dimensions.

The differences in the diagram from the original one are that in the diagram on Fig. 1,a the optical system *1*, and photohead *2* are fixed, and the component to be measured *3* moves, entering one after another from the feeder *4* to the zone of measurement and from there to the conveyor *10* for further sorting. These changes have arisen out of the necessity to build the measuring device in an assembly line to be used for measuring small diameters of components of the electric motors. Simultaneously the efficiency of the photoelectronic apparatus has also been improved.

Efficiency of the automat for the measurement of linear dimensions is determined by the following equation:

$$Q=6\cdot 10^4 V/(1+\varepsilon)L, \text{ pieces/minute,} \tag{1}$$

where V—linear velocity of the displacement of components, m/sec;
L—length being measured, mm;
ε—coefficient which is equal to:

$$\varepsilon=(L_n-L)/L. \tag{2}$$

Here, L_n—quantity which is determined by the complete displacement of the carriage (Fig. 1,a).

Let us rearrange the efficiency equation (1), by adding to it the fundamental kinematic parameters of the diagrams for calculating the velocity of displacement:

$$Q=n_m h/i_{ms}L_n \text{ pieces/minute,} \tag{3}$$

where n_m—number of rotations of the motor *5*, rpm;
h—pitch of the screw *8* mm;
i_{ms}—transmission ratio of the gears *6*, *7* from the motor to the screw.

As an example of the preliminary evaluation of the accuracy of measurement, let us take an error caused by the discreteness of the adopted method of measurement.

This error may be due to counting of an extra impulse by the ECI or omission of one impulse during counting:

$$\Delta L_m=\pm C; \tag{4}$$

$$C=h/ki_{ms}, \tag{5}$$

where, k—number of holes in the rotor *9* of the electronic-mechanical generator for counting impulses.

For the given automat, kinematic synchronization between the frequency of impulses of the generator and the velocity of displacement of the component under examination (velocity of the light control) is accomplished with the help of screw and gear transmission.

Let us consider the points, which must be taken into consideration during the selection of different mechanisms for this purpose. Let us compare some variants of the drive, which transform the rotating motion of the rotor of the generator into the translatory motion of the component in the zone of measurement. Besides gear-screw transmission, used in the diagram of Fig. 1,a let us consider the gear transmission (see Fig. 1,b) and also the gear-rack transmission (see Fig. 1,c).

For the diagram, given in the Fig. 1,b we have following equation for the efficiency Q and the value of scale division C:

$$Q=2\cdot \pi n_m R/i_{mR}L_n \text{ pieces/minute}, \tag{6}$$

$$C=2\pi R/ki_{mR}, \tag{7}$$

where R—radius of the rotor, that moves the component during measuring process (Fig. 1,b);

i_{mR}—transmission ratio from the motor to the transporting rotor.

The value of the radius R should be chosen from the condition that the length of the arc of the displacement during the measurement approaches the length of the chord. For small values of the central angle α, this occurs with a higher degree of accuracy. Thus:

$$R=L/\alpha. \tag{8}$$

If value of α is taken as $\alpha\leqslant 4°$, then the error does not exceed 0.02%. In this case, if $L=2$ mm, and $\alpha=2°$, we have $R\approx 60$ mm.

Equations for Q and C in the case of diagrams in which gear-rack mechanisms are used, are the same as equations (6) and (7). As is clear from the diagram (Fig. 1,c) R—radius of pitch circle of the gear, which drives the rack is determined from the laws of motion of gear drives.

Let us consider the conditions under which the devices, considered by us would have similar efficiency and value of impulse. We obtain this by equating the equations (3) with (6) and (5) with (7), and get one common condition:

$$h/i_{ms}=2\pi R/i_{mR}. \tag{9}$$

Thus, if we assume that the device shown in Fig. 1,a has parameters $h=0.5$ mm and $i_{ms}=5$, then a similar device shown in Fig. 1,b having the same efficiency and same error, fulfills the following equation at $R=60$ mm:

$$i_{mR}=2\pi R i_{ms}/h\approx 3800.$$

Thus to provide the same efficiency for the same value of impulse, the automat shown in Fig. 1,b must have a reduction gear with high transmission ratio as compared to the one already considered.

An analysis of equations (3), (5) - (7) and (9) reveals that at higher values of the impulse C, equal to 1 mm or more, the characteristics of the gear transmission is preferable to the gear-screw transmission, with all other conditions remaining the same, because this results in higher efficiency.

Such characteristics prove to be effective, for example, during the measurements of big areas.

On the other hand, designs with the gear-screw transmission are considerably simpler for measuring the linear dimensions with high degree of accuracy of the order of 5-10 microns.

Gear-rack transmission makes it possible (see Fig. 1,c) to reduce the transmission ratio of the reduction gear due for a decrease in the value of R.

All the diagrams considered above are characterized by the fact that rotor of the generator of counting impulses is situated on the axis of the motor. Location of the motor in the middle of the kinematic chain (from the rotor of the generator to the link which carries the component to the zone of measurement) cannot change the above conclusions. Similarly, it may be pointed out that the final selection of one or the other kinematic chains should be done on the basis of comparison of absolute values of total errors of measurement.

2. Accuracy Calculations for an Automat for Checking and Measuring Linear Dimensions

Calculations for checking the accuracy of measurement of linear dimensions for an automat have been carried out on the basis of the consideration of random errors, whose limiting values may be constrained by the selection of tolerances. On the basis of the theory of accuracy [3], practical limiting values of errors of measurement for a given coefficient of risk z for a group of similar devices (4) is determined from the equation:

$$\Delta L=\sum_{i=1}^{m}\Delta_{ci}+\sum_{m+1}^{n}M_jP_j\pm z\sqrt{\sigma_D^2P_D^2+\sum_{m+1}^{n-1}\sigma_j^2P_j^2}, \qquad (10)$$

where, n—overall number of primary errors of the device;

Δ_{ci}—systematic error, caused by the special features of the accepted method of measurement, which approximates the given law of transformation;

m—overall number of systematic errors in the device;

M_j—mean value (mathematical anticipation) of random primary errors;

σ_j—mean square deviations of the random primary errors;

σ_D—mean square deviations of the errors, determined by the discreteness;

P_j, P_D—coefficients of influence of primary errors.

Let us assume that all primary errors are mutually independent, expressions M_jP_j and σ_jP_j (10) are linear functions of the primary errors of the device and error ΔL obeys the normal law of distribution.

Mean square deviation of the error, caused by the discreteness of the method of measurement has been obtained in equation (10). Making use

of equation (4) and putting limiting permissible error of measurement δ in place of ΔL, we get:

$$\left(\delta-\sum_{1}^{m}\Delta_{ci}-\sum_{m+1}^{n-1}M_jP_j\right)^2=z^2\left(\lambda_D^2C^2+\sum_{m+1}^{n-1}\sigma_j^2P_j^2\right). \tag{11}$$

Let us assume that the error of discreteness is analogous to the error of rounding off during counting from the scale. Consequently, its distribution follows the law of equal probability, i.e.

$$\alpha_D=0;\ M_D=0;\ \lambda_D=0.58,$$

where α_D—coefficient of relative asymmetry;
M_D—mean value of the error of discreteness;
λ_D—relative mean square deviation.

Coefficient of risk is usually taken as $z=3$ in the calculations because it gives insignificantly small value of the probability of random errors from exceeding the calculated limit, and is equal to $\pm 0.13\%$.

It is convenient to write equation (11) for analysis in the following form:

$$\delta_n^2=A^2+\lambda_D^2C^2, \tag{12}$$

where

$$\delta_n={}^1/_3\left(\delta-\sum_{1}^{m}\Delta_{ci}-\sum_{m+1}^{n-1}M_jP_j\right);$$

$$A^2=\sum_{m+1}^{n-1}\sigma_j^2P_j^2.$$

Equation (12) allows us to determine the value of error of discreteness for the given value of limiting permissible error and for the known instrumental error of the device.

A graph, constructed on the basis of the equation (12) is given in Fig. 2. For the diagram of the automat, given in Fig. 1,a expression (12) may be uesd for the determination of parameters of the device, for example k, in the following way:

$$k=\lambda_D h/i_{ms}\sqrt{{}^1/_9\left(\delta-\sum_{1}^{m}\Delta_{ci}-\sum_{m+1}^{n-1}M_jP_j\right)^2-\sum_{m+1}^{n-1}\sigma_j^2P_j^2}. \tag{13}$$

A similar equation for the diagram in Fig. 1,b is of the form:

$$k=2\pi\lambda_D R/i_{mR}\sqrt{{}^1/_9\left(\delta-\sum_{1}^{m}\Delta_{ci}-\sum_{m+1}^{n-1}M_iP_i\right)^2-\sum_{m+1}^{n-1}\sigma_j^2P_j^2}. \tag{14}$$

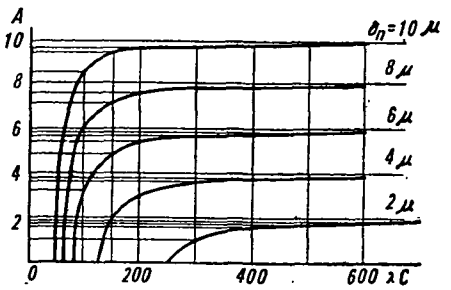

Fig. 2. Determination of limiting error of measurement.

An analysis, of the fundamental sources of errors of automats with photoelectronic devices has made it possible to establish a common number n of primary errors of these devices, having maximum values and also to calculate the induction coefficients P_i.

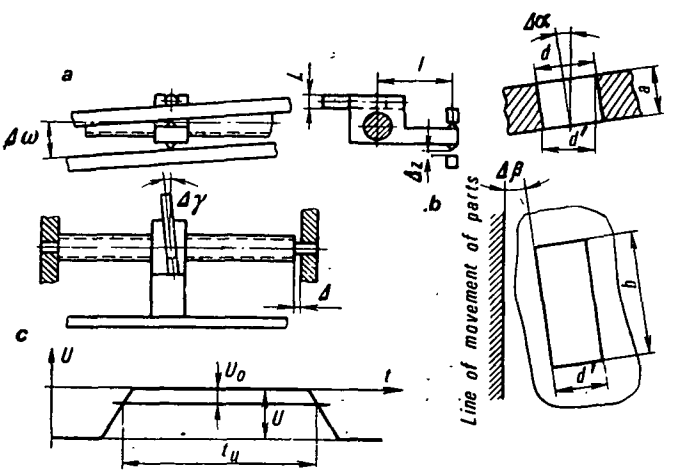

Fig. 3. Determination of induction coefficients of primary errors of the device.

General expression for the equation of accuracy of the automat, which checks linear dimensions and is constructed according to the diagram on Fig. 1,a is written as:

$$\Delta L = P_1\Delta h_c + P_2\Delta h_\Sigma + P_3\Delta\omega + P_4\Delta_3 + P_5\Delta_M + P_6\Delta\gamma^2 + P_{7,8}(\Delta\varphi_2 - \Delta\varphi_1) + P_3\Delta\alpha + P_{10}\Delta\beta, \quad (15)$$

where induction coefficients are equal to:

$$P_1 = 1; \quad P_2 = L/D; \quad P_3 = hL/2\pi l; \quad P_4 = h/2\pi l; \quad P_5 = 1; \quad P_6 = L/2;$$
$$P_{7,8} = h/\pi m z_2; \quad P_9 = \xi_A d/\mu_0(2u_0/u - 1); \quad P_{10} = \xi_B d/\mu_0(2u_0/u - 1);$$

where Δh_0—cyclic error of the pitch of the screws;
Δh_Σ—accumulated error of the pitch of the screw for a length D;
l—distance from the axis of rotation of the screw up to the point of contact of the tail of the nut with the guides (see Fig. 3,a);
$\Delta\omega$—angle of inclination of the guides to the axis of the screw (see Fig. 3,a);
Δ_3—guaranteed fitting clearance of the tail of the nut of guides (see Fig. 2,a);
Δ_γ—angle of obliquity of the component in the setting fixture;
Δ_M—axial play of the screw in the bearings;
z_2—number of teeth in the driven gear;
$\Delta\varphi_1$, $\Delta\varphi_2$—errors of location of the driving and driven gears respectively;
d—width of the diaphragm of the optical system (Fig. 3,b);
μ_0—magnification of the photohead lens;
ξ_A, ξ_B—coefficients, defining the parameters of the diaphragm $\xi_A=a/d$; $\xi_B=B/d$;
a—thickness of the diaphragm;
B—length of the diaphragm;
$\Delta\alpha$—angle of obliquity of the axis of the diaphragm of the optical system;
$\Delta\beta$—angle of inclination of the diaphragm to the direction of motion of the job;
u—full output voltage of the photomultiplier;
u_0—output voltage of the photomultiplier at the start of counting impulses (Fig. 3, c).

Error of discreteness does not figure in the equation (15) because of the above mentioned reasons.

Data of the accurate calculation of the device, used for measuring the jobs of cylindrical form of small diameters ($L\approx 2$ mm) and based on the diagram of Fig. 1,a is given in Table 1. Selection of α_i and δ_i is based on [5].

Calculations reveal the importance of manufacturing error of the screw among other forms of errors. Accuracy of devices made according to other diagrams (see Fig. 1,b and 1,c) are calculated similarly.

3. Method of Selection of Parameters of Automats for Measuring Linear Dimensions

Basic data for the design of automats for checking linear dimensions are:

1) efficiency Q, pieces/min;
2) range of measurement or checking $L_{min}-L_{max}$, mm;
3) maximum permissible error of measurement in the given range, δ, micron.

Table 1. Data for the calculation of the accuracy of devices for measuring components of small diameters

Primary error		Induction coefficient		Coefficient of relative asymmetry, α_j	Relative mean square deviation, λ_j	Coordinates of the middle of the tolerance zone Δ_{0j}, mm	Half of the tolerance zone δ_j, mm	Mean value of the deviations M_j, mm	Mean square deviation σ_j, mm	σ_j^2, $\times 10^4$ mm^2	$\sigma_j^2 P_j^2$, $\times 10^8$ mm^2
Symbol	Absolute value, mm	Expression	Numerical value								
Δh_c	0.003	P_1	1	−0.28	0.38	0	0.003	−0.00084	0.00114	0.013	130
Δh_Σ	0.005	L/D	0.12	−0.28	0.38	0.0025	0.0025	0.0018	0.00095	0.009	1.3
Δ_ω	0.0002	$hL/2\pi l$	0.006	−0.28	0.38	0	0.0002	0.000056	0.000066	0.000044	0.00001
Δ_3	0.044	$h/2\pi l$	0.002	0	0.33	−0.006	0.022	−0.006	0.0073	0.53	0.02
Δ_ω	0.001	P_5	1	0	0.33	0	0.001	0	0.0003	0.0009	9
$\Delta\gamma^2$	0.0002	$L/2$	1.5	0	0.33	0	0.0002	0	0.000066	0.000044	0.99
$\Delta\varphi_1$	0.035	$h/\pi m z_2$	0.0035	−0.28	0.38	0.0175	0.0175	0.0127	0.007	0.49	0.06
$\Delta\varphi_2$	0.070		0.0035	−0.28	0.38	0.035	0.035	0.0252	0.013	1.69	0.17
$\Delta\alpha$	0.017	$\xi_A d/\mu_0(2U_0/U-1)$	0.001	0	0.33	0	0.017	0	0.0056	0.31	0.0031
$\Delta\beta$	0.017	$\xi_B d/\mu_0(2U_0/U-1)$	0.012	0	0.33	0	0.017	0	0.0056	0.31	0.447

REMARKS: $M_\Sigma = -0.00046$ mm $+\Delta_c = -0.00046 + 0.00033 = -0.00013$ mm $= -0.13$ micron; $3\sigma_\Sigma = \pm 0.00345$ mm $= \pm 3.45$ micron; $M_\Sigma \pm 3\sigma_\Sigma = -0.13 \pm 3.45$ micron. Systematic error $\Delta_c = d/M_0(2U_0/U-1)$ is calculated with $U_0 = 1$ volt; $U = 1.5$ volt.

Instead of the range of measurements, $L_{\min}$ to $L_{\max}$ and permissible error of measurement δ, the relative error may be given:

$$P_L = \Delta L \cdot 100\%/L.$$

It is required to select the kinematic scheme of the automat and the basic kinematic parameters n_D, h, i_{ms}, k for the diagram in Fig. 1,a. This problem is solved in the following sequence:

1. On the basis of the initial data and taking into consideration equations (3), (6), (5), (7) and (9), the suitability of the selected scheme of the drive is evaluated.

2. For the given (range) $L_{\min} - L_{\max}$ and using the condition of location of feeders, the outgoing conveyor, etc. coefficient ε is determined.

3. From equations (3) and (6) or making use of the diagram given in Fig. 4 and from the known values of Q and L_n, n_D, h and i_{ms} are selected.

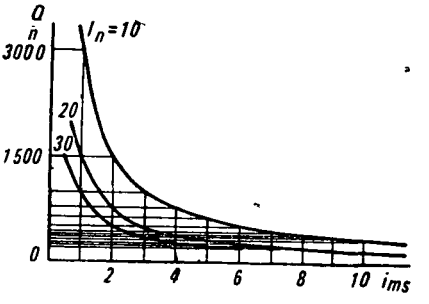

Fig. 4. Nomogram for selecting i_{ms} from δ.

The rpm of the motor n_m and pitch of the screw h is determined on the basis of the general evaluation of the device; n_m is calculated from the consideration of obtaining minimum size, power, cost and absence of special requirements from the driven mechanisms (design of movable supports, "pulsations" of the shafts, balancing of rotors, etc.).

The pitch of the screw is selected so as to obtain the minimum transmission ratio of the reduction gear and suitable manufacturing accuracy from cost considerations.

4. On the basis of equations (10)-(15) and table, precise calculation of the schematic diagram of the device is carried out. During this phase, a number of parameters characteristic of the design of the different units of the device and specifications of the optical and electronic units are determined. Calculations may be made a number of times with consecutive correction in the tolerances of different units, if instrumental error, determined from the table, exceeds the maximum permissible error of measurement.

5. From equations (13) and (14), number of holes in the disc of the generator of counting impulses is determined.

4. Special Features of the Design of Automats for Checking and Measuring Area

Machines and devices for measuring area and based on the photoelectronic numerical impulse method are described in [1-2]. They are based on the calculation of the number of impulses of a special generator on gradual luminous development of the area. Efficiency of the device for measuring area is expressed as:

$$Q=k_A F/t,\ \text{m}^2/\text{sec}, \tag{16}$$

where F—area of the luminous development;
t—time of measurement, sec;
k_A—coefficient of utilization of the area;

We determine F and t while measuring according to Fig. 5.

$$F=A_c X, \tag{17}$$

where A—length of scanning (see Fig. 5);
X—maximum value of the abscissa of the figure to be measured, when the axes are placed, as shown in Fig. 5;

$$t_0=t_c+t_m, \tag{18}$$

where t_0—time of a single measurement;
t_c—time of a single scanning run;
t_m—time spent in the displacement of the figure being measured, by one pitch ΔX along *ox* axis.

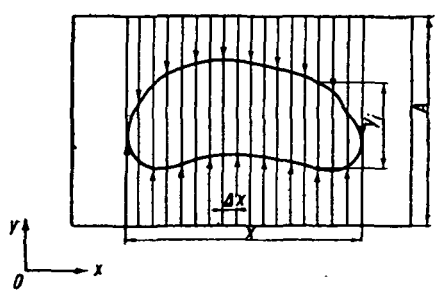

Fig. 5. Diagram of photoelectronic measurement of area.

Let us take:

$$t_m=\mu t_c, \tag{19}$$

where μ—coefficient which determines the relationship between the time of scanning and the time of displacement for pitch ΔX.

Then

$$t=(1+\mu)NA/V, \text{ sec}$$

or

$$t=(1+\mu)NA/3.6\times 10^3 V, \text{ hours}, \tag{20}$$

where N—number of measurements, equal to the number of runs of the scanning device.

In this case,

$$Q=3.6\times 10^3\times k_A XV/(1+\mu)N, \text{ m}^2/\text{hour}. \tag{21}$$

If the kinematic diagram of the drive of the scanning device corresponds to the diagram of Fig. 1,a then we have:

$$Q=0.6\times 10^2\times k_A Xn_m h/i_{ms}(1+\mu)N, \text{ m}^2/\text{hour}. \tag{22}$$

For the selection of the basic parameters of the device, for measuring the area, it is necessary to add to equation (22), the expression for the determination of the value of one impulse:

$$C=h\Delta x/ki_{ms}. \tag{23}$$

Expression for the calculation of the number of measurements N, in general case will be:

$$N=f[P_{aF}],$$

where P_{aF}—error of the approximation of the curve, which confines the given figure.

On the basis of the equations (22) and (23) the most expeditious method for the determination of the basic parameters of the given device may be worked out. Earlier, during the selection of the basic parameters of the device for the determination of linear dimensions, number of parameters exceeded the number of equations and some parameters were selected on the basis of general evaluation (n_m, h).

This guarantees the solution of a similar problem while designing a device meant for the measurements of areas, regardless of the fact that here it is necessary to satisfy more conditions.

References

1. Sklyadnev, B. N. Analiz i sintez fotoelectronnoi mashiny dlya izmereniya ploshchadei ploskikh figur (Analysis and Synthesis of Photoelectronic Machines for the Measurement of Areas of Plane Figures). Kandidatskaya dissertatsiya, Moscow, 1958.

2. SKLYADNEV, B. N., B. N. YURUKHIN and YU. I. EVTEEV. Sintez electronno-mekhanicheskikh ustroistv dlya avtomaticheskogo beskontaktnogo opredeleniya geometricheskikh parametrov ploskikh figur (Synthesis of Electronic-mechanical Devices for Automatic Noncontacting Determination of Geometrical Parameters of Plane Figures). Sbornik *Mekhanika mashin*, No. 3-4, Izd-vo Nauka, 1966.
3. BRUEVICH, N. G. Tochnost' mekhanizmov (Accuracy of Mechanisms). Moscow-Leningrad, GITTL, 1946.
4. BORODACHEV, N. A. Obosnovanie metodiki rascheta dopuskov i oshibok razmernykh i kinematicheskikh tsepei (Basis of the Method of Calculating Tolerances and Errors of Dimensional and Kinematic Chains). Parts I and II, Izd-vo AN SSSR, 1943, 1946.
5. KOROTKOV, V. P. and B. A. TAITS. Osnovy metrologii i tochnosti mekhanizmov priborov (Fundamentals of Metrology and Accuracy of Mechanisms of Instruments). Mashgiz, 1961.

L. P. Storozhev

A NOMOGRAPHICAL METHOD FOR THE SYNTHESIS OF MULTIPLE CONTOUR PLANE HINGED-LEVER MECHANISMS

In this article, some kinematic and dynamic properties of slider-crank mechanisms are discussed and systematization carried out. Charts of functions of its displacement and velocities are described. The kinematic diagram of a device for the analysis and synthesis of flat-guide hinged-lever mechanisms is constructed. Nomographical method of synthesis of a few types of multiple link plane hinged-lever mechanisms with one degree of mobility is investigated through two numerical examples. Solutions of these problems develop the nomographical method of synthesis of plane transmission and flat guides hinged-lever mechanisms [1-3].

1. Systematization, Properties and Charts of the Slider-Crank Mechanism

Systematization, properties and charts of the displacement and velocity functions of the hinged four-link mechanism are given in reference [2]. Similar problems may be solved for the slider-crank mechanism, if we assume the following symbols:

r—length of the driving link A_0A, taken as the unit link;

l—relative length of the connecting rod AB;

a—relative length of the axial, measured from the support A_0 with positive sign upward and negative sign downward;

xA_0y—cartesian system of coordinates; the abscissa is directed toward the right from the support A_0 and is parallel to the guides of the slider and the ordinate is directed upward;

x—abscissa of point B;

φ and β—angles, measured from the positive direction of the abscissa

in the counter clockwise direction which determine the position of links A_0A and AB;

α_1 and α_2—acute angles, measured from the connecting rod AB in the counter clockwise direction which give the directions of velocity vectors of points A and B.

Slider-crank mechanism is formed by the combination of conventional mechanism V and I [2]. Some features of this mechanism may be found out by superimposing on each other the geometrical positions of free elements of conditional mechanisms with different dimensions of the mechanism. According to these features, all slider-crank mechanisms are divided into three groups, each of which has a specific number of variants depending on the relative position of links.

Number of variants and types of motion of links for each group of slider-crank mechanisms are given in Table 1.

Table 1. Variants of execution and types of motion of the slider-crank mechanisms

No.	No. of executions	Types of motion of links		
		link A_0A	connecting rod AB	slider B
I	4	Oscillating rotary motion with respect to the axis, inclined at an angle to the axis A_0x	Plano-parallel motion, in whose rotary motion, connecting rod performs complete rotations	Linear-oscillatory motion with respect to the point, that does not coincide with the support A_0
II	2	Oscillating rotary motion with respect to the axis	Plano-parallel motion, in whose rotary motion, connecting rod performs complete rotations	Linear-oscillatory motion with respect to the support A_0
III	4	Rotary motion	Plano-parallel motion in whose rotary motion, connecting rod oscillates with respect to an axis inclined to axis A_0x	Linear-oscillatory motion with respect to the point, that does not coincide with the support A_0

From the same geometrical positions, boundaries of existence of all the three types of slider-crank mechanisms are determined.

Boundaries of these regions are shown by thick lines in Fig. 1, which are designated respectively as *I, II, III* for mechanisms with positive values of the axial a and I', II', III'—for mechanism with the negative values of the axial a.

Zones confined and divided by thick lines A, B, C, D and E correspond to five types of limiting slider-crank mechanisms.

Mechanisms of line A belong to the first type. In these mechanisms, links A_0A and AB are stretched into a straight line when angles φ and β take values 0° and 180° and are equal to each other or differ from each other by 180°.

Mechanisms corresponding to lines B belong to the second type. In these mechanisms, links A_0A and AB are along a straight line if angles φ and β take values 90° and 270° and differ from each other by 180°.

Mechanism situated at the point K will belong to the mechanisms of third type. These mechanisms are characterized by the property that links A_0A and AB stretch into a straight line when angles φ and β are equal to 0, 90°, 180° and 270° and are equal between themselves or are different by 180°, links A_0A and also AB can rotate as a single link when points B and A_0 coincide. Lines D have a structure which we conventionally consider as limiting-slider-crank mechanisms of fourth type with infinitely small length of the connecting rod AB. Similarly, structures and not mechanisms correspond to lines E, which we consider as a limiting slider-crank mechanisms of 5th type with the axial that differs from the sum of the lengths of the links A_0A and AB by an infinitely small value.

This convention makes it possible for us to investigate the limiting mechanisms of the 4th and 5th types.

Points for mechanisms with the following dimensions (Table 2) are marked by circles with numbers in Fig. 1.

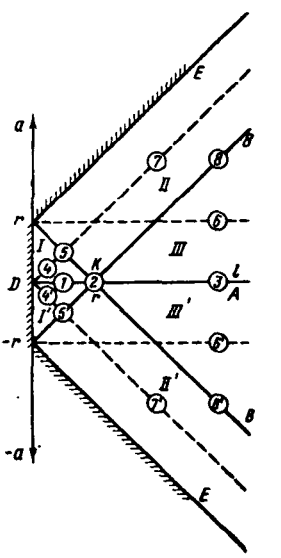

Fig. 1.

Table 2. Relative dimensions of slider-crank mechanisms

No. of mechanism	Relative dimensions		No. of mechanism	Relative dimensions	
	l	a		l	a
1	0.5	0	5	0.5	±0.5
2	1	0	6	3	±1
3	3	0	7	2	±2
4	0.25	±0.25	8	3	±2

REMARKS: For mechanisms 1-8 $r=1$.

These mechanisms along with all the limiting mechanisms of 4th and 5th types are investigated with the help of nomograph [1].

From the results of the analysis, 5 charts of displacement function are constructed:

$$\beta=\beta(\varphi),\ x=x(\varphi),\ \alpha_1=\alpha_1(\varphi),\ \alpha_2=\alpha_2(\varphi) \text{ and } \alpha_2=\alpha_2(\alpha_1).$$

A number of kinematic and dynamic properties of slider-crank mechanisms may be investigated by an analysis of these charts. A few of these are given below:

1. Charts of the displacement function $\alpha_2=\alpha_2(\alpha_1)$ of the slider-crank mechanisms, superimposed on the chart of velocities [1] represents the chart of velocities of this mechanism.

2. Each slider-crank mechanism with different variants of execution reproduces identical displacement and velocity functions.

3. For every monotonic change in the dimensions of mechanisms within the limits of each of the three fields of its existence, there occurs a monotonic change in the graphs of the displacement and velocity functions. When those dimensions are reached, which correspond to the limiting mechanisms, then all graphs of displacement and velocity functions change discontinuously.

4. For all the slider-crank mechanisms, under investigation (including limiting mechanisms of 4th and 5th type), extreme values with respect to the dimension x, angles φ, β, α_1 and α_2 and ratios of velocities $m_1=v_B:v_A$ and $m_2=v_{BA}:v_A$ have different values.

For the sake of brevity, extreme values of these quantities for only 3 mechanisms are given in Table 3.

5. For every monotonic change of dimensions of the mechanism within the limits of each region, there corresponds a monotonic change of extreme values of all quantities given in Table 3. When these dimensions are achieved for limiting mechanisms, then all these quantities change non-discontinuously.

6. Corresponding to the dotted lines starting from the origin of coordinates (see Fig. 1), there are slider-crank mechanisms whose links can be so located that at angle $\varphi=0°$, 180° and 360°, angle β takes the value 90° and 270°. Corresponding to the dotted lines parallel to abscissa there are slider-crank mechanisms whose links can be so located that at angle $\varphi=90°$, 270°, angle β takes value 0°, 180° and 360°. The point of intersection of these lines will represent slider-crank mechanism for which, angles φ and β take all these values.

However, all these mechanisms are not the limiting ones, because these are not characterized by an abrupt change in graphs of displacement and velocity functions.

7. For investigating those slider-crank mechanisms which do not have graphs on these charts, new graphs may be constructed on these charts by proportional interpolation between dimensions of mechanisms of one region or lines and coordinates of their graphs (see Fig. 1).

These data about systematization, properties and charts are the reference material which may be used for the study and design of all slider-crank mechanisms.

Table 3. Extreme values of relative dimensions, angles and of ratios of velocities of the slider-crank mechanisms

No. of the mechanism	Type of execution	Extreme values of the quantities						
		φ^0	x	β^0	α_1^0	α_2^0	m_1	m_2
1	*a*	330; 30	0.5; 1.5	0; 360	−90; 90	−90; 90	$-\infty;\infty$	$-\infty;\infty$
	b	150; 210	−0.5; −1.5					
2	*a*	0; 360	−2; 2	0; 360	−90; 90	−90; 90	$-\infty;\infty$	$-\infty;\infty$
	b	0; 360	0		90	—	0	1
3	*a*	0; 360	2; 4	340; 20	−90; 90	−19; 19	−1.07; 1.07	−1; 1
	b	0; 360	−4; −2	160; 199				

2. Apparatus for Drawing Connecting Rod Curves

Connecting rod curves of a number of plane mechanisms have applications in engineering. In many of these the required curve is generated by some point C of the connecting rod AB which performs plano-parallel motion and forms a rotating pair with the rotating link A_0A. From such mechanisms, let us separate imaginary mechanism A_0AC, which will conventionally form the mechanism V[2]. In this conventional mechanism let us take link A_0A as the unit link and let us designate the relative dimension of AC as $l=AC : A_0A$ and angle $CAB-\Theta$.

We adopt the same system of measuring angles as in the case of slider-crank mechanism. Then the displacement function $\beta'=\beta'(\varphi)$ for the link AC of the conventional mechanism will remain the same as the displacement function $\beta=\beta(\varphi)$ for the connecting rod AB, but these functions will differ from each other by a constant angle Θ. These assumptions form the basis of calculation of the kinematic diagram of the apparatus which is designed for drawing the connecting rod curves according to the given function $\beta=\beta(\varphi)$ and for drawing the graph $\beta'=\beta'(\varphi)$ as per the connecting rod curve.

Kinematic diagram of the mechanism of the device is shown in Fig. 2.

Let us imagine that this mechanism is divided into two independent mechanisms: a differential gear mechanism which solves the problem of compensation and the mechanism of coordinator. The driving link of the first mechanism is the pin E with the slider *5*, plate *4* and gear *3*. Let us move slider along plate for setting and adjusting the dimension l and rotate the plate with respect to gear *3* for setting and adjusting the angle β'.

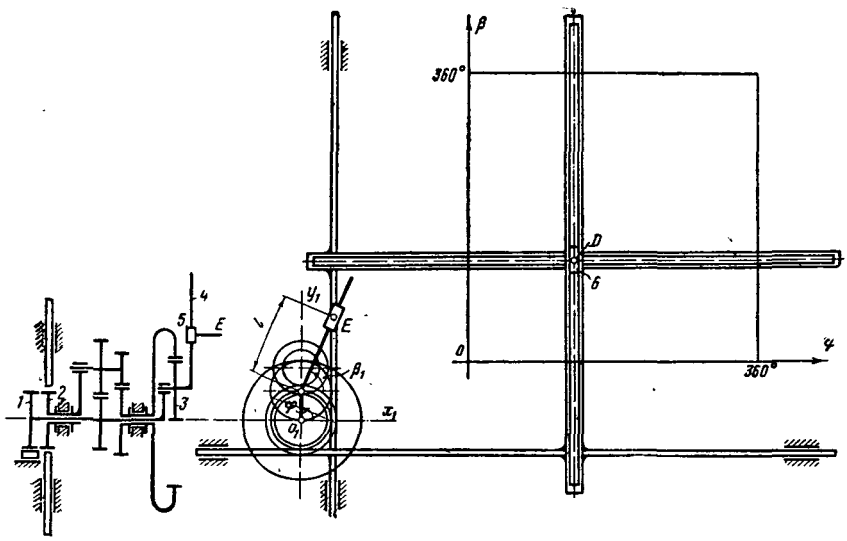

Fig. 2.

Number of teeth of the gears may be taken as follows:

$$z_4=z_5=z_{12}=43,\ z_7=20,\ z_{7'}=12,\ z_8=40,\ z_9=48 \text{ and } z_{10}=86.$$

Their modules of meshing may assume any value but it will be definitely similar for all the gears and radii of the pitch circles of gears *1*, *2* and *3* will be equal to the length of the unit link of the imaginary mechanism. Moreover, the value of the module determines the stroke of the slider of the coordinator and hence determines the dimensions of the chart.

For example for module $m=1$ mm, charts have dimensions 135×135 mm, at $m=2$ mm it is 270×270 mm, etc. At the same time, length of the link A_0A must be respectively equal to 21.5 mm, 43 mm, etc. Driving link of the coordinator is pin D with the slider *6*.

For drawing the connecting rod curve from the chart of the function $\beta=\beta(\varphi)$, it is necessary to place the chart on the apparatus in such a way so that their coordinate axes coincide. Set dimension l and angle β' of the given mechanism on the apparatus and draw its graph by the pin D. Then pin E will draw the required connecting rod curve. For drawing other connecting rod curves of the same mechanism, we change the dimension l

or angle β' and draw the same graph. Thus we can draw the whole group of connecting rod curves of any hinged four-link mechanism, slider-crank, quick-return, and of other fundamental and multiple link mechanisms which contain conventional mechanism *V*.

For drawing the graph of function $\beta'=\beta'(\varphi)$ as per the given connecting rod curve, it is necessary to draw this curve with a pantograph in accordance with the link of unit length, determine its position with respect to the axes $x_1O_1y_1$ of the apparatus, set the dimension l and then draw the given curve with the pin E. Then pin D will draw the required graph.

It is clear from the above statement that for any given connecting rod curve, a number of graphs may be made which may be used for the selection of guiding mechanisms according to charts.

Consequently, the above mentioned apparatus considerably simplified the solution of problems of synthesis and analysis of plane guiding hinged lever mechanisms by approximate methods.

3. Nomographical Method of Synthesis of Multiple Contour Plane Hinged Lever Mechanisms

Existing charts of displacement and velocity functions for the hinged four-link mechanisms [2], nomograph and chart of velocities of plane four-link mechanisms [1], atlas for the kinematic calculations of slider-crank mechanisms [4] and those described in this article charts of position and velocity functions of slider-crank mechanisms, apparatus for drawing the connecting rod curves and other auxiliary and reference material provide the nomographical method of analysis and synthesis of transmitting and guiding plane basic mechanisms with one degree of mobility.

So far the problem of compilation of similar material for all plane-hinged lever mechanisms has not been attempted.

However, existing material proved to be sufficient for solving the problems of synthesis and analysis of a whole family of plane multiple-link mechanisms by the nomographical method. Mechanisms which are classified into plane basic mechanisms with one degree of mobility and conventional mechanisms of first and second class, belong to the category of these mechanisms.

Let us term all such mechanisms as multiple contour plane hinged-lever mechanisms with one degree of mobility. The synthesis of these mechanisms by the nomographical method is given below through two numerical examples.

Example 1. Select according to the charts, plane hinged-lever mechanism with one degree of mobility whose working cycle corresponds to two revolutions of the driving link rotating uniformly, for which the driven link performs reciprocating motion, and during one rotation of the driving link, the driven link nearly moves with constant velocity.

It is quite evident that not even a single one of the basic mechanisms can generate the given motion. That means that the required mechanism must be multiple contour and in the simplest case must be a six-link mechanism formed by connecting conventional mechanism of the second class to the basic mechanism.

A study of such mechanisms reveals that the plane mechanism, shown in Fig. 3 can approximately generate the given motion.

This mechanism can be separated into two basic mechanisms; a hinged four-link A_0ABB_0 and slider-crank mechanism B_0CD. The problem of synthesis for each one of the basic mechanisms must be formulated separately.

According to the given condition of the problem let us write the given displacement function for the whole of the mechanism approximately:

$$k(x-x_0)=\varphi-\varphi_0\,, \tag{1}$$

where, φ_0 and x_0—initial data;

$\varphi-\varphi_0$—angular displacement of the driving link A_0A;

k—constant coefficient of proportionality;

$x-x_0$—relative displacement of the driven slider D.

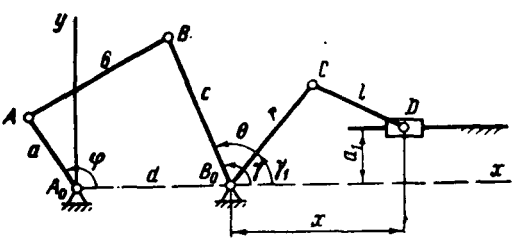

Fig. 3.

This function must be considered as a complex one, which can be assumed to be made of two functions, which are the given displacement functions for each basic mechanism separately. Then for the slider-crank mechanism we can write the equation:

$$x-x_0=x\,(\varphi_1), \tag{2}$$

and for the hinged four-link mechanism:

$$\gamma=\gamma(\varphi-\varphi_0), \tag{3}$$

where $\varphi_1=\gamma-\Theta$.

Let us express the given velocity function for the whole of the mechanism in the following form:

$$v_D : v_A=\text{const.} \tag{4}$$

There is no need of working out the velocity function for the basic mechanisms. During the selection of basic mechanisms according to chart, approximation functions are the graphs of displacement and velocity functions drawn on those very charts. However, it is not possible to determine functions (2) and (3) by function (1) and the additional conditions. That is why the graph of the approximation function of displacement of one of the basic mechanisms must be selected by the additional constraint. Then according to the given function (1) and the selected graph of the approximation function, we draw the graph of the given displacement function for the second basic mechanism.

At the same time it must be taken into consideration that a great number of graphs of the given displacement function for the slider-crank mechanism may be drawn according to the selected graph of approximation function of displacement of the hinged four-link mechanism, but only one graph of the given function of displacement of the hinged four-link mechanism may be drawn according to the selected graph of approximation function of displacement of the slider-crank mechanism.

Proceeding from this, we select the hinged four-link mechanism with relative dimensions as $a=1$, $b=d=2$ and $c=3$ in conformity with the charts of displacement function $\gamma=\gamma(\varphi)$. By its characteristic functions this mechanism satisfies the additional constraint formulated in the problem. This mechanism belongs to the limiting hinged four-link mechanisms of first type.

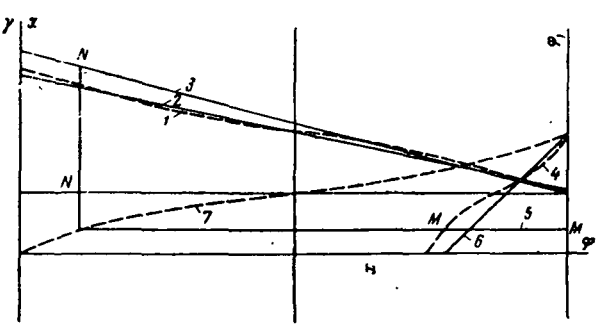

Fig. 4.

Its relative dimensions satisfy the following relationships:

$$\begin{aligned} &a=b-c+d;\\ &a<c+d-b;\\ &a<b+c-d. \end{aligned} \tag{5}$$

In this mechanism, one complete oscillation of the rocker arm B_0B corresponds to two rotations of the crank A_0A. At $\varphi=0°$ and $\gamma=180°$, all

the links are in a straight line. During motion of the rocker arm B_0B in one direction, crank A_0A completes more than one revolution and during its motion in the other direction, crank A_0A completes less than one revolution. In the first case ratio of velocities $m_1=v_B : v_A$ is nearly unity and in the second case it exceeds this value considerably. All this is determined from the charts of hinged four-link mechanisms.

In Fig. 4, where

$$1-k'(x-x_0)=\varphi-\varphi_0\,;$$
$$2-k_1(x-x_0)=\varphi-\varphi_0\,;$$
$$3-k(x-x_0)=\varphi-\varphi_0\,;$$
$$4-(x-x_0)=x(\varphi_1)\,;$$
$$5-MM=MN\,;$$
$$6-x=x_0=x'(\varphi),$$

is shown the graph of function $\gamma=\gamma(\varphi)$, (curve 7) of the hinged four-link mechanisms and graph of the given function (1) for any value of coefficient k (all constructions must be done in the same scale as that of chart).

According to these graphs as shown in Fig. 4, a graph of the given function (2) for the slider-crank mechanism is made, and as per additional kinematic and dynamic conditions, a slider-crank mechanism is selected from these charts.

Thus after a thorough investigation of charts, a known limiting slider-crank mechanism of the 31st type is selected with the relative dimensions $r=1$, $l=3$ and $a=0$. This mechanism approximately generates the given function in the region $\varphi_{10}=41°$ to $\varphi_1=119°$.

The graph of the approximation function of displacement $x-x_0=x'(\varphi_1)$ is shown in the same figure. From the data obtained for the approximation function of displacement of basic mechanisms, a graph of the displacement function $k'(x-x_0)=\varphi-\varphi_0$ for the whole of the mechanism is drawn according to the known sequence. From this graph, a graph of the given function $k_1(x-x_0)=\varphi-\varphi_0$ is made keeping in mind the averaging of the deviations of the approximation function. Coefficient of proportionality k_1 and the modulus of maximum deviation of the approximation function (which compared to the given one does not exceed 1%) are determined.

Approximate function of velocity for the whole of the mechanism is expressed in the following form:

$$m=v_D/v_A=(B_0C/B_0B)m_1'm_1'', \qquad (6)$$

where $m_1'=v_B : v_A$, $m_1''=v_D : v_C$—ratios of velocities which are taken from the chart of velocities of the hinged four-link mechanism and of the slider-crank mechanism for a number of positions of the whole of the mechanism.

Ratio $B_0C : B_0B$ is selected in this manner: the dimensions of the hinged four-link mechanism can be arbitrary but they must satisfy the values of the relative dimensions, *a, b, c, d* which have been selected already and determine the dimension B_0B; dimension B_0C is determined from the absolute given value of the stroke of the slider *h* and from the relative value of this stroke $x_{max}-x_0$, which is determined from the chart and is 1.24 in the given example, i.e.

$$B_0C=h/(x_{max}-x_0). \tag{7}$$

Modulus of maximum deviation of the approximate function of velocity from the given one is calculated according to formula:

$$L=2(m_{max}-m_{min})/(m_{max}+m_{min}). \tag{8}$$

In this case, its value is 20%.

From the example it is clear that corresponding to the insignificant deviation of the approximation function of displacement with respect to the given one, there is a considerable deviation of the function of velocity with respect to the given one. This relationship is not incidental and it must be taken as a rule. Thus during the synthesis of mechanisms according to the given function of velocity, deviations with respect to the given function of displacement must be minimum.

From an analysis of charts of basic mechanisms it is clear that maximum approximation may be achieved by changing their kinematic parameters. For example, an increase in the relative dimension *l* causes a minor decrease of deviations. Variation of kinematic parameters of the hinged four-link mechanism (which must satisfy the relationship (5)) gives far better results. Best approximations are obtained after a number of trials and analysis of functions of deviations.

The above mentioned sequence of selection of mechanisms according to the charts shows that it can be used for all multi-contour mechanisms with one degree of mobility which are divided into the basic mechanisms with simultaneous consideration of different additional conditions of synthesis.

Example 2. Let us select a six-link mechanism (Fig. 5), which has link D_0D-crank and dwell, corresponding to angle $\varphi_1-\varphi_0=90°$ of rotation of the driving crank A_0A.

This mechanism may be separated into a hinged four-link mechanism $A_0AC'BB_0$, which is the fundamental guiding mechanism and a conventional one of second class $C'DD_0$. Let us formulate the problem of synthesis for each of these mechanisms separately.

In the given section $\varphi_1-\varphi_0$, point C' of the connecting rod *AB* of the hinged four-link mechanism approximately describes an arc of the circle

whose radius is equal to the length of the link CD. At the moment when the link D_0D stops, point D must nearly coincide with the center of curvature C of the connecting rod curve in the section of approximation.

This problem has multiple solutions and the most suitable may be selected from the condition of best approximation or according to the additional conditions which will be described below.

Let us consider the solution to this problem by using the above mentioned apparatus. For this we draw a number of concentric circles (Fig. 6) from any point D' as center and assume that these circles are drawn by a point C_1 of the conventional mechanism $A_{01}A_1C_1$ whose points A_{01}, A_1 and C_{12} respectively coincide with the points A_0, A and C of the hinged four-link mechanism A_0ACBB_0. Then with pin E of the apparatus (see Fig. 2), draw these circles with different dimensions of l and O_1D' and a number of graphs of displacement functions $\beta''=\beta''(\varphi'')$, which generate the conventional mechanism $A_{01}A_1C_1$. Theoretically infinite number of these graphs may be drawn, by this method.

Actually, free selection of the relative dimensions of l, O_1D' of the radius of the circle and the possibility of drawing circles with constant relative dimension $A_{01}A_1$, equal to the radius of the pitch circle of gear *1* of the apparatus makes it possible to change all the kinematic parameters of the mechanism under investigation and to draw the whole set of these graphs with this apparatus.

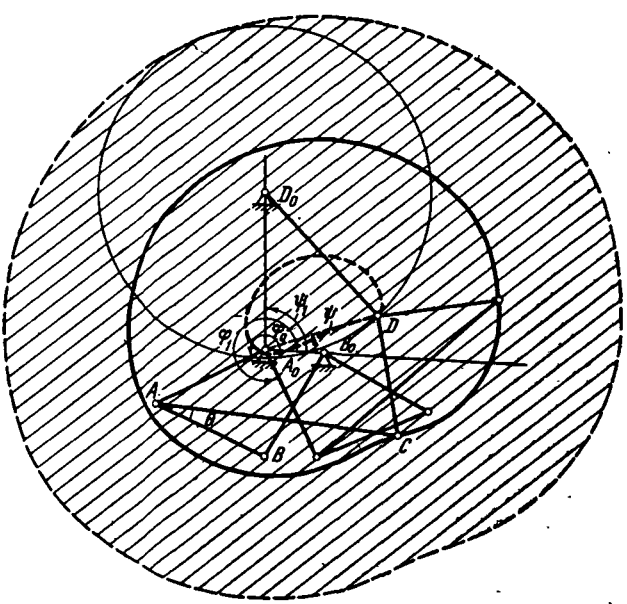

Fig. 5.

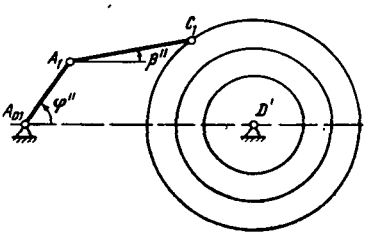

Fig. 6.

Graphs drawn by this method will be the graphs of the given displacement function for the hinged four-link mechanism A_0ACBB_0 [3]. If the point D' is considered stationary the formed figure $A_{01}A_1C_1D'$ is considered a hinged four-link mechanism whose chart of displacement function $\beta=\beta(\varphi)$ is already given.

Consequently, the selection of the dimensions of the figure under consideration is facilitated by this chart and the graphs of this, which are not shown in the chart, can be drawn quickly and simply by means of the apparatus. According to these graphs, the chart of function $\beta=\beta(\varphi)$ and the additional conditions, we may select both of the hinged four-link mechanisms.

Their relative dimensions will become the relative dimensions of the desired mechanism, which in the present case are: $a=b=c=2d=0.5l=d=1$. Positions of the links of the mechanism, corresponding to the section of approximation are given by the angles $\varphi_0=210°$, $\varphi_1=300°$, $\Theta=18°$ and $\psi=20°$.

Selection of the relative dimensions a_1, d_2 and the angle ψ_1 must be done according to additional conditions. One additional kinematic condition of the turning of the link D_0D is formulated in the problem. For this, we draw the connecting rod curve of the point C of the hinged four-link mechanism A_0ACBB_0 with the help of the apparatus, break up the mechanism at the kinematic pair D and draw the geometrical location (in Fig. 5 this place is shaded) of the possible positions of that free element of the pair D, which belongs to the link CD. Afterward, on this geometrical location we place geometrical location of the possible position of the other free element of the pair D in such a way that the latter touches the boundary limits of the former, as shown in the figure. By this we determine the required values $a_1=1.4$; $d_2=1.3$ and $\psi_1=93°$. An analysis of the mechanism thus obtained reveals that the given kinematic condition has only one possible solution.

In the kinematic parameters of the six-link mechanism, determined by this method, dwell of the link D_0D exactly corresponds to the given section of approximation. Deviations have not been detected during graphical constructions.

From the examples analyzed, it is clear that with the application of different charts, nomographs and apparatus, i.e., with the application of the nomographic method, different problems of synthesis of many multiple contour mechanisms with one degree of mobility may be solved and at the same time additional conditions for their design should be taken into consideration.

References

1. Storozhev, L. P. Primenenie nomogramm dlya sinteza ploskikh chetyrekhzvennikov (Application of Nomographs for the Synthesis of Plane Four-link Chains). Sbornik *Teoriya mashin i mekhanizmov*, vyp. 103, Izd-vo Nauka, 1964.
2. Storozhev, L. P. Karty dlya analiza i sinteza sharnirnykh chetyrekhzvennikov (Charts for the analysis and synthesis of hinged four-link chains). *Izv. vuzov. Mashinostroenie*, No. 4, 1965.
3. Storozhev, L. P. Primenenie nomogrammy i kart dlya sinteza ploskikh napravlyayushchikh sharnirnykh chetyrekhzvennikov (Application of Nomographs and Charts for the Synthesis of Flat-guides of Hinged Four-link Chains). Sbornik *Mekhanika Mashin*, vyp. 3, 4, Izd-vo Nauka, 1966.
4. Artobolevskii, I. I. Atlas po kinematicheskomu raschetu krivoshipno-shatunnykh mekhanizmov (Atlas for Kinematic Calculation of Slider-Crank Mechanisms). Izd-vo AN SSSR, 1942.

B. S. Sunkuev

TECHNIQUES FOR SYNTHESIZING ADJUSTABLE LEVER MECHANISMS

Adjustable lever transmission mechanisms are in wide use in industrial machinery. However, there are no techniques of universal applicability to the synthesis of this class of mechanisms [1, 7].

The development of a universal method of synthesis of adjustable lever transmission mechanisms, which are in wide use in light industry has been undertaken in this article.

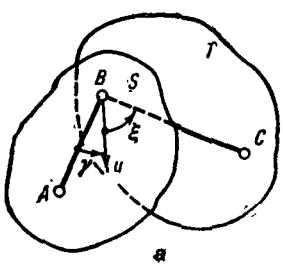

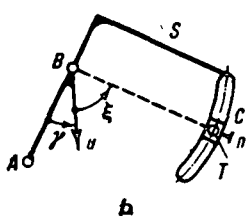

Fig. 1. Diagram of the adjustable link.

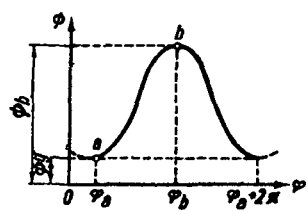

Fig. 2. Graph of the displacement function.

The diagram of an adjustable mechanism is shown in Fig. 3,a. Consider the regulated link *1* of this mechanism as a kinematic pair (Fig. 1,a). One of the links *S* of the pair carries on it a hinge *A* and the other link *T* carries hinge C_a. During operation a definite relative position of the links must be fixed in the adjustable link by forming a rigid connection in the kinematic pair.

For accomplishing the rigid connection in the pair AB_aC_a, one of the links, for example link *S* is made in the form of a crank with a slot, drawn in the form of an arc of a circle with the center B_a (Fig. 1,b) and the other

link T, in the form of a slide block fitted in the groove of this crank with a screw n.

For subsequent analysis let us represent the adjustable link by a straight line passing through A and B_a and rigidly connected with the crank. At the same time, let us represent the hinge B_a by a continuous circle to differentiate it from those hinges, which are not connected rigidly. Relative positions of the links S and T are determined by the angle ξ, which is the angle between an auxiliary line B_au, belonging to the crank and the line B_aC_a of the slider. The position of the line B_au with respect to line AB_a is fixed with the help of the angle γ.

Let us study the graph of displacement function of the transmission mechanism (Fig. 2). We should note that ordinates ψ_a and ψ_b of extreme points a and b of the graph show extreme positions of the driven link of the adjustable mechanism for the given adjustment, and abscissa φ_a and φ_b of these points determine the corresponding positions of the driving link. The abscissa φ_a and φ_b are denoted as phases of the extreme positions of the driven links.

In the subsequent analysis, the synthesis of only those swinging adjustable mechanisms are considered for which it is sufficient to determine the graph of the displacement function with coordinates φ_a, ψ_a, φ_b, ψ_b of extreme points a and b. It is assumed that the length of the graph between these points does not measurably impair the technological process being performed.

In this case, let us denote the coordinates of the extreme points a and b as characteristics of displacement function.

For the class of mechanisms being analyzed, regulation is undertaken to change one or few characteristics of the displacement function. In general with the change of one characteristic in the adjustable mechanism, all other characteristics change arbitrarily.

In the process of synthesis of adjustable mechanisms, it is necessary that as one characteristic is changed the other characteristics should change according to the given functional relationship or remain unchanged.

In addition, it is often necessary to establish the functional relationship between one of the characteristics and the angle ξ (see Fig. 1,b), i.e. to define the scale of regulation. If the above mentioned conditions are correlated with different characteristics of the displacement function, we are in a position to explore the problems of synthesizing adjustable mechanisms.

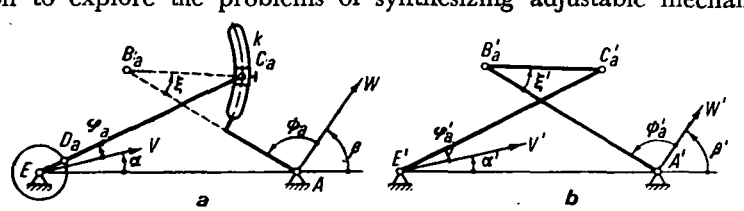

Fig. 3. Diagrams of the adjustable four-link and auxiliary mechanisms.

A general method for solving the above mentioned problems is given below. In order to illustrate this method, let us solve the following problem of synthesis of the adjustable swinging four-link mechanism ED_aC_aA, shown in Fig. 3,a in its dead center position. Let us measure the angle of rotation of the driving crank φ from the axis EV and angle ψ of rotation of the driven link from axis AW. The position of the axes EV and AW with respect to the support EA is given by angles α and β respectively. Let us denote the angles of rotation of the driving and the driven links in the dead center position by an index a.

During regulation, the following functional relationship is to be fulfilled:

$$\psi_a = F(\varphi_a) \tag{1}$$

in the given interval $[\varphi_a^0, \varphi_a^m]$.

Let us rigidly connect the links ED_a and D_aC_a of the mechanism in the position in which these are shown in the Fig. 3,a and establish the rigid connection between the links, contained in the adjustable link. As a result of this transformation, we get a new auxiliary hinged four-link mechanism $E'C_a'B_a'A'$ (Fig. 3). Parameters of the diagrams of the auxiliary and adjustable four-link mechanisms are related through the following equations:

$$E'C_a' = ED_a + D_aC_a; \tag{2}$$

$$C_a'B_a' = C_aB_a; \tag{3}$$

$$B_a'A' = B_aA; \tag{4}$$

$$E'A' = EA. \tag{5}$$

We select link $E'C_a'$ as the driving link in the auxiliary mechanism and select $E'V'$ and $A'W'$ as reference axes for angles φ_a' of the rotation of driving link and angles ψ_a' of rotation of the driven link. Positions of axes $E'V'$ and $A'W'$ with respect to the support $E'A'$ are found with the help of the angles α' and β'.

Let us consider these angles equal to:

$$\alpha' = \alpha; \tag{6}$$

$$\beta' = \beta. \tag{7}$$

Then the displacement function of the auxiliary mechanism will be identical to the relationship:

$$\psi_a = f(\varphi_a),$$

reproduced by the adjustable mechanism.

Parameters of the diagram of auxiliary four-link mechanism are determined from the condition of approximation of the displacement function to the given equation (1) in the given interval ($\varphi_0'^0=\varphi_a^0$, $\varphi_a'^m=\varphi_a^m$). Subsequently we get the parameters of the diagram of the required adjustable four-link mechanism from equations (2)-(7), in which the given equation (1) between the characteristics ψ_a and φ_a is approximately followed.

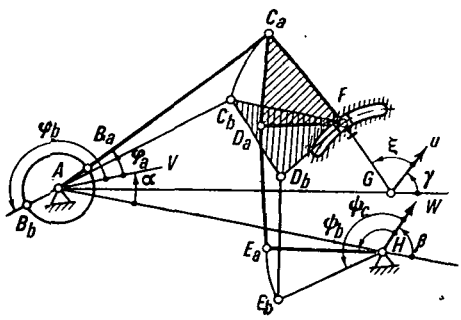

Fig. 4. Diagram of the adjustable six-link mechanism.

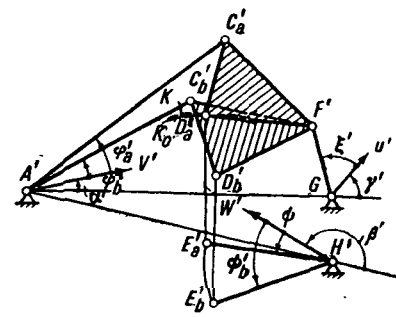

Fig. 5. Diagram of the auxiliary ten-link mechanism.

The essence of this method for solving the problems of synthesis of adjustable mechanisms is summarized below:

1) the given adjustable mechanism is transformed into an auxiliary non-adjustable mechanism, which reproduces the given function to the required constant degree of accuracy:

$$y=F(x) \tag{8}$$

in the given interval (x^0, x^m) where x and y are characteristics of the function of displacement or angle ξ;

2) a relationship is established between the parameters of the adjustable and the auxiliary mechanisms which allows to determine the parameters of the diagram of the adjustable mechanism completely or partially if parameters of the diagram of the auxiliary mechanism are known;

3) problem of the synthesis of the auxiliary non-adjustable mechanism is solved as per the condition of reproduction of the given relationship (8);

4) After determining the parameters of the diagram of the auxiliary mechanism on the basis of known equations, the parameters of the diagram of the adjustable mechanism are determined.

Calculation of the parameters of the diagram of auxiliary mechanism may be accomplished through known methods of the synthesis of lever mechanisms (8).

The following example illustrates that the synthesis of adjustable

mechanism according to the above mentioned method reduces to the correct selection of auxiliary mechanism.

One may be faced with the following problem in the design of conveyors for industrial processes: it is required to determine the parameters of the diagram of a six-link mechanism (Fig. 4), in which the swing of the driven link is regulated from 0 to the given value of ψ_{ab}. Coordinate of one of the extreme positions, for example ψ_a, and phases φ_a and φ_b remain unchanged during this:

$$\psi_a=\psi_1=\text{const}\,; \tag{9}$$

$$\varphi_a=\varphi_1=\text{const}\,; \tag{10}$$

$$\varphi_b=\varphi_2=\text{const}, \tag{11}$$

and angle ξ varies within the given limits (ξ^0, ξ^m).

Let us return to Fig. 4, in which the adjustable six-link mechanism is shown in the dead center positions. The angle of rotation φ of the driving link AB_a is measured from the axis AV, and the angle of rotation φ of the driven link is measured from the axis HW. We determine the position of the axis AV with respect to the support AG by angle α, and the position of the axis HW with respect to the support AH by angle β. Let us represent the hinges and angles φ and ψ in one of the dead centers of the mechanism with index a and in the other by index b.

Let us measure the angle ξ which affects the regulation, from the axis Gu, and the position of the latter (axis Gu) with respect to the support AG by angle γ.

Let us carry out the following transformation in the dead center a: we rigidly connect the links AB_a and B_aC_a and eliminate the rigid connection between the links FG and AG, contained in the adjustable link. As a result, we get a new mechanism $A'C'_aF'G'D'_aE'_aH'$ (Fig. 5).

Parameters of the diagram of this auxiliary mechanism are determined from the equations:

$$A'C'_a=AB_a+B_aC_a\,; \tag{12}$$

$$\Delta C'_aD'_aF'=\Delta C_aD_aF\,; \tag{13}$$

$$F'G'=FG; \tag{14}$$

$$D'_aE'_a=D_aE_a\,; \tag{15}$$

$$E'_aH'=E_aH\,; \tag{16}$$

$$\Delta A'G'H'=\Delta AGH. \tag{17}$$

By a similar transformation of the adjustable six-link mechanism in second dead center, we get second auxiliary six-link mechanism $A'C_b'F'G'D_b'E_b'H'$. Dimensions of the links of the latter will be the same as they were in the first auxiliary mechanism:

$$\Delta C_b'D_b'F'=\Delta C_a'D_a'F'\,; \tag{18}$$

$$D_b'E_b'=D_a'E_a'\,; \tag{19}$$

$$E_b'H'=E_a'H'. \tag{20}$$

Lengths of the links $F'G'$ and $A'G'H'$ are determined from the equations (14) and (17) and lengths of the link $A'C_b'$ from the equation:

$$A'C_b'=B_aC_a-AB_a. \tag{21}$$

We connect the auxiliary mechanisms in such a way that link $F'G'$ and hinges A' and H' are common in these. As a result of this we get a new auxiliary mechanism, a ten-link mechanism (see Fig. 5). Lengths of the links of the ten-link mechanism are determined from equation (12)-(21). In the auxiliary ten-link mechanism, we measure angles of rotation and φ_a', φ_b' of the rockers $A'C_a'$ and $A'C_b'$ from the axis $A'V'$, angles ξ' of the rotation of the rocker $F'G'$, from the axis $G'u'$. Positions of the axes $A'V'$ and $G'u$ with respect to the support $A'G'$ may be determined by angles α' and γ' respectively. Let us take these angles equal to:

$$\alpha'=\alpha\,; \tag{22}$$

$$\gamma'=\gamma. \tag{23}$$

Then displacement function of the auxiliary ten-link mechanism $\varphi_a'=f(\xi')$ will become the identity $\varphi_a=f(\xi)$, reproduced in the adjustable mechanism, while displacement function $\varphi_b'=f(\xi')$ of the same ten-link mechanism will be the relationship $\varphi_b-\pi=f(\xi)$ which is reproduced in the

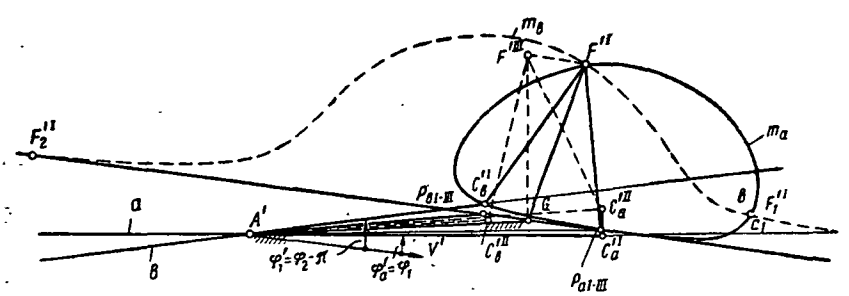

Fig. 6. Design of an auxiliary mechanism.

adjustable mechanism. From this it follows that if conditions (10) and (11) are fulfilled for adjustable mechanism, rockers $A'C_a'$ and $A'C_b'$ must remain stationary during the rotation of the driving link $F'G'$ in the corresponding auxiliary mechanism. As this is not possible, equation (10) and (11) cannot be satisfied exactly.

Let us consider the case when a variation, of φ_a and φ_b within the given limits $(\varphi_1, \varphi_1+\Delta\varphi_a)$ and $(\varphi_2, \varphi_2-\Delta\varphi_b)$ respectively, is allowed.

Approximate solution can be described in the form of the solution of synthesis of two four-link mechanisms $A'C_a'F'G'$ and $A'C_b'F'G'$. In these four-link mechanisms, supports $A'G'$ and the driven connecting rod $F'G'$ are the common elements and lengths of the cranks are equal, $C_a'F'=C_b'F'$.

The problem is defined as follows: In the first four-link mechanism, during its transition from first position $A'C_a'^{I}F'^{I}G'$ (Fig. 6) to second $A'C_a'^{III}F'^{III}G'$, to the rotation of the driving link $A'C_a'$ through an angle $\varphi_{aI-III}=\Delta\varphi_a$, must correspond the rotation of the driven link $F'G'$ by an angle $\xi'_{I-III}=\xi^M-\xi^0$; in the second four-link mechanism, during its transition from first position $A'C_b'^{I}F'^{I}C'$, to the second position $A'C_b'^{III}F'^{III}G'$, to the angle of rotation $\varphi_{bI-III}=-\Delta\varphi_b$ of the driving link $A'C_b'$ must correspond the similar angle, as in the case of first four-link mechanism, angle of rotation ξ'_{I-III} of the driven link $F'G'$.

The following design sequence may be suggested.

For the first four-link mechanism $A'C_a'F'G'$ with the given $\varphi_{aI-III}=\Delta\varphi_a$ and $\xi'_{I-III}=\xi^M-\xi^0$ we find pole P_{aI-III} of the finite rotation that corresponds to the position $A'C_a'^{I}$ and $A'C_a'^{III}$ of the driving link with respect to the first position $F'^{I}G'$ of the driven link (see Fig. 6).

Position of the reference axis $A'V'$ for angles φ'_a and φ'_b is selected arbitrarily. Line a—a, which lags behind the axis $A'V'$, by an angle φ_1 will give the geometrical position of the hinges $C_a'^{I}$. Giving any position to the hinge $C_a'^{I}$ on the line a—a and making use of the pole P_{aI-III} and angle:

$$\theta_{aI-III}/2=(\Delta\varphi_a-\xi'_{I-III})/2,$$

we get the position of the hinge F'^{I} of the driven link.

In a similar way for the given $\varphi_{bI-III}=-\Delta\varphi_b$, $\xi'_{I-III}=\xi^M-\xi^0$ and the same support $A'G'$, pole P_{bI-III} may be found out, which corresponds to the positions $A'C_b'^{I}$ and $A'C_b'^{III}$ of the driving link, with respect to the first position $F'^{I}C'$ of the driven link. Geometrical position of hinges $C_b'^{I}$ is determined by the line b—b, lagging behind from the axis $A'V'$ by an angle $\varphi_2-\pi$. If we have arbitrary positions $C_b'^{I}$ of hinge C_b' on the line b—b; then in general case we get a hinge F'^{I} which does not coincide with the similar one of the first mechanisms and the length of the link $C_b'^{I}F'^{I}$ is not equal to the length of the link $C_a'^{I}F'^{I}$ of the first four-link mechanism.

To avoid an arbitrary selection of the hinge $C_a'^{I}$ on the straight line a—a in the first mechanism and similarly the hinge $C_b'^{I}$ on the straight line b—b

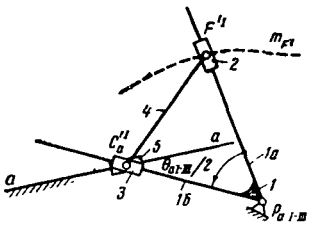

Fig. 7. Diagram of the mechanism for drawing the locii m_a and m_b.

in the second four-link mechanism, we find their positions for which hinges F'^{I} of the mechanisms coincide and lengths of the links C'_aF' and C'_bF' are equal to each other.

For this we draw the geometrical position of hinges F'^{I} for a set of such four-link mechanisms $A'C'_aF'G'$ in which conformity between the positions of the driving and driven links given by the angles φ_{aI-III} and ξ'_{I-III} is fulfilled; besides hinges C'^{I}_a lie on the straight line a—a and lengths of the connecting rods are equal to the given length l.

It may be noted that in the set of all the four-link mechanisms, connecting rods $C'^{I}_aF'^{I}$ are visible from the pole P_{aI-III} at an angle of Θ_{aI-III}. Let us take an auxiliary mechanism (Fig. 7) whose double-arm lever *1* rotates around P_{aI-III} and angle between the arms *1a* and *1b* is equal to $\Theta_{aI-III}/2$. Sliding blocks *2* and *3*, connected between themselves by the link *4* of the length l slide along arms *1a* and *1b*. A second block *5* is situated on the axis of the block *3* and this block *5* moves along stationary guides a—a. In this mechanism, upon the rotation of double arm lever arlund hinge P_{aI-III}, point F'^{I} traces the required locus hinges of the first four-link mechanism.

Subsequently, we draw the locus m_b of hinges F'^{I} of such four-link mechanisms $A'C'_bF'G'$, in which given conformity between the positions of the driving and driven links is fulfilled, hinges $C_b'^{I}$ lie on the line b—b, and lengths of connecting rods $C'^{I}_bF'^{I}$ are equal to l. For this, we make use of the same auxiliary mechanism (see Fig. 7) by putting the center of rotation of the lever *1* at the pole P_{bI-III} and by taking angle between the arms *1a* and *1b* equal to $\Theta_{bI-III}/2$ and by selecting line b—b as guide of the slider *5*. Point F'^{I} of the mechanism will trace the required locus m_b.

Curves m_a and m_b represent connecting rod curves of some slider-crank mechanisms [9] and are tricircular curves of fourth order, two such curves have up to 12 actual points of intersection. In Fig. 6, these curves intersect at three points: F'^{I}, F'_1, and F'^{I}_2. Let us select one of the points, for example F'^{I} as common hinge of the required mechanisms. Corresponding hinges C'^{I}_a and C'^{I}_b are found out with the help of poles P_{aI-III}, P_{bI-III} and angles Θ_{aI-III}, Θ_{bI-III}.

Let us reconsider the diagram of auxiliary ten-link mechanism (see Fig. 5). Angles of rotation ψ_a' and ψ_b' of the rockers $E_a'H'$ and $E_b'H'$ are measured from the axis $H'W'$, and position of the latter with respect to the support $A'H'$ is determined by angle β'.

Take this angle equal to:

$$\beta'=\beta. \tag{24}$$

Then displacement function $\psi_a'=f(\xi')$ of the auxiliary ten-link mechanism will be identical to the relationship $\psi_a=f(\xi)$, reproduced in the adjustable mechanism and displacement function $\psi_b'=f(\xi')$ will be the relationship $\psi_b=f(\xi)$, accomplished in the adjustable six-link mechanism.

In accordance with [5], condition $\psi_{ab}=0$ at $\xi=0$ is satisfied for the adjustable six-link mechanism (see Fig. 4) when hinges F and E_a coincide.

For the fulfillment of equation (9), it is necessary that in the auxiliary ten-link mechanism (see Fig. 5) rocker $E_a'H'$ should remain stationary during the rotation of the link $F'G'$ between the positions given by angles ξ^0 and ξ^m. In this case curve k, traced by the point D_a' of the connecting rod of the four-link mechanism $A'C_a'F'G'$, during transition of later from the position $A'C_a'F'^{I}G'$ to $A'C_a'^{III}F_a'^{III}G'$, must coincide with the arc of the circle k_0 drawn from the point E_a' with the radius $E_a'D_a'$.

Taking this into consideration, the unknown parameters of the diagram of auxiliary ten-link mechanism are determined from the following condition: hinge E_a' coincides with F'^{I} and is the center of rotation for three positions $F'^{I}C_a'$, $F'^{II}C_a'^{II}$ and $F'^{III}C_a'^{III}$ of the rocker $F'C_a'$, shown in the Fig. 8 (position $F'^{II}C_a'^{II}$ is obtained at $\xi'^{II}=\xi^0/2+\xi^m/2$), and hinge D_a' will be a circular point corresponding to this center.

Poles P_{I-II} and P_{I-III} and angles of rotation Θ_{I-II} and Θ_{I-III} for the above mentioned positions of the rocker have been determined in Fig. 8

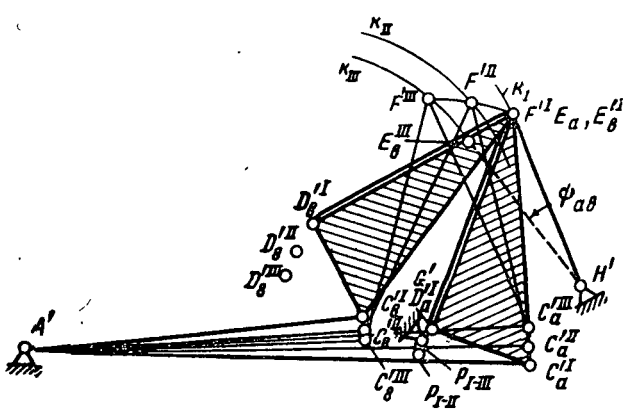

Fig. 8. Design of the auxiliary ten-link mechanism.

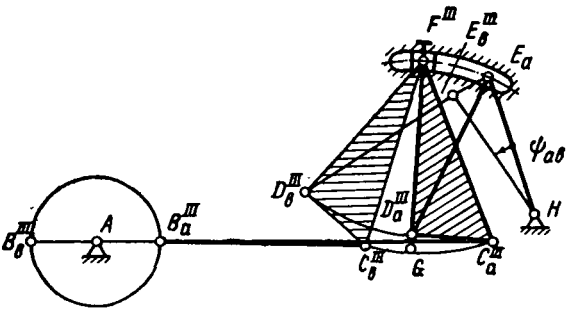

Fig. 9. Diagram of the adjustable six-link mechanism.

and also position $D_a'^{I}$ of the hinge D_a' is also found out. Afterward, positions of hinges $D_b'^{I}$, $D_b'^{II}$, $D_b'^{III}$ of the auxiliary ten-link mechanism are obtained on the basis of the equation (18). Arcs k_{II} and k_{III}, drawn with radii $D_a'^{I}E_a'$ from points $D_b'^{II}$ and $D_b'^{III}$ represent the locii of hinges $E_b'^{II}$ and $E_b'^{III}$.

Hinge $E_b'^{III}$ is selected in such a way that point of intersection of the segment $E_a'E_b'^{III}$ and of the arc k_{II} must lie inside the segment. Taking $E_a'E_b'^{III}$ as base, we draw an isosceles triangle with the vertex angle as ψ_{ab}. Vertex point will give the stationary hinge H' of the auxiliary ten-link mechanism.

An adjustable six-link mechanism designed according to the method discussed in this article is drawn to scale in Fig. 9, and is characterized by the following given conditions:

$$\varphi_a \approx 8° \approx \text{const}; \quad \varphi_b \approx 195° \approx \text{const}; \quad \Delta\varphi_a = 2°; \quad \Delta\varphi_b = -2°; \quad \psi_a = 0 = \text{const}; \quad \psi_{ab} = 0 \text{ to } 17°; \quad \xi^0 = 0 \text{ and } \xi^M = 20°.$$

References

1. Schnarbach, K. Getriebe mit verstellbarem Hub und einer festen Umkehrstellung, *Getriebetechnik*, **9**, No. 10, 1941, S. 447, 448.
2. Tao, D. C. Adjustable four-bar linkage for variable output velocity, *Transactions of the Seventh Conference of Mechanisms, Machine design*, **34**, No. 30, 1962.
3. Kraus, R. Verstellbare Kurbelschwinggetriebe, *Getriebetechnik*, **10**, No. 1, 1941, S. 33-36.
4. Kraus, R. Kurbelschwinggetriebe mit Zeitversetallung fur Hin— und Rückgang der Schwinge, *Getriebetechnik*, **10**, No. 2, 1942, S. 81.

5. HAIN, K. Im Lauf verstellbare Kurbelgetriebe fur veranderliche Arbeitsbedingungen, VDI, *Zeitschrift*, **107**, No. 6, 1965.
6. LOHSE, P. Zur Konstruktion von im Lauf verstellbarem Gelenkgetrieben, *Konstruktion*, **6**, 1954, No. 7, S. 392.
7. KRAUS, R. Kurbelgetriebe mit Hub und Zeitverstellung, *Getriebetechnik*, **10**, No. 4, 1942, S. 173.
8. ARTOBOLEVSKII, I. I., N. I. LEVITSKII and S. A. CHERKUDINOV. Sintez ploskikh mekhanizmov (Synthesis of Plane Mechanisms). Fizmatgiz, 1959.
9. CHERKUDINOV, S. A. Mekhanizmy dlya vycherchivaniya geometricheskikh mest metricheskogo sinteza svyazannykh s parametron r (Mechanisms for drawing locii of metric synthesis connected with the parameter r). *Trudy LPA*, vyp. 11, Leningrad, 1939.

K. V. Tir and *D. N. Senik*

AN APPROXIMATE TECHNIQUE FOR THE SYNTHESIS OF DISK CAM MECHANISMS

In spite of considerable research in recent years on cam mechanisms a satisfactory method of engineering synthesis of these mechanisms has not yet been developed. Design of new machines requires both knowledge and rationalization of calculations of main cyclic mechanisms, including those of cam mechanisms.

Research by the authors in the Department of Polygraphic Machines of the Ukrainian Polygraphic Institute, involves the development of a method of engineering synthesis of cam mechanisms. Synthesis of disk cam mechanisms with reciprocating follower (Fig. 1,a) and oscillating roller follower (Fig. 1,b) are discussed in this article.

One of the authors, D. N. Senik has undertaken extensive parametric investigation of values of pressure angles of a cam mechanism with oscillating follower for one complete kinematic cycle with the variation of the given angle of swing of the oscillating follower by 5° within the range 10° to 60°, and with the relative initial dimensions of cams $\rho_0=r_0/l$, where r_0—value of minimum radius-vector of pitch curve and l—base-distance between the axes of rotation of the disk cam and of the oscillating follower ($\rho_0=0.2$; 0.4; 0.6; 0.8) with the change in relative lengths of the oscillating follower $\beta=b_p/l$, where b_p is the length of the oscillating follower (determined by the condition of limiting the pressure angles at extreme points $\alpha_N > -60°$ and $\alpha_{mk}<60°$).

In this case,

$$\beta_{\min}=\sqrt{1-0.25\rho_0^2}-0.866\rho_0^2$$

$$\beta_{\max}=\sqrt{1-0.25\rho_0^2}+0.866\rho_0^2.$$

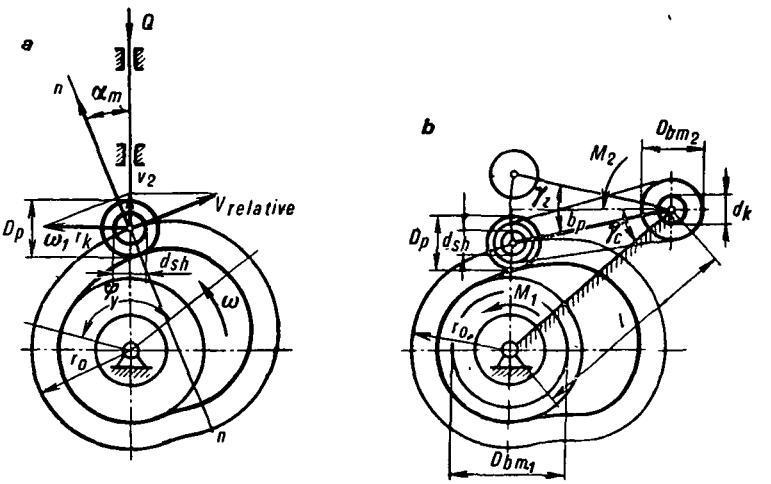

Fig. 1. Diagram of disk cam mechanisms with reciprocating (*a*) and oscillating followers (*b*).

Investigations were conducted for laws of periodic motion K and C_0 (acceleration diagrams—cosine curve and sine curve), Sh—Shun's polynom and 0307/1.5—trigonometric law differing by constant of peak values of velocity of *B* from 1.57 to 2.

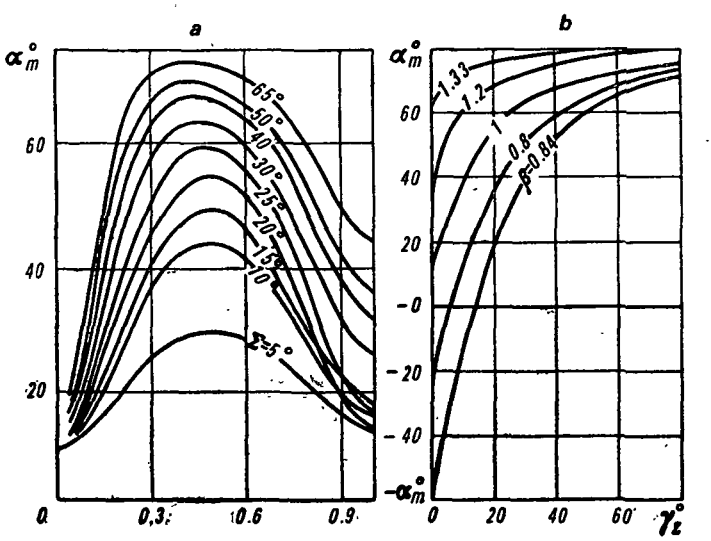

Fig. 2. Graphs of the variations of pressure angle α (*k*) for the oscillating mechanisms at $\beta=1$; $\varphi_y=60°$; $\rho_0=0.4$ and with the law of motion c_0 corresponding values of swing angles γ_Σ are shown on the curves (*a*) and generalized graphs of variation of peak pressure angles $\alpha_m(\gamma_\Sigma)$ at $\rho_0=0.4$; $\varphi_y=60°$ and at various relative lengths of the oscillating follower $\beta=b_p/l$ (*b*).

To illustrate this, graphs of variation of the pressure angles α with respect to the relative time $k=\varphi/\varphi_y$ for the law of motion C_0, $\beta=1$; $\varphi_y=60°$; $\rho_0=0.4$ with different values of angular swing of the oscillating followers γ_Σ (given on the respective lines) are shown in Fig. 2,a.

A systematic index card of similar graphs of 240 structural diagrams of mechanisms, for the above mentioned four rules of motion, has been compiled by D. N. Senik. The values of the peaks of pressure angles α_m for interpolation have been consolidated on the graphs shown in Fig. 2,b.

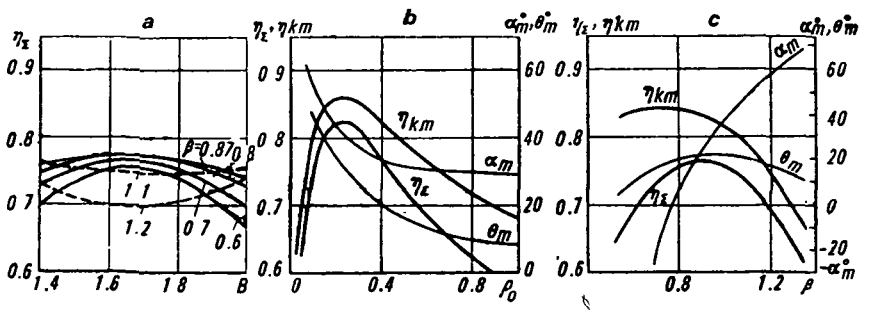

Fig. 3. Cyclic efficiency of the cam mechanisms with oscillating follower η_Σ at $\varphi_y=90°$; $\gamma_\Sigma=10°$ and coefficients of friction $f_1=0.05$ (sharp edge-cam), $f_{02}=0.01$ (oscillating follower-pivot):

a—$\eta_\Sigma(B, \beta)$ *at* $\rho_0=0.4$ *and* $p=50$ *for different laws of motion, differing by the constant of peak value of velocity of* $B=v_m/ST^{-1}$; b—$\eta_\Sigma(\rho_0)$, $\beta=1$, $p=50$, η_Σ*—curve of cyclic efficiency,* $\eta_{k,m}$*—curve of maximum instantaneous efficiencies*; c—$\varepsilon_\Sigma(\beta)$, $\rho_0=0.4$, $p=50$; *law of motion for graphs* b, c—*Shun's polynom.*

From the standpoint of permissible pressure angle α_m, these graphs offer the possibility of being easily oriented for accepting alternative structural diagram of mechanisms.

Generalized nomographs for determination of α_m in the case of using any other laws of motion and different combinations of geometrical parameters β, ρ_0, γ_Σ and φ_y, have been formulated by D. N. Senik.

The utilization of the graphs on Fig. 2,a and the existing graphs of instantaneous efficiency of cam mechanisms η_k, as a function of pressure angle, α offers the possibility of determining η_k in each phase of the cycle.

Simplification of the procedure for determining the function η_k (k) permits analytical determination of the values of cyclic efficiency η_Σ according to equation:

$$\eta_\Sigma=\int_0^1 p_k b_k d_k \Big/ \left(\int_0^{k_1} (u_k/\eta_k')\, d_k+\int_{k_1}^1 u_k \eta_k' dk\right).$$

Here $k=\varphi/\varphi_y$—relative time (k_1—corresponds to the change of sign of u_k from "plus" to "minus"): $u_k=(p_k+c_k')b_k$—positional invariant of similarity of

total power N_Σ : $u_k=N_\Sigma/mS^2T^3$, where m—mass, S—swing of displacement and T—its duration for the driven link; $p_k=P_{cm}/mST^{-2}$—Newton's number (relative force); $c_k=a/ST^{-2}$—positional invariant of similarity of acceleration and $b_k=v/ST^{-1}$—positional invariant of similarity of velocity of the driven link; η_k' and η_k''—instantaneous efficiencies of the mechanism during consumption and release of energy to the system.

Some results of the analytical investigation of cyclic efficiencies η_Σ of the cam mechanisms with oscillating follower [1], prepared according to these signs are given in the Fig. 3.

Fig. 3,a—$\eta_\Sigma=f_1(B)$, where $B=\omega_{2m}/\gamma_\Sigma T^{-1}$—constant of peak of velocity;

Fig. 3,b—$\eta_\Sigma=f_2(\rho_0)$, where ρ_0—relative initial dimensions of the radius-vector of the pitch curve;

Fig. 3,c—$\eta_\Sigma=f_3(\beta)$, where $\beta=b_p/l$—relative length of the oscillating arm.

This information may assist the designer during the selection of concrete diagrams of mechanisms.

For the purpose of checking the practicality of the suggested method of analytical calculation of cyclic efficiency, testing of cam mechanisms on the special stand designed and manufactured in UPI, were carried out by D. N. Senik with the assistance of K. V. Tir.

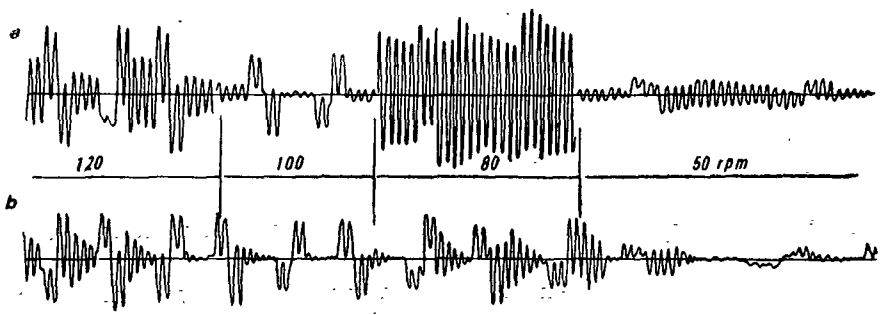

Fig. 4. Oscillograms of recordings of accelerations of the driven inertia disk for the variation of number of rotations of the cam in minute (during running down) from 120 to 0 rpm:
a—*for ball bearings;* b—*for slide bearings. Law of reverse motion of the disk*—C_0.

A method for the determination of cyclic efficiencies by running down of the cam shaft with a flywheel (rotor) fitted on it was proposed. Calibration of the moment of inertia of the rotor was carried out by the method of trifilar suspension. The initial speed of the rotor was brought to 120 rpm with calibration by the stroboscopic method. Kinetic energy, accumulated by the rotor, following disconnection of the electromagnetic coupling of the drive, was utilized on the working of the spring loaded oscillating cam mechanism in conjunction with inertia loading (kinematically closed pair of coupled cam with double roller oscillating follower). Cams were machined by milling on a special precision dividing head with an accuracy up to 0.02 mm, utiliz-

ing the method of small graduations (from 0.5-1°) in rough and finish passes.

The effect of laws of periodic motion, geometric parameters of mechanisms, the type of bearings (of sliding friction or of rolling friction) was studied on the cyclic efficiency [2].

Values of the cyclic efficiencies were determined using the dynamic equation of work:

$$\Phi=(A_{kin\,0}-zA_L-E_I\omega_{red}^2)/zA_L,$$

where $\Phi=1/\eta_\Sigma''-\eta_\Sigma'$ (η_Σ' and η_Σ''—cyclic efficiencies at outstroke and return stroke of the oscillating follower).

$A_{kin\,0}$ —kinetic energy of the rotor at the time of start of the running down;

A_L—total work lost on friction due to static forces during one rotation of the rotor;

$E_I\cong 4E_D\mathcal{J}\gamma_\Sigma/\varphi_y^2$—work lost during one rotation of the shaft on friction due to kinetic loads (due to inertia forces) [3, 4];

$\omega_{red}^2=\omega_0^2+\omega_1^2+,\ldots,+\omega_{z-1}^2+\omega_z^2$—reduced angular velocity of the rotor;

z—number of rotations of the rotor during the period of running down, determined by the indicator of complete rotations and by the index of incomplete fractions of rotation.

For kinematically closed cams:

$$E_D=A_{kin\,0}-zA_L/N_0\omega_{red}^2,$$

where $N_0=2\mathcal{J}\gamma^2{}_\Sigma/\varphi_y^2$($\gamma_\Sigma$—angular swing of the oscillating follower;

φ_y—rise angle;

$\mathcal{J}$—moment of inertia of the mass, driven by oscillating followers).

Experimental investigations confirmed the proximity of analytical evaluations of the cyclic efficiencies to the real value on correct selection of the coefficients of friction. During running down the rotor passed through the zone where the number of revolutions continuously changes from 120 to 0 rpm.

Oscillograms of the torques, on the shaft of the oscillating follower during the period of running down, are given in Fig. 4. The upper oscillogram is for the shaft of the oscillating follower on the roller bearings and the lower one is for the shaft on the slide bearing, damping the forced elastic torsional vibrations of the shaft due to friction. All other conditions of the experiment remained unchanged. Growth of the amplitude of torsional vibrations as it approaches near resonance conditions is very typical in such cases.

1. Approximate Engineering Synthesis of Disk Cam Mechanisms with Reciprocating Follower

It is known that the tangent of the maximum pressure angle of the disk cam mechanism with the reciprocating follower is approximately determined by the equation:

$$\tan \alpha_m \approx v_m/\omega_1 r_c = B/\varphi_y r_{c0}, \tag{1}$$

where $\varphi_y=\omega_1 T$; $v_m=BS/T$; $r_{c0}=r_c/S$—relative mean radius vector of the pitch curve of the cam;

$B=v_m/ST^{-1}$—constant of the peak of the velocity of the follower;

v_m—maximum velocity;

S—swing (stroke);

T—period of single-value displacement of the follower;

φ_y—angle of withdrawal, i.e., angle of rotation of the cam during the time T with angular velocity ω_1.

From equation (1) it follows that for the condition of prevention of jamming:

$$r_{c_0}^{\mathrm{I}} \geqslant B/\varphi_y \tan[\alpha_m]. \tag{2}$$

Instructions concerning the selection of permissible pressure angle $[\alpha_m]$ exist in technical literature. For the calculation of $r_{c_0}^{\mathrm{II}}$ from the condition of contact strength an approximate working equation developed by K. V. Tir [3, 4], based on the generalization of investigations on minimum radii of curvature of pitch curves of the cam, is used:

$$0.92 r_{m0}^2/(r_{m_0}+C/\varphi_y^2) \geqslant [R_{\min}] = n_3 D_R/2S = n_3 q d_{w0}/2, \tag{3}$$

where, D_R—diameter of the roller;

n_3—safety factor for preventing the sharpening of the cam profile;

C—constant of the peak of acceleration.

This equation after substituting $r_{m0}=r_{c0}+0.5$, $D_R=qd_w$, where $q\approx 2.1$ —geometrical parameter, d_w—diameter of the pin of the roller, $d_{w0}=d_w/S$ and $\varphi_w=b_{rol}/d_w$—geometrical parameter of the roller (b_{rol}—width), and after solving with respect to r_{c0} takes the form:

$$r_{c0}^{\mathrm{II}} \geqslant q_1 \sqrt{P_{\Sigma m0}} \left[1+\sqrt{1+2C/q_1\sqrt{P_{\Sigma m0}}\,\varphi_y^2} \right] - 0.5. \tag{4}$$

Here,

$P_{\Sigma m0}=P_{\Sigma m}/[\sigma_{sp}]S^2$—strength criterion of similarity;

$P_{\Sigma m}$—maximum design load on the roller;

$[\sigma_{sp}]$—permissible specific pressure between the roller and the journal;

$q_1=0.272\,n_3\,q/\sqrt{\varphi_w}$ —complex geometrical parameter, which may be taken as $q_1\simeq 1$ at $n_3=1.8$; $q=2.1$ and $\varphi_w\approx 1$.

C—constant of the peak of acceleration of the follower, which is determined by the selected law of motion.

From the condition of proximity of the roller of the follower and bush the hub of the cam,

$$r_{c_0}^{II}\geqslant(D_R+D_{\text{bush }1})/2S+0.5=0.5(D_{R0}+D_{\text{bush }1.0}+1). \tag{5}$$

Geometrical parameter of the roller $D_{r0}=D_R/S$—is found, as known, in the form

$$D_{R0}=D_R/S=qd_w/S=q\sqrt{P_{\Sigma m}/\varphi_w[\sigma_{sp}]S^2}=q\sqrt{P_{\Sigma m0}/\varphi_w}. \tag{6}$$

Geometrical parameter of the bush of the hub of the cam will be:

$$D_{\text{bush }1.0}=D_{\text{bush}}/S\approx(1.6\text{ to }1.8)d_G/S=(1.6\text{ to }1.8)d_{r0}, \tag{7}$$

where parameter 1.6 is selected for steel and 1.8 for iron cams. Relative diameter of the main shaft $d_{r0}=d_r/S$ is calculated from strength consideration:

$$M_{\text{cal}}=N_m/\omega_1=P_{\Sigma m}\cdot v_m/\omega_1=0.2d_G^3[\tau_v].$$

After substituting $V_p=BS/T$ and solving with respect to d_{G0}, we find:

$$d_{G0}=d_{G0}/S=\sqrt{P_{\Sigma m}BS/0.2\varphi_v[\tau_v]S^3}\approx 1.7\sqrt[3]{P_{\Sigma m0}B/\varphi_v[\sigma_0]}, \tag{8}$$

where $[\sigma_0]=[\sigma_{sp}]/[\tau_v]\approx 0\,4$.

Taking into consideration equations (6), (7) and (8) relationship (5) takes the form:

$$r_{c_0}^{III}\geqslant 0.5[q/\sqrt{\varphi_w}\sqrt{P_{\Sigma m0}}+(2.72-3.06)\sqrt[3]{P_{\Sigma m0}B/\varphi_v[\sigma_0]}+1]. \tag{9}$$

And thus, generalizing the known relationships in the complex $B_v=B/\varphi_v$ and $C_v=C/\varphi_v^2$, we find three relationships which determine the mean relative radius of pitch curve of the cam according to limiting criterions from the conditions:

1) Prevention of the jamming according to equation (2), dimension which does not depend on $P_{\Sigma m0}$

$$r_{c_0}^{I}>B_v/\tan[\alpha_m]; \tag{10a}$$

2) Contact strength at $q_1\approx 1$

$$r_{c_0}^{II}\geqslant\sqrt{P_{\Sigma m0}}\left[1+\sqrt{1+2C_v/\sqrt{P_{\Sigma m0}}}\right]-0.5=f_{II}(P_{\Sigma m0},C_v); \tag{10b}$$

3) Proximity of roller with the bush of the hub of the cam when $[\sigma_0] \approx 0.4$, $\varphi_w = 1$ and $q \approx 2.1$

$$r_{c0}^{III} > 1.05\sqrt{P_{\Sigma m0}} + (1.00 - 1.13)\sqrt[3]{P_{\Sigma m0} B_v} + 0.5 = f_{III}(P_{\Sigma m0}, B_v). \quad (10c)$$

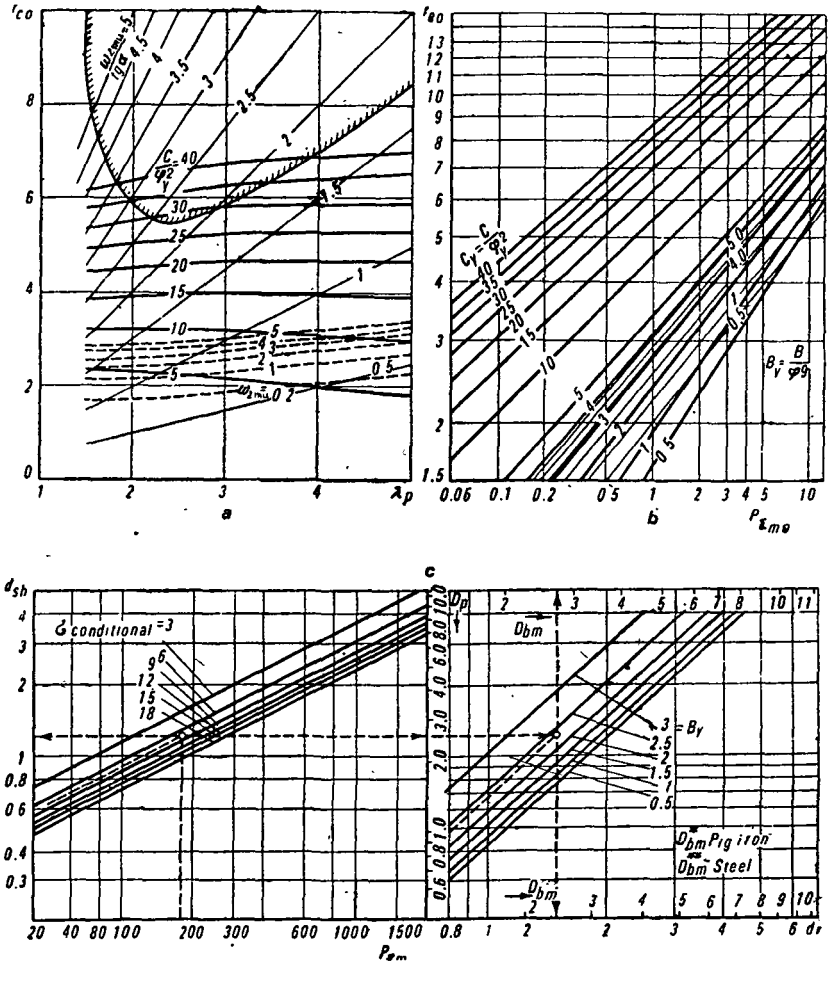

Fig. 5. Charts of blocking contours for the engineering synthesis of disk cam mechanisms with oscillating followers:

a—*for mechanisms with oscillating follower with the angle of swing of the follower* $\gamma_\Sigma = 30°$; $\lambda_p = b_p/d_k$—*relative length of the oscillating follower;* r_{c0}—*relative mean radius of pitch curve of the cam;* b—*for mechanisms with the reciprocating follower;* $P_{\Sigma m0} = P_{\Sigma m}/[\sigma_{sp}]S^2$—*similarity criterion of the strength;* c—*nomographs for the selection of components of cam mechanisms.*

Values of kinematic criterions of similarity $B_y=B/\varphi_y$ and $C_y=C/\varphi_y^2$, the permissible maximum pressure angle $[\alpha_m]$[1] and the strength criterion of similarity $P_{\Sigma m0}=P_{\Sigma m}/[\sigma_{sp}]S^2$ are known according to the given conditions and the selected law of motion B or C, and therefore relationships (10a)-(10c) are solved for lower limits identically.

Of the three so determined dimensions of r_{c0}, one is maximum and limiting. The remaining two inequalities are satisfied upon the selection of this limiting dimension.

As is apparent from equation (10), if we plot the value $r_{c0}=r_c/S$ along the ordinate and the complex criterion of strength similarity $P_{\Sigma m0}=P_{\Sigma m}/[\sigma_{sp}]S^2$ along abscissa then $r_{c_0}^{I}$ is independent of the latter and is expressed by a horizontal line (then $r_{c_0}^{I}=B_y/\tan[\alpha_m]$, and does not depend on $P_{\Sigma m0}$), and $r_{c_0}^{II}$ is expressed by a number of curves each for a value of $C_y=C/\varphi_y^2$ and $r_{c_0}^{III}$ is expressed similarly by a number of curves, each for a value of $B_y=B/\varphi_y$.

The chart of blocking contours obtained is applicable for any sort of initial indices of periodic motion. In Fig. 5,b (cast iron cams) it is drawn on the logarithm graph with averaging, which are usually adopted during calculation of polygraphical machines. On the basis of the method of drawing the graphs described above, similar charts may be developed which may be applicable to the strength norms adopted in other fields of the national economy, as well as for steel cams [5-14].

2. Engineering Synthesis of Disk Cam with an Oscillating Follower

A diagram of the mechanism is shown in Fig. 1,b. As a physical module of measurement of all linear dimensions of the components of the mechanism, it is best to select the diameter d_k of the shaft of the oscillating follower, which can be determined (irrespective of the structural diagram of the mechanism), from the conditional calculation for torsion as per the lower permissible stress (τ_y'') from the equation given below:

$$d_k=\sqrt[3]{|K_D J_\Sigma \varepsilon+M_{st}|_{\max}/0.2[\tau_y'']}, \tag{11}$$

where, K_D—dynamic-response factor;

J_Σ—moment of inertia of the mass, transformed to the oscillating follower;

ε—angular acceleration of the oscillating follower;

M_{st}—moment of static forces;

$[\tau_y'']$—conditional permissible torsional stress for the shaft of the oscillating follower.

[1] Method of selection of (α_m) (see in [3, 4]). This takes into consideration cam mechanisms approaching the optimum power condition of the work.

Using the above value of d_k, we can express all other linear dimensions of the components of the mechanism in terms of their geometrical parameters in the form:

$$l_i = q_i d_k, \tag{12}$$

where $q_i = l_i/d_k$ is determined from the condition of uniform strength of the components considered.

The main variable parameter for the mechanisms, which differ from others as demonstrated in the diagram, in the sense that direction of tangential velocity of the point of the follower (center of the roller) in the mean position of the oscillating follower ($\gamma = \gamma_\Sigma/2$), passes through the center of the cam, is the length of the oscillating follower b_p which in the future we will express in terms of the geometrical parameter $\lambda_p = b_p/d_k$.

Taking, as above (see also [3, 4]) $b_w = \varphi_w d_w$ and $D_p = q d_w$, where $\varphi_w = \sqrt{0.2[\sigma_u]/[\sigma_{sp}]}$—geometrical parameter of the journal and $q = D_p/d_w \approx 2.1$—geometrical parameter of the diameter of the roller, let us express the maximum load on the roller, taking strength into consideration:

$$Q_m = M_{\Sigma m}/b_p \cos[\alpha_m] = \varphi_w d_w^2 [\sigma_{sp}]. \tag{13}$$

Accordingly let us introduce the loading moment from strength consideration:

$$M_{\Sigma m} = 0.2 d_k^3 [\tau_y''].$$

Solving equation (13) with respect to $\vartheta_w = d_w/d_k$, we find

$$\vartheta_w = d_w/d_k = \sqrt{0.2[\tau_y'']/\varphi_w \lambda_p [\sigma_{sp}] \cos[\alpha_m]} = A_1/\sqrt{\lambda_p}, \tag{14}$$

where, $\lambda_p = b_p/d_k$—variable geometrical parameter of the length of the oscillating follower, and $A_1 = \sqrt{0.2(\tau_y'')/\varphi_w [\sigma_{sp}] \cos[\alpha_m]}$—strength criteria.

As follows from the previous conclusions that,

$$\vartheta_p = D_p/d_k = q\vartheta_w = qA_1\sqrt{\lambda_p} = A_2/\sqrt{\lambda_p}. \tag{15}$$

Geometrical parameter of the diameter of the main shaft is determined from the condition of conservation of energy:

$$M_{1m}\omega_1\eta_k = |M_{\Sigma 2}\omega_2|_{\max}, \tag{16}$$

where M_{1m}—maximum torque on the main shaft;

η_k—instantaneous efficiency of the mechanism;

$M_{\Sigma 2}$—total torsional moment on the shaft of the oscillation follower;

ω_2—its angular velocity.

Expressing $|M_{\Sigma 2} \cdot \omega_2|_{\max} = \mu M_{\Sigma 2m} \cdot \omega_{2m}$, where, $\mu = |M_{\Sigma 2} \cdot \omega_2|_{\max}/M_{\Sigma 2m} \cdot \omega_{2m}$ for the given laws of motion of the oscillating shaft and of variation of

statical loading-strictly determined dimensionless criterion ($\mu \leqslant 1$) and substiting in the equation (16) $M_{1m}=0.2d_G^3[\tau_y']$ and $M_{\Sigma 2m}=0.2d_k^3[\tau_y'']$, we get:

$$\vartheta_G=d_G/d_k=\sqrt[3]{[\tau_y'']\cdot\omega_{2mu}\cdot\mu/\eta_k[\tau_y']}=A_3\sqrt[3]{\omega_{2mu}}, \tag{17}$$

where $\omega_{2mu}=\omega_{2m}/\omega_1$—invariant of similarity of the peak of angular velocity of the oscillating shaft, which is expressed in the form below, after the introduction of the constant of peak of angular velocity of the oscillating follower B in the calculation,

$$\omega_{2mu}=B\gamma_\Sigma\omega_1/\omega_1\varphi_y=B\gamma_\Sigma/\varphi_y.$$

This dimensionless complex has important significance in the generalized criterion calculations.

Geometrical parameters of the bushes of the hub of the cam and of the lever of the oscillating follower can be determined easily on the basis of the norms, used in machine design:

for oscillating follower

$$D_{\text{bush}\cdot k}=(1.6-1.8)d_k=\vartheta_{\text{bush}\cdot k}d_k,$$

i.e.

$$\vartheta_{\text{bush}\cdot k}=(1.6-1.8),$$

and for the cam

$$D_{\text{bush}\cdot G}=1.6-1.8)\vartheta_G d_k=\vartheta_{\text{bush}\cdot G}d_k, \tag{18}$$

i.e.,

$$\vartheta_{\text{bush}\cdot G}=(1.6-1.8)A_3\sqrt[3]{\omega_{2mu}},$$

where coefficient 1.6 is taken for steel, and 1.8 for cast iron components.

Since the geometrical parameters of components are known, let us formulate the engineering synthesis of disk cam mechanism with oscillating follower.

Condition of elimination of the possibility of jamming of the mechanism—for the diagram under consideration with sufficient engineering approximations, considering the value of $\tan\alpha_m$ can be expressed in the form,

$$\tan\alpha_m\approx v_{2m}/\omega_1 r_c^{\mathrm{I}}=B\gamma_\Sigma\omega_1 b_p/\varphi_y'\omega_1 r_c^{\mathrm{I}}=\omega_{2mu}b_p/r_c^{\mathrm{I}}\leqslant\tan[\alpha_m],$$

from where we determine the necessary geometrical parameter of the mean radius of the cam:

$$r_{c0}^{\mathrm{I}}=r_c^{\mathrm{I}}/d_k\geqslant\omega_{2mu}\cdot\lambda_p/\tan[\alpha_m], \tag{19}$$

where $r_{c0}^{\mathrm{I}}=f_{\mathrm{I}}(\omega_{2mu}/\tan[\alpha_m],\ \lambda_p)$.

If we consider that ratio $r_{c0}^{\mathrm{I}}/\lambda_p=\tan\gamma_c$, where γ_c—angle between the base line distance O_1O_2 and the axis of the oscillating follower in the mean position, then we get the hyperbolic relationship:

$$\tan\gamma_c\tan[\alpha_m]\geqslant\omega_{2mu}. \tag{20}$$

Condition of proximity of the roller with he shaft of the oscillating follower is written in the form $l_p > D_p/2 + D_{lim}/2$, where D_{lim}—limiting diameter of components, situated on the opposite side of the roller on the shaft of the the oscillating follower.

Dividing both sides of the inequality by d_k we get:

$$\lambda_p > \vartheta_p/2 + \vartheta_{lim}/2 = A_2/2\sqrt{\lambda_p} + \vartheta_{lim}/2$$

or

$$\lambda_p - A_2/2\sqrt{\lambda_p} > \vartheta_{lim}/2. \tag{21}$$

If there are no components on the shaft of the oscillating follower on the opposite side of the roller, then $\vartheta_{lim}=1$. In the presence of the bush of the hub of the lever (see above), $\vartheta_{lim}=1.6\text{-}1.8$.

Condition of proximity of the roller with the bush of the hub of the cam is written in the form of inequality:

$$r_c^{II} > \sqrt{[(D_p + D_{hub\,1})/2]^2 + b_p^2(1-\cos(\gamma_\Sigma/2))^2} + b_p \sin(\gamma_\Sigma/2)$$

or in the criterion form:

$$r_{c_0}^{II} > \sqrt{[(\vartheta_p + \vartheta_{hub\,1})/2]^2 + \lambda_p^2(1-\cos(\gamma_\Sigma/2))^2} + \lambda_p \sin(\gamma_\Sigma/2), \tag{22}$$

i.e. $r_{c_0}^{II} = f_{II}(\gamma_\Sigma, \omega_{2mu}, \lambda_p)$.

Condition of contact strength of the cam may be formulated, if in the first approximation, evaluation of the minimum radii of curvature of the convex part of the pitch curve of the cam of the disk cam mechanism with the reciprocating follower is utilized.

Substituting in equation (3), $S = b_p\,\gamma_\Sigma = \lambda_p d_k \gamma_\Sigma$, we find:

$$t_{c_0}^{III} = r_c^{III}/d_k = \vartheta_p' + \sqrt{(\vartheta_p')^2 + 2\vartheta_p'(C/\varphi_y^2)\gamma_\Sigma\lambda_p} - 0.5\lambda_p\gamma_\Sigma,$$

where $\vartheta_p' = n_3\vartheta_p/3.68 = 0.272 n_3\vartheta_p$.

In this way:

$$r_{c_0}^{III} = f_{III}(\gamma_\Sigma, \lambda_p, C/\varphi_y^2, n_3). \tag{23}$$

Condition of proximity of the cam with the shaft of the oscillating follower (in that case, if the nose of the cam during its rotation approaches the surface of the shaft of the oscillation follower) may be written from the analysis of the diagram in Fig. 1,b in the form of the inequality:

$$\sqrt{(r_{c_0}^{IV} + \lambda_p \sin(\gamma_\Sigma/2))^2 + \lambda_p^2(1-\cos(\gamma_\Sigma/2))^2} - \vartheta_p/2 \leqslant \lambda_p/\cos\gamma_c - 0.5\vartheta_{lim} \tag{24}$$

or with the consideration, that at $\gamma_\Sigma \leqslant 60°$ $(1-\cos(\gamma_\Sigma/2))^2 < 0.02$,

$$\text{i.e. } r_{c_0}^{IV} + \lambda_p \sin(\gamma_\Sigma/2) - \vartheta_p/2 \leqslant \lambda_p/\cos\gamma_c - 0.5\vartheta_{lim}. \tag{25}$$

Substituting $\cos\gamma_c=1/\sqrt{1+(r_{c_0}^{IV}/\lambda_p)^2}$ in equation (25) and solving with respect to $r_{c_0}^{IV}$, we get:

$$r_{c_0}^{IV}\leqslant\lambda_p[1-(\sin(\gamma_\Sigma/2)-\vartheta_p-\vartheta_{lim}/2\lambda_p)^2]/2(\sin(\gamma_\Sigma/2)-\vartheta_p-\vartheta_{lim}/2\lambda_p)=f_{IV}(\gamma_\Sigma,\lambda_p), \tag{26}$$

because in equation (15), $\vartheta_p=A_2/\sqrt{\lambda_p}$.

Comparing expressions (19), (22), (24) and (26), we find that if a concrete constant value is given to the angular swing γ_Σ, then because of the introduction of geometrical parameters in the calculations, in the form of some functions of $\lambda_p=b_p/d_k$, $[\alpha_m]$, and generalized complexes $\omega_{2mu}=B\gamma_\Sigma/\varphi_v$ and $C_y=C/\varphi_y^2$, four inequalities for $r_{c_0}^i$ may be determined.

Considering $\gamma_\Sigma=$const (5, 10,..., 55, 60), we express $r_{c_0}^i$ in the form of a function from the conditions;

a) eliminating of jamming

$$r_{c_0}^{I}=f_I(\omega_{2mu}/\tan[\alpha_m],\lambda_p);$$

b) proximity of the roller with the bush of the hub of the cam

$$r_{c_0}^{II}=f_{II}(\omega_{2mu},\lambda_p);$$

c) escape of the cam from the possibility of self intersection of the line of the actual profile and the contact strength (at $n_3=1.5$)

$$r_{c_0}^{III}=f_{III}(C/\varphi_y^2,\lambda_p);$$

d) proximity of the cam and of the shaft of the oscillating followers

$$r_{c_0}^{IV}=f_{IV}(\lambda_p).$$

The results obtained by K. V. Tir, offer the possibility of drawing the charts of blocking contours, in which values of the relative mean radii of the cam $r_{c_0}^i=r_c^i/d_k$ are plotted along the ordinate and variable relative length of the oscillating follower $\lambda_p=b_p/d_k$ along abscissa.

Calculation and drawing of 12 charts for γ_Σ from 10° up to 60° with an interval of 5° have been carried out by D. N. Senik.

On the chart, for example the one with $\gamma_\Sigma=30°$ given in Fig. 5,a, functions $r_{c_0}^I=f_1(\lambda_p)$ from the condition of preventing the mechanism from jamming are expressed for each concrete given value of $\omega_{2mu}/\tan[\alpha_m]=B\gamma_\Sigma/\varphi_v\times\tan[\alpha_m]$ in the form of the rising ray shown by the thin continuous lines.

The actual selected value of r_{c_0} must be more than $r_{c_0}^\lambda$—the lower limit determined in this ray.

Relationships $r_{c_0}^{II}(\lambda_p)$, determined by the conditions of proximity of the roller and of the bush of the hub of the cam are expressed by the dotted lines with the respective values of ω_{2mu} (0.2; 1, . . .; 5) shown on the lines. Here too, it is necessary to fulfill the condition $r_{c_0} > r_{c_0}^{II}$ for the given value of ω_{2mu}. Functions $r_{c_0}^{III} = f_{III}(\lambda_p)$, determined from the condition of contact strength of the pair roller-cam are expressed by a set of curves drawn by thick lines with the given concrete values of C/φ_y^2 shown on these lines. In this case also, condition $r_{c_0} > r_{c_0}^{III}$ must be fulfilled.

Curve drawn by the thick line and hatched with vertical lines on the upper side represents the function $r_{c_0}^{IV} = f_{IV}(\lambda_p)$, which expresses the condition of proximity of the cam with the shaft of the oscillating follower. Here, in contrast to previous cases, condition $r_{c_0} < r_{c_0}^{IV}$ should be fulfilled.

If charts of blocking contours made by the authors and shown in Fig. 5,a for $\gamma_\Sigma = 30°$ and suitable for any initial laws of periodic motion, are used then synthesis of disk cam with oscillating follower is accomplished easily.

After determination of the similarity criteria $\omega_{2mu}/\tan[\alpha_m]$ and $C_y = C/\varphi_y^2$ and selection of permissible pressure angle $[\alpha_m]$ we find from the chart, zone of possible combinations of r_{c_0} and λ_p above the lines $[r_{c_0}^{I}]$, $[r_{c_0}^{II}]$, $[r_{c_0}^{III}]$, and below $r_{c_0}^{IV}$ for the given conditions.

Following strength calculation of the conditional diameter of the shaft of the oscillating follower d_k from equation (11), we will determine the dimensions of the rest of the components by multiplying with geometrical parameters for the given values of r_{c_0}, λ_p, $[\alpha_m]$, $\omega/_{2mu}$, and C/φ_y^2 with the determined physical module of measurement, d_k.

With the aim of rationalizing engineering calculations for the determination of dimensions of components of the mechanism, the nomograph made by the authors (see Fig. 5,c) may be used on which the method for the determination of diameters of the pin d_w, roller D_p, main shaft d_G and of the bush of the cam (D_{hub}^{*}—for cast iron and D_{hub}^{**}—for steel cams) according to the value of the maximum design total load on the roller $P_{\Sigma m}$ is given.

Existing norms of strength and wear resistance have been observed in this case, because geometrical parameters of the components have been determined from that consideration. Conditions of proximity of the components of equal strength have also been considered as follows from the method of drawing of the chart. The last requirements completely block the zone of the free selection of $r_{c_0}^{i}(\lambda_p)$ in a number of cases, which testifies the impossibility of combining the given values of γ_Σ, γ_y, B and C.

This method of engineering synthesis of disk cam mechanisms facilitates the calculations, necessary during the variation of their structural diagrams, draft and technical projects of cyclic machines in the design departments of machine plants and scientific research organizations.

References

1. Senik, D. N. Vliyanie struktury kulachkovykh mekhanizmov na tsiklovye k.p.d. (Effect of the Design of Cam Mechanisms on Cyclic Efficiency). Sbornik *Poligrafiya i izdatel'skoe delo*, No. 1. L'vov. Izd. LGU imeni Ivanovo Franko, 1964.
2. Senik, D. N. Energetichna efektivnist' kulachkovikh mekhanizmiv pri chistodinamichnomu navantazhenni (Effectiveness of Cam Mechanisms). Sbornik *Poligrafiya i vidavnicha sprava*, No. 2, L'vov, Vid. LDU, imeni Ivanovo Franko, 1965.
3. Tir, K. V. Kompleksnyi raschet kulachkovykh mekhanizmov (Complex Calculation of Cam Mechanisms). Moscow-Kiev, Mashgiz, 1958.
4. Tir, K. V. Mekhanika poligraficheskikh avtomatov (Mechanics of Polygraphic Automats). Izd-vo Kniga, 1965.
5. Kozhevnikov, S. N. Vybor parametrov kulachkovykh mekhanizmov (Selection of parameters of cam mechanisms). *Trudy Dnepropetr. metallurg. in-ta*, vyp. 32, 1954.
6. Levitskii, N. I. Metody rascheta kulachkovykh mekhanizmov (Methods of Calculation of Cam Mechanisms). Mashgiz, 1954.
7. Levitskii, N. I. Kulachkovye mekhanizmy (Cam Mechanisms). Izd-vo Mashinostroenie, 1964.
8. Orlikov, M. L. Kulachkovye mekhanizmy mashin-avtomatov (Cam Mechanisms of Automatic Machines). Mashgiz, 1955.
9. Popov, S. A. Proektirovanie kulachkovykh mekhanizmov s vrashchayushchimsya tolkatelem (Design of Cam Mechanisms with Rotary Followers). Izd. MVTU, 1958.
10. Rotbart, G. A. Kulachkovye mekhanizmy (Cam Mechanisms). Sudpromgiz, 1960.
11. Tir, K. V. K voprosu o profilirovanii kulachkov poligraficheskikh mashin (Problems Concerning Profiling of Cams of Polygraphic Machines). Kand. diss. Moscow Izd. MPI, 1952.
12. Tir, K. V. Metod invariantov podobiya v mekhanike mashin (Method of Invariants of Similarity in the Mechanics of Machines). Doctoral dissertation, L'vov, Izd. LPI, 1963.
13. Shaumyan, G. A. Avtomaty i avtomaticheskie linii (Automats and Automatic Lines). Mashgiz, 1961.
14. Yudin, V. A. K voprosu ob opredelenii razmerov kulachkovogo mekhanizma s kachayushchimsya tolkatelem pri silovom zamykanii vysshei pary (Problem concerning determination of dimensions of cam mechanisms with oscillatory follower by closing higher pairs). *Trudy Mosk. in-ta khimicheskogo mashinostroeniya*, **17**, No. 3, 1958.

K. A. Tonoyan

THE PROBLEM OF EXISTENCE OF THE CRANK IN THE SPATIAL FOUR-LINK MECHANISM WITH TWO TURNING AND TWO SPHERICAL PAIRS

Calculation of the geometrical conditions of turning of links of the spatial four-link mechanism with two turning and two spherical pairs is one of the most difficult problems in the analysis of this mechanism.

A number of articles [1-9] are devoted to this problem.

Procedures given below offer a possibility of separating double crank mechanisms from the crank-rockers.

Let us select the system of coordinates $Oxyz$ (Fig. 1) in such a way so that z-axis is directed along the shortest distance OE between the axes of rotation OA and ED, and x-axis along OA. Angles φ and Φ of the rotation of links AB and DC are found with the help of straight lines parallel to the z-axis in the counter clockwise direction, if seen along the directions AO and DE. Parameters of the kinematic diagram of the mechanisms are: a, b, c, e, f, g, α.

Substituting the coordinates of the points B and C:

$$x_B=f; \qquad x_C=g\cos\alpha+c\sin\alpha\sin\psi;$$
$$y_B=-a\sin\varphi; \qquad y_C=g\sin\alpha-c\cos\alpha\sin\psi;$$
$$z_B=a\cos\varphi; \qquad z_C=e+c\cos\psi$$

in the equation:

$$b^2=(x_C-x_B)^2+(y_C-y_B)^2+(z_C-z_B)^2,$$

and after transformation we get the displacement function of the mechanism $\psi=F(\varphi)$ in implicit form, i.e.

$$ag\sin\alpha\cdot\sin\varphi-ae\cos\varphi-cf\sin\alpha\cdot\sin\psi+ce\cos\psi-ac\cos\alpha\cdot\sin\varphi\sin\psi-$$
$$ac\cos\varphi\cdot\cos\psi+\frac{1}{2}(a^2+c^2+e^2+f^2+g^2-b^2-2fg\cos\alpha)=0. \qquad (1)$$

1. Types of the Mechanism According to Conditions of Turning of Links

Differentiating equation (1) with respect to φ, we get:

$$d\psi/d\varphi = a(g\sin\alpha\cdot\cos\varphi + e\sin\varphi - c\cos\alpha\cdot\cos\varphi\cdot\sin\psi + c\sin\cdot\varphi\cos\psi)/c(f\sin\alpha\cdot\cos\psi + e\sin\psi + a\cos\alpha\cdot\sin\varphi\cdot\cos\psi - a\cos\varphi\cdot\sin\psi). \quad (2)$$

In the extreme position of the link AB,

$$d\varphi/d\psi = 0$$

and from equation (2):

$$f\sin\alpha\cos\psi + e\sin\psi + a\cos\alpha\sin\varphi\cos\psi - a\cos\varphi\sin\psi = 0. \quad (3)$$

Equation (3) represents some function $\psi = P(\varphi)$ in implicit form with range of existence $-\infty < \varphi < \infty$. Any branch $\psi = p(\varphi)$ of the function $\psi = P(\varphi)$ is a continuous and periodic function with period 2π.

Let us determine the condition at which $\psi = p(\varphi)$ changes in the range $-\infty < p(\varphi) < \infty$.

Dividing both parts of the equation (3) by $\cos\psi$ and substituting

$$\sin\varphi = 2\tan\varphi/2/(1+\tan^2\varphi/2), \qquad \cos\varphi = (1-\tan^2\varphi/2)/(1+\tan^2\varphi/2),$$

we get,

$$[f\sin\alpha + (a+e)\tan\psi]\tan^2\varphi/2 + 2a\cos\alpha\tan\varphi/2 + f\sin\alpha + (e-a)\tan\psi = 0,$$

from where keeping in mind that function $p(\varphi)$ exists in the zone $-\infty < \varphi < \infty$, the necessary and sufficient condition for the given condition $-\infty < p(\varphi) < \infty$ is:

$$(a\cos\alpha)^2 - [f\sin\alpha + (a+e)\tan\psi]\,[f\sin\alpha + (e-a)\tan\psi] \geqslant 0.$$

After transformation:

$$(a^2-e^2)\tan^2\psi - 2ef\sin\alpha\tan\psi + a^2\cos^2\alpha - f^2\sin^2\alpha \geqslant 0. \quad (4)$$

For any value of ψ, equation (4) is true if the following conditions are fulfilled simultaneously:

$$a^2 - e^2 > 0. \quad (5)$$

$$(ef\sin\alpha)^2 - (a^2-e^2)\,(a^2\cos^2\alpha - f^2\sin^2\alpha) \leqslant 0. \quad (6)$$

From equation (6):

$$e^2\cos^2\alpha + f^2\sin^2\alpha - a^2\cos^2\alpha \leqslant 0,$$

from where,

$$a^2 \geqslant e^2 + f^2\tan^2\alpha. \quad (7)$$

If equation (7) is satisfied, equation (5) is also satisfied except in the case when $\alpha=0$ and $e=a$, but then equation (4) is realized: consequently, inequality (7) is the necessary and sufficient condition for $-\infty<p(\varphi)<\infty$. Proceeding from this, we formulate the following theorem.

Theorem 1. *The necessary and sufficient condition for the nonexistence of the crank rocker mechanism with crank AB is*:

$$a^2\geqslant e^2+f^2\tan^2\alpha.$$

Proof. Let there be a crank-rocker mechanism with the crank AB. Then the branch $\psi=f(\varphi)$ of the function $\psi=F(\varphi)$ will be a continuous and finite function.

For the condition stated in the theorem, function $\psi=p(\varphi)$ varies in the range $-\infty<p(\varphi)<\infty$ [see Fig. 2, where *1*—$\psi=p(\varphi)$; *2*—$\psi=f(\varphi)$].

Let us form an auxiliary function:

$$g(\varphi)=p(\varphi)-f(\varphi),$$

which is continuous and varies in the range $-\infty<g(\varphi)<\infty$, therefore a point $\varphi=\varphi_0$ is found out where function $g(\varphi)$ equals zero and consequently:

$$p(\varphi_0)=f(\varphi_0)=\psi_0,$$

and this means that the system of equations (1) and (3) has actual solution $\varphi=\varphi_0$, $\psi=\psi_0$, with the help of which the extreme position of the link AB, is determined. As this does not agree with the stated assumption, the mechanism cannot be crank-rocker mechanism with the crank AB.

We may note that the geometric condition corresponds to equation,

$$a^2\geqslant e^2+f^2\tan^2\alpha,$$

of theorem 1; axis ED passes through the circle AB or intersects the circle AB.

Under the condition:

$$a^2=e^2+f^2\tan^2\alpha,$$

link AB may occupy any position $0\leqslant\varphi<2\pi$, only at $b=B_0C_0$ (see Fig. 3), but will not be a crank because in the position AB_0, link DC freely rotates around axis ED and without external forces mechanism will not move out of this position.

In the extreme position of the link DC,

$$d\psi/d\varphi=0.$$

From equation 2, we get:

$$g\sin\alpha\cdot\cos\varphi+e\sin\varphi-c\cos\alpha\cdot\cos\varphi\sin\psi+c\sin\varphi\cdot\cos\psi=0. \qquad (8)$$

Similarly, considering the system of equation (1) and (8), we prove the next theorem.

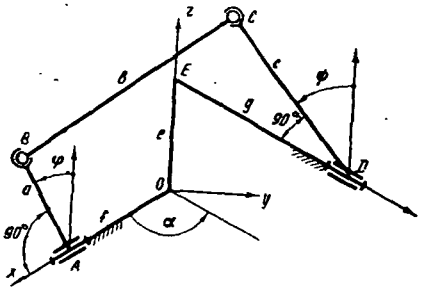

Fig. 1.

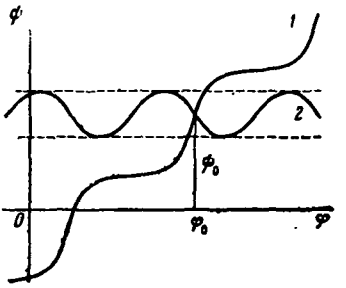

Fig. 2.

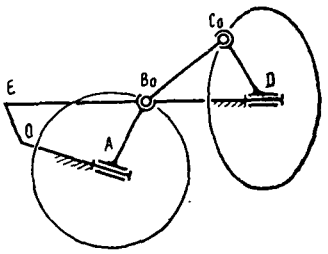

Fig. 3.

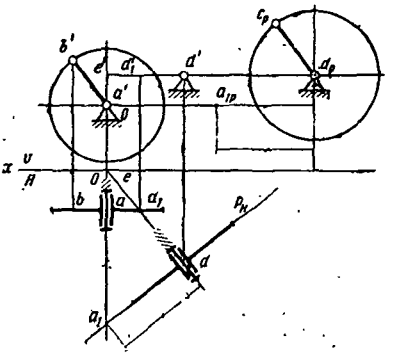

Fig. 4.

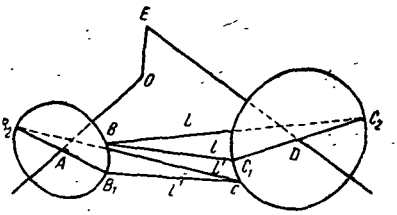

Fig. 5.

Theorem 2. *The necessary and sufficient condition for the nonexistence of the crank-rocker mechanism with the crank DC is:*

$$c^2 \geqslant e^2 + g^2 \tan^2\alpha.$$

Generalizing the above statement, depending upon parameters a, c, e, f, g and α, mechanisms with two turning and two spherical pairs can be classified as per conditions of turning in 4 types (see Table 1).

Mechanisms of the type shown in Fig. 3 are obtained from the equations of Table 1.

Type of the mechanism is easily determined graphically with the consideration of the fact, that on drawing the kinematic diagram of the mechanism in orthogonal projections (see Fig. 4), the expression $\sqrt{e^2+f^2\tan^2\alpha}$ corresponds the line $a'd_1'$ and the expression

$$\sqrt{e^2+g^2\tan^2\alpha}$$

corresponds to the line $d_p a_{1p}$ in the plane P, superposed with the frontal plane of projection.

The mechanism shown in the Fig. 4 is of type 3.

2. Conditions of Existence of Crank

Let us disconnect link BC from links AB and DC. Then points B and C can occupy any position on the circles AB and DC (see Fig. 5).

Let us consider the distance λ between points B and C, as a function $\lambda=\lambda(\varphi, \psi)$ of two variables. Function $\lambda(\varphi, \psi)$ is determined by the equation:

$$\begin{aligned}\lambda^2=&2ag\sin\alpha\cdot\sin\varphi-2ae\cos\varphi-2cf\sin\alpha\cdot\sin\psi+2ce\cos\psi-\\&2ac\cos\alpha\cdot\sin\varphi\cdot\sin\psi-2ac\cos\varphi\cdot\cos\psi+a^2+\\&c^2+e^2+f^2+g^2-2fg\cos\alpha,\end{aligned}\tag{9}$$

which is obtained from equation (1) by the substitution of the length of the connecting rod b by the variable distance λ between the points B and C.

Critical points of the function $\lambda=\lambda(\varphi, \psi)$ are found from the condition:

$$\partial\lambda/\partial\varphi=0,\quad \partial\lambda/\partial\psi=0.\tag{10}$$

From equation (9) we get:

$$\lambda\partial\partial/\partial\varphi=a(g\sin\alpha\cos\varphi+e\sin\varphi-c\cos\alpha\cos\varphi\sin\psi+c\sin\varphi\cdot\cos\psi),$$

$$\lambda\partial\lambda/\partial\psi=-c(f\sin\alpha\cos\psi+e\sin\psi+a\cos\alpha\sin\varphi\cos\psi-a\cos\varphi\sin\psi).$$

Comparing these relationships with equations (3) and (8), we have, that under the condition $\partial\lambda/\partial\varphi=0$ variables φ and ψ satisfy equation (8) and under the condition $\partial\lambda/\partial\psi=0$, these variables satisfy equation (3).

In this way, critical points of the function $\lambda(\varphi, \psi)$ are determined by solving the system of equations (3) and (8).

Let us introduce the following symbols (see Fig. 5):

l—minimum distance of some point B to the points of circle DC;

L—maximum distance of some point B to the points of circle DC;

l'—minimum distance of some point C to the points of circle AB;

L'—maximum distance of some point C to the points of circle AB.

Table 1. Types of mechanisms with two rotary and two spherical pairs, depending on the parameters

Types of mechanism	Possible type of crank mechanism	Condition of type	Ratios of extremes		Condition of the existence of crank
1	Double crank	$a^2>e^2+f^2\tan^2\alpha$ $c^2>e^2+g^2\tan^2\alpha$	$l_{max}=l'_{max}$ $L_{min}=L'_{min}$	$l_{max}<L_{min}$	$l_{max}<b<L_{min}$
2	Crank-rocker with crank AB	$a^2<e^2+f^2\tan^2\alpha$ $c^2>e^2+g^2\tan^2\alpha$			$l_{max}<b<L_{min}$
3	Crank-rocker with crank DC	$a^2>e^2+f^2\tan^2\alpha$ $c^2<e^2+g^2\tan^2\alpha$	$l_{max}=L'_{min}$ $L_{min}=l'_{max}$	$L_{min}<l_{max}$	$L_{min}<b<l_{max}$
4	Crank-rocker with crank AB or DC	$a^2<e^2+f^2\tan^2\alpha$ $c^2<e^2+g^2\tan^2\alpha$		—	—

Distances l and L are determined from the condition $\partial\lambda/\partial\psi=0$. From Fig. 5 it is clear that for the condition $\partial\lambda/\partial\psi=0$, there corresponds a geometrical condition: tangents to the circle DC at the points C_1 and C_2 are perpendicular to the lines BC_1 and BC_2 and this means that lines BC_1 and BC_2 are normals to the circle DC at points C_1 and C_2, i.e. these lie in the same plane with axis ED.

Similarly distances l' and L' are determined from the condition $\partial\lambda/\partial\varphi=0$ and lines CB_1 and CB_2 will be normal to the circle AB at points B_1 and B_2, i.e. they lie in one plane with the axis OA. If critical point of the function $\lambda\ (\varphi, \psi)$ is calculated from the condition (10), then on the basis of the above statement we note that critical value of λ represents a line which will be common normal to the circles AB and DC, i.e. from one side it lies in one plane with the axis OA and from the other side it is situated in another plane with the axis ED.

Let us consider the variable distances l, l' and L and L' as functions $l=l(\varphi)$, $L=L(\varphi)$, $l'=l'(\psi)$ and $L'=L'\ (\psi)$.

Functions $l(\varphi)$ and $L(\varphi)$ are determined as parts of function $\lambda(\varphi, \psi)$ with the additional requirement that variables φ and ψ satisfy the condition $\partial\lambda/\partial\psi=0$. That is why condition $\partial\lambda/\partial\varphi=0$ is satisfied in the critical points of the functions $l(\varphi)$ and $L(\varphi)$.

Similarly functions $l'(\psi)$ and $L'(\psi)$ represent parts of the function $\lambda(\varphi, \psi)$ with the additional condition $\partial\lambda/\partial\varphi=0$ and in the critical points of these functions, condition $\partial\lambda/\partial\psi=0$ is fulfilled.

In this way, critical points of functions $l(\varphi)$, $L(\varphi)$, $l'(\psi)$ and $L'(\psi)$ are determined by equation (10). Thus critical value of the function $\lambda(\varphi, \psi)$ is the critical value of one of the functions $l(\varphi)$ or $L(\varphi)$ as well as critical value of one of the functions $l'(\psi)$ or $L'(\psi)$.

From the definitions of functions $l(\varphi)$, $L(\varphi)$, $l'(\psi)$ and $L'(\psi)$ and geometrical consideration, it follows that these are single-valued continuous and finite functions.

Let us denote maximum and minimum values of these functions by the symbols $l_{\min}$, $l_{\max}$, $L_{\min}$, $L_{\max}$, $l'_{\min}$, $l'_{\max}$, $L'_{\min}$ and $L'_{\max}$.

It is evident that :

$$l_{\min}=l'_{\min}=\lambda_{\min}, \qquad L_{\max}=L'_{\max}=\lambda_{\max}, \tag{11}$$

where $\lambda_{\min}$ and $\lambda_{\max}$—minimum and maximum values of λ.

Zones of existence of the mechanism depend on the length of the connecting rod and are determined from the condition:

$$l_{\min}<b<L_{\max}. \tag{12}$$

Extreme values $l_{\max}$, $L_{\min}$, $l'_{\max}$ and $L'_{\min}$ represent the minimum and maximum of the function $\lambda(\varphi, \psi)$. These extreme values are conditions of existence of cranks in the given mechanism.

Let us show that depending on the length of the connecting rod, area of existence of crank AB is determined by the condition:

$$l_{max}<b<L_{min}. \tag{13}$$

Let the length of the connecting rod not fulfill the condition (13). Let us consider the case:

$$l_{min}<b<l_{max}.$$

If the function $l(\varphi)$ is continuous, then in some point $\varphi=\varphi_0$ we shall have $b=l(\varphi_0)$; this means that in the position of the mechanism with angle $\varphi=\varphi_0$ variables φ and ψ satisfy equation (3) and consequently link AB is in the extreme position. That is why in the given case, link AB cannot be crank.

Similarly, we can prove that line AB is not the crank under the condition,

$$L_{min}<b<L_{max}.$$

In a similar way, it may be shown that range of existence of crank $ABDC$ is determined from equation:

$$l'_{max}<b<L'_{min}. \tag{14}$$

Theorem 3. *In the interval* (l_{max}, L_{min}) *functions* $l'(\psi)$ *and* $L'(\psi)$ *cannot take the critical values.*

Proof. Let us consider two possible cases.

1) $l_{max}<L_{min}$ (Fig. 6): Let function $l'(\psi)$ or $L'(\psi)$ have critical value λ_0 in the interval $l_{max}<\lambda_0<L_{min}$. This means that λ_0 will be the critical value of one of the functions $l(\varphi)$ or $L(\varphi)$. But as in the given case $l(\varphi)$ and $L(\varphi)$ in the interval (l_{max}, L_{min}) do not exist, so the existence of critical value λ_0 of functions $l'(\psi)$ and $L'(\psi)$ is not possible.

2) $l_{max}>L_{min}$ (Fig. 7): From Fig. 5 it is clear that points B, lying on the surface of the tore with the guiding circle DC with the circular section of radius l satisfy the condition $l=L=$const. As surface of the tore and circle intersect in not more than 4 points, so the maximum number of points B, which satisfy the condition $l=L=$const, is equal to 4.

This means any straight line on the graph of functions $l(\varphi)$ and $L(\varphi)$ and parallel to the abscissa (see Fig. 7) intersects the curves $l(\varphi)$ and $L(\varphi)$ in not more than 4 points.

It is clear from Fig. 7 that any straight line, parallel to the abscissa in the interval (l_{max}, L_{min}), intersects curves $l(\varphi)$ and $L(\varphi)$ in 4 points: M_1, M_2, M_3 and M_4. Therefore, not even one of these points in the interval (l_{max}, L_{min}) can be a multiple because a multiple point is equal to 2 points of intersection (we may note that contact point of the surface of the tore with the circle corresponds to the multiple point).

Thus, functions $l(\varphi)$ and $L(\varphi)$ in the interval $(l_{\max}, L_{\min})$ do not have critical values. Consequently, existence of critical values of functions $l'(\psi)$ and $L'(\psi)$ in the given interval is also not possible.

Similarly we can prove the following theorem.

Theorem 4. *Functions* $l(\varphi)$ *and* $L(\varphi)$ *cannot have critical values in the interval* $(l'_{\max}, L'_{\min})$.

On the basis of this theorem, we will show that it is necessary to have the following relations between the extremes $l_{\max}$, $L_{\min}$, $L'_{\min}$ and $l'_{\max}$:

$$l_{\max}=l'_{\max}, \qquad L_{\min}=L'_{\min} \tag{15}$$

or

$$l_{\max}=L'_{\min}, \qquad L_{\min}=l'_{\max}. \tag{16}$$

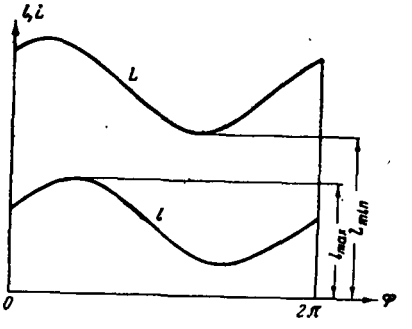

Fig. 6.

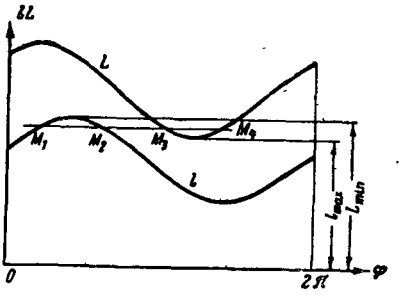

Fig. 7.

Let us consider the following cases:

1) Let the mechanism be a double-crank mechanism; then length of the connecting rod fulfills equations (13) and (14). Keeping in mind theorems 3 and 4, we get, that equations (13) and (14) are satisfied simultaneously, if equations (15) are satisfied.

In the given case we get a double crank mechanism by the variation of the length of the connecting rod, if the same lies in the interval $(l_{\max}, L_{\min})$ and in the reverse case—a double-rocker mechanism.

2) Let mechanism be a crank-rocker with the crank AB. In this case, length of the connecting rod satisfies equation (13).

On the basis of [9] we may note that in the extreme positions AB_1C_1D and AB_2C_2D of the crank-rocker mechanism, section B_1C_1 will definitely be the distance of the type l', if section B_2C_2 represents distance of the type L' and vice versa. Hence the length of the connecting rod must satisfy the condition:

$$L'_{\min}<b<l'_{\max}.$$

Keeping in mind theorems 3 and 4, we get that the above condition and equation (13) are simultaneously satisfied only when equations (16) are true.

In the given case, we get the crank-rocker mechanism with the crank AB by the variation of the length of the connecting rod; if the length of the connecting rod is contained in the interval (l_{max}, L_{min}) and otherwise, a double-rocker mechanism results.

3) Let the mechanism be crank-rocker mechanism with the crank DC. Analysis of this case is similar to the previous one.

Thus, it is necessary that equations (15) or (16) are satisfied for the extreme values l_{max}, L_{min}, l'_{max} and L'_{min}.

If equation (15) is satisfied, depending on the length of the connecting rod, the mechanism may be double-crank or a double-rocker mechanism. With equation (16) satisfied, depending on the length of the connecting rod, the mechanism may be double-rocker or,

1) crank-rocker with crank AB, if $l_{max} < L_{min}$,

2) crank-rocker with crank DC, if $L_{min} < l_{max}$.

On the basis of equation (16) and equation (14), the condition of existence of crank-rocker mechanism with the crank DC will be expressed in the form:

$$L_{min} < b < l_{max}. \tag{17}$$

Relations between the extremes l_{max}, L_{min}, l'_{max} and L'_{min} and conditions of existence of the crank are given in the last two columns of the Table 1.

In this way, determination of the zones of existence of the mechanism and crank depending on the length of the connecting rod reduces to the determination of extreme values l_{min}, l_{max}, L_{min} and L_{max}.

For the calculation of the above mentioned extreme values, we solve the system of equations (3) and (8), and substituting the values of variables φ and ψ in the equation (9), we determine the critical value of λ. The minimum of the values of λ represents l_{min}, and maximum—L_{max}. To find l_{max} and L_{min} from the other values of λ, it is necessary to take into consideration that if the value of $\lambda(\varphi_0, \psi_0)$ represents the distance of the type l, then:

$$\lambda(\varphi_0, \psi_0) < \lambda(\varphi_0, \psi'_0), \tag{18}$$

where ψ_0' takes any value, not equal to ψ_0.

Taking $\psi_0' = k\pi/2$, where $k=0, 1, 2, \ldots$, this gives us the possibility of calculating $\lambda(\varphi'_0, \psi'_0)$ without laborious calculations.

For example, let system of equations (3) and (8) have six real solutions: $\varphi=\varphi_1$, $\psi=\psi_1$, $\varphi=\varphi_2$, $\psi=\psi_2$, $\ldots$, $\varphi=\varphi_6$, $\psi=\psi_6$, substituting these solutions in the equation (9), we get six values for λ: λ_1 λ_2, λ_3, λ_4, λ_5 and λ_6. Now let $\lambda_1 < \lambda_2 < \lambda_3 \ldots, < \lambda_6$, then we have $l_{min} = \lambda_1$ and $L_{max} = \lambda_6$. Let only λ_5 from the values λ_2, λ_3, λ_4, λ_5 not satisfy the condition (18). This means that λ_2, λ_3, λ_4 represent distances l and λ_5 distance L. Therefore, in the given case, $l_{max} = \lambda_4$ and $L_{min} = \lambda_5$.

It may be noted that in general the set of equations (3) and (8) may be solved only by the numerical methods.

Let us show the graphical determination of extremes l_{min}, l_{max}, L_{min} and L_{max}. For this we make use of the method of circular projections of geometrical drawing. Let us draw a plane T through the axis OA (Fig. 8), and take this as plane of projections. Let us take arcs of circles as projecting rays which have common axis OA. To each point in the space will correspond two projections in the plane T. Let us project the circles AB and DC on the plane T. Circular projections of the circle AB is represented by points B_1 and B_2 of the circle DC two curves: γ and the curve symmetrical to γ with respect to axis OA (this curve is not shown in the figure).

For definiteness, we always place curve γ on the right side of the OA.

Let BC represent l_{max} in Fig. 8. The circular projection of the straight line BC will be B_1C_T. Let us draw a sphere of radius BC with the center in the point B. Circular projection of this sphere on the plane T, will be a circle β, with the center at point B_1 and radius equal to BC. Since the tangent to the circle DC at the point C is perpendicular to the straight line BC, then the sphere touches the circle DC in the point C. Hence the circle β touches the curve γ, which is located completely outside the circle β.

Thus, in the given case of location of circles AB and DC, extreme value l_{max} is the minimum distance of the point B_1 to the curve γ.

Carrying out similar analysis for the rest of the extreme values, we find that with any relative location of circles AB and DC;

1) minimum distance of the point B_2 to the curve γ will be l_{min}.

2) maximum distance of the point B_1 to the curve γ will be L_{max}.

3) minimum distance λ_1 of the point B_1 to the curve γ and maximum distance λ_2 of the point B_2 to the curve γ are l_{max} and L_{min}.

Depending on the relative position of circles AB and DC, relationships $l_{max}=\lambda_1$ and $L_{min}=\lambda_2$ or $l_{max}=\lambda_2$ and $L_{min}=\lambda_1$ are observed.

For the determination of l_{max} and L_{min} we note that if the mechanism is of the types 1, 2, and 3 then it is not difficult to find l_{max} and L_{min} from Table 1 as per the correlations of λ_1 and λ_2, and if the mechanism is of the type 4, from the Fig. 8 it is clear that always $l_{max}=\lambda_1$, and hence $L_{min}=\lambda_2$.

Let us consider the example of determination of extreme distances. Let us draw circles AB and DC of the given mechanism in orthogonal projections (Fig. 9), and by the plano parallel motion, superpose the plane P of the circle DC with the frontal plane of the projections.

Draw a horizontal plane T through the axis OA and project circles AB and DC on the plane T with the arcs of circles having common axis OA. Points b_1 and b_2 are projections of circle AB and curve γ is the projection of circle DC. Method of drawing the points 2_0 of the curve γ is shown in

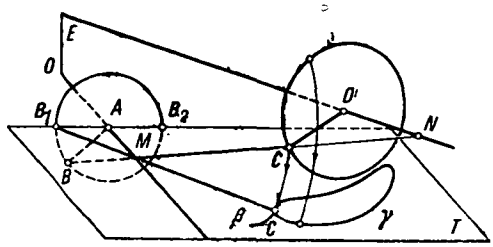

Fig. 8.

figure. Since the mechanism is of the type four in the given case, so for the extreme l_{max} corresponds a minimum distance of the point b_1 to the curve γ. It is not difficult to determine the rest of the extreme values after the determination of l_{max}.

Lengths l_{min}, l_{max}, L_{min} and L_{max} make it possible to establish the limits of variation of b for the existence of the crank and mechanism, and also point out the link which can be a crank. For the indicated length of the connecting rod, shown in Fig. 8, the mechanism is a crank-rocker with the crank DC.

For determining the conditions of existence of the crank, let us consider the particular case $f=g=0$. This mechanism is given in [10] where special charts for the determination of the condition of rotation of links are given, which makes it possible to calculate the extreme positions of links.

In the given case, parameter e is equal to the distance d between the points A and D.

Keeping in mind that in this case, four mechanisms with the angles α, $\alpha_1=\pi-\alpha$, $\alpha_2=\pi+\alpha$ and $\alpha_3=2\pi-\alpha$ are perfectly similar, we take:

$$0\leqslant\alpha\leqslant\pi/2.$$

We locate the mechanism in the system of coordinates $Oxyz$ in such a way, so that the following condition is observed.

$$a\leqslant c. \tag{19}$$

Depending on the ratio of parameters c and d, curve γ has three characteristic forms on the plane (Fig. 10). In Fig. 10, straight line AM is the axis of rotation of the link AB and AN-line of intersection of the plane of rotation of the link AB with the plane T.

At $c\leqslant d$, curve γ completely lies in the circle *1* and touches the circle *1* in points C_1 and C_2 (Fig. 10,a).

At $c>d$, curve completely lies in the area bounded by the arc of the circle *1* and the straight line *3* (Fig. 10,b) or it lies in the area bounded by the arcs

of the circles *1* and *2* (Fig. 10,c). As in the case of Fig. 10,b in case of Fig. 10,c also point D may lie inside or outside the area bounded by the curve γ.

This case and also determination of areas of variation of parameters, corresponding to the form in Fig. 10,b or 10,c of the curve γ, will not be considered because these are only necessary during detailed investigation of conditions of turning of links.

Complete analysis of conditions of turning of links has not been carried out in the given paper because in this case it would have been necessary to take into consideration some other conditions which are a hindrance from the point of view of practical utilization of these conditions.

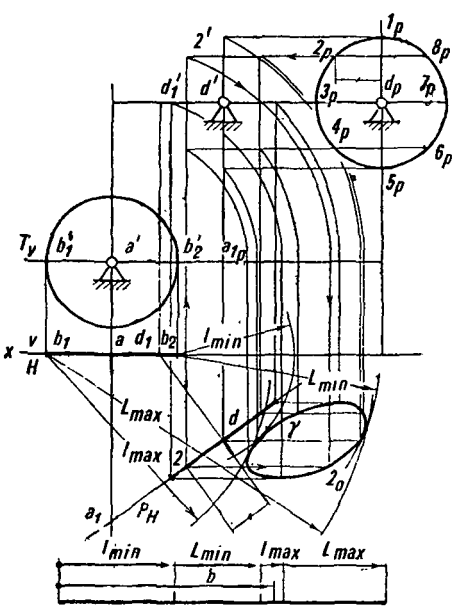

Fig. 9.

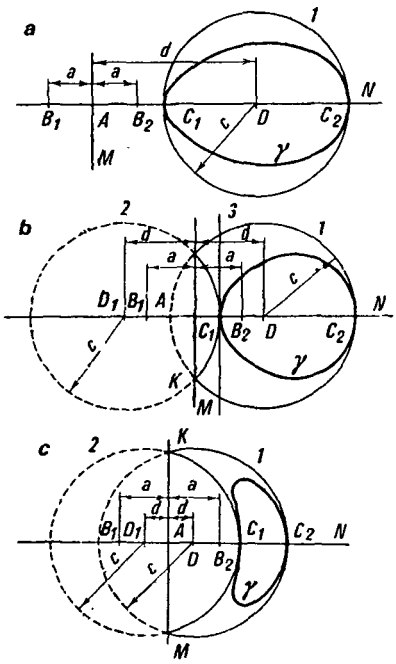

Fig. 10.

It may be noted that in all cases, straight line AN is axis of symmetry of the curve γ.

Let us study the different forms of the mechanism.

Type 1. From Table 1, we have conditions:

$$d<a\,, \qquad d<c. \tag{20}$$

In this case, curve γ is of the form shown in Fig. 10,b or 10,c and length DD_1 is less than B_1B_2. Considering that $l_{max}<L_{min}$ for the given form then from Fig. 10 we get:

$$L_{min}\leqslant B_1C_1=a+c-d, \qquad l_{max}>B_2C_2=d+c-a. \tag{21}$$

In the given case, for the existence of double-crank mechanism, necessary and sufficient condition is:

$$l_{max}<b<L_{min},$$

and from equations (21) we have necessary condition, i.e.

$$b<a+c-d, \qquad b>d+c-a, \tag{22}$$

from where,

$$d+b<a+c, \qquad d+c<a+b. \tag{23}$$

Thus, in the particular case $f=g=0$ at $0<\alpha<\pi/2$, set of relationships:

$$d+a<b+c \qquad d+b<a+c \qquad d+c<a+b \tag{24}$$

is necessary but not sufficient condition for the existence of double-crank mechanism. The first inequality of set (24) has been derived taking into consideration equation (20).

When $\alpha=0$ (plane hinged four-link mechanism), curve γ is reduced to the line C_1C_2 and inequality (21) takes the form:

$$L_{min}=a+c-d, \qquad l_{max}=d+c-a. \tag{25}$$

Consequently, in this case the set of inequalities (24) will be necessary and sufficient condition for the existence of double-crank mechanism which does not contradict Grashof's condition.

When $\alpha=\pi/2$, curve γ takes the form of the arc of circles *1* and *2*. From Fig. 10 we have:

$$l_{max}=L_{min}=B_1K=B_2K.$$

Hence in the given case, a double-crank mechanism is not possible, because for $b=B_1K$ we get the mechanisms of the form shown in Fig. 3.

From Fig. 10 it is evident that when $\alpha\neq\pi/2$

$$l_{max}<B_1K<L_{min}.$$

This means that at $b=B_1K$ mechanism will become double-crank. From Fig. 10 we have,

$$B_1K=\sqrt{AK^2+AB_1^2}, \qquad AK^2=D_1K^2-AD_1^2,$$

with the consideration of the fact that $AD_1=d$; $AB_1=a$ and $D_1K=c$, we get:

$$B_1K=\sqrt{a^2+c^2-d^2}.$$

Thus the mechanism is double-crank if the system of equations (24) and

$$b=\sqrt{a^2+c^2-d^2},$$

hold good.

From Fig. 10 it is evident that for constant values of a, c and d with the increase in the values of α, $L_{\min}$ decreases and $l_{\max}$ increases, i.e. field of existence of double-crank mechanism decreases.

Thus, set of equations (24) for the double-crank mechanism is necessary and sufficient condition when $\alpha=0$ and is necessary but not sufficient condition when $\alpha\neq 0$; with the increase in α, field of existence of double-crank mechanism decreases and finally when $\alpha=\pi/2$ double-crank mechanism is not possible.

Type 2. From Table 1, we have the condition:

$$a<d, \qquad c>d. \tag{26}$$

In this case curve γ will have the form of Fig. 10,b or 10,c and length DD_1 will become more than B_1B_2. Considering, that for the given type $l_{\max}<L_{\min}$, we have from Fig. 10:

$$\begin{aligned} L_{\min}&=B_2C_2=d-a+c,\\ l_{\max}&=B_1C_1=c-d+a. \end{aligned} \tag{27}$$

From equations (27), we write the condition of existence of crank-rocker mechanism with the crank AB,

$$b<d-a+c, \qquad b>c-d+a,$$

from where,

$$\begin{aligned} a+b&<c+d,\\ a+c&<b+d. \end{aligned} \tag{28}$$

When $\alpha=\pi/2$ and $b=B_1K$ we get the mechanism of type shown in Fig. 3. It may be noted that instead of equation (26), the following condition may be added to inequalities (28)

$$a+d<b+c. \tag{29}$$

Type 3. From Table 1 we have the conditions,

$$a>d, \quad c<d,$$

but since these relationships do not agree with equation (19), we shall not consider this type.

Type 4. From Table 1 we have the following conditions:

$$a<d, \quad c<d. \tag{30}$$

In this case, curve γ has the path as shown in Fig. 10,a. From Fig. 10 we get:

$$\begin{aligned} l_{\max}&=B_1C_1=a+d-c, \\ L_{\min}&=B_2C_2=d+c-a. \end{aligned} \tag{31}$$

From equations (31), we will find the condition of existence of crank-rocker mechanism with crank AB

$$\begin{aligned} b&>a+d-c, \\ b&<d+c-a, \end{aligned}$$

from where,

$$\begin{aligned} a+b&<c+d, \\ a+d&<b+c. \end{aligned} \tag{32}$$

It may be noted that instead of equations (30) the following condition may be added to equations (32):

$$a+c<b+d. \tag{33}$$

From equations (28), (29), (32) and (33) we get the following: In the particular case $f=g=0$, for any α, set of inequalities:

$$\begin{aligned} a+b&<c+d, \\ a+c&<b+d, \\ a+d&<b+c, \end{aligned} \tag{34}$$

is the necessary and sufficient condition of existence of the crank-rocker mechanism with the crank AB, with the exception of the mechanism of the type in Fig. 3, which are obtained at the simultaneous fulfilment of the condition:

$$\alpha=\pi/2, \; c\geqslant d \text{ and } b=\sqrt{a^2+c^2-d^2}.$$

References

1. Dzhabua, G. A. Analiticheskoe issledovanie chetyrekhzvennogo prostranstvennogo mekhanizma (Analytical Investigation of Four Link Spatial Mechanism). Tbilisi. Izd-vo Tsodna, 1963.
2. Egorov, V. V. Graficheskii metod opredeleniya polozhenii prostranstvennykh mekhanizmov (Graphical method of determination of positions of spatial mechanisms). *Trudy seminara po teorii mashin i mekhanizmov,* vyp. 25. Izd-vo AN SSSR, 1949.

3. KOZHEVNIKOV, S. N. K voprosu o kinematike i sinteze prostranstvennykh krivoshipno-koromyslovykh mekhanizmov (Problem of the kinematics and synthesis of spatial crank-rocker mechanisms). *Trudy seminara po teorii mashin i mekhanizmov,* vyp. 9, Izd-vo AN SSSR, 1947.
4. LANGE, O. I. Usloviya sushchestvovaniya krivoshipa v chetyrekhzvennom i krivoshipno-shatunnom prostranstvennykh mekhanizmakh (Conditions of existence of crank in four link and crank slider spatial mechanisms). *Izv. vuzov. Mashinostroenie,* No. 9, 1965.
5. LEBEDEV, P. A. Usloviya sushchestvovaniya krivoshipa v prostranstvennykh chetyrekhzvennikakh (Conditions of existence of crank in spatial four-link mechanism). *Izv. vuzov. Tekhnologia legkoi promyshlennosti,* No. 5, 1966.
6. LIBERG, L. A. K voprosu o graficheskom sposobe opredeleniya radiusa krivoshipa prostranstvennogo chetyrekhzvennika (A graphical method for the retermination of radius of crank of spatial four link mechanism). *Trudy seminara po teorii mashin i mekhanizmov,* vyp. 85, Izd-vo AN SSSR, 1961.
7. TAVKHELIDZE, D. S. K voprosu o sushchestvovanii krivoshipa i dvykh krivoshipov v prostranstvennykh mekhanizmakh (Existence of a crank in spatial four link mechanism). *Trudy seminara po teorii mashin i mekhanizmov,* vyp. 9, Izd-vo AN SSSR, 1947.
8. TARKHANOV, K. S. Usloviya provorachivaemosti krivoshipa v prostranstvennom chetyrekhzvennike (Conditions of Rotation of Crank in Spatial Four Link Mechanism). Sbornik *Voprosy teorii mashin i mekhanizmov, Trudy MVTU im. Baumana,* vyp. 65, 1955.
9. TSVIYAK, P. B. K voprosu ob issledovanii i proektirovanii prostranstvennykh mekhanizmov pervoi gruppy s nizshimi parami grafoanaliticheskimi metodami (Investigation and design of spatial mechanisms of first group with lower pairs by graphical and analytical methods). *Trudy seminara po teorii mashin i mekhanizmov,* vyp. 62, Izd-vo AN SSSR, 1956.
10. HARRISBERGER, L. Simple technique for synthesizing space crank mechanisms used in transmitting angular motion between two skewed shafts. *Machine Design,* **36**, No. 21, 1964.

Yu. V. Epshtein and *V. A. Novgorodtsev*

FUNCTIONS WITH MINIMUM DEVIATIONS FROM ZERO IN PROBLEMS OF SYNTHESIS OF CAM MECHANISMS

Point M on the driven link of the cam mechanism where the force of productive resistance is applied and the law of motion is optimum—satisfies two conditions:

a) Point M does not have natural oscillations during dwell, acceleration or deceleration.

b) The maximum module of the function, which represents numerically the main condition of synthesis for which it is particularly important to use the best available solution.

Let us denote the function, whose maximum module has been minimized as the main characteristic of the mechanism. This gives along with the condition (a) the significance of the optimum which changes with different working regions. The problem will be solved with the help of an algorithm, which is applicable for all the main characteristics currently in use [1].

If the cam mechanism is of the multiple-link type, the kinematic chain, driven by the cam, will have a large number of natural frequencies. Hence for fulfilling the conditions (a) and (b), it is necessary to have a large number of free parameters. The solution may be obtained through the exponential polynomial as a function of the simplest calculation, which is convenient for computing machines. By increasing the exponent of the polynomial, practically any number of free parameters may be put in the problem. Either the polynomial, with minimum deviation from zero or the function with minimum deviation from zero, is formed by means of the algorithm. But the polynomial is used in the calculation procedure. The algorithm is programmed for a digital computer.

Polynomials with minimum deviation from zero, were first used by Ya. L. Geronimus [2] in the problems of synthesis of cam mechanisms. They provide the best solution for the problems and are convenient to use because

of their simplicity. If dimensionless coefficients of the polynomials are given to the designer, then the complex procedure for finding out the optimum is reduced to the calculation of the coordinates of the points of the cam profile. The mathematical concepts of P. L. Chebyshev [3] form the siasis of these polynomials on which the most prospective method of synthesis c based. Foreign researchers have not investigated this method.

1. Let us consider point M to be the point of applibation of the masses and forces of the chain, driven by the cam, and assume that after satisfying the condition (a), all natural frequencies, except one, say the ν-th may be neglected in the spectrum of natural frequencies of the chain. Then the system, which is dynamically equivalent to the cam mechanisms, is of unit mass (Fig. 1,a). The constants of the system must be selected in such a way, that its natural frequency would be:

$$\nu^2=(c+c^*)/m,$$

where,

m—mass of the chain, driven by the cam, reduced to the point M;

c—rigidity of the chain;

c^*—rigidity of the spring, closing the higher pair.

Let

h—swing of the point M during starting motion,

T—period of the starting motion,

α—coefficient of damping of vibrations,

q_1—coordinate of point M (it is assumed that this point moves either in a straight line or along the arc of the circle).

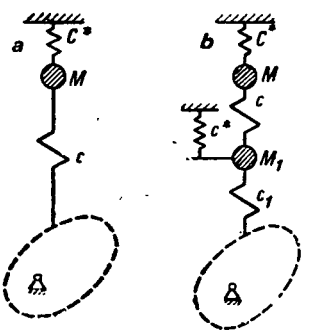

Fig. 1.

Let us put:

$$q_1(t)=q_1(0)+\xi_1(t),$$

$$q(t)=q(0)+\xi(t),$$

and let us introduce dimensionless quantities in the problem under consideration:

$$y=\xi_1/h, \qquad \tilde{y}=\xi/h, \qquad k=t/T,$$

and write differential equation of motion of the equivalent system in terms of these quantities. We have:

$$y''+\beta_1 y'+\beta_2 y=\beta_2 Q(k), \tag{1}$$

where, $\beta_1=\alpha T/m$, $\beta_2=\nu^2 T^2$.

Right hand side of the equation (1) is expressed as:

$$Q(k)=(\tilde{y}\ (k)-F(y)/ch)\ c/\ (c+c^*), \tag{2}$$

where $F(y)$—algebraic sum of the reduced forces of all the resistances of the chain and the constant component of the elastic force of the closing spring.

In [1], it has been shown that if in the interval of starting motion ($0\leqslant k\leqslant 1$), the solution of the heterogeneous equation (1) conforms to the zero initial conditions $y(0)=y'(0)=y''(0)=0$, and in the interval of dwell ($k\geqslant 1$) solution of the same equation satisfies the initial conditions $y(1)=1, y'(1)=y''(1)=0$, the condition (a) of optimum is completely fulfilled.

It may be stressed that dynamic conditions of the sufficiently common cam mechanisms, preferably belonging to automats are such that for making the optimum law more accurate, it is necessary to add to the system s degrees of freedom where, s—number of frequencies of the spectrum of the chain driven by the cam, which cannot be neglected in the problem.

Let $s=2$ and let coordinates y and y_1, where y again represents the coordinate of point M (Fig. 1,b), describe the motion of the equivalent system. Masses m and m_1, of the equivalent system and rigidity c and c_1, of the elastic constraints of the system are found by using the theory of small vibrations [4, 5] so that the following equations are satisfied:

$$\nu^2=(c+c^*)/m, \qquad \nu_1^2=(c+c_1+c_1^*)/m_1, \tag{3}$$

where, ν and ν_1—given numbers, c^*—rigidity of the closing spring, if the movable end of the spring is fastened to the system of the mechanism in such a way that it is necessary to connect it with the mass m in the equivalent system, and c_1^*—if the same end of the spring is to be connected with the mass m_1 (Fig. 1,b).

The system of differential equations of motion of the equivalent system is expressed as:

$$\begin{aligned} &m_1 y_1''/T^2-c(y-y_1)+c_1(y_1-\tilde{y})+c_1^* y_1=0,\\ &my''/T^2+\alpha/Ty'+c(y-y_1)+c^*y=-F(y)/h, \end{aligned} \tag{4}$$

where, α, T, $F(y)$ have the same meaning as given earlier.

In these equations $c^*=0$, if the movable end of the closing spring is connected with the mass m_1 and $c_1^*=0$ if it is connected with mass m.

Eliminating coordinate y_1 and derivatives of this coordinate from the system of equations (4) we get,

$$y^{IV}+\beta_1 y^{III}+\beta_2 y^{II}+\beta_3 y^{I}+\beta_4 y=\beta_4 Q(k), \tag{5}$$

where, $\beta_1=\alpha T/m$; $\beta_2=(\nu^2+\nu_1^2)T^2$; $\beta_3=\beta_1\nu_1^2T^2$; $\beta_4=(\nu^2\nu_1^2+c^2/mm_1)\ T^4$.
Right hand side of the equation (5) is equal to:

$$Q(k)=[c_1/m_1\tilde{y}(k)-1/ch(\nu_1^2F+F''/T^2)]cT^4\beta_4 m. \tag{6}$$

If the equivalent system has s degrees of freedom, then the differential equation, describing the motion of m is of the order $2s$. Our formulation permits solution if forces of friction and damping have been brought to the point M and only to the point M.

2. Let the motion of the point M follow the region dwell-start-dwell. Let us solve the differential equation (5) in two intervals: firstly in the interval of start and then in that interval of dwell which proceeds after the start. We combine both the solutions in the point $k=1$ in such a way, that initial conditions for the second solution are those values which are obtained by putting $k=1$ in the first solution.

Let us represent the function (6) in the form of polynomial of degree n:

$$Q(k)=\sum_{i=0}^{n} a_i k^i \quad (0\leqslant k\leqslant 1), \tag{7}$$

where, a_i $(i=0,\ 1,\ \ldots,n)$—for the time being are unknown numbers, satisfying the conditions:

$$Q(0)=0, \quad Q(1)=1. \tag{8}$$

These conditions prevent the function (6) from being noncontinuous in points $k=0$ and $k=1$. Particular solution of the heterogeneous equation (5) will be found in the form of polynomial of degree n:

$$y^*(k')=\sum_{i=0}^{n} b_i k^i \quad (0\leqslant k\leqslant 1). \tag{9}$$

Coefficients of the polynomials (7) and (9) are linearly connected. By putting both the polynomials in the equation (5) and equating the coefficients of similar powers of k on both sides of the resulting expression, we have:

$$a_i=b_i+\frac{1}{\beta_4}\sum_{g=1}^{4}\beta_g b_{i+g}\prod_{j=1}^{g}(i+j), \tag{10}$$

where $b_i=0$ for all $i\geqslant n+1$.

General solution of the homogeneous equation, corresponding to the heterogeneous equation (5) will be:

$$\Upsilon = C_1 e^{\gamma_1 k} + C_2 e^{\gamma_2 k} + C_3 e^{\gamma_3 k} + C_4 e^{\gamma_4 k}, \tag{11}$$

where $\gamma_i (i=1, 2, 3, 4)$—roots of the characteristic equation.

According to the conditions of the problem, each of the roots is different from 0 and it can be so arranged that there are no multiple roots. Our homogeneous equation with constant coefficients has a singular solution if the number of initial conditions is equal to the number of roots.

Let all the initial conditions be zero, i.e.

$$y(0)=y'(0)=y''(0)=y'''(0)=0. \tag{12}$$

Then general solution of the homogeneous equation is identically equal to zero. Making use of the expressions (9) and (11), we find that $b_i=0$, $(i=0, 1, 2, 3)$. Substituting in the equation (5), $k=0$ and after fulfilling the first of the conditions (8), we get:

$$y^{IV}(0)=0, \tag{13}$$

from where, $b_4=0$. Returning to the heterogeneous equation (5), we have:

$$y(k)=y^*(k)+\Upsilon=\sum_{i=0}^{n} b_i k^i \quad (0 \leqslant k \leqslant 1). \tag{14}$$

Successively differentiating the expression (14) four times and putting $k=1$, we get:

$$y(1)=\sum_{i=5}^{n} b_i; \qquad y'(1)=\sum_{i=5}^{n} i b_i; \qquad y''(1)=\sum_{i=5}^{n} (i-1) i b_i, \tag{15}$$

$$y'''(1)=\sum_{i=5}^{n} (i-2)(i-1) i b_i; \qquad y^{IV}(1)=\sum_{i=5}^{n} (i-3)(i-2)(i-1) i b_i.$$

The characteristic polynomial has the same four roots in the interval of dwell and in order that the homogeneous equation, corresponding to the heterogeneous equation (5) in the interval of running down similarly had a singular solution, it is necessary that this solution is subjected to four new initial conditions.

It has already been shown that these initial conditions may be obtained by putting $k=1$ in the solution (14) and in the expressions obtained by differentiating equation (14). After plotting the function $\tilde{y}(k)$ which gives the cam, profile, coefficients a_i $(i=5, 6, \ldots, n)$ of the polynomial (7)

and b_i ($i=5, 6, \ldots, n$) of the polynomial (9) are realized in such a way that new initial conditions may be expressed in the following way:

$$y(1)=1, \qquad y'(1)=y''(1)=y'''(1)=0. \tag{16}$$

The solution of the homogeneous equation in the nterval of start (acceleration) is identically equal to zero and condition (a) of optimum will be completely satisfied.

Substituting condition (16) in expression (15), we get 4 linear correlations which must be compiled by the coefficients b_i ($i=5, 6, \ldots, n$).

Putting $k=1$ in equation (5) and on the basis of expression (16) and the second condition (8), we get:

$$y^{IV}(1)=0. \tag{17}$$

This result puts another linear constraint on the coefficients b_i ($i=5, 6, \ldots, n$).

If the equivalent system has s degrees of freedom, then condition (a) will be completely satisfied when:

$$\begin{gathered} y(0)=y'(0)=y''(0)=,\ldots,=y^{(\rho-1)}(0)=0, \\ y(1)=1, y'(1)=y''(1)=,\ldots,=y^{(\rho-1)}(1)=0, \end{gathered} \tag{18}$$

where, $\rho=2s+1$.

Expressions (18) have to be satisfied even in the case when the elasticity of links of the mechanism is neglected; in this case $\rho \geqslant 2$. Keeping in mind all the problems arising in actual practice, let us define the terms being used in our problem, which are new in the technical literature.

Let y—coordinate of point M of the cam mechanism. Let us call the function $y(k)$ as the polydynamic law of motion of point M, if it is a polynomial of degree n so that conditions (18) are fulfilled. If in addition the function $y(k)$ reduces the main characteristic of the mechanism to a minimum we denote it as the optimum polydynamic law.

3. Considering all the known main characteristics in practice, we form four problems:

Problem 1. Main characteristic is the derivative $y^{(r)}(r=1, 2)$.

Problem 2. Main characteristic is the product $y' \cdot y''$[6] (maximum power module of the system of forces of inertia of the chain, driven by the cam, are minimized).

Problem 3. In the segment (0.5; 1) basic characteristic will be the fraction $y''(k)/y(k)$, if the tachogram in this segment is symmetrical (maximum modulus of the effective component of reaction of the cam, applied to the follower is minimized; it is assumed that the system of the follower moves under the action of this component of reaction of the cam only).

Problem 4. Main characteristic, if $s=1$, will be the fraction $mh/(T^2y''+c^*hy+F)$: ρ_{red}, where ρ_{red} is the reduced radius of curvature of element of the higher pair, and ρ_{red} is expressed as a function of y, four first derivatives of y and the constants of the mechanism occurring in the Hertz formula (maximum modulus of maximum contact stresses in the elements of higher pair is minimized).

Important from the practical point of view, the problem of the wear resistance of the profile connected with the occurrence of sliding and rolling of the roller along the profile is given in [7]. This problem poses another main characteristic (which can be considered as condition *b*). This has not been investigated by the authors so far.

Problem 1, with the simplest main characteristic, is transformed to the well known mathematical problem of V. A. Markov, about the formation of polynomial of given degree n in the given range and with minimum deviation from zero, whole coefficients comply with the linear relationship $m \leqslant n$. This problem does not have a general solution. Algorithm given in [1] solves this problem, approximately with sufficient accuracy for engineering purposes. In three other problems, the unknown function will be the one which has minimum deviation from zero.

For problems 1, 2 and 3, the solution obtained on the digital computer is of a general type suitable for all mechanisms having the given main characteristic. Constants of problem 4 depend on the specific properties of each mechanism, and for each mechanism it is necessary to repeat all the calculations. The authors have so far solved this problem only for flat followers, using the formula of Ya. L. Geronimus for the radius of curvature of the cam profile, which is convex at all its points.

The algorithm may be so changed that problem 4 is stated in form that rigidity of the spring which closes the higher pair serves the role of variable parameters.

If coefficients of the polynomial $y(k)=\sum_{i=0}^{n} b_i k^i$ are known to the designer, then using the relationship (10), he may determine the coefficients of the polynomial $Q(k)=\sum_{i=0}^{n} a_i k^i$; and subsequently calculate the coordinates $\tilde{y}(k)$ of the cam profile step by step according to the formula (2) if $s=1$ and according to formula (6) if $s=2$. It is necessary to express the function $\tilde{y}(k)$ in the analytical form if the cam is machined on numerically controlled machines.

4. The algorithm, described in [1], is based on splitting of the unknown polynomial $y(k)$ of n-th degree into two polynomials:

$$y(k)=y_0(k)+b_n y_D(k), \tag{18a}$$

where, $y_0(k)$—polynomial fulfilling only the condition (18), and

$y_D(k)$—polynomial of degree n, whose main coefficient is equal to one and others are connected among themselves by the linear relationship resulting again from the condition (18) if in this condition we put $y_D(1)=0$.

Constant b_n is varied on the digital computer and in the interval (0, 1), it has $(n-2\rho)$ roots either of the polynomial $y_D(k)$ or of the p-th derivative of this polynomial, where p is equal to the number of roots which lie in the interval (0, 1). The first round of variation is accomplished when the maximum inter module maximums of the main characteristic found on the i-th stage of the first process will become different by some given and sufficiently small value ε from the maximum module found on the previous $(i-1)$-th stage. These calculations are repeated for other arbitrarily selected initial conditions of the varying roots.

Machine calculations for first problem only may be carried out by means of a stronger algorithm, which does not place any limitations on the degree of extreme polynomial. Coefficients of the polynomial satisfy 2ρ linear relationships, where 2ρ—number of conditions of (18).

During calculations $n+1-2\rho$ roots of 1st derivative of the first extreme polynomial are varied. Without giving proof, we only state that,

1) polynomial $y(k)$ always has odd degree;

2) all variable roots lie in the interval (0, 1);

3) number of points of deflection of the extreme polynomial in the interval 0, [1] in our problem is expressed as:

$$\mu=(n+1)/2-\rho+d, \tag{19}$$

where, $d=1$, if $r=1$; if $r=2$ and fraction $(n+1)/2$—even number, then $d=2$ and $d=1$ when this fraction is an odd number.

Calculations on the digital computer are completed when all the value of μ of the points of deflection have been attained.

5. Coefficients and module-maximums of polynomials, for problems 1 and 2, are given in [1]. Similarly values of maximums of module of polynomials, fulfilling only condition (a) for the same number of conditions (18) are also given in [1].

Thus for example, in problem 1 when $r=1$, optimization decreases $\max y'(k) \,\|\, (0\leqslant k\leqslant 1)$ nearly by 35%.

Let us return to the problem 3. We shall solve an example of a mechanism, whose equivalent system has 1 degree of freedom. From the conditions of the problem $F(y)=0$; if, in addition we put in the equation (1) $\alpha=0$, we get:

$$y''+\nu^2T^2y=cT^2/m\tilde{y} \qquad (0\leqslant k\leqslant 1). \tag{20}$$

Let us resolve the reaction of the cam, applied to the system of the follower into two components (effective and noneffective components). Let us express the effective component in the form:

$$R_E(k)=R_E(0)+c^*h(\tilde{y}-y) \qquad (0\leqslant k\leqslant 1). \tag{21}$$

Making use of the equation (19), we have:

$$R_E(k)=R_E(0)+mh/T_2[y''(k)+ay(k)] \qquad (0\leqslant k\leqslant 1), \tag{22}$$

where,
$$a=c^*T^2/m. \tag{23}$$

With expression (22), the noneffective component may be expressed as:

$$R_L=R_E(k)\tan\delta, \tag{24}$$

where, δ—pressure angle.

Let maximum module of angle δ be rigidly standardized by means of two parameters of the kinematic diagram of the mechanism, which are nonexistent in our problem. Let us consider the binomial $y''(k)+ay(k)$ as the main characteristic. If maximum module of this binomial will be minimized in the interval (0, 1), then it may be stated that the region of friction of elements of the higher pair will be improved radically along with the minimization of maximum dynamic stresses in the elastic elements of the equivalent system.

For this form of the problem, constant c^*, appearing in expression (22), becomes the sought after parameter and constant $R_E(0)$ existing in the same expression will fulfill a single role: it provides the reserve of elastic force, which closes the higher pair, when the relationship given below is satisfied even for one single point k_1 of the interval (0, 1)

$$y''(k_1)+ay(k_1)=0. \tag{25}$$

Then all along the interval [0, 1] we have:

$$y''(k)+ay(k)\geqslant 0. \tag{26}$$

The following formulation may be given to the problem: if graph of the derivative $y'(k)$ is symmetrical with respect to the point $k=0.5$, it is required to convert the maximum module of the positive polynomial (26) into minimum in the interval (0,1).

Let us express the expression (26) in the form:

$$ay(k)\geqslant -y''(k). \tag{27}$$

One of the typical graphs of function—$y''(y)$ is drawn in Fig. 2, and it is symmetrical with respect to the point $y=0.5$.

It follows from the relationship (27) that straight line ay will be the external tangent to the graph and straight line $a(y-1)$ will also be its external tangent because of the symmetry of the graph.

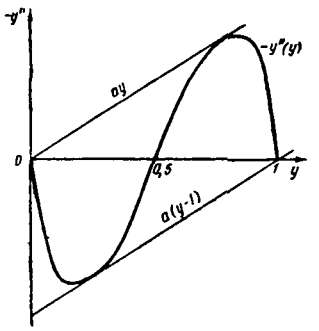

Fig. 2.

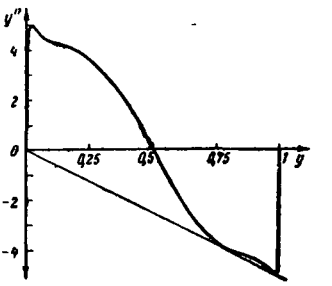

Fig. 3.

From Fig. 2 we have

$$\max|y''(k)+ay(k)|=a \qquad (0\leqslant k\leqslant 1). \tag{28}$$

In the interval (0.5; 1), the following equation is satisfied

$$a=\max|y''(k)/y(k)|. \tag{29}$$

We see that numerator of the expression $y''(k)$ $(0.5\leqslant k\leqslant 1)$ performs the role of main characteristic. Polynomial of degree $n=9$ which converts the maximum module of this characteristic into minimum in the interval (0.5; 1) and constructed by means of the common algorithm on the digital computer. "Minsk-2" is expressed as:

$$y(k)=24.316914\,k^3-131.891785\,k^4+406.695315\,k^5-$$
$$734.518757\,k^6+753.548442\,k^7-4077.64453\,k^8+90.614324\,k^9.$$

Graph of the function $y(k)$ is given in Fig. 3. Number of points of deflection of the function y''/y from 0 in the interval (0.5; 1) is equal to two.

If polynomial $y(k)$ satisfied only the condition a of the optimum then it has degree $n=5$ and

$$\max|y''(k)/y(k)|=6.152 \ (0.5\leqslant k\leqslant 1).$$

If condition (a) and condition (b) of the optimum are satisfied then at $n=9$:

$$\max|y''(k)/y(k)|=5.065 \quad (0.5\leqslant k\leqslant 1).$$

Rigidity of the closing spring is easily determined with the help of equations (23) and (29).

6. If $s=1$, then for conditions (18) $\rho=3$ and at points $k=0$ and $k=1$ discontinuity of the derivative $\tilde{y}'(k)$ takes place. This will lead to a rigid collision of the elements of higher pair and may possibly distort the optimum law of motion of the point M. Rigid collision may be avoided by putting $\rho=4$. This will increase the module-maximum of the extreme polynomial and consequently will lower the effect of optimization. It is true that module-maximum may be lowered by increasing the degree of the polynomial. However one may question whether

it is always necessary to avoid the rigid collision, if it impairs the dynamics of the chain, driven by the cam. Impact phenomena are closely connected with contact stresses in the zone of impact of the higher pair and in cach case a valid and sound solution may be given for each problem using standard equations.

7. For the evaluation of the effect of manufacturing errors of the profile of the cam on the optimum laws, experiments on special stands fitted with cam mechanisms were carried out for the case where follower of the mechanism performs translatory motion. Constants of the driven chain were selected in such a way that this chain is transformed into a unit mass equivalent system, with high degree of accuracy. Two sets of cams were manufactured with an equal degree of accuracy. Cams of the first group were profiled according to the cycloidal law for which extensive experimental data is available. This law is recommended for fast mechanisms. Cams of the second set were profiled according to the optimum law, determined for problem 1 at $r=2$, $n=9$ and $\rho=3$. All the constants of the equation (1) were found out experimentally.

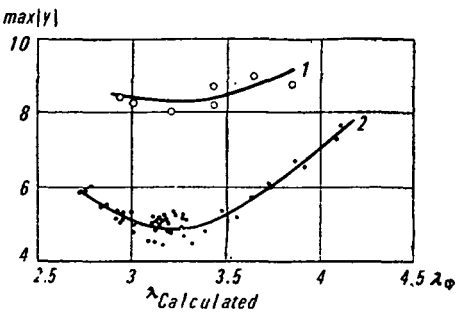

Fig. 4.

Graphs of the function $L(\lambda_\varphi)$, where $L=\max|y''|$ and λ_φ—actual number of free vibrations of the follower during the start, are drawn in Fig. 4, according to experimental data. Curve *1* is calculated for cycloidal and curve *2* for optimum polydynamic laws. During profiling of the cam, $\lambda_{calc}=3.183$ was taken.

It is clear from Fig. 4 that the effect of optimization is preserved at those values of λ_φ which are sufficiently close to λ_{calc}. Profile of the cams was machined with the tolerance of the order of 0.02 mm; in the design regime, effect of error of the profile on the properties of optimum law was not detected. During the profiling of cams, optimum law with main characteristic $y''(k)$ was selected, as this characteristic is particularly sensitive to the technological errors of the profile.

References

1. Novgorodtsev, V. A. and Yu. V. Epshtein. Optimizatsiya polidinamicheskikh zakonov dvizheniya vedomogo zvena kulachkovykh mekhanizmov (Optimization of Polydynamic Laws of Motion of Driven Link of Cam Mechanisms). Sbornik *Teoriya mekhanizmov i mashin*, vyp. 3, Kharkov, Izd-vo KhGU, 1967.
2. Geronimus, Ya. L. Dinamicheskii sintez mekhanizmov po Chebyshevu (Dynamic Synthesis of Mechanisms According to Chebyshev). Kharkov, Izd-vo KhGU, 1958.
3. Chebyshev, P. L. Polnoe sobranie sochinenii (Complete Collection of Articles). Volume II, Izd-vo AN SSSR, 1948.
4. Panovko, Ya. G. Prikladnaya teoriya kolebanii (Applied Theory of Vibrations). Mashgiz, 1958.
5. Korchemnyi, L. V. Mekhanizmy gazoraspredeleniya dvigatelya (Distribution Mechanisms of Engines). Izd-vo Mashinostroenie, 1964.
6. Tir, V. E. Komplekenyi raschet kulachkovykh mekhanizmov (Complex Calculation of Cam Mechanisms). Mashgiz, 1958.
7. Yudin, V. A. Analiz i sintez mekhanizmov (Analysis and synthesis of mechanisms). *Trudy 3-go soveshchaniya po osnovnym problemam teorii mashin i mekhanizmov*, Mashgiz, 1963.

ABSTRACTS

UDC 621.01

Kinematic Analysis of the Steering Linkage of an Automobile. N. I. Aleksishvili. Sbornik "Analysis and Synthesis of Mechanisms" (Analiz i sintez mekhanizmov). Izdatel'stvo Nauka, 1970, pages 7-13.

Conditions of efficiency of the steering linkage of an automobile having 4 kinematic pairs of 5th class are investigated in this paper, taking into consideration the possible deviations and errors in the dimensions of links of the linkage. A method for compensating for manufacturing or assembly errors of an automobile steering linkage by maintaining a prescribed clearance allowance in the turning pairs is proposed here.

A relationship is derived, which makes it possible to calculate the amount of clearance necessary to compensate for the deviations in the dimensions of the links of the steering mechanism of an automobile. Equations and procedures of calculation are intended to serve as an algorithm for solving the given problem with the help of digital computers.

Illustrations 4. References 3.

UDC 621.01

New Methods of Synthesis of Mechanisms for Reproducing and Enveloping Curves. E. G. Berger. Sbornik "Analysis and Synthesis of Mechanisms" (Analiz i sintez mekhanizmov). Izdatel'stvo Nauka, 1970, pages 13-21.

The proposed methods of synthesis of mechanisms are based on the theory of enveloping and the generalized transformation of curves. A curve is considered as enveloping a set of straight lines, constrained by definite geometrical conditions. The analysis gives proofs of three theorems.

On the basis of these methods, mechanisms for formation of sheet of Descartes and lemniscates of Bernoulli with the simultaneous enveloping of hyperbola and cubic parabola have been found and also for the formation

and enveloping of conical sections, enveloping of quadratic and semi-cubical parabolas and others.

The methods described give new insights in the synthesis of mechanisms. Illustrations 5. References 11.

UDC 621.01

Determination of Momentum in Three-link Mechanisms with a Higher Pair of the 4th Class. L. N. Borisenko. Sbornik "Analysis and Synthesis of Mechanisms" (Analiz i sintez mekhanizmov). Izdatel'stvo Nauka, 1970, pages 21-28.

Motion of a plane with respect to a point has been considered. During selection of motion of the plane, as described in paragraph 1, curves appear to be centroids in relative motion, while the curvature of curves are same at their point of contact. In addition the diameter of the rotating circle and both the parameters of the curve of circular points in the relative motion have been found.

For the three link mechanism, an inversion has been carried out in such a way, that driving link 1 becomes a support and profiles of the driving and driven links are conjugated roulettes. A moving system of coordinates connected with the plane has been specified, and diagrams of velocities, accelerations and angular momentum are drawn successively. In addition the absolute velocity, acceleration and angular momentum of a fixed point (before inversion) of the hinge of the driven link are known as well as the acceleration and angular momentum of ICV (Instantaneous Center of Velocity) in relative motion. Similarly the acceleration and projection on the polar tangent of the angular momentum of ICV in the plane are determined.

Examples illustrating determination of the angular momentum in plane cam mechanisms are presented.

Illustrations 3. References 5.

UDC 621.01

A Method of Calculating the Change in Primary Dimensions of Mechanisms due to Wear for the Purpose of Estimating Their Reliability. E. I. Vorob'ev. Sbornik "Analysis and Synthesis of Mechanism" (Analiz i sintez mekhanizmov). Izdatel'stvo Nauka, 1970, pages 28-35.

Change in tolerances of cam mechanism with the reciprocating follower have been determined by a method of calculation which takes into account abrasive and fatigue wear.

Equations for the determination of accidental loads of driven link of the mechanism have been obtained which can be used for evaluating the reliability of these mechanisms.

Illustrations 2. References 14.

UDC 621.01

Calculation of Kinematic Parameters of Radial-Piston Multipass Hydraulic Motors with Guide Block Profile Consisting of Arcs of Circles. A. S. Gel'man, Yu. A. Danilov, L. V. Krymova and A. M. Makeev. Sbornik "Analysis and Synthesis of Mechanisms" (Analiz i sintez mekhanizmov). Izdatel'stvo Nauka, 1970, pages 35-42.

Problems of kinematics of radial piston multipass hydraulic motors with guide block profile determined by normal and tangential components of absolute velocity and acceleration of the piston group of hydraulic motors are considered in this article. Motion of the roller on the convex, concave, linear and concentric parts of the profile has been considered.

Introduction of the transitional parameter-pressure angle, has made it possible to simplify the analytical expressions considerably, and to express these in a form, suitable for engineering practice.

Effect of the angular acceleration of the shaft on the amount of linear acceleration of piston group has been considered. Results have been generalized and put in a tabular form. An example is presented.

Tables 2. Illustrations 4. References 6.

UDC 621.835

Nomographs for Selecting Optimal Laws of Motion of the Driven Links of Cam Mechanisms. M. M. Gernet. Sbornik "Analysis and Synthesis of Mechanisms" (Analiz i sintez mekhanizmov). Izdatel'stvo Nauka, 1970, pages 42-48.

Cyclograms of automats may be consolidated by means of the application of rational laws of motion of the driven links and thus their efficiency may be increased. Selection of points is constrained by the limiting maximum values of the velocities and accelerations of driven links.

In this article, equations for selecting the optimum motion have been derived and nomographs drawn for determining relative duration of starting up (acceleration) u, and the positions of the center of gravity of the areas of accelerations λ_1 and λ_2 for motion with double portion tachograms as per the given maximum velocity, for motions with three section tachograms; for determining relative duration of uniform motion according to a given maximum velocity, for determining the relative duration of start up u and the positions of the center of gravity of the graphs of accelerations in case of $\lambda_1=\lambda_2=\lambda$, for laws with double section tachograms, for laws of motion with three section tachograms and for direct and inverse relationship of the maximum accelerations, maximum velocity and relative duration of start up.

Illustrations 7. References 3.

UDC 621.01

Design of a Four-link Mechanism for Reproducing a Given Motion. N. M. Guseinov and S. I. Gamrekeli. Sbornik "Analysis and Synthesis of Mechanisms" (Analiz i sintez mekhanizmov). Izdatel'stvo Nauka, 1970, pages 49-57.

Problems connected with the design of plane hinged four-link mechanisms for a given law of motion have been examined in this article.

The authors have come to the conclusion that a pragmatic method of solving the different problems of the synthesis of hinged four-link mechanisms involves the use of modeling.

This analysis clearly shows that modeling of four link hinged mechanisms makes it possible to form all possible variants of contours of the four-link mechanisms, and investigate these by varying the parameters. From these investigations, a conclusion can be made. Mechanical variation and selection of parameters for the given conditions simplifies the problem for the designer and scientists who have to spend considerable time on the design of plane four-link mechanisms.

Illustrations 6. References 6.

UDC 621.835

Synthesis of Cam Lever Mechanisms for Different Types of Motions of Driven Links. R. P. Dzhavakhyan. Sbornik "Analysis and Synthesis of Mechanisms" (Analiz i sintez mekhanizmov). Izdatel'stvo Nauka, 1970, pages 57-70.

The problem of synthesis of five-link lever cam mechanisms, in which

it is possible to regulate (both at rest and during motion) the stroke and phases of motion of the driven link, independently or according to a functional relationship, is investigated in this article.

Variation of parameters of motion of the driven link for a fixed profile of the cam is accomplished by varying the parameters of the four-link lever mechanism, which drives the cam into nonuniform motion or by varying the relative position of the cam and link.

Illustrations 6. References 8.

UDC 621.835

Effects of Errors in the Working Profile of the Cam on Velocity and Acceleration of the Follower. E. N. Dokuchaeva. Sbornik "Analysis and Synthesis of Mechanisms" (Analiz i sintez mekhanizmov). Izdatel'stvo Nauka, 1970, pages 70-81.

The effect of dimensional errors in the working profile of the cam on the law of motion of the roller follower (without the consideration of its elasticity) has been analyzed in this article. Irregularities on both smooth surfaces as well as surface with sharp turnings have been investigated.

Analytical expressions for the additional velocity and acceleration of the follower depending on the geometrical form of errors of the design profile and values of the radii of the roller of the follower have been determined. The article describes methods to determine the optimum value of the radius of the roller of the follower and how to increase or decrease it.

Illustrations 6. References 5.

UDC 621.01

Kinematic Study of Spatial Mechanisms by the Technique of Vector Analysis. Yu. M. Zingerman. Sbornik "Analysis and Synthesis of Mechanisms" (Analiz i sintez mekhanizmov). Izdatel'stvo Nauka, 1970, pages 81-88.

For the kinematic analysis of a rigid body, 6 vector projections of each basic vector must be known. If two links of the spatial mechanism are connected to form a kinematic pair, for transition from link to link, a number of vector projections equal to the number of degrees of freedom for relative motion of these links is "lost".

In this article the problem of determination of common vector projections of basic kinematic vectors, during the analysis of relative motion of

two links forming the given pair is solved, for eight commonly used kinematic pairs. Rules established in this paper have been applied for the kinematic analysis of a number of spatial mechanisms.

Table 1. Illustrations 4. References 7.

UDC 621.833

A Method of Analytical Synthesis of Plane Toothed Lever Mechanisms. V. S. Karelin. Sbornik "Analysis and Synthesis of Mechanisms" (Analiz i sintez mekhanizmov). Izdatel'stvo Nauka, 1970, pages 88-104.

Connecting equations of points of the given curve, form the basis of the method of synthesis given in this paper. These equations can be written in a matrix form which is denoted in this article as the Vandermond type of determinant. Exploring the properties of this determinant, three theorems have been proposed which allow us to simplify considerably the synthesis and exclude the differences between the methods of approximation for simple and multiple interpolation of sub-assemblies.

Similarly a theorem has been proposed in this article which shows that deviation of the limiting curve from the given curve is maximum out of all possible deviations in the given interval of approximation.

The method of analytical synthesis of the plane epicyclic mechanisms allows us to considerably simplify the synthesis of mechanism which are approximately directed along the straight line or a curve of second order.

Illustrations 6. References 10.

UDC 621.01

Two Simple Methods of Regulating Motion of the Driven Link in Three-dimensional Single Contour Mechanisms. A. A. Kasamanyan. Sbornik "Analysis and Synthesis of Mechanisms" (Analiz i sintez mekhanizmov). Izdatel'stvo Nauka, 1970, pages 104-112.

In cases, where it is required to keep the position of the driving and driven axes unchanged, the methods of regulation given below are considered to be the simplest of all existing methods.

Regulation by rearrangement of the driving or driven link around its fixed axis. This has been used in one of the spatial lever mechanisms already considered by the author.

In order to accomplish regulation during motion, a diagram of the

mechanism with the number of degrees of freedom more than one is taken.

The selected methods of regulation are illustrated through examples of simplest mechanisms, in which driving and driven links are those links which belong to the support and form a cylindrical pair with it.

A case is given, when it is expeditious to use the spatial regulating mechanism instead of a plane regulating one.

Illustrations 6. References 4.

UDC 621.833

Synthesis of a Toothed Lever Transmission Mechanism. A. E. Kropp. Sbornik "Analysis and Synthesis of Mechanisms" (Analiz i sintez mekhanizmov). Izdatel'stvo Nauka, 1970, pages 112-119.

A toothed-lever transmission mechanism is described here, which allows to change smoothly the velocity and torque on the driving shaft of the actuating machine under load without the use of any sort of frictional devices.

It is shown that the necessary relationship between the transmission ratio of the mechanism and the position of the regulating part may be obtained over a wide range. In particular, this property is used for obtaining the ideal pulling characteristic of the transporting machine. Under normal operating conditions when the transmission mechanism is not decelerating design relationships for the synthesis of four-link basic mechanisms are stated for a given mean transmission ratio, as well as for the variable mean transmission ratio.

For the range of operations analysed for the transmission mechanism, the equations for the calculation of velocities and accelerations of its driven links are given.

Illustrations 3. References 5.

UDC 621.01

Design of Three Dimensional Four-link Mechanisms Conforming to the Travel of the Driven Link and Coefficient of Increase in Velocity of the Reverse Stroke. V. I. Kulyugin. Sbornik "Analysis and Synthesis of Mechanisms" (Analiz i sintez mekhanizmov). Izdatel'stvo Nauka, 1970, pages 119-127.

Graphical and analytical methods of solving some problems of synthesis of the spatial crank-rocker mechanism of a general type conforming to a prescribed travel of the driven link and coefficient of increase of the velocity

of reverse stroke, are presented in this paper. In addition, the method of drawing the fields of possible location of the center of the hinge connecting crank with the connecting rod, which considerably facilitates the selection of location of the center of the hinge and fulfills not only the geometric but also the kinematic conditions of the problem, has also been given.

Illustrations 4. References 7.

UDC 621.01

Classification of Slotted Bar and Lever Mechanisms of Discontinuous Motion. P. G. Kukharenko. Sbornik "Analysis and Synthesis of Mechanisms" (Analiz i sintez mekhanizmov). Izdatel'stvo Nauka, 1970, pages 127-141.

Necessary and sufficient conditions of motion, instantaneous stop and dwell of links in the slotted bar-lever mechanisms have been analysed in this paper. Equations for the determination of coordinates of the profile of the linear rocker have been derived and peculiarities of the method of synthesis of mechanisms with curvilinear profile of the driven link have been shown.

A classification of 38 single position and multiple position mechanisms is given and displacement functions of some mechanisms with reciprocating, rocking and rotary motions of the driven link have been found out. These mechanisms make it possible to have the desired law of motion, and also vary the ratio of the duration of motion to the duration of stopping over a wide range and can be synthesized for realizing regulated dwell.

Reference materials provided in the article may be used for designing mechanisms with intermittent motion for automats.

Tables 4. Illustrations 6. References 17.

UDC 621.01

Peculiarities of the Lagrangian Method in the Synthesis of Mechanisms. N. I. Levitskii and Yu. L. Sarkisyan. Sbornik "Analysis and Synthesis of Mechanisms" (Analiz i sintez mekhanizmov). Izdatel'stvo Nauka, 1970, pages 142-147.

In this article integral expressions of Lagrangian multiples have been obtained on the basis of well known theorem about mean values. These expressions make it possible to make use of their equality to zero with sufficient accuracy, thus leading to the linearization of the nonlinear systems mentioned here.

An important property for the quadratic synthesis of the hinged mechanisms has been established: conditions of minimum-quadratic integral with some approximation, do not depend on equations of constraints, to which the nonlinear members of the approximation polynomials are subjected. The equations given here are identically satisfied within the limits of the assumptions.

Approximate simultaneous systems of linear equations whose number is equal to the number of unknowns and of nonlinear equations of constraints have been obtained. A method for solving the heterogeneous and homogeneous systems of equations for quadratic synthesis of mechanisms is given.

Examples of calculations of 4 and 5 parameters of the four-link mechanism for reproducing the logarithmic function are given. In the case of calculation of five parameters, zero approximation provides for the approximate coincidence of the function, which is generated by the designed mechanism with the given function.

Applications of Newton's method and the method of iteration for the accurate synthesis of hinged mechanisms have also been considered.

Illustration 1. References 3.

UDC 621.835

Design of Cam Elements of Electrical Switches. D. M. Lukichev, V. A. Nikonorov and Z. S. Gazizova. Sbornik "Analysis and Synthesis of Mechanisms" (Analiz i sintez mekhanizmov). Izdatel'stvo Nauka, 1970, pages 148-153.

Equations for determining parameters of the cam element and its kinematic diagram are given in this article. Similar calculations for the spring have been undertaken based on the condition of providing normal working of the contactor (switch).

Besides electrical wear, mechanical wear has great significance for the contactors operating at small values of current.

The consideration of wear of contacts and in kinematic pairs, during design of the pitch curve of the cam plate has also been made by the authors.

Illustrations 5. References 3.

UDC 621.01

Synthesis of Cam-Planetary-Connecting Rod Mechanism with Reverse Stroke and Stop. L. B. Maisyuk. Sbornik "Analysis and Synthesis of Mechanisms" (Analiz i sintez mekhanizmov). Izdatel'stvo

Nauka, 1970, pages 153-161.

Synthesis of a cam-planetary-connecting rod mechanism with complex single-sided motion is analyzed by considering the maximum torque on the driving link of the mechanism.

Conditions for selecting an optimal group of mechanisms with minimum values of the coefficient of maximum velocity of the follower, have been obtained.

Equations for calculating the transitional sections of displacement function from motion to dwell and from dwell to motion are derived, so as to eliminate hard impacts on the driven link. Analytical relationships for calculating the displacement of the follower of the inversed cam group, contained in the combined mechanism have been found out.

Equations in explicit form for the calculation of analogs of velocity and acceleration of the follower have been obtained. Method of calculation of cam-planetary-connecting rod mechanism has been given and an example of calculation of its parameters is also included.

Illustrations 4. References 5.

UDC 621.01

Determination of the Zones of Existence of Slotted Lever Mechanisms. V. A. Mamedov. Sbornik "Analysis and Synthesis of Mechanisms" (Analiz i sintez mekhanizmov). Izdatel'stvo Nauka, 1970, pages 161-165.

A method for determining the boundaries of the zone of existence of slotted lever mechanism has been considered in this article. A flow diagram and a computer program for the calculation of basic parameters of the mechanism in the universal algorithmic language ALGOL-60 is also given. These calculations can be used for solving other problems of synthesis of such mechanisms.

Results show that for determining limiting values of angle of rotation, corresponding to the condition that discriminant is equal to zero, a cubical equation of cos α is obtained, which determines the boundary of the zone of existence as per the condition that discriminant is equal to zero.

Illustration 1. References 5.

UDC 621.01

Three-Dimensional Five-link Hinged Mechanisms. P. G.

M u d r o v. Sbornik "Analysis and Synthesis of Mechanisms" (Analiz i sintez mekhanizmov). Izdatel'stvo Nauka, 1970, pages 166-170.

A hinged five-link spatial mechanism is formed by the combination of two mechanisms. Geometrical parameters of the five-link mechanism may easily be determined proceeding from the structures of combined Bennett mechanisms. The kinematics of the five-link mechanism may also be determined depending on the method of their formation. On this basis, the author obtained equations for the determination of position, velocity and acceleration of the driven link, which are convenient to use.

An analysis of the equations for the calculation of angular velocity of the driven link made it possible to determine the conditions, for which it is possible to obtain a five-link mechanism with two cranks, in which one crank performs two rotations for one rotation of the other; and a five-link mechanism with one crank and one balancer where the stroke of the balancer (angle of rotation) may exceed 180°.

Illustrations 4. References 4.

UDC 621.01

Kinematic Study of Three-dimensional Three-link Lever Mechanisms Using Analytical Methods. Z. S. N a t s v l i s h v i l i. Sbornik "Analysis and Synthesis of Mechanisms" (Analiz i sintez mekhanizmov). Izdatel'stvo Nauka, 1970, pages 171-180.

Relationships between kinematic parameters of three-link mechanisms of zero family with such modification as common in machine building and instrumentation have been established in the present study. Equations have been derived for the functional relationship of displacements, velocities, accelerations, relative velocities and accelerations, and angular velocities and accelerations of driven links with the angles of rotation of the driving links.

From the results, tables have been developed and corresponding kinematic diagrams have been drawn, which provide insight into the motion of different links of the mechanisms.

Tables 3. Illustrations 6. References 7.

UDC 621.01

An Approximate Method for Synthesizing a Hinged Lever Amplifying Mechanism of a Molding Press. M. S. R o z o v s k i i, E. N. D o k u c h a e v a and V. G. L a p t e v a. Sbornik "Analysis and

Synthesis of Mechanisms" (Analiz i sintez mekhanizmov). Izdatel'stvo Nauka, 1970, pages 180-189.

An approximate method of synthesis of the amplifying mechanism of a press, used for molding models is considered in this article. The kinematic diagram of this mechanism differs from ordinary diagrams of amplifying mechanisms with a "bending" lever in that during the working part of the stroke of the driven link of the mechanism, a nearly constant transmission ratio is provided. The problem includes the determination of dimensions of the six-link mechanism—seven parameters. For solving this problem, the accurate but complex relationship between the transmission ratio and parameters of the mechanism is replaced by an approximate relationship which is a complete third degree polynomial of the angle of rotation of one of the connecting rod.

Simplification of the coefficients of each variable of the polynomial is carried out by making a number of assumptions, which have insignificant effect on the accuracy of the result. Moreover, a number of approximate relationships are used. As a result five equations for seven unknown geometrical parameters of the mechanism are found. Introduction of two conditions of optimization made it possible to obtain simple approximate relationships for the determination of all seven unknown parameters of the mechanism, which made it possible to solve the problem of its synthesis.

An example of the synthesis of mechanism is given.

Illustrations 6.

UDC 621.01

Dynamic Force Analysis of Plane-Mechanisms in Three-dimensional Space. K. F. Saskii. Sbornik "Analysis and Synthesis of Mechanisms" (Analiz i sintez mekhanizmov). Izdatel'stvo Nauka, 1970, pages 190-202.

An ordinary double-carrier group, if considered as a plane kinematic chain, is statically determinate. But in each kinematic pair of the fifth class in general the reaction force consists of three components of forces and two components of moments. Thus during static calculations, there are 15 unknowns whereas for two links of the above mentioned group only 12 equations can be formed. In the present article an effort is made to consider the statics of "plane" Assur groups from three-dimensional point of view. For solving the problem, a method of initial parameters in matrix form is used.

Basic equations are derived after providing the physical conception of the method. Kinematic parameters (linear and angular displacements)

of any section of the spatial bar type linkage (which in reality is the "plane" mechanism), and force factors (forces and moments) are expressed in terms of these parameters of the initial section.

Matrix form of the problem makes it possible to solve it conveniently on a digital computer.

General matrix relationships obtained for any spatial bar type linkage have been used for the double-carrier Assur group of the first type and a method for determining fifteen components of reactions in three turning pairs is derived.

The problem of accuracy of position of this group is solved, by considering the elastic deformation of its links.

Illustrations 6. References 2.

UDC 621.01

Analysis of the Structural and Technical Errors of Six-link Mechanisms in the Dwell Zone. V. I. Sergeev, S. A. Cherkudinov and I. G. Oleinik. Sbornik "Analysis and Synthesis of Mechanisms" (Analiz i sintez mekhanizmov). Izdatel'stvo Nauka, 1970, pages 202-213.

Presently, rational design of the modern machines is possible only through the calculation of structural and kinematic errors. Methods for the determination of structural errors of a six-link mechanism and of kinematic error due to errors of lengths and clearances are considered here.

Results provide guidelines for the selection of tolerances on lengths and clearances in the elements of the mechanisms.

A comparative analysis of the structural and kinematic errors of mechanisms has been undertaken.

Tables 2. Illustrations 8. References 7.

UDC 621.835

Fundamentals of the Theory of Dynamic Synthesis of Cam Mechanisms. P. V. Sergeev. Sbornik "Analysis and Synthesis of Mechanisms" (Analiz i sintez mekhanizmov). Izdatel'stvo Nauka, 1970, pages 214-219.

Mathematical techniques for the dynamic synthesis of cam mechanisms for different dynamic conditions have been presented in this article. It has been shown that this problem leads to the selection of design parameters of

cam mechanism whose extreme and limiting values for the given dynamic conditions coincide. This problem involves the selection of parameters of functions for their extreme values, which is equivalent to the classical problem of finding the extreme values of the function. For solving the problem of synthesis of parameters of the function it is proposed to use the auxiliary function, whose properties are established by the theorem, which is formulated and proved for the most general case. It is shown that the determination of parameter of initial function for the given value of its extreme leads to the determination of extreme value of the auxiliary function.

The proposed method of dynamic synthesis is independent of design conditions and is universally applicable to any structural diagrams of plane and spatial cam mechanisms with one and two degrees of freedom.

This method makes it possible to solve many problems of synthesis, for which there were no direct solutions available previously.

Illustrations 4. Reference 1.

UDC 621.01

Kinematic and Force Analysis of Spatial Mechanisms of Pneumatic and Hydraulic Drive for Stopcocks of Gas Mains of Type Du 1000. A. V. Sinev, I. Z. Brodotskaya and I. S. Charnaya. Sbornik "Analysis and Synthesis of Mechanisms" (Analiz i sintez mekhanizmov). Izdatel'stvo Nauka, 1970, pages 219-227.

The problem of determination of forces in the links of mechanisms taking into account friction forces is solved in order to identify the zone of jamming and determine the loss due to friction.

Force analysis of the mechanism is carried out by forming a generalized spiral equation of equilibrium (by equating to zero the main vector of forces and moments for each link of the mechanism taking into consideration the mutual reactions in links and the frictional forces caused during the relative motion of links).

The spiral calculations made it possible to effectively determine the position of links in space and their relative motion. A method for calculating the forces in links of the mechanism considering friction forces has been developed.

Illustrations 6. References 3.

UDC 621.01

Design of Automats with Photoelectronic Devices for the

Control and Measurement of Linear Dimensions and Areas. B. N. Sklyadnev, B. N. Yurukhin, Yu. I. Evteev and E. I. Astakhov. Sbornik "Analysis and Synthesis of Mechanisms" (Analiz i sintez mekhanizmov). Izdatel'stvo Nauka, 1970, pages 228-237.

This article deals with the selection of basic parameters of automats of specified efficiency and accuracy. A comparative evaluation of different kinematic diagrams of automats has been undertaken. An example considering primary errors of the device is given.

Results may be used in the design of automats with photoelectronic devices for the control and measurement of different geometrical parameters.

Table 1. Illustrations 5. References 5.

UDC 621.01

A Nomographical Method for the Synthesis of Multiple Contour Plane Hinged-lever Mechanisms. L. P. Storozhev. Sbornik "Analysis and Synthesis of Mechanisms" (Analiz i sintez mekhanizmov). Izdatel'stvo Nauka, 1970, pages 237-247.

All plane slider-crank mechanisms are divided into three groups, depending on the dimensions of links and characteristic motion of links. The zone of existence of each group and of whole mechanism is determined analytically and graphically. Limiting slider-crank mechanism of 5 types correspond to the limits of these zones. This systematization defines 8 slider crank mechanisms with different dimensions, which have different graphs of displacement functions and velocities. Five charts of displacement functions and one chart of absolute and relative linear velocities are constructed from graphs in the article. A number of kinematic and dynamic properties of this mechanism have been established by a study of these charts.

Two problems of synthesis of multiple contour plane mechanisms with one degree of mobility have been analyzed by the nomographical method.

Tables 3. Illustrations 6. References 4.

UDC 621.01

Techniques of Synthesizing Adjustable Lever Mechanisms. B. S. Sunkuev. Sbornik "Analysis and Synthesis of Mechanisms" (Analiz i sintez mekhanizmov). Izdatel'stvo Nauka, 1970, pages 247-255.

A method of synthesizing adjustable lever transmission mechanisms for

a specified variation in the extreme positions of the driven link and corresponding position of the driving link is described. The latter have been termed as phases of extreme positions of the driven link.

The essence of the method is that adjustable mechanisms may be converted into an auxiliary nonadjustable one, which simulates the regulation of the original mechanism. Synthesis of the nonadjustable auxiliary mechanism is carried out initially. This is converted into the adjustable mechanism and parameters of the latter are determined.

Existing methods of synthesis can be employed during synthesis of the auxiliary mechanism.

Solution of two problems of synthesis with the application of the herein mentioned method is given as an illustration.

Illustrations 9. References 7.

UDC 621.835

An Approximate Technique for the Synthesis of Disk Cam Mechanisms. K. V. Tir and D. N. Senik. Sbornik "Analysis and Synthesis of Mechanisms" (Analiz i sintez mekhanizmov). Izdatel'stvo Nauka, 1970, pages 255-267.

Change in pressure angle during a kinematic cycle according to the four laws of motion has been studied in this article for 240 structural diagrams. For diagrams not included in this set, graphs of maximum pressure angles α_m have been obtained by interpolation. Nomographs for selecting cam dimensions and instantaneous efficiency as a function of the given conditions have also been drawn.

All generalizations have been made on the basis of the method of similarity invariants for the mechanisms. This makes it possible to draw charts of blocking contour (as a result of the insertion of a number of new generalized criterions) for central cam mechanisms with reciprocating and oscillating followers which are valid for any law of motion under any conditions of loading of the mechanism. These charts take into account the necessary conditions for preventing jamming of the mechanism, the tensile strength and wear resistance of elements of components and also conditions of proximity which put limitations on the selection of the structural diagram.

Tables and nomographs of geometrical parameters of components have been drawn which enable thorough calculation of the mechanism to be undertaken in 20 minutes.

Illustrations 5. References 14.

UDC 621.01

The Problem of Existence of the Crank in the Spatial Four-link Mechanism with Two Turning and Two Spherical Pairs. K. A. Tonoyan. Sbornik "Analysis and Synthesis of Mechanisms" (Analiz i sintez mekhanizmov). Izdatel'stvo Nauka, 1970, pages 267-280.

Geometrical conditions of turning of links of spatial four-link mechanism with two spherical and two turning pairs have been considered.

Conditions have been defined which permit the separation of the field of existence of double-crank mechanism from crank-rocker mechanisms and point out the link in the definite zone of variation of parameters of the mechanism, in which it can be a crank.

Analytical and graphical calculations for the limits of variation of the length of the connecting rod necessary for the existence of crank and mechanism are given. Conditions of turning of links have been obtained for one particular case and these conditions resemble Grasgaf's conditions for plane hinged four-link mechanism.

Illustrations 10. References 10.

UDC 621.835

Functions with Minimum Deviations from Zero in Problems of Synthesis of Cam Mechanisms. Yu. V. Epshtein and V. A. Novgorodtsev. Sbornik "Analysis and Synthesis of Mechanisms" (Analiz i sintez mekhanizmov). Izdatel'stvo Nauka, 1970, pages 280-288.

During synthesis of cam mechanisms, functions with minimum deviation from zero are used. An algorithm for defining a polynomial or a function having minimum deviation from zero has been developed for calculating the polynomial. The algorithm has been programmed for a digital computer.

A unit mass system, dynamically equivalent to the cam mechanism is considered. Experiments were undertaken on a special stand provided with a cam mechanism, for determining the effect of manufacturing errors on the optimal profile of a cam.

Illustrations 4. References 7.